INFLAMMASOME SIGNALLING DURING *SALMONELLA* TYPHIMURIUM INFECTION

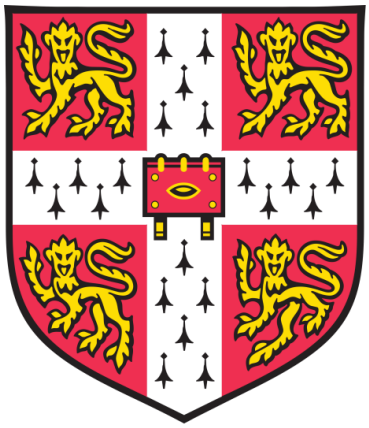

Milton César de Almeida Pereira

Churchill College

University of Cambridge

This dissertation is submitted for the degree of Doctor of Philosophy

April 2018

INFLAMMASOME SIGNALLING DURING *SALMONELLA* TYPHIMURIUM INFECTION

Milton César de Almeida Pereira

Summary

The innate immune system is the first line of defence against infection. It is comprised of physicochemical barriers and a variety of cell types including macrophages and dendritic cells. Pathogens express specific pathogen associated molecular patterns (PAMP) which are recognised by pattern recognition receptors (PRR) on macrophages to initiate an innate immune response. Gram-negative bacteria such as *Salmonella enterica* serovar Typhimurium express a range of bacterial PAMPs recognised by Toll-like receptors (TLRs) including lipopolysaccharides (LPS) recognised by TLR-4 and lipoproteins by TLR-2. The activation of TLRs results in activation of nuclear factor κB (NF-κB) to drive transcription of mRNA coding for pro-inflammatory proteins such as tumor necrosis factor α (TNF-α) and pro-interleukin (IL) 1β. Myeloid cells also possess intracellular PRRs including the nucleotide-binding domain and leucine-rich repeat (NLR) family. NLR family CARD domain-containing protein 4 (NLRC4) and NLR family pyrin domain-containing protein 3 (NLRP3) are the main NLRs engaged in recognising *S*. Typhimurium infection, leading to formation of the inflammasome.

The inflammasome is a macromolecular complex assembled in the cytoplasm, and usually contains a NLR, the structural protein apoptosis-associated speck-like protein containing a CARD (ASC) and effector enzymes such as cysteine-dependent aspartate-directed protease (caspase) -1 and caspase-8. This structure is responsible for processing the cytokines pro-IL-1β and pro-IL-18 to their mature form and is involved in triggering a pro-inflammatory process of cell death termed pyroptosis. The formation of the inflammasome therefore results in cell death and secretion of proinflammatory cytokines which play important roles in controlling infections. Inflammasome activity must be tightly coordinated, as its dysregulation is associated with a variety of auto-inflammatory and auto-immune diseases.

The signalling events leading to inflammasome assembly are poorly understood and the molecules involved in fine-tuning its activity are only beginning to be discovered. The aim of

this thesis was to discover new molecules involved in inflammasome activation and/or in keeping its activity in check. To achieve this goal, I performed *S*. Typhimurium infection assays in primary bone marrow derived macrophages (BMDM) derived from C57BL/6 mice wild type (WT) and compared the resulting cellular viability, intracellular bacteria counts and IL-1β production to that of BMDMs derived from C57BL/6 mice lacking proteins involved with, or suspected to be involved with, innate immune activity. Amongst the proteins I studied, caspase recruitment domain 9 (CARD9) inhibited inflammasome-mediated IL-1β production. Multiple independent genome-wide association studies link this protein to inflammatory pathologies such as Crohn's disease, but its role in canonical inflammasomes was largely unexplored.

To investigate how CARD9 inhibits inflammasome-mediated IL-1β production I have conducted assays in WT and *Card9*$^{-/-}$ BMDMs, including stimulation of specific NLRs with their purified ligands, infection with bacterial strains deficient in NLRC4 activation, and infection assays in presence of pharmacological inhibitors. By employing these approaches, I observed that CARD9 has a negative role on NLRP3-dependent IL-1β production. Specifically, in response to activation of the NLRP3 by *Salmonella* infection, CARD9 negatively regulates pro-IL-1β transcription, and decreases IL-1β processing by inhibiting spleen tyrosine kinase (SYK)-mediated NLRP3 activation and represses caspase-8 activity in the inflammasome. CARD9 expression is suppressed in the course of *S.* Typhimurium infection which may act as a mechanism to increase IL-1β production during the infection.

In conclusion, I have established a connection between CARD9 and IL-1β production by the canonical NLRP3 inflammasome and elucidated some of the mechanisms involved in this process. I have also found evidence that other proteins are likely to be involved in inflammasome regulation and the elucidation of their roles will be addressed in future studies.

Declaration and statement of length

This dissertation is the result of my own work and includes nothing which is the outcome of work done by others except where specifically indicated in the text. This work has not been submitted in whole or in part for consideration for any degree, diploma or any other qualification at this, or any other university.

This thesis does not exceed the word limit of 60,000 words excluding figures, tables, appendices and bibliography.

Milton César de Almeida Pereira

April 2018

Acknowledgements

First, I would like to thank Professor Clare Bryant for her supervision, support and encouragement throughout my PhD. I would also like to thank all the colleagues who helped me along the way: Zsofi Digby, Dan Levy, Dr. Charlotte Macleod, Dr. Panagiotis Tourlomousis, Dr. Lee Hopkins, Dr. Martyn Symmons, Dr. John Wright, Dr. Tom Monie, Dr. Bettina Lee, Dr. Christine Hinz and Professor Jerry Wells. My sincere thanks to Dr. Vishva Dixit and Dr. Nobuhiko Kayagaki for the summer internship opportunity at Genentech.

I am grateful to Coordenação de Aperfeiçoamento de Pessoal de Nível Superior (CAPES, Brazil) for their financial support and for giving me the opportunity to study at the University of Cambridge.

I would like to thank my parents for always believing in me. A very special thank you to all the wonderful people who were around me in the past few years: Catherine, Caroline, Henrique, Thais, Júlia, Rebecca, Sun, Aušrinė, Alessandra, Charlotte, Thiago, Yasmin, Sarah, Rosie and Luíza.

Lastly, I am very grateful to Lou Reed, Patti Smith, Caetano Veloso, Belchior, Simon Jeffes, Courtney Barnett, Lucy Dacus, Mac DeMarco, Marisa Monte and Paul Simon. Without them, writing this thesis would have been a very dull endeavour.

Table of contents

List of abbreviations

AIM2	Absent in melanoma 2
ALR	AIM2-like receptors
AP-1	Activator protein 1
ASC	Apoptosis-associated Speck-like protein containing a CARD
AUC	Area under the curve
BCL10	B-cell lymphoma/leukemia-10
Bid	BH3 interacting-domain death agonist
BIR	Baculovirus inhibitor repeat
BMDC	Bone marrow derived dendritic cells
BMDM	Bone marrow derived macrophages
BRCC3	BRCA1/BRCA2-Containing Complex Subunit 3
BTK	Bruton Tyrosine Kinase
β-TRCP	β-Transducin repeat-containing protein
CARD	Caspase recruitment domain
Caspase	Cysteine-dependent aspartate-directed protease
CBP	CREB-binding protein
CD	Cluster of differentiation
cGAMP	Cyclic GMP-AMP
cGAS	Cyclic GMP-AMP synthase
CIITA	MHC class II transcriptional activator
COX	Cyclooxygenase
DAMP	Danger associated molecular pattern
DAP	Diaminopilemic acid
DD	Death Domain
DED	Death effector domain
DFNA5	Deafness autosomal dominant 5
DHX9	DExH-Box helicase 9
DISC	Death Inducing Signalling Complex
DMEM	Dulbecco's modified Eagle's medium
ds	Double strand
ERK	Extracellular signal-regulated kinases
FADD	Fas-associated protein with death domain

FAF1	FAS-associated factor-1
FcR	Fragment crystallisable receptor
FIIND	Function to Find
GAPDH	Glyceraldehyde 3-phosphate dehydrogenase
GPA	Gentamicin protection assay
GWAS	Genome-wide association studies
HET-E	Incompatibility locus protein from *Podospora anserina*
HIN	Hematopoietic expression, interferon-inducible nature, and nuclear localization
HIV-1	human immunodeficiency virus 1
IBD	Inflammatory bowel diseases
ICE	Interleukin conversion enzyme
IFN	Interferon
IkB	Inhibitor of NF-κB
IKK	IκB kinase
IL	Interleukin
iNOS	Inducible Nitric Oxide Synthase
IPAF-1	ICE Protease-activating Factor 1
IRAK	Interleukin-1 receptor-associated kinase
IRF3	Interferon regulatory transcription factor 3
ITAM	Tyrosine-based activation motif
JNK	C-Jun N-terminal kinases
LeTx	Lethal Toxin
LPS	Lipopolysaccharides
LyGPI	Ly GDP-dissociation inhibitor
MAL	MyD88-adaptor-like
MALT1	Mucosa-associated lymphoid tissue lymphoma translocation protein 1
MAPK	Mitogen-associated protein kinases
MAVS	Mitochondria Antiviral Signalling
MDA5	Melanoma differentiation-associated protein
MDP	Muramyl dipeptide
MEF	Mouse embryonic fibroblasts
MHC	Major histocompatibility complex
MLKL	Mixed lineage kinase domain-like
MyD88	Myeloid differentiation primary response gene 88
NACHT	NAIP, CIITA, HET-E and TP1

NAIP	NLR family, apoptosis inhibitory protein
NAIP	Neuronal apoptosis inhibitory protein
NALP	LRR and PYD domains-containing protein
NBD	Nucleotide binding domain
NEMO	NF-κB essential modulator
NES	Nuclear export sequence
NF-kB	Nuclear factor κB
NK	Natural Killer
NLR	Nucleotide-binding domain and leucine-rich repeat
NLRC	NLR family CARD domain-containing protein
NLRP	NLR family pyrin domain-containing protein
NLS	Nuclear leading sequence
NO	Nitric Oxide
NOD	Nucleotide-binding oligomerization domain-containing protein
NOS	Nitric Oxide Synthase
PAMP	Pathogen associated molecular pattern
PARP	Poly-(ADP-Ribose) polymerase (PARP)
PGE2	Prostaglandin E2
PIDD	p53-inducible protein with death domain
PKA	Protein kinase A
PKC	Protein Kinase C
PP2A	Protein Phosphatase 2A
PRR	Pattern recognition receptor
PS	Phosphatidylserine
PTM	Post-translational modifications
PYD	Pyrim domain
Pyk2	Proline-rich tyrosine kinase 2
RAIDD	(RIP)-associated ICH-1/CED-3 homologous protein with a death domain
RANTES	Regulated on activation, normal T cell expressed and secreted
RHD	Rel Homology Domain
RIG-I	Retinoic acid-Inducible Gene-I
RIPK	Receptor-interacting serine/threonine-protein kinase
RLR	RIG-I-like Receptors
ROS	Reactive oxygen species
RUBICON	RUN domain Beclin-1-interacting cysteine-rich-containing
SCF	Skp1-cullin-F-box protein

SCV	*Salmonella* cointaining vacuole
SEM	Standard error of the mean
SHP	Small heterodimer partner
siRNA	Small interfering RNA
SLC15	Solute carrier family 15
SopB	*Salmonella* outer protein B
SPI	*Salmonella* pathogenicity island
SPRY	Spi-A kinase and ryanodine receptor
ss	Single strand
STAT1	Signal transducer and activator of transcription 1
STING	Stimulator of interferon genes
SYK	Spleen tyrosine kinase
T3SS	Type 3 secretion system
TBK1	TANK-binding kinase-1
TIR	Toll/Interleukin-1 receptor homology domain
TLR	Toll-like receptor
TNFR	Tumor necrosis factor receptor
TNFR	Tumor necrosis factor receptor
TNF-α	Tumor necrosis factor α
TP1	Telomerase-associated protein 1
TRADD	Tumor necrosis factor receptor type 1-associated death domain protein
TRAF	TNF receptor associated factor
TRAM	TRIF-related adaptor molecule
TRIF	TIR-domain-containing adapter-inducing interferon-β
TRIM	Tripartite Motif Containing protein
WT	Wild type
XIAP	X-linked IAP

List of figures

List of tables

Chapter 1

Introduction

1.1. Innate immunity

Microbial diversity is unprecedented, with an estimated one trillion species occupying a wide range of environments (Locey and Lennon, 2016). The human body, in particular, is inhabited by 10,000 different microbial species (Huttenhower et al., 2012) with an estimated ratio of human to bacterial cells of one to one (the more dramatic and often cited one to ten ratio lacks empirical support) (Sender et al., 2016). Most of these bacteria reside in the gastrointestinal tract and are either commensal or symbiotic. Commensal microorganisms benefit from the host while the host is neither harmed nor benefitted. Symbionts are microorganisms that have co-evolved with the host in a mutually beneficial way. They are provided with a favourable habitat and, through the host's diet, non-digestible material which they degrade to produce energy and nutrients essential for their growth. In turn, certain end-products of this fermentation, such as short chain fatty acids and vitamins, play important physiological, metabolic and protective roles in the host's gut health. Furthermore, symbiotic bacteria compete with pathogenic bacteria for nutrients and space preventing them from colonising the gastrointestinal tract (Pickard et al., 2017).

In addition to commensals and symbionts, we are also exposed to a large number of microbes with pathogenic potential, which, however, rarely cause disease. This is not only due to competition with the gut microbiota as mentioned above, but also due to the protective effect of the innate immune system. This system is the first line of defence against invading organisms and is formed by numerous components such as physical and chemical barriers, nonspecific antimicrobial molecules and numerous cell types such as macrophages and dendritic cells. Although it is nonspecific and conserved throughout evolution, it is highly efficient at eliminating threats before compromising the host's health.

Different cells of the innate immune system recognise bacteria by using pattern recognition receptors (PRR), which detect conserved pathogen associated molecular patterns (PAMP) of foreign origin and danger associated molecular patterns (DAMP) of host origin. Once activated, PRRs trigger specific cellular signalling events leading to a pro-inflammatory response important for clearing the infection (Janeway and Medzhitov, 2002; Schroder and Tschopp, 2010). At the heart of this response lies the production of cytokines and chemokines together with the induction of various forms of programmed host's cell death

(Figure 1.1). In the context of a wide range of infectious agents, programmed cell death is beneficial to the host: an infected cell “commits suicide” and interrupts the pathogen’s life cycle and/or alerts neighbouring cells to the pathogen (Grootjans et al., 2017; Lamkanfi and Dixit, 2014).

Apoptosis is the most well-defined form of programmed cell death triggered by both intrinsic and extrinsic signals, occurring both in physiological conditions (for instance during development), and in pathologies including infections. Morphologically, apoptotic cells undergo shrinkage due to enzymatic cleavage of cytoskeletal proteins, membrane blebbing, chromatine condensation and nuclear fragmentation (Kerr et al., 1972). This death program is executed by different cysteine-aspartic protease (caspase) enzymes. An important feature of this process is the translocation of phosphatidylserine (PS) to the outer leaflet of the plasma membrane, acting as a signal for phagocytes to “clear” the apoptotic cell (Fadok et al., 1992). This process is considered immunologically silent as apoptotic cells do not generally release their intracellular contents and are quickly cleared by phagocytosis.

Unlike the immunologically silent apoptosis, pyroptosis is an orchestrated form of cell death that involves the production and release of pro-inflammatory cytokines interleukin (IL)-1β and IL-18. Although the mechanisms of cytokine release are not clear, it is possible that the release of intracellular contents including cytokines occurs after the loss of membrane integrity. Pyroptosis is triggered by caspase 1 cleavage of the protein gasdermin D to its active form which create pores in the cellular membrane (Aglietti et al., 2016; Kayagaki et al., 2015; Shi et al., 2015). This results in rapid cytoplasmic swelling with subsequent cell rupture and release of intracellular contents that can act as danger signals to “alert” neighboring cells (Cunha and Zamboni, 2013). This form of cell death is associated with the formation of macromolecular complexes known as inflammasomes. Pyroptosis is thought to be important for host protection against a number of intracellular pathogens, as the rupture of the cell in an inflammatory context releases the invading pathogen into the extracellular space where it can be destroyed by other immune cells, such as neutrophils (Lamkanfi and Dixit, 2014; Miao et al., 2010).

Necroptosis is a form of cell death typically associated with pathological processes where cells are rapidly stressed. Necroptosis involves rapid cytoplasmic swelling resulting in plasma membrane and organelle breakdown and is thought to trigger inflammation due the release of DAMPs. Mechanistically, this form of cell death involves proteins such as caspase-8, receptor-interacting serine/threonine-protein kinase (RIPK)-1, RIPK-3 and mixed lineage kinase domain-like (MLKL) (Grootjans et al., 2017; Krysko et al., 2008). Necroptosis can also be triggered by infectious agents and play a role in clearing the infection. For

instance, RIPK3-dependent necroptosis is thought to be important in the clearance of cytomegalovirus infections (Upton et al., 2008).

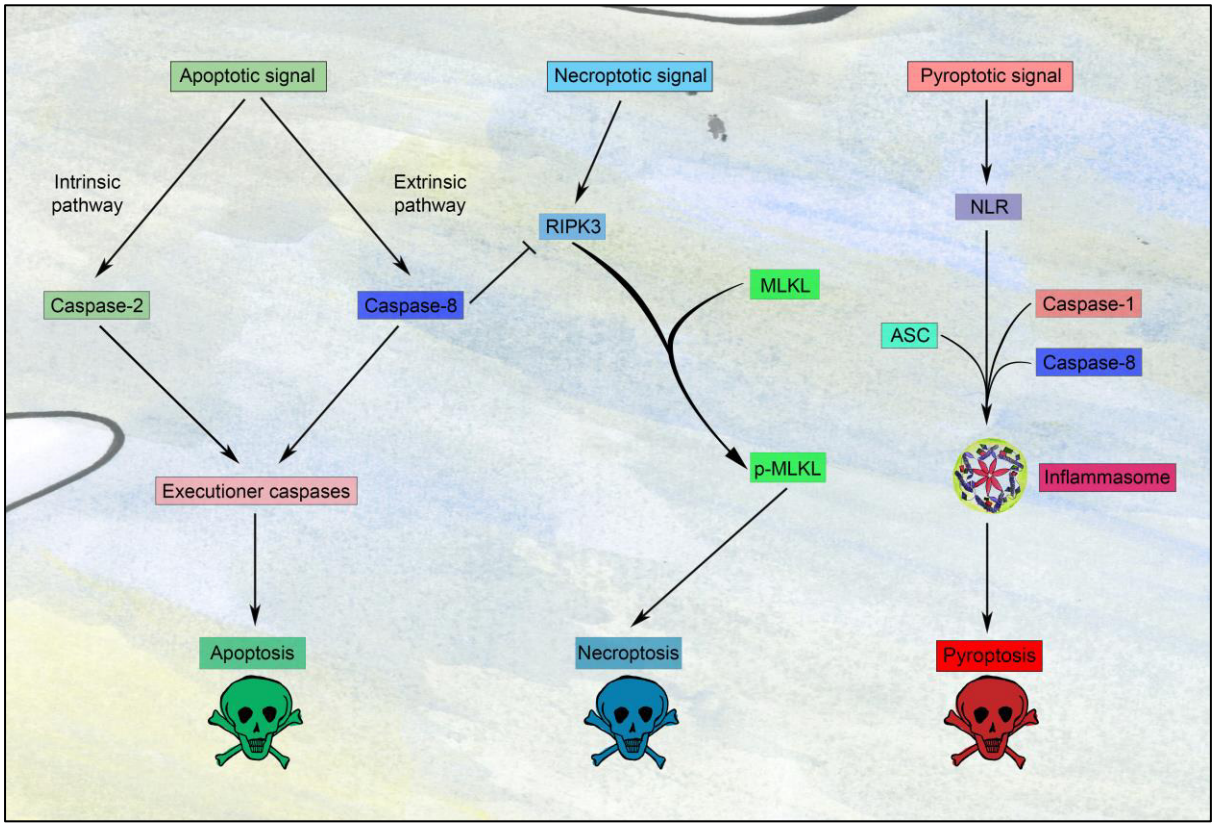

Figure 1.1: Programmed cell-death. Overview of apoptosis, necroptosis and pyroptosis, with some of the key-players highlighted.

1.2. Toll-like Receptors

The family of Toll-like receptors (TLRs) consists of transmembrane proteins usually expressed in myeloid cells such as macrophages and dendritic cells. Twelve of these receptors have been so far identified in mammals and are located either on the surface of the plasma membrane (TLR 1, 2, 4, 5, 6, 10 and 11) or in endosomes (TLRs 3, 4, 7, 8, 9, 12 and 13). TLRs can initiate and modulate important biological responses, such as phagocyte activation and induction of inflammation, therefore contributing to the resolution of infection (Monie et al., 2009).

Different TLRs recognizes different PAMPs. For example, TLR4 recognises lipopolysaccharide (LPS) present in the outer membrane of Gram negative bacteria

(Hoshino et al., 1999; Poltorak et al., 1998). TLR5 and TLR11 recognises bacterial flagellar proteins (Feuillet and Medjane, 2006; Hayashi et al., 2001; Mathur et al., 2012). TLR9 recognises non-methylated CpG motifs, a common feature in the DNA of numerous microorganisms (Hemmi et al., 2000; Klinman et al., 1996). TLR2 and TLR1 heterodimers recognise triacylated proteins (Takeuchi et al., 2002) while diacylated proteins are recognised by TLR2 and TLR6 heterodimers (Takeuchi et al., 2001). Viral single stranded (ss) DNA is recognised by either TLR7 or TLR8 (Heil, 2004; Lund et al., 2004). Profilin from Toxoplasma gondii is recognised by TLR11 and TLR12 dimers (Koblansky et al., 2013). Finally, bacterial rRNA is recognised by TLR13 (Oldenburg et al., 2012). Table 1.1 and Figure 1.2 summarise the different TLRs discussed above.

Table 1.1: TLRs and their main adaptor(s), cellular location and PAMPs.

Toll-like receptor	Adaptor	Cellular location	PAMP
TLR1	MyD88	Plasma membrane	Triacylated lipoproteins (Dimer TLR1/TLR2)
TLR2	MyD88	Plasma membrane	Lipoproteins (Heterodimer with TLR1 or TLR6)
TLR3	TRIF	Endosomes	dsRNA
TLR4	MyD88/TRIF	Plasma membrane	LPS
TLR5	MyD88	Plasma membrane	Flagella proteins
TLR6	MyD88	Plasma membrane	Diacylated lipoproteins (Dimer TLR6/TLR2)
TLR7	MyD88	Endosomes	ssRNA
TLR8	MyD88	Endosomes	ssRNA
TLR9	MyD88	Endosomes	Non-methylated CpG DNA
TLR10	MyD88	Plasma membrane	Unknown
TLR11(*)	MyD88	Plasma membrane	Flagellin
TLR12(*)	MyD88	Endosomes	Profilin
TLR13(*)	MyD88	Endosomes	Bacterial 23S rRNA

(*) Absent in humans.

Upon activation, the TLRs form homo- or heterodimers and recruit the adaptors Myeloid Differentiation primary response gene 88 (MyD88) or TIR-domain-containing adapter-inducing interferon-β (TRIF), in some cases via the adaptors MAL (MyD88-adaptor-like) or TRAM (TRIF-related adaptor molecule), respectively. With the exception of TLR3, every TLR signals through MyD88, while the TRIF branch is only activated by TLR3 and TLR4 (Kawai and Akira, 2011). MyD88 ultimately leads to activation of nuclear factor-κB (NF-κB) and mitogen-associated protein kinases (MAPK) and TRIF-dependent pathways leads to

activation of NF-κB and interferon regulatory transcription factor 3 (IRF3) (Kawai and Akira, 2010).

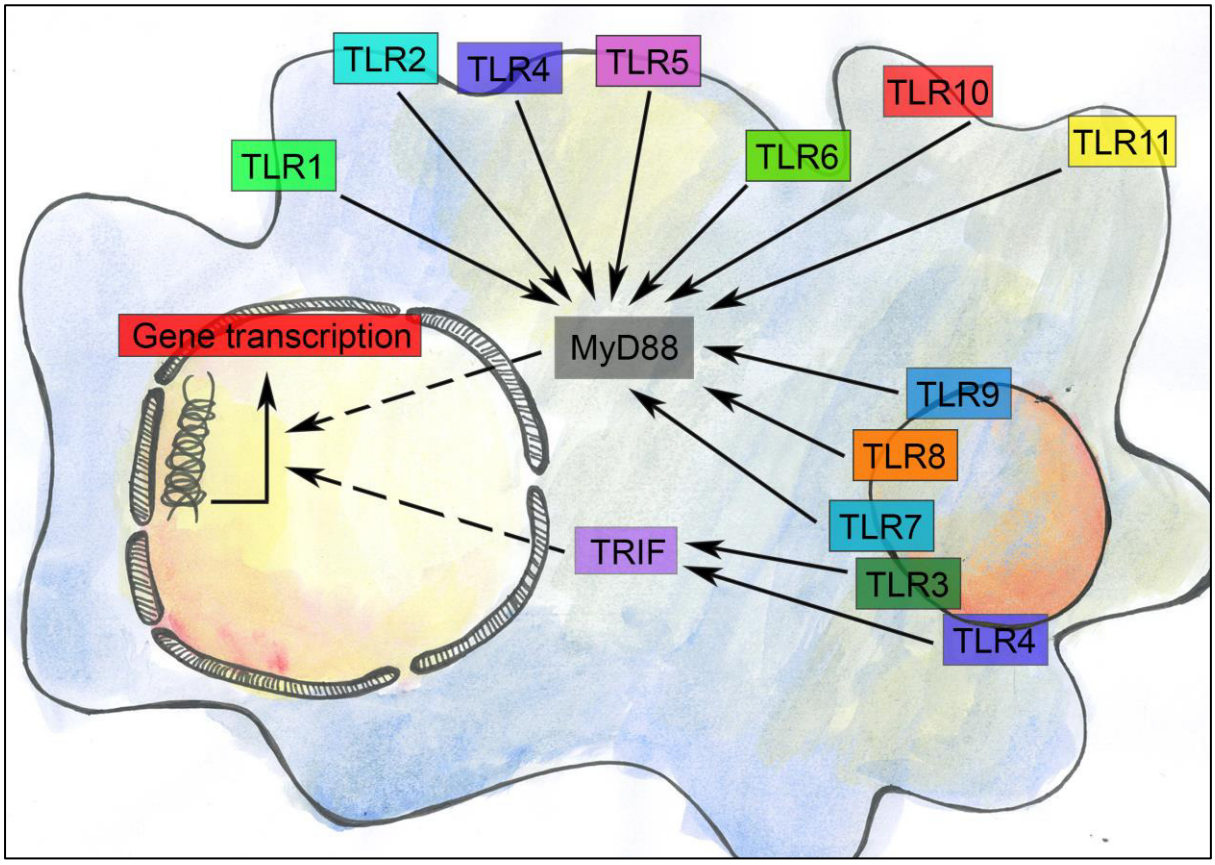

Figure 1.2: Toll-like receptors, their cellular localization and main adaptors.

Downstream to MyD88 and TRIF, NF-κB is the main family of transcription factors activated by PAMPs. NF-κB is a homo- or heterodimer that can be formed by the subunits RelA, c-Rel, RelB, p50 and p52, all of which contain a Rel Homology Domain (RHD), allowing them to interact with the DNA. In resting cells, the NF-κB dimer is sequestered in the cytosol by the protein Inhibitor of NF-κB (IκB), that masks NF-κB nuclear leading sequence (NLS), blocking its interaction with nuclear importins (Jacobs and Harrison, 1998). Upon activation, IκB is phosphorylated by the IκB kinases (IKK) IKK1/IKK2 complex, followed by ubiquitination and degradation in the proteasome (Tergaonkar, 2006). This causes NF-κB to translocate to the nucleus where it can interact with enhancers such as p300/CBP (CREB-binding protein), allowing the transcription of target genes to occur. Over time, newly synthetized IκBα is translocated to the nucleus, where it binds to NF-κB and interacts with exportins due to its nuclear export sequence (NES), completing the NF-κB cycle (Huang et al., 1999).

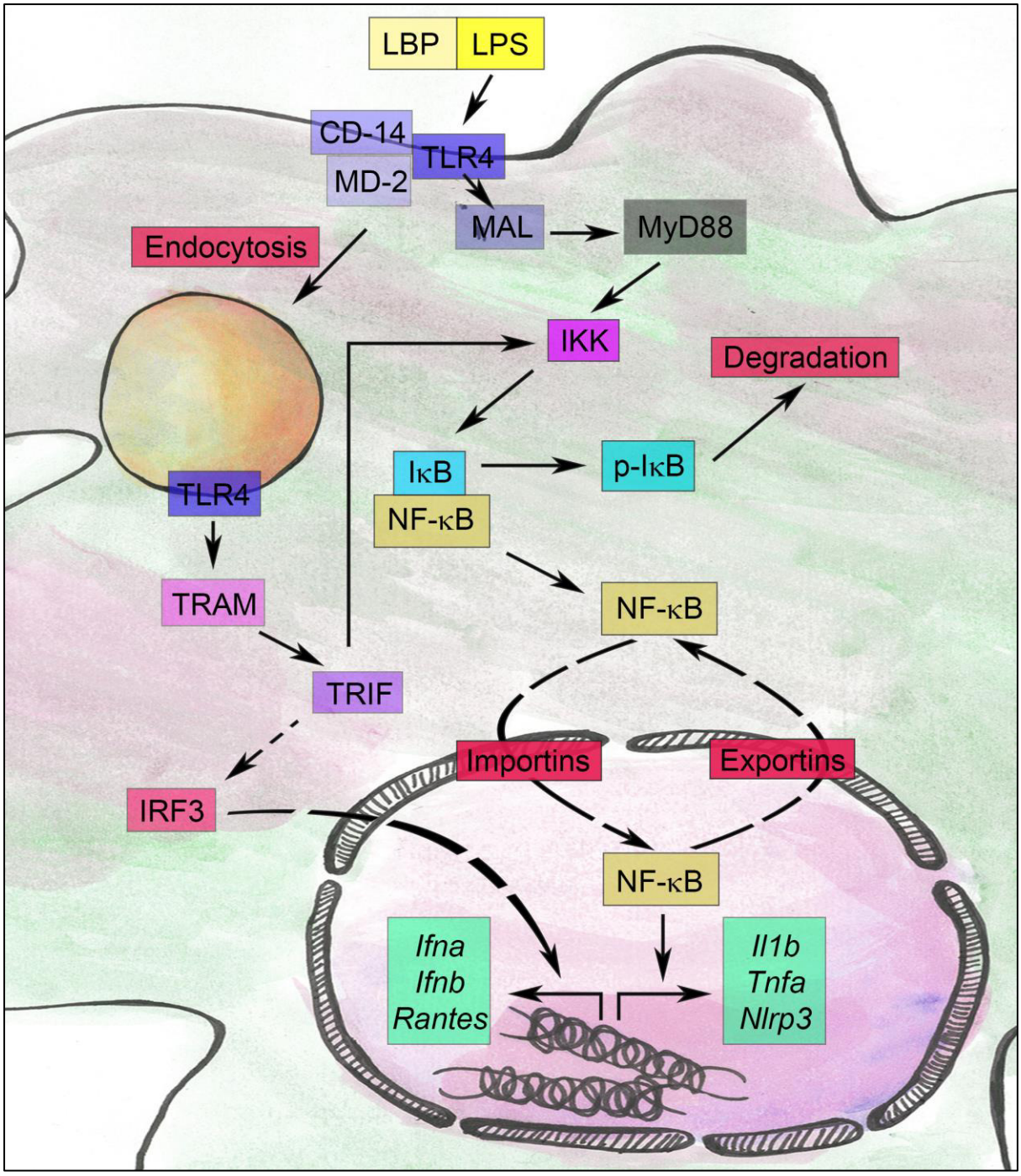

Figure 1.3: The NF-κB pathway, as exemplified by TLR4 activation. TLR4 activation leads to Mal/MyD88-dependent activation of NF-κB signalling. On a later stage, the receptor undergoes endocytosis leading to TRAM/TRIF-dependent activation of IRF3 and NF-κB.

The TLR4 signalling pathway is unique in that it can be both TRIF- and MyD88-dependent. LPS is solubilized by the LPS-binding protein (LBP) (Tobias et al., 1986), and transferred to the receptor cluster of differentiation (CD)-14 present in the membrane of numerous myeloid

cells (Wright et al., 1990). The LPS/CD-14 complex interacts with TLR4 and the MD-2 co-receptor resulting in the recruitment of the adaptor MAL. MAL, in turn, mediates the interaction with MyD88, triggering the recruitment of IL-1 associated protein kinases (IRAK) and early phase NF-κB translocation (Burns et al., 1998; Horng et al., 2002; Shimazu et al., 1999), upregulating the transcription of genes that code for proteins such as NLRP3, pro-IL-1β, cyclooxygenase-2 (COX-2) and TNF-α (Bauernfeind et al., 2009; Hiscott et al., 1993; Libermann and Baltimore, 1990; Shakhov et al., 1990; Ueda and Yamamoto, 1995). Next, TLR4 is endocytosed allowing TRIF to be recruited through the adaptor TRAM. This results in a delayed stimulation of NF-κB and the IRF3 pathway, which upregulates the transcription of genes such as *Ifna*, *Ifnb* and *Rantes* (Fitzgerald et al., 2003; Kagan et al., 2008; Lin et al., 1999; Yamamoto et al., 2002; Yoneyama et al., 1998) (Figure 1.3).

1.3. Nucleotide-binding domain and leucine-rich repeat-containing proteins

Nucleotide-binding domain and leucine-rich repeat-containing (NLR) proteins are located in the cytoplasm of a variety of cell types and can act as PRRs by recognizing PAMPs and DAMPs or by modulating a variety of signalling pathways associated with innate immunity, such as the formation of the inflammasome. Members of this family usually contain C-terminal LRR and a N-terminal nucleotide-binding domain, either a caspase-recruitment domain (CARD) or PYRIN domain (PYD), although some members possess a baculovirus inhibitor repeat (BIR) domain or a domain with no clear homology to any described domain. Members of this family also contain the NACHT domain, named after some of its constituent proteins: NAIP, CIITA, HET-E and TP1 (acronyms for neuronal apoptosis inhibitory protein, MHC class II transcriptional activator, incompatibility locus protein from *Podospora anserina*, and telomerase-associated protein) (Koonin and Aravind, 2000), that bind oligonucleotides to initiate oligomerization. Table 1.2 (modified from Proell et al., 2008) lists some of the NLRs and their constituent domains.

Table 1.2: NLR proteins and their domains. Caspase-recruitment domain (CARD), Pyrin Domain (PYD), baculovirus inhibitor repeat (BIR), domain present in NAIP, CIITA, HET-E and TP1 (NACHT), function to find (FIIND), leucine rich repeats (LRR).

NLR	Domains
NOD1	CARD-NACHT-LRR
NOD2	CARD-CARD-NACHT-LRR
NLRC3	CARD-NACHT-LRR
NLRC4	CARD-NACHT-LRR
NLRC5	CARD-NACHT-LRR
NLRA	CARD-NACHT-LRR
NLRP1	PYD-NACHT-LRR-FIIND-CARD
NLRP2	PYD-NACHT-LRR
NLRP3	PYD-NACHT-LRR
NLRP4	PYD-NACHT-LRR
NLRP5	PYD-NACHT-LRR
NLRP6	PYD-NACHT-LRR
NLRP7	PYD-NACHT-LRR
NLRP8	PYD-NACHT-LRR
NLRP9	PYD-NACHT-LRR
NLRP10	PYD-NACHT
NLRP11	PYD-NACHT-LRR
NLRP12	PYD-NACHT-LRR
NLRP13	PYD-NACHT-LRR
NLRP14	PYD-NACHT-LRR
NAIP	BIR-NACHT-LRR
NLRX1	X-NACHT-LRR
CIITA	X-NACHT-LRR

In addition to NLRs, absent in melanoma-2 (AIM2)-like receptor (ALR) and RIG-I-like receptor (RLR) are also intracellular PRRs involved in the recognition of intracellular nucleic acids (Rathinam and Fitzgerald, 2016; Yoneyama et al., 2015).

1.3.1. The inflammasome

One of the most important functions of both NLRs and ALRs is the recognition of PAMPs and DAMPs which trigger signalling events leading to the assembly of the inflammasome. Ultimately the inflammasome is observed as a speck-like macromolecular protein complex (which appears as a ring-shaped structure in super resolution microscopy of the endogenous complex) in the cytoplasm of the cell (Man et al., 2014). It contains a polymer of the adaptor apoptosis-associated speck-like protein containing a CARD (ASC), acting as a platform for

the activation of caspase-1, which in turn catalyses the conversion of pro-IL-1β and pro-IL-18 to their active forms IL-1β and IL-18, respectively (Martinon et al., 2002). Inflammasome assembly also results in cleavage of gasdermin D that create pores in the cellular membrane executing pyroptosis (Aglietti et al., 2016; Kayagaki et al., 2015; Lamkanfi and Dixit, 2014; Man et al., 2014; Masumoto et al., 1999; Shi et al., 2015). The ring-shaped structure containing a NLR, ASC and caspase-1 is known as a canonical inflammasome (Figure 1.4). The less well characterised non-canonical inflammasomes may or may not contain ASC and a contains a non-caspase-1 enzyme, such as caspase-8 or caspase-11 (human caspase 4/5) and are assembled in specific contexts. For example, the caspase-8 non-canonical inflammasome is assembled during fungal infections as a result of dectin-1 activation, a C-type lectin (Gringhuis et al., 2012), whereas the caspase-11 non-canonical inflammasome is formed upon recognition of intracellular LPS (Kayagaki et al., 2013, 2011). Currently, the following canonical inflammasomes were described: NLRP1, NLRP3, NLRC4, AIM2, NLRP9 and Pyrin (Agostini et al., 2004; Fernandes-Alnemri et al., 2009; Mariathasan et al., 2004; Martinon et al., 2002; Xu et al., 2014; Zhu et al., 2017).

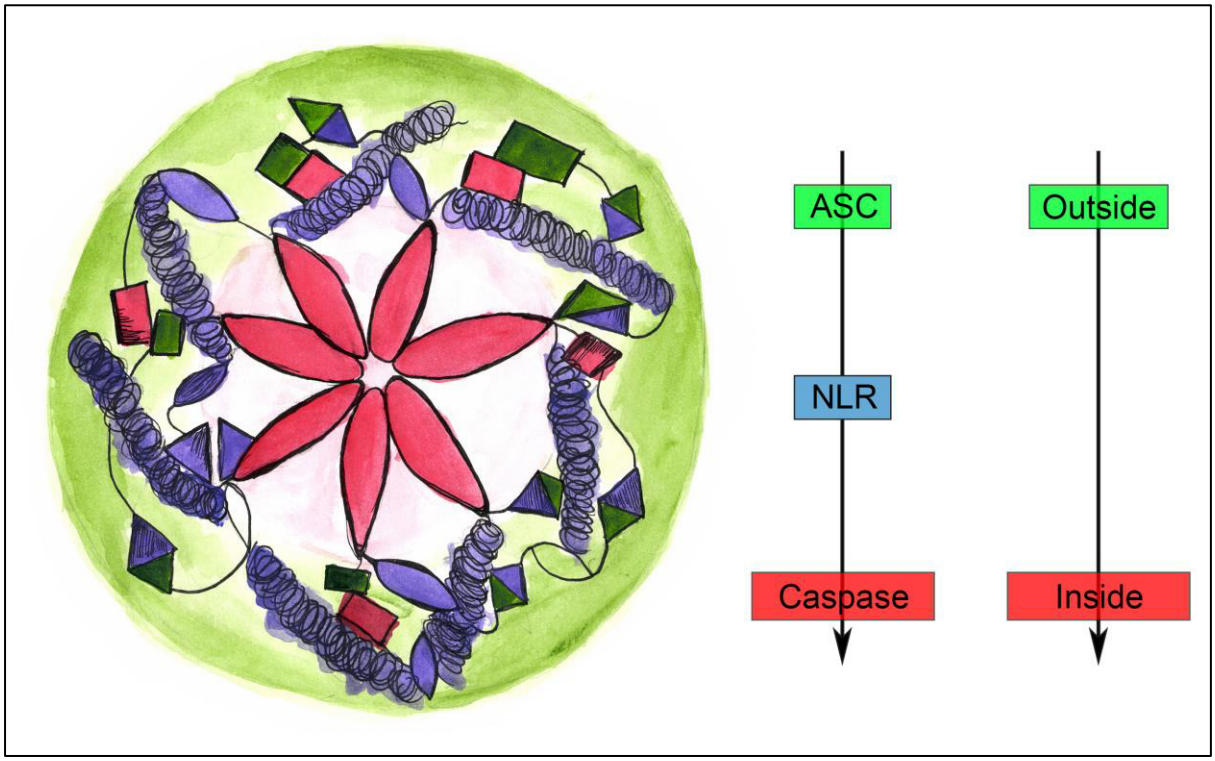

Figure 1.4: The inflammasome. Ring-shaped model as suggested by super resolution microscopy in physiological conditions. Multiple molecules of ASC form a platform on the outer surface of the inflammasome, with caspase-1 enzymes located in the core of the structure and NLR molecules between ASC and caspase-1.

The exact structure of the inflammasome is currently a topic of debate. Super resolution microscopy experiments conducted in cells using antibodies against proteins present in the endogenous inflammasome reveal a ring-shaped structure formed by polymeric ASC, with NLRs on the inside surface and caspase-1 and caspase-8 forming the core of this structure. Pro-IL-1β is also seen in the core, in contact with the enzymatically active caspases (Man et al., 2014) (Figure 1.4). The same structure is not observed *in vitro* and in cells overexpressing some of the components of the inflammasome. In these systems, cryo-electron microscopy reveals PYD domains from AIM2 and NLRP3 nucleate ASC, allowing ASC to recruit multiple copies of caspase-1 through CARD-CARD interactions, forming characteristic filamentous structures (Lu et al., 2014). Although rings are seen in THP-I cells not overexpressing any proteins, the investigators claim these ring structures are artefactual (Lu et al., 2014).

In vivo, different inflammasomes play a key role against a number of pathogens. Pyroptosis of infected cells could contribute to controlling the infection by exposing intracellular pathogens to circulating phagocytes, in a IL-1β and IL-18 rich-environment (Lamkanfi and Dixit, 2014). These cytokines have a very potent inflammatory potential (Slaats et al., 2016). IL-18 enhances the induction of Th1 polarization, priming natural killer (NK) cells to produce more interferon (IFN)-γ which is of extreme importance in clearing intracellular pathogens (Chaix et al., 2008; Slaats et al., 2016). IL-1β is responsible for inducing COX2 expression, a key enzyme in the synthesis of the eicosanoid prostaglandin E2 (PGE_2) responsible for enhancing Th17 polarization by upregulating IL-17 in CD4+ cells (Boniface et al., 2009). IL-1β upregulates the production of IL-6, another cytokine involved in Th17 polarization (Korn et al., 2008).

The production of pro-inflammatory cytokines such as IL-1β and IL-18 by the inflammasome must be tightly regulated. Deficient production of these cytokines is detrimental to the host in the context of infections caused by bacterial pathogens such as *Salmonella enterica* serovar Typhimurium (Sebastiani et al., 2002; Srinivasan et al., 2007), and excessive production of these cytokines are associated with a worse outcome in several infectious diseases such as tuberculosis (G. Zhang et al., 2014). Unresolved and/or excessive inflammation caused by inflammasome activation is linked to several inflammatory diseases such as vitiligo, psoriasis, type I diabetes, colitis and Chron's disease (Cobrin and Abreu, 2005; Siegmund et al., 2001; Zhong et al., 2013). For example, the missense mutation c.1009A>T, encoding p.Thr337Ser in the nucleotide binding domain of the NLRC4 gene causes an early-onset recurrent fever flares and macrophage activation syndrome, with spontaneous inflammasome formation and exacerbated IL-1β and IL-18 production (Canna et al., 2014).

Another NLRC4 gain-of-function mutation described occurs in the HD1 domains of the protein, substituting the amino acid valine at the 341 position for an alanine, and causing chronic inflammation and enterocolitis (Romberg et al., 2014). Several mutations in the NLRP3 gene are also linked to a variety of diseases, such as Muckle-Wells Syndrome, familial cold autoinflammatory syndrome, and other diseases featuring symptoms such as fever and cold sensitivity (Aganna et al., 2002; Dodé et al., 2002; Hoffman et al., 2001).

1.3.2. NLRP3

NLRP3 (also known as Cryopyrin, and NACHT, LRR and PYD domains-containing protein (NALP) 3) is a cytoplasmic 118 kDa protein containing a N-terminal PYD domain, a NACHT domain and a C-terminal LRR. It was first discovered in the context of familial cold auto-inflammatory syndrome and Muckle-Wells syndrome which are both pathological conditions associated with excessive inflammation (Hoffman et al., 2001).

NLRP3 is involved in assembling a canonical inflammasome containing ASC, caspase-1 and caspase-8 (Agostini et al., 2004; Gurung et al., 2014; Man et al., 2013) in response to a wide array of pathogens including gram-negative and gram-positive bacteria such as *Staphylococcus aureus*, *Listeria monocytogenes*, *Escherichia coli*, *S.* Typhimurium, fungi such as *Candida albicans*, viruses such as influenza A, and parasites including the helminth *Schistosoma mansoni* and the amoeba *Entamoeba histolytica*. NLRP3 is, therefore, a rather promiscuous sensor, able to respond to infectious agents that are evolutionary distant from one another (Table 1.3). This suggests that NLRP3 is unlikely to detect specific PAMPs but, instead, recognizes DAMPs of endogenous origin, secondary to cellular or tissue injury (Lamkanfi and Dixit, 2012).

Table 1.3: Examples of pathogens that can activate the NLRP3 inflammasome.

Microorganism	Type	Reference
Adenovirus	dsDNA virus	(Muruve et al., 2008)
Aspergillus fumigatus	Fungus	(Saïd-Sadier et al., 2010)
Candida albicans	Fungus	(Gross et al., 2009)
Chlamydia pneumoniae	Gram-negative bacteria	(He et al., 2010)
Chlamydia trachomatis	Gram-negative bacteria	(Abdul-Sater et al., 2009)
Dermatophagoides pteronyssinus	Arthropod	(Dai et al., 2011)
Encephalomyocarditis virus	ssRNA virus	(Rajan et al., 2011)
Entamoeba histolytica	Protozoa	(Mortimer et al., 2015)
Escherichia coli	Gram-negative bacteria	(Brereton et al., 2011)
Influenza A virus	ssRNA virus	(Allen et al., 2009)
Klebsiella pneumoniae	Gram-negative bacteria	(Willingham et al., 2009)
Listeria monocytogenes	Gram-positive bacteria	(Kim et al., 2010)
Modified Vaccinia Virus Ankara	dsDNA virus	(Delaloye et al., 2009)
Mycobacterium marinum	Mycobacteria	(Carlsson et al., 2010)
Mycobacterium tuberculosis	Mycobacteria	(Mishra et al., 2010)
Neisseria gonorrhoeae	Gram-negative bacteria	(Duncan et al., 2009)
Porphyromonas gingivalis	Gram-negative bacteria	(Huang et al., 2009)
Salmonella enterica serovan Typhimurium	Gram-negative bacteria	(P. Broz et al., 2010)
Schistosoma mansoni	Helminth parasite	(Ritter et al., 2010)
Staphylococcus aureus	Gram-positive bacteria	(Craven et al., 2009)
Trypanosoma cruzi	Protozoa	(Gonçalves et al., 2013)
Vesicular stomatitis virus	ssRNA virus	(Rajan et al., 2011)
Vibrio cholerae	Gram-negative bacteria	(Toma et al., 2010)
Vibrio vulnificus	Gram-negative bacteria	(Toma et al., 2010)

The list of DAMPs capable of triggering NLRP3 inflammasome assembly is also very long and includes ATP, cholesterol and uric acid crystals, glucose, amyloid β, hyaluronan, and low intracellular potassium concentration as triggered by foreign molecules such as the ionophore nigericin (Davis et al., 2011b; Mariathasan et al., 2006; Martinon et al., 2006; Pétrilli et al., 2007). It is likely that NLRP3 does not directly interact with these DAMPs, but no co-receptor protein has been described thus far. The bacterial ligands responsible for NLRP3 activation are only now beginning to emerge, a consistent theme is that potassium efflux is important in NLRP3 activation in *Salmonella* infections: blocking K^+ efflux reduces IL-18 production, indicative of an adverse effect on inflammasome activity (Franchi et al., 2007). The glycolytic enzyme hexokinase can also act as a stress sensor in some conditions. This enzyme is usually located in the mitochondrial outer membrane and it is also capable of interacting with N-acetylglucosamine due to its similarity with D-glucose. This interaction causes the release of hexokinase from the mitochondria to the cytosol where it triggers NLRP3 inflammasome formation via an unknown mechanism that does not involve

K^+ efflux (Wolf et al., 2016). There is also evidence to suggest that bacterial mRNA may act as an NLRP3 activator, although it is still unclear how relevant this response is in the context of bacterial infections (Sander et al., 2011).

The production of reactive oxygen species (ROS) by the complex NADPH oxidase appears to be key for the activation of the NLRP3 inflammasome. For instance, ATP activates the NLRP3 inflammasome via the purinergic receptor P2X7R leading to the production of ROS by NADPH oxidase, as shown by the lower IL-1β production upon NADPH oxidase pharmacological inhibition or when ROS scavengers are present (Cruz et al., 2007; Hewinson et al., 2008). Similarly, ROS produced by NADPH oxidase appears to be involved in the activation of the NLRP3 inflammasome by a variety of other stimuli, such as nigericin, silica and asbestos, as well as infectious agents (Cassel et al., 2008; Dostert et al., 2008; Hewinson et al., 2008; Tóth et al., 2017). ROS production is also potentially involved in the oxidation of mitochondrial DNA, which is released from the mitochondria in stress situations and activates the NLRP3 inflammasome (Shimada et al., 2012).

In vitro in mouse cells, a "licensing step" is required before DAMPs can induce NLRP3 inflammasome formation in macrophages and dendritic cells. In this step, the transcription of *Nlrp3*, as well as *Il1b*, is upregulated by activation of the NF-κB pathway, as NLRP3 is only weakly expressed in those cells under physiological conditions (Bauernfeind et al., 2009). Nevertheless, NLRP3 expression is not negligible (Heng and Painter, 2008; Hoffman et al., 2001), and transcriptional regulation is not the only event that occurs during the licensing step. This has been demonstrated in experiments where LPS priming was done too fast for protein synthesis to occur, or was performed in the presence of protein synthesis inhibitors or transcription inhibitors (Fernandes-Alnemri et al., 2013; Juliana et al., 2012; Lin et al., 2014; Walle et al., 2014). During non-transcriptional priming, deubiquitination was described as necessary for NLRP3 activation. In resting cells, the NLRP3 pool is kept in an inactive state by ubiquitination at the LRR domain, a post-translational modification involving the binding of the 8.5 kDa protein ubiquitin to an amino acid side-chain. Upon TLR4 stimulation and signalling through MyD88/IRAK1, the NLRP3 pool is deubiquitinated by the K63 deubiquitinase BRCA1/BRCA2-Containing Complex Subunit 3 (BRCC3), allowing NLRP3 activation to occur (Fernandes-Alnemri et al., 2013; Juliana et al., 2012; Lin et al., 2014; Py et al., 2013).

At the end of this priming step, the intracellular concentration of NLRP3 is greatly enhanced and the protein is found in a de-ubiquitinated state, ready to respond to several DAMPs. Although we still do not have a complete picture of the signalling events involved in NLRP3 inflammasome activation, studies on the post-translational modifications (PTM) of

inflammasome components have provided some evidence. In primed macrophages, stimulation of the NLRP3 inflammasome causes ASC to be phosphorylated at tyrosine 144 via spleen tyrosine kinase (SYK), enhancing the assembly of the ASC speck and subsequent cytokine production. Interestingly, this phosphorylation is not mediated by SYK in dendritic cells and suggests that the signalling events in inflammasome formation is cell type-dependent (Hara et al., 2013). It is currently unclear how SYK controls ASC phosphorylation, with evidence suggesting that SYK can either directly bind and phosphorylate ASC (Lin et al., 2015), or it can act via phosphorylation and activation of proline-rich tyrosine kinase 2 (Pyk2), which in turn binds and phosphorylates ASC (Chung et al., 2016). In addition to SYK and Pyk2, Bruton Tyrosine Kinase (BTK) was also linked to NLRP3 inflammasome activity. BTK was found to interact and promote ASC speck formation in a variety of cell lines, and *in vivo* BTK inhibitors were capable of protecting mice from ischaemic brain injury, a pathology linked to NLRP3 (Ito et al., 2015).

Different PTMs can also inhibit inflammasome activity. For example, direct phosphorylation of NLRP3 by protein kinase A (PKA) negatively regulates inflammasome activity. Upon PGE_2 stimulation, PKA is activated and catalyses the phosphorylation of NLRP3 at serine 295, disrupting inflammasome activity (Mortimer et al., 2016). The nitrosylation of cysteine residues is a PTM responsible for modulating the function of several proteins including proteins related to innate immunity. It is caused by an increase in the local nitric oxide (NO) concentration due to enhanced nitric oxide synthase (NOS) activity (Hess and Stamler, 2012). NLRP3 was found to be inhibited by NO-induced S-nitrosylation, explaining the antagonistic effect that IFN-γ has in inflammasome signalling. This is because IFN-γ enhances the expression of inducible NOS (iNOS), therefore increasing intracellular NO concentration and inhibiting the inflammasome (Hernandez-Cuellar et al., 2012; Mishra et al., 2012). How exactly this inhibition occurs is largely unknown. For example, there is no data on which cysteine residues are modified and whether S-nitrosylation inhibits speck formation, caspase recruitment or cytokine maturation.

Further fine-tuning of the NLRP3 inflammasome is achieved by autophagy of inflammasome components. In particular, NLRP3 and AIM2 inflammasomes can be targeted for autophagy via ubiquitination of ASC which is recognized by p62 and directed for engulfment and subsequent degradation by the autophagosome (Shi et al., 2012). This suggests that the relationship between inflammasome activation and autophagy is antagonistic, a hypothesis that is further strengthened by the observation that caspase-1 can inhibit autophagy by cleaving the adaptor TRIF which triggers autophagy via Beclin 1 (Jabir et al., 2014; Shi and Kehrl, 2008).

Molecules capable of negatively and positively regulating inflammasome activity by modulating the first and second steps of NLRP3 activation are still being discovered. For instance, A20 is a protein known to increase the susceptibility to rheumatoid arthritis with a mechanism linked to negative regulation of *Nlrp3* transcription. Patients with an aberrant A20 have a higher NLRP3 expression and consequentially a lower NLRP3 activation threshold (Walle et al., 2014). In contrast, the small heterodimer partner (SHP) acts as a negative regulator of the second phase of NLRP3 activation by inhibiting the binding of NLRP3 to ASC, thus preventing speck formation (Yang et al., 2015).

Figure 1.5 summarises some of the events in NLRP3 inflammasome activation.

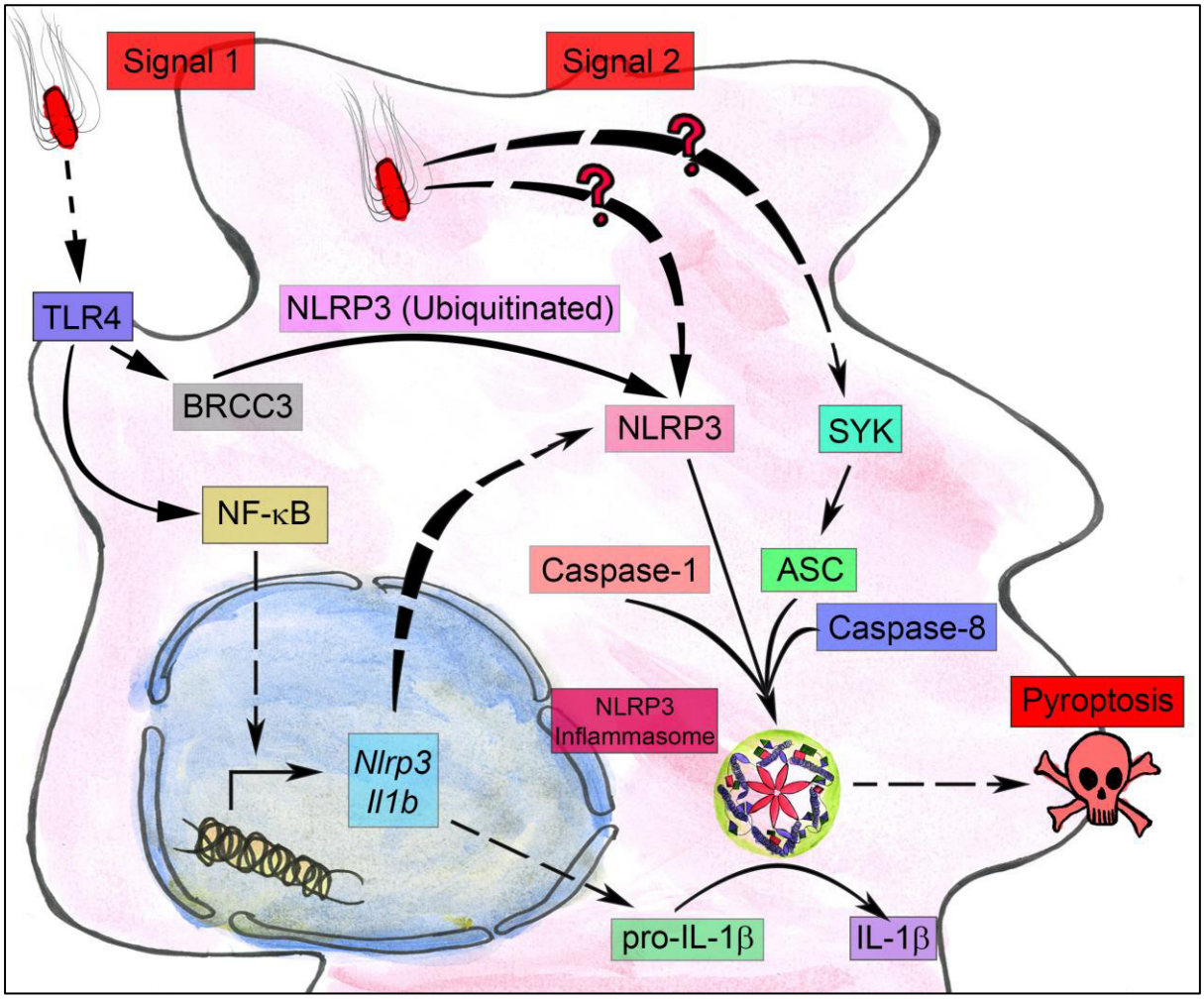

Figure 1.5: The NLRP3 inflammasome. Upon stimuli by molecules involved in cellular and tissue damage, NLRP3 recruits ASC and enzymes such as caspase-1 to form the NLRP3 inflammasome. How PAMPs and DAMPs trigger the assembly of this inflammasome remains unclear.

1.3.3. NLRC4

NLRC4 (also known as IPAF or CARD12) is a CARD-containing NLR constitutively expressed as different splice variants in different cell types with the 116 kDa variant the most commonly expressed in immune cells (Masumoto et al., 2003; Poyet et al., 2001). NLRC4 is involved in the assembly of a canonical inflammasome containing ASC, caspase-1 and caspase-8 (Man et al., 2013; Mariathasan et al., 2004) and interestingly NLRC4 is also capable of directly interacting with caspase-1, an interaction that is possibly involved in speck-independent pyroptosis (Petr Broz et al., 2010b). Unlike NLRP3, NLRC4 inflammasome formation does not require a priming step due the fact that NLRC4 is constitutively expressed in a variety of immune cells such as macrophages and dendritic cells (Heng and Painter, 2008; Mariathasan et al., 2004).

This inflammasome is involved in the innate immune response against pathogens such as *S*. Typhimurium, *Shigella flexneri*, *Anaplasma phagocytophilum*, *Pseudomonas aeruginosa*, *Burkholderia thailandensis*, *Legionella pneumophila* (Lamkanfi and Dixit, 2012; Pedra et al., 2007) (Table 1.4). In contrast to the very broad activation repertoire of NLRP3, NLRC4 can recognise either directly or indirectly a small set of PAMPs commonly present in intracellular flagellated or type 3 secretion system (T3SS)-containing bacterial pathogens, such as flagellin (Franchi et al., 2006; Miao et al., 2006).

Table 1.4: Example of pathogens capable of activating the NLRC4 inflammasome.

Microorganism	Type	Reference
Anaplasma phagocytophilum	Gram-negative bacteria	(Pedra et al., 2007)
Burkholderia thailandensis	Gram-negative bacteria	(Miao et al., 2010)
Klebsiella pneumoniae	Gram-negative bacteria	(Cai et al., 2012)
Legionella pneumophila	Gram-negative bacteria	(Amer et al., 2006)
Listeria monocytogenes	Gram-positive bacteria	(Wu et al., 2010)
Pseudomonas aeruginosa	Gram-negative bacteria	(Sutterwala et al., 2007)
Salmonella enterica serovar Typhimurium	Gram-negative bacteria	(Mariathasan et al., 2004)
Shigella flexneri	Gram-negative bacteria	(Suzuki et al., 2007)
Yersinia pseudotuberculosis	Gram-negative bacteria	(Brodsky et al., 2010)

The recognition of bacterial PAMPs by NLRC4 is indirect and mediated by the N-terminal BIR-containing family of neuronal apoptosis inhibitory proteins (NAIP). Four NAIP paralogues are constitutively expressed in mice (NAIP 1, 2, 5 and 6) whereas only one NAIP

protein is expressed in human cells (Diez et al., 2003). In mice, NAIP1 recognises the needle protein of the T3SS, NAIP2 recognises the basal rod component of the T3SS, NAIPs 5 and 6 recognise flagellin and the single NAIP expressed in humans is responsible for recognition of the T3SS needle protein (Kofoed and Vance, 2011; Rayamajhi et al., 2013; Yang et al., 2013; Zhao et al., 2016, 2011). *In vitro* structural studies of NAIP/NLRC4 interaction allowed researchers to develop models explaining the early stages of NLRC4 inflammasome formation. In this model, the NAIP/ligand binding occurs at the nucleotide-binding domain (NBD) and it is required for the subsequent NAIP/NLRC4 co-oligomerization (Tenthorey et al., 2014), as illustrated by NAIPs 2 and 5. A single NAIP molecule interacts with flagellin, which then interacts with NLRC4 and induces a change from the closed auto-inhibitory conformation to an open active conformation. The open conformation propagates the recruitment of multiple copies of NLRC4 and culminates in the formation a stacked open disk-like filamentous structure capable of recruiting caspase-1 (Diebolder et al., 2015; Halff et al., 2012; Hu et al., 2015, 2013; Tenthorey et al., 2017; Zhang et al., 2015).

Many of the events that lead to the activation of the NLRC4 inflammasome are not well characterized, but PTMs are likely to play a role in this process. Protein Kinase C isoform δ (PKCδ)-dependent NLRC4 phosphorylation occurs in a conserved serine residue (Ser 533) in response to flagellin and *S*. Typhimurium. This phosphorylation event is triggered by flagellin, but does not depend on NAIP5 (Matusiak et al., 2015; Qu et al., 2012). It is unlikely however that this phosphorylation event is required for NLRC4 inflammasome formation at all times, since NAIP2-dependent NLRC4 activation occurs independently of PKCδ (Suzuki et al., 2014).

Figure 1.6 summarises the signalling events leading to the NLRC4 inflammasome assembly.

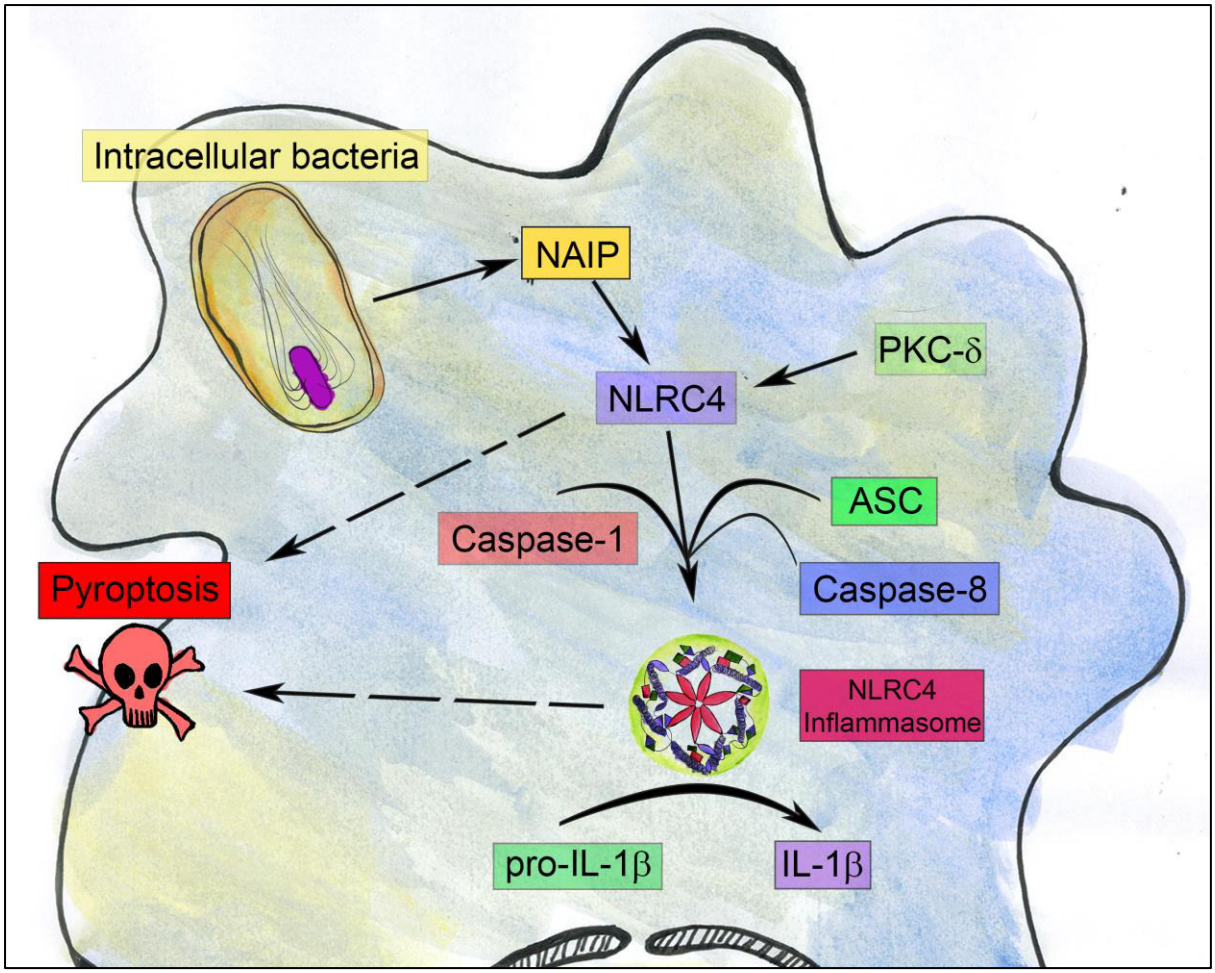

Figure 1.6: The NLRC4 inflammasome. PAMPs from intracellular bacteria are recognized by NAIPs to engage NLRC4 which subsequently recruits ASC resulting in the assembly of the NLRC4 inflammasome which stimulates pyroptosis and pro-IL-1β processing. Alternatively, pyroptosis may occur independently of ASC.

1.3.4. NLRP1a-c

Also known as NALP1, NLRP1 interacts with ASC and caspase-1 to form a canonical inflammasome in response to signals such as *Bacilus anthracis* Lethal Toxin (LeTx), ATP depletion and *Toxoplasma gondii* infection (Boyden and Deitrich, 2006; Cirelli et al., 2014; Liao and Mogridge, 2013; Martinon et al., 2002). In mice the *Nlrp1* gene has suffered duplication events throughout evolution and different strains have up to three paralogue genes (*Nlrp1 a, b* and *c*) with different expression patterns and allelic variants, each responding to different signals with different affinities (Boyden and Deitrich, 2006).

Its structure is somewhat unique amongst NLRs: NLRP1 contains a N-terminal PYR domain (present in humans but not in mouse and rat), NACHT, NACHT associated domain (NAD),

LRR domain and CARD domain, in addition to the unusual “function to find” domain (FIIND) between the LRR and CARD domains (D’Osualdo et al., 2011).

NLRP1 is “primed” by autoproteolysis at the FIIND domain, and the resulting fragments remain associated as inactive dimers until further stimulation occurs (Frew et al., 2012). In response to LeTx, specific alleles of *Nlrp1b* can be proteolytically cleaved at the N-terminal (Levinsohn et al., 2012), which in turn triggers the recruitment of ASC through the CARD domain of NLRP1 (Finger et al., 2012), caspase-1 activation and cytokine production (Cordoba-Rodriguez et al., 2004). In the context of ATP depletion, however, NLRP1 N-terminal proteolysis is not required (Liao and Mogridge, 2013). This could be explained by the fact that some NLRP1 variants contain an ATP-binding domain that is exposed during ATP depletion, stimulating its auto-proteolytical activity and inflammasome formation (Neiman-Zenevich et al., 2014) (Figure 1.7).

1.3.5. NLRC3

Although their activation typically initiates inflammation, some NLRs can also have anti-inflammatory properties. NLRC3 is such an example. This 114 kDa protein contains a N-terminal NBD followed by a LRR. It is expressed in the cytoplasm of cells related to the immune system such as T-cells and macrophages, and acts as an inhibitor of MyD88-dependent NF-κB signalling (Conti et al., 2005). During MyD88 signalling, TNF receptor associated factor (TRAF) 6 is conjugated to the lysine 63 (K63) of ubiquitin, allowing it to activate the IKK complex (Deng et al., 2000). During LPS stimulation, NLRC3 negatively regulates the transcription of NF-kB related genes, such as *Tnf*, *Il1b*, *Il6* and *Il12*, by inhibiting TRAF6 K63-ubiquitination (Schneider et al., 2012).

In addition to NF-κB, NLRC3 is also an inhibitor of the stimulator of interferon genes (STING) pathway. In the STING pathway, viral DNA is recognized by cyclic GMP-AMP synthase (cGAS), an enzyme that in turn catalyses the production of the second messenger cyclic GMP-AMP (cGAMP) in the cytoplasm. cGAMP then interacts with STING in the endoplasmatic reticulum, leading to its association with TANK-binding kinase-1 (TBK1). TBK1 then translocates to perinuclear regions and phosphorylates proteins such as IRF3 and NF-κB, modulating this way the transcription of immunologically relevant genes (Barber, 2015; Gao et al., 2013). NLRC3 can physically interact with both STING and TBK1, blocking the pathway (L. Zhang et al., 2014) (Figure 1.8).

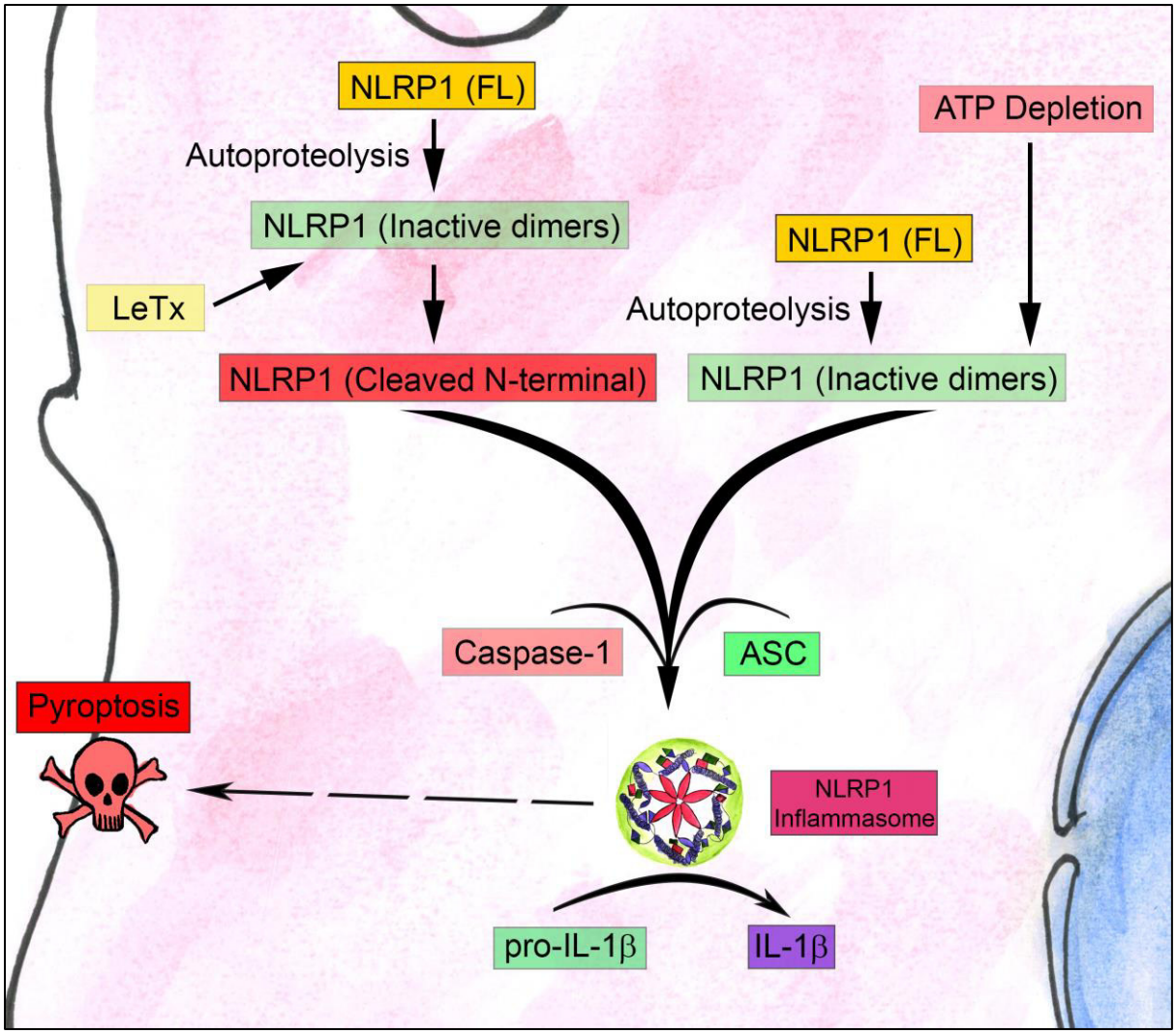

Figure 1.7: The NLRP1 inflammasome. The NLRP1 FIIND domain is involved in autoproteolysis, priming NLRP1 to respond to stimuli such as LeTx. Further proteolytic events are required for NLRP1 assembly in response to LeTx but not in response to ATP depletion.

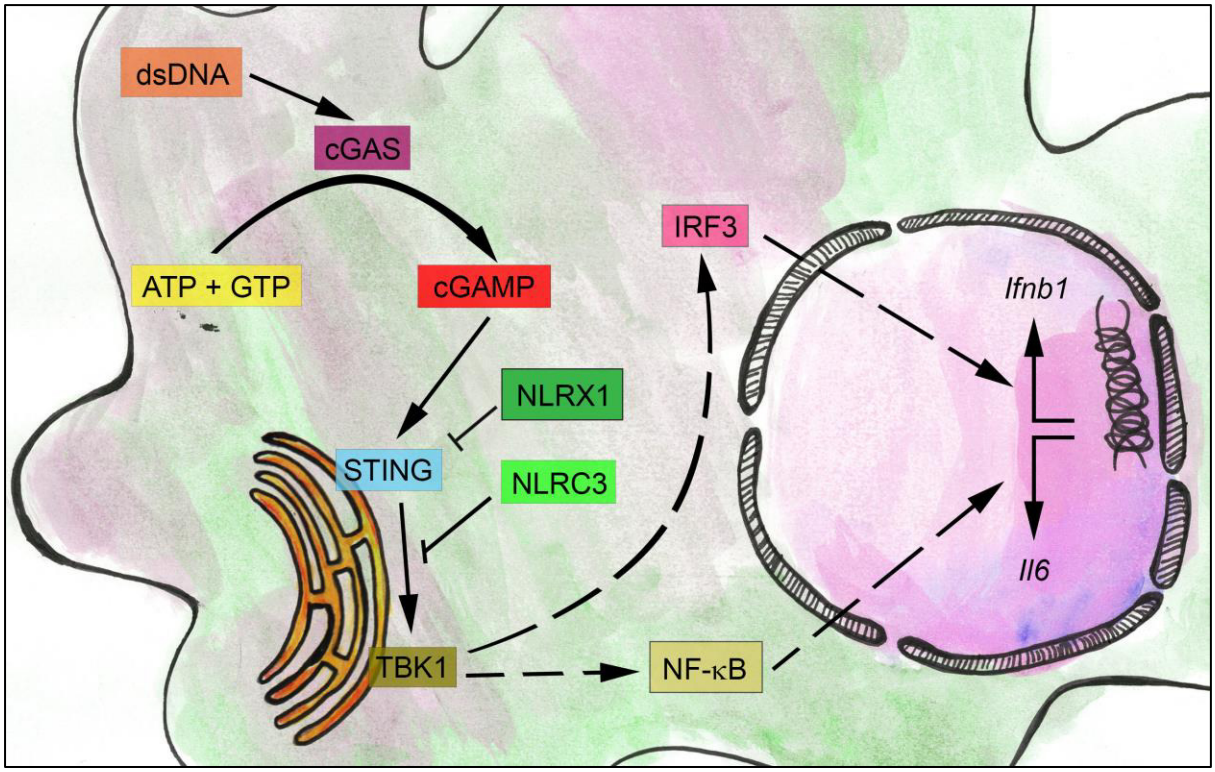

Figure 1.8: The STING pathway. Recognition of dsDNA by cGAS triggers the production of the second messenger cGAMP, responsible for activating STING and subsequent NF-κB and IRF3 activation. NLRC3 and NLRX1 modulate this pathway by inhibiting STING/TBK1 interaction.

1.3.6. NLRX1

NLRX1 is a 108 kDa protein containing a NBD and a LRR domains, in addition to a N-terminal mitochondrial targeting sequence (Tattoli et al., 2008), responsible for NLRX1 localization at the mitochondrial outer membrane, where NLRX1 acts as a negative regulator of viral responses. During single-stranded RNA virus infections, the cytoplasmic receptor retinoic acid-inducible gene-I (RIG-I) recognizes foreign nucleic acids and activates the mitochondria antiviral signalling protein (MAVS). MAVS activates IRF3 and stimulates the formation of the CARD9/B-cell lymphoma/leukemia-10 (BCL10) complex, responsible for NF-κB activation (Poeck et al., 2010; Seth et al., 2005; Yoneyama et al., 2004). In this context, NLRX1 is capable of physically interacting with MAVS, disrupting the RIG-I/MAVS interaction and inhibiting the pathway (Allen et al., 2011; Moore et al., 2008). NLRX1 also inhibits the NF-κB pathway by blocking TRAF3 and TRAF6 (Allen et al., 2011). Interestingly, NLRX1 is itself a target of negative regulation by the protein FAS-associated factor-1

(FAF1), which competes for NLRX1 binding and consequentially increases MAVS signalling (Kim et al., 2017) (Figure 1.9).

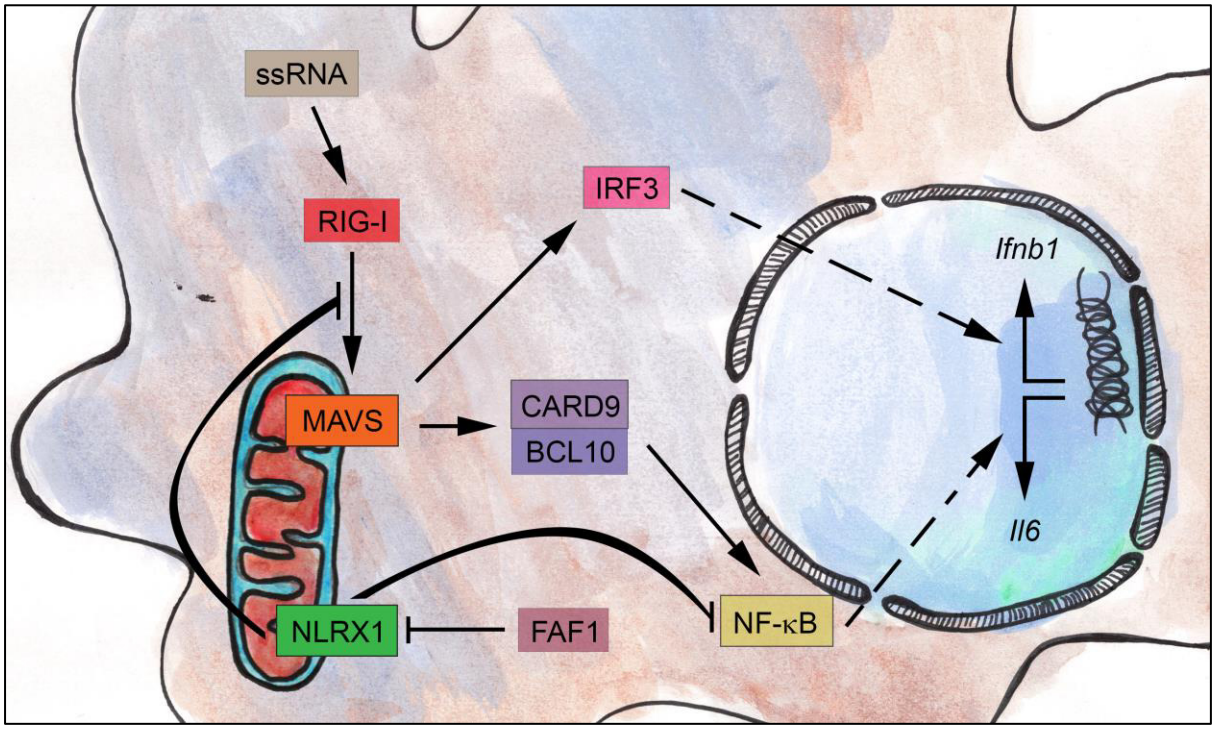

Figure 1.9: RIG-I pathway. ssRNA is recognized by RIG-I and ultimately leads to NF-kB and IRF3 activation. NLRX1 blocks the IRF3 branch of the pathway by inhibiting RIG-I and MAVS interaction and the NF-κB branch by interacting with TRAF3 and TRAF6.

A study using genome wide small interfering RNA (siRNA) analysis identified NLRX1 as an early-stage regulator of human immunodeficiency virus 1 (HIV-1) replication (Zhou et al., 2008), a pathogen known to stimulate the STING pathway discussed above (Gao et al., 2013). In this context NLRX1 assumes a role similar to that of NLRC3. The reverse-transcribed DNA of HIV-1 triggers STING activation and subsequent association with TBK1, leading to the expression of proteins such as IFN-β, RANTES (regulated on activation, normal T-cell expressed and secreted) and IL-6. This process is disrupted by NLRX1 which blocks the pathway by physically interacting with STING (Guo et al., 2016) (Figure 1.8).

1.3.7. NLRC5

Studies in human-derived cell lines suggested a role for NLRC5 in controlling type I interferon-responses to viruses. This is because, first, NLRC5 is upregulated in response to double stranded RNA stimulation, second, knocking this protein down by interfering RNA technology reduced type I interferon responses and, third, its overexpression and oligomerization stimulated those responses (Kuenzel et al., 2010; Neerincx et al., 2010). A different study however identified NLRC5 as a negative regulator of NF-κB signalling. In particular, NLRC5 acted by competing with NF-κB essential modulator (NEMO) for IKKα/IKKβ interaction, inhibiting their phosphorylation and kinase activity which is necessary for NF-κB signalling (Cui et al., 2010). The same study also identified NLRC5 as a negative regulator of type I interferon responses, possibly by inhibiting the cytoplasmic sensors RIG-I and the RLR melanoma differentiation-associated protein 5 (MDA5). Equally, generation of *Nlrc5*$^{-/-}$ mice by different groups also raised conflicting reports regarding NLRC5 role in NF-κB and type I interferon responses (Kumar et al., 2011; Tong et al., 2012).

In terms of inflammasome biology, a study reported that NLRC5 possesses inflammasome-like activity, and the fact that ASC and caspase-1 are required for that activity strongly suggests that NLRC5 can form a canonical inflammasome (Davis et al., 2011a). Mechanistically, the authors suggested that NLRC5 collaborates with NLRP3 to trigger inflammasome formation in response to bacterial PAMPs, most likely by physically interacting with NLRP3 through NLRC5's NBD. The study however was performed in human macrophage cell lines either overexpressing or having NLRC5 knocked down. Moreover, the physical interaction between NLRC5 and NLRP3 was demonstrated in the HEK293T overexpression system. In this system, high concentration of one of the proteins can lead to "forced" non-physiological interactions. These findings should, therefore, be interpreted with caution and further confirmation for the occurrence of this inflammasome is required.

1.3.8. NLRP6

NLRP6 contains a N-terminal PYD followed by NACHT and LRR domains and was originally described as an activator of caspase-1 and NF-κB signalling, and colocalises with ASC in speck structures (Grenier et al., 2002). However, the study in question used a HEK293T overexpression model and later studies using BMDMs from genetically altered mice demonstrated that *Nlrp6*$^{-/-}$ cells have enhanced NF-κB signalling and unaltered IL-1β production upon *L. monocytogenes, E. coli and S. Typhimurium* infections (Anand et al.,

2012). Currently, evidence for the existence of the NLRP6 inflammasome in more physiological settings is lacking.

1.3.9. NOD1 and NOD2

The first NLRs described, NOD1 (NLRC1, CARD4) and NOD2 (NLRC2, CARD15) are cytoplasmic proteins containing a CARD domain followed by a second CARD (NOD2 only), NACHT, NAD and LRR domains (Girardin et al., 2001). NOD1 recognizes meso-diaminopilemic acid (DAP), a structure found in the cell wall of gram-negative bacteria, whereas NOD2 recognizes muramyl dipeptide (MDP), a motif found in the cell wall of both gram-positive and gram-negative bacteria (Chamaillard et al., 2003; Girardin et al., 2003).

Bacterial wall components are transported from endosomal compartments by the solute carrier family 15 (SLC15) A3 and SLC15A4, allowing them to be recognized by NOD1 and NOD2 (Kim et al., 2008). These NLRs then oligomerize and interact with RIPK2 and X-linked IAP (XIAP) (Abbott et al., 2004; Krieg et al., 2009), which promotes IKK activation resulting in NF-κB signaling (Fritz et al., 2006). In addition to the NF-κB pathway, NOD2 recruits the adaptor CARD9 to stimulate the MAPKs p38 and c-Jun N-terminal kinase (JNK) (Hsu et al., 2007), via interaction with the NOD2 NACHT domain and the linker region between NACHT and CARD domains (Parkhouse et al., 2014). JNK and p38 regulate the activity of the transcription factor activator protein 1 (AP-1), which in turn acts on *il1b* transcription, further linking NOD2 to the priming event required for inflammasome activation (Arthur and Ley, 2013; Roman et al., 2000) (Figure 1.10).

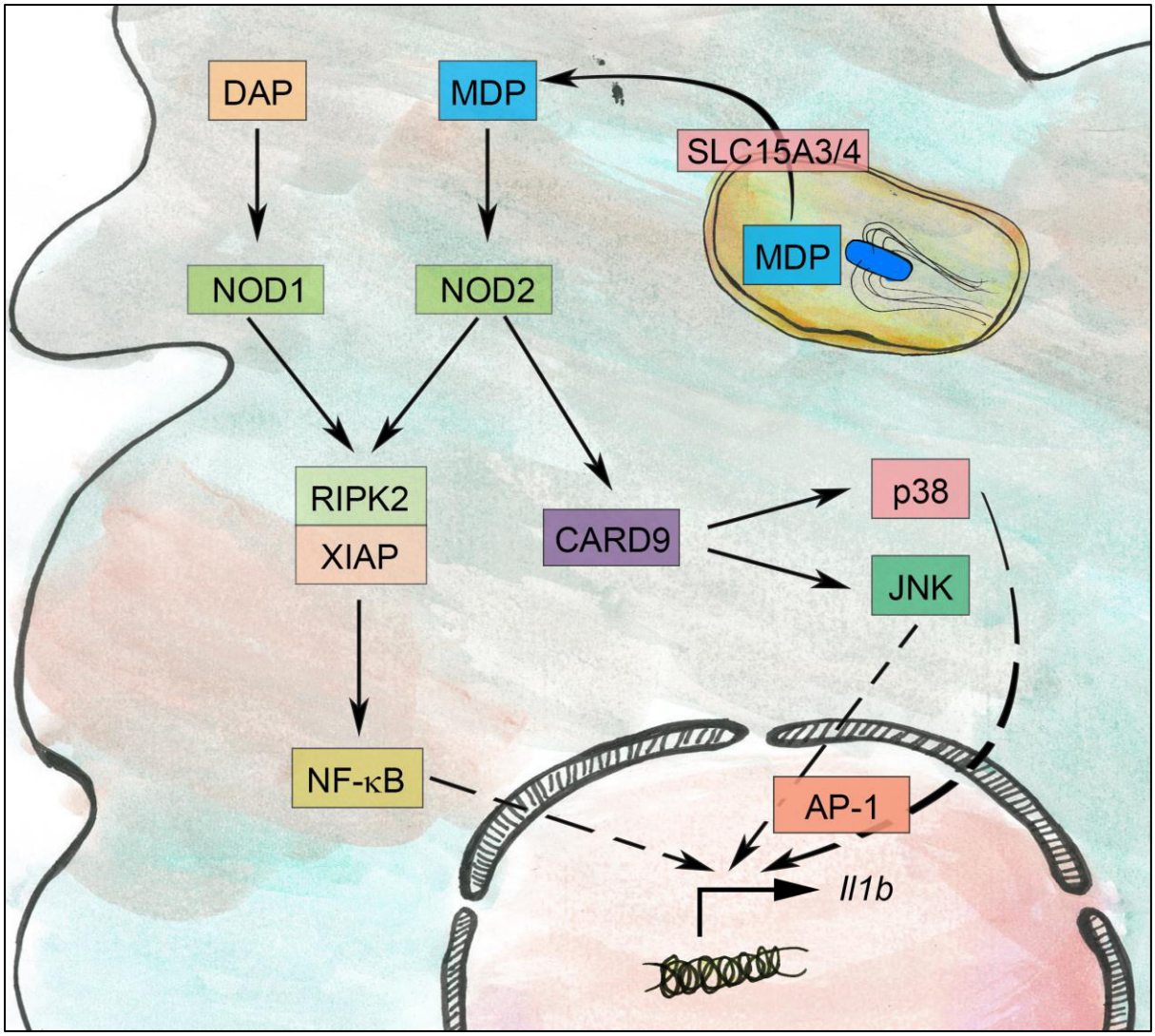

Figure 1.10: NOD1/2 signalling. Components of the bacterial cell wall are recognized by NOD1/2, leading to RIPK2 and XIAP-dependent NF-kB activation. Additionally, NOD2 activates p38 and JNK signalling via CARD9.

1.3.10. AIM2

AIM2 is an interferon-inducible 39 kDa protein containing a N-terminal PYD domain and a HIN domain (acronym for hematopoietic expression, interferon-inducible nature, and nuclear localization) (Schattgen and Fitzgerald, 2011). The ability of AIM2 to recognize cytoplasmic DNA was discovered by combining proteomic (proteins capable of interacting with DNA) and genomic (transcripts induced by IFN-β) screens (Bürckstümmer et al., 2009). It is now established that AIM2 is one of the main receptors to trigger inflammasome formation in response to cytoplasmic dsDNA in murine cells (Bürckstümmer et al., 2009; Fernandes-Alnemri et al., 2009; Hornung et al., 2009). In human myeloid cells, however, AIM2 is not

involved in dsDNA sensing. This role is instead performed by cGAS/STING, which triggers cell death and subsequent activation of the NLRP3 inflammasome (Gaidt et al., 2017)

The HIN domain of AIM2 contains two adjacent oligonucleotide and oligosaccharide-binding folds capable of interacting electrostatically with DNA. This interaction triggers the recruitment and oligomerization of ASC through the AIM2 PYD, forming a structure capable of recruiting caspase-1. This macromolecular structure, termed the AIM2 inflammasome, is responsible for dsDNA-induced cell death and maturation of pro-inflammatory cytokines such as IL-1β and IL-18 (Fernandes-Alnemri et al., 2009; Hornung et al., 2009; Rathinam et al., 2010). Interestingly, in addition to AIM2 activation in response to viral infections, certain microbial pathogens such as *Francisella tularensis* and *L. monocytogenes* can also activate this inflammasome (Rathinam et al., 2010; Warren et al., 2010) (Figure 1.11).

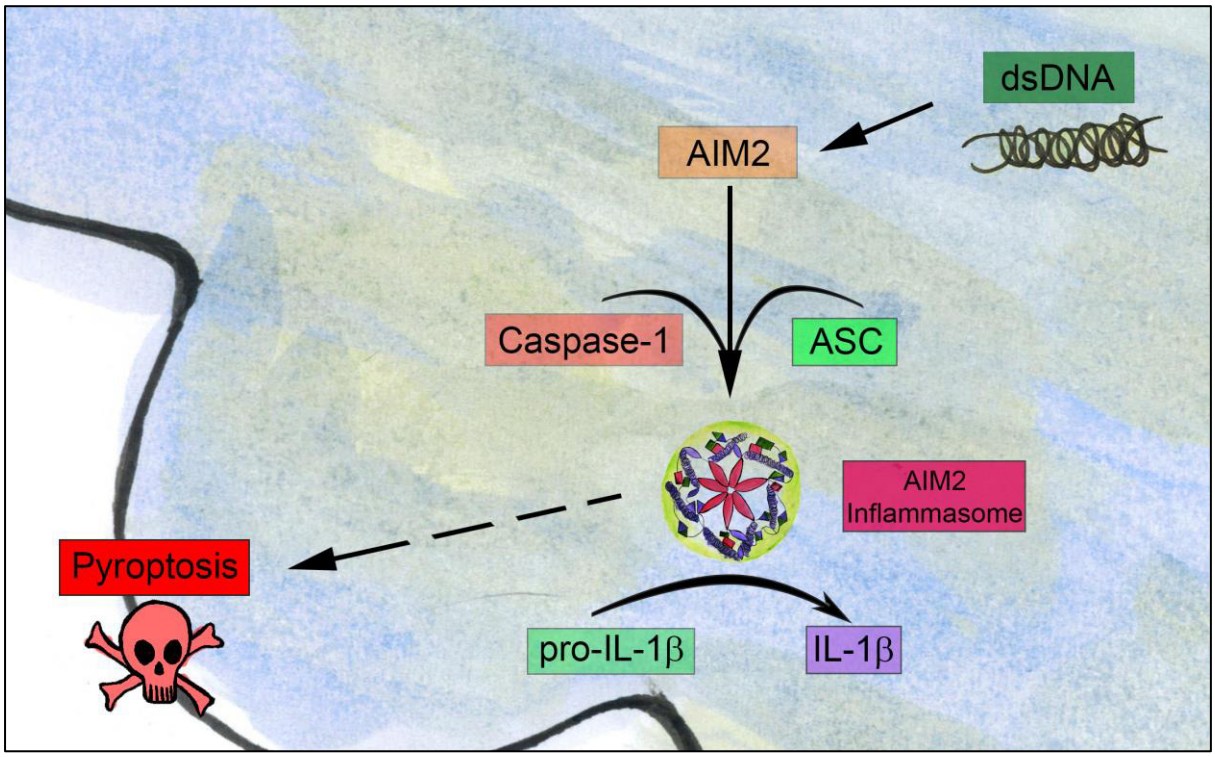

Figure 1.11: The AIM2 inflammasome. In murine cells, AIM2 recognizes cytoplasmic dsDNA, leading to assembly of the AIM2 inflammasome.

1.4. Caspases

Caspases are cysteine peptidases that cleave their substrate exclusively after an aspartic acid residue within a somewhat variable recognition motif (Pop and Salvesen, 2009). They were originally discovered in the context of cytokine maturation (Cerretti et al., 1992;

Nicholson et al., 1995) and play an important role in the development of innate immunity. Not only do they mediate the production of potent, biologically active pro-inflammatory cytokines, but they also drive different forms of host cell death. In humans, 12 caspases have been described so far (caspase-1 to caspase-10, caspase-12 and caspase-14). Based on their main function, caspases can be subdivided into three distinct groups: the pro-inflammatory caspases (caspase-1, -4, -5 and caspase-12), pro-apoptotic caspases (caspase-2, -3, -6, -7, -8, -9 and caspase-10) and those with no clear pro-inflammatory or pro-apoptotic function (caspase-14) (Table 1.5). (Julien and Wells, 2017; Shalini et al., 2014; van Raam and Salvesen, 2012).

Structurally, caspases contain a C-terminal catalytic domain and a N-terminal prodomain usually containing a death fold motif, either a CARD (present in caspase-1, -2, -4, -5, -9, -11, and caspase-12) or a death effector domain (DED) (caspase -8 and caspase-10). The CARD or DED domains are involved in homotypic protein-protein interactions and, therefore, confer specificity in regard to their interaction partners. This allows the pro-apoptotic caspases to be further grouped into initiator caspases containing either CARD or DED domains (caspase-2, -8, -9 and caspase-10) and executioner caspases lacking specific pro-domain motifs (caspase-3, -6 and caspase-7) (Shalini et al., 2014).

Table 1.5: Caspases in humans and mice.

Protein	Human	Mouse	Pro-domain motif	Function
Caspase-1	+	+	CARD	Inflammation
Caspase-2	+	+	CARD	Apoptosis
Caspase-3	+	+	-	Apoptosis
Caspase-4	+	-	CARD	Inflammation
Caspase-5	+	-	CARD	Inflammation
Caspase-6	+	+	-	Apoptosis
Caspase-7	+	+	-	Apoptosis
Caspase-8	+	+	DED	Apoptosis
Caspase-9	+	+	CARD	Apoptosis
Caspase-10	+	-	DED	Apoptosis
Caspase-11	-	+	CARD	Inflammation
Caspase-12	+	+	CARD	Inflammation
Caspase-14	+	+	-	Other

However useful, the classifications described above fail to consider the functional complexity and redundancy seen among caspases. A characteristic example is caspase-8 which was originally described as pro-apoptotic (Muzio et al., 1996). However, it was later found that, first, caspase-8 can be enzymatically active and cleave pro- IL-1β to its active form (Maelfait et al., 2008), and, second, it can regulate a distinct form of cell death termed necroptosis (Bell et al., 2008).

1.4.1. Caspase-1

The first and most well-studied pro-inflammatory caspase is caspase-1. Its first name was Interleukin Converting Enzyme (ICE) because it was originally described as an enzyme capable of converting pro-IL-1β into its mature form (Cerretti et al., 1992). Caspase-1 is expressed as a 45 kDa pro-enzyme containing a N-terminal CARD, a p20 subunit and a C-terminal p10 subunit. Upon stimulation pro-caspase-1 oligomerizes to catalyise its own proteolysis and the resulting p20 and p10 fragments assemble into two p20/p10 heterodimers to form the active caspase-1 tetramer (Wilson et al., 1994). Caspase-1 activation is a process that depends on inflammasome assembly requiring ASC polymerization (Mariathasan et al., 2004; Srinivasula et al., 2002) which acts as a platform for pro-caspase-1 recruitment and activation through CARD-CARD interactions (Srinivasula et al., 2002).

Caspase-1 is the main effector enzyme in canonical inflammasomes. Upon assembly of the inflammasome, caspase-1 is recruited to the ASC speck through CARD-CARD interactions (Srinivasula et al., 2002), where it enzymatically converts pro-IL-1β and pro-IL-18 to their mature forms (Cerretti et al., 1992). Canonical inflammasomes also stimulate pyroptosis in a caspase-1 dependent manner, although the molecules responsible for this process are not completely understood. Gasdermin D, the main executioner of pyroptosis upon activation of the non-canonical caspase-11 inflammasome, is also cleaved by caspase-1 leading to cell death. However, gasdermin D is not the sole pyroptosis executioner upon canonical inflammasome activation (Kayagaki et al., 2015). It is possible that other members of the gasdermin family could be involved in pyroptosis. Although no evidence was found for caspase-1 cleavage of gasdermin A, B, C (Shi et al., 2015), and deafness autosomal dominant 5 (DFNA5, also known as gasdermin E) (Rogers et al., 2017), it is possible that these proteins are involved in cell death in specific contexts, as there is precedent for other members of the gasdermin family to be used as a caspase substrate. For example, It was demonstrated that during apoptosis caspase-3 can cleave DFNA5 causing secondary

necroptosis/pyroptosis, although the physiological relevance of this finding is still unclear (Rogers et al., 2017; Wang et al., 2017).

1.4.2. Caspase-2

The presence of functional redundancy amongst caspases is further illustrated by caspase-2; despite being one of the most conserved caspases across species (Lamkanfi et al., 2002), caspase-2 knockout mice are only mildly impaired in regulating apoptosis (Bergeron et al., 1998). It is, therefore, challenging to study the precise role of this enzyme in the development of innate immune responses.

Despite this limitation, *in vitro* studies have shown that upon stimulation with a variety of apoptosis-inducing agents, caspase-2 is recruited and activated in a macromolecular complex termed the PIDDosome, containing (RIP)-associated ICH-1/CED-3 homologous protein with a death domain (RAIDD) and the p53-inducible protein with death domain (PIDD) (Berube et al., 2005; Tinel, 2004). The PIDDosome then acts as an initiator in the intrinsic apoptotic pathway by activating BH3 interacting-domain death agonist (Bid) which permeabilizes the mitochondria allowing cytochrome c to be released to the cytosol (Paroni et al., 2002; Robertson et al., 2002). Cytochrome c then binds to ICE protease-activating factor-1 (IPAF-1) forming the apoptosome (Zou et al., 1999) which cleaves pro-caspase-9 to its mature form. Caspase-9 continues the amplifying cascade by cleaving and activating the apoptosis executioner caspases -3, -6 and -7 (Li et al., 1997). Some of the key events of the apoptosis signalling pathway are illustrated in figure 1.12.

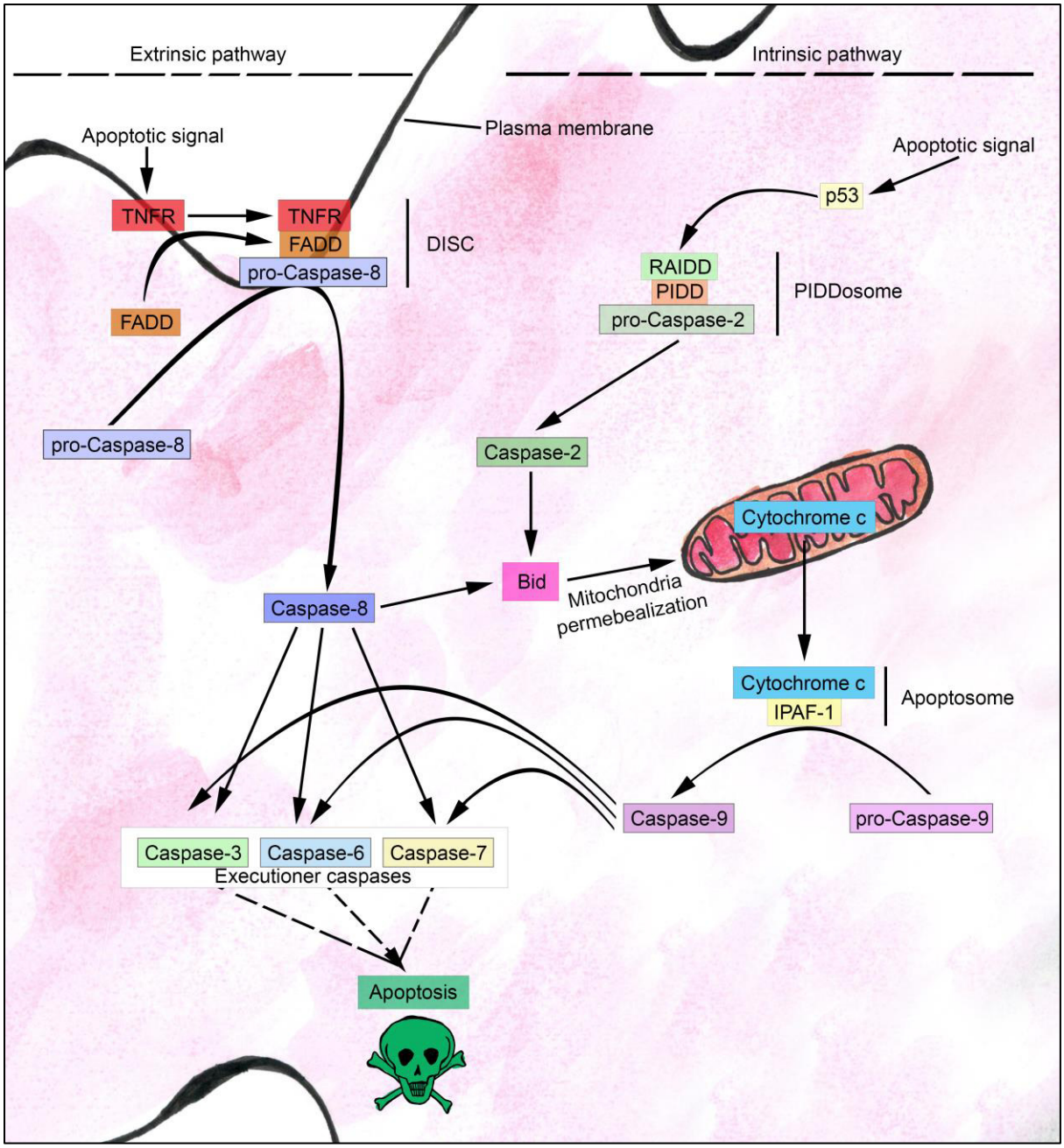

Figure 1.12: Intrinsic and extrinsic apoptotic pathways. Extracellular apoptotic signals engage the extrinsic apoptotic pathway, resulting in the formation of the protein complex DISC and caspase-8-dependent activation of the executioner caspases -3, -6 and -7. Intracellular apoptotic signals trigger activation of caspase-2 via the PIDDosome, resulting in cytochrome c release from the mitochondria and activation of executioner caspases via caspase-9.

Links between this caspase and proinflammatory forms of cell death, including pyroptosis, have also been also described. *Brucella suis* is capable of inducing a caspase-1-independent and caspase-2-dependent proinflammatory cell death in macrophages, featuring some characteristics of pyroptosis such as IL-1β release (Chen et al., 2011). Another report linked NLRP3 activation to the mitochondria-destabilizing role of caspase-2 (Bronner et al., 2015). Induction of mitochondrial ROS production in response to endoplasmic reticulum stress signals the recruitment of NLRP3 to the mitochondria, independently of ASC, and triggers the cleavage and activation of caspase-2 and the pro-apoptotic protein Bid. Activation of caspase-2 and Bid subsequently induces permeabilization of the mitochondria which allows mitochondrial DAMPs to be released to the cytosol and activate the canonical NLRP3 inflammasome.

1.4.3. Caspase-8

Caspase-8 is classically regarded as an apoptosis initiator in the extrinsic apoptotic pathway. In this pathway, a membrane death receptor such as the tumor necrosis factor receptor (TNFR) interacts with a pro-apoptotic stimulus, an event that stimulates the receptor to homodimerize and triggers a conformational change in its cytoplasmic portion (Scott et al., 2009; L. Wang et al., 2010). This conformational change allows for homotypic death domain interactions between the receptor and Fas-associated protein with Death Domain (FADD) (Chinnaiyan et al., 1995; Kischkel et al., 1995). Following its recruitment, FADD's Death Effector Domain (DED) recruits pro-caspase-8 (Kischkel et al., 1995; Muzio et al., 1996) forming a protein complex known as Death Inducing Signalling Complex (DISC). In this complex, pro-caspase-8 is then dimerised and cleaved resulting in the release of the p18 fragment which represents the active form of the enzyme. (Medema et al., 1997; Muzio, 1998), events required for the activation of this protease (Oberst et al., 2010; van Raam and Salvesen, 2012).

Upon caspase-8 activation, apoptosis may occur via the intrinsic or extrinsic pathways: In the extrinsic pathway, caspase-8 directly activates the executioner caspase-3 (Enari et al., 1996; Scaffidi et al., 1998), which, in turn, cleaves and activates numerous targets such as Poly-(ADP-Ribose) polymerase (PARP) (Nicholson et al., 1995). In the intrinsic pathway, activated caspase-8 cleaves Bid which translocates to the mitochondria and stimulates the release of cytochrome c (Cosulich et al., 1997; Li et al., 1998). Figure 1.12 summarises the signalling events leading to apoptosis.

Caspase-8 deletion in mice was found to be lethal *in utero* (Varfolomeev et al., 1998), and this embryonic lethality is rescued by co-deletion of caspase-8 and RIPK3, suggesting that caspase-8 is required to prevent RIPK3-induced cell death (Kaiser et al., 2011; Oberst et al., 2011). Upon stimulation of receptors such as TNF receptor 1 (TNFR1), FADD and tumor necrosis factor receptor type 1-associated death domain protein (TRADD) are recruited in the cytoplasmic region of the receptor through DD homotypic interactions (Boldin et al., 1995; Hsu et al., 1996b). This complex is then capable of recruiting RIPK1 and, when caspase-8 is absent or inactivated, RIPK1 recruits RIPK3 to what is now termed the necroptosome (Cho et al., 2009; Hsu et al., 1996a; Stanger et al., 1995). This complex is then capable of phosphorylating MLKL leading to necroptotic cell death (Zhao et al., 2012). In this pathway, caspase-8 acts by cleaving RIPK1 and RIPK3 to their inactive forms thus preventing the oligomerization of the full-length RIPK1/3 and, therefore, blocking necroptosis (Li et al., 2012). Figure 1.13 summarises RIPK3-dependent necroptosis.

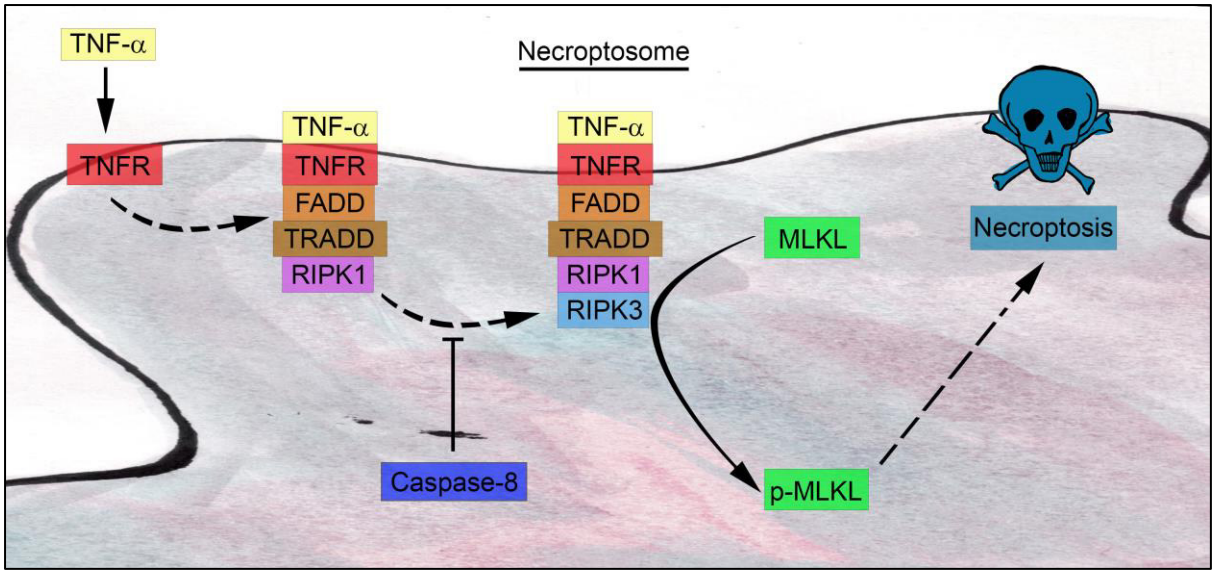

Figure 1.13: RIPK3-dependent necroptosis. In situations where caspase-8 is absent or inactivated, the multiprotein complex known as the necroptosome can be formed. This complex is responsible for the RIPK3-dependent phosphorylation of MLKL leading to necroptotic cell death.

Caspase-8 was also implicated in pro-IL-1β processing using HEK293T system overexpressing this enzyme (Maelfait et al., 2008). The first evidence for such a role in a more physiological setting came from studies of the dectin-1 pathway (Gringhuis et al.,

2012). During fungal infections, the C-type receptor dectin-1 recognizes polysaccharides such as curdlan (Yoshitomi et al., 2005) and triggers the activation of spleen tyrosine kinase (SYK). This enzyme then phosphorylates various targets such as protein kinase C-γ (PKC-γ) and induces the production of ROS (Rogers et al., 2005; Strasser et al., 2012; Underhill et al., 2005). Active PKC-γ phosphorylates the adaptor CARD9, which mediates the formation of a complex with BCL10 and mucosa-associated lymphoid tissue lymphoma translocation protein 1 (MALT1), resulting in activation of NF-κB and thus modulating the production of proinflammatory cytokines such as IL-6, pro-IL-1β, TNF-α and IL-23 in dendritic cells (Gross et al., 2006; LeibundGut-Landmann et al., 2007; Strasser et al., 2012). Dectin-1 activation by curdlan derived from *Candida albicans* is able to stimulate IL-1β production in BMDCs by the formation of a non-canonical inflammasome, without caspase-1 recruitment (Gringhuis et al., 2012). In this case, the activation of dectin-1 stimulates SYK and allows the adaptor CARD9 to interact with BCL10 and MALT1 as described above. This interaction can stimulate NF-κB and upregulate the expression of pro-IL-1β. Caspase-8 and ASC are then recruited to the CARD9-BCL10-MALT1 complex, allowing pro-IL-1β to be processed (Gringhuis et al., 2012). Figure 1.14 illustrates the dectin-1 pathway in dendritic cells in response to fungal infections.

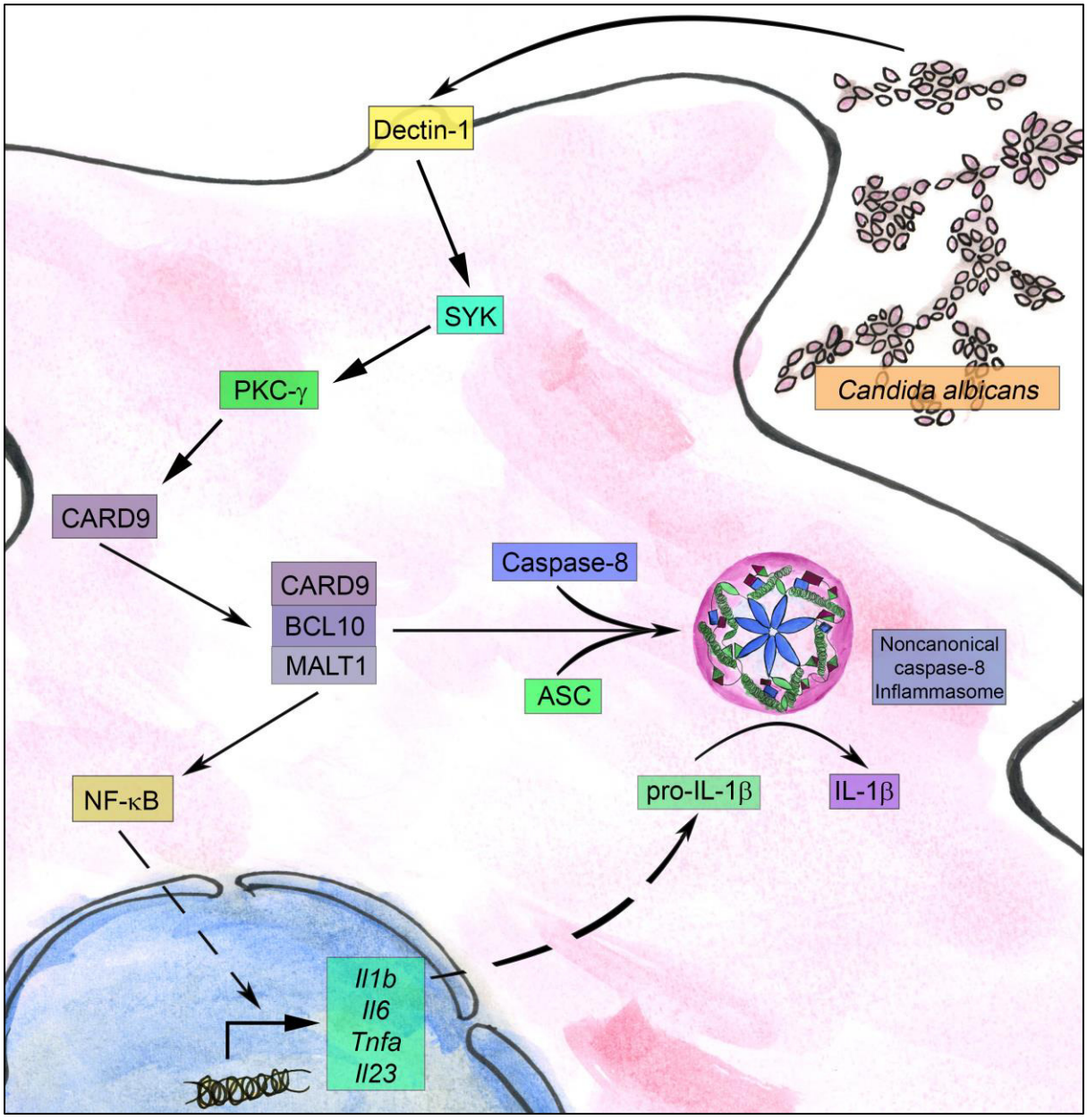

Figure 1.14: The dectin-1 pathway. The C-type lectin receptor dectin-1 recognises fungal PAMPs and activates NF-kB and noncanonical caspase-8 inflammasome formation via SYK and CARD9.

Caspase-8 is also involved in the formation of canonical inflammasomes. FADD and caspase-8 can modulate the expression of inflammasome-related genes such as *Nlrp3* and *il1b*, thus affecting the priming step of the NLRP3 inflammasome activation (Gurung et al., 2014). Pro-caspase-8 is recruited to the inflammasome during both NLRC4 and NLRP3 activation (Man et al., 2014), where it is processed to mature caspase-8 in an ASC-dependent fashion. Mature caspase-8 then cleaves pro-IL-1β to IL-1β but it is not involved

either in pyroptosis or in IL-18 processing during *Salmonella* infection (Man et al., 2013). The observation that caspase-8 is not involved in pyroptosis was made in cells expressing caspase-1/11, known to be the major players in this response (Mariathasan et al., 2004). In the absence of caspase-1/11, caspase-8 triggers cell death in the context of NAIP/NLRC4 activation, further illustrating the extensive redundancy found in this protein family (Lee et al., 2018; Mascarenhas et al., 2017; Schneider et al., 2017).

1.4.4. Caspase-11 (Human caspase-4 and -5)

Analogous to human caspase-4 and -5, caspase-11 was originally described as an enzyme capable of activating caspase-1 (Wang et al., 1998). Its expression is induced by LPS via the production of interferon β (Broz et al., 2012; Wang et al., 1998). In 2011, researchers demonstrated that the *caspase-1*$^{-/-}$ mouse strain widely used in the field of innate immunity was in fact a caspase-1 and caspase-11 double knockout, since their proximity in the chromosome made it difficult for these genes to be segregated by recombination (Kayagaki et al., 2011).

We now know that, upon infection with pathogens such as *E. coli* and *C. rodentium*, caspase-11 can form a non-canonical inflammasome responsible for IL-1β maturation (Kayagaki et al., 2011). There is also evidence to suggest that this enzyme is involved in the TLR4-independent response to LPS from bacteria that escape the cytoplasmic vacuole, raising the possibility of developing new therapeutic strategies in conjunction with TLR4 antagonists (Aachoui et al., 2013; Case et al., 2013; Hagar et al., 2013; Kayagaki et al., 2013). One of the hypotheses regarding this response is that caspase-11 itself could act as an intracellular PRR that can recognise LPS and trigger the assembly of the non-canonical inflammasome (Shi et al., 2014). As a result, caspase-11 oligomerizes and cleaves the full length gasdermin D to a N-terminal p30 fragment which creates pores in the membrane leading to cell death (Aglietti et al., 2016; Kayagaki et al., 2015; Liu et al., 2016; Shi et al., 2015). In addition to its role in non-canonical pyroptosis, gasdermin D may also link caspase-11 to the NLRP3 inflammasome. This is because caspase-11-dependent cleavage of gasdermin D can activate the NLRP3 inflammasome. Although the details of this activation are still unknown, it is likely that this mechanism is responsible for the caspase-11-dependent IL-1β production (Kayagaki et al., 2015) (Figure 1.15).

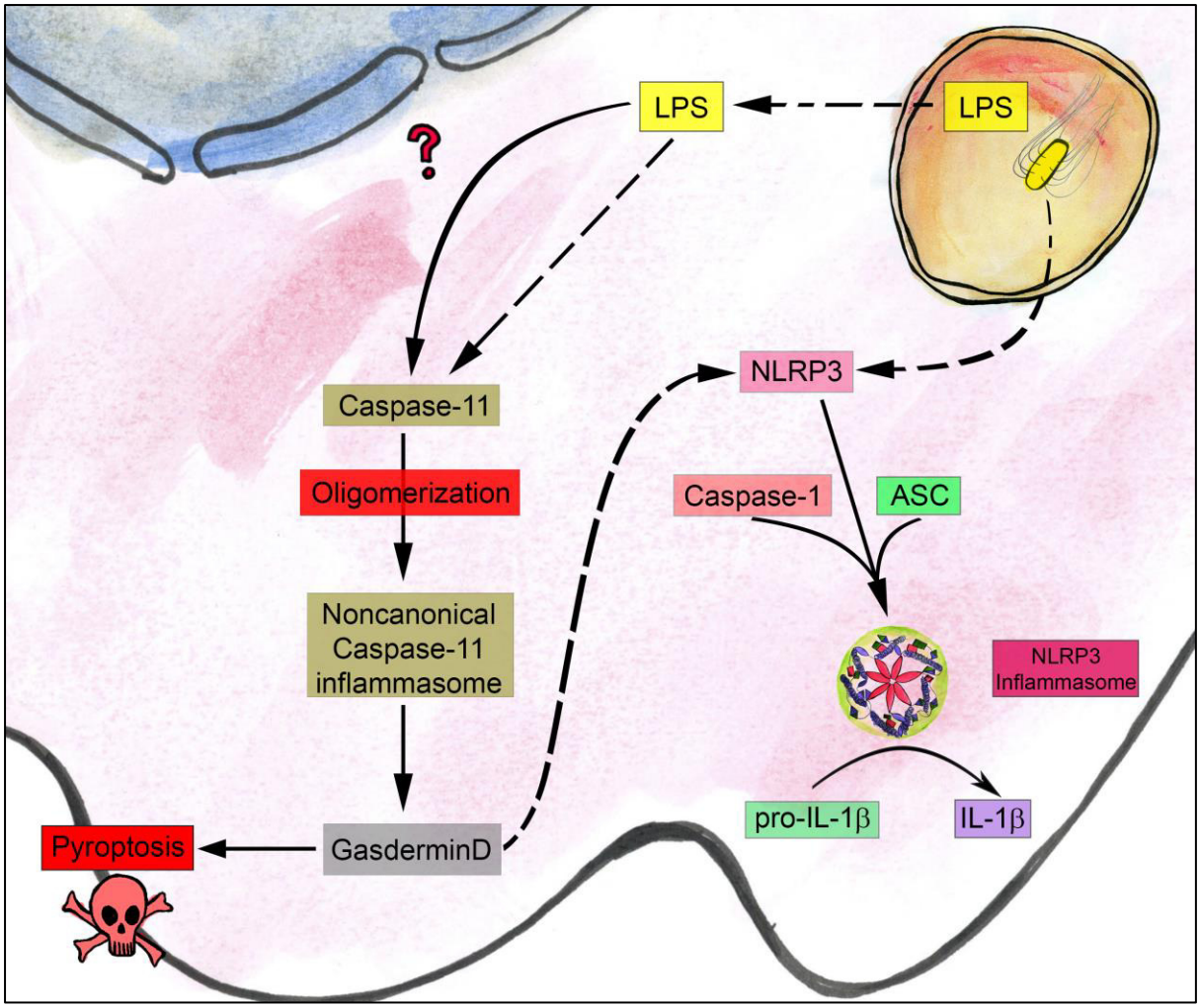

Figure 1.15: Non-canonical caspase-11 inflammasome. Cytosolic LPS is the PAMP responsible for caspase-11 oligomerization resulting in the formation of the noncanonical caspase-11 inflammasome. This inflammasome then triggers pyroptosis and canonical NLRP3 activation via gasdermin D.

1.4.5. Caspase-12

Caspase-12 was originally described as an inflammatory caspase due its high amino acid sequence identity with caspase-1 and -11 (-1, -4 and -5 in humans). *Caspase-12* mRNA is transcribed in most tissues, especially in the lungs and skeletal muscle (Van De Craen et al., 1997). The full length caspase-12 protein is 48 kDa and consists of three domains: a N-terminal prodomain containing a CARD, a large catalytic subunit and a C-terminal small catalytic subunit (Lamkanfi et al., 2004).

In animal models, initial studies using *caspase-12* knockout mice reported an inhibitory effect of this caspase in the production of pro-inflammatory cytokines IL-1β and IL-18, rendering

caspase-12$^{-/-}$ mice resistant to LPS-induced sepsis, possibly due a physical interaction between caspase-12 and caspase-1 (Saleh et al., 2006). The same group later reported an additional caspase-12 anti-inflammatory role by blocking the NOD2 pathway (LeBlanc et al., 2008).

In contrast, caspase-12 can also exhibit inflammatory properties in the context of viral infections. As discussed previously, upon recognition of RNA viruses in the cytoplasm, RIG-I undergoes ubiquitination, leading to interaction with MAVS and subsequent type I interferon responses. Notably, caspase-12 was found to stimulate tripartite motif containing protein 25 (TRIM25)-mediated RIG-I ubiquitination, positively regulating this antiviral pathway (P. Wang et al., 2010). However, it was recently discovered that the *caspase-12*$^{-/-}$ mice used by most experimenters so far were in fact deficient in both caspase-12 and caspase-11. The use of caspase-12 single knockout mice failed to reproduce the anti-inflammatory phenotype previously described, although the inflammatory response to RNA virus infection was not re-evaluated (Vande Walle et al., 2015).

1.5. *Salmonella* Typhimurium

Salmonella enterica, subspecies *enterica*, is a flagellated, facultative anaerobic, gram negative bacillus. It is of great significance in terms of public health because it can infect humans and animals and cause diseases of varying clinical manifestations. Amongst these, typhoid fever affects an estimated 21.7 million people while paratyphoid fever affects around 5.4 million people worldwide. In both cases, the highest percentage of people affected live in low-income countries (Crump and Mintz, 2010).

S. enterica is divided into more than 50 serogroups (based on the O antigen) and more than 2400 serological variants (based on flagellar H antigen) (Grimont and Weill, 2007). Some serovars are of particular interest in human and animal health for causing invasive forms of the disease, such as the serovars Typhi (*Salmonella* Typhi) and Typhimurium (*Salmonella* Typhimurium). *S*. Typhi is only capable of infecting humans and it is the main pathological agent of typhoid fever, a disease endemic in areas with poor sanitary conditions and whose symptoms include fever, malaise, anorexia, nausea, abdominal discomfort and myalgia, (Parry et al., 2002). *S*. Typhimurium, on the other hand, is capable of infecting humans and several other species, causing different syndromes in different hosts. In humans, *S*. Typhimurium causes an enteric disease whose symptoms are enteritis and diarrhoea, whereas in mice it is responsible for a disease similar to human typhoid fever (Bryan Coburn et al., 2007; Santos, 2014).

Due to host specificity difficulties in establishing an animal model to study *S*. Typhi, most studies investigating the host's immune responses against *S*. *enterica* are conducted in mice infected with *S.* Typhimurium. The development of animal models to study S. Typhi is however necessary and some progress has been made in recent years. For instance, the receptor TLR11 is absent in humans but present in mice, and *S*. Typhi can successfully colonise *Tlr11*$^{-/-}$ mice and cause a disease very similar to human typhoid fever (Mathur et al., 2012). Despite that, the use of *S*. Typhimurium is still preferred for safety reasons and the fact that for every gene of interest the experimenters would need to generate the knockout strain in *Tlr11*$^{-/-}$ animals, which is a laborious and time-consuming process.

S. Typhimurium infection in mice usually occurs by ingestion of contaminated food or water. The bacteria first colonise the intestinal lumen and after adhering to the epithelium, they can invade enterocytes and dendritic cells of the intestinal epithelium and macrophages of the submucosa. From there, they access the systemic circulation and subsequently spread to the whole body. Upon entering the host cell, the pathogen modifies the surface of the vacuole that contains it to form the *Salmonella* containing vacuole (SCV) in which it can evade several host cell defence mechanisms. From inside the SCV, the bacteria can inject into the cytoplasm an ample array of effector molecules that can modulate several cellular processes. A plethora of virulence factors are involved in the invasion process described above, such as flagella and fimbria involved in cell adhesion and invasion; T3SS, important for the modification of the SCV and secretion of a variety of molecules; and finally different effector molecules secreted into the cytosol that can affect a variety of cell signaling events. (de Jong et al., 2012). Many of these virulence factors are encoded by genes in specific regions of the *Salmonella spp.* chromosome known as *Salmonella* pathogenicity islands (SPI). These SPI vary in quantity and composition between different *Salmonella* serovars (Marcus et al., 2000). SPI-1 and SPI-2 are amongst the most well-studied SPIs. SPI-1 codes for a T3SS that translocate bacterial proteins across the host plasma membrane and is required for cellular invasion (Que et al., 2013). The expression of SPI-1 proteins are required for host NLRC4 activation (Lara-Tejero et al., 2006). SPI-2 codes for a distinct T3SS responsible for injecting effector molecules in the host cytosol across the SCV, modulating hosts cellular responses and increasing bacterial proliferation (Jennings et al., 2017).

1.5.1. *S.* Typhimurium and innate immunity

TLR4 appears to be of particular importance against infection with *S*. Typhimurium. Both *in vivo* and *in vitro*, TLR4 signalling is key for inducing the pro-inflammatory response and

controlling bacterial burden (Hoshino et al., 1999; Poltorak et al., 1998; Talbot et al., 2009). In addition to TLR4, TLR2 also plays a complementary role in controlling *S*. Typhimurium infections. TLR2 mRNA levels are upregulated in the spleen and liver of *Salmonella*-infected mice, in a TLR4-dependent manner (Tötemeyer et al., 2005, 2003). Mice lacking TLR2 and/or TLR4 have higher bacterial burden and decreased survival in comparison to WT controls, whereas deficiency in other TLRs does not appear to significantly increase susceptibility to infection (Arpaia et al., 2011; Jessen et al., 2014). TLR5 recognizes bacterial flagellin (Hayashi et al., 2001), but it is not required for controlling systemic *S*. Typhimurium infection in mice although it may be important in recognising bacteria during the enteric phase of an infection (Feuillet and Medjane, 2006; Vijay-Kumar et al., 2006). Flagellin also drives inflammasome activation through NLRC4, limiting the infection (Franchi et al., 2006; Lage et al., 2013; Lai et al., 2013; Miao et al., 2006).

TLRs are not the only players in the defense against *Salmonella spp*. (Royle et al., 2003). Caspase-1 is also an important component of the innate immune response against *Salmonella*. This is because *caspase-1*$^{-/-}$ mice harbor significantly more bacteria in their internal organs and succumb to infection earlier than WT controls. It is likely that the protective effect of caspase-1 is mediated via IL-18, which confers resistance during the systemic phase of the infection, and IL-1β, which is involved in resistance during the intestinal phase of the infection (Lara-Tejero et al., 2006; Raupach et al., 2006). The transcription of IL-1α, IL-1β and IL-18 are strongly upregulated in various organs in mice infected with *S.* Typhimurium (Sebastiani et al., 2002). *Salmonella* infection also drives caspase 1 recruitment to the inflammasome upon NLRC4 and/or NLRP3 stimulation (P. Broz et al., 2010; Man et al., 2014; Mariathasan et al., 2004).

NLRC4 and NLRP3 are both activated by salmonellae. *In vitro* evidence links NLRP3 inflammasome activation to *S*. Typhimurium infection, although, unlike NLRC4, the bacterial PAMPs or host DAMPs responsible for this effect is unknown (P. Broz et al., 2010; Man et al., 2014).

The role of NLRs in *Salmonella* infection *in vivo* is not as well characterized as that observed *in vitro*. Inflammasome activation is involved in host defense against this pathogen, because caspase-1, ASC, IL-1β and IL-18 are all involved in restricting microbial growth *in* vivo (Lara-Tejero et al., 2006; Raupach et al., 2006). *Nlrc4*$^{-/-}$ and WT mice had similar bacterial burden and survival rates in a *S*. Typhimurium oral infection model (Lara-Tejero et al., 2006), and similarly no difference was found between WT and *Nlrp3*$^{-/-}$ mice (Sutterwala et al., 2006). Mice deficient in both NLRs, however, exhibited a phenotype very similar to that of *caspase-1*$^{-/-}$ mice with increased bacterial burden in the spleen, liver, and lymph nodes, as well as

impaired IL-18 production (P. Broz et al., 2010). Using a subclinical *S*. Typhimurium infection model, it was observed that both NLRP3 and NLRC4 are involved in controlling bacterial burden as both knockout strains are more susceptible to infection than the WT controls (Man et al., 2014). Accordingly, the same study observed that both NLRC4 and NLRP3 are relevant *in vitro*. By using super resolution microscopy to visualise inflammasome assembly, the authors found that upon *Salmonella* infection of bone marrow derived macrophages, NLRC4 and NLRP3 are recruited to the same ASC speck (Man et al., 2014). Further studies revealed that NLRP3 is recruited to the inflammasome speck downstream to NLRC4, although the signalling events leading to this dual recruitment are not fully understood (Qu et al., 2016).

S. Typhimurium-derived flagellin is also capable of stimulating IL-1α production in BMDM, a pro-inflammatory cytokine important in controlling bacteremia, that is associated with non-canonical inflammasome formation and stimulates a novel form of cell death. This form of cell death has morphological features similar to apoptosis and autophagy and involves the release of cathepsin B and D into the cytosol (Lage et al., 2013). It is unknown at the moment how important this form of cell death is during *S*. Typhimurium infections, but it could occur in response to bacteria that escapes the SCV. Similarly, the induction of the non-canonical caspase-11 inflammasome could also play a role in inducing cell death upon LPS release from the SCV into the cytosol (Kayagaki et al., 2011). At the moment it is unclear how important these events are in the course of salmonellosis in physiological conditions, but it could complement the NLRC4 response (Broz et al., 2012).

Various lines of evidence suggest a role for NOD2 during *S*. Typhimurium infection. NOD1 and NOD2 are also potentially involved in NF-κB signalling in response to bacterial T3SS protein SipA *in vitro*. *In vivo* however, *Nod1*$^{-/-}$*Nod2*$^{-/-}$ mice produce less *Ifng* and *Tnfa upon S. Typhimurium* oral infection, but no statistically significant difference was observed between WT and ΔSipA *S*. Typhimurium. An independent study found a similar pattern, where NOD1 and NOD2 absence dampened *in vivo* production of pro-inflammatory cytokines, an effect that was dependent of the T3SS, although the identity of the effector molecule remained unknown (Geddes et al., 2010; Keestra et al., 2011). It was later demonstrated that SipA is not required for NOD2 activation during *Salmonella* infections, as bacterial MDP can escape the SCV and reach the cytosol via the transporters SLC15A3 and SLC15A4, leading to NOD2-dependent activation of the NF-κB pathway (Nakamura et al., 2014).

Figure 1.16 summarises key aspects of the innate immune response triggered by *S*. Typhimurium.

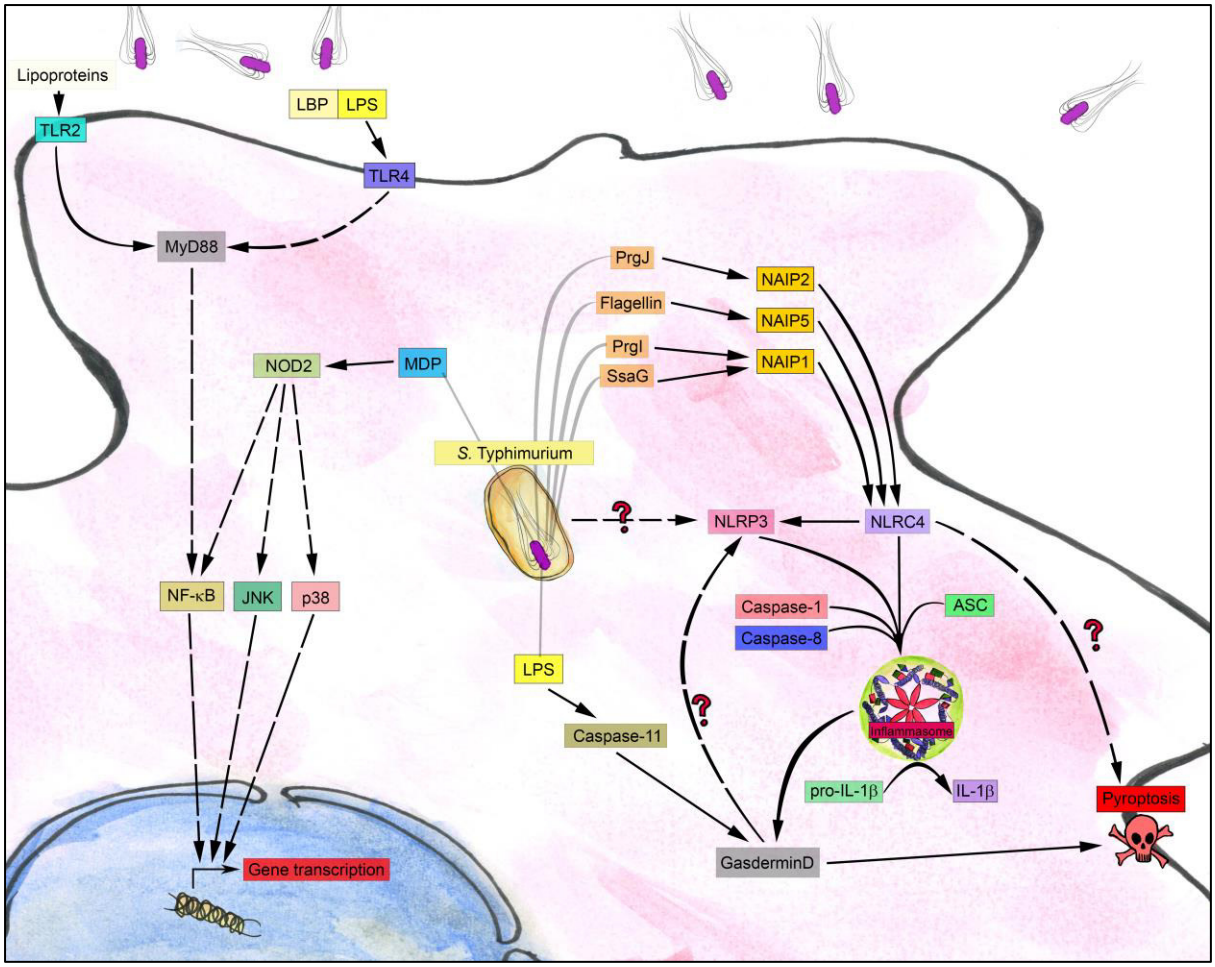

Figure 1.16: Innate immune pathways activated in response to *S.* Typhimurium infection. Amongst others, TLR2/4, NOD2, NLRC4 and NLRP3 are activated upon S. Typhimurium infection.

Bacterial molecules that are capable of modulating inflammasome activity to benefit the pathogen have been described in several genera such as *Yersinia*, *Pseudomonas*, *Mycobacterium* and *Francisella* (Taxman et al., 2010). *S*. Typhimurium is also capable of avoiding detection by either regulating inflammasome activation or directly inhibiting it. For example, upon infection, *S*. Typhimurium downregulates its flagellin expression thus avoiding recognition by the NLRC4 inflammasome (Cummings et al., 2006, 2005). The protein *Salmonella* outer protein B (SopB) is a virulence factor encoded by SPI-1, and can inhibit NLRC4 inflammasome activation, although the mechanism is largely unknown (Hu et al., 2017). In B-cells, *S*. Typhimurium downregulates the host NLRC4 expression, thus inhibiting pyroptosis. This inhibition involves a protein encoded in the bacterial SPI-1, although its identity is still unknown (Perez-Lopez et al., 2013).

It has been shown that the regulatory NLRs NAIP12 and NLRP6 can dampen immune responses against *Salmonella*. First, mice deficient for these NLRs are more resistant than WT to *Salmonella* infection. Second, LPS-primed macrophages from such mice have higher NF-κB and ERK activation in response to the *Salmonella* infection (Anand et al., 2012; Zaki et al., 2014). It is possible that *S*. Typhimurium stimulates these NLRs in order to avoid detection and therefore prolong its survival into the cell. However, this hypothesis remains to be tested.

1.6. AIMS

Despite their importance in modulating innate immune responses, very little is known about the signalling events leading to inflammasome formation and the regulatory mechanisms that finely tune their activation. Novel canonical and non-canonical inflammasomes are still being discovered as illustrated by the recently described NLRP9 inflammasome in the context of viral infections (Zhu et al., 2017). It is possible that other, not well characterised NLRs can form inflammasomes and/or act as regulators of the already known inflammasomes, such as NLRP3 and NLRC4.

Once the inflammasome is formed, little is known about its components, their exact role and their interactions. For example, work done in our lab and by others identified caspase-8 as a molecule recruited to the inflammasome, contributing to IL-1β production (Gurung et al., 2014; Man et al., 2014, 2013). The functional redundancy of caspases suggests it is possible that other caspases are also recruited to the inflammasome. Other proteins that contain CARD or pyrin domains could also be recruited to the inflammasome.

The importance of inflammasome activation in the host response against *S*. Typhimurium, (Petr Broz et al., 2010a; Lara-Tejero et al., 2006; Man et al., 2014) make this pathogen a good model for studying the signalling events involved in the activation and regulation of the NLRC4 and NLRP3 inflammasomes.

The aims my thesis were to:

1. Determine whether NLRs, caspases and CARD domain containing proteins not known to be important in inflammasome formation might be important regulators of its activation. To do this I used *in vitro S*. Typhimurium infection assays of bone marrow derived macrophages from mice lacking specific NLRs, caspases, or other adaptor proteins relevant to innate immunity.

2. Determine how proteins identified in Aim 1 would modify inflammasome formation in response to infection by *S*. Typhimurium and other pathogens.

Chapter 2

Material and methods

2.1. Mice

WT C57BL/6 mice were obtained from Charles River, UK. *Caspase-1*$^{-/-}$*-11*$^{-/-}$, *Nlrc4*$^{-/-}$, *Nlrp3*$^{-/-}$ and *Pycard*$^{-/-}$ mice on a C57BL/6 background were produced by Millenium Pharmaceuticals and obtained from Kate Fitzgerald (University of Massachusetts). *Card9*$^{-/-}$ mice on a C57BL/6 background, originally produced by Xin Lin (University of Texas) (Hsu et al., 2007), were provided by David Underhill (Cedars-Sinai Medical Center). *Nod2*$^{-/-}$ mice were provided by Peter Murray (St. Jude Children's Research Hospital). *Nlrc3*$^{-/-}$, *Nlrc5*$^{-/-}$, *GasderminD*$^{-/-}$, *GasderminD*$^{-/-}$*Dfna5*$^{-/-}$, *Nlrp6*$^{-/-}$, *Nlrx1*$^{-/-}$, *Pidd*$^{-/-}$, *Nlrp1a-c*$^{-/-}$, *Caspase-2*$^{-/-}$, *Caspase-11*$^{-/-}$ and *Caspase-12*$^{-/-}$ were produced by Genentech. *Caspase-1*$^{-/-}$*-11*$^{-/-}$*Nlrc4*$^{-/-}$ were generated in house by crossing *Caspase-1*$^{-/-}$*-11*$^{-/-}$ and *Nlrc4*$^{-/-}$ *animals.* Mice were backcrossed on a C57BL/6 background for at least 8 generations.

All animals were housed under specific pathogen-free conditions and all work involving live animals complied with the University of Cambridge Ethics Committee regulations under Home Office Project License number 80/2572.

2.2. Cell isolation and culture

Mice were killed by cervical dislocation, they were then sprayed with ethanol 70% for sterilization and their hind legs without the skin were aseptically removed and placed in Dulbecco's modified Eagle's medium (DMEM) on ice. In a laminar flow cabinet, muscle and connective tissue surrounding the bones were removed, the tibia and femur were separated at the knee joint with the proximal and distal epiphysis removed. For bone marrow derived macrophages (BMDM) culture, bone marrow was flushed out using BMDM growth media (DMEM supplemented with 10% HyClone® (Thermo Fisher Scientific), 20% L929 conditioned media and 5 mM L-Glutamine (Sigma)) with the help of a 2 mL syringe and a size 25G needle. Collected cells were centrifuged at 300 x G for 10 minutes at 15 ^{o}C and resuspended in BMDM growth media. For bone marrow derived dendritic cells (BMDC), the bone marrow was flushed out using BMDC growth media (RPMI 1640 supplemented with 10% FCS, 50 µM 2-Mercaptoethanol and 1000 U/mL GM-CSF (PeproTech). BMDMs and BMDCs were then cultured at 37 ^{o}C under 5% CO_2 atmospheric conditions, in Petri dishes

(9cm diameter, 10 mL per dish) with the addition of equal volume of the appropriate media after 2 days in culture and completely replenishing the media after 4 days in culture.

After 6 to 8 days in culture, the petri dishes containing BMDCs or BMDMs were washed three times in plain media, the cells were then carefully scraped and resuspended in complete media. Next, the cells were counted with a hemocytometer, diluted in complete media to a concentration of 10^6 cells/mL and specific number of cells were plated, as described in each individual experiment. In all cases, the plates were incubated overnight at 37 ^oC under 5% CO_2. Every experiment was conducted using cells cultured for 7 to 9 days.

L929 conditioned media was prepared by growing L929 cells to confluence for 2 weeks, in RPMI 1640 (Sigma) supplemented with 10% Hyclone® and 5 mM L-Glutamine. The culture supernatant was collected and sterilized by filtration through 0.22 µm filters (Milipore).

WT and *Card9*$^{-/-}$ immortalized bone marrow derived macrophages were obtained from Katherine A. Fitzgerald (University of Massachusetts) and cultured in DMEM containing 10% fetal bovine serum (Sigma) and 5 mM L-Glutamine.

2.3. *In vivo* infections

The attenuated *S*. Typhimurium strain M525P was grown statically for 18 hours at 37 ^oC in LB Broth (Sigma), then washed and resuspended in D-PBS (Sigma). 1.90 to 2.04 x10^4 CFU/mouse were administered systemically via the lateral tail vein to both male and female mice with ages ranging from 8 to 16 weeks, while control mice were inoculated with PBS only. At days 1, 3 and 7 post-infection, the animals were euthanized, and their spleens and livers were aseptically removed.

Livers were homogenized in 10 mL sterile water using a Colworth stomacher. To obtain single cell suspensions from the spleen, the whole organ was disrupted through a 70 µm cell strainer (BD Biosciences) using the inner part of a 2 mL syringe. Cell suspensions were then centrifuged at 300 x G for 10 minutes, the supernatant was collected for quantification of cytokines and bacterial burden, and the pellet was resuspended in 1 mL of Red Blood Cell lysis buffer (Sigma) and incubated for 10 minutes at room temperature. To stop the reaction, suspensions were toped up to 15 mL with RPMI and then centrifuged at 300 x G for 10 minutes. Supernatant was discarded and the cell pellet was washed once more with 15 mL of RPMI. The purified splenocytes were then lysed for 10 minutes in ice using buffer containing 10 mM Tris pH 7.4, 150 mM NaCl, 5 mM EDTA, 1% Triton X-100, 10 mM NaF, 1 mM $NaVO_4$, 20 mM PMSF, Phosphatase inhibitor cocktail 3 (1 in 100 dilution, Sigma) and

Protease inhibitor cocktail (1 in 100 dilution, P8340, Sigma). The proteins were probed by immunoblotting as described below.

Bacterial burden was quantified by serially diluting (10-fold) the organ homogenates in PBS, plating the appropriate dilutions on LB agar plates followed by overnight incubation at 37 °C. The *in vivo* infections were conducted by Dr. Panagiotis Tourlomousis.

2.4. Cell stimulation and infection

Salmonella Typhimurium strain SL1344, *Escherichia coli* strain P19A, and *Listeria monocytogenes* strain EGD-e were cultured to log phase. This was done by pre-culturing the bacteria for 17.5 hours in 5 mL LB broth (Sigma) at 37 ^{o}C and 200 rpm, followed by a 1 in 10 dilution of the pre-culture in LB broth and further culture for 2 hours (*S*. Typhimurium and *E. coli*) or 3 hours (*L. monocytogenes*). The bacteria were then centrifuged for 10 min at 4,300 x G and resuspended in BMDM or BMDC growth media. Next, the bacteria solutions were diluted to the adequate concentrations in BMDM or BMDC growth media and used for infections.

For gentamicin protection assays (GPA), the bacteria solutions were added to 200,000 BMDM or BMDC cells, adhered to 3 different 96 wells plates at the indicated multiplicity of infection (MOI). Infections using S. Typhimurium SL1344 Δ*fliC*Δ*fljB*Δ*prgJ* included a centrifugation step (5 min at 1,000 x G) to allow the non-motile bacteria to infect the cells. The infection was carried out for an hour at 37 ^{o}C and 5% CO_2. Next, the supernatant was collected and replaced with complete media containing 50 µg/mL gentamicin, followed by 1 hour incubation at 37 ^{o}C and 5% CO_2. Gentamicin is an antibiotic that is unable to cross the eukaryotic plasma membrane, thus killing off the extracellular bacteria. This allows for quantification of intracellular bacteria later in the assay.

After the 50 µg/mL gentamicin incubation, the first plate (2 hours total infection time) had its supernatant collected, and intracellular bacteria counts and cell viability assays were carried out as described below. The remaining 2 plates had their supernatants collected and replaced with complete media containing 10 µg/mL gentamicin. This concentration of the antibiotic has bacteriostatic effects on the bacteria released to the supernatant during the infection, whilst not toxic to eukaryotic cells in the incubation times used in this assay. The second plate was incubated at 37 ^{o}C for another 4 hours (6 hours total infection time) and the third plate was incubated at 37 ^{o}C for another 22 hours (24 hours total infection time). After incubations, both plates had their supernatants collected and intracellular bacteria

counts and cell viability assays were carried out as described below. Culture supernatants were collected and either stored at -80 ^{o}C or used immediately for cytokine quantification.

Selected experiments required the use of BMDMs or BMDCs primed with LPS. This was performed by incubating the cells in growth media containing 200 ng/mL ultrapure LPS from *Escherichia coli* O111:B4 (InvivoGen) for 3 hours at 37 ^{o}C and 5% CO_2, followed by washing in LPS-free media. For stimulation experiments, the LPS-primed cells were incubated with Nigericin 10 µM (Sigma), ATP 5 mM (Sigma), Poly(dA:dT)/LyoVec 2 µg/mL (Invivogen), MDP 10 µg/mL (Sigma) or 60 ng ultrapure flagellin from *Salmonella* Typhimurium (Invivogen). Before applying it to the cells, 1.5 µg of flagellin was mixed with 2.5 µL Profect-P1 reagent (Target Systems) in a final volume of 500 µL in plain media, and incubated at room temperature for 20 minutes for formation of a lipid-protein complex that allows flagellin to be delivered into the cytosol. Zymosan A from *Saccharomyces cerevisae* (Sigma) and NaClO-oxidized zymosan were used at a concentration of 100 µM. NaClO-oxidized zymosan was prepared by incubating 0.05 g of Zymosan in 0.1 M NaOH with 0.5% NaClO at 4 ^{o}C for 24 hours with gentle agitation, followed by centrifugation at 3000 x G for 5 minutes and re-suspension of the sediment in PBS. Table 2.1 summarises the treatments used in this thesis.

Table 2.1: Treatments commonly used in this project.

Treatment	Concentration	time (minutes)
Muramyl Dipeptide (MDP)	10 µg/mL	60
ATP	5 mM	30
Nigericin	10 µM	60
Flagellin	60 ng per 200.000 cells	60
Poly(dA:dT)/LyoVec	2 µg/mL	240
Zymosan	100 µM	60
Oxidized-Zymosan	100 µM	60

For inhibition experiments, a pre-incubation step was carried out before the cells were stimulated or infected, according to each specific inhibitor (Table 2.2). For dectin-1 blocking experiments, LPS-primed cells were incubated for one hour at 37 ^{o}C with BMDM growth media containing anti-dectin-1 2A11 (Abd Serotec) diluted 1 in 10 (100 µg/mL final concentration). Equal volume of *S.* Typhimurium at appropriate MOI was added without removing the media and the infection carried out as detailed above.

Table 2.2: Concentrations and pre-incubation times of the inhibitors used in this project.

Inhibitor	Concentration	Manufacturer	Pre-incubation time (minutes)	Target
3-Methyladenine (3MA)	2.5 mM	Sigma	15	Autophagy
Anti-Dectin-1 2A11	100 µg/mL	Abd Serotec	60	Dectin-1 Receptor
Epoxomicin	1 µM	Sigma	60	Proteasome
Glibenclamide	200 µM	Sigma	15	NLRP3
MCC950	10 µM	Cayman	15	NLRP3
R406	1 µM	Cayman	60	SYK
SB203580	10 µM	Tocris	30	p38
SP600125	10 µM	Tocris	30	JNK
SR11302	10 µM	Tocris	30	AP1
Z-IETD-FMK	10 µM	BD Biosciences	0	Caspase-8

2.5. Cellular viability assays and intracellular bacteria counts

BMDM and BMDC cytotoxicity was measure using the CytoTox 96 Non-Radioactive Cytotoxicity Assay (Promega). Briefly, adherent cells were first washed three times in pre-warmed non-supplemented DMEM and then incubated with 40 µL per well of Triton X-100 0.5% for 15 minutes at 4 ^{o}C. Cells were then scraped off the bottom of each well using a multichannel mechanical pipette. From this, 10 µL were used for intracellular bacteria counts and another 10 µL for cellular viability.

For intracellular bacteria counts, 10 µL of the scraped-cell solution were serially 10 fold diluted in PBS. The dilutions ranging from 10^{-2} to 10^{-4} were plated in LB agar and incubated overnight at 37 ^{o}C. The CFUs were then manually counted.

Another 10 µL of the scraped-cell solution were transferred to a new plate already containing 105 µL Triton X-100 1.2% and incubated at 37 ^{o}C for 1 h. Next, 25 µL were transferred to a new plate already containing 25 µL PBS, and 50 µL of CytoTox reagent was added and gently mixed. After 30 minutes of incubation at room temperature, 50 µL of stop solution was added and absorbance at 492 nm was quantified using a plate reader. Cellular viability was then calculated in relation to a standard curve containing 100% viability (200,000 uninfected cells) serially 2-fold diluted to 6.25% viability (12,500 uninfected cells).

2.6. Cytokine quantification

Secreted cytokines in the cell culture supernatants after appropriate dilution in growth media were quantified by enzyme linked immunosorbent assay (ELISA). All cytokines were measured according to the manufacter's instructions. Mouse IL-1β was measured by the OptEIA Mouse IL-1β Set (BD Biosciences) or mouse IL-1β Tissue culture kit (Meso Scale Discovery). Mouse IL-18 was measured by the mouse IL-18 ELISA kit (MBL International), while for mouse TNF-α the TNF-α DuoSet ELISA kit (R&D Systems) was used.

2.7. Immunofluorescence

For immunofluorescence assays, BMDMs were prepared as described above and 100,000 cells were plated overnight into 8-chambers glass slides (Thermo Fisher Scientific).

After stimulations, BMDMs were washed three times in PBS and fixed in -20 ^{o}C methanol for 5 minutes or 4% paraformaldehyde for 15 minutes at room temperature. Cells were washed three times in pre-warmed PBS and then blocked in PBS (Sigma) containing 10% normal goat serum (Dako) and 0.1% saponin (Sigma) for 1 h at 37 ^{o}C. After blocking for non-specific protein binding, cells were stained with the primary antibody solution (1:500 dilution in PBS containing 10% goat serum), anti-ASC produced in rabbit (Enzo) for 50 minutes at 37 ^{o}C. Cells were then washed three times in pre-warmed PBS and stained with the secondary antibody solution (1:1000 dilution in PBS containing 10% goat serum, anti-rabbit Alexa-fluor 568 produced in goat (Invitrogen)) for 40 minutes at 37 ^{o}C. After three more washes with pre-warmed PBS, cells were counterstained in DAPI mounting medium (Vecta Labs).

For CARD9 and ASC co-colocalization experiments, after incubation with anti-ASC primary and Alexa-fluor 568 secondary antibody, cells were washed three times in PBS and blocked once again in PBS containing 1% BSA and 0.1% saponin. Staining was then carried out as before, using anti-CARD9 (Santa Cruz, 1:300 dilution) and anti-Rabbit-Alexa 430 (1:1000 dilution in PBS containing 1% BSA, Invitrogen). Counterstaining with DAPI was performed as described above. Table 2.3 summarises the antibodies used in this thesis.

To stain for active caspase-8 and caspase-1, LPS-primed BMDMs were stimulated with nigericin, the cell supernatant was then replaced by media containing 0.5X FLICA caspase-8 or caspase-1 reagent (ImmunoChemistry Technologies) and incubated for one hour at 37 ^{o}C. After carefully washing three times with PBS, immunofluorescence staining was performed as described above. Cells were imaged using a Leica DM6000 B fluorescence microscope.

2.8. Immunoprecipitation, protein precipitation and immunoblot

Proteins from cell culture supernatants and spleen homogenates were precipitated using methanol and chloroform. Briefly, one volume of the sample was vortexed for 20 seconds with one volume of methanol at -20 ^{o}C and 0.25 volume of chloroform, followed by centrifugation (4 ^{o}C, 16000 x G for 12 minutes). The intermediate phase containing the precipitated proteins was collected, washed twice in -20 ^{o}C methanol, left in the fume hood for roughly 10 minutes until dry and resuspended in 2x concentrated Pierce™ Lane Marker Reducing Sample Buffer (Life Technologies).

Cells were lysed for 10 minutes in ice using buffer containing 10 mM Tris pH 7.4, 150 mM NaCl, 5 mM EDTA, 1% Triton X-100, 10 mM NaF, 1 mM $NaVO_4$, 20 mM PMSF, Phosphatase inhibitor cocktail 3 (1 in 100 dilution, Sigma) and Protease inhibitor cocktail (1 in 100 dilution, P8340, Sigma). Protein levels were quantified using Pierce™ BCA Protein Assay Kit (Life Technologies) and adjusted to 600 µg/mL for immunoprecipitation or within the range of 250 to 2500 µg/mL for immunoblotting. The samples were then used for co-immunoprecipitation assays (described below) or incubated for 5 minutes at 100 ^{o}C with Pierce™ Lane Marker Reducing Sample Buffer (Life Technologies) for immunoblotting. Gels were loaded with 20 µL of the sample per lane, with a final protein mass ranging from 5 to 50 µg.

For co-immunoprecipitation assays, 10,000,000 BMDMs adhered to Petri dishes were primed with LPS and stimulated with nigericin or infected with *S.* Typhimurium as described above. After treatments, cells were washed three times with PBS at 4 ^{o}C. The cells were then reversibly cross-linked with 5 mM DTBP (Fisher Scientific) for 30 minutes at 4 ^{o}C then lysed as described above. Protein concentration was adjusted to 600 µg/mL and 800 µL was incubated overnight with 2 µL antibody (goat anti-ASC, (sc-33958, Santa Cruz); rabbit anti-CARD9 (mouse preferred) (12283, Cell Signaling); mouse anti-SYK (MA1-19332, Thermo Fisher Scientific)) and 20 µL of Protein A/G PLUS-agarose beads (Santa Cruz). The remainder of the protein sample was stored for use as protein input controls for the immunoblotting. After incubation, the beads were washed four times in lysis buffer, re-suspended in Pierce™ Lane Marker Reducing Sample Buffer (Life Technologies), incubated for 5 minutes at 100 ^{o}C, centrifuged for 1 minute at 5000 x G and the supernatant used for immunoblotting.

Immunoblots were probed using the following primary antibodies: caspase-1 p10 (mouse) (sc-514, Santa Cruz) 1 in 500; cleaved caspase-8 (rabbit) (8592, Cell Signaling) 1 in 500; caspase-8 (rabbit) (IG12, Enzo) 1 in 500; IL-1β (goat) (AF-401, R&D Systems) 1 in 1000; SYK (mouse) (MA1-19332, Thermo Fisher Scientific) 1 in 1000; p-SYK (rabbit) (2711, Cell

Signaling) 1 in 1000; ASC (rabbit) (AL177, Enzo) 1 in 2000; β-Actin (mouse) (AB3280, ABCAM) 1 in 2500; CARD9, mouse preferred (rabbit) 1 in 1000 (12283, Cell Signaling). The secondary antibodies used were: anti-goat IgG-HRP (sc-2922, Santa Cruz) 1 in 5000; anti-mouse IgG-HRP (7076, Cell Signaling) 1 in 6000; anti-rabbit IgG-HRP (A24537, Thermo Fisher Scientific) 1 in 6000 as appropriate. Table 2.3 summarises the different antibodies and how they were used in this work.

2.9. Reactive oxygen species (ROS) assay

BMDMs were seeded in 96-well white opaque plates (OptiPlate-96, PerkinElmer) at a density of $2x10^5$ cells per well and left overnight at 37 ^oC and 5% CO_2 in BMDM growth media without phenol red. BMDMs were then washed three times with $DPBS^+$ solution (Dulbecco PBS supplemented with 100 mg/L Ca^{2+}, 100 mg/L Mg^{2+}, 1 g/L glucose and 4 mM sodium bicarbonate). Next, 80 µL of $DPBS^+$ was added to each well, incubated at 37 ^oC for 3 minutes, followed by addition of 100 µL DBPS+ containing 320µM luminol and 37.5U/mL HRP and immediately afterwards 20 µL of $DBPS^+$ (control), zymosan in $DPBS^+$ (final concentration 100 µg/mL), *S.* Typhimurium or *L.* monocytogenes (both in $DPBS^+$, MOI 50) were added and chemioluminescence at 425 nm was recorded every 2 minutes for 120 minutes.

2.10. Quantitative PCR (qPCR)

Primers were selected based on previous work done by others and uploaded to the primer bank database (http://pga.mgh.harvard.edu/primerbank/index.html) (Spandidos et al., 2009). Table 2.4 summarizes the primers employed. The reverse transcriptase and PCR reaction were carried out in a single step according to manufacturer instructions (SensiFAST™ One-Step Real-Time PCR, Biolab).

Table 2.3: Antibodies, their concentrations and dilutions used in this work.

Antibody	Host	Manufacturer	Original concentration	Dilution	Use
anti-ASC AL177	Rabbit	Enzo	1 mg/mL	1 in 500	Immunofluorescence
anti-ASC AL177	Rabbit	Enzo	1 mg/mL	1 in 2000	Immunoblot
anti-ASC sc33958	Goat	Santa Cruz	0.2 mg/mL	1 in 400	Immunoprecipitation
anti-β-Actin AB3280	Mouse	ABCAM	0.2 mg/mL	1 in 2500	Immunoblot
anti-CARD9 12283	Rabbit	Cell Signaling	0.1 mg/mL	1 in 400	Immunoprecipitation
anti-CARD9 12283	Rabbit	Cell Signaling	0.1 mg/mL	1 in 1000	Immunoblot
anti-CARD9 sc49408	Rabbit	Santa Cruz	0.2 mg/mL	1 in 300	Immunofluorescence
anti-Caspase-1 p10 sc-514	Mouse	Santa Cruz	0.2 mg/mL	1 in 500	Immunoblot
anti-Caspase-8 IG12	Rabbit	Enzo	0.2 mg/mL	1 in 500	Immunoblot
anti-cleaved Caspase-8 8592	Rabbit	Cell Signaling	0.2 mg/mL	1 in 500	Immunoblot
anti-Dectin-1 2A11 MCA2289	Rat	Abd Serotec	0.1 mg/mL	1 in 10	Inhibition assay
anti-goat IgG-HRP sc-2922	Rabbit	Santa Cruz	0.4 mg/mL	1 in 5000	Immunoblot
anti-IL-1b	Goat	R&D Systems	0.2 mg/mL	1 in 1000	Immunoblot
anti-mouse IgG-HRP 7076	Horse	Cell Signaling	1 mg/mL	1 in 6000	Immunoblot
anti-p-SYK 2711	Rabbit	Cell Signaling	1 mg/mL	1 in 1000	Immunoblot
anti-rabbit alexa fluor 430	Goat	Invitrogen	2 mg/mL	1 in 1000	Immunofluorescence
anti-rabbit alexa fluor 568	Goat	Invitrogen	2 mg/mL	1 in 1000	Immunofluorescence
anti-rabbit IgG-HRP A24537	Goat	Thermo Scientific	1 mg/mL	1 in 6000	Immunoblot
anti-SYK MA1-19332	Mouse	Thermo Scientific	1 mg/mL	1 in 400	Immunoprecipitation
anti-SYK MA1-19332	Mouse	Thermo Scientific	1 mg/mL	1 in 1000	Immunoblot

Table 2.4: Pair of primers used for the qPCR experiments.

Gene	Forward (5'-3')	Reverse (5'-3')	Amplicon size (bp)	Primer Bank ID
Bcl-10	CTTCAAGTAGAAAACGGGCTGG	GCACCTAGAGAGGTTGTTGGT	233	6753166a1
Card9	TCCAGACGGAGAGCCGATTA	CCTGGGTGAACTGTCTTCCAA	101	147904863c3
Caspase-1	ACAAGGCACGGGACCTATG	TCCCAGTCAGTCCTGGAAATG	237	6753282a1
Caspase-8	TGCTTGGACTACATCCCACAC	TGCAGTCTAGGAAGTTGACCA	169	33859520a1
Fadd	GCGCCGACACGATCTACTG	TTACCCGCTCACTCAGACTTC	215	6753812a1
Gapdh	AGGTCGGTGTGAACGGATTTG	TGTAGACCATGTAGTTGAGGTCA	123	6679937a1
Malt-1	GGACAAAGTCGCCCTTTTGAT	TCCACAGCGTTACACATCTCA	165	27370250a1
Naip5	TGCCAAACCTACAAGAGCTGA	CAAGCGTTTAGACTGGGGATG	203	5932014a1
Nlrc4	TTGAAGGCGAGTCTGGCAAAG	GGCGCTTCTCAGGTGGATG	125	146198620c2
Nlrp3	ATTACCCGCCCGAGAAAGG	TCGCAGCAAAGATCCACACAG	141	22003870a1
Pro-il-18	GTGAACCCCAGACCAGACTG	CCTGGAACACGTTTCTGAAAGA	202	6680412c1
Pro-il-1β	TTCAGGCAGGCAGTATCACTC	GAAGGTCCACGGGAAAGACAC	75	118130747c2
Pycard	CTTGTCAGGGGATGAACTCAAAA	GCCATACGACTCCAGATAGTAGC	154	31560222a1
Rantes	GCTGCTTTGCCTACCTCTCC	TCGAGTGACAAACACGACTGC	104	7305461a1
Syk	CTACCTGCTACGCCAGAGC	GCCATTAAGTTCCCTCTCGATG	103	6755706a1
TNF-α	CCCTCACACTCAGATCATCTTCT	GCTACGACGTGGGCTACAG	61	7305585a1
β-actin	GGCTGTATTCCCCTCCATCG	CCAGTTGGTAACAATGCCATGT	154	6671509a1

The infection was carried out for 1 hour using 6-well plates with $1.6x10^6$ BMDMs per well, at an MOI of 5, followed by another hour of incubation in media containing 50 μg/mL gentamicin. The supernatant was collected to confirm IL-1β production, and after 2 washes with PBS, cells were detached from the wells by scrapping in the presence of 1 mL RNA protect cell reagent (QIAGEN). The cell lysis and RNA isolation were performed as described by the manufacturer (RNAEasy, QIAGEN), followed by enzymatic DNA cleavage as described by the manufacturer (Ambion®, Life Technologies).

Gene transcription analyses was carried out using GAPDH and β-actin as reference genes, employing Pfaffl method correcting for reaction efficiency (Pfaffl, 2001), according to equation 1:

$$(1)\quad \text{Fold increase} = \frac{\text{Efficiency (Target)}^{\text{CT(target,untreated)}-\text{CT(target,treated)}}}{\text{Efficiency (Reference)}^{\text{CT(ref,untreated)}-\text{CT(ref,treated)}}}$$

2.11. Schematic diagrams

The individual graphical elements used in the schematic diagrams in this thesis were hand drawn by Caroline R. Paié, and later assembled into the final figures using Adobe Photoshop CC 2014 (Adobe Systems Incorporated).

2.12. Statistical analysis

Statistical analysis was performed using the software Prism 6.0 (GraphPad Software) as indicated for each individual experiment. In summary, and depending on the number of experimental groups, the data type and the number of qualitative variables, statistical difference was determined using either unpaired t-test, one-way analysis of variance (ANOVA) with Tukey's post-test, or two-way ANOVA with Bonferroni post-test. In this work, a p value below 0.05 was considered significant.

Chapter 3

Elucidation of pathways involved in inflammasome signalling during *Salmonella* Typhimurium infection

3.1. Introduction

Caspase-1, ASC, IL-1β and IL-18 are all important in the host response against *S*. Typhimurium *in vivo* (Lara-Tejero et al., 2006; Raupach et al., 2006). In particular, *S*. Typhimurium activates both the NLRC4 and NLRP3 inflammasomes (Broz et al., 2010a; Man et al., 2014). In myeloid cells *in vitro*, *S*. Typhimurium stimulates NLRC4 early during infection, triggering rapid pyroptosis, IL-1β and IL-18 release, whilst NLRP3 is recruited on a later stage contributing to optimal cytokine production (Man et al., 2014). In this context, NLRC4 activation not only induces pyroptosis in an ASC-independent fashion (Broz et al., 2010b), but also signals the recruitment of NLRP3 to the ASC speck (Man et al., 2014; Qu et al., 2016). Caspase-1 and caspase-8 are both recruited to the ASC-speck in response to *Salmonella* infection showing somewhat redundant activities: caspase-1 is involved in IL-1β/IL-18 production and pyroptosis, whereas caspase-8 is involved in IL-1β production (Man et al., 2013). The role of other caspases during *Salmonella* infection is not very well characterised.

Activation of the NLRC4 inflammasome is achieved upon recognition of several *Salmonella* PAMPs by NAIPs, such as flagellin recognized by NAIP5, PrgJ by NAIP2, PrgI and SsaG by NAIP1 (hNAIP in humans) (Miao et al., 2010; Yang et al., 2013; Zhao et al., 2016, 2011). Less clear, however, is how *S*. Typhimurium activates the NLRP3 inflammasome. It is possible that bacterial mRNA triggers NLRP3 inflammasome assembly, although the physiological relevance for this remains unclear (Sander et al., 2011). Another hypothesis involves NLRP3 activation by cellular stress signals such as high citrate concentration (Wynosky-Dolfi et al., 2014) or low intracellular potassium concentration (Franchi et al., 2007).

Although it is well established that inflammasomes play an important role in controlling bacterial infections, very little is known about molecules that finely tune this response. For instance, SYK is involved in phosphorylating ASC at tyrosine 144, leading to an increase in inflammasome activity (Gross et al., 2009; Hara et al., 2013; Lin et al., 2015) and, similarly, NLRC4 is activated by phosphorylation at serine 533 by a mechanism involving PKC-δ (Qu et al., 2012). Other molecules including SHP and A20 are capable of inhibiting

inflammasome activity, the first acts by physically interacting with the inflammasome whilst the second inhibits transcription events important for inflammasome activity (Walle et al., 2014; Yang et al., 2015).

Since there are still gaps in our understanding on how inflammasomes operate in the context of *Salmonella* infection, this chapter will focus on better characterising the events leading to NLRC4 and NLRP3 inflammasome activation and assembly. It will also investigate whether other molecules such as NLRs and caspases could be involved in the immune response against *Salmonella* infection. To achieve this, BMDMs from wild-type and various knockout strains were infected *in vitro* with *S.* Typhimurium and the effects on cell viability, intracellular microbial load and levels of cytokines such as IL-1β were assessed.

3.2. Results

The assay used in this body of work is the gentamicin protection assay (GPA). During this assay, BMDMs are infected with *Salmonella* at different MOIs for one hour, after which cell culture supernatant is replaced by fresh medium containing 50 μg/mL gentamicin. At this high concentration, gentamicin will kill all extracellular bacteria. However, and at least for short exposure times, this antibiotic cannot cross the plasma membrane to access the cytosol of the cell and, for this reason, intracellular bacteria are not affected and can be enumerated as a means to assess microbial invasiveness. After 1 h incubation in the presence of 50 μg/mL gentamicin, cell culture supernatant is replaced by fresh medium containing 10 μg/mL gentamicin. At this low concentration, gentamicin has a bacteriostatic rather than a bactericidal effect on extracellular bacteria and it is less likely to gain access the cell cytosol. In this way, intracellular bacteria will not be killed by the antibiotic and can still be enumerated at later time points, such 6 h and 24 h after infection. Apart from enumeration of intracellular bacteria, this assay also allows for cell viability to be assessed indirectly via measurement of LDH and levels of cytokines present in the supernatant to be determined by ELISA.

LDH is an enzyme responsible for converting lactate to pyruvate and is constitutively expressed in most cells, including mammalian cells and bacteria. A possible pitfall in the GPA is that bacterial LDH could interfere with the quantification of eukaryotic cellular viability. This is unlikely, as the cells are lysed at 37 ^{o}C using 1.2% Triton X-100, a non-ionic detergent. This condition is not enough to lysis bacteria, and harsher treatments including boiling would be required (Sung et al., 2003). To confirm that the lysis method used in the GPA is incapable of lysing the bacteria, I have compared LDH activity from BMDMs treated

with Triton X-100 (200,000 to 12,500 cells) to that of bacteria treated in the same conditions (1,000,000 to 1,000 bacteria). In BMDMs, the resulting LDH activity was proportional to the number of cells lysed, whereas no LDH activity was observed when bacteria are treated with Triton X-100, regardless the number of bacteria treated. This suggests that despite the presence of live bacteria inside the cells during the GPA, bacterial LDH does not contribute to the total amount of LDH quantified. This is either due the fact that the Triton X-100 incubation is not enough to cause bacterial lysis or that bacterial cells express much less LDH compared to eukaryotic cells, so the bacterial contribution in this assay is negligible (Figure 3.1). In either case, the LDH activity measured in the GPA correlates primarily to eukaryotic cellular viability.

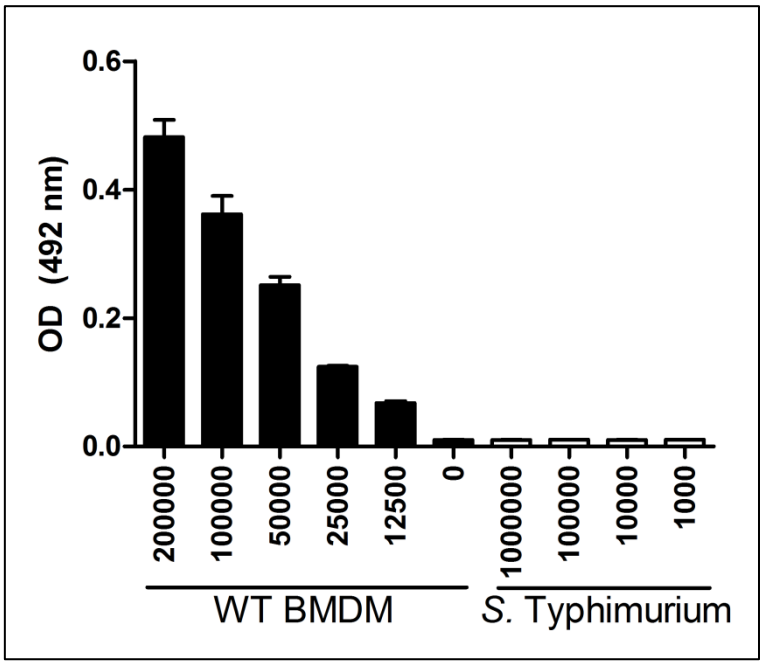

Figure 3.1: *S*. Typhimurium microbial cells does not contribute to the amount of LDH released during the GPA. LDH activity measured after one hour incubation with Triton X-100 1.23% at 37 ^{o}C, as described in material and methods under "Cell stimulation and infection". Data represent the mean from three independent experiments while error bars show the standard error of the mean (s.e.m.).

3.2.1. NLRC4, Caspase-1 and Caspase-11

The NLRC4 inflammasome is quickly assembled in BMDMs in response to *Salmonella* infection to drive pyroptosis and IL-1β production (Man et al., 2014). It has been shown that

this NLRC4-dependent rapid pyroptotic cell death does not depend on ASC (Broz et al., 2010b). Less clear however is the role of caspase-1/11 in ASC-independent and NLRC4-mediated cell death and if other enzymes, including other caspases, are involved in this process. To answer this question, cell viability of WT, *Caspase-1$^{-/-}$Caspase-11$^{-/-}$*, *Nlrc4$^{-/-}$* and *Nlrc4$^{-/-}$Caspase-1$^{-/-}$Caspase-11$^{-/-}$* BMDMs was assessed in response to infection with *Salmonella*.

As expected, *Caspase-1$^{-/-}$Caspase-11$^{-/-}$* BMDMs at 2 and 6 hours after infection were more resilient to cell death in comparison to WT controls. This occurs because caspase-1 is the pyroptosis executioner caspase in the NLRC4 inflammasome (Poyet et al., 2001). *Nlrc4$^{-/-}$* cells exhibited increased survival in comparison to *Caspase-1$^{-/-}$Caspase-11$^{-/-}$* at 2 and 6 hours after infection. This suggests that upon *Salmonella* infection, NLRC4 triggers cell death independent of caspase-1/11, as previously observed (Broz et al., 2010b). Interestingly, *Nlrc4$^{-/-}$Caspase-1$^{-/-}$Caspase-11$^{-/-}$* cells were even more resilient to cell death than *Nlrc4$^{-/-}$* cells but only moderately and only at 2 hours after infection, suggesting that early in the infection NLRC4 can trigger cell death via different pathways, one of which involves Caspase-1/11 (Figure 3.2). Interestingly, however, is that at 24 hours post-infection at MOI 10 and 50, substantial cell death occurs in all knockout strains. Thus, it is possible that other proteins such as NLRs and caspases could be involved in driving cell death in *S.* Typhimurium infections. In the context of the NLRC4 and NLRP3 inflammasomes, caspase-8 is not involved in pyroptosis when caspase-1 is present (Man et al., 2013). Possible roles for caspase-2 and caspase-12, as well as other NLRs, are going to be investigated later in this chapter.

Intracellular bacteria count followed a similar pattern to that observed in cell viability. Overall, *Nlrc4$^{-/-}$* and *Nlrc4$^{-/-}$Caspase-1$^{-/-}$Caspase-11$^{-/-}$* BMDMs showed increased bacteria burden in comparison to WT controls, possibly a consequence of the increased number of viable cells. *Caspase-1$^{-/-}$Caspase-11$^{-/-}$* also showed increased intracellular bacteria counts, but not as much as the other knockout strains (Figure 3.2).

No consistent differences in Il-1β production was observed between *Nlrc4$^{-/-}$, Caspase-1$^{-/-}$ Caspase-11$^{-/-}$* and *Nlrc4$^{-/-}$Caspase-1$^{-/-}$Caspase-11$^{-/-}$* (Figure 3.3), suggestive that Caspase-1/11 activation downstream NLRC4 is necessary for IL-1β production upon *Salmonella* infection. Thus, the data suggests that the NLRC4-dependent and caspase-1/11-independent death pathway does not contribute significantly to IL-1β production. It is likely that at 6 and 24 hours post infection, NLRP3 and caspase-8 are involved in IL-1β production (Figure 3.3) (Man et al., 2013).

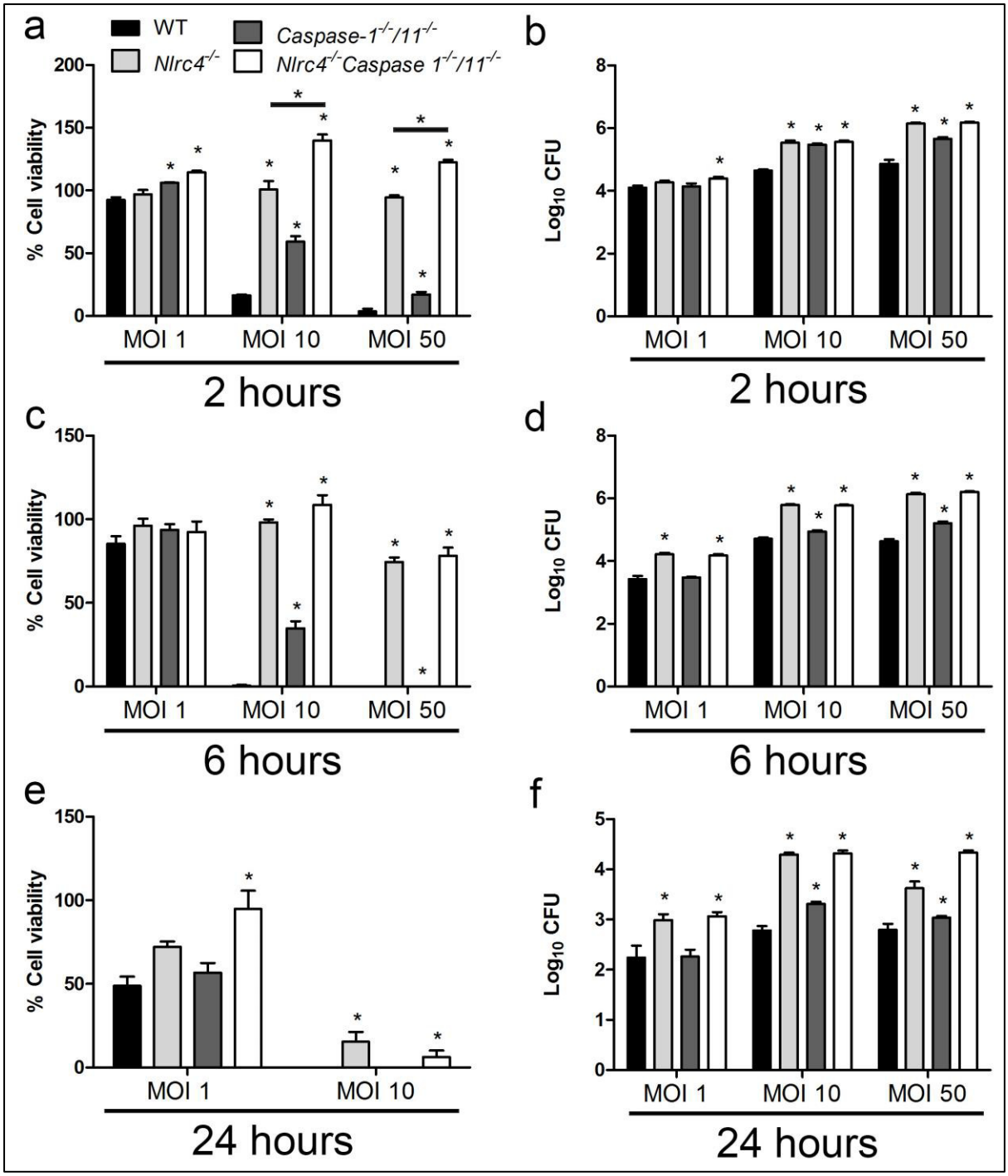

Figure 3.2: NLRC4 and Caspase-1/Caspase-11 are involved in cell death and intracellular bacteria counts in BMDMs infected with *S*. Typhimurium SL1344. (a), (c) and (e) Cellular viability (as measured by LDH release) and (b), (d) and (f) intracellular bacteria counts of WT, *Nlrc4*$^{-/-}$, *Caspase-1*$^{-/-}$*Caspase-11*$^{-/-}$ *and Nlrc4*$^{-/-}$/*Caspase-1*$^{-/-}$*Caspase-11*$^{-/-}$ BMDMs after infection with *S*. Typhimurium at MOIs 1, 10 and 50 for 2 (a-b), 6 (c-d) and 24 (e-f) hours. * $p<0.05$ (one-way ANOVA with Tukey's multiple comparisons test). Data represent the mean from three independent experiments while error bars show the s.e.m.

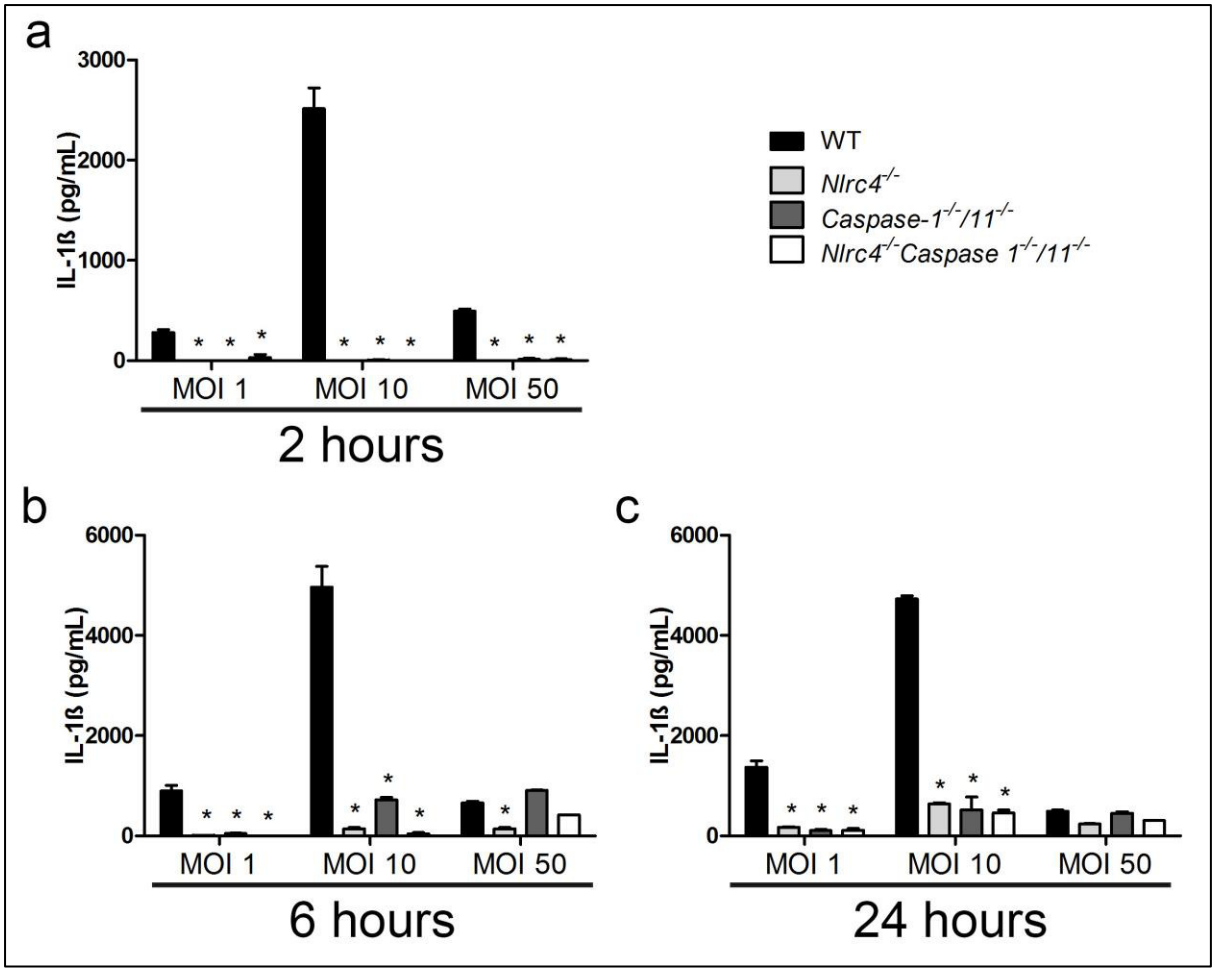

Figure 3.3: NLRC4 and Caspase-1/Caspase-11 are essential for IL-1β production in BMDMs infected with *S*. Typhimurium SL1344. IL-1β secretion (as measured by ELISA) of WT, *Nlrc4*$^{-/-}$, *Caspase-1*$^{-/-}$*Caspase-11*$^{-/-}$ *and Nlrc4*$^{-/-}$/*Caspase-1*$^{-/-}$*Caspase-11*$^{-/-}$ BMDMs after infection with *S*. Typhimurium at MOIs 1, 10 and 50 for 2 (a), 6 (b) and 24 (c) hours. * $p<0.05$ (one-way ANOVA with Tukey's multiple comparisons test). Data represent the mean from three independent experiments while error bars show the s.e.m.

3.2.2. Caspase-11

Caspase-11 was first described as an accessory caspase capable of activating caspase-1 (Wang et al., 1998). The role of this enzyme in inflammasome biology was revisited when it was discovered that the very popular *caspase-1*$^{-/-}$ mice were actually deficient in both caspase-1 and caspase-11 due the proximity of these genes in the chromosome (Kayagaki et al., 2011). Generation of caspase-1 and caspase-11 single knockouts led to the discovery that caspase-11 can form a non-canonical inflammasome and may act as an intracellular PRR sensing cytosolic LPS (Hagar et al., 2013; Kayagaki et al., 2013, 2011; Shi et al.,

2014). How relevant these responses are in the context of *Salmonella* infection *in vitro* have not been so far investigated.

Infection of *caspase-11*$^{-/-}$ BMDMs revealed no differences in intracellular bacteria, cellular viability or IL-1β production in comparison to WT controls (Figure 3.4-5). This however does not rule out an effect of caspase-11, because the rapid and robust NLRC4-driven response could be masking a potentially delayed caspase-11-dependent effect. To check this hypothesis, two different experimental approaches could be employed. The first one makes use of macrophages derived from *Nlrc4*$^{-/-}$*Caspase-11*$^{-/-}$ mice. The second one relies on the use of a bacterial strain that cannot activate NLRC4. Our laboratory does not possess *Nlrc4*$^{-/-}$*Caspase-11*$^{-/-}$ mice. For this reason, I infected wild-type and *Caspase-11*$^{-/-}$ cells with SL1344 *S.* Typhimurium Δ*fliC*Δ*fljB*Δ*prgJ*. This triple knockout microbial strain lacks flagella and PrgJ, a type III secretion system inner rod protein, thus it fails to activate NLRC4 (Man et al., 2014).

In the absence of NLRC4 activation, little to no cell death is observed at 2 and 6 hours post infection (Figure 3.6), whilst IL-1β production only starts to be reliably detected at 6 hours post infection (Figure 3.7). *Caspase-11*$^{-/-}$ BMDMs infected with *S.* Typhimurium Δ*fliC*Δ*fljB*Δ*prgJ* showed impaired cell death and increased intracellular bacteria counts at 24 hours post infection (Figure 3.6). Additionally, *caspase-11*$^{-/-}$ had deficient IL-1β production at 6 and 24 hours post infection (Figure 3.7). Taken together, the data suggests that caspase-11 is involved in the innate response against *Salmonella in vitro*. A possible explanation for these effects involves the formation of the non-canonical caspase-11 inflammasome due the release of LPS into the cytosol (Kayagaki et al., 2011). Another hypothesis is that caspase-11 could potentially be involved with the canonical NLRP3 inflammasome, which is activated later in the infection (Man et al., 2014). These hypotheses were not tested thus far.

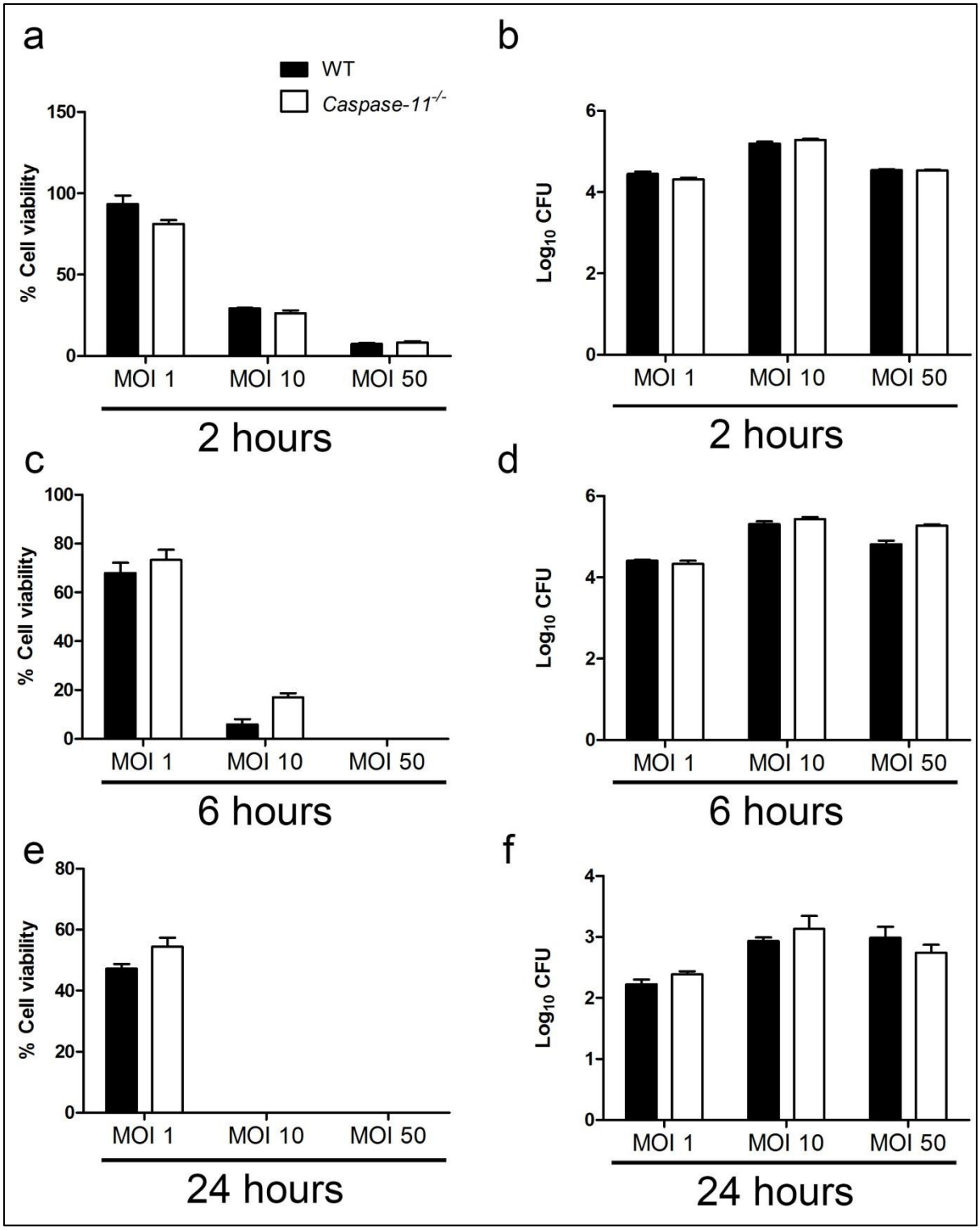

Figure 3.4: Caspase-11 has no effect on cellular viability and intracellular bacteria counts in BMDMs infected with *S.* Typhimurium SL1344. (a), (c) and (e) Cellular viability (as measured by LDH release) and (b), (d) and (f) intracellular bacteria counts of WT and *Caspase-11*$^{-/-}$ BMDMs after infection with *S*. Typhimurium at MOIs 1, 10 and 50 for 2 (a-b), 6 (c-d) and 24 (e-f) hours. $p>0.05$ unpaired t-test. Data represent the mean from two independent experiments while error bars show the s.e.m.

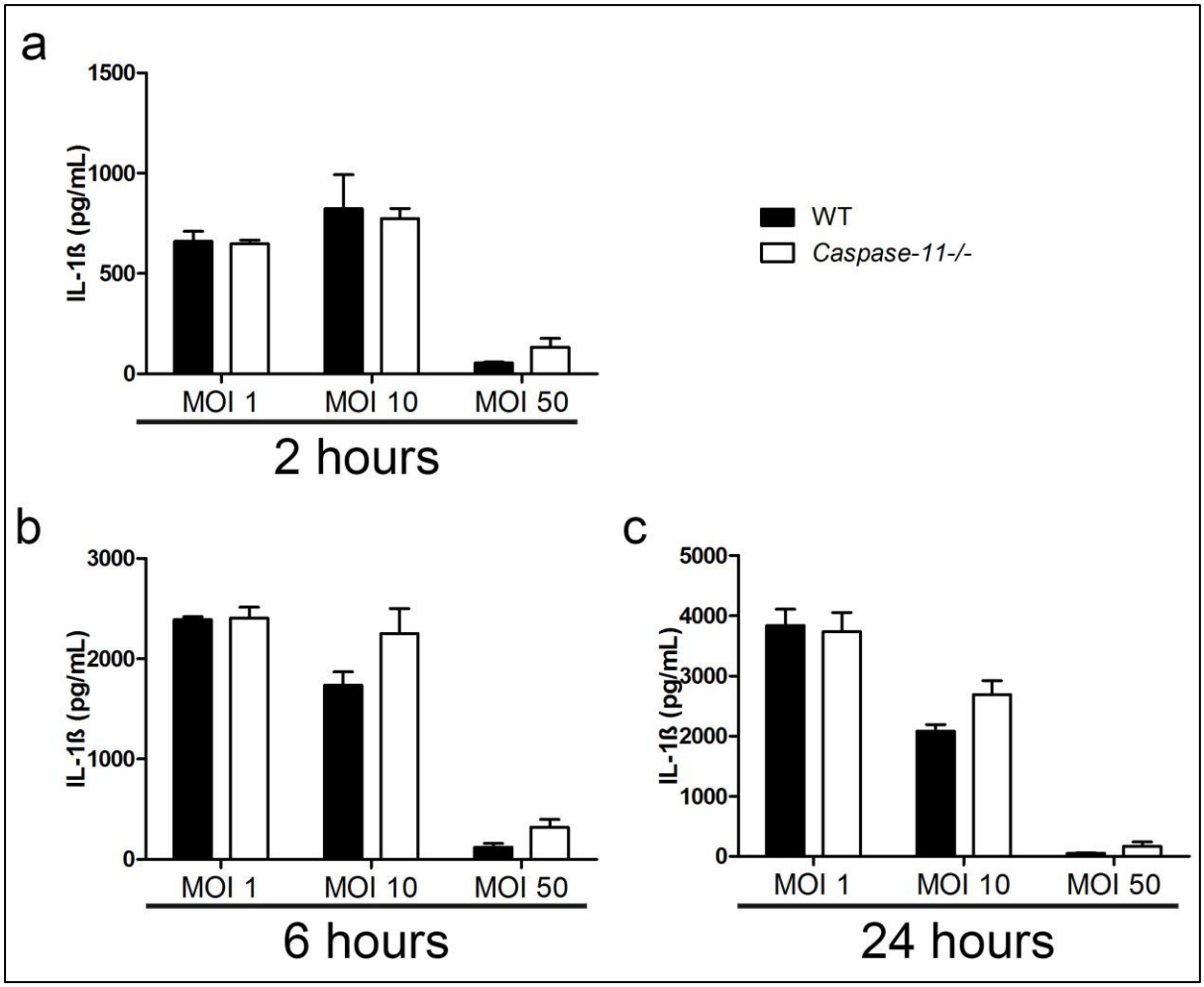

Figure 3.5: Caspase-11 has no effect on IL-1β production in BMDMs infected with *S.* Typhimurium SL1344. IL-1β secretion (as measured by ELISA) of WT *and Caspase-11*$^{-/-}$ BMDMs after infection with *S.* Typhimurium at MOIs 1, 10 and 50 for 2 (a), 6 (b) and 24 (c) hours. $p>0.05$ unpaired t-test. Data represent the mean from two independent experiments while error bars show the s.e.m.

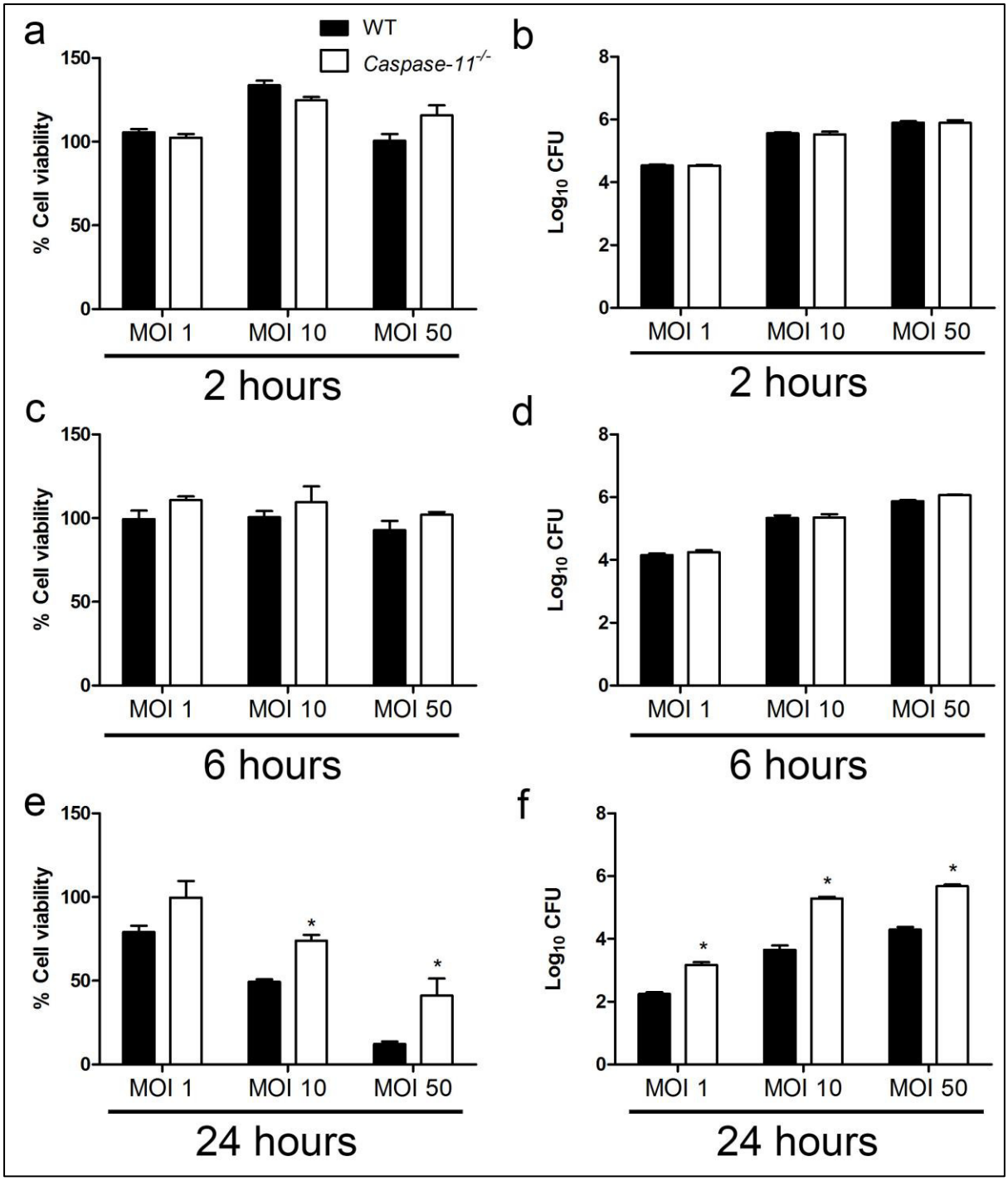

Figure 3.6: Caspase-11 is involved in cell death and intracellular bacteria counts at later time points in BMDMs infected with *S.* Typhimurium Δ*fliC*Δ*fljB*Δ*prgJ*, deficient in NLRC4 activation. (a), (c) and (e) Cellular viability (as measured by LDH release) and (b), (d) and (f) intracellular bacteria counts of WT and *Caspase-11*$^{-/-}$ BMDMs after infection with *S*. Typhimurium Δ*fliC*Δ*fljB*Δ*prgJ* at MOIs 1, 10 and 50 for 2 (a-b), 6 (c-d) and 24 (e-f) hours. * $p<0.05$ unpaired t-test. Data represent the mean from two independent experiments while error bars show the s.e.m.

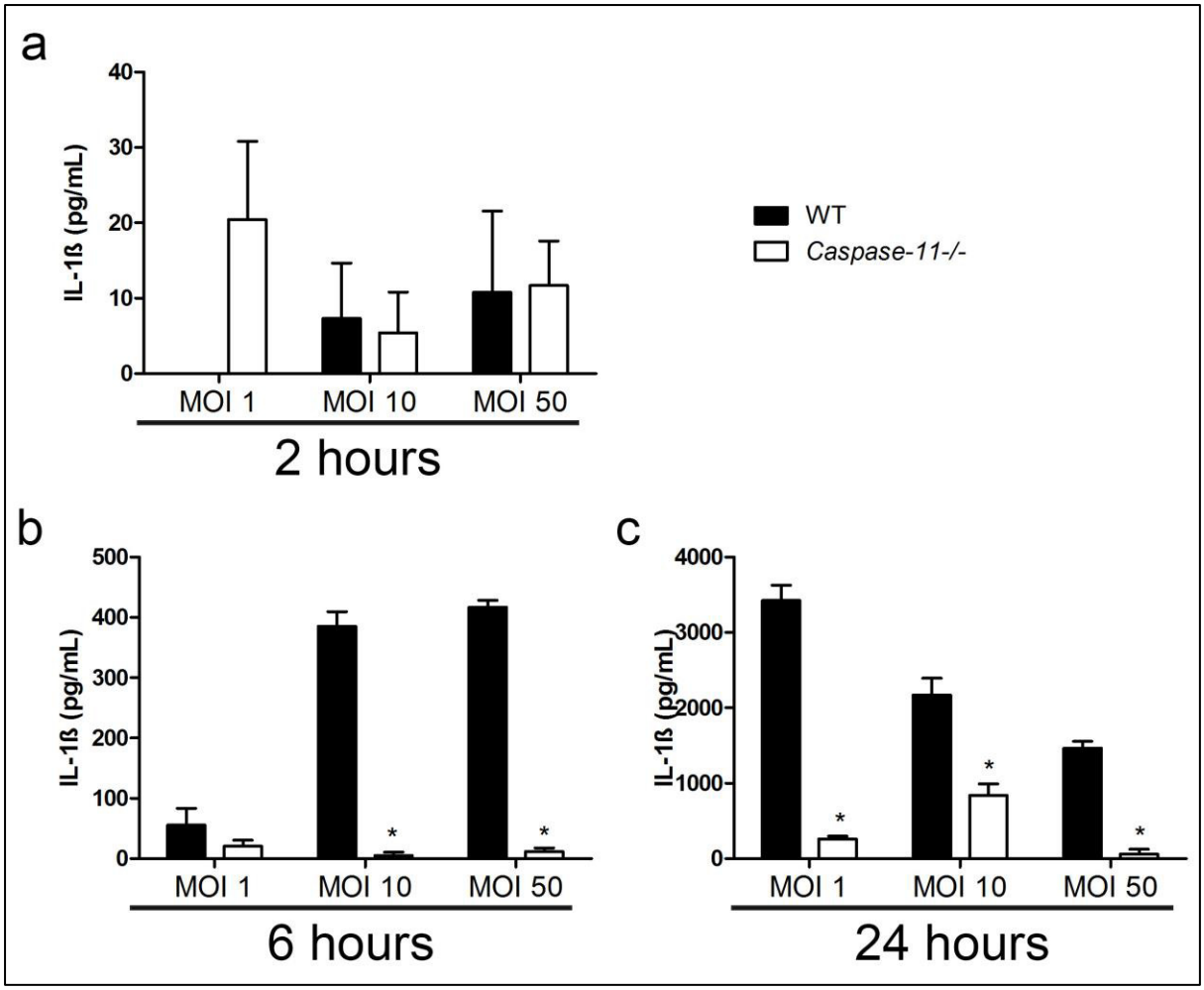

Figure 3.7: Caspase-11 is involved in IL-1β production in BMDMs infected with *S.* Typhimurium Δ*fliC*Δ*fljB*Δ*prgJ*, deficient in NLRC4 activation. IL-1β secretion (as measured by ELISA) of WT *and Caspase-11*$^{-/-}$ BMDMs after infection with *S*. Typhimurium Δ*fliC*Δ*fljB*Δ*prgJ* at MOIs 1, 10 and 50 for 2 (a), 6 (b) and 24 (c) hours. * $p<0.05$ unpaired t-test. Data represent the mean from two independent experiments while error bars show the s.e.m.

3.2.3. NLRC3 and NLRC5

NLRC3 and NLRC5 are CARD-containing NLRs which act as inhibitors of innate immune pathways, with NLRC3 inhibiting NF-κB and cGAS/STING and NLRC5 inhibiting NF-κB and RIG-I (Cui et al., 2010; Schneider et al., 2012; Tong et al., 2012; Zhang et al., 2014). These studies however focused on specific TLR ligands or viruses, and their role in bacterial infections, including *S.* Typhimurium, remains unknown.

Cellular viability of *Nlrc3*$^{-/-}$ and *Nlrc5*$^{-/-}$ BMDMs infected with *Salmonella* was similar to that of WT cells at MOIs 10 and 50 in all time points. At MOI 1, however, *Nlrc3*$^{-/-}$ and *Nlrc5*$^{-/-}$ cells exhibited a decrease in cellular viability at all time points which reached statistical significance ($p<0.05$ one-way ANOVA) at 24 hours only (Figure 3.8). This suggests that both NLRC3 and NLRC5 are negative modulators of *Salmonella*-induced cell death at later time-points. The lack of significant differences at MOIs 10 and 50 are possibly due the extensive cell death observed at these MOIs, making it difficult to detect effects that result in increased cell death.

The increased cell death was accompanied by a decrease in IL-1β production in both *Nlrc3*$^{-/-}$ and *Nlrc5*$^{-/-}$ BMDMs. At MOIs 1 at 2 and 6 hours, WT BMDMs produced twice as much IL-1β as the knockout strains. At MOI 10, the IL-1β produced by both *Nlrc3*$^{-/-}$ and *Nlrc5*$^{-/-}$ are only slightly above the detection limit (16 pg/mL), whilst WT controls produced around 50 pg/mL at 2 hours and 100 pg/mL at 6 hours (Figure 3.9). No differences were observed at 24 hours and in all time points infected with MOI 50 (Figure 3.9). The impaired IL-1β production in *Salmonela*-infected *Nlrc3*$^{-/-}$ and *Nlrc5*$^{-/-}$ BMDMs could potentially be a consequence of decreased cellular viability. Quantification of IL-18, however, made this hypothesis unlikely. If the increased cell death was responsible for the observed decrease in IL-1β production, a similar trend would be expected for IL-18. Upon *S.* Typhimurium infection, WT, *Nlrc3*$^{-/-}$ and *Nlrc5*$^{-/-}$ produced the same amount of IL-18 at all time points and MOIs investigated (Figure 3.10). Whilst the cell viability data supports a role for NLRC3 and NLRC5 as NF-κB inhibitors, the IL-1β data suggests that it is possible that NLRC3 and NLRC5 are involved in activating NF-κB signalling during *S.* Typhimurium infection. Further experimentation is required to elucidate how NLRC3 and NLRC5 are involved in these processes.

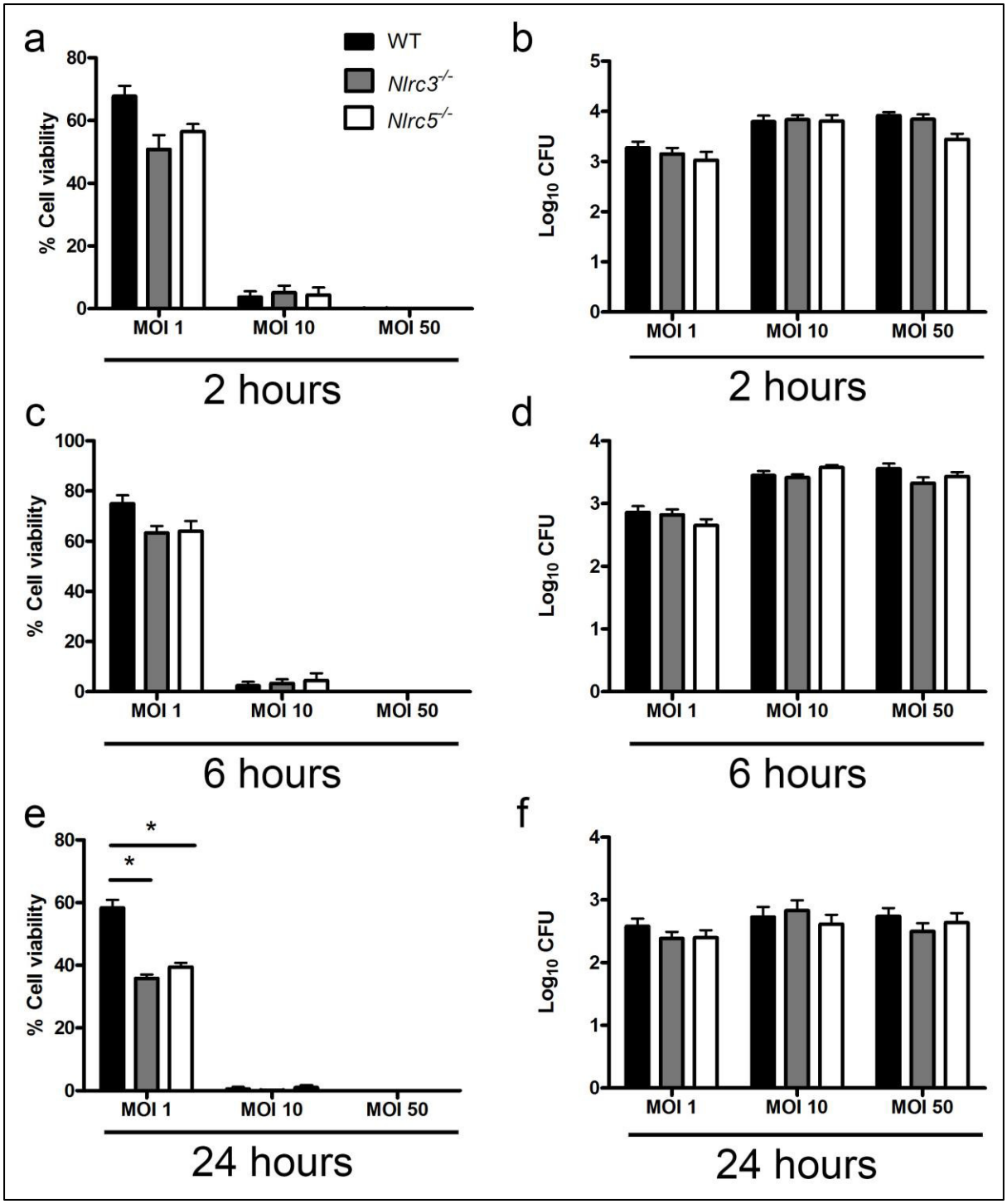

Figure 3.8: NLRC3 and NLRC5 are involved in cell death at later time points in BMDMs infected with *S.* Typhimurium SL1344, without affecting intracellular bacteria counts. (a), (c) and (e) Cellular viability (as measured by LDH release) and (b), (d) and (f) intracellular bacteria counts of WT, *Nlrc3*$^{-/-}$ *and Nlrc5*$^{-/-}$ BMDMs after infection with *S.* Typhimurium at MOIs 1, 10 and 50 for 2 (a-b), 6 (c-d) and 24 (e-f) hours. * $p<0.05$ one-way ANOVA with Tukey's multiple comparisons test. Data represent the mean from three independent experiments while error bars show the s.e.m.

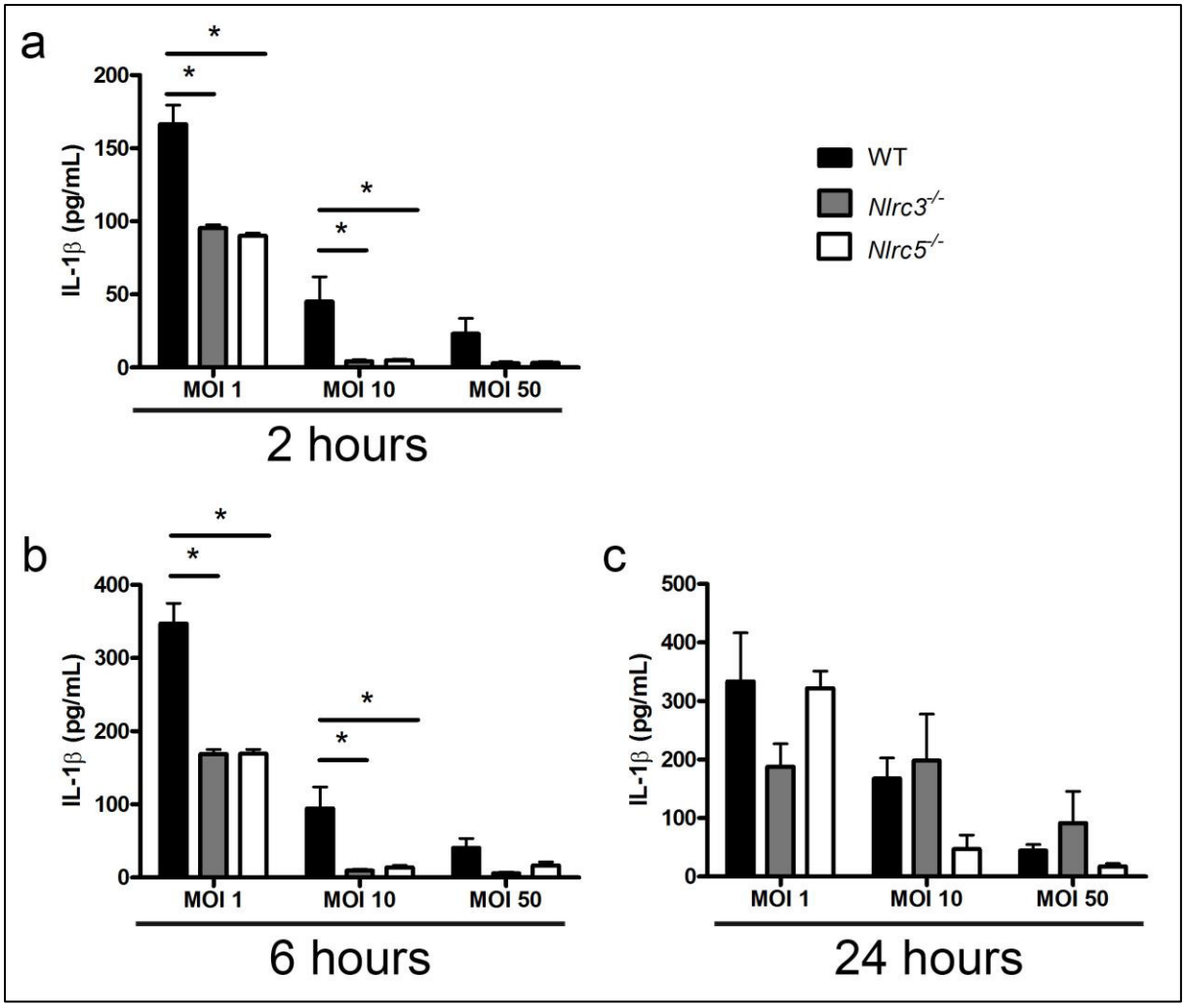

Figure 3.9: NLRC3 and NLRC5 are involved in IL-1β production in BMDMs infected with *S.* Typhimurium SL1344. IL-1β secretion (as measured by Luminex™) of WT, *Nlrc3*$^{-/-}$ *and Nlrc5*$^{-/-}$ BMDMs after infection with *S*. Typhimurium at MOIs 1, 10 and 50 for 2 (a), 6 (b) and 24 (c) hours. * $p<0.05$ one-way ANOVA with Tukey's multiple comparisons test. Data represent the mean from three independent experiments while error bars show the s.e.m.

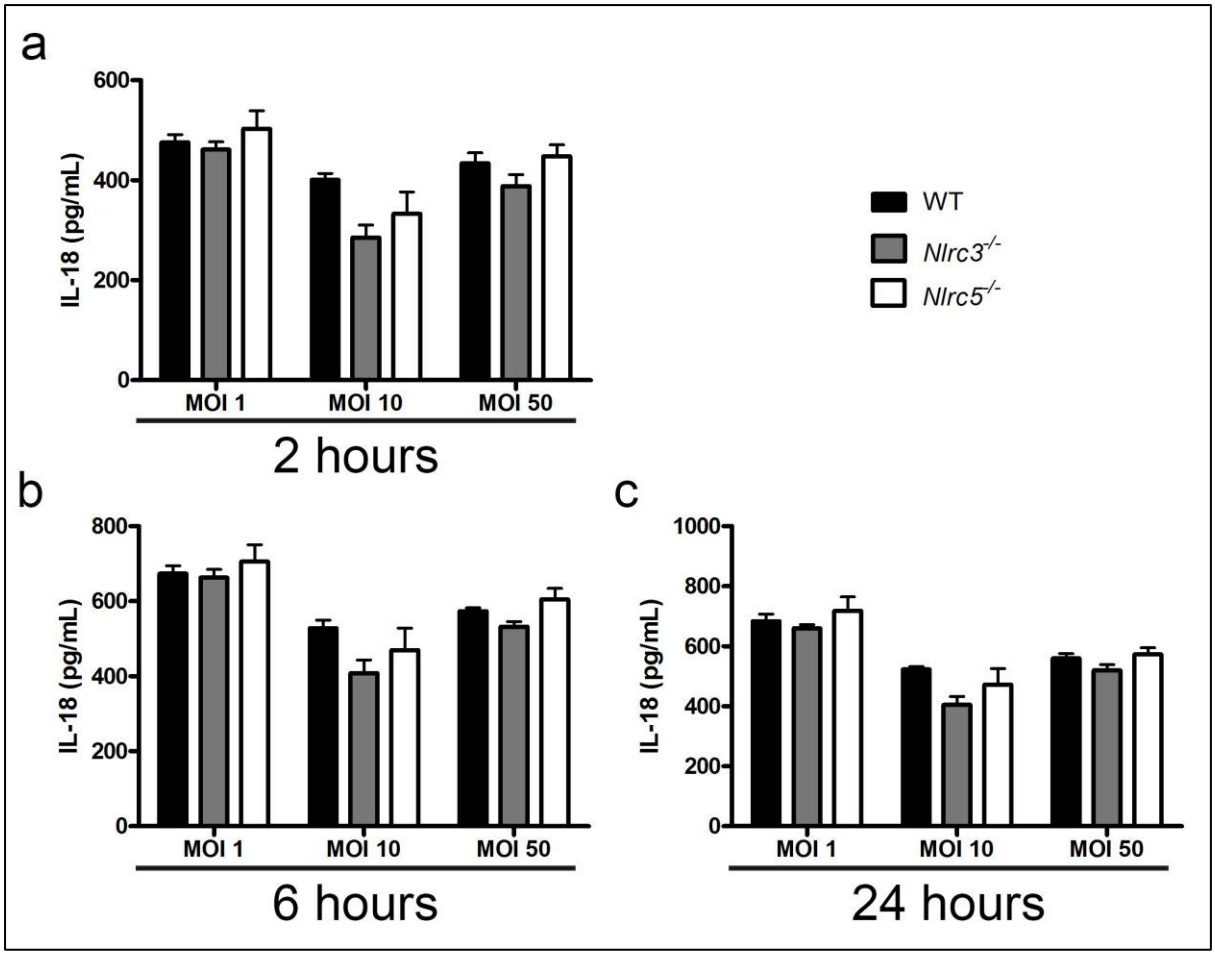

Figure 3.10: NLRC3 and NLRC5 are not involved in IL-18 production in BMDMs infected with *S.* Typhimurium SL1344. IL-18 secretion (as measured by ELISA) of WT, *Nlrc3*$^{-/-}$ *and Nlrc5*$^{-/-}$ BMDMs after infection with *S*. Typhimurium at MOIs 1, 10 and 50 for 2 (a), 6 (b) and 24 (c) hours. $p>0.05$ one-way ANOVA. Data represent the mean from three independent experiments while error bars show the s.e.m.

3.2.4. Gasdermin D and DFNA5

As previously discussed, pyroptosis is a form of cell death characterised by membrane rupture and release of intracellular contents including inflammatory cytokines and DAMPs into the extracellular space. Upon activation of the caspase-11 non-canonical inflammasome, gasdermin D is the main executioner of pyroptosis: it is cleaved by caspase-11, allowing its N-terminal fragment to create pores in the plasma membrane leading to cell lysis (Aglietti et al., 2016; Kayagaki et al., 2015; Liu et al., 2016; Shi et al., 2015). Upon activation of canonical inflammasomes, however, it is not clear if gasdermin D is the sole mediator of cell lysis (Kayagaki et al., 2015).

Upon infection with *S.* Typhimurium, *GasderminD*$^{-/-}$ BMDMs were more resilient than WT to cell death only at MOI 10 and only at 2 post infection. However, a substantial number of *GasderminD*$^{-/-}$ cells were still lysed at MOI 10, while they did not survive the infection with MOI 50 any better than WT BMDMs. This suggests that gasdermin D is not the only executioner of pyroptosis during *Salmonella* infection (Figure 3.11).

DFNA5, also known as gasdermin E, could be playing a role in mediating pyroptosis during canonical inflammasome activation. This protein belongs to the gasdermin family and was recently described as a caspase-3 target during apoptosis, causing secondary cell lysis (Rogers et al., 2017; Wang et al., 2017). This protein could, therefore, be involved in *Salmonella*-induced pyroptosis. Infection of both *GasderminD*$^{-/-}$ and *GasderminD*$^{-/-}$*/Dfna5*$^{-/-}$ BMDMs, however, revealed no difference in cellular viability between them (Figure 3.11).

Gasdermin D is also involved in IL-1β release. This is shown by the impaired production of this cytokine in comparison to WT controls at all time points and MOIs analysed (Figure 3.12). Pore formation is one of the proposed mechanisms for IL-1β secretion (Fink and Cookson, 2006), so it is feasible that the decrease in membrane integrity due gasdermin D activity accounts for the IL-1β released to the supernatant. This effect is, however, specific to IL-1β, as IL-18 production was similar between WT and *GasderminD*$^{-/-}$ BMDMs (Figure 3.19). No differences in IL-18 nor IL-1β production were detected between *GasderminD*$^{-/-}$ and *GasderminD*$^{-/-}$*/Dfna5*$^{-/-}$ (Figure 3.11-13), suggesting that DFNA5 plays no role in these processes.

Differences in intracellular bacteria counts in *Salmonella*-infected *GasderminD*$^{-/-}$ and *GasderminD*$^{-/-}$*/Dfna5*$^{-/-}$ BMDMs in comparison to WT controls were inconsistent and no statistically significant difference was observed (Figure 3.11).

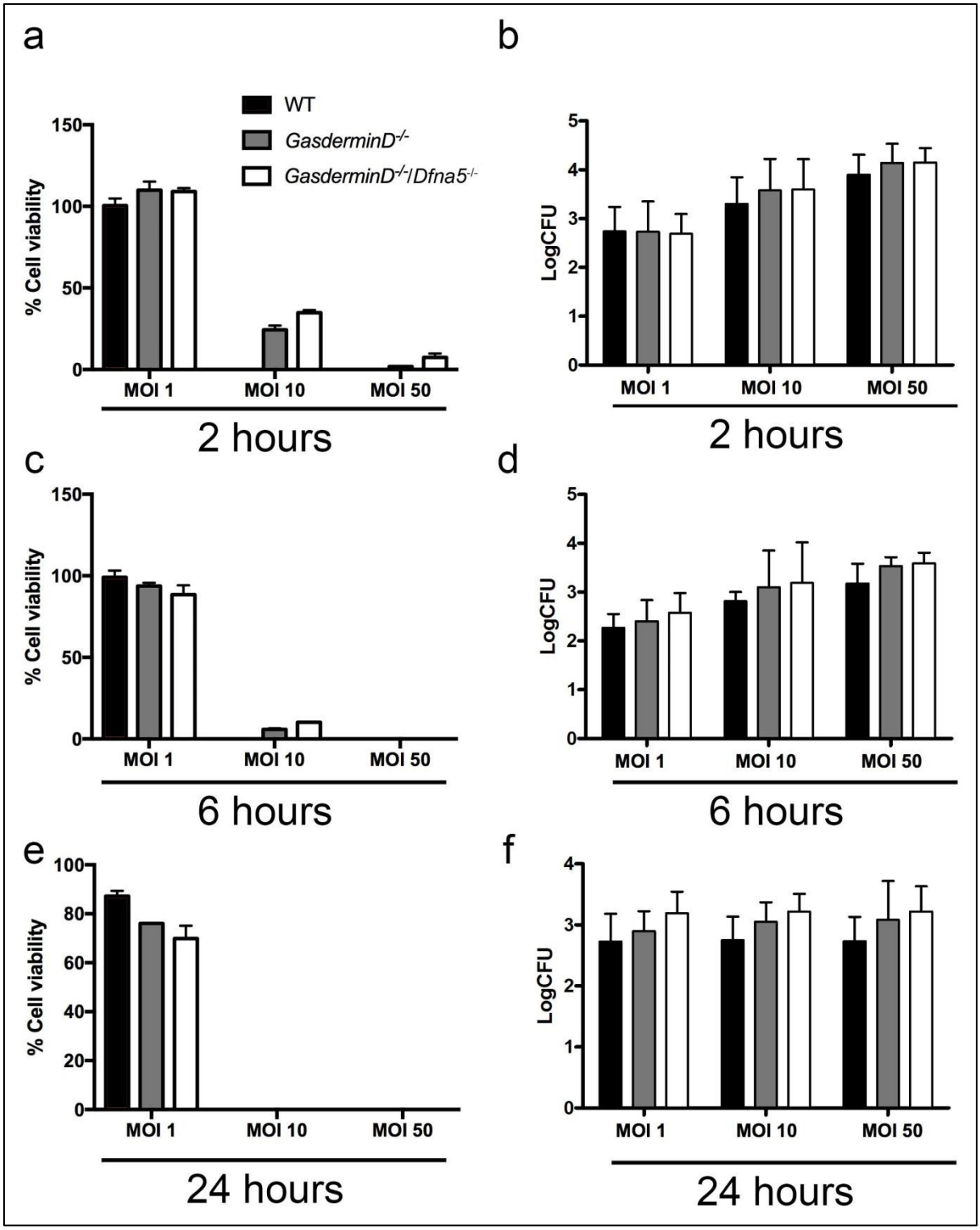

Figure 3.11: Neither Gasdermin D or DFNA5 has an effect on cellular viability and intracellular bacteria counts in BMDMs infected with *S*. Typhimurium SL1344. (a), (c) and (e) Cellular viability (as measured by LDH release) and (b), (d) and (f) intracellular bacteria counts of WT, *GasderminD$^{-/-}$ and GasderminD$^{-/-}$/Dfna5$^{-/-}$* BMDMs after infection with *S*. Typhimurium at MOIs 1, 10 and 50 for 2 (a-b), 6 (c-d) and 24 (e-f) hours. Data represent the mean from four independent experiments while error bars show the s.e.m.

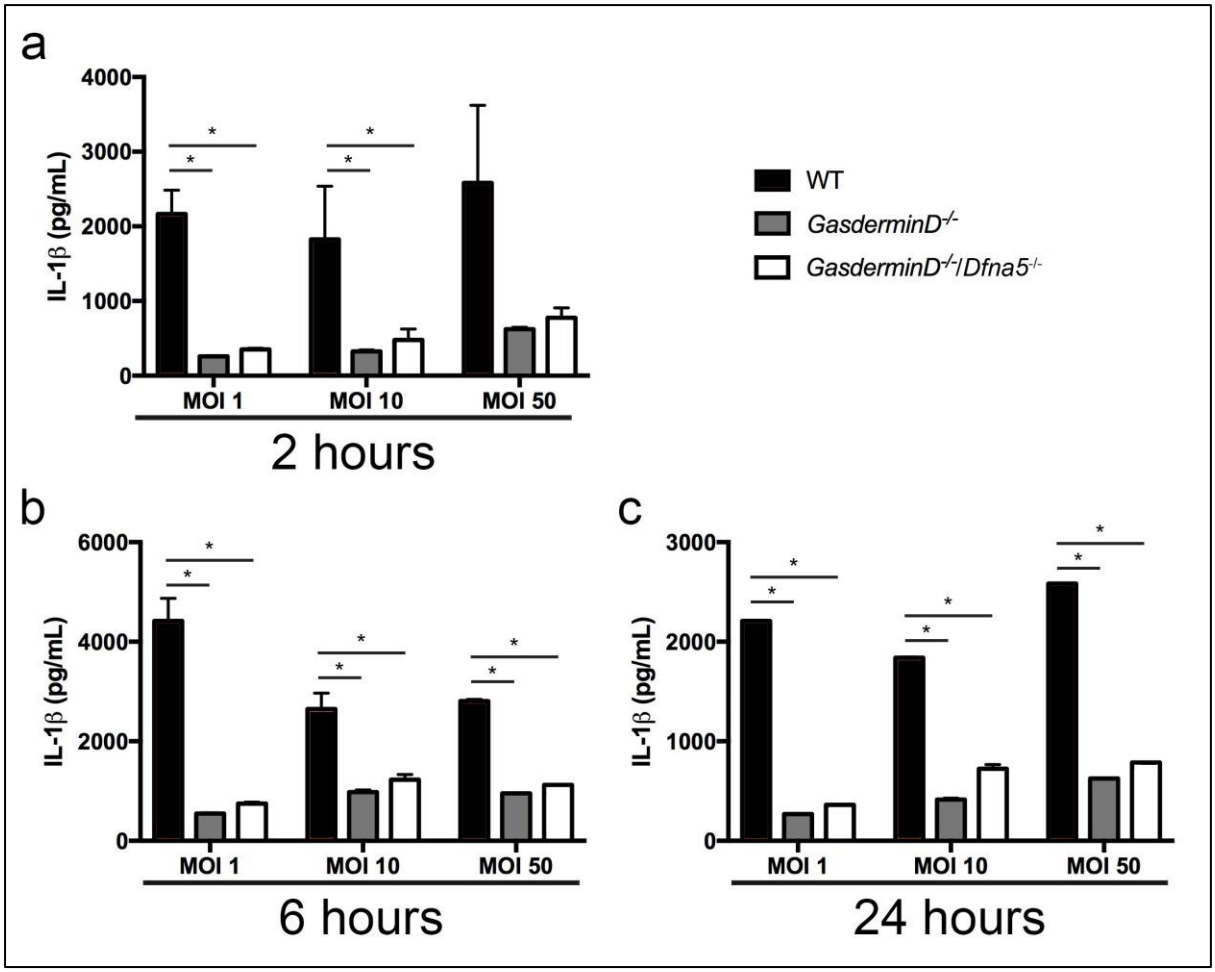

Figure 3.12: Gasdermin D, but not DFNA5, suppresses IL-1β production in BMDMs infected with *S*. Typhimurium SL1344. IL-1β secretion (as measured by Luminex^{TM}) of WT, *GasderminD$^{-/-}$ and GasderminD$^{-/-}$/Dfna5$^{-/-}$* BMDMs after infection with *S*. Typhimurium at MOIs 1, 10 and 50 for 2 (a), 6 (b) and 24 (c) hours. * $p<0.05$ one-way ANOVA with Tukey's multiple comparisons test). Data represent the mean from four independent experiments while error bars show the s.e.m.

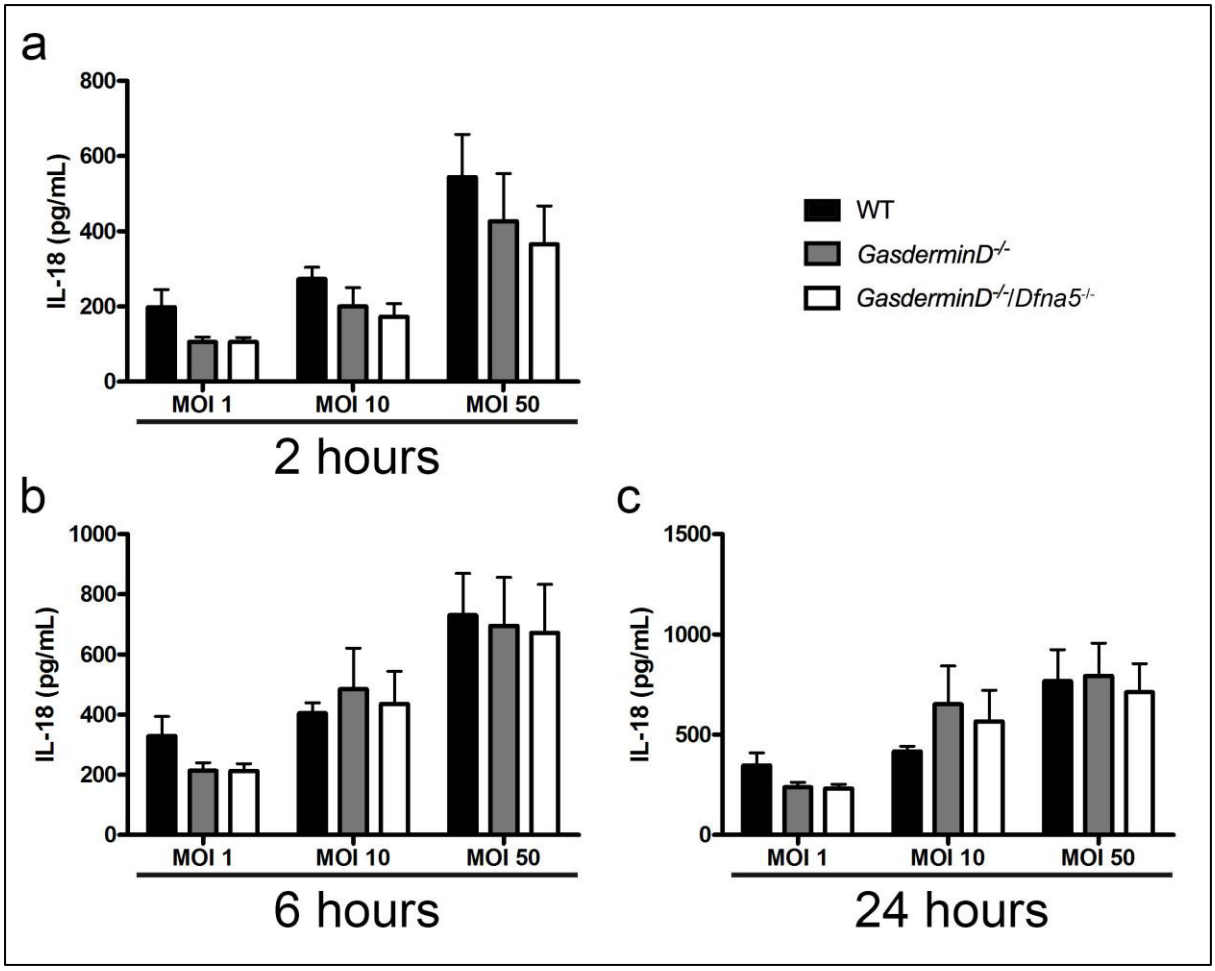

Figure 3.13: Neither Gasdermin D or DFNA5 have any effect on IL-18 production in BMDMs infected with *S*. Typhimurium SL1344. IL-18 secretion (as measured by ELISA) of WT, *GasderminD$^{-/-}$ and GasderminD$^{-/-}$/Dfna5$^{-/-}$* BMDMs after infection with *S*. Typhimurium at MOIs 1, 10 and 50 for 2 (a), 6 (b) and 24 (c) hours. $p>0.05$ one-way ANOVA. Data represent the mean from four independent experiments while error bars show the s.e.m.

Because NLRC4 is the single most potent inducer or early pyroptosis in BMDMs infected with *Salmonella*, its dramatic effect could mask more subtle contributions from other players, such as DFNA5. To address this, WT, *GasderminD$^{-/-}$* and *GasderminD$^{-/-}$/Dfna5$^{-/-}$* macrophages were infected with *S*. Typhimurium Δ*fliC*Δ*fljB*Δ*prgJ*, a microbial mutant that cannot activate NLRC4 (Man et al., 2014). Cellular viability was found to be similar between all three genotypes for all MOIs and time points tested (Figure 3.14). In this setting, no cell death is observed at 2 hours (as illustrated in Figure 3.6). Taken together, the data suggests that DFNA5 is not involved in inflammasome biology in the context of *Salmonella* infection, thus no further work was done with cells from these mice.

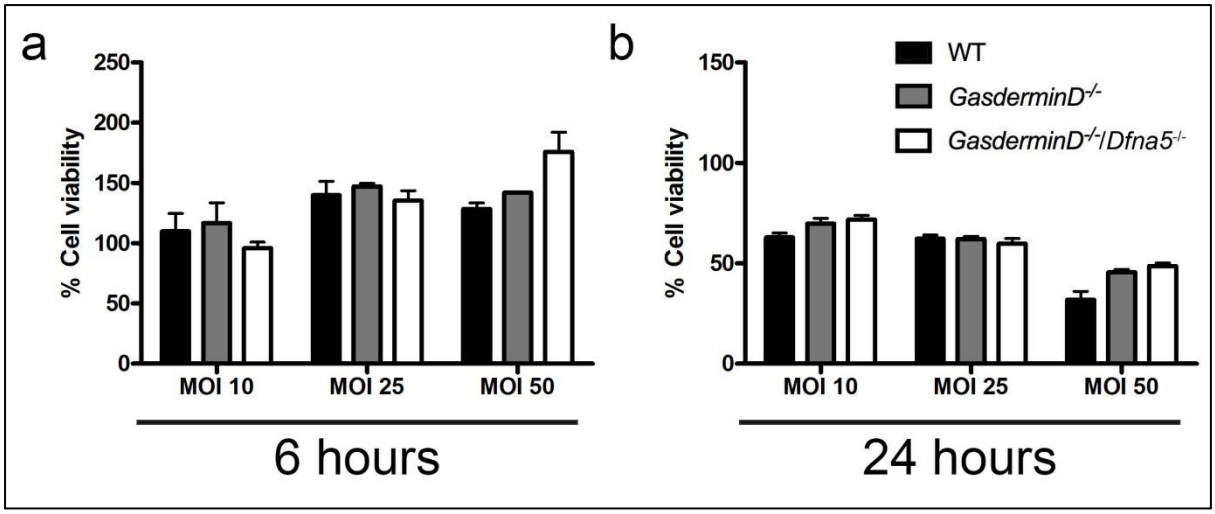

Figure 3.14: Neither Gasdermin D or DFNA5 have any effect on cellular viability in BMDMs infected with *S.* Typhimurium Δ*fliC*Δ*fljB*Δ*prgJ*, deficient in NLRC4 activation. Cellular viability (as measured by LDH release) of WT, *GasderminD*$^{-/-}$ *and GasderminD*$^{-/-}$ */Dfna5*$^{-/-}$ BMDMs after infection with *S.* Typhimurium Δ*fliC*Δ*fljB*Δ*prgJ* at MOIs 10, 25 and 50 for 6 (a) and 24 (b) hours. No cell death is observed at 2 hours. $p>0.05$ one-way ANOVA. Data represent the mean from two independent experiments while error bars show the s.e.m.

3.2.5. NLRP6 and Caspase-12

Overexpression of NLRP6 results in the formation of inflammasome-like structures that contain ASC and activated caspase-1 (Grenier et al., 2002). This finding, however, could not be confirmed under more physiological conditions (Anand et al., 2012). The same two studies also reported conflicting results regarding the role of this NLR in NF-κB signalling. This controversy makes NLRP6 an interesting protein to study in the context of *Salmonella* infection.

Like caspase-11, caspase-12 was originally described to play a role in sepsis. In particular, caspase-12 knockout mice were found to be more resilient to sepsis and have lower levels of IL-18 and IL-1β when compared to WT controls (Saleh et al., 2006). It was recently discovered, however, that the caspase-12 knockout mice used in the original studies were in fact deficient for both caspase-11 and caspase-12 (Vande Walle et al., 2015). It is, therefore, necessary to re-evaluate the role(s) of caspase-12 in microbial infection.

Infection of *caspase-12*$^{-/-}$ and *Nlrp6*$^{-/-}$ BMDMs with *S.* Typhimurium revealed no differences in cellular viability (Figure 3.15) and IL-1β secretion (Figure 3.16) when compared to WT cells at all MOIs and time-points investigated.

The lack of involvement of caspase-12 and NLRP6 in inflammasome dependent host responses to *Salmonella* meant no further work was done with cells from these mice.

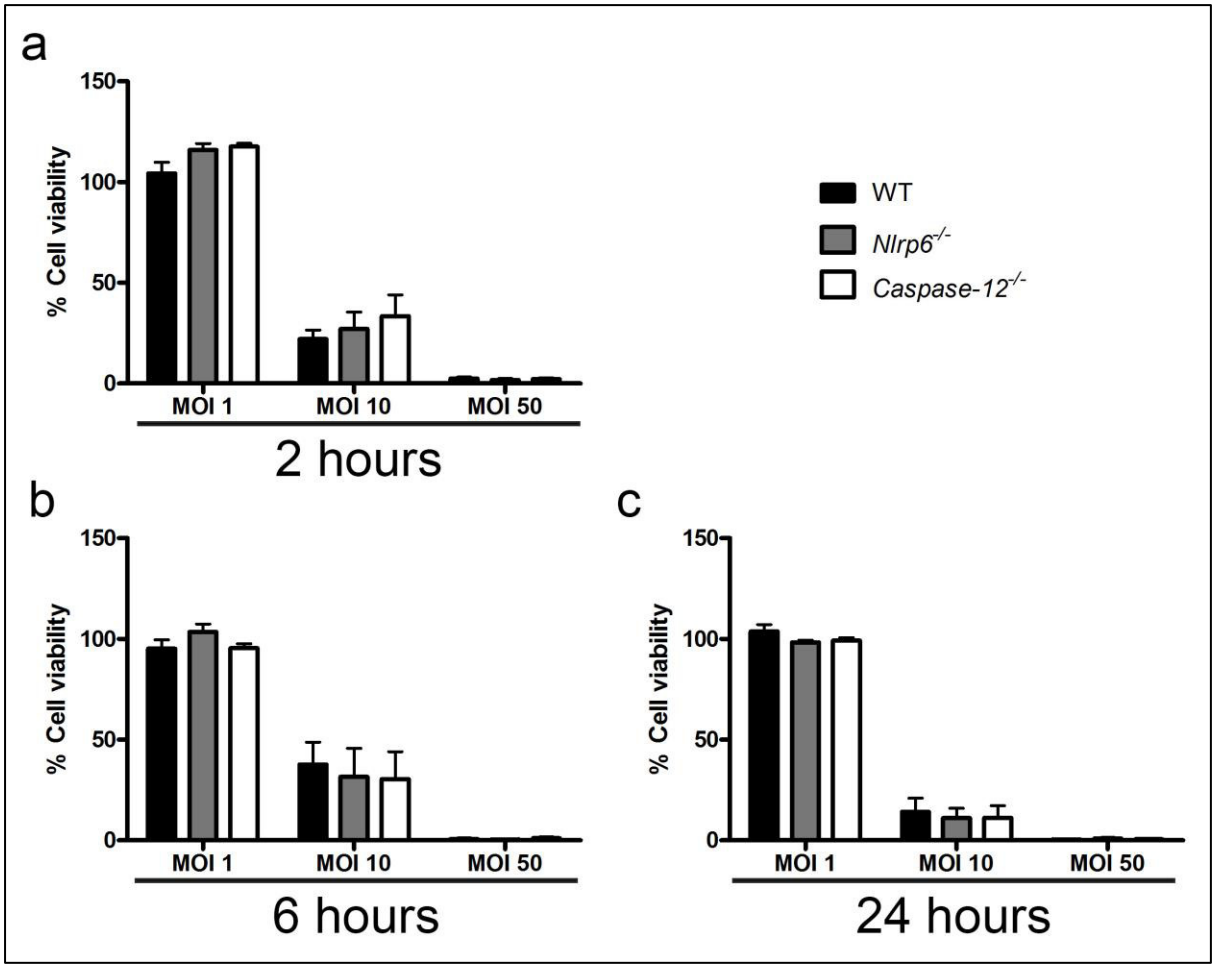

Figure 3.15: NLRP6 and Caspase-12 have no effect on cellular viability in BMDMs infected with *S.* Typhimurium SL1344. Cellular viability (as measured by LDH release) of WT, *Nlrp6*$^{-/-}$ *and Caspase-12*$^{-/-}$ BMDMs after infection with *S*. Typhimurium at MOIs 1, 10, and 50 for 2 (a), 6 (b) and 24 (c) hours. $p>0.05$ unpaired t-test. Data represent the mean from two independent experiments while error bars show the s.e.m.

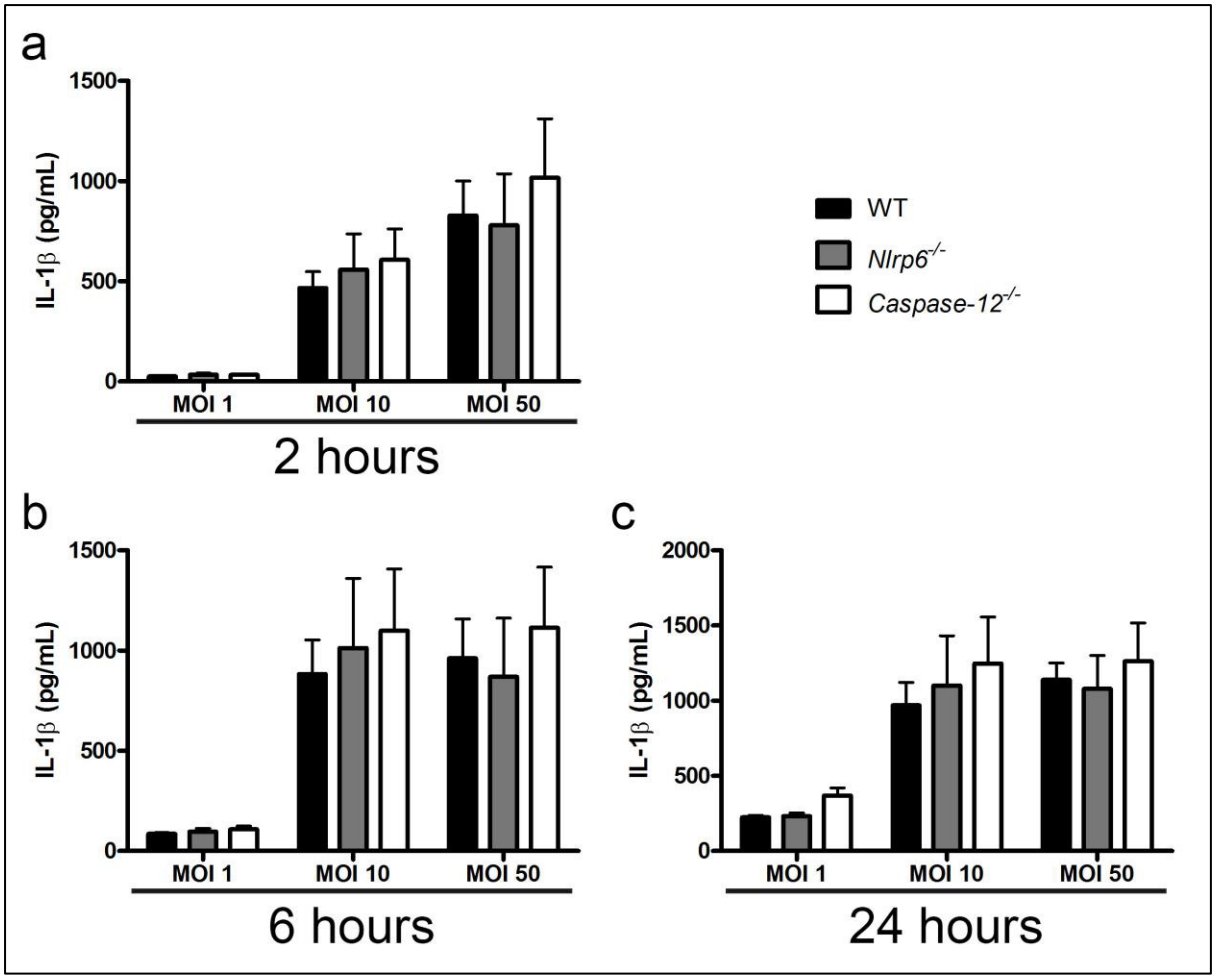

Figure 3.16: NLRP6 and Caspase-12 have no effect on IL-1β production in BMDMs infected with *S.* Typhimurium SL1344. IL-1β secretion (as measured by Luminex^{TM}) of WT, *Nlrp6*$^{-/-}$ *and Caspase-12*$^{-/-}$ BMDMs after infection with *S.* Typhimurium at MOIs 1, 10 and 50 for 2 (a), 6 (b) and 24 (c) hours. $p>0.05$ unpaired t-test. Data represent the mean from two independent experiments while error bars show the s.e.m.

3.2.6. NLRX1 and PIDD

NLRX1 is a mitochondrial outer membrane protein that acts as a negative regulator in the responses against viruses. This NLR acts by inhibiting the interaction between RIG-I and MAVS in the context of viral ssRNA infections, resulting in decreased IRF3 and NF-κB responses (Moore et al., 2008). This NLR can also inhibit NF-κB signalling via interaction with TRAF3 and TRAF6 (Allen et al., 2011). NF-κB signalling is important in the host response against *Salmonella* infections, so it is possible that NLRX1 could be relevant in the innate immune response against bacteria. The role of this protein in the context of pathogens such as *Salmonella* remains unknown.

In the intrinsic apoptotic pathway, the PIDDosome is a macromolecular complex composed of PIDD and RAIDD. It activates caspase-2, which results in cytochrome c release from the mitochondria into the cytoplasm (Paroni et al., 2002; Robertson et al., 2002). So far, no links between PIDD and *Salmonella* infection have been described, although it is possible that its effect on caspase-2 activation and, as a result, on apoptosis could have an impact on the infection outcome (Jesenberger et al., 2000).

GPAs using *S*. Typhimurium revealed no statistically significant differences in cellular viability between WT and *Nrlx1*$^{-/-}$ or *Pidd*$^{-/-}$ cells (Figure 3.17). However, *Pidd*$^{-/-}$ BMDMs showed an increase in IL-1β production at the MOI 50 when measured at 6 and 24 hours post infection (Figure 3.18). The reasons for the difference in IL-1β production between WT and *Pidd*$^{-/-}$ BMDMs are yet unknown, but it is possible that it involves caspase-2. The role of caspase-2 in the context of *Salmonella* infection is going to be explored later.

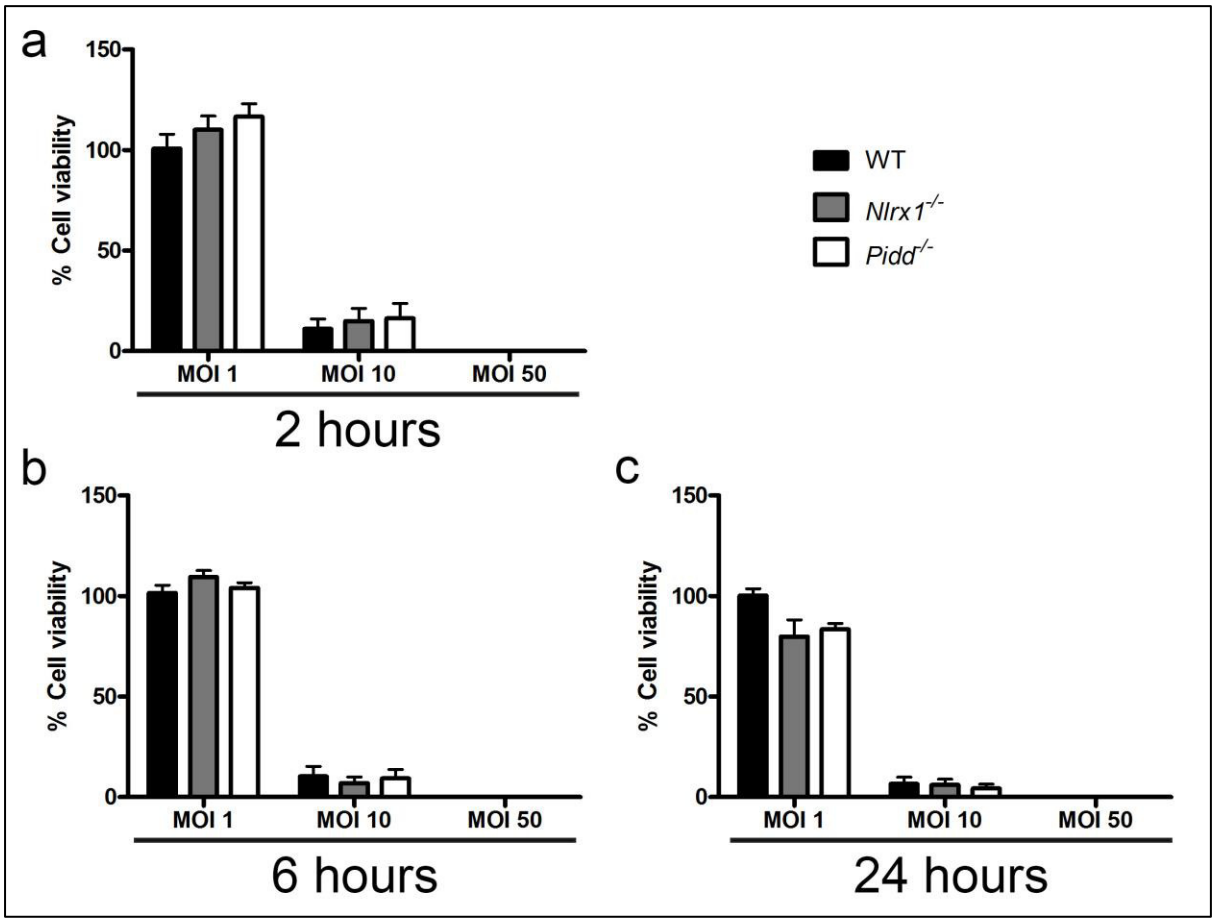

Figure 3.17: NLRX1 and PIDD have no effect on cellular viability in BMDMs infected with *S*. Typhimurium SL1344. Cellular viability (as measured by LDH release) of WT, *Nlrx1*$^{-/-}$ *and Pidd*$^{-/-}$ BMDMs after infection with *S*. Typhimurium at MOIs 1, 10, and 50 for 2 (a), 6 (b) and 24 (c) hours. $p>0.05$ unpaired t-test. Data represent the mean from two independent experiments while error bars show the s.e.m.

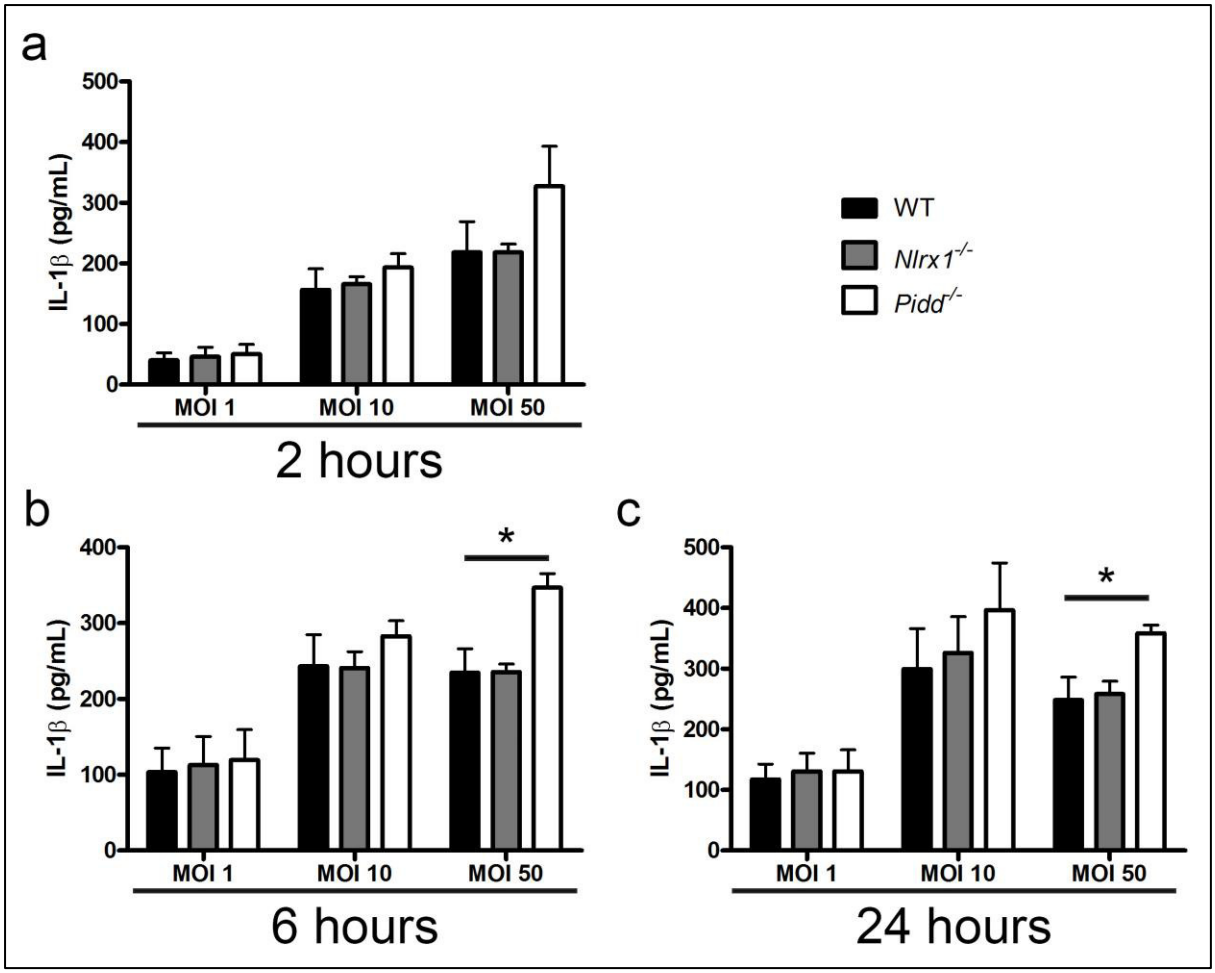

Figure 3.18: NLRX1 has no effect on IL-1β production in BMDMs infected with *S.* Typhimurium SL1344, whilst PIDD absence enhances IL-1β production in specific conditions. IL-1β secretion (as measured by Luminex^{TM}) of WT, *Nlrx1$^{-/-}$ and Pidd$^{-/-}$* BMDMs after infection with *S*. Typhimurium at MOIs 1, 10 and 50 for 2 (a), 6 (b) and 24 (c) hours. * $p<0.05$ unpaired t-test. Data represent the mean from two independent experiments while error bars show the s.e.m.

3.2.7. NLRP1a-c

Although NLRP1 was the first inflammasome to be described (Martinon et al., 2002), very few studies have examined its role in inflammasome activation triggered by *Salmonella*. Previously, researchers compared the mechanisms of caspase-1 activation in cells challenged with either *S*. Typhimurium or *Bacilus anthracis* Lethal Toxin (LeTx). They concluded that although caspase-1-mediated cell death occurred in both cases, it was very likely that LeTx and *S*. Typhimurium stimulated different mechanisms of caspase-1 activation with the first using NLRP1 and the latter NLRC4 as the primary NLR (Fink et al., 2008). This

study however did not directly investigate the possibility that different NLRP1 paralogues could be activated during *S.* Typhimurium infection. To investigate this, I conducted GPAs in BMDMs from mice lacking the NLRP1 paralogues a, b and c.

Nlrp1a-c$^{-/-}$ BMDMs infected with *Salmonella* showed no differences in cellular viability or IL-1β production when compared with WT cells (Figures 3.19-3.20). It is therefore unlikely that this NLR is involved in inflammasome activation during *S*. Typhimurium infection, so no further work was carried out in cells from these mice.

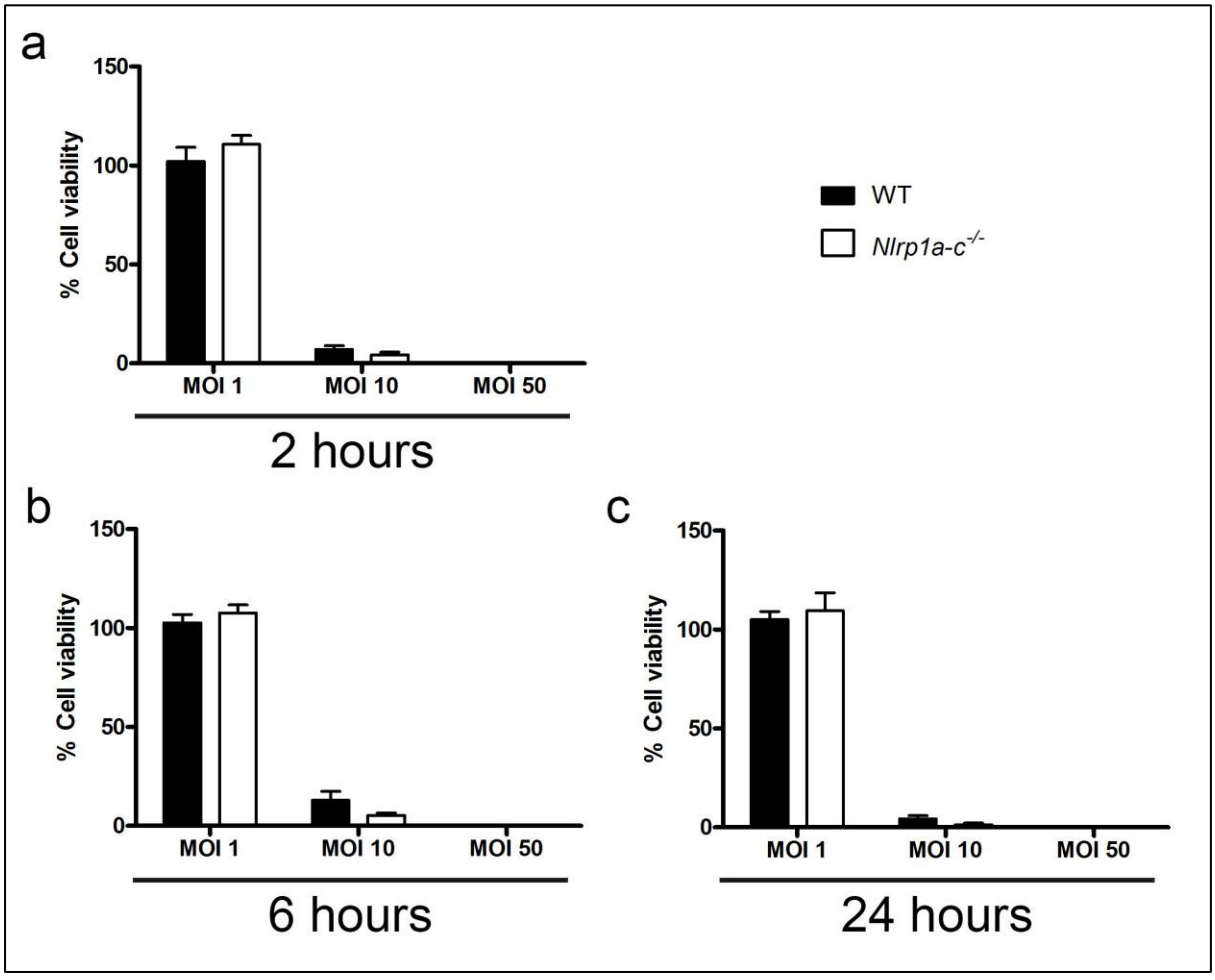

Figure 3.19: NLRP1a-c has no effect on cellular viability in BMDMs infected with *S.* Typhimurium SL1344. Cellular viability (as measured by LDH release) of WT and *Nlrp1a-c*$^{-/-}$ BMDMs after infection with *S*. Typhimurium at MOIs 1, 10, and 50 for 2 (a), 6 (b) and 24 (c) hours. $p>0.05$ unpaired t-test. Data represent the mean from two independent experiments while error bars show the s.e.m.

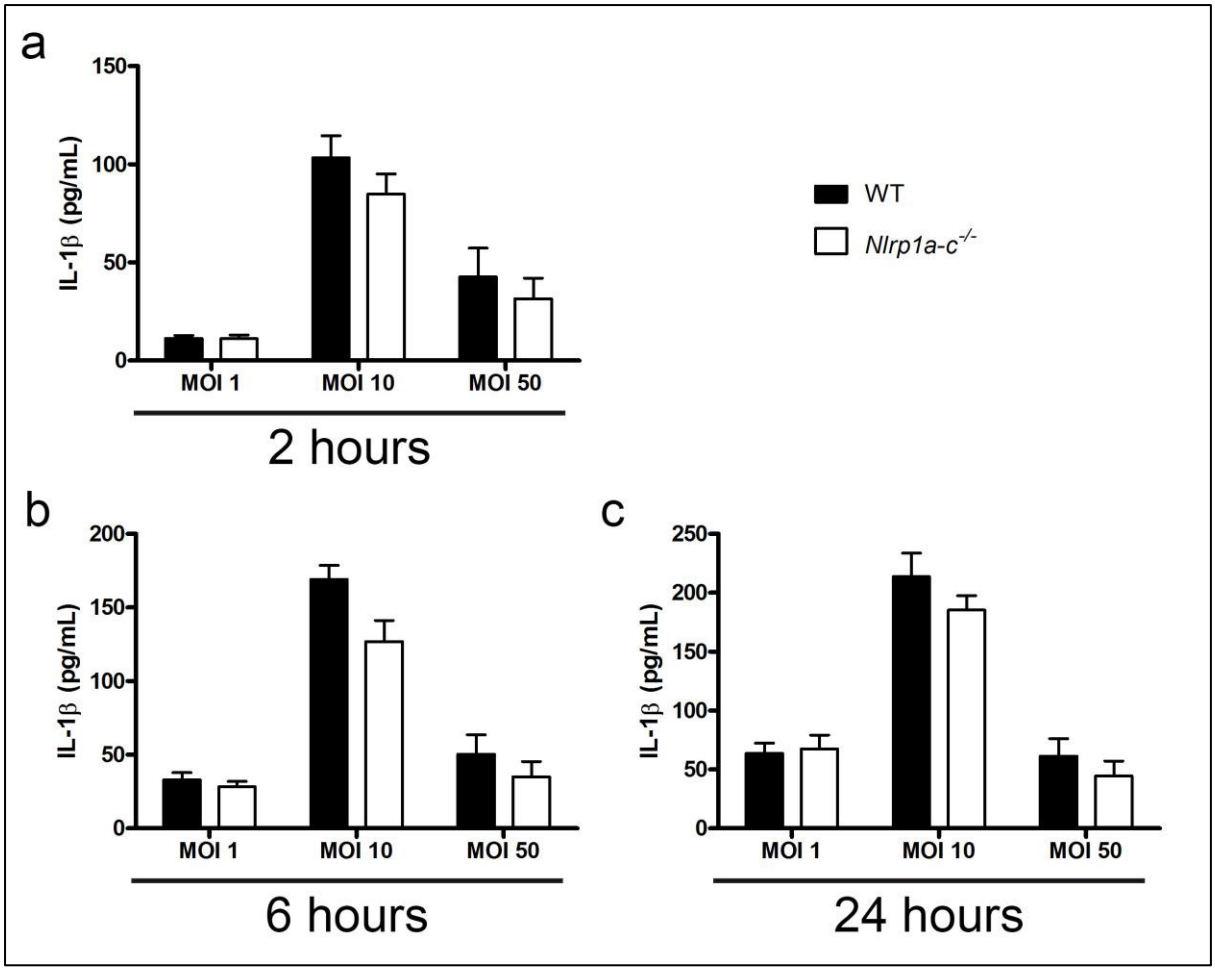

Figure 3.20: NLRP1a-c has no effect on IL-1β production in BMDMs infected with *S.* Typhimurium SL1344. IL-1β secretion (as measured by Luminex^{TM}) of WT, *Nlrp1a-c*$^{-/-}$ BMDMs after infection with *S.* Typhimurium at MOIs 1, 10 and 50 for 2 (a), 6 (b) and 24 (c) hours. $p>0.05$ unpaired t-test. Data represent the mean from two independent experiments while error bars show the s.e.m.

3.2.8. Caspase-2

Caspase-2 is an enzyme involved in apoptosis triggered by several stimuli (Bergeron et al., 1998). Briefly, upon stimulation this enzyme is recruited and activated in the PIDDosome, a molecular complex containing PIDD and RAIDD. This leads to mitochondria permeabilization and release of cytochrome c initiating the intrinsic apoptotic pathway.

Little is known, however, about the role of caspase-2 in inflammasome activation by *Salmonella*. A study using an infection model with *S.* Typhimurium transitioning from the stationary to logarithmic phase described a marginal, albeit statistically significant, contribution of caspase-2 to what it was then termed “apoptosis” (Jesenberger et al., 2000).

This study, however, was published before inflammasomes were described, and it is possible that the form of programmed cell death triggered by *Salmonella* and described by the authors as “apoptosis” was in fact pyroptosis, at least in part of the cell population. The occurrence of extensive functional redundancy between caspases, as illustrated by caspase-8 in the inflammasome (Man et al., 2013) together with published data supporting a role for caspase-2 in *Salmonella* infections (Jesenberger et al., 2000) prompted me to investigate whether caspase-2 is involved in *Salmonella*-induced inflammasome formation. Importantly, the GPA conducted in this work used log-phase bacteria, which stimulate NLRC4 inflammasome assembly due to the expression of SPI-I genes (Lara-Tejero et al., 2006).

S. Typhimurium infection of *caspase-2*$^{-/-}$ and WT BMDMs showed similar cellular viability and intracellular bacterial numbers in all MOIs and time points tested (Figure 3.21). IL-1β production, however, was decreased in *caspase-2*$^{-/-}$ BMDMs in comparison to WT controls in most conditions, particularly at MOIs 10 and 50 at 6 hours post-infection (Figure 3.22). On the contrary, there was no statistically significant difference in IL-18 production between WT and *caspase-2*$^{-/-}$ macrophages (Figure 3.23). This pattern involving decreased IL-1β production without relevant differences in IL-18 production and cell viability is strikingly similar to that observed in *caspase-8*$^{-/-}$/*Ripk3*$^{-/-}$ BMDMs infected with *S.* Typhimurium (Man et al., 2013). There, the authors reported that caspase-8 is recruited to the inflammasome, where it acts only on IL-1β production, whilst caspase-1 acts on the production of IL-1β, IL-18 and in pyroptosis. It is possible, therefore, that caspase-2 assumes a similar role to caspase-8 in the inflammasome, further illustrating the concept of redundancy among caspases.

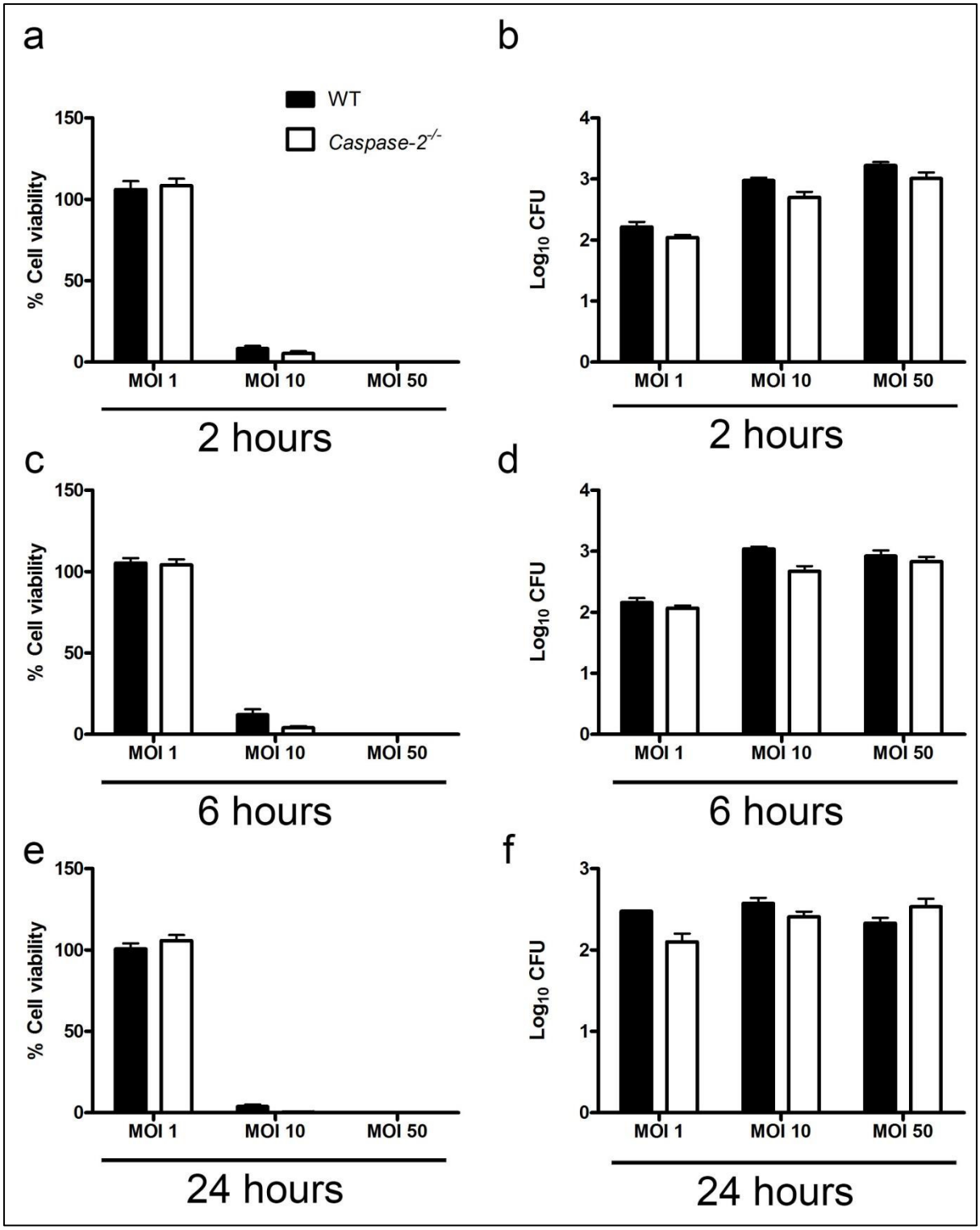

Figure 3.21: Caspase-2 has no effect on cellular viability and intracellular bacteria counts in BMDMs infected with *S.* Typhimurium SL1344. (a), (c) and (e) Cellular viability (as measured by LDH release) and (b), (d) and (f) intracellular bacteria counts of WT and *Caspase-2*$^{-/-}$ BMDMs after infection with *S*. Typhimurium at MOIs 1, 10 and 50 for 2 (a-b), 6 (c-d) and 24 (e-f) hours. $p>0.05$ unpaired t-test. Data represent the mean from three independent experiments while error bars show the s.e.m.

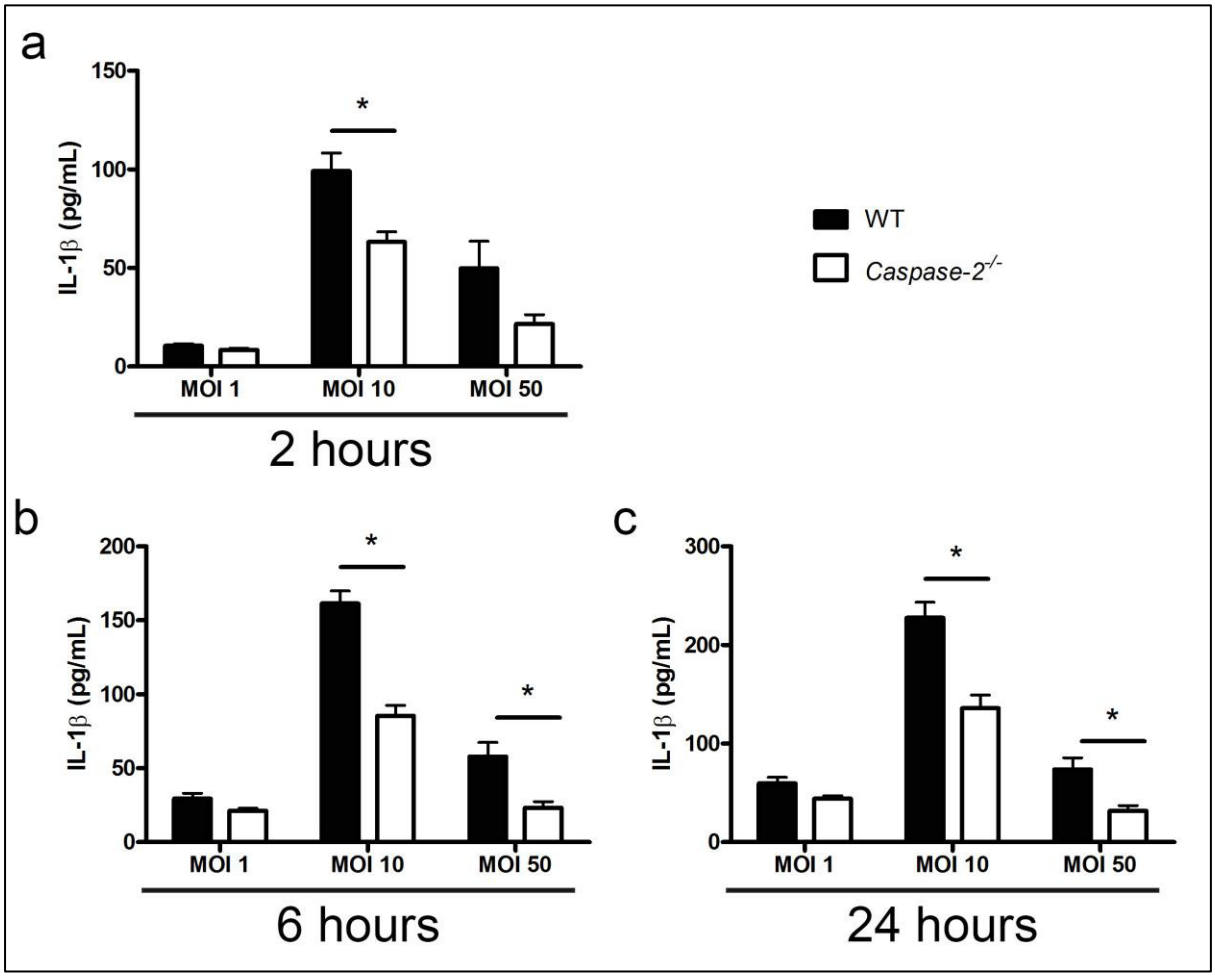

Figure 3.22: Caspase-2 is involved in IL-1β production in BMDMs infected with *S.* Typhimurium SL1344. IL-1β secretion (as measured by Luminex^{TM}) of WT and *Caspase-2*$^{-/-}$ BMDMs after infection with *S.* Typhimurium at MOIs 1, 10 and 50 for 2 (a), 6 (b) and 24 (c) hours. * $p<0.05$ unpaired t-test. Data represent the mean from three independent experiments while error bars show the s.e.m.

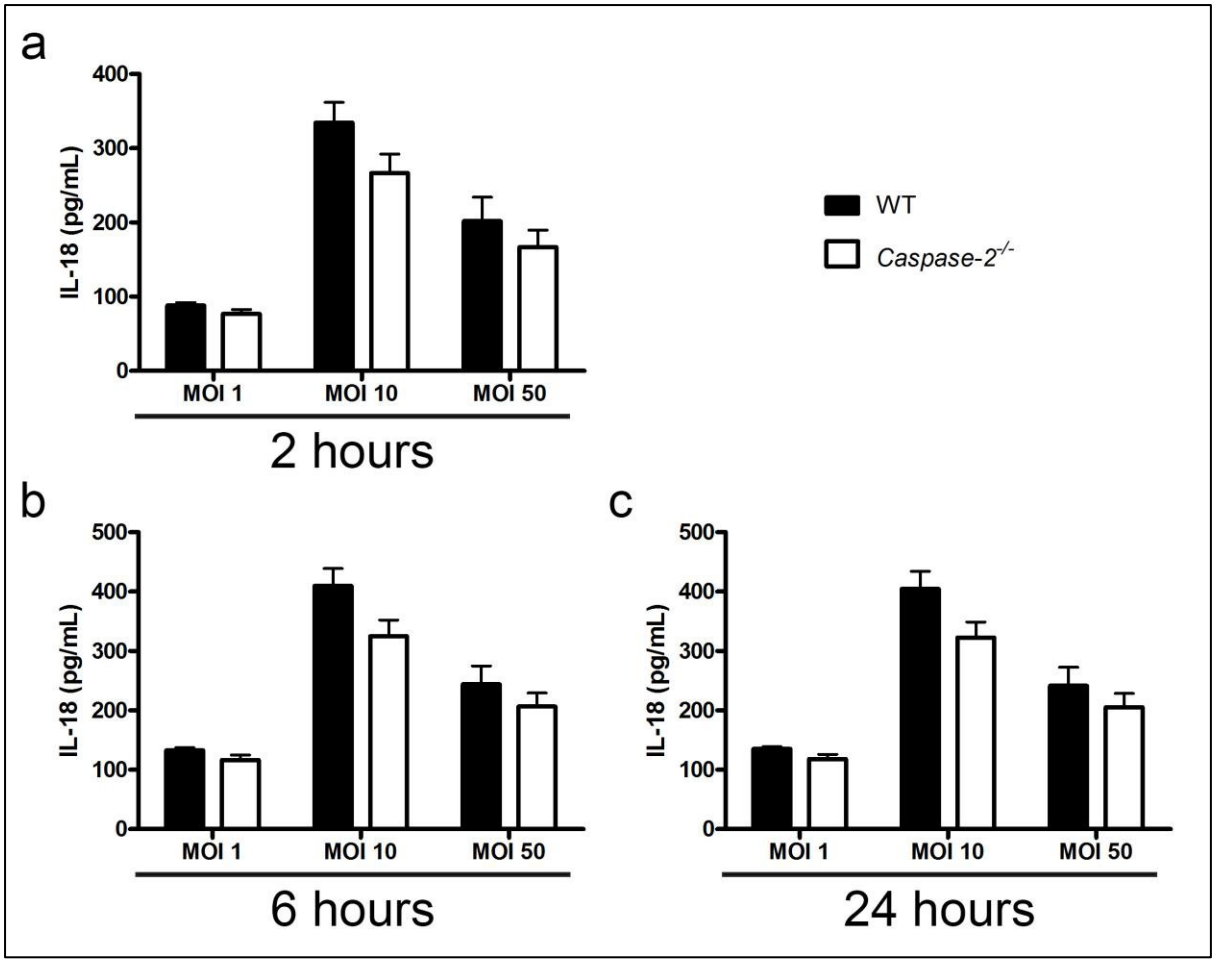

Figure 3.23: Caspase-2 has no effect on IL-18 production in BMDMs infected with *S.* Typhimurium SL1344. IL-1β secretion (as measured by ELISA) of WT and *Caspase-2*$^{-/-}$ BMDMs after infection with *S*. Typhimurium at MOIs 1, 10 and 50 for 2 (a), 6 (b) and 24 (c) hours. $p>0.05$ unpaired t-test. Data represent the mean from three independent experiments while error bars show the s.e.m.

3.2.9. CARD9

CARD9 is an adaptor protein originally described in the context of NF-κB signalling in HEK293T cells, where it forms a signalling platform with BCL10 and MALT1 (Bertin et al., 2000). Later, the formation of CARD9 complexes was described in other contexts. For instance, in the dectin-1 pathway in dendritic cells, the receptor dectin-1 recognizes PAMPs from the fungal wall and signals the activation of SYK and subsequent CARD9 phosphorylation, leading to NF-κB translocation via the formation of the CARD9/MALT1/BCL10 signalling complex (Gross et al., 2006). Similarly, the formation of the CARD9/MALT1/BCL10 complex was observed downstream fragment crystallisable receptor

(FcR)-γ activation (Hara et al., 2007). In the context of viral infections, RIG-I recognises viral nucleic acids and activates MAVS, which in turn signals the formation of a CARD9/BCL10 complex responsible for NF-κB activation (Poeck et al., 2010).

In bacterial infections, CARD9 was described as an adaptor in the NOD2 pathway, linking this NLR to MAPKs activation without affecting NF-κB (Hsu et al., 2007). CARD9 is also a positive regulator of ROS production by the NADPH complex in response to intracellular bacterial infections (Wu et al., 2009). No work has thus linked CARD9 to canonical inflammasomes.

In comparison to WT controls, infection of *Card9*$^{-/-}$ BMDMs with *S*. Typhimurium revealed only a marginal increase in cellular viability and intracellular bacterial numbers only at MOI 10 and only at 2 hours post-infection (Figure 3.24). *Nlrc4*$^{-/-}$ cells, in contrast, showed a marked increase in viability and intracellular bacterial numbers, illustrating the importance of this NLR in the context of *Salmonella* infection (Figure 3.24). The production of IL-1β was, however, significantly increased in *Card9*$^{-/-}$ macrophages (Figure 3.25). For example, *Card9*$^{-/-}$ cells produced up to four times more IL-1β than WT cells at 24 hours post-infection at MOI 10. *Nlrc4*$^{-/-}$ cells, as expected, were critically impaired in IL-1β production (Figure 3.25).

To rule out the possibility that this increase in cytokine production is a consequence of the marginally higher cellular viability in *Card9*$^{-/-}$ BMDMs, the cytokine TNF-α was also quantified. TNF-α levels were increased in the *Nlrc4*$^{-/-}$ compared to WT cell cultures (Figure 3.26), presumably as a consequence of their increased survival rates (Figure 3.24). In accordance with the viability data, *Card9*$^{-/-}$ cells secreted more TNF-α only at MOI 10 and only at 2 hours post-infection (Figure 3.26). The increase in the amount of IL-1β produced by *Card9*$^{-/-}$ macrophages, therefore, cannot be explained by an increase in cellular viability alone. The rapid effect that CARD9 has on IL-1β production suggests that this protein may inhibit NLRC4-mediated cytokine production, since early IL-1β produced is largely dependent on this NLR (Man et al., 2014). How exactly CARD9 inhibits the inflammasome, and which inflammasome it inhibits, is going to be the focus of the next chapters.

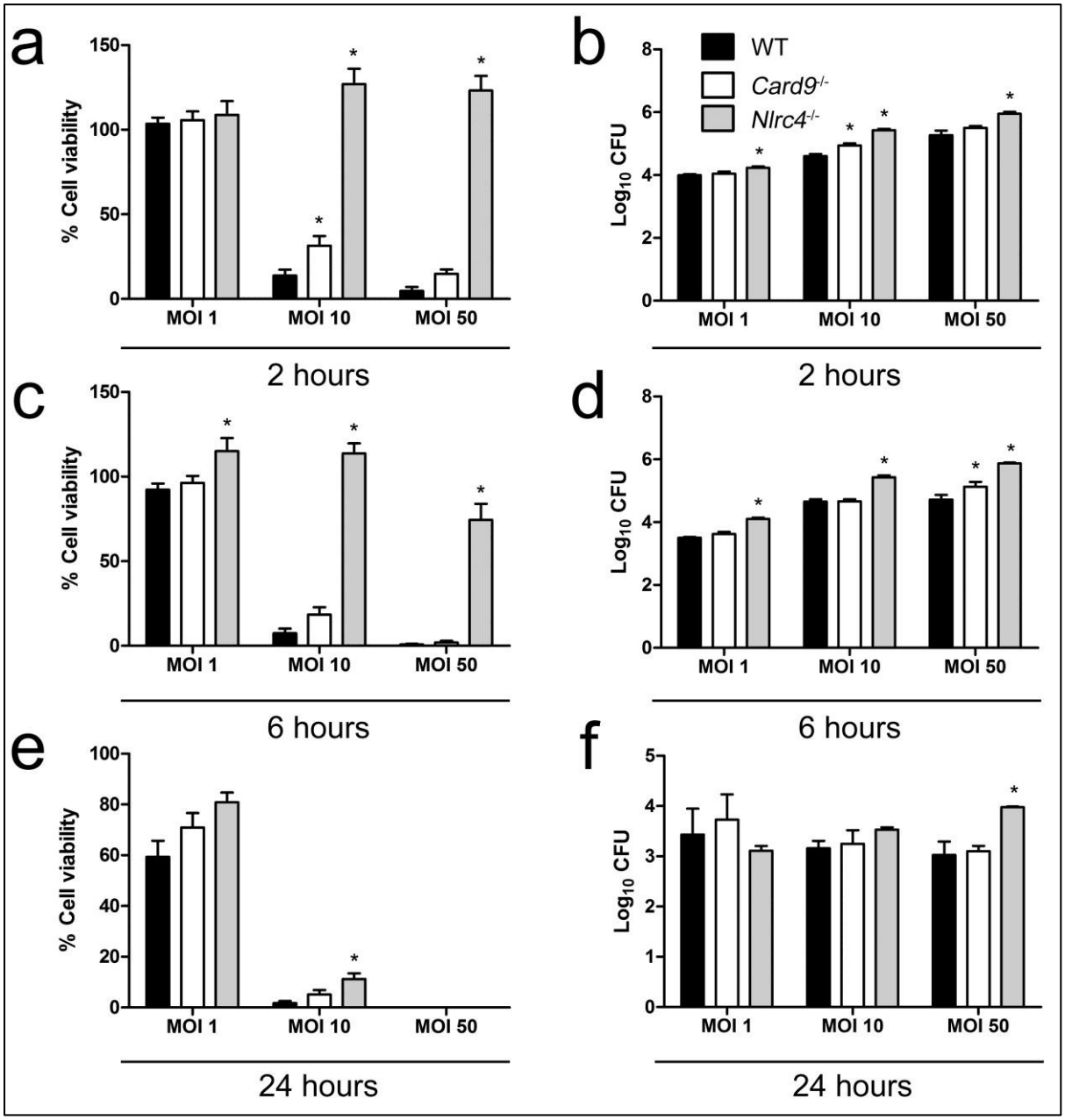

Figure 3.24: CARD9 has a mild effect on cellular viability and intracellular bacteria counts in BMDMs infected with *S.* Typhimurium SL1344. (a), (c) and (e) Cellular viability (as measured by LDH release) and (b), (d) and (f) intracellular bacteria counts of WT, *Nlrc4*$^{-/-}$ and *Card9*$^{-/-}$ BMDMs after infection with *S*. Typhimurium at MOIs 1, 10 and 50 for 2 (a-b), 6 (c-d) and 24 (e-f) hours. * $p<0.05$ one-way ANOVA with Tukey's multiple comparisons test. Data represent the mean from five independent experiments while error bars show the s.e.m.

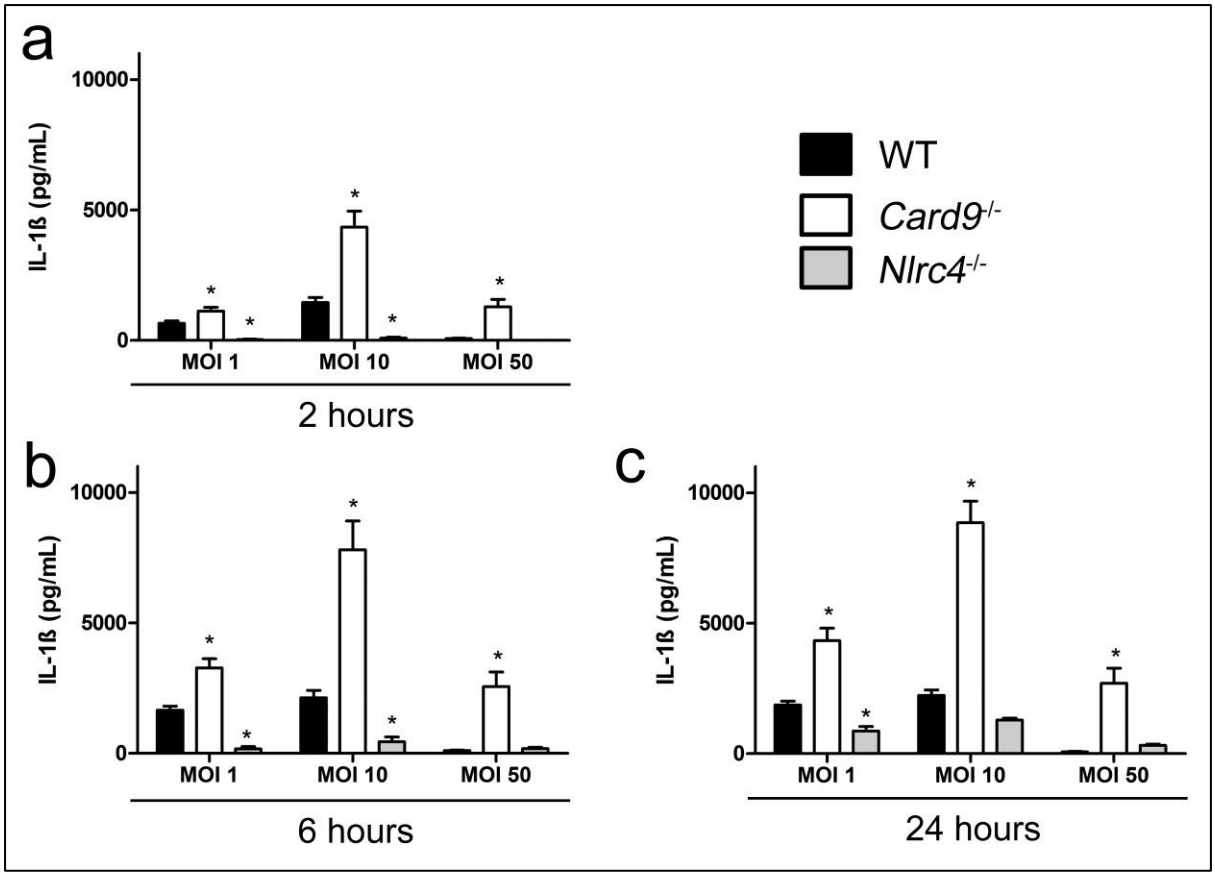

Figure 3.25: CARD9 loss promotes IL-1β production in BMDMs infected with *S.* Typhimurium SL1344. IL-1β secretion (as measured by ELISA) of WT, *Nlrc4*$^{-/-}$ and *Card9*$^{-/-}$ BMDMs after infection with *S*. Typhimurium at MOIs 1, 10 and 50 for 2 (a), 6 (b) and 24 (c) hours. * $p<0.05$ one-way ANOVA with Tukey's multiple comparisons test. Data represent the mean from five independent experiments while error bars show the s.e.m.

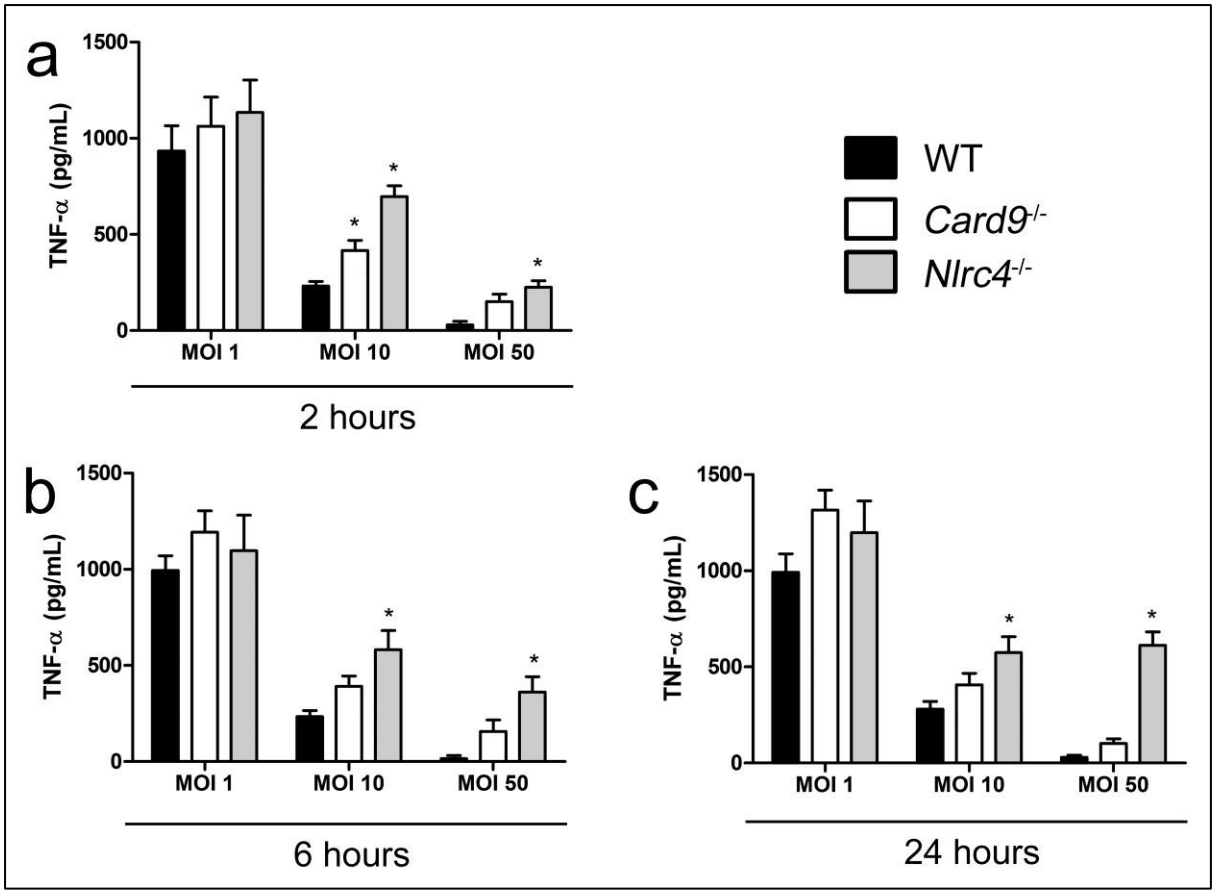

Figure 3.26: CARD9 has no effect on TNF-α production in BMDMs infected with *S.* Typhimurium SL1344 in most conditions. TNF-α secretion (as measured by ELISA) of WT, *Nlrc4*$^{-/-}$ and *Card9*$^{-/-}$ BMDMs after infection with *S*. Typhimurium at MOIs 1, 10 and 50 for 2 (a), 6 (b) and 24 (c) hours. * $p<0.05$ one-way ANOVA with Tukey's multiple comparisons test. Data represent the mean from five independent experiments while error bars show the s.e.m.

3.3. Discussion

The signalling events leading to NLRC4 and NLRP3 activation upon *S*. Typhimurium infection are not well understood. This is why, in this chapter, I investigated the effect of several NLRs, caspases and related proteins in the activation of the inflammasome induced by *Salmonella*. To achieve this, I performed GPA on BMDMs obtained from 15 genetically altered strains of mice. Table 3.1 qualitatively summarises the data on cellular viability, intracellular bacterial numbers and IL-1β obtained from these experiments.

Table 3.1: GPA data summary. Qualitative summary of cellular viability, intracellular bacteria and IL-1β production of various BMDM knockout strains infected with *S.* Typhimurium SL1344 WT (WT) or *S.* Typhimurium Δ*fliC*Δ*fljB*Δ*prgJ* (TKO) in relation to WT BMDMs unless otherwise noted.

Strain	*S.* Typhimurium	In relation to BMDM	Cell viability	Intracellular bacteria	IL-1β
Card9$^{-/-}$	WT	WT	Similar/Increase	Similar/Increase	Increase
Card9$^{-/-}$	WT	*Nlrc4*$^{-/-}$	Decrease	Decrease	Increase
Caspase-1$^{-/-}$*Caspase-11*$^{-/-}$	WT	WT	Increase	Increase	Decrease
Caspase-11$^{-/-}$	WT	WT	Similar	Similar	Similar
Caspase-11$^{-/-}$	TKO	WT	Increase	Increase	Decrease
Caspase-12$^{-/-}$	WT	WT	Similar	Similar	Similar
Caspase-2$^{-/-}$	WT	WT	Similar	Similar	Decrease
GasderminD$^{-/-}$	WT	WT	Increase	Similar	Decrease
GasderminD$^{-/-}$	TKO	WT	Similar	No data	Similar
GasderminD$^{-/-}$*Dfna5*$^{-/-}$	WT	*GasderminD*$^{-/-}$	Similar	Similar	Similar
GasderminD$^{-/-}$*Dfna5*$^{-/-}$	TKO	*GasderminD*$^{-/-}$	Similar	Similar	Similar
GasderminD$^{-/-}$*Dfna5*$^{-/-}$	WT	WT	Increase	Similar	Decrease
GasderminD$^{-/-}$*Dfna5*$^{-/-}$	TKO	WT	Similar	No data	Similar
Nlrc3$^{-/-}$	WT	WT	Decrease	Similar	Decrease
Nlrc4$^{-/-}$	WT	WT	Increase	Increase	Decrease
Nlrc4$^{-/-}$Caspase-1$^{-/-}$Caspase-11$^{-/-}$	WT	WT	Increase	Increase	Decrease
Nlrc4$^{-/-}$Caspase-1$^{-/-}$Caspase-11$^{-/-}$	WT	*Nlrc4*$^{-/-}$	Increase	Similar	Similar
Nlrc4$^{-/-}$Caspase-1$^{-/-}$Caspase-11$^{-/-}$	WT	*Caspase-1*$^{-/-}$*Caspase-11*$^{-/-}$	Increase	Increase	Similar
Nlrc5$^{-/-}$	WT	WT	Decrease	Similar	Decrease
Nlrp1a-c$^{-/-}$	WT	WT	Similar	Similar	Similar
Nlrp6$^{-/-}$	WT	WT	Similar	Similar	Similar
Nlrx1$^{-/-}$	WT	WT	Similar	Similar	Similar
Pidd$^{-/-}$	WT	WT	Similar	Similar	Increase

Amongst these 15 mouse strains, *Caspase-12*$^{-/-}$, *Nlrp1a-c*$^{-/-}$, *Nlrp6*$^{-/-}$ and *Nlrx1*$^{-/-}$ BMDMs showed no differences in cellular viability, intracellular counts and IL-1β production when compared to WT macrophages. These results do not completely rule out potential contributions for these proteins during *Salmonella* infection for two reasons. First, the GPA employed throughout this chapter used macrophages derived from bone marrow, which is a very specific subset of immune cells. The use of other cell types such as bone marrow-derived dendritic cells, neutrophils, or even peritoneal macrophages could have potentially yielded different results. Second, and perhaps more importantly, *in vitro* infection with *S.* Typhimurium strongly engages the NLRC4 pathway, causing rapid cell death and cytokine release and potentially masking subtle contributions of other players not involved in this pathway. This problem can be circumvented if cells are infected with a *S*. Typhimurium strain that is deficient in activating the NLRC4 inflammasome. Indeed, this approach was used in this chapter to investigate the effect of caspase-11 and DFNA5 in the activation of the inflammasome induced by the *S*. Typhimurium mutant Δ*fliC*Δ*fljB*Δ*prgJ*, as it will be discussed in more detail below.

Caspase-1/11 is known to significantly contribute to pyroptotic cell death, IL-1β production and infection clearance (Brennan and Cookson, 2000; Hersh et al., 1999; Monack et al., 2001), a result that was reproduced in this work in BMDMs *in vitro* (Figure 3.2-3.3). NLRC4, however, appears to have an even more prominent role in regulating cell death upon *Salmonella* infection. The reason for this is that NLRC4 triggers cell death independent of caspase-1/11 (Broz et al., 2010b). The cumulative effect, however, of these 3 proteins had not been so far evaluated. BMDMs lacking NLRC4, caspase-1 and caspase-11 were more resilient to cell death than BMDMs lacking NLRC4 or Caspase-1/11 alone, confirming that NLRC4 drives multiple cell death pathways upon *Salmonella* infection, one involving ASC and caspase-1/11 (Mariathasan et al., 2004), and others independent of these proteins (Broz et al., 2010b). Interestingly, cell death still occurred later in the infection even in the absence of NLRC4, Caspase-1 and Caspase-11 (Figure 3.2). It is possible that in the absence of these proteins, other NLRs and caspases could be involved in driving cell death. It has been already shown that recruitment of caspase-8 to the inflammasome is not important for pyroptosis in response to *S*. Typhimurium infection (Man et al., 2013). The same applies for caspases -2 and -12, since BMDMs from *caspase-2*$^{-/-}$ and *caspase-12*$^{-/-}$ mice were infected with *Salmonella* and showed no differences in cellular viability in comparison to WT controls (Figure 3.15, 3.21). The data on caspases -8, -2 and -12, however, were generated in the context of NLRC4 activation. So, it is possible that in the absence of NLRC4 these caspases could drive cell death in response to *Salmonella* infection.

The caspase-1-deficient mice widely used in innate immunity studies were in fact deficient for both caspase-1 and caspase-11. This means that the role of these caspases must be re-evaluated in a variety of settings, including *S.* Typhimurium infection. Infection of *caspase-11*$^{-/-}$ BMDMs with log-phase *Salmonella* (figure 3.3 and 3.4) showed no significant difference regarding cell death and IL-1β production when compared to WT cells. To make sure that the dominant effect of NLRC4 does not mask any potential contribution of caspase-11, I infected macrophages with the *S.* Typhimurium mutant Δ*fliC*Δ*fljB*Δ*prgJ*, which cannot activate NLRC4. In this case, caspase-11 appears to contribute to *Salmonella*-induced cell death at later time points (figure 3.5). Similar conclusions were reported previously using an *in vitro* infection model with stationary phase *S*. Typhimurium. There, the authors found that caspase-11 is involved in NLRC4-independent cell death after 17 hours infections (Broz et al., 2012). The role of caspase-11 *in vivo* is, however, less clear, as *caspase-11*$^{-/-}$ and WT mice showed similar susceptibility to the infection whilst caspase-1 appeared to play a fundamental role in clearing the infection (Broz et al., 2012).

In the absence of NLRC4 activation, caspase-11 also had a very clear effect on IL-1β production. Cells lacking caspase-11 were impaired at secreting this cytokine, and once again the result was more pronounced after 24 hours of infection (figure 4.6). Similarly, 17-hours infection with stationary-phase *S.* Typhimurium Δ*fliG* also showed a role for caspase-11 in IL-1β production (Broz et al., 2012). It is interesting to note that similar findings were reported using LPS-primed macrophages during infection with *Legionella pneumophila*: *Caspase-11*$^{-/-}$ BMDMs infected with mutants incapable of activating the NLRC4 inflammasome exhibited an increase in cell survival and a substantial decrease in IL-1β production when compared to WT macrophages (Case et al., 2013).

It is unclear how exactly caspase-11 controls IL-1β production and cell death in the absence of NLRC4 stimulation. One explanation is that caspase-11 was originally described as an activator of caspase-1; its absence could therefore block caspase-1 activation which drives IL-1β maturation and cell death (Wang et al., 1998). Caspase-11 is also a key component of a non-canonical inflammasome responsible for the maturation of IL-18 and IL-1β, although the physiological relevance of this inflammasome in the context of *Salmonella* infection in macrophages is still unknown (Kayagaki et al., 2011; Knodler et al., 2014; Shi et al., 2014). Another hypothesis is that caspase-11 is required for canonical NLRP3 inflammasome activation via gasdermin D, and caspase-11 deficiency could lead to deficient NLRP3 activation in my experimental setting (Kayagaki et al., 2015). In summary, caspase-11 is not required for optimal inflammasome activation in response to infection with *S*. Typhimurium. It

does, however, appear to contribute to inflammasome activation only when NLRC4, is not activated.

The noncanonical caspase-11 inflammasome is known to trigger the cleavage and activation of gasdermin D, a protein responsible for creating pores in the plasma membrane, thus mediating pyroptosis (Kayagaki et al., 2015; Shi et al., 2015). Its role as the executioner of pyroptosis appears to be complemented by a yet unknown molecule during canonical NLRP3 inflammasome activation (Kayagaki et al., 2015). The data I generated from infecting *GasderminD*$^{-/-}$ BMDMs with *S.* Typhimurium corroborated this; although cellular viability in *GasderminD*$^{-/-}$ BMDMs was higher than that of WT controls, a significant amount of cell death was still observed (Figure 3.11). Two conclusions can be extracted from this. First, gasdermin D is indeed involved in NLRC4-mediated cell death. This complements a previous report using flagellin from *P. aeruginosa* that suggested that gasdermin D has an early effect on cell death mediated by NLRC4 (Kayagaki et al., 2015). Similarly, I observed that early in the *Salmonella* infection, gasdermin D is involved in cell death, whereas this effect is not observed at later time points (Figure 3.11). Second, since early cell death is still observed in the absence of Gasdermin D, other pyroptosis executioners are likely to exist.

The identity of this pyroptosis executioner is still unknown. I hypothesised that the gasdermin-related protein DFNA5 could play this role, but the data did not support a role for DFNA5 in *Salmonella*-dependent pyroptosis as *GasderminD*$^{-/-}$*/Dfna5*$^{-/-}$ and *GasderminD*$^{-/-}$ BMDMs showed similar cell death upon *Salmonella* infection. It is, however, possible that DFNA5 executes pyroptosis in a caspase-3-dependent fashion in other contexts (Rogers et al., 2017; Wang et al., 2017).

Interestingly, the production of IL-1β was greatly impaired, but not completely blocked, in both *GasderminD*$^{-/-}$ and *GasderminD*$^{-/-}$*/Dfna5*$^{-/-}$ BMDMs when compared to WT controls (Figure 3.12). It is unclear how gasdermin D controls IL-1β production. It is conceivable that the lower IL-1β detected in the supernatant is secondary to a decrease in membrane pore formation, a process that involves gasdermin D (Aglietti et al., 2016). IL-1β lacks a secretion signal sequence (Auron et al., 1984), and pore-formation is one of the proposed mechanisms for IL-1β release (Fink and Cookson, 2006). Thus, lower cell death would cause a decrease in IL-1β detected in the supernatant. This hypothesis is contradicted by the IL-18 data, where both gasdermin D and DFNA5 had no effect on IL-18 production in all time points and MOIs (Figure 3.13). Since IL-18 also lacks a secretion signal sequence (Kohka et al., 1998), the discrepancy between IL-1β and IL-18 detected in the supernatant makes the “cytokine decreases as consequence of decreased pore formation” hypothesis less likely.

The literature on NLRC3 and NLRC5 suggests that these NLRs act as inhibitors of innate immune pathways, with NLRC3 inhibiting NF-κB and cGAS/STING (Schneider et al., 2012; Zhang et al., 2014) and NLRC5 inhibiting NF-κB and RIG-I signalling (Cui et al., 2010; Tong et al., 2012). Analysis of cellular viability during *Salmonella* infection appear to support a role for NLRC3 and NLRC5 as NF-κB inhibitors. Generally, upregulation of NF-κB signalling results in increased cell death due to upregulation of genes such as *Nlrp3* and *Tnfa* (Bauernfeind et al., 2009; Shakhov et al., 1990). Upon *Salmonella* infection, NLRC3 and NLRC5 inhibited cell death (Figure 3.8), an effect that could be attributed to their potential role as NF-κB negative regulators. Analysis of cytokine production, however, suggests the opposite. Upon *Salmonella* infection, NLRC3 and NLRC5 stimulates IL-1β production without affecting IL-18 (Figure 3.9-10), an effect that could be attributed to a positive effect on NF-κB signalling, as *Il1b* is a NF-κB-inducible gene whereas *Il18* is constitutively expressed (Hiscott et al., 1993; Puren et al., 1999).

It is important to notice that previous work done in LPS-primed macrophages derived from *Nlrc5*$^{-/-}$ mice infected with *S*. Typhimurium showed no difference in IL-1β production in relation to WT controls (Kumar et al., 2011). This could be explained by the fact that the priming was done using high LPS concentration for a long period of time (500 ng/mL for 24 hours), potentially masking subtle effects NLRC5 could have in the NF-κB pathway. Additionally, Kumar and collaborators employed *S*. Typhimurium at MOI 50, an experimental condition not ideal for studying small effects, since this MOI kills BMDMs very early in the infection. In line with this, I was unable to detect statistically significant differences in cellular viability, intracellular counts, IL-1β and IL-18 production in *Nlrc3* and *Nlrc5* knockout macrophages at MOI 50, regardless of the time point analysed. Further experimentation is now required to confirm that NLRC3 and NLRC5 are involved in cell death upon *S*. Typhimurium infection at later time points. Analysis of gene transcription by qPCR and stimulation of *Nlrc3*$^{-/-}$ and *Nlrc5*$^{-/-}$ BMDMs by canonical NLRP3 ligands, such as ATP and nigericin, could possibly improve our understanding on how these NLRs affect cellular viability during infection.

Functional redundancy between caspases is of relevance to inflammasome biology. This is illustrated by caspase-1 and caspase-11, both involved in triggering pyroptosis in a number of settings and by the fact that caspase-8 and caspase-1 are both involved in processing pro-IL-1β to its mature form (Kayagaki et al., 2011; Man et al., 2013). Less clear, however, is how other caspases affect this process. Infection of *caspase-2*$^{-/-}$ BMDMs revealed no difference in cellular viability in comparison to WT controls (Figure 3.21). This observation contradicts data generated in a previous study, according to which infection of *caspase-2*$^{-/-}$

BMDMs with *S*. Typhimurium showed a small albeit statistically significant impairment in cell death (Jesenberger et al., 2000). This difference could be explained by the fact that the authors used bacteria transitioning from stationary to logarithmic phase. Stationary phase bacteria is known to sub optimally stimulate the NLRC4 pathway due to lower expression of SPI-I proteins (Lara-Tejero et al., 2006). The activity of the NLRC4 inflammasome could, therefore, be masking a potential role for caspase-2 in cellular viability in my experimental setting. Of note however is the observation that IL-1β production is slightly impaired in *caspase-2*$^{-/-}$ BMDMs whereas IL-18 production remained unaltered (Figures 3.21-3.22). This follows a very similar pattern to that observed in *caspase-8*$^{-/-}$*/Ripk3*$^{-/-}$ cells when compared to *Ripk3*$^{-/-}$ and WT BMDMs; IL-1β production was impaired but IL-18 production and the degree of cellular viability were the same (Man et al., 2013). These observations imply a complementary role for caspase-2 during inflammasome activation.

Interestingly, this role is probably unrelated to the well-established effect of caspase-2 in apoptosis. This is because I found that PIDD, which is located upstream of caspase-2 in the intrinsic apoptotic pathway, did not affect cellular viability and intracellular bacteria counts. IL-1β production is, however, increased at MOI 50 upon 6 and 24 hours of infection where PIDD appeared to significantly inhibit IL-1β production (Figures 3.17-3.18). Assuming that caspase-2 indeed possess a role in inflammasome-regulated IL-1β processing, it is possible that the inhibitory effect of PIDD on IL-1β production occurs due to competition; in the presence of PIDD, caspase-2 can either interact with the PIDDosome or with the inflammasome and once PIDD is removed from the system (as in *Pidd*$^{-/-}$ BMDMs), a higher amount of caspase-2 is available to interact with the inflammasome, thus increasing IL-1β production. At the moment, this hypothesis is speculative, and more work is needed to establish if caspase-2 is actively involved in the activation of the *Salmonella*-induced inflammasome and whether PIDD plays a role in this process.

Despite evidence that the dectin-1 pathway could recognise bacterial PAMPs (Jackson et al., 2014), little is known about this receptor and its downstream adaptors in the context of inflammasome formation in response to *Salmonella*. For this reason, I examined the role of CARD9 in this process and I found that it had a profound inhibitory effect on IL-1β production. According to the well-established paradigm of inflammasome activation, one could expect that CARD9 would also have an inhibitory effect on pyroptotic cell death, since IL-1β production and pyroptosis are usually coupled processes. This, however, was clearly not the case. On the contrary, CARD9 was found to marginally promote cell death upon *S.* Typhimurium infection. This unexpected inhibitory activity of CARD9 in IL-1β production also

contradicts its roles as a positive regulator of inflammatory pathways such as NF-κB and MAPK (Bertin et al., 2000; Hsu et al., 2007; Poeck et al., 2010).

In the dectin-1 pathway, in addition to its involvement in NF-κB activation, CARD9 mediates the assembly of a noncanonical inflammasome containing caspase-8, responsible for IL-1β processing (Gringhuis et al., 2012). Little is known about the link between CARD9 and canonical inflammasomes. Previous work found no evidence of CARD9 involvement in IL-18 production mediated by AIM2 and NLRP3 (Hara et al., 2013). CARD9 is also not involved in NLRP3 activation in LPS-primed primary dendritic cells (Gross et al., 2009). Due to the unexpected impact of CARD9 on IL-1β production which is uncoupled from cell death, I decided to further investigate the role of CARD9 in regulating inflammasome activation upon *S.* Typhimurium infection.

Chapter 4

CARD9 regulation of canonical inflammasome activation

4.1. Introduction

CARD9 is a 62 kDa protein containing a N-terminal CARD followed by a coiled coil domain and expressed in several different tissues including the spleen (Bertin et al., 2000). Its role in innate immunity was first described in the context of NF-κB signalling, in which the authors used HEK293T overexpression systems to study the physical interaction between CARD9 and BCL10. This interaction activates NF-κB signalling via the IKK complex (Bertin et al., 2000). Later it was demonstrated that the CARD9/BCL10 interaction is physiologically relevant in the context of fungal infections in dendritic cells. Fungal pathogens such as *Candida albicans* contain the PAMP β-glucan that is recognised by dectin-1, a plasma membrane receptor containing a immunoreceptor tyrosine-based activation motif (ITAM). Upon recognition of its ligand, dectin-1 is phosphorylated and recruits spleen tyrosine kinase (SYK) (Gross et al., 2006). SYK is then activated and stimulates protein kinase C-δ (PKC-δ), responsible for phosphorylating CARD9 at threonine 231. This phosphorylation event allows CARD9 to interact with BCL10 and MALT1 forming a complex that stimulates the phosphorylation and activation of TAK1, responsible for activating NF-κB signalling via IKK phosphorylation. Interestingly CARD9 appears to modulate specific aspects of the dectin-1/SYK signalling pathway, as phagocytosis of zymosan particles is dependent on dectin-1 and SYK but independent of CARD9 (Gross et al., 2006; Strasser et al., 2012). The role of CARD9 in the NF-κB pathway is highly context-dependent, as illustrated by the fact that in macrophages CARD9/MALT1/BCL10 plays no role in NF-κB translocation despite the reasonably high expression of these proteins (Goodridge et al., 2009).

Studies in T-cells suggests that dectin-1 is a PRR that recognises bacterial β-(1,3)-glucan. In those cells, dectin-1 recognises the purified antigen, resulting in the production of IL-2 and facilitating antigen presentation (Jackson et al., 2014). It is unclear if this response is relevant *in vivo*, and if other cell types such as macrophages are able to recognise bacterial PAMPs via dectin receptors.

In addition to its role in the regulation of gene transcription via NF-κB, CARD9 is also involved in the assembly of a non-canonical inflammasome upon dectin-1 stimulation in dendritic cells. There, fungal pathogens such as *C. albicans* are recognised by the C-type lectin dectin-1, triggering the upregulation in the transcription of genes such as *Il1b* via

assembly of the CARD9/MALT1/BCL10 complex. This complex then recruits ASC and caspase-8 and results in the production of pro-inflammatory cytokines such as IL-1β (Gringhuis et al., 2012).

Other ITAM proteins employ CARD9 as an adaptor whilst transducing extracellular signals. In myeloid cells such as dendritic cells and macrophages, the ITAM-containing adaptors fragment crystallisable receptor (FcR)-γ and DNAX activating protein of 12 kDa (DAP12) are recruited by a number of receptors, allowing CARD9 to be activated via SYK, as described above. This phenotype is only observed in myeloid cells, as lymphocytes and natural killer (NK) cells employ the adaptor CARD11 instead and CARD9 deficiency has no impairment in the activation of FcR-γ and DAP12-associated ITAM receptors (Hara et al., 2007; Hara and Saito, 2009).

Upon viral infection, CARD9 acts as an adaptor in the RIG-I and Rad50 pathways. RIG-I interacts with viral dsRNA, leading to its activation by K63 ubiquitination and subsequent activation of MAVS forming the CARD9/BCL-10 complex responsible for activating NF-κB signalling (Poeck et al., 2010; Seth et al., 2005). In response to foreign dsDNA such as poly(dA:dT), the cytoplasmic protein Rad50 acts as a PRR in dendritic cells and triggers the formation of the CARD9/BCL10 complex that upregulates pro-IL-1β expression. CARD9 in the context of viral infections thus acts by controlling the transcription of pro-inflammatory cytokines (Roth et al., 2014). Interestingly, the CARD9 antiviral response appears to be specific to the RIG-I pathway, as CARD9 does not modulate AIM2 inflammasome activity nor is it involved in the cGAS/STING pathway (Roth et al., 2014).

Termination of CARD9/MALT1/BCL10 signalling is achieved by the RUN domain Beclin-1-interacting cysteine-rich-containing (Rubicon). Upon dectin-1 or RIG-I activation the CARD9/MALT1/BCL10 signalling complex is formed, whilst in parallel Rubicon is unphosphorylated and changes its binding partner from 14-3-3β to CARD9. The Rubicon/CARD9 interaction results in the disruption of the interactions between CARD9/MALT1/BCL10 and termination of signalling (Yang et al., 2012).

Genome-wide association studies link *CARD9* mutations to the development of inflammatory diseases such as colitis and Crohn's disease (Balzola et al., 2012; Beaudoin et al., 2013; Hong et al., 2015; Zhernakova et al., 2008). As discussed previously, *NOD2* mutations are also strongly linked to those conditions (Hugot et al., 2001; Uniken Venema et al., 2017). Mechanistically, CARD9 is an adaptor in the NOD2 signalling pathway. Upon NOD2 stimulation, CARD9 interacts with the NACHT domain of NOD2 leading to activation of the MAPKs p38 and JNK, but it is not involved in NF-κB signalling in the context of NOD2

signalling (Hsu et al., 2007; Parkhouse et al., 2014). The activation of MAPKs further illustrate the context-dependent activity of CARD9, as in lymphocytes this adaptor is not involved in MAPK signalling (Hara et al., 2007). Figure 4.1 illustrates some of the roles of CARD9 in dendritic cells.

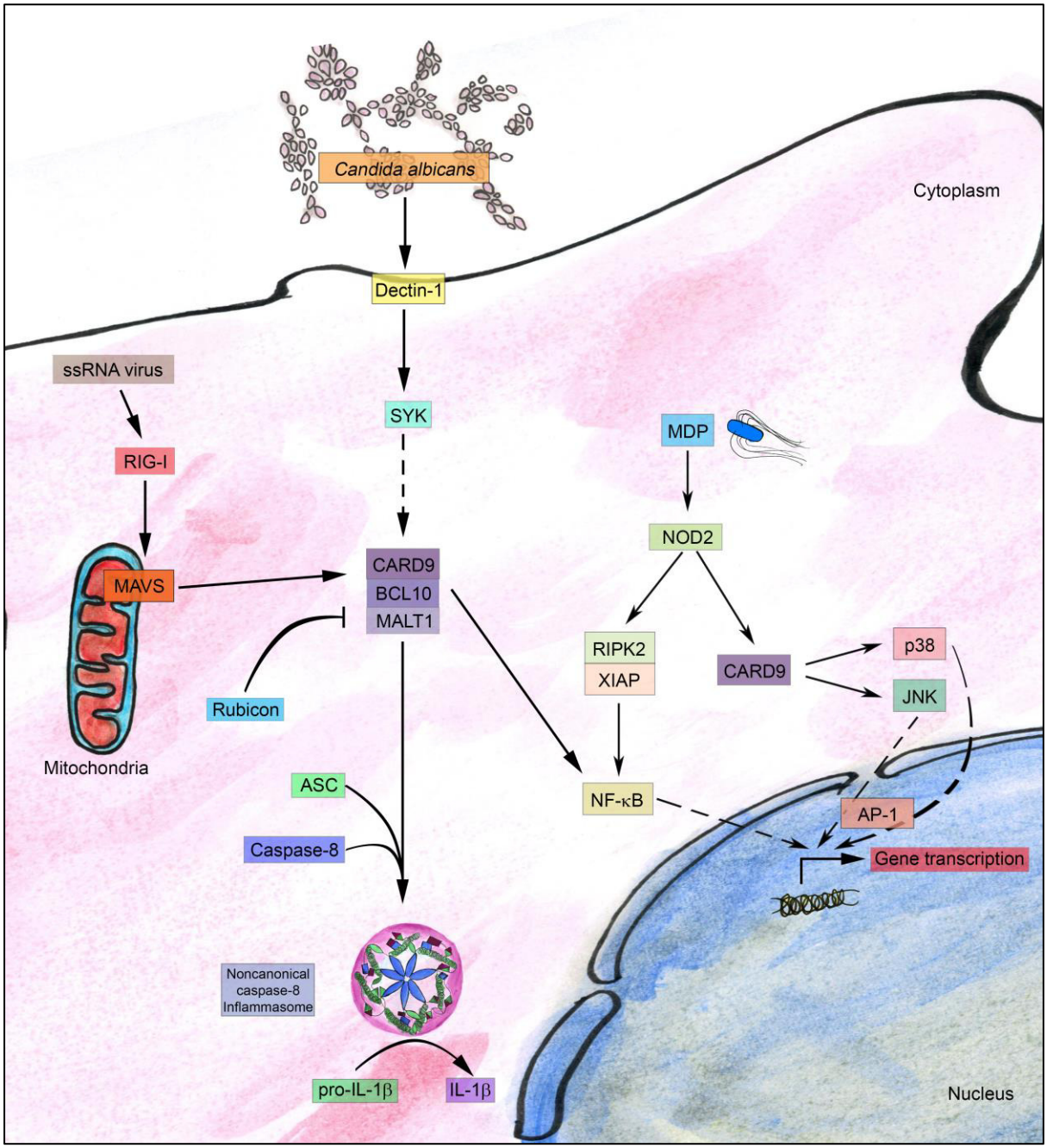

Figure 4.1: CARD9 as an adaptor in innate immunity. CARD9 involvement in the RIG-I pathway, non-canonical inflammasome formation, and NOD2 signalling in the response against ssRNA viruses, *C. albicans* and MDP respectively. CARD9 role in non-canonical inflammasome formation was only studied in dendritic cells.

CARD9 is also involved in the clearance of invasive bacterial pathogens by stimulating the production of ROS. This production is, in large part, controlled by the NADPH oxidase complex which is activated by the Rho-family GTPase Rac1. Upon infection, Rac1 is activated by GTP and is recruited to the membrane together with various NADPH complex proteins, forming a complex responsible for ROS production. This process is inhibited by the protein Ly GDP-dissociation inhibitor (LyGPI). In this context, CARD9 disrupts LyGDI inhibition of the ROS-producing complex and plays a key role in ROS production in macrophages in response to *E. coli*, *L. monocytogenes* and *S.* Typhimurium, but is not involved in ROS production in response to zymosan nor *C. albicans* (Figure 4.2) (Gross et al., 2009; Wu et al., 2009).

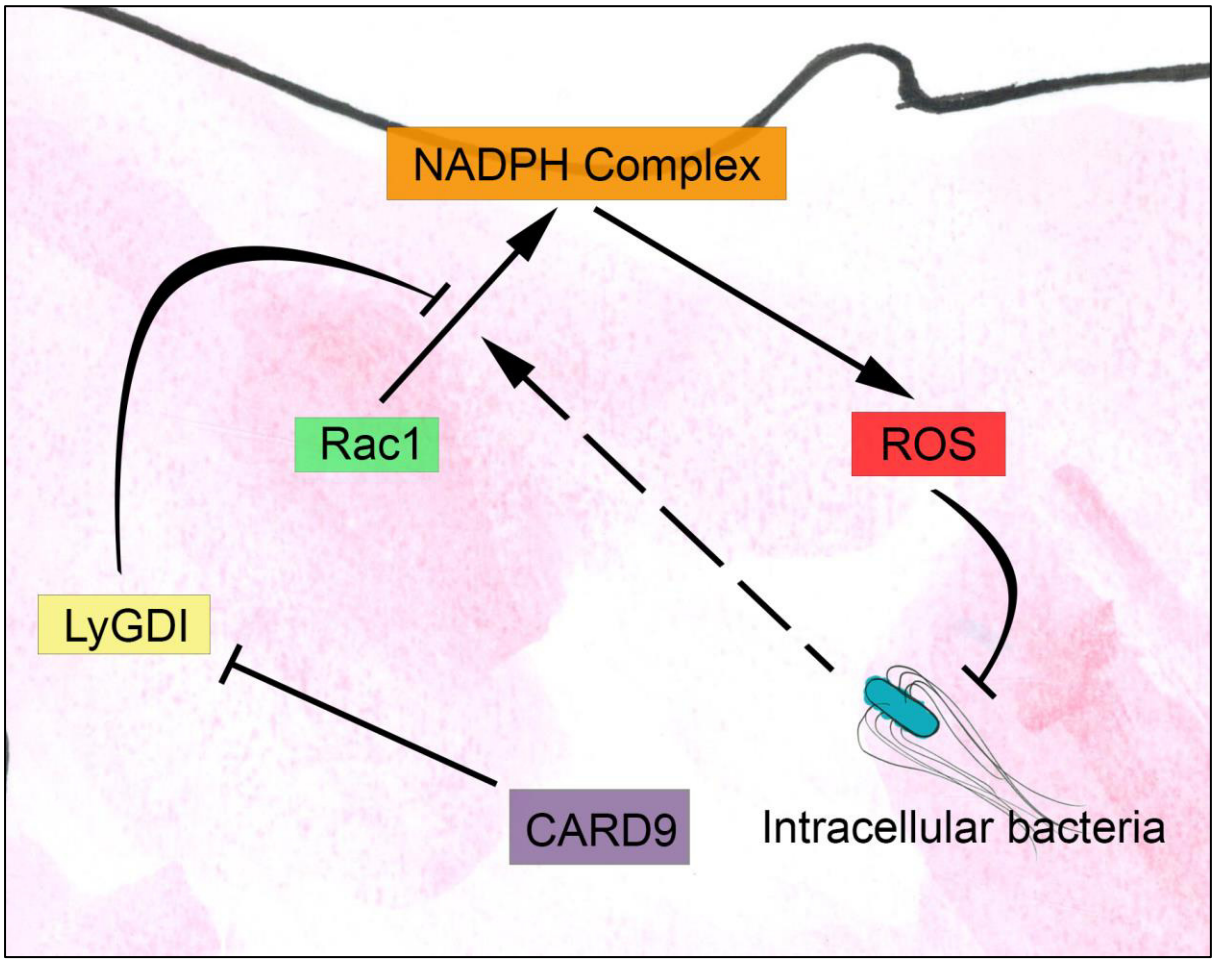

Figure 4.2: CARD9 and ROS production. CARD9 stimulates the production of ROS in response to intracellular bacteria by inhibiting LyGDI, thus increasing NADPH oxidase activity.

With respect to Mycobacteria infection, CARD9 appears to adopt an anti-inflammatory role. In a model of aerosol *Mycobacterium tuberculosis* infection, *Card9*$^{-/-}$ mice succumbed earlier to the disease and demonstrated a higher quantity of pro-inflammatory cytokines in the serum and lungs. These findings were linked by the authors to a deficiency in IL-10 production by the CARD9 knockout animals (Dorhoi et al., 2010).

The various roles that CARD9 plays during infection suggests that when it comes to innate immunity, all roads lead to CARD9 (Colonna, 2007). Evidence linking CARD9 to canonical inflammasomes, however, is missing, although some evidence in the literature from SYK studies suggest a possible role for CARD9. Upon *C. albicans* infection of BMDCs, CARD9 is involved in regulating pro-IL-1β expression via formation of a complex with BCL10 and MALT1 and activation of NF-κB (Gross et al., 2006). When BMDCs are initially primed with LPS, however, causing them to express great quantities of pro-IL-1β, CARD9 has no effect on NLRP3-mediated IL-1β production (Gross et al., 2009). In BMDMs, stimulation of the NLRP3 inflammasome by nigericin and stimulation of the AIM2 inflammasome by poly(dA:dT) in *Card9*$^{-/-}$ revealed similar IL-18 production in comparison to WT controls, albeit the production of IL-1β was not investigated (Hara et al., 2013).

In the previous chapter, I showed during *S*. Typhimurium infection of *Card9*$^{-/-}$ BMDMs there was a substantial increase in IL-1β production relative to their WT counterparts. This was not coupled to TNF-α production, suggesting a specific effect on IL-1β production, and was unlikely to be a consequence of the marginal increase in cellular viability (Figure 3.24-26). This was a surprising finding since the CARD9 functions thus far described suggests that this protein predominantly plays a key pro-inflammatory role in cell signalling, although whether it plays a role in canonical inflammasome activation in macrophages is unknown.

This chapter will focus on the elucidation of which inflammasomes CARD9 is capable of fine-tuning during *Salmonella* infection to explain the elevated IL-1β production seen in Chapter 3. Part of the data presented in this chapter was successfully published (Pereira et al., 2016) (Appendix 18).

4.2. Results

The enhanced IL-1β production from BMDMs after *S.* Typhimurium infection suggests a previously unknown role for CARD9 in the innate immune response to bacteria.

NLRC4 and NLRP3 are the main NLRs activated in response to *Salmonella* infection (Man et al., 2014), both capable of forming inflammasomes and converting pro-IL-1β to IL-1β. One of the differences between these two NLRs *in vitro* is the timing at which they are activated. In unprimed WT BMDMs, NLRC4-mediates IL-1β production as early as two hours post-infection. This contrasts with the NLRP3 inflammasome, that induces IL-1β production at later time points (Man et al., 2014). In primed macrophages both NLRC4 and NLRP3 can be activated at the same time (Man et al 2014). In the infection assays presented in the previous chapter (Figure 3.26-28), unprimed *Card9*$^{-/-}$ BMDMs produced more IL-1β than the WT controls throughout the course of the experiment. Since a significant difference in cytokine production is observed as early as 2 hours post-infection, I hypothesized that CARD9 acts as an inhibitor of the NLRC4 inflammasome.

To test whether CARD9 inhibits NLRC4 activation, WT, *Card9*$^{-/-}$, *Nlrc4*$^{-/-}$ and *Nlrp3*$^{-/-}$ BMDMs were primed with LPS (200 ng/mL for 3 hours) prior to transfection with ultrapure flagellin from *S*. Typhimurium, a NLRC4 ligand, for one hour. Next, I quantified cellular viability and the levels of IL-1β production. Flagellin transfection had no effect on BMDM cell viability (Figure 4.3 a), while marked IL-1β production was observed in all mouse lines except the NLRC4 knockout negative controls. Interestingly, WT, NLRP3 and CARD9 knockouts secreted similar IL-1β quantities into the supernatant (Figure 4.3 b). Taken together these results do not support a link between flagellin-activated NLRC4 and CARD9.

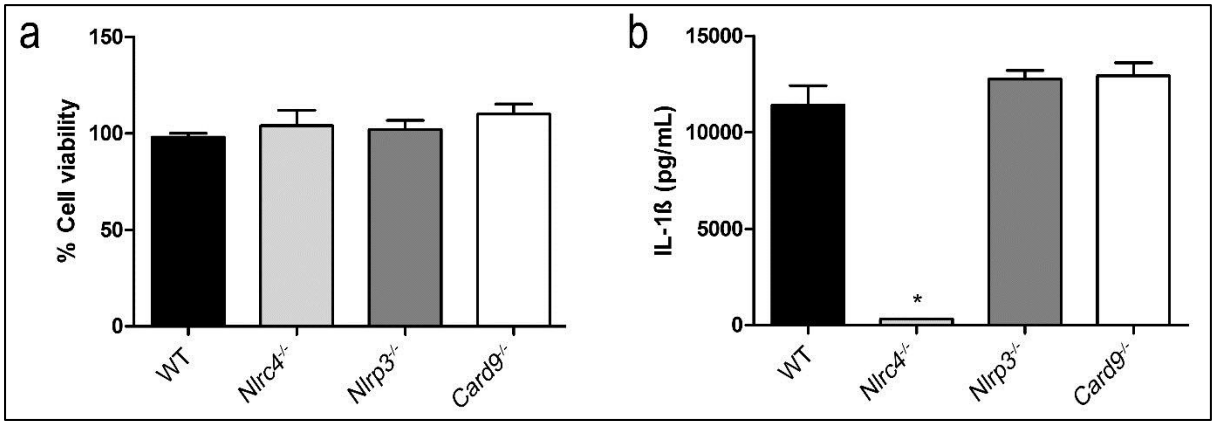

Figure 4.3: CARD9 does not influence flagellin activated NLRC4-mediated IL-1β production and cellular viability in LPS-primed BMDMs. WT, *Nlrc4*$^{-/-}$, *Nlrp3*$^{-/-}$ and *Card9*$^{-/-}$ LPS-primed BMDMs (200 ng/mL for 3 hours) were transfected with 60 ng ultrapure flagellin for one hour followed by analysis of cellular viability (as measure by LDH release) (a) and IL-1β production (as measured by ELISA) (b). * $p<0.05$ one-way ANOVA with Tukey's multiple comparisons test. Data represent the mean from three independent experiments while error bars show the s.e.m.

Salmonella also activates NLRC4 through its SPI protein PrgJ as well as via flagellin. To further investigate a possible link between NLRC4 and CARD9, GPAs were conducted using *S*. Typhimurium SL1344 *ΔfliCΔfljBΔprgJ*. This non-motile *Salmonella* mutant is deficient in NLRC4 activation (Man et al., 2014). If CARD9 acts by negatively regulating NLRC4 activity, then infection with the *ΔfliCΔfljBΔprgJ* mutant would stimulate similar IL-1β production in WT and *Card9*$^{-/-}$ BMDMs, presumably via NLRP3.

In this set of GPAs, WT and CARD9 knockout unprimed BMDMs were infected with *S*. Typhimurium *ΔfliCΔfljBΔprgJ* or with the parental *S*. Typhimurium SL1344 strain, at an of MOI 10. The plates were then centrifuged to allow for both the motile and amotile bacteria to contact the cell surface at the same time and allowed to infect the cells for up to 24 hours. Cellular viability and IL-1β production were determined at 2, 6 and 24 hours post-infection. WT and *Card9*$^{-/-}$ BMDMs showed similar patterns of cell viability post infection, regardless of the bacterial strain used and at all time-points studied (Figure 4.4 a-c). Although the original infection assays revealed a slight increase in cell viability in *Card9*$^{-/-}$ macrophages (Figure 3.24), this difference was absent in this set of experiments possibly due the fact that a centrifugation step was carried out to allow the *S*. Typhimurium *ΔfliCΔfljBΔprgJ* infection to occur, and thereby potentially increasing the infectivity of the WT bacteria as well. This observation, however, does not affect the conclusions drawn from this set of experiments.

The levels of IL-1β, however, remained increased in *Card9*$^{-/-}$ BMDMs regardless of the bacteria strain used. Infection with *S.* Typhimurium SL1344 increased IL-1β production in CARD9 knockout macrophages compared to WT controls, by 2 hours post infection. Similarly, in cells infected with the triple mutant *S*. Typhimurium *ΔfliCΔfljBΔprgJ*, IL-1β production was enhanced in *Card9*$^{-/-}$ BMDMs, most notably at 6 and 24 hours post-infection. Interestingly, infection with this bacterial strain caused no detectable IL-1β production at 2 hours in WT BMDMs, but at this time point the level of cytokine produced by *Card9*$^{-/-}$ BMDM*s* exceeded the detection limit (150 pg/mL detected, with a detection limit around 16 pg/mL). At 6 and 24 hours, *Card9*$^{-/-}$ macrophages produced 2.5 times more IL-1β than the WT controls for both bacterial strains (Figure 4.4 d-f). The ratio of IL-1β produced by *Card9*$^{-/-}$/WT BMDMs was similar regardless of the bacteria strain used. Since *ΔfliCΔfljBΔprgJ* does not activate the NLRC4 inflammasome, the data suggests that the enhanced IL-1β production observed in *Card9*$^{-/-}$ BMDMs in the context of *Salmonella* infection does not require NLRC4. This is consistent with the flagellin transfection data (Figure 4.3) and therefore the hypothesis that CARD9 regulates the NLRC4 inflammasome is unlikely.

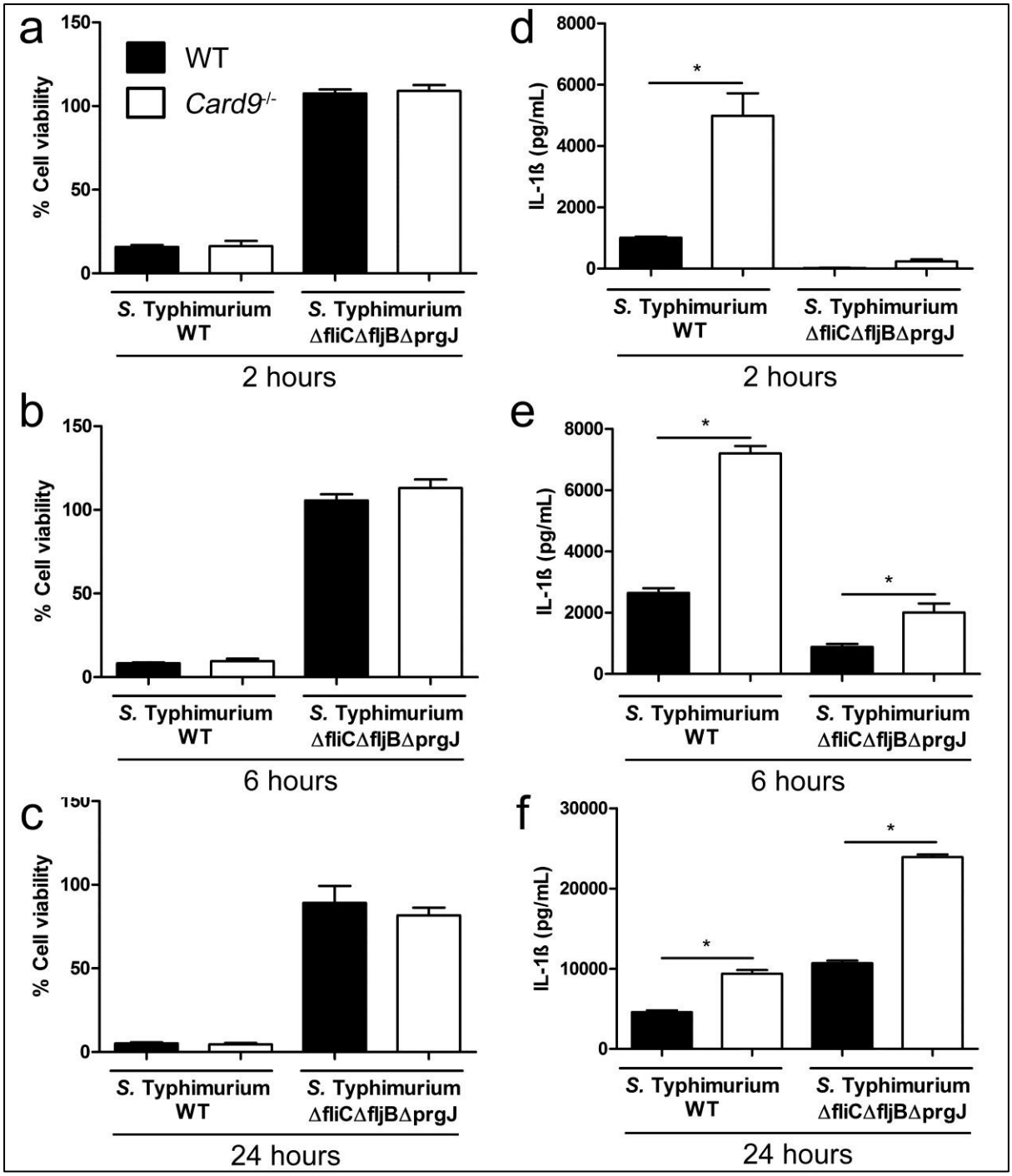

Figure 4.4: Cellular viability and IL-1β production in WT and *Card9*$^{-/-}$ BMDMs infected with *S.* Typhimurium SL1344 WT and *ΔfliCΔfljBΔprgJ* further suggest that NLRC4-mediated IL-1β production is unlikely to be controlled by CARD9. Cellular viability (a-c) and IL-1β production (d-f) from unprimed BMDMs after infection with *S.* Typhimurium WT or the NLRC4 activation deficient mutant *ΔfliCΔfljBΔprgJ* at MOI 10 for 2 (a,d), 6 (b,e) and 24 (c,f) hours. * $p<0.05$ in comparison to WT (one-way ANOVA with Tukey's multiple comparisons test). Data represent the mean from three independent experiments while error bars show the s.e.m.

In the dectin-1 pathway, CARD9 links SYK to NF-κB signalling and to the noncanonical caspase-8 inflammasome (Gringhuis et al., 2012). Although there is some evidence that dectin-1 can function as a *Salmonella* PRR in T cells (Jackson et al., 2014), this link was not established, to my knowledge, in macrophages. I hypothesized that CARD9 could potentially modulate the IL-1β production in macrophages through the dectin-1 pathway.

To test this hypothesis, I infected macrophages in presence of a dectin-1 blocking antibody. First, to verify if the antibody was suitable for functional assays, I have performed dectin stimulation assays in LPS-primed BMDMs using the dectin ligand zymosan. Oxidised zymosan was also included in this experiment, as primary macrophages are known to be better stimulated by the oxidised form of this molecule (Saijo et al., 2007). Next, cellular viability, IL-1β and TNF-α production were quantified. In this experiment, no difference in cellular viability was detected, whilst TNF-α production decreased in WT BMDMs incubated with ox-zymosan in presence of the blocking antibody. CARD9 knockout macrophages produced substantially less TNF-α and were not influenced by the presence of the blocking antibody, indicative that CARD9 is important in the response against ox-zymosan (Figure 4.5). No IL-1β was detected in any of the zymosan or ox-zymosan treatments. This suggests that the anti-dectin-1 antibody is suitable for functional assays.

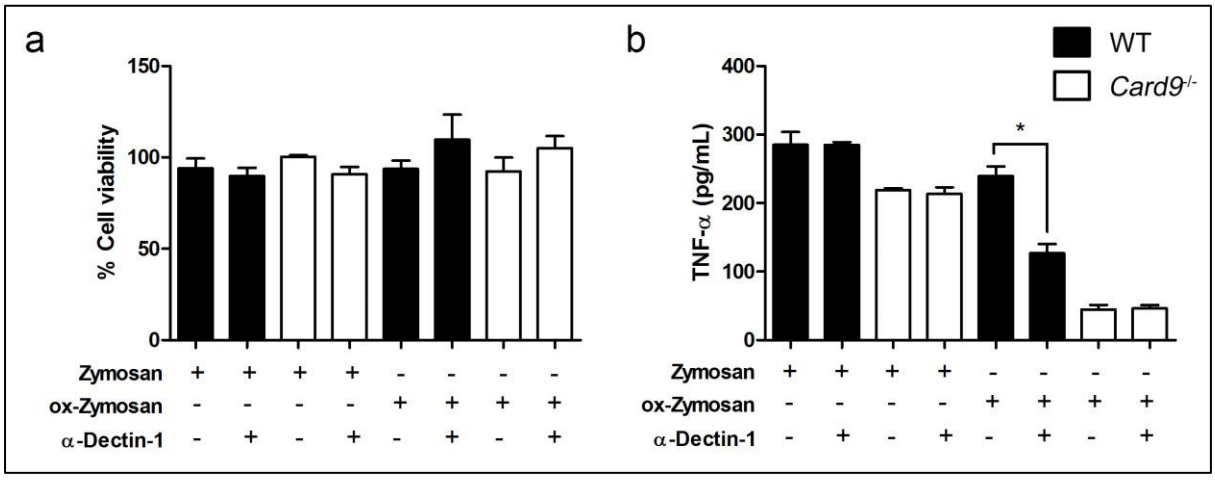

Figure 4.5: Anti-Dectin-1 antibody blocks TNF- induced by oxidised-zymosan in WT BMDMs. Cellular viability (a) and TNF-α production (b) from LPS-primed (200 ng/mL for 3 hours) WT and *Card9*$^{-/-}$ BMDMs after one-hour stimulation with 100 µg/mL zymosan or oxidized zymosan. No IL-1β was detected in any of the treatments. * $p<0.05$ in comparison to WT (one-way ANOVA with Tukey's multiple comparisons test). Data represent the mean from three independent experiments while error bars show the s.e.m.

Next, LPS-primed WT and *Card9*$^{-/-}$ BMDMs were infected with *S*. Typhimurium for one hour in presence or absence of dectin blocking antibody, followed by cellular viability measurement and culture supernatants collection for cytokine (IL-1β and TNF-α) quantification. The use of LPS-priming allows for quicker inflammasome activation during *Salmonella* infection, which is ideal for experiments using inhibitors or neutralizing antibodies where long exposure to these molecules could have adverse effects on the cells. Upon infection, *Card9*$^{-/-}$ BMDMs produced more IL-1β than the WT cells, but the presence or absence of anti-dectin failed to elicit any difference in cellular viability or levels of IL-1β and TNF-α (Figure 4.6). Possible interpretations of these results would be that dectin-1 is not a PRR during *S.* Typhimurium infections in macrophages, or at least its activity does not result in IL-1β or TNF-α production therefore it is unlikely this receptor is a candidate for the CARD9-mediated IL-1β inhibition.

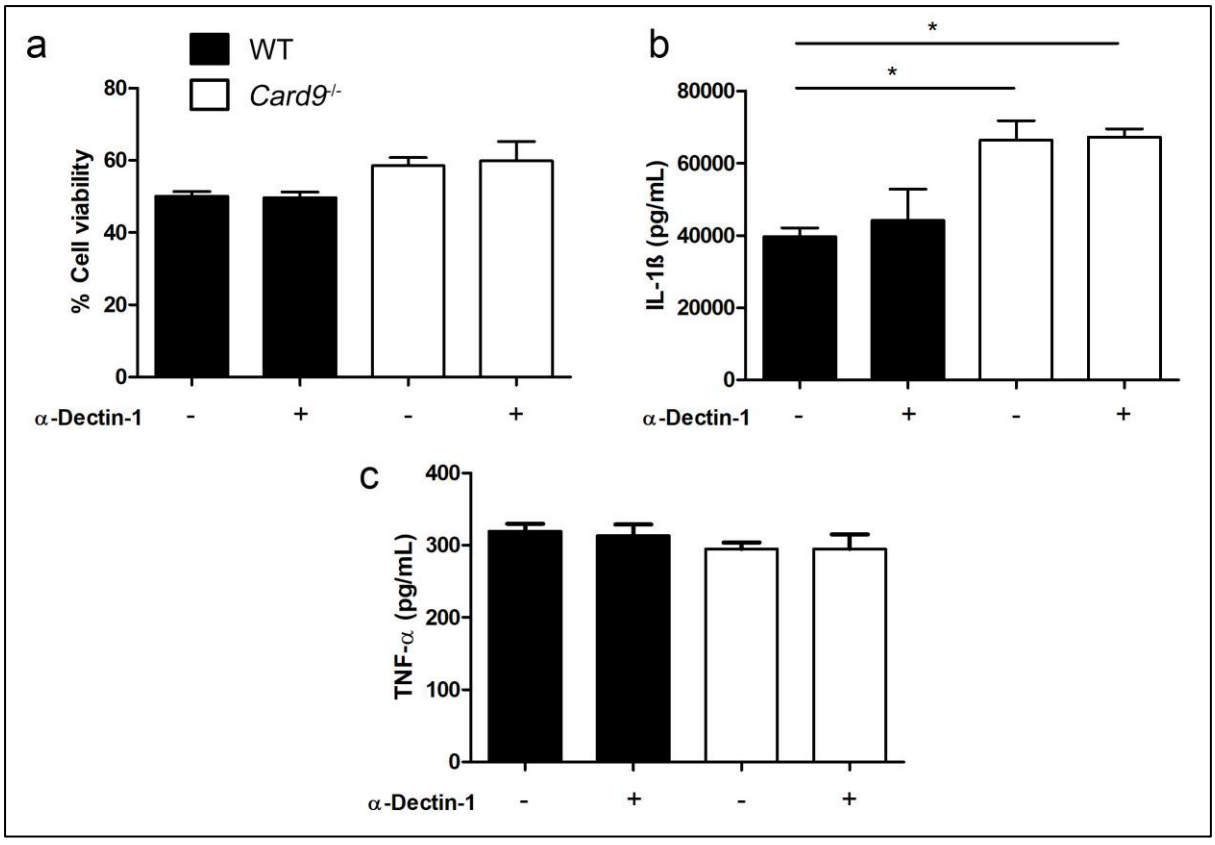

Figure 4.6: Dectin-1 neutralisation does not affect IL-1β production in BMDMs infected with *S*. Typhimurium. Cellular viability (a), IL-1β (b) and TNF-α production (c) from LPS-primed (200 ng/mL for 3 hours) WT and *Card9*$^{-/-}$ BMDMs after one hour infection with *S.* Typhimurium at MOI 10. * $p<0.05$ in comparison to WT (one-way ANOVA with Tukey's multiple comparisons test). Data represent the mean from three independent experiments while error bars show the s.e.m.

Upon infection, bacterial DNA is thought to act as a PAMP triggering IL-1β production via the AIM2 inflammasome. This pathway however appears to be of little relevance during *S.* Typhimurium infections (Rathinam et al., 2010; Warren et al., 2010). Researchers also failed to link the adaptor CARD9 to AIM2 inflammasomes in dendritic cells (Roth et al., 2014). Although it is unlikely that AIM2 is involved in CARD9 regulation of IL-1β production I tested whether AIM2 ligands could induce greater IL-1β production in CARD9 knockout BMDMs compared to WT controls. WT and *Card9*$^{-/-}$ BMDMs were primed with LPS (3 hours, 200 ng/mL) then transfected the AIM2 ligand poly(dA:dT) and the cellular viability and IL-1β production quantified. AIM2 stimulation led to no differences in cellular viability nor IL-1β production between WT and *Card9*$^{-/-}$ cells (Figure 4.7). This result is in agreement with previous reports that AIM2 is not involved in the response against *Salmonella* and that CARD9 is not involved in AIM2 signalling (Roth et al., 2014).

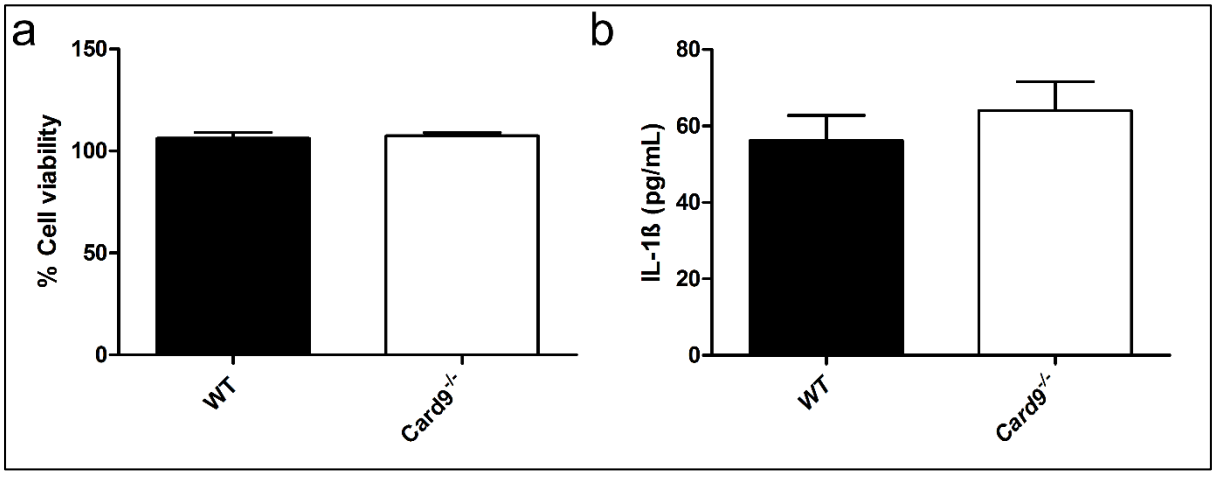

Figure 4.7: WT and CARD9 knockout LPS-primed BMDMs have similar cellular viability and IL-1β production after AIM2 stimulation with poly(dA:dT). Cellular viability (a) and IL-1β production (b) from LPS-primed (200 ng/mL for 3 hours) WT and *Card9*$^{-/-}$ BMDMs after four hours stimulation with 2 µg/mL poly(dA:dT). * p>0.05 (unpaired t-test). Data represent the mean from three independent experiments while error bars show the s.e.m.

During the infection process, *S*. Typhimurium engages both the NLRC4 and the NLRP3 inflammasome (Broz et al., 2010; Man et al., 2014). NLRC4 stimulation and infection assays using a *Salmonella* mutant deficient in NLRC4 activation failed to demonstrate a link between CARD9 and IL-1β produced by this inflammasome (Figure 4.3-4). I therefore

determined whether NLRP3 was important in the inhibitory effect that CARD9 exerts on IL-1β production during *Salmonella* infection.

Unprimed WT and CARD9 knockout macrophages were infected with *S*. Typhimurium at MOI 10 for 2 and 6 hours in presence or absence of the drug glibenclamide. This drug is a sulfonylurea commonly used in human medicine for the treatment of type 2 diabetes, but it also has an inhibitory effect on the NLRP3 inflammasome (Lamkanfi et al., 2009). After infection, cellular viability and IL-1β production in the supernatant was quantified. Upon infection, glibenclamide had no discernible effect on the cellular viability in both WT and *Card9*$^{-/-}$ BMDMs. Similarly, the drug had no effect on IL-1β released by *Salmonella*-infected WT BMDMs, confirming that in WT BMDMs infected with *Salmonella*, NLRP3 is not involved in IL-1β production early in the infection (Man et al., 2014). In contrast, glibenclamide inhibited IL-1β production at 2 and 6 hours in CARD9 knockout BMDMs, thus upon NLRP3 inhibition the resulting IL-1β secretion was similar between WT and *Card9*$^{-/-}$ (Figure 4.8). This suggested that CARD9 inhibits NLRP3 and that in the absence of the former, NLRP3 activation *in vitro* occurs as early as 2 hours post *Salmonella* infection, a time point that usually only involves NLRC4 activation during *S.* Typhimurium infection (Man et al., 2014).

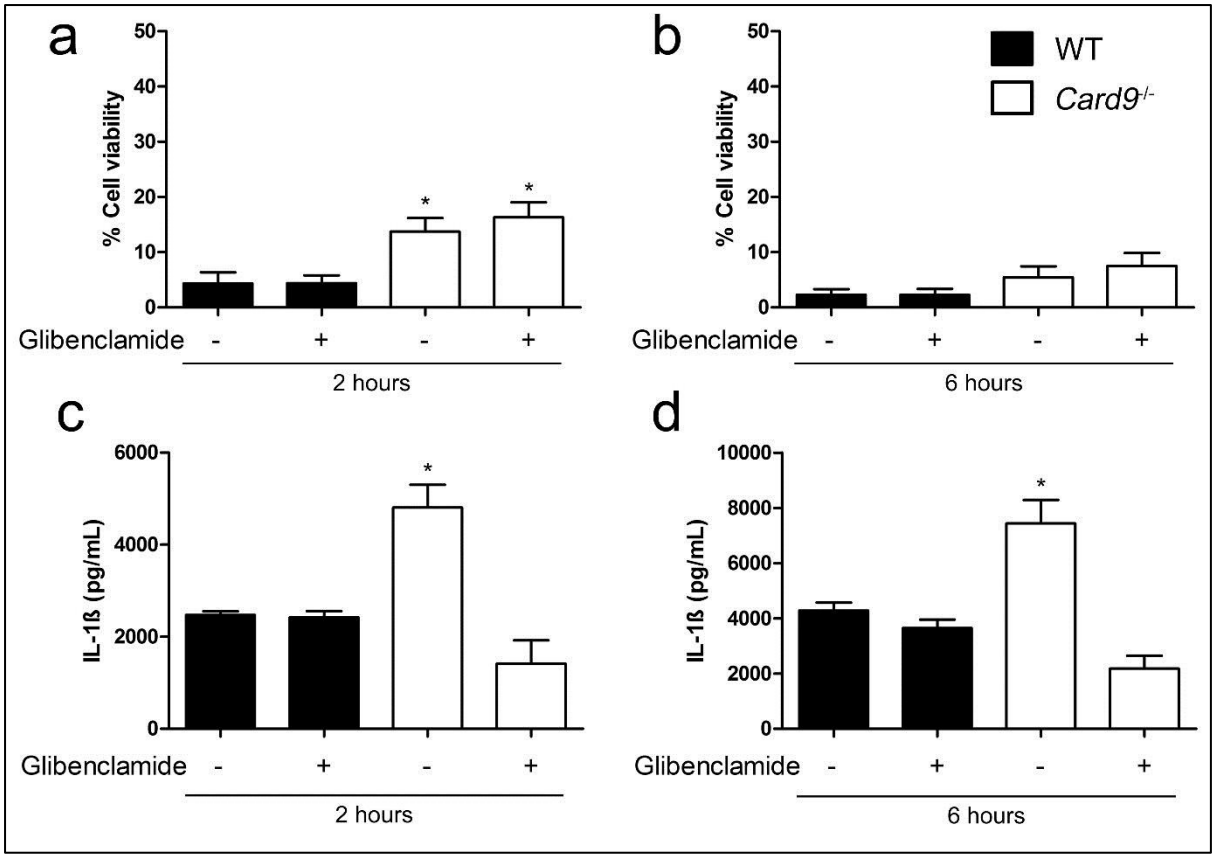

Figure 4.8: NLRP3 inhibition with glibenclamide decreases IL-1β production in *Card9*$^{-/-}$ but not in WT BMDMs. Cellular viability (a-b) and IL-1β production (c-d) from unprimed BMDMs after infection with *S*. Typhimurium at MOI 10 for 2 (a,c) and 6 (b,d) hours in the presence of 200 μM glibenclamide. * $p<0.05$ in comparison to WT (one-way ANOVA with Tukey's multiple comparisons test). Data represent the mean from three independent experiments while error bars show the s.e.m.

More recently researchers have reported the development of MCC950, a potentially specific NLRP3 inhibitor (Coll et al., 2015). To further confirm the link between NLRP3 and CARD9, I performed a NLRP3 inhibition assay using MCC950. Using the same experimental design as for the glibenclamide experiment (Figure 4.8) similar data was obtained with IL-1β production unaffected in WT cells treated with MCC950, whilst *Card9*$^{-/-}$ BMDMs produce less IL-1β at 2 and 6 hours upon MCC950 inhibition. The resulting IL-1β production when the inhibitor is present is similar between WT and *Card9*$^{-/-}$ macrophages (Figure 4.9). This corroborates the glibanclamide data and further suggests that CARD9 inhibits NLRP3-mediated IL-1β production.

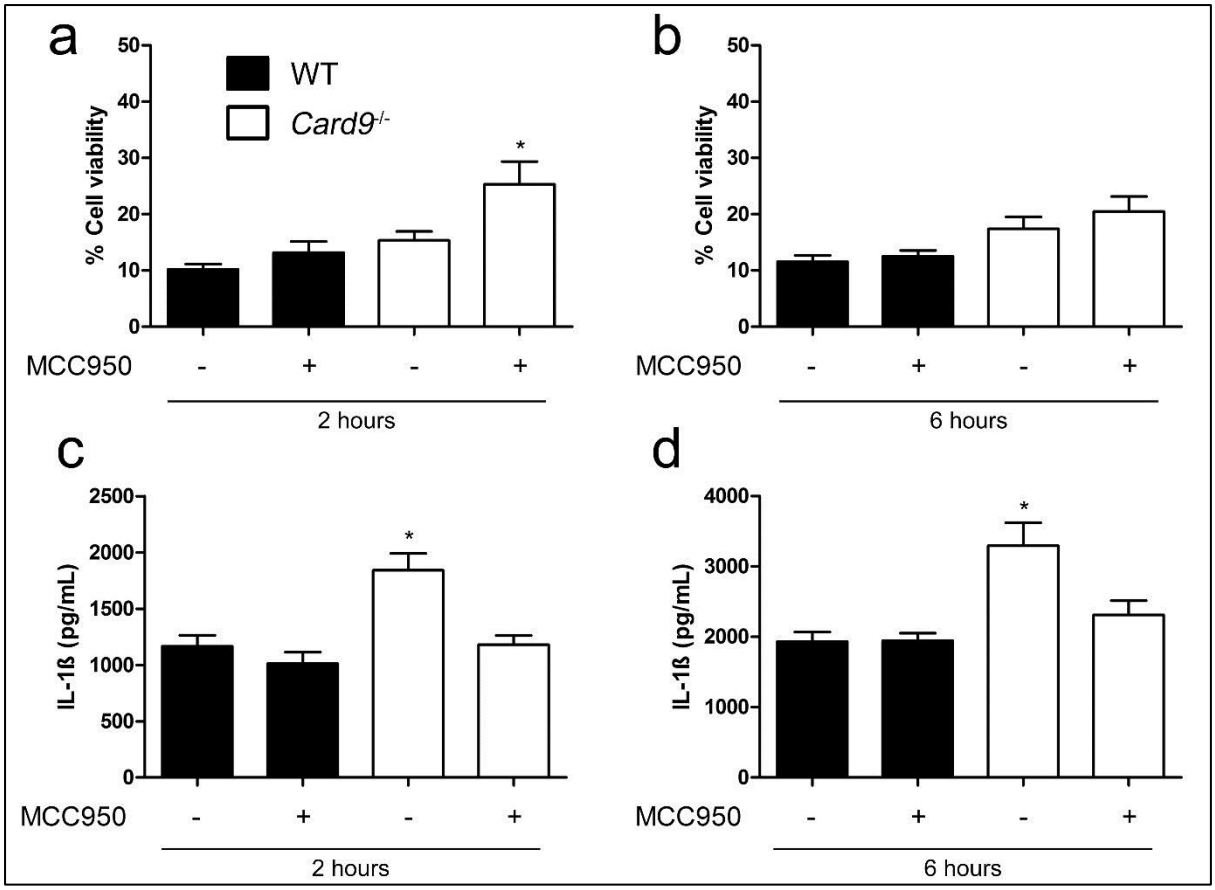

Figure 4.9: NLRP3 inhibition with MCC950 decreases IL-1β production in *Card9*$^{-/-}$ but not in WT BMDMs. Cellular viability (a-b) and IL-1β production (c-d) from unprimed BMDMs after infection with *S*. Typhimurium at MOI 10 for 2 (a,c) and 6 (b,d) hours in presence of 10 μM MCC950. * $p<0.05$ in comparison to WT (one-way ANOVA with Tukey's multiple comparisons test). Data represent the mean from three independent experiments while error bars show the s.e.m.

To provide further evidence that CARD9 inhibits IL-1β production via the NLRP3 inflammasome, I investigated whether the IL-1β production in WT and *Card9*$^{-/-}$ BMDMs was similar after stimulation with canonical NLRP3 activators such as the ionophore nigericin (Mariathasan et al., 2006). WT, *Card9*$^{-/-}$, *Nlrp3*$^{-/-}$ and *Nlrc4*$^{-/-}$ BMDMs were primed with LPS (200 ng/mL for 3 hours), and then stimulated for one hour with nigericin. After stimulation, cellular viability and IL-1β present in the supernatants were quantified. Similar cell viability was observed in WT, *Card9*$^{-/-}$ and *Nlrc4*$^{-/-}$ macrophages, whilst *Nlrp3*$^{-/-}$ BMDMs were protected from cell death, as expected, because pyroptotic cell death is impaired in this knockout mouse line post nigericin stimulation (Figure 4.10 a). Similarly, IL-1β production is greatly impaired in *Nlrp3*$^{-/-}$ cells following nigericin treatment. WT and *Nlrc4*$^{-/-}$ BMDMs

produced two times less IL-1β than *Card9*$^{-/-}$ macrophages (Figure 4.10 b). This once again suggests that the IL-1β production mediated by NLRP3 is inhibited by CARD9, whilst pyroptosis remains unnaffected.

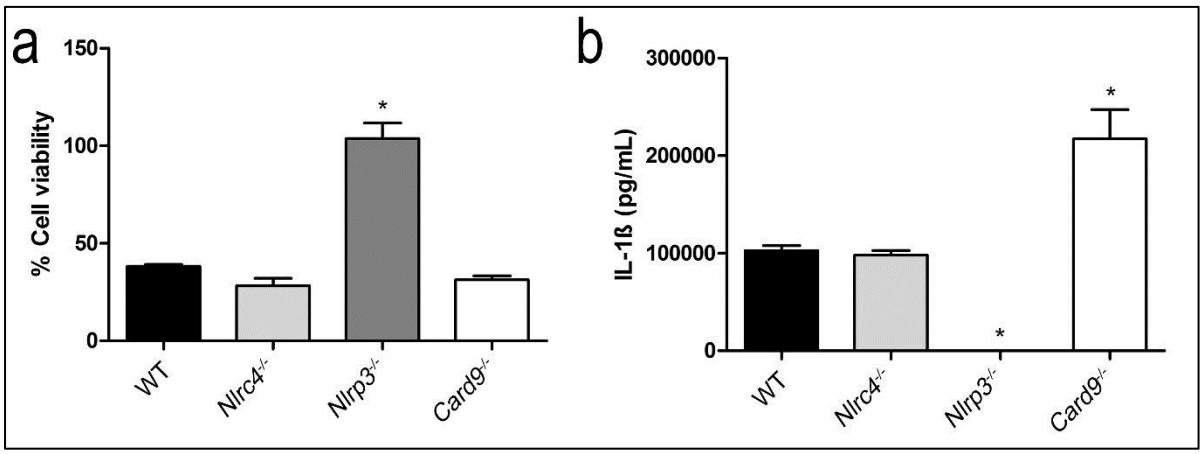

Figure 4.10: CARD9 influences NLRP3-mediated IL-1β production but not cellular viability in response to nigericin stimulation of LPS-primed BMDMs. WT, *Nlrc4*$^{-/-}$, *Nlrp3*$^{-/-}$ and *Card9*$^{-/-}$ LPS-primed BMDMs (200 ng/mL for 3 hours) were incubated with 10 μM nigericin for one hour followed by analysis of cellular viability (as measure by LDH release) (a) and IL-1β production (as measured by ELISA) (b). * $p<0.05$ in comparison to WT (one-way ANOVA with Tukey's multiple comparisons test). Data represent the mean from three independent experiments while error bars show the s.e.m.

Finally, to further substantiate the CARD9/NLRP3 link, I have conducted another NLRP3 stimulation assay using a different stimulus. In LPS-primed macrophages, ATP is a DAMP that triggers the assembly of the canonical NLRP3 inflammasome via the purinergic receptor P2X7R and production of ROS by NADPH oxidase (Cruz et al., 2007; Hewinson et al., 2008; Mariathasan et al., 2006). Here, WT, *Nlrp3*$^{-/-}$ and *Card9*$^{-/-}$ BMDMs were primed with LPS (200 ng/mL for 3 hours), stimulated with 5 mM ATP for 30 minutes, and then cellular viability and IL-1β production were quantified. At this concentration and incubation time, ATP did not cause any loss in cellular viability in all mouse lines analysed. In comparison to WT controls the levels of IL-1β production were decreased in *Nlrp3*$^{-/-}$ macrophages and enhanced in *Card9*$^{-/-}$ (Figure 4.11). The increased level of IL-1β production in *Card9*$^{-/-}$ macrophages upon NLRP3 stimulation provides additional evidence that the adaptor CARD9 inhibits the NLRP3 inflammasome.

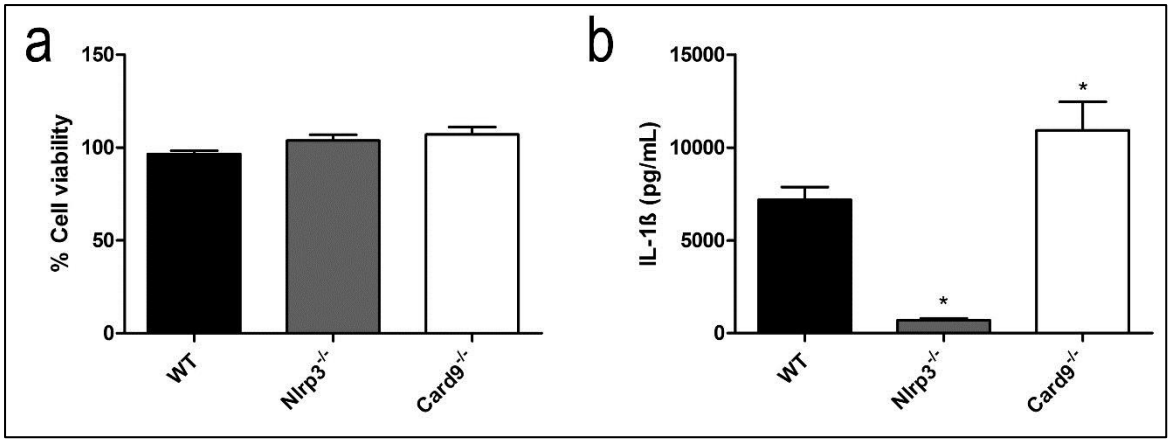

Figure 4.11: CARD9 influences NLRP3-mediated IL-1β production but not cellular viability in response to ATP stimulation of LPS-primed BMDMs. WT, *Nlrp3*$^{-/-}$ and *Card9*$^{-/-}$ LPS-primed BMDMs (200 ng/mL for 3 hours) were incubated with 5 mM ATP for 30 minutes followed by analysis of cellular viability (as measure by LDH release) (a) and IL-1β production (as measured by ELISA) (b). * $p<0.05$ in comparison to WT (one-way ANOVA with Tukey's multiple comparisons test). Data represent the mean from three independent experiments while error bars show the s.e.m.

The data above (Figures 4.8-11) supports the hypothesis that CARD9 negatively regulates the activity of the NLRP3 inflammasome both during *S.* Typhimurium infection of unprimed macrophages and after direct stimulation by canonical NLRP3 ligands in LPS-primed macrophages. To further consolidate this finding and to investigate whether CARD9 is relevant in other infection models known to activate the NLRP3 inflammasome, I infected cells with the enteropathogenic *E. coli* strain P19A. *E. coli* activates the NLRP3 inflammasome (Brereton et al., 2011), but little work was done to characterize the enteropathogenic P19A strain.

To confirm that this strain activates the NLRP3 inflammasome, I have conducted GPAs in unprimed WT, *Nlrp3*$^{-/-}$, *Nlrc4*$^{-/-}$ and *Caspase-1*$^{-/-}$*/11*$^{-/-}$ BMDMs using *E. coli* P19A at MOI 10. Upon 2 and 6 hours of infection, cellular viability and IL-1β production were assayed. The P19A strain caused cell death as early as 2 hours post-infection in WT and *Nlrc4*$^{-/-}$ macrophages, whilst *Nlrp3*$^{-/-}$ and *Caspase-1*$^{-/-}$*/11*$^{-/-}$ macrophages were protected (Figure 4.12 a). At 6 hours, *Nlrp3*$^{-/-}$ macrophages remained with near 100% cell viability (Figure 4.12 c). At 2 hours, *E. coli* P19A induced IL-1β production in both WT and NLRC4 knockout BMDMs, whilst this production was below detection limit in *Nlrp3*$^{-/-}$ and *Caspase-1*$^{-/-}$*/11*$^{-/-}$ macrophages (Figure 4.12 b). No IL-1β was detected in *Nlrp3*$^{-/-}$ cells at 6 hours (Figure 4.12 d). Taken

together, this GPA confirms that *E. coli* P19A activates the NLRP3 inflammasome *in vitro* as early as 2 hours post infection. This bacterial strain is, therefore, suitable to study any links between CARD9 and NLRP3.

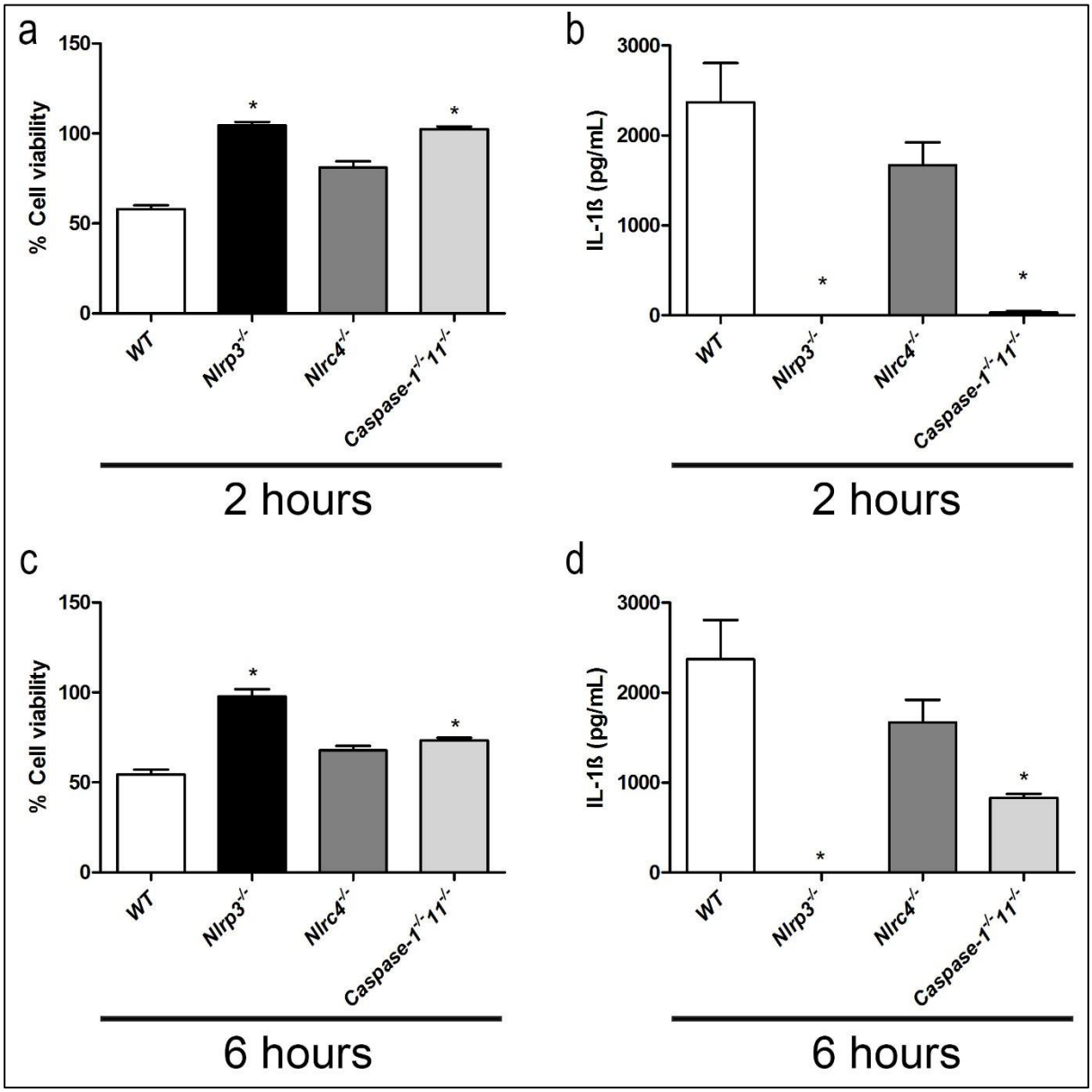

Figure 4.12: NLRP3 and Caspase-1/11, but not NLRC4, are important in triggering cell death and IL-1β release during *E. coli* strain P19A infection. (a,c) Cellular viability (as measured by LDH release) and (b,d) IL-1β release in WT, *Nlrp3*$^{-/-}$, *Nlrc4*$^{-/-}$ and *Caspase-1*$^{-/-}$ *Caspase-11*$^{-/-}$ BMDMs after infection with *E. coli* P19A at MOI 10 for 2 (a-b), and 6 (c-d) hours. * $p<0.05$ in comparison to WT (one-way ANOVA with Tukey's multiple comparisons test). Data represent the mean from two independent experiments while error bars show the s.e.m.

WT and *Card9*$^{-/-}$ BMDMs were infected with *E. coli* P19A (MOIs 1, 10 and 50 for 2 and 6 hours) and analysed for cell viability, intracellular bacteria and cytokine production (IL-1β and TNF-α). At both 2 and 6 hours post-infection, *E. coli* P19A caused similar levels of cell death in WT and CARD9 knockout macrophages, whilst no differences in intracellular bacteria counts was observed (Figure 4.13). ELISA of the cell culture supernatants showed a significant increase in IL-1β production in CARD9 knockout BMDMs in comparison to WT controls, whilst TNF-α production in both macrophage strains remained similar (Figure 4.14). CARD9 therefore inhibits the production of IL-1β without affecting pyroptosis or the production of pro-inflammatory cytokines such as TNF-α in response to both *E. coli* and *S* Typhimurium. Since *E. coli* activates the NLRP3 inflammasome, it is likely that CARD9 inhibits this inflammasome.

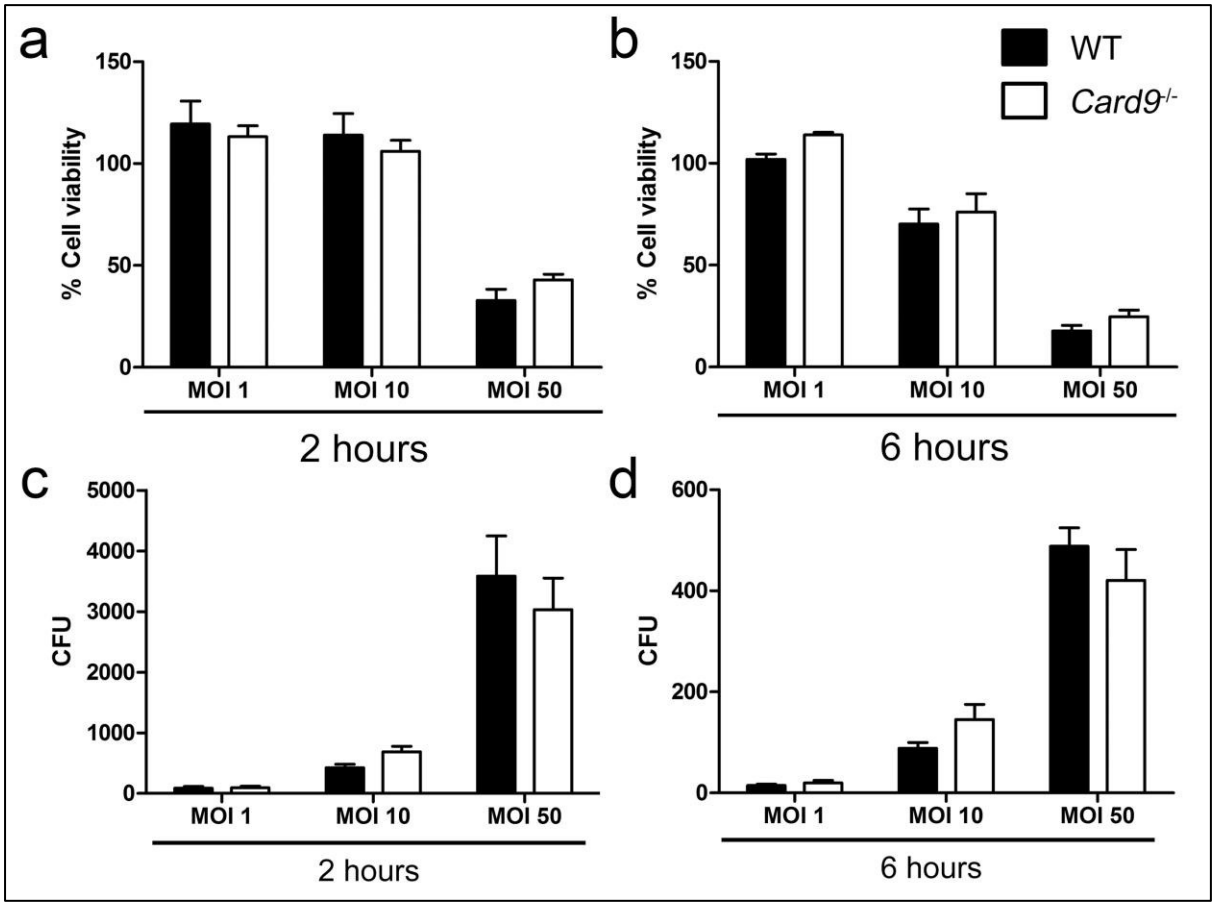

Figure 4.13: CARD9 has no effect on cellular viability and intracellular bacteria counts in BMDMs infected with *E. coli* P19A. (a,b) Cellular viability (as measured by LDH release) and (c,d) intracellular bacteria counts of WT, *and Card9*$^{-/-}$ BMDMs after infection with *E. coli* P19A at MOIs 1, 10 and 50 for 2 (a-c) and 6 (b-d) hours. * $p<0.05$ in comparison to WT (one-way ANOVA with Tukey's multiple comparisons test). Data represent the mean from two independent experiments while error bars show the s.e.m.

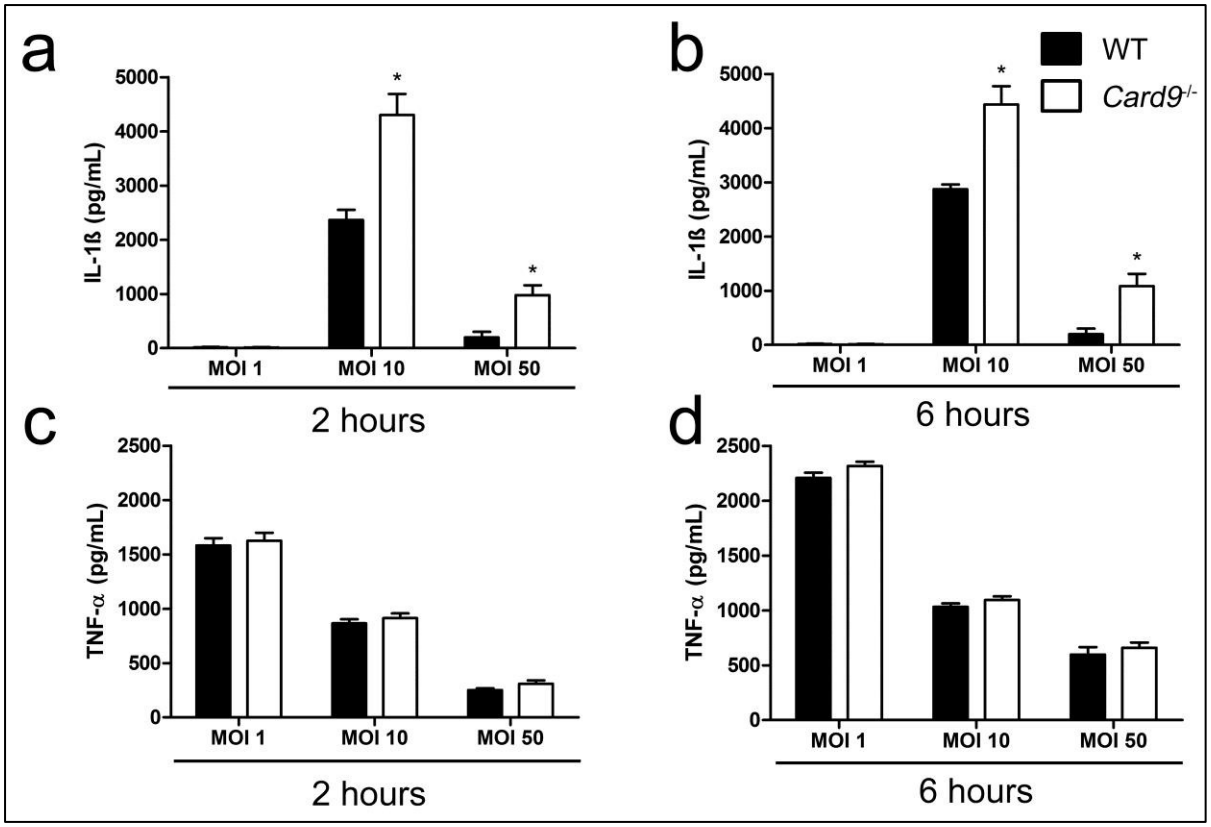

Figure 4.14: CARD9 affects IL-1β but not TNF-α production in BMDMs infected with *E. coli* P19A. IL-1β secretion (as measured by ELISA) (a,b) and TNF-α secretion (as measured by ELISA) (c,d) of WT, and *Card9*$^{-/-}$ BMDMs after infection with *E. coli* P19A at MOIs 1, 10 and 50 for 2 (a-c) and 6 (b-d) hours. * $p<0.05$ in comparison to WT (one-way ANOVA with Tukey's multiple comparisons test). Data represent the mean from two independent experiments while error bars show the s.e.m.

Having established a link between NLRP3 and CARD9, I sought to investigate the mechanistic basis for how CARD9 negatively regulates this inflammasome. A possible mechanism for controlling NLRP3 activity is by CARD9 physically interacting with this inflammasome or some of its components. In practical terms, if a protein interacts with the assembled inflammasome, then this protein might be expected to co-localise with the ASC speck at the microscopic level. I therefore used immunofluorescence localisation of CARD9 and ASC as a first approach to investigate the mechanism(s) involved in NLRP3 inhibition by CARD9. WT, *Pycard*$^{-/-}$ (ASC negative) and *Card9*$^{-/-}$ BMDMs were primed with LPS (200 ng/mL for 3 hours). Next, the NLRP3 inflammasome was stimulated with nigericin (5 μM for 30 minutes), the cells fixed in methanol and immunostained for ASC and CARD9. DAPI was

used for nuclei counterstaining and the preparations were then visualised under an epifluorescence microscope.

As expected, WT and *Card9*$^{-/-}$ BMDMs formed ASC specks after stimulation with nigericin, while *Pycard*$^{-/-}$ BMDMs do not (Figure 4.15, red arrows). CARD9 was present as aggregates in the cytosol of both unstimulated WT and ASC knockout BMDMs but not in *Card9*$^{-/-}$ cells. These aggregates continued to be observed after nigericin stimulation and appear to be unrelated to the ASC specks. The lack of ASC/CARD9 colocalization suggests that CARD9 is not recruited to the ASC speck (Figure 4.15, green arrows).

The CARD9 antibody showed non-specific background staining in *Card9*$^{-/-}$ BMDMs. This staining, however, is much fainter than that observed in WT and *Pycard*$^{-/-}$ cells. Additionally, no CARD9 aggregates were observed in *Card9*$^{-/-}$ macrophages (Figure 4.15). To further verify the specificity of the CARD9 antibody, I performed an immunoblot assay using protein lysate from WT and *Card9*$^{-/-}$ cells probed with the same anti-CARD9 antibody used in the immunofluorescence assay. The immunoblot revealed one major protein band with an apparent molecular weight under 75 kDa, presumably CARD9 which is not present in the CARD9 knockout strain (Figure 4.16).

Immunofluorescence and immunoblotting are fundamentally different techniques. Immunoblot, in most conditions, disrupts the protein structure thus altering the capability of the antibody to bind the protein. But Figure 4.16, taken together with the fainter signal and lack of aggregates observed in *Card9*$^{-/-}$ in Figure 4.15, suggests that the anti-CARD9 antibody employed is specific enough for the purposes of this investigation and supporting the conclusion that there is no evidence of co-localisation of CARD9 and ASC.

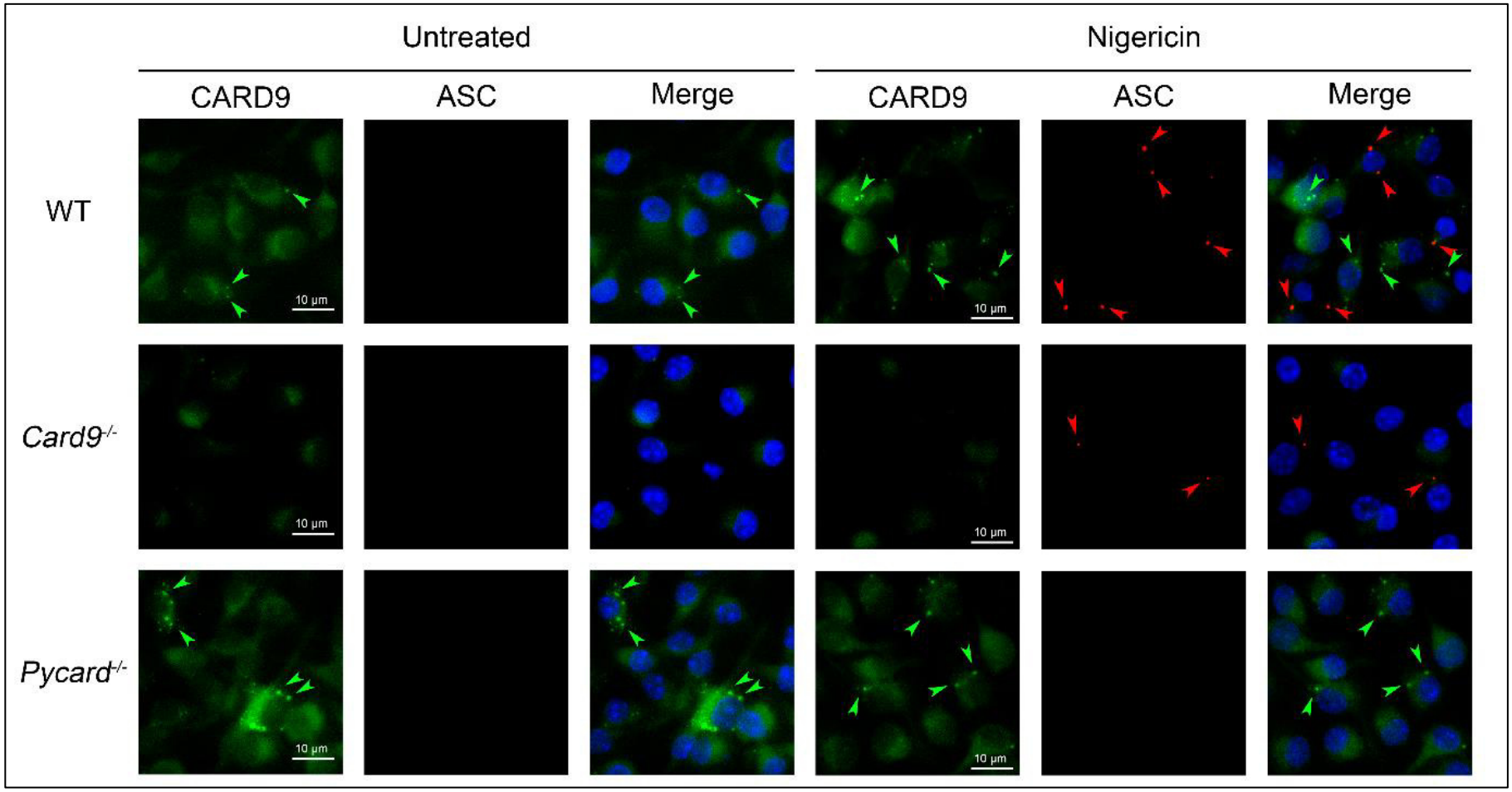

Figure 4.15: CARD9 and ASC do not co-localize in LPS-primed BMDMs after stimulation with nigericin. ASC (red) and CARD9 (green) and nuclei (blue) visualization in WT, *Card9*$^{-/-}$ and *Pycard*$^{-/-}$ LPS-primed BMDMs (200 ng/mL for 3 hours) after 30 minutes stimulation with 5 µM nigericin. Images are representative of three independent experiments.

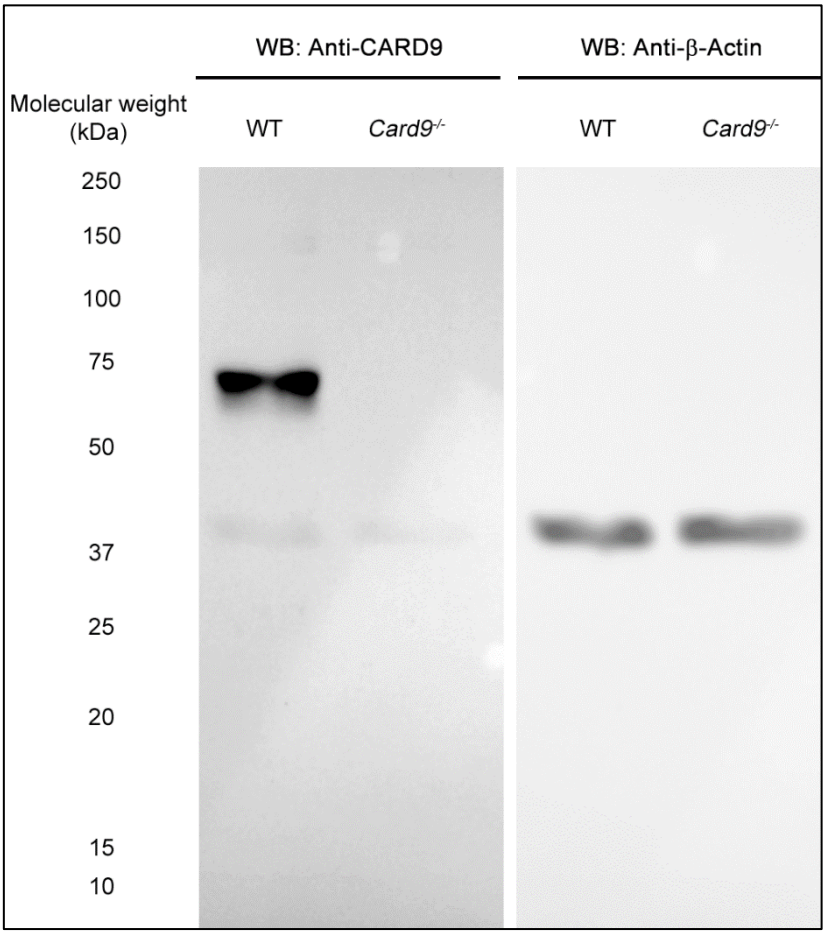

Figure 4.16: Specificity of the anti-CARD9 antibody. Immunoblot of protein samples extracted from WT and *Card9*$^{-/-}$ BMDMs and probed with anti-Card9 and anti-β-Actin. The image is representative of two independent experiments.

Whilst ASC and CARD9 do not co-localise at the ASC speck, it is possible that both proteins interact either upstream or downstream of ASC speck formation. To test whether there is cross talk upstream of ASC speck formation co-immunoprecipitation assays were conducted using anti-ASC, anti-CARD9 and anti-SYK antibodies as bait. In this set of experiments, SYK was chosen due its reported relevance in both NLRP3 inflammasomes and CARD9 signalling (Gross et al., 2009; Hara et al., 2013).

WT BMDMs were primed with LPS (200 ng/mL for 3 hours) and infected with *S.* Typhimurium (MOI 10, 30 minutes) or stimulated with nigericin (10 μM, 30 minutes), and after successive washes in cold PBS, the cells were fixed in 5 mM DTBP for 30 minutes to

preserve labile protein-protein interactions. After fixation, the cells were lysed, and the protein lysate was incubated with protein A/G agarose beads with one of the “bait” antibodies, anti-SYK, anti-CARD9 or anti-ASC. After overnight incubation, the beads were washed, the proteins eluted and subjected to immunoblotting. The protein lysates pre-incubated with the agarose beads were also subjected to immunoblotting, to confirm that the protein input was similar in all treatments.

The co-immunoprecipitations revealed that SYK interacts (directly or indirectly) with both ASC and CARD9 in unstimulated cells, but no evidence of ASC and CARD9 interaction was observed (Figure 4.17, Appendix 1-3). After *S*. Typhimurium infection or nigericin treatment, ASC interacted preferentially with phosphorylated SYK (p-SYK) as previously described (Lin et al., 2015). CARD9, however, appears to interact preferably with unphosphorylated SYK after infection or nigericin stimulation (Figure 4.17, Appendix 1-3). These co-immunoprecipitation patterns further suggest that CARD9 does not interact directly with ASC, and its inhibitory role occurs upstream ASC speck formation. One possibility is that CARD9 interacts with SYK. Since the CARD9/SYK/p-SYK interactions changes whether the inflammasome is stimulated or not, it is feasible that SYK is somehow involved in the CARD9 regulation of the NLRP3 inflammasome. This possibility will be explored later in this thesis.

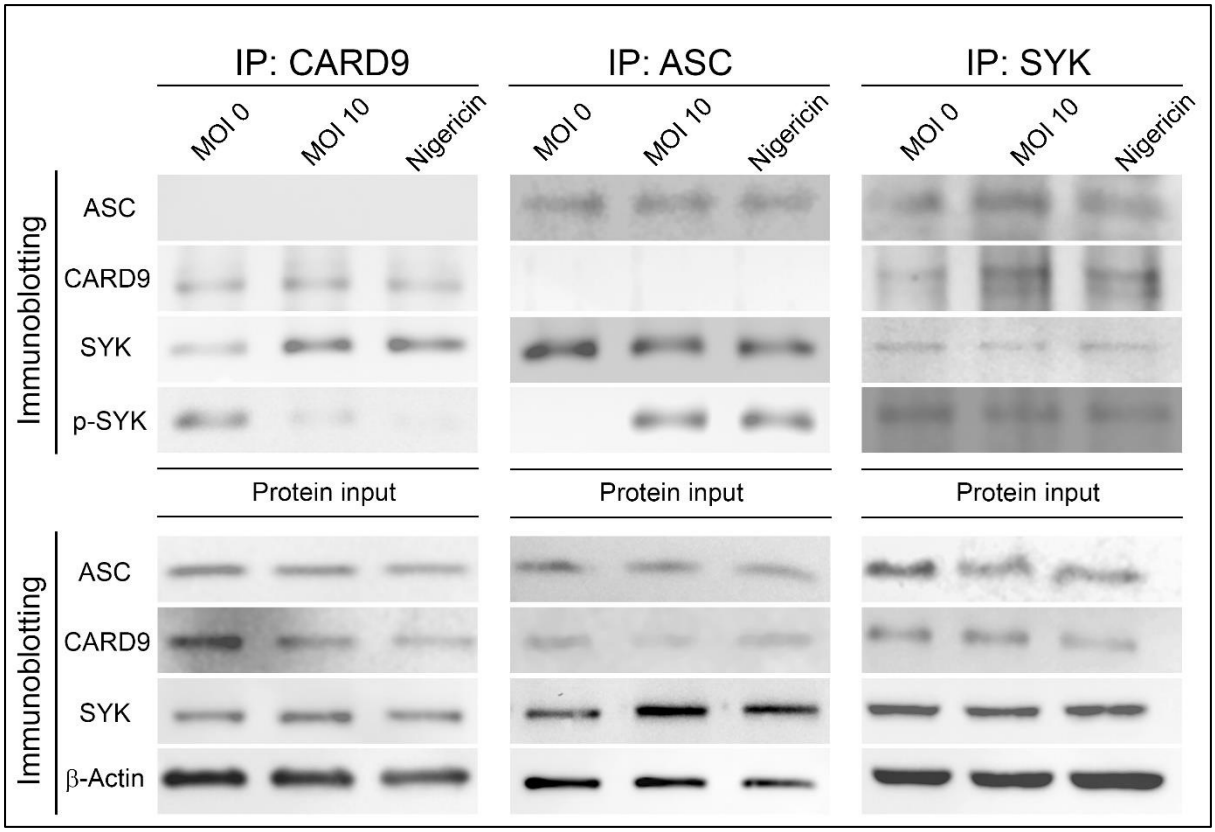

Figure 4.17: Co-immunoprecipitation assays shows no evidence of association between ASC and CARD9, while different phosphorylation states of SYK affects its interaction with both proteins. Co-immunoprecipitation of ASC, CARD9 and SYK from cell lysates of uninfected, *S*. Typhimurium-infected (MOI 10, 30min) or nigericin-stimulated (10 μM, 30min) LPS-primed BMDMs (200 ng/mL for 3 hours). Image representative of three independent experiments.

As an additional control for the co-immunoprecipitation assays, protein lysates extracted from *Card9*$^{-/-}$ and *Pycard*$^{-/-}$ BMDMs were subjected to co-immunoprecipitation using as bait CARD9 and ASC antibodies respectively. Briefly, CARD9 knockout BMDMs were primed with LPS, and then stimulated with *S.* Typhimurium at MOI 10 or nigericin. The cells were then washed, fixed with DTBP, lysed, and the protein lysate was subjected to co-immunoprecipitation using anti-CARD9 as bait. Immunoblot of the proteins eluted from the agarose beads failed to detect ASC, CARD9 or SYK. This indicates that the co-immunoprecipitations discussed on Figure 4.17 are not due to non-specific interactions with the antibody. Similar results were obtained using *Pycard*$^{-/-}$ BMDMs and anti-ASC as bait (Figure 4.18, Appendix 4).

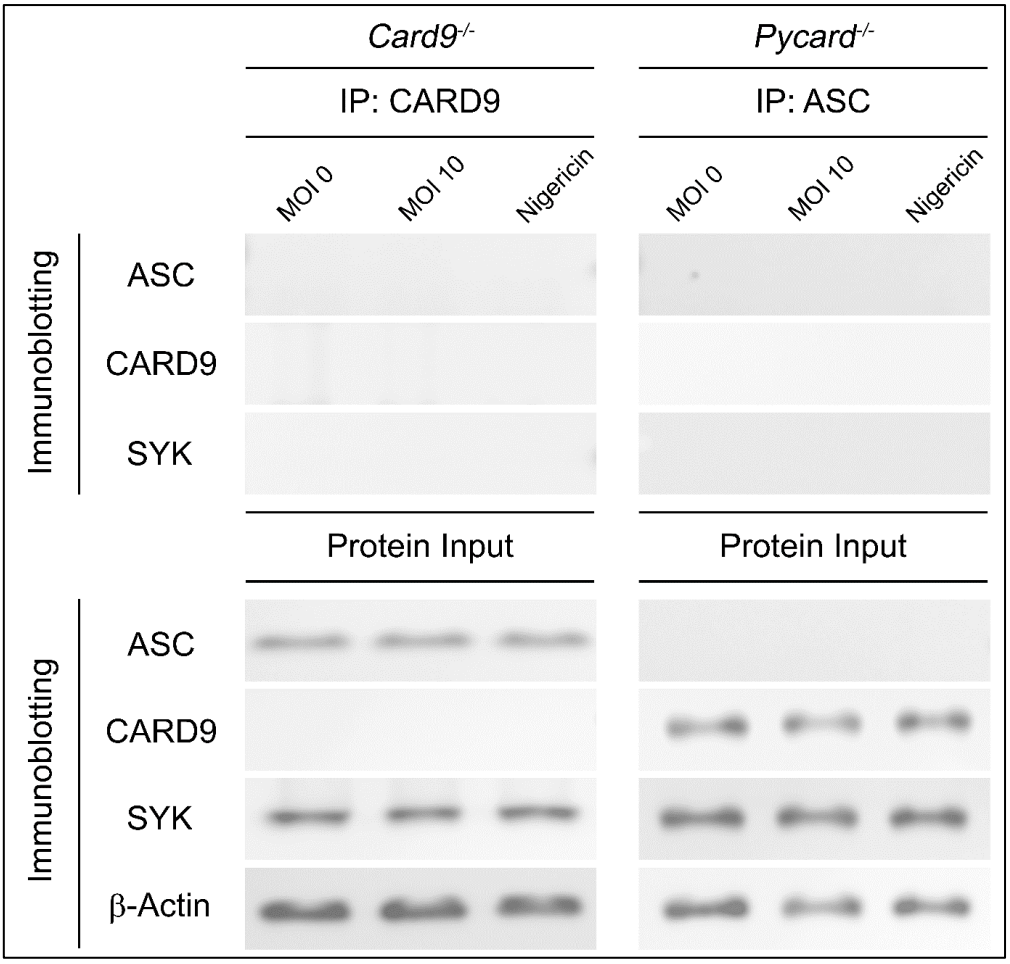

Figure 4.18: Knockout controls for the co-immunoprecipitation assays reveals no unspecific immunoprecipitation. Immunoprecipitation of CARD9 from *Card9*$^{-/-}$ and immunoprecipitation of ASC from *Pycard*$^{-/-}$ cell lysates of uninfected, *S*. Typhimurium-infected (MOI 10, 30min) or nigericin-stimulated (10 mM, 30min) LPS-primed BMDMs (200 ng/mL for 3 hours). Image representative of three independent experiments.

Since CARD9 does not co-localize with the ASC speck, it is likely that its role as a negative regulator of inflammasome activation occurs upstream of speck formation. One possibility is that absence of CARD9 increases ROS-mediated activation of the NLRP3 inflammasome (Cruz et al., 2007). This hypothesis however is not consistent with previous reports, as CARD9 knockout BMDMs have lower ROS production in response to intracellular bacteria such as *L. monocytogenes* and *E. coli* (Wu et al., 2009). The study in question however has not analysed ROS production by BMDMs in response to *S.* Typhimurium, prompting me to repeat their ROS experiments and include *S*. Typhimurium infection.

WT and *Card9*$^{-/-}$ BMDMs were seeded in opaque plates, and after washes with DPBS^{+} buffer, the cells were stimulated with 100 µg/mL zymosan, *L. monocytogenes* at MOI 50 or *S.* Typhimurium at MOI 50. Luminescence produced by luminol oxidation was followed as a readout of ROS produced by the cells. The luminescence was monitored in real time for a period 120 minutes.

ROS production in WT and *Card9*$^{-/-}$ BMDMs upon zymosan stimulation was similar throughout the experiment (Figure 4.19 a-b). *Card9*$^{-/-}$ macrophages, however, had impaired ROS production during *L. monocytogenes* infection for most of the time course (Figure 4.19 c-d). Similar to *L. monocytogenes* infection, *Card9*$^{-/-}$ BMDMs showed substantial impairment in ROS production during *S.* Typhimurium infection (Figure 4.19 e-f). These results are in agreement with previous publication (Wu et al., 2009), and since ROS production is impaired in CARD9 knockout macrophages, it unlikely that ROS production is the mechanism for increased NLRP3-mediated IL-1β production in *Card9*$^{-/-}$.

CARD9 is a regulator of the NF-κB pathway under specific conditions and in certain cell types (Bertin et al., 2000). It is possible, therefore, that the CARD9 effect observed in NLRP3-mediated IL-1β production is attributable to an increase in pro-IL-1β expression. To investigate whether *Card9*$^{-/-}$ BMDMs produce more pro-IL-1β that the WT controls, immunoblot analysis of uninfected cells was conducted. Briefly, protein lysates were prepared from WT, *Card9*$^{-/-}$ and *Pycard*$^{-/-}$ BMDMs and immunoblots were probed with antibodies raised against pro-IL-1β, SYK, caspase-8, CARD9 and ASC. Uninfected cells had similar expression levels of pro-caspase-1, pro-caspase-8 and SYK, while pro-IL-1β was undetectable by immunoblotting in all three mouse lines. As expected, ASC is not expressed in *Pycard*$^{-/-}$ and is expressed at similar levels in WT and CARD9 knockouts. Similarly, CARD9 is not expressed in *Card9*$^{-/-}$ and expressed at similar levels in WT and *Pycard*$^{-/-}$ BMDMs (Figure 4.20, Appendix 5). Furthermore, the pool of pro-caspase-1 and pro-caspase-8 are similar in all BMDMs strains, with no detectable active caspase-1 or -8. This suggests that CARD9 does not alter the level of pro-IL-1β protein expression in unstimulated cells, and whatever differences observed in IL-1β production and caspase activity upon inflammasome activation occur during the inflammasome activation process.

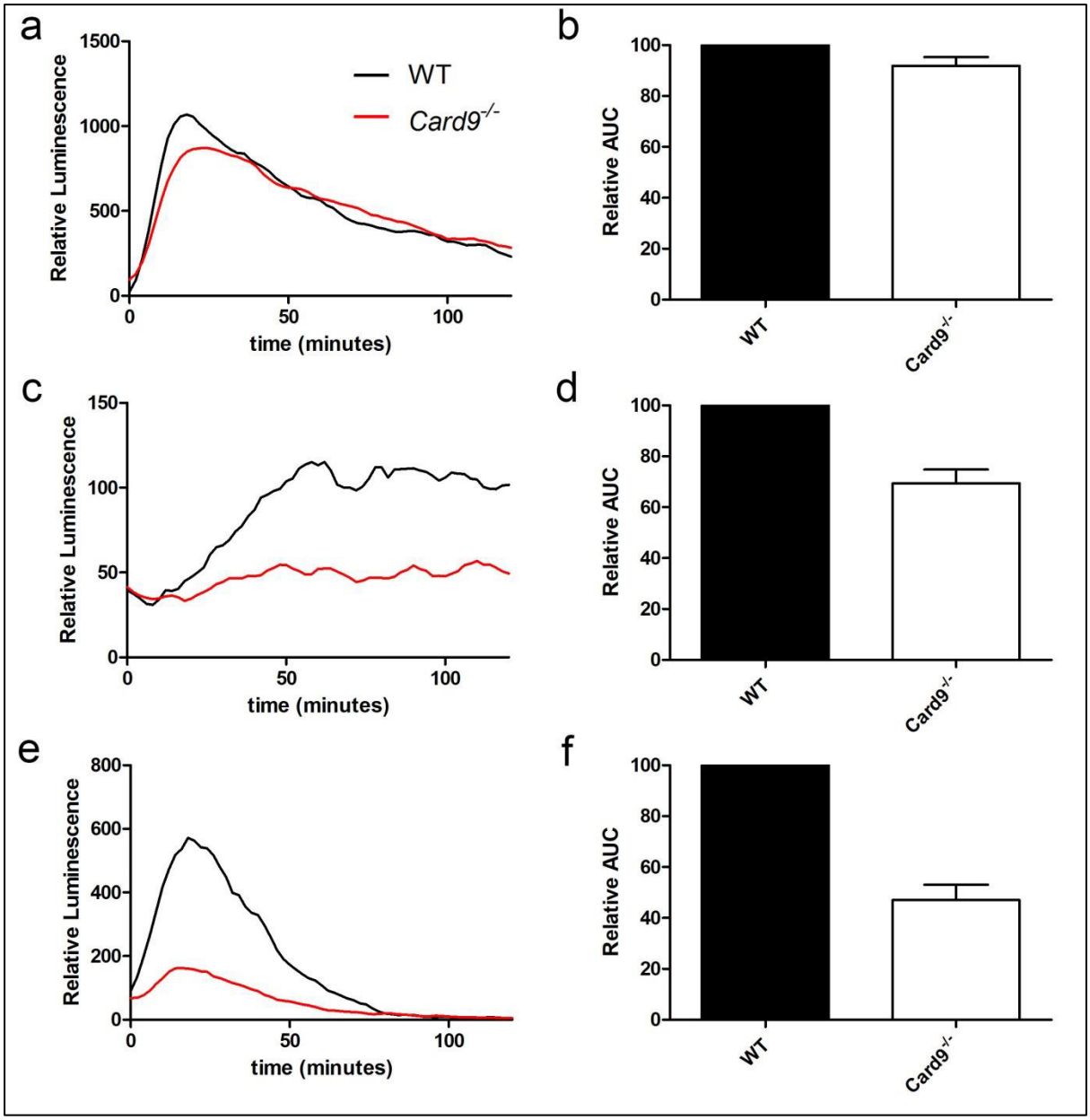

Figure 4.19: CARD9 is required for ROS production in BMDMs during infection with *S.* Typhimurium SL1344, *L. monocytogenes* but not in BMDMs stimulated with zymosan. (a,c,e) ROS production and area under the curve (AUC) in relation to WT (b, d, f) in BMDMs stimulated with (a, b) Zymosan 100 µM or (c, d) infected with *L. monocytogenes* at MOI 50 or (e, f) *S.* Typhimurium at MOI 50. Images (a), (c) and (e) are representative of four independent experiments. Data from (b), (d) and (f) represent the mean from four independent experiments while error bars show the s.e.m.

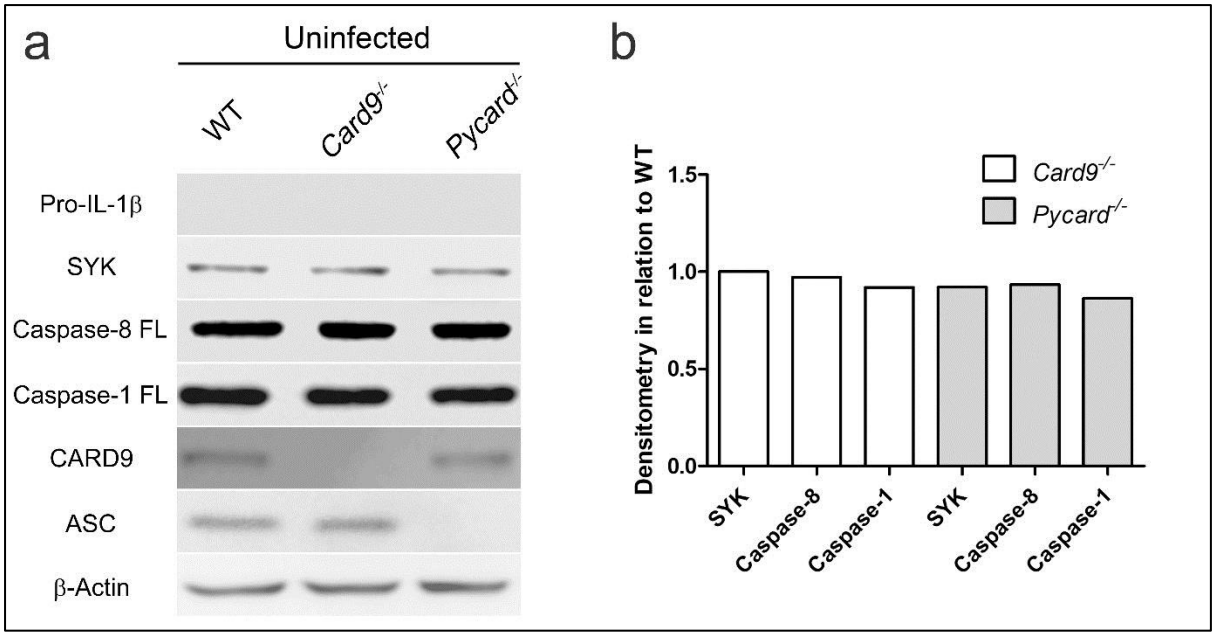

Figure 4.20: Immunoblot analysis of WT, *Card9*$^{-/-}$ and *Pycard*$^{-/-}$ BMDMs reveals similar expression levels in uninfected BMDMs. Uninfected BMDMs were lysed and probed for Pro-IL-1β, SYK, Caspase-8 full length, Caspase-1 full length, CARD9, ASC and β-Actin. Immunoblot (a) and its densitometry in relation to WT (b). Image and densitometry are representative of three independent experiments.

To test whether CARD9 influences protein expression upon infection, immunoblotting analysis of WT, *Card9*$^{-/-}$ and *Pycard*$^{-/-}$ unprimed BMDMs infected with *S*. Typhimurium at MOI 5 for 2 and 6 hours was performed. This MOI was chosen to avoid excessive cell death as viable cells are required for subsequent protein analysis. In addition, analysis of proteins present in the supernatant was undertaken to one, confirm the ELISA data regarding the IL-1β increase in *Card9*$^{-/-}$ BMDMs, and second, to study the pattern of caspase-1 and caspase-8 activation.

Upon *Salmonella* infection, an increase in IL-1β in the supernatant was observed in WT and *Card9*$^{-/-}$, while *Pycard*$^{-/-}$ IL-1β production was below detection limit. CARD9 knockout macrophages, as expected, had higher IL-1β levels in the supernatant than the WT control at 2 and 6 hours post-infection. In the cell lysate fraction, a small increase in pro-IL-1β was observed in *Card9*$^{-/-}$ BMDMs in comparison to both WT and *Pycard*$^{-/-}$ controls. This suggests that increased expression is a potential mechanism for the IL-1β increase observed in CARD9 knockout macrophages. Interestingly, the cell lysate fraction also revealed a small increase in SYK and pro-caspase-8 expression, proteins known to be important both in

inflammasome biology and CARD9 signalling (Gringhuis et al., 2012; Gurung et al., 2014; Hara et al., 2013; Man et al., 2013; Underhill et al., 2005). A small increase in caspase-8 was observed in the supernatant of *Card9*$^{-/-}$ BMDMs in comparison to WT and ASC knockout macrophages. Caspase-1 in the supernatant and pro-caspase-1 in the cell lysate were found to be expressed at similar levels in WT and *Card9*$^{-/-}$ BMDMs. This finding is in accordance with the cell viability data where this parameter is found to be similar in most MOIs and time points between the two mouse lines (Figure 4.21, Appendix 6-8).

This set of immunoblots reveals that the differences between *Salmonella*-infected WT and *Card9*$^{-/-}$ occur in IL-1β production and possibly in pro-IL-1β expression as well. The increase in active caspase-8 in the supernatants of CARD9 knockout macrophages suggests increased activity of this enzyme, which could contribute to the enhanced IL-1β production. Equally, the possible differences in pro-IL-1β, SYK and caspase-8 expression suggests that CARD9 can act at the transcriptional level. These possible mechanisms are going to be further investigated in the next chapter of this thesis.

To further characterize this response, *in vivo* systemic infection assays were conducted in WT and *Card9*$^{-/-}$ C57BL/6 mice using a sub-lethal *S*. Typhimurium infection model with the strain M525P. At days 1, 3 and 7 post-infection, the liver and spleen microbial load showed no statistically significant difference between the mouse lines (Figure 4.22). Failure to demonstrate overall differences in bacteria burden in *Card9*$^{-/-}$ in this infection model does not rule out that CARD9 plays a regulatory role in context of bacterial infections *in vivo*, so I decided to focus on IL-1β analysis as a readout for inflammasome activation. Unfortunately, ELISA analysis of serum failed to detect IL-1β in any of the animals. This is consistent with other published studies, where the authors were unable to detect IL-1β in the serum of infected WT animals (Broz et al., 2010).

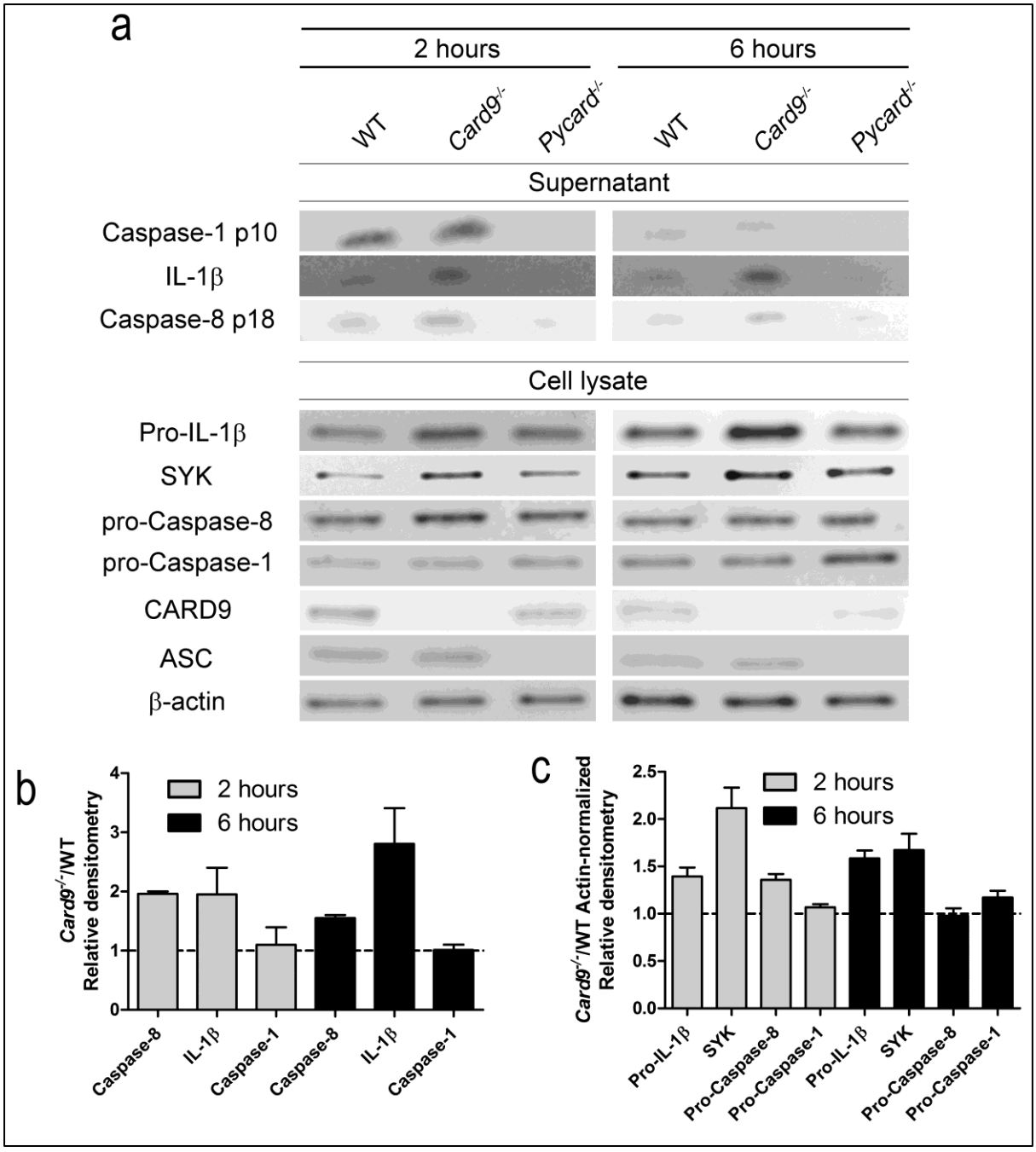

Figure 4.21: Immunoblot analysis of WT, *Card9*$^{-/-}$ and *Pycard*$^{-/-}$ BMDMs reveals differential expression levels after BMDMs infection in both the cell lysates and culture supernatants. BMDMs from WT, *Card9*$^{-/-}$ and *Pycard*$^{-/-}$ mice were infected with *S.* Typhimurium at MOI 5 for 2 and 6 hours, lysed and probed for Pro-IL-1β, SYK, Caspase-8, Caspase-1, CARD9, ASC and β-Actin and the supernatant was precipitated and probed for IL-1β, Caspase-1 and Caspase-8. (a) Immunoblot and (b) densitometric analysis in the culture supernatants (b) and cell lysates (c). Image (a) is representative of three independent experiments. Data from (b) and (c) are from three independent experiments (mean and s.e.m.).

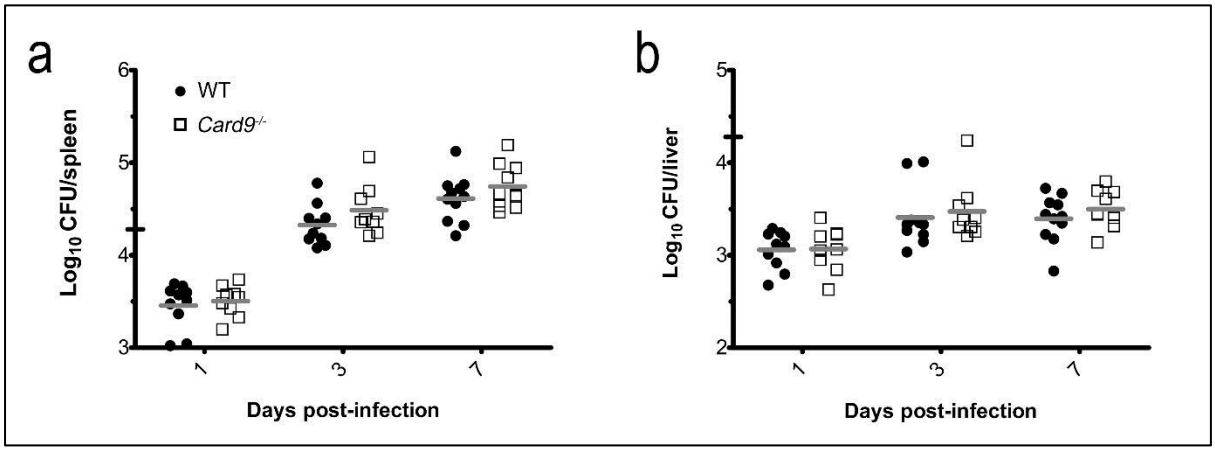

Figure 4.22: *S*. Typhimurium-infected WT and *Card9*$^{-/-}$ mice have similar bacteria burden in spleen and liver. Bacteria burden in the spleen (a) and liver (b) after C57BL/6 WT and *Card9*$^{-/-}$ infection with *S*. Typhimurium M525P strain (1.90 to 2.02 x10^4 CFU/mouse). p>0.05 unpaired t-test. Data represent the mean from two independent experiments using four to six mice per genotype, plus two negative controls per genotype, while error bars show the s.e.m.

Due to the technical difficulty in detecting IL-1β in animal serum by ELISA, I performed immunoblotting analysis of splenocyte populations pooled from the different mice. On days 1, 3 and 7 post infections, spleens were excised and the heterogenous spleen cell population was harvested. After extensive washes, the cells were lysed, and the protein sample was subjected to immunoblotting and probed for pro-IL-1β and caspase-1. At day 7 post-infection, immunoblot analysis revealed an increase in pro-IL-1β expression in *Card9*$^{-/-}$ mice splenocytes, whereas no significant differences were observed with regards to caspase-1 full length or p10 fragment (Figure 4.23, Appendix 9). Again, no mature IL-1β was detected by this method, probably due the relative low concentration of this protein in the sample.

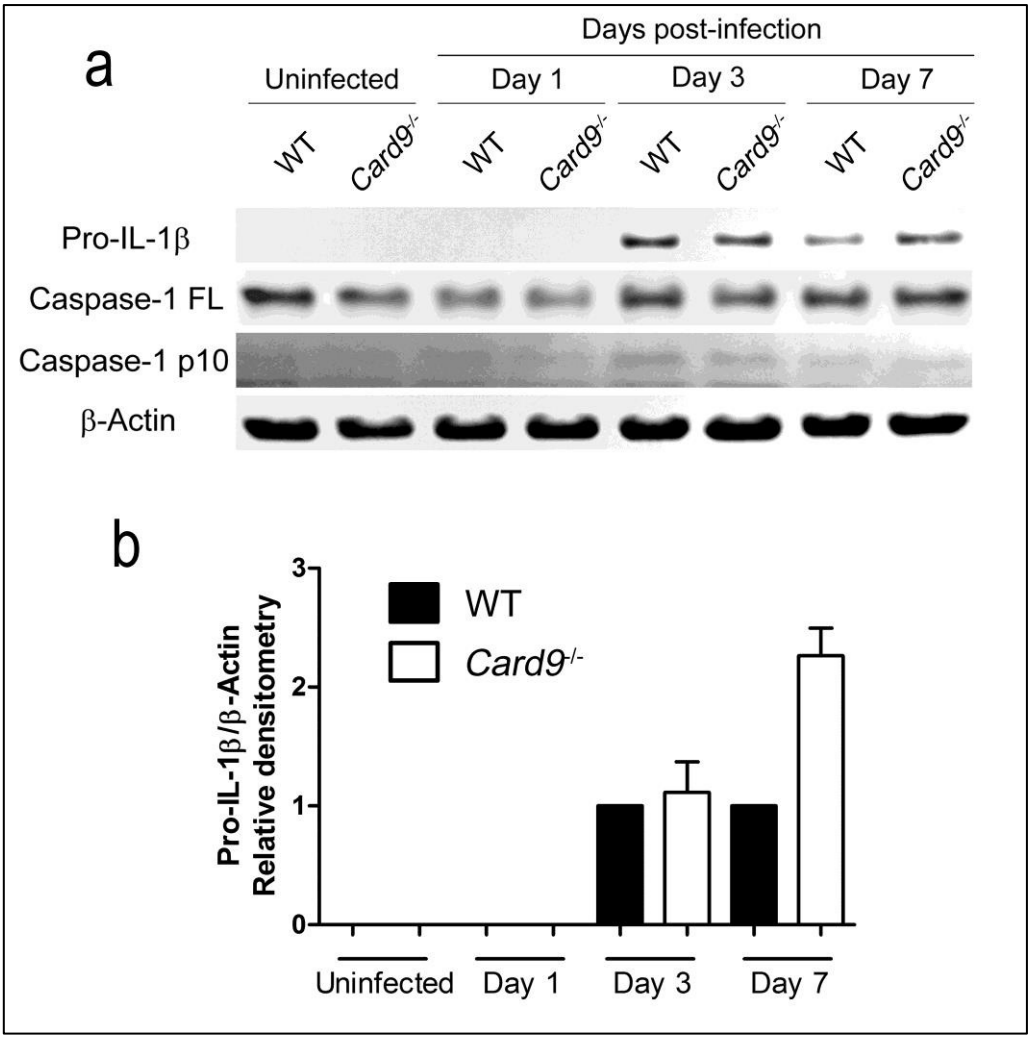

Figure 4.23: CARD9 is involved in Pro-IL-1β production in spleen cells derived from *S.* Typhimurium-infected mice. (a) Immunoblot analysis of pro-IL-1β, caspase-1 and β-actin in spleen cells isolated from infected WT and *Card9*$^{-/-}$ C57BL/6 mice after intravenous infection with *S*. Typhimurium M525P (1.90 to 2.02 x10^4 CFU/mouse) and pro-IL-1β/β-Actin densitometric analysis in relation to WT (b). (a) Representative immunoblot from two independent experiments, using cells pooled from four to six mice per genotype, plus two negative controls per genotype. Mice were from 8 to 16 weeks old, both male and female. (b) Data represent the mean from two independent experiments while error bars show the s.e.m.

Even though IL-1β detection by ELISA in the serum is problematic, the detection of this cytokine *in vivo* has been previously reported using organ homogenates (Yang et al., 2015). Encouraged by such reports, I tried to detect IL-1β by ELISA of spleen homogenates. IL-1β detection from spleen homogenates gave a clean data set. In spleen homogenates, IL-1β production was enhanced at day 3 and 7 post-infection in both WT and *Card9*$^{-/-}$ animals. At day 7, a visual increase in IL-1β production in *Card9*$^{-/-}$ in relation to WT was observed. This difference however was not statistically significant (p = 0.0519, unpaired t-test) (Figure 4.24).

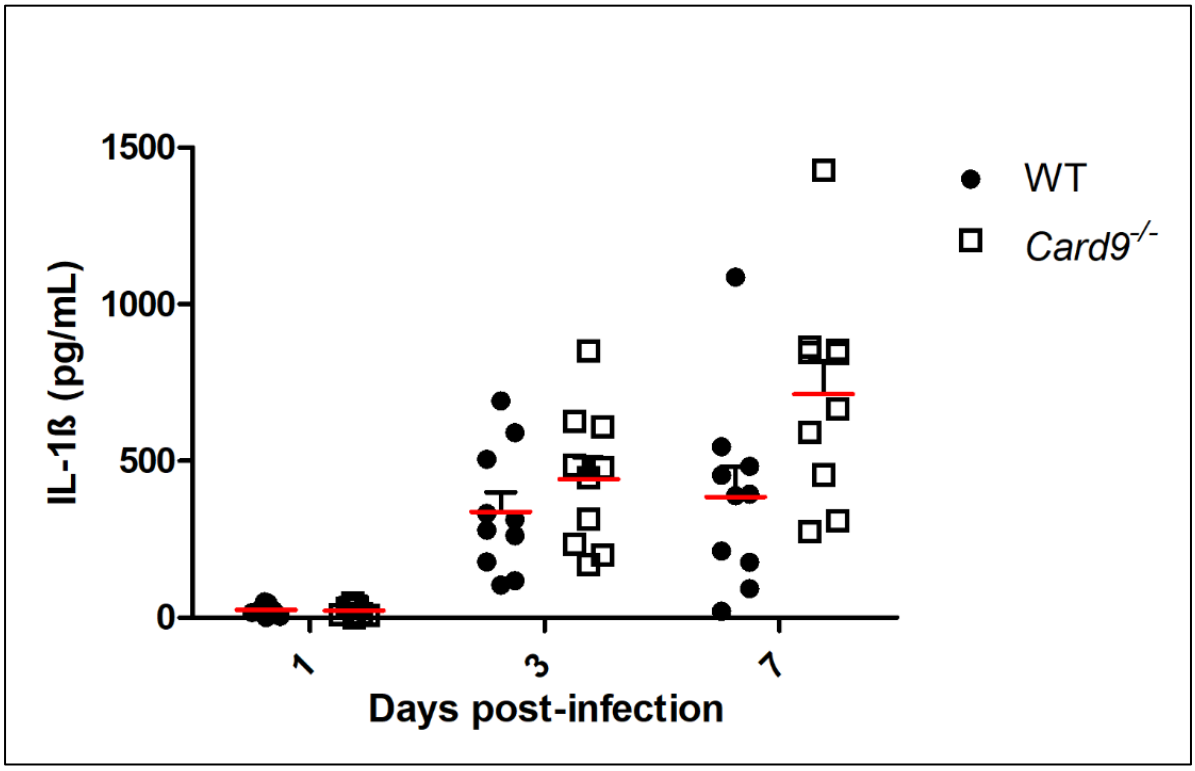

Figure 4.24: IL-1β in spleen homogenates of *S.* Typhimurium-infected WT and *Card9*$^{-/-}$ mice. IL-1β quantified by ELISA in spleen homogenates of C57BL/6 WT and *Card9*$^{-/-}$ mice infected with *S.* Typhimurium M525P (1.90 to 2.02 x10^4 CFU/mouse), at days 1, 3 and 7 post-infection. p>0.05 unpaired t-test. Data represent the mean from two independent experiments using four to six mice per genotype, plus two negative controls per genotype, while error bars show the s.e.m.

4.3. Discussion

Upon *in vitro Salmonella* infection the level of IL-1β produced by *Card9*$^{-/-}$ BMDMs under certain conditions, is approximately four times higher than that observed in WT macrophages, without accompanying increase in cellular viability, intracellular bacteria or TNF-α production (Figure 3.24-25). This role for CARD9 as a negative regulator of inflammasome activity was surprising, as most of the biological functions thus far reported for CARD9 place this protein as a key-adaptor in the positive regulation of inflammatory responses such as NF-κB signalling, ROS production and noncanonical caspase-8 assembly (Bertin et al., 2000; Gringhuis et al., 2012; Wu et al., 2009). *In vivo*, no effect of CARD9 was observed in bacteria burden in the liver and spleen when compared to WT controls, but a visual, albeit not statistically significant, increase in IL-1β is observed in *Card9*$^{-/-}$ spleen homogenates and a statistically significant increase in pro-IL-1β in splenocytes are observed, indicating that this finding could be potentially relevant at the organism level (Figure 4.22-24). As the work presented in this chapter was being concluded, researchers reported increased *Il1b* transcription in the gut upon colitis induction in *Card9*$^{-/-}$ mice in relation to WT controls. Since the microbiota plays an essential role in colitis pathophysiology, their findings further substantiate the notion that CARD9 is capable of decreasing IL-1β production *in vivo* (Lamas et al., 2016).

In this chapter, my goal was to elucidate which inflammasome(s) are regulated by CARD9 upon *Salmonella* infection and to investigate the mechanisms involved in this regulation. *S.* Typhimurium infection is known to primarily activate two NLRs, NLRC4 and NLRP3 (Broz et al., 2010; Man et al., 2014). *In vitro*, NLRC4 is activated by the bacteria during the early stages of infection (Man et al., 2014), making it the most likely target for the observed CARD9 negative regulation on IL-1β, as this effect is observed as early as 2 hours post-infection. Surprisingly, careful experimentation revealed that CARD9 has no effect on NLRC4 activation, either by flagellin transfection or by analysing the IL-1β production profile upon infection with *S.* Typhimurium SL1344 Δ*fliC*Δ*fljB*Δ*prgJ*, which is deficient in NLRC4 activation (Figure 4.3-4). Alternatively, the CARD9 effect could occur by negative modulation of the dectin-1 pathway or the AIM2 inflammasome, as dectin-1 is a potential Salmonella PRR and AIM2 is capable of recognizing bacterial DNA (Jackson et al., 2014; Rathinam et al., 2010; Warren et al., 2010). Both these possibilities were unlikely, as *S*. Typhimurium is not known to engage these pathways, and upon experimentation these possibilities were discarded (Figure 4.5-7).

It is possible that the effects of CARD9 on *Salmonella*-induced inflammasome activity may be indirect, for example, by regulating the autocrine production of anti-inflammatory

cytokines such as IL-10, which is reduced in *Card9*$^{-/-}$ neutrophils infected with *M. tuberculosis* (Dorhoi et al., 2010). An IL-10-mediated effect of CARD9 on *Salmonella*-induced IL-1β production from BMDMs, however, is unlikely as elevated IL-1β production occurs within the first 2 hours of infection, whereas IL-10 production occurs at later time-points in the infection (Foster et al., 2008). Nonetheless, this possibility was not formally addressed.

The NLRC4-independent increase in IL-1β production in *Card9*$^{-/-}$ macrophages could potentially be explained by CARD9 fine-tuning the NLRP3 inflammasome activity. Infection of WT and CARD9 knockout primary macrophages in the presence of the NLRP3 inhibitors glibenclamide or MCC950 appeared to support a role for CARD9 in NLRP3 activation. Upon infection in the presence of these inhibitors, the level of IL-1β production is decreased in *Card9*$^{-/-}$ BMDMs to the level observed in WT cells. Interestingly, these inhibitors failed to decrease the IL-1β production in WT cells at these time-points (Figure 4.8-9), possibly because in WT cells infected with *S.* Typhimurium *in vitro*, the NLRP3 inflammasome is engaged at later time-points and as a consequence the inhibitors have no effect early in the infection (Man et al., 2014). This timing indicates that CARD9 absence decreases the NLRP3 activation-threshold possibly by influencing the "signal 1" required for NLRP3 activation, either by controlling transcription events or by regulating non-transcriptional priming of the NLRP3 inflammasome.

Although NLRP3 expression is induced upon infection (Bauernfeind et al., 2009), its basal expression levels in unprimed macrophages is, however, not negligible (Heng and Painter, 2008; Hoffman et al., 2001). Thus, an early response of the NLRP3 inflammasome could not be ruled out based on expression levels alone. The use of an alternative pathogen capable of activating the NLRP3 inflammasome early in the infection further corroborates these findings. *E. coli* is a gram-negative bacteria reported to activate the NLRP3 inflammasome (Brereton et al., 2011) and in this chapter it was found that the pathogenic strain P19A triggers cell death and IL-1β production in unprimed macrophages independent of NLRC4 and dependent of NLRP3 as early as 2 hours post-infection (Figure 4.12). Infection of WT and *Card9*$^{-/-}$ BMDMs using this *E. coli* strain further consolidates the observation that CARD9 negatively regulates IL-1β production via the NLRP3 inflammasome and importantly, this effect is not exclusive to *Salmonella* infections and could be a general theme in the innate immune response against gram-negative bacteria (Figure 4.13-14).

Investigation of the link between CARD9 and NLRP3 in LPS-primed macrophages supports the overall conclusions discussed above. Stimulation of the canonical NLRP3 inflammasome with nigericin or ATP revealed increased IL-1β production in *Card9*$^{-/-}$ BMDMs in comparison

to WT or *Nlrp3*$^{-/-}$ controls (Figure 4.10-11). These experiments are important not only for supporting the previous CARD9/NLRP3 conclusions but also for suggesting that the mechanism involved occurs not only at the transcriptional "signal 1", and CARD9 potentially affects "signal 2" as well. Priming with LPS in these conditions presumably stimulates pro-IL-1β production and NLRP3 priming at similar rates in WT and *Card9*$^{-/-}$ BMDMs, thus the increased IL-1β secretion observed in CARD9 knockouts are due a more efficient pro-IL-1β to IL-1β catalysis. The "signal 2" hypothesis as well as the assumption that pro-IL-1β levels are similar in both cell strains after LPS-priming are going to be formally addressed in the next chapter.

Next, I started investigating possible mechanism(s) for the inhibitory function that CARD9 has on IL-1β production. Previously described negative regulators of inflammasome activity perform their inhibitory functions by multiple mechanisms, including direct inhibition in the ASC speck, inhibition of transcriptional events, and by modulation of PTMs important in NLRP3 biology (Hernandez-Cuellar et al., 2012; Mishra et al., 2012; Walle et al., 2014; Yang et al., 2015). My first approach was to investigate if CARD9 can physically interact with the ASC speck. Upon stimulation of LPS-primed BMDMs with nigericin, immunofluorescence microscopy revealed that CARD9 and ASC do not co-localize in the inflammasome speck (Figure 4.15). Co-immunoprecipitation assays appear to confirm this finding, as no interaction between ASC and CARD9 was found in my experimental settings. Interestingly however, SYK co-immunoprecipitated with both ASC and CARD9 in untreated cells, while after treatment with nigericin or infection with *S*. Typhimurium ASC interacted preferentially with p-SYK, while the CARD9/SYK interaction appears to occur preferentially with unphosphorylated SYK (Figure 4.17). The SYK/ASC and SYK/CARD9 interactions are not totally unexpected, as this kinase is known to be involved in NLRP3 inflammasome biology and CARD9 signalling (Gross et al., 2009; Hara et al., 2013; Lin et al., 2015), but they hint to a possible mechanism: after infection or stimulation with nigericin, SYK is phosphorylated and activated, catalysing ASC phosphorylation in the context of NLRP3 inflammasome activation. The preferential interaction of CARD9 with SYK here suggests that CARD9 can act by inhibiting SYK phosphorylation and consequentially CARD9 absence can increase NLRP3-inflammasome activity.

ROS production by NADPH oxidase is a mechanism involved in activation of the NLRP3 inflammasome (Cruz et al., 2007; Dostert et al., 2008; Hewinson et al., 2008), thus increased ROS in *Card9*$^{-/-}$ could potentially explain the increased IL-1β production in this strain upon *Salmonella* infection. The literature, however, suggests that upon intracellular bacteria challenge, CARD9 plays a role in stimulating NADPH oxidase thus increasing ROS

production, with CARD9 knockout macrophages producing less ROS than WT controls (Wu et al., 2009). The study in question did not include ROS-quantification experiments using *S.* Typhimurium specifically, so the ROS/IL-1β hypothesis could not be entirely dismissed based on this study alone. Furthermore, WT and *Card9*$^{-/-}$ ROS quantification upon *S.* Typhimurium challenge revealed that CARD9 knockout BMDMs have deficient ROS production in comparison to WT, similar to what is observed in *L. monocytogenes* (Figure 4.19) (Wu et al., 2009). In summary, since ROS production in CARD9 knockout BMDMs is deficient, it is unlikely that ROS is the mechanism involved in the increased NLRP3-dependent IL-1β production in *Card9*$^{-/-}$.

How then does CARD9 inhibit the NLRP3 inflammasome? It is possible that CARD9 knockout BMDMs have a higher pro-IL-1β expression even in unstimulated cells. This is unlikely to be the case, as the concentration of this pro-cytokine was below the detection limit in WT and *Card9*$^{-/-}$ BMDMs (Figure 4.20). Upon *Salmonella* infection however, CARD9 knockout macrophages express more pro-IL-1β than the WT cells and the amount of IL-1β in the supernatant was also higher in *Card9*$^{-/-}$ BMDMs. This is not caused by increase in active caspase-1, as shown by the presence of similar levels of the caspase-1 p10 fragment in the supernatant of both cell types (Figure 4.21). The lack of increase in active caspase-1 is consistent with the *in vivo* immunoblots presented in figure 4.23, where no increase in caspase-1 FL nor p10 fragment are observed, and consistent with the cell viability data, where the cell death in WT and CARD9 knockout is similar in most conditions (Figure 3.24). The immunoblot in figure 4.21 revealed a slight increase in pro-caspase-8 in infected *Card9*$^{-/-}$ BMDMs, as well as increased caspase-8 in the supernatant. This finding is particularly intriguing, as caspase-8 was described as having a complementary role in IL-1β production in the NLRP3 inflammasome, without affecting pyroptosis (Gurung et al., 2014; Man et al., 2013), making this enzyme a candidate for explaining the observed CARD9 phenotype. SYK, another enzyme known to be involved in NLRP3 inflammasome and CARD9 signalling (Gross et al., 2009; Hara et al., 2013) was also found to be marginally upregulated (Figure 4.21). The significant of these findings are going to be further explored in the next chapter.

In summary, the work presented in this chapter has established CARD9 as an inhibitor of NLRP3-mediated IL-1β production in primary macrophages (Figure 4.25). The possible mechanisms involved in this inhibition are going to be investigated in further details in the following chapter.

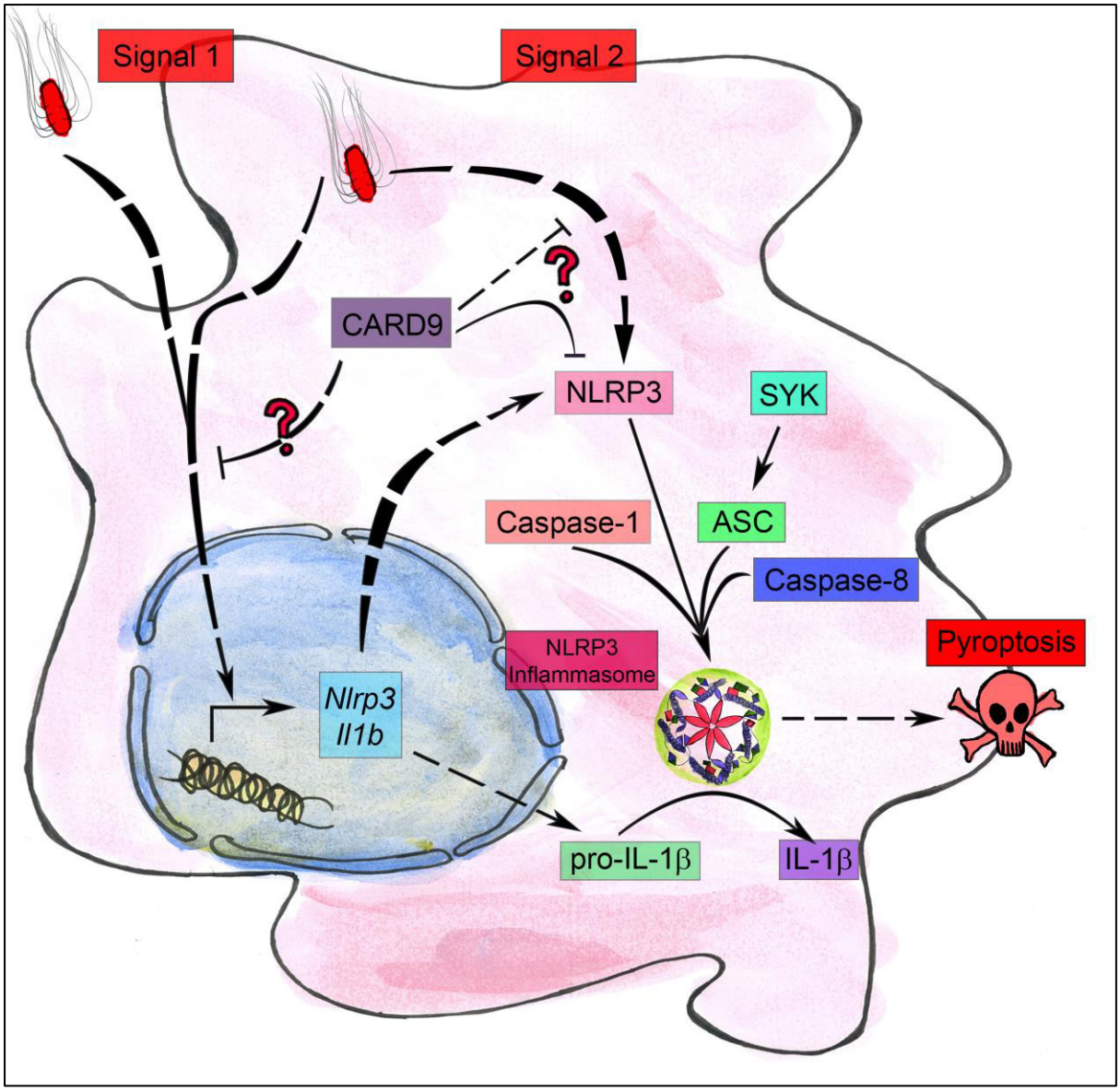

Figure 4.25: CARD9 inhibits NLRP3-dependent IL-1β production. Production of IL-1β triggered by nigericin, ATP and by gram-negative bacteria such as *E. coli* and *S.* Typhimurium is inhibited by CARD9.

Chapter 5

Molecular mechanism for CARD9 regulation of the NLRP3 inflammasome

5.1. Introduction

One of the main features of the NLRP3 inflammasome is the way in which it is activated. In macrophages, *in vitro* inflammasome assembly comprises two distinct steps. First, a priming event "licenses" the NLRP3 inflammasome to respond to DAMPs. This step occurs via upregulation of protein expression of key-components such as NLRP3 itself, as well as post-translational modifications including NLRP3 de-ubiquitination (Bauernfeind et al., 2009; Juliana et al., 2012). Second, a DAMP triggers the assembly of the NLRP3 inflammasome, leading to IL-1β and IL-18 production, as well as pyroptotic cell death (Agostini et al., 2004).

Both steps follow complex signalling events. The licensing step requires the activation of another PRR, such as TLR4, which results in the upregulation of key-genes via NF-κB, as well as relevant post-translational modifications (Bauernfeind et al., 2009; Juliana et al., 2012). The signalling events involved in the second step are less well understood. Little is known about how exactly NLRP3 is activated and the elucidation of the molecular events regulating its activity remains an ongoing task. Amongst the proteins described that modulate NLRP3 inflammasome activity is SYK. This kinase is responsible for phosphorylating ASC at tyrosine 144 in its CARD domain, resulting in enhanced cytokine production (Hara et al., 2013). SYK however is not essential for inflammasome activity, and other kinases such as Pyk2 and BTK were also previously described as possessing similar roles (Chung et al., 2016; Ito et al., 2015).

Once activated, caspase-1 and caspase-8 are recruited to the inflammasome (Agostini et al., 2004; Gurung et al., 2014; Man et al., 2014, 2013). Both enzymes are capable of converting pro-IL-1β to IL-1β, whereas only caspase-1 is involved in the production of IL-18 and pyroptosis (Man et al., 2013). It is not clear whether specific conditions can favour the recruitment of one caspase over the other although most experimental evidence points to caspase-1 being the predominant caspase in inflammasome formation (Martinon et al., 2002).

Evidence presented in the previous chapter suggests that CARD9 regulation of NLRP3-mediated IL-1β production could occur at both steps of NLRP3 activation. Protein expression of *Salmonella*-infected BMDMs reveals an increase in pro-IL-1β expression in *Card9*$^{-/-}$ cells, suggestive of a CARD9 role in controlling *Il1b* transcription (Figure 4.23). Furthermore,

nigericin and ATP stimulation experiments revealed that CARD9 inhibits the NLRP3 inflammasome even after LPS-priming (Figure 4.12-13), a situation where pro-IL-1β availability is unlikely to play a role. This suggests that CARD9 may fine-tune the second step of NLRP3 activation.

These two possible mechanisms are not mutually exclusive, as precedent exists in the literature for CARD9 acting in signalling pathways both transcriptionally and non-transcriptionally. For instance, NOD2 stimulation activates the MAPKs p38 and JNK via CARD9 (Hsu et al., 2007), and dectin-1 activation leads to the formation of the CARD9/BCL10/MAL1 complex, responsible for NF-κB activation (Gross et al., 2006). In both cases CARD9 regulates gene transcription. Non-transcriptional signalling events controlled by CARD9 include ROS-production via the NADPH complex (Wu et al., 2009) and non-canonical IL-1β production in the dectin-1 pathway (Gringhuis et al., 2012).

The aim of this chapter is to investigate at which stage(s) of NLRP3 activation CARD9 acts, and to elucidate the possible mechanisms involved in this inhibition. Part of the data presented in this chapter was successfully published (Pereira et al., 2016) (Appendix 18).

5.2. Results

The immunoprecipitation pattern observed in figure 4.19 suggests a possible role of SYK in the enhanced IL-1β production observed in *Card9*$^{-/-}$ BMDMs. In that experiment, it was observed that after inflammasome stimulation, CARD9 interacts with the unphosphorylated form of SYK, whilst p-SYK interacts with ASC, where previous studies have shown it functions in ASC phosphorylation and enhancing cytokine production (Hara et al., 2013; Lin et al., 2015).

To test whether SYK plays a significant role in the *Card9*$^{-/-}$ phenotype, NLRP3 was stimulated in LPS-primed BMDMs by nigericin or infection with *S.* Typhimurium in the presence or absence of the SYK inhibitor R406. Cellular viability and IL-1β in the culture supernatant were quantified. SYK inhibition decreased IL-1β production in both WT and *Card9*$^{-/-}$ BMDMs stimulated with nigericin or infected with bacteria, without affecting cell viability (Figure 5.1). This inhibition was more noticeable in *Card9*$^{-/-}$ BMDMs, and upon SYK inhibition the resulting IL-1β output was similar in WT and CARD9 knockout macrophages. This suggests that the enhanced IL-1β production observed in *Card9*$^{-/-}$ macrophages indeed involves SYK (Figure 5.1).

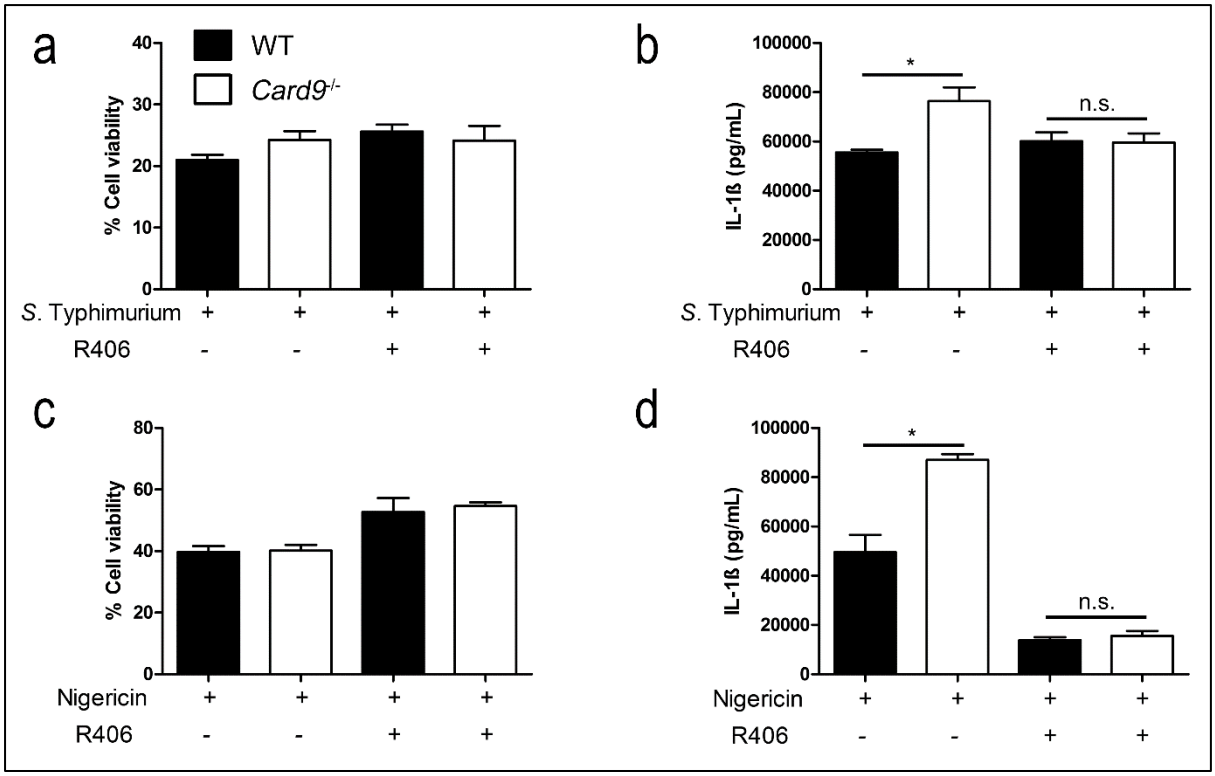

Figure 5.1: SYK is involved in the CARD9 regulation of the NLRP3 inflammasome in BMDMs. LPS-primed BMDMs (200 ng/mL for 3 hours) were infected with *S*. Typhimurium at MOI 10 for one hour (a,b) or stimulated with 5 μM nigericin for one hour (c,d) in presence of SYK inhibitor R406 (1 μM). (a,c) Cellular viability and (b,d) IL-1β production. * $p<0.05$, n.s. Not significant (one-way ANOVA with Tukey's multiple comparisons test). Data represent the mean from three independent experiments while error bars show the s.e.m.

An alternative explanation for this result would be that CARD9 knockout macrophages respond differently to priming with LPS in the conditions used in this thesis, potentially expressing more pro-IL-1β than their WT counterpart. A consequence for this would be increased IL-1β production due to the increase in substrate concentration. To address this possibility, WT and *Card9*$^{-/-}$ BMDMs were primed with 200 ng/mL LPS for 3 hours, then the cells were lysed and the proteins analysed by immunoblot. No significant differences in pro-IL-1β expression were observed between WT and CARD9 knockout BMDMs. The proteins SYK, caspase-1 and caspase-8 were also expressed at similar levels between both cell types upon LPS treatment (Figure 5.2). Since the levels of these proteins are also similar in unprimed cells (Figure 4.22, Appendix 10), it is unlikely that the results obtained from experiments using LPS-primed cells are attributable to differences in pro-IL-1β availability.

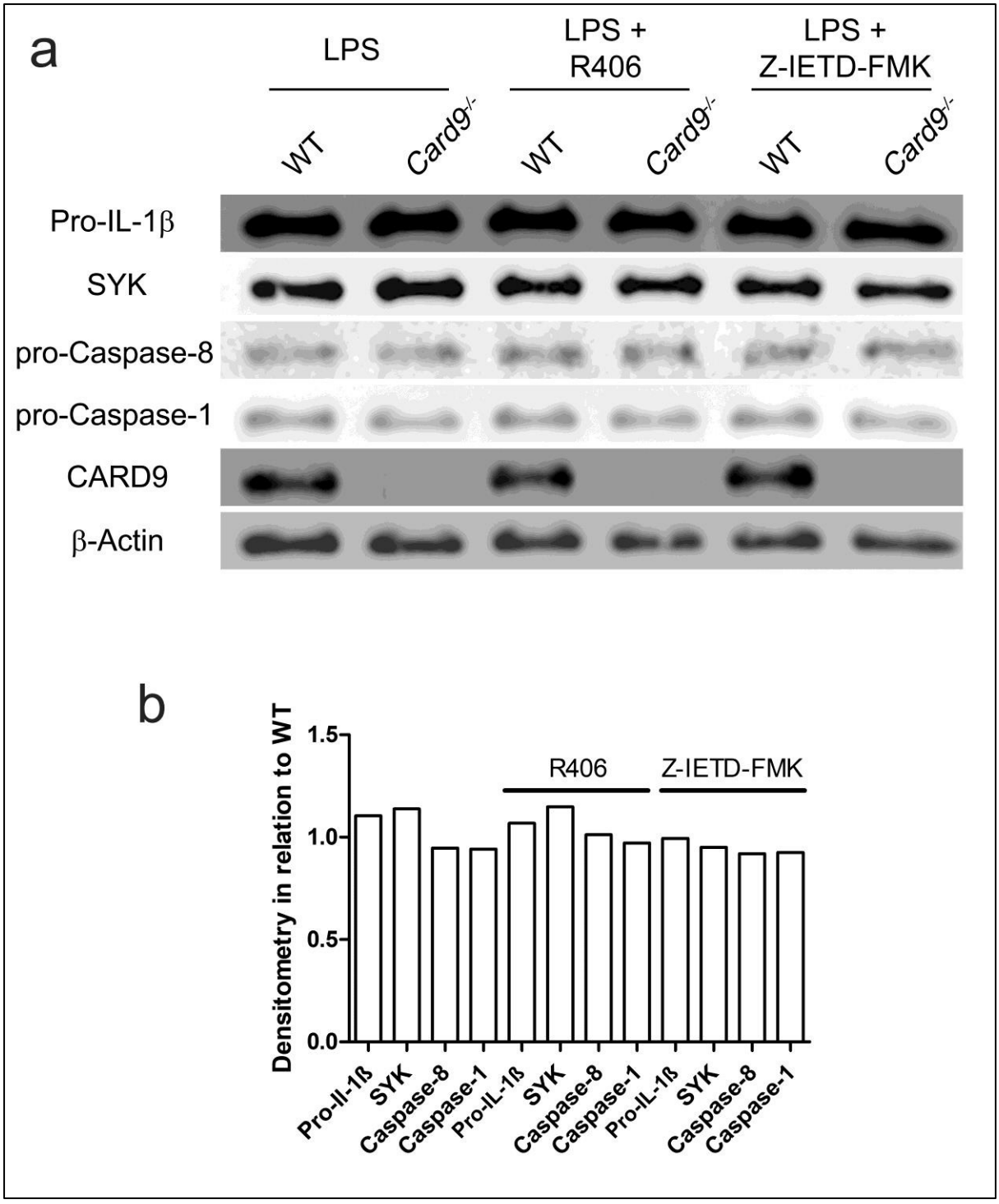

Figure 5.2: Expression levels of CARD9 and inflammasome constituents in LPS-primed WT and *Card9*$^{-/-}$ BMDMs in the presence or absence of SYK or Caspase-8 inhibitors. (a) Immunoblot analysis of pro-IL-1β, SYK, caspase-8, caspase-1, CARD9 and β-actin in LPS-primed WT and *Card9*$^{-/-}$ BMDMs (200 ng/mL for 3 hours) with an additional hour of incubation with SYK inhibitor R406 (1 μM) or caspase-8 inhibitor Z-IETD-FMK (10 μM) and (b) its densitometry in relation to WT. Figure and densitometry are representative of three independent experiments.

SYK activity is involved in NLRP3 inflammasome activation in macrophages but not in dendritic cells (Hara et al., 2013). If SYK is indeed involved in CARD9 inhibition of the NLRP3 inflammasome, it is possible that this phenotype is different in dendritic cells. To test this hypothesis, bone marrow derived dendritic cells (BMDC) were prepared from WT and *Card9*$^{-/-}$ mice and infected with *S.* Typhimurium at MOI 10 for 2, 6 and 24 hours. The supernatants were then collected for IL-1β quantification and cell viability assays. Similar to my observations in macrophages, infection of WT and *Card9*$^{-/-}$ BMDCs with *Salmonella* revealed no statistically significant difference in cellular viability at 6 and 24 hours, whilst *Card9*$^{-/-}$ BMDCs have slightly increased cell viability at 2 hours. IL-1β production by WT and *Card9*$^{-/-}$, however, had no significant difference, a phenotype not observed in macrophages (Figure 5.3).

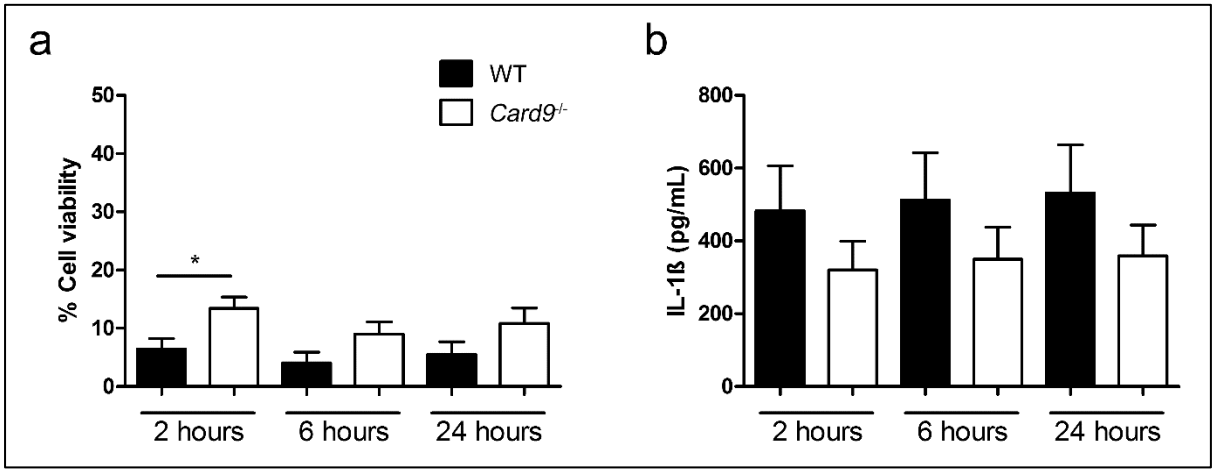

Figure 5.3: CARD9 has no effect on IL-1β production in BMDCs infected with *S.* Typhimurium. (a) Cellular viability (as measured by LDH release) and (b) IL-1β release in WT, *and Card9*$^{-/-}$ BMDCs after infection with *S.* Typhimurium at MOI 10 for 2, 6 and 24 hours. * $p<0.05$ one-way ANOVA with Tukey's multiple comparisons test. Data represent the mean from three independent experiments while error bars show the s.e.m.

It is possible that any potential differences between the activation of the NLRP3 inflammasome of WT and *Card9*$^{-/-}$ dendritic cells could be masked by the effects of activating the NLRC4 inflammasome, the main NLR responsible for early IL-1β produced *in vitro* during *Salmonella* infections (Man et al., 2014). To better address the potential of a cell-specific role for CARD9 in fine-tuning the NLRP3 inflammasome LPS-primed WT and CARD9 knockout BMDCs were stimulated with nigericin. These experiments showed no difference in cellular

viability nor IL-1β production (Figure 5.4). Addition of the SYK inhibitor R406 had no effect in either cell type (Figure 5.4). These data are in agreement with a cell type specificity for CARD9 regulation of inflammasome activity possibly due the different role that SYK undertakes in macrophages and dendritic cells.

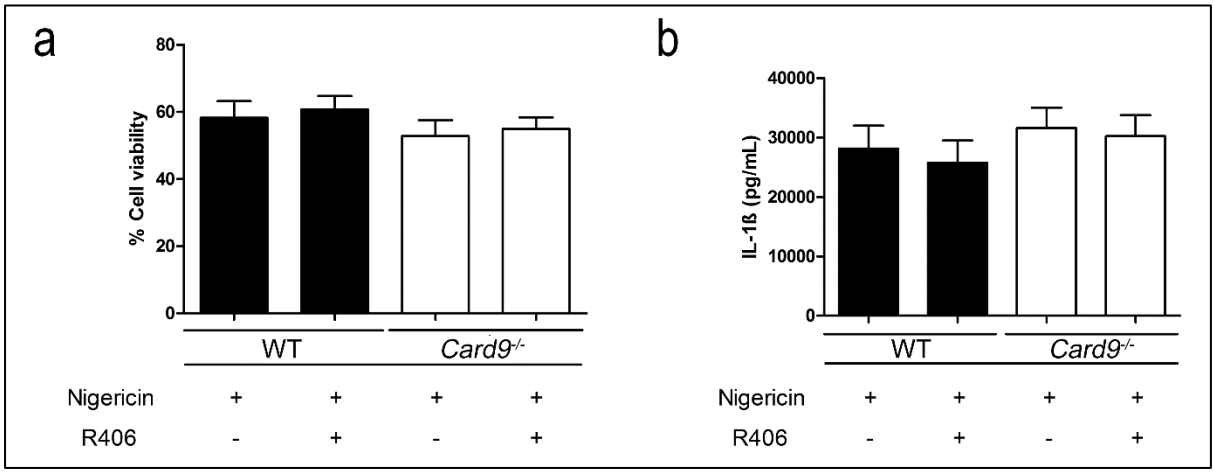

Figure 5.4: SYK is not involved in the regulation of the NLRP3 inflammasome in BMDCs. LPS-primed BMDCs (200 ng/mL for 3 hours) were stimulated with 5 μM nigericin for one hour in presence of SYK inhibitor R406 (1 μM). (a) Cellular viability and (b) IL-1β production. $p>0.05$ one-way ANOVA. Data represent the mean from three independent experiments while error bars show the s.e.m.

The co-immunoprecipitation pattern observed in figure 4.17 suggests that upon NLRP3 stimulation, CARD9 interacts preferentially with unphosphorylated SYK. It is possible, therefore, that CARD9 interaction with unphosphorylated SYK can influence the phosphorylation state of SYK. To verify SYK phosphorylation levels, LPS-primed WT and CARD9 knockout BMDMs were either left unstimulated, infected with *S*. Typhimurium or treated with nigericin. Post treatment, total cellular proteins were carefully extracted in presence of protease and phosphatase inhibitors and immunoblot assays were performed using antibodies raised against total SYK or phosphorylated SYK (Y525/526). In *Card9*$^{-/-}$ BMDMs, the levels of Y525/526 phosphorylated SYK (p-SYK) in relation to total SYK is greater than that observed in WT controls, with or without inflammasome stimulation (Figure 5.5, Appendix 11). This suggests that the enhanced SYK phosphorylation observed in CARD9 knockout macrophages results in enhanced cytokine production by the inflammasome.

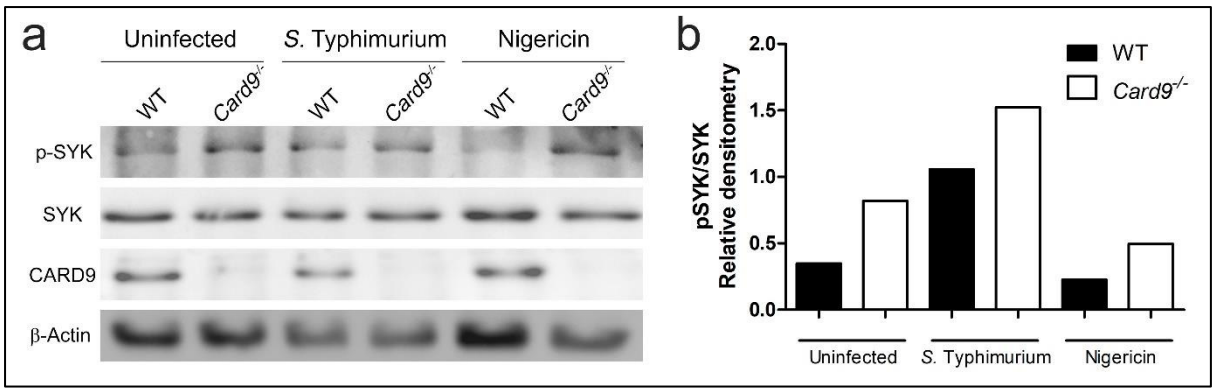

Figure 5.5: CARD9 absence increases phosphorylated SYK (Y519/520) in relation to total SYK. WT and *Card9*$^{-/-}$ LPS-primed BMDMs were infected with *S.* Typhimurium at MOI 10 for 2 hours or stimulated with 10 μM nigericin for 30 minutes, the cell lysate was then subjected to immunoblotting and the membrane probed for p-SYK (Y519/520), total SYK, CARD9 and β-Actin. Immunoblot (a) and its relative p-SYK/SYK densitometry (b). Data representative of three independent experiments.

The enhanced IL-1β production in CARD9 knockout BMDMs without a proportional increase in cell viability suggests that there is not an increase in caspase-1 activity, as this enzyme is involved in triggering pyroptosis. It is possible, however, that caspase-8 activity is upregulated in *Card9*$^{-/-}$ macrophages, as caspase-8 can cleave pro-IL-1β to IL-1β without affecting cell viability in response to *S.* Typhimurium infection (Man et al., 2013). To test this hypothesis, LPS-primed WT and *Card9*$^{-/-}$ BMDMs were infected with *S.* Typhimurium or stimulated with nigericin in presence of the caspase-8 inhibitor z-ietd-fmk. Irrespective of the stimuli used, caspase-8 inhibition does not affect cell viability. Upon caspase-8 inhibition, the IL-1β production decreased in both WT and *Card9*$^{-/-}$ BMDMs, with the resulting IL-1β levels similar in both cell types (Figure 5.6). This suggests that the increased IL-1β production observed in CARD9 knockout macrophages is likely to involve caspase-8 activity.

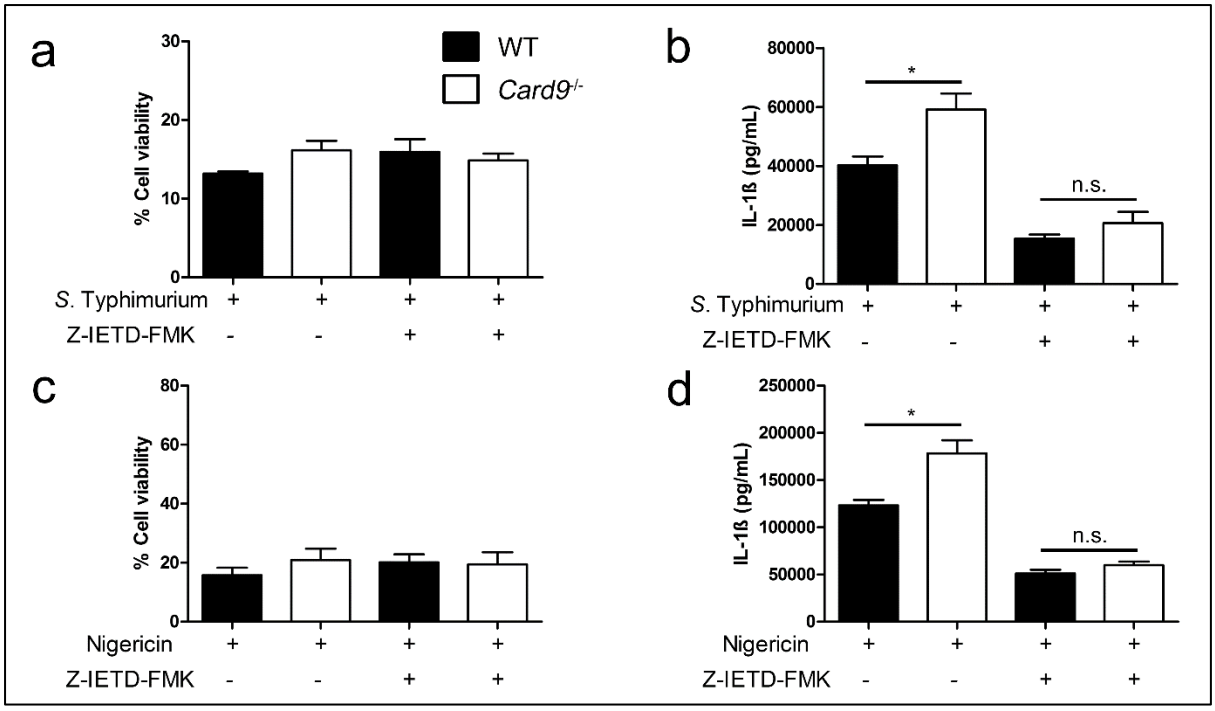

Figure 5.6: Caspase-8 is involved in the CARD9 regulation of the NLRP3 inflammasome in BMDMs. LPS-primed BMDMs (200 ng/mL for 3 hours) were infected with *S*. Typhimurium at MOI 10 for one hour (a,b) or stimulated with 5 μM nigericin for one hour (c,d) in presence of caspase-8 inhibitor Z-IETD-FMK (10 μM). (a,c) Cellular viability and (b,d) IL-1β production. * $p<0.05$, n.s. Not significant (one-way ANOVA with Tukey's multiple comparisons test). Data represent the mean from three independent experiments while error bars show the s.e.m.

Ideally, I would have investigated the links between CARD9, SYK, Caspase-8 and IL-1β production by using cells with multiple simultaneous knockout mutations. Since our laboratory does not possess *Syk*$^{-/-}$ or *Caspase-8*$^{-/-}$*/Ripk3*$^{-/-}$ mice strains, breeding animals with *Card9*$^{-/-}$ to obtain useful strains was not a viable option. Instead, I used an immortalized bone marrow derived macrophages (iBMDM), a system with the potential for genetic manipulation. To validate this system, I attempted to replicate in WT and *Card9*$^{-/-}$ iBMDMs the GPA data I originally produced in primary macrophages (Figure 3.24-26). Both WT and CARD9 knockout iBMDMs exhibited similar cellular viability after 2 and 6 hours of infection. Surprisingly, the infection assays using WT and *Card9*$^{-/-}$ iBMDMs failed to replicate the IL-1β data observed in primary macrophages, with no statistically significant difference in the production of this cytokine, despite the visual difference suggesting an impairment in IL-1β production by *Card9*$^{-/-}$ iBMDMs (Figure 5.7).

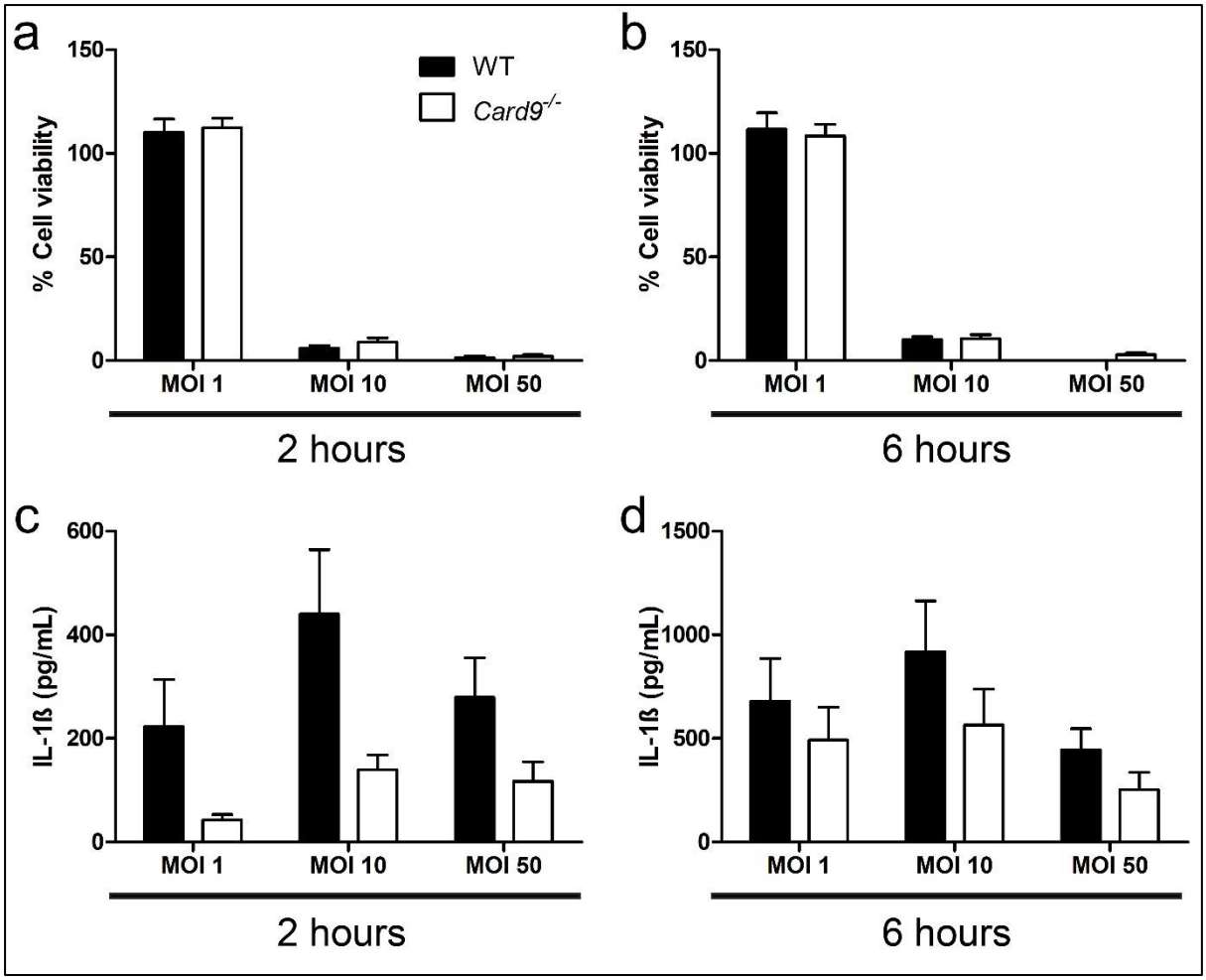

Figure 5.7: *Card9*$^{-/-}$ iBMDMs do not behave like primary *Card9*$^{-/-}$ BMDMs during *S.* Typhimurium infection. Cellular viability (as measured by LDH release) (a,b) and IL-1β (as measured by ELISA) (c,d) of WT and *Card9*$^{-/-}$ iBMDMs infected with *S.* Typhimurium at MOIs 1, 10 and 50 for 2 (a,c) and 6 (b,d) hours. $p>0.05$ unpaired t-test. Data represent the mean from three independent experiments while error bars show the s.e.m.

One explanation for this difference lies in the expression pattern of proteins likely to be involved in the CARD9 inhibition of the NLRP3 inflammasome. To check for differences in protein expression, cell lysates derived from unstimulated WT and *Card9*$^{-/-}$ iBMDMs were subjected to immunoblot and probed with antibodies raised against SYK, CARD9 and ASC. In *Card9*$^{-/-}$ iBMDMs, SYK was found to be expressed at lower levels compared to that observed in WT iBMDMs, despite having similar levels of ASC (Figure 5.8, Appendix 12). This result further links SYK activity to IL-1β production (Hara et al., 2013). Moreover, it suggests that the use of immortalized cells would not be useful for my work. To circumvent this problem, I continued my work in primary cells using pharmacological inhibitors.

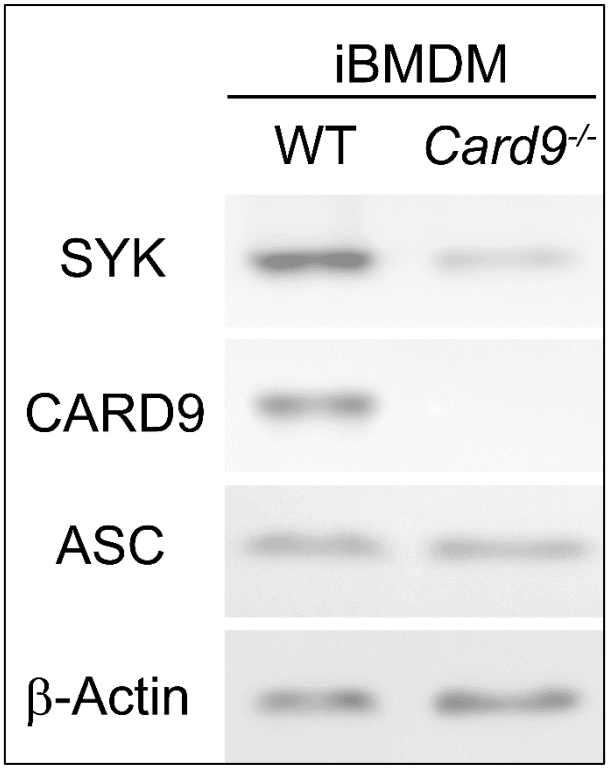

Figure 5.8: *Card9*$^{-/-}$ immortalized bone-marrow derived macrophages have deficient SYK expression. WT and *Card9*$^{-/-}$ iBMDMs were cultured for 7 days, proteins were extracted, subjected to immunoblotting and the membrane was probed for total SYK, CARD9, ASC and β-Actin. Immunoblot (a) and densitometry (b). Data representative of 2 independent experiments.

To further understand how SYK, caspase-8, and CARD9 are involved in controlling IL-1β production, I used immunofluorescence microscopy to stain for active caspase-8 and caspase-1 specks upon nigericin treatment of LPS-primed WT and *Card9*$^{-/-}$ BMDMs in the presence or absence of the SYK inhibitor R406. Both active enzymes were stained using the FLICA active substrate reagents relatively specific for either caspase-1 or caspase-8. This set of experiments assumes that the caspase specks observed under the microscope are the active enzymes recruited to the inflammasome foci. To support this assumption, *Pycard*$^{-/-}$ (ASC negative) BMDMs were included as negative controls, and as expected, the number of cells scored positive for caspase-1 and caspase-8 specks in *Pycard*$^{-/-}$ is very low, with any positive staining being most likely artefactual because specific foci were not apparent. (Figure 5.9).

Upon treatment, the percentage of cells containing caspase-1 specks was similar in WT and *Card9*$^{-/-}$ BMDMs (around 15%) (Figure 5.9 c), whereas the percentage of cells positive for

caspase-8 specks was higher in *Card9*$^{-/-}$ cells (Figure 5.9 b). This result is suggestive of increased caspase-8 recruitment to the inflammasome in *Card9*$^{-/-}$ cells. SYK inhibition decreased the percentage of caspase-8 positive cells in both WT and *Card9*$^{-/-}$ BMDMs and caused WT and *Card9*$^{-/-}$ macrophages to behave similarly. No statistically significant difference was observed in the percentage of caspase-1 positive cells post SYK inhibition, suggesting that this kinase is relevant in signalling the recruitment of caspase-8 to the inflammasome, but not for not caspase-1 (Figure 5.9). The increase in caspase-8 recruited to the inflammasome is most likely to be involved in the enhanced IL-1β production observed in CARD9 knockout BMDMs, as this enzyme can process pro-IL-1β to its mature form (Man et al., 2013).

The experiments described above were performed in LPS-primed cells. Under these conditions, the levels of pro-IL-1β are similar between WT and *Card9*$^{-/-}$ BMDMs (Figure 5.2), and the resulting differences in IL-1β production are unlikely to be due differential gene transcription and protein expression. In unprimed cells, however, a potential effect of CARD9 on protein expression could not be ruled out. Immunoblotting of unprimed WT, *Card9*$^{-/-}$ and *Pycard*$^{-/-}$ (ASC negative) BMDMs showed increased pro-IL-1β expression in *Card9*$^{-/-}$ macrophages upon *S.* Typhimurium infection (Figure 4.23), suggesting that gene transcription could potentially contribute to the *Card9*$^{-/-}$ phenotype. To test whether this was the case, WT and *Card9*$^{-/-}$ primary macrophages were infected with *S*. Typhimurium at MOI 5 for one hour. Total RNA was then extracted in order to quantify gene transcription by quantitative PCR (qPCR). The MOI chosen is lower than the one used in the initial GPAs (Figures 3.24 to 3.26) to avoid excessive cell death and increase the amount of RNA extracted. The different experimental conditions had no effect on the phenotype, as CARD9 knockout BMDMs continued to produce, as expected, more IL-1β than the WT controls (Figure 5.10).

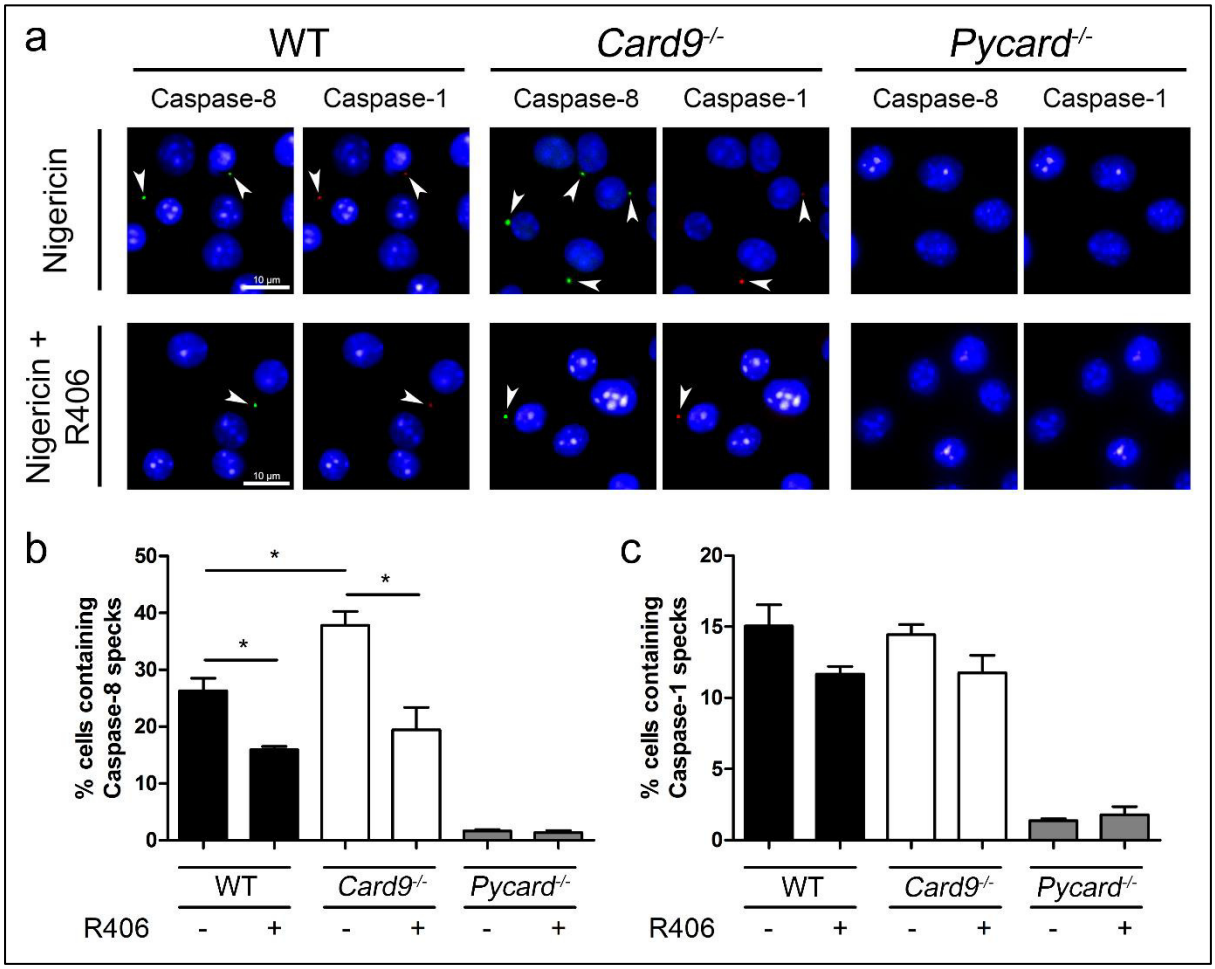

Figure 5.9: SYK inhibition decreases the percentage of cells containing caspase-8 specks upon NLRP3 stimulation with nigericin. WT, *Card9*$^{-/-}$ and *Pycard*$^{-/-}$ LPS- BMDMs (200 ng/mL for 3 hours) were stimulated with 5 µM nigericin for 30 minutes in presence of caspase-1 and caspase-8 FLICA substrates and with or without 1 µM of the SYK inhibitor R406. (a) Arrowheads pointing to FLICA-stained caspase-1 and caspase-8 specks in stimulated cells. (b) Percentage of cells containing caspase-8 specks and (c) percentage of cells containing caspase-1 specks. (a) Image is representative of three independent experiments. (b,c) * $p<0.05$ one-way ANOVA with Tukey's multiple comparisons test. Data represent the mean from three independent experiments while error bars show the s.e.m.

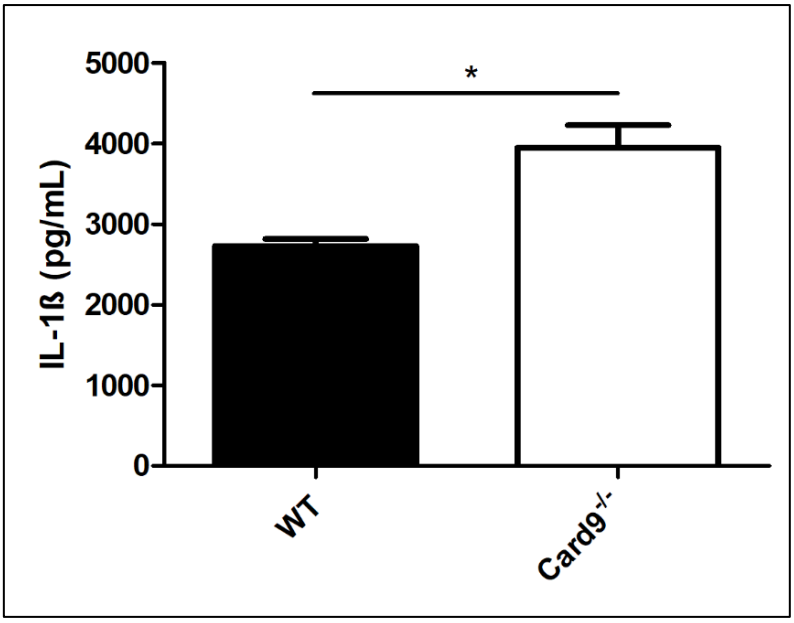

Figure 5.10: *Card9*$^{-/-}$ BMDMs produce more IL-1β than WT cells under the conditions used for the qPCR experiments. 1.6x10^{6} per well WT and *Card9*$^{-/-}$ BMDMs were plated in 6-wells plates and infected with *S.* Typhimurium at MOI 5 for 2 hours. The supernatant was collected and IL-1β was measured by ELISA. The cells were then washed, scraped, and used for RNA extraction. * $p<0.05$ one-way ANOVA with Tukey's multiple comparisons test. Data represent the mean from three independent experiments while error bars show the s.e.m.

At the mRNA level in unstimulated WT and CARD9 knockout cells, no differences were observed in the transcription of genes coding for pro-IL-1β, pro-IL-18, caspase-1, caspase-8, NLRP3, NLRC4, ASC, Bcl-10, MALT-1, SYK, TNF-α, RANTES, FADD and NAIP5 (Figure 5.11). This set of genes were selected because of their functional links with either CARD9 and/or inflammasomes. Attempts to quantify additional transcripts such as those coding for dectin-1, IFN-β and caspase-11 failed possibly due to low transcriptional level and/or unsuitable primers, and as a consequence were not included in this thesis.

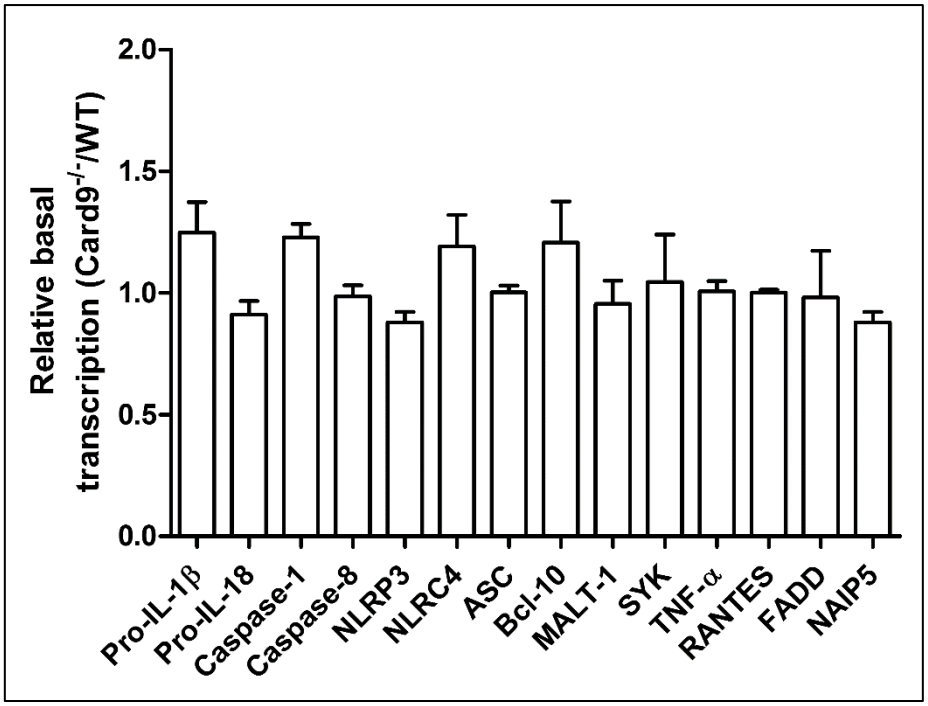

Figure 5.11: *Card9*$^{-/-}$ and WT BMDMs have no differences in the basal transcription of the genes studied in this work. Basal transcriptional levels of Pro-IL-1β, Pro-IL-18, Caspase-1, Caspase-8, NLRP3, NLRC4, ASC, Bcl-10, MALT-1, SYK, TNF-α, RANTES, FADD and NAIP5 in uninfected *Card9*$^{-/-}$ BMDMs in relation to uninfected WT cells. GAPDH and β-Actin were used as reference genes. Data represent the mean from three independent experiments while error bars show the s.e.m.

Upon *Salmonella* infection, the transcription level of genes encoding for pro-IL-1β, NLRP3, TNF-α, RANTES, MALT-1 and pro-IL-18 increased in both WT and *Card9*$^{-/-}$ cells (Figure 5.12-13). However, *Il1b* (encoding for pro-IL-1β) increased significantly more in CARD9 knockout BMDMs in comparison to WT controls, (i.e. a 1300-fold increase in *Card9*$^{-/-}$ BMDMs compared to an 800-fold increase in WT BMDMs) (Figure 5.12 a). Post infection, the transcription of genes encoding for SYK and caspase-8 increased marginally in *Card9*$^{-/-}$ BMDMs, whilst the levels of those transcripts remained unchanged in the WT counterpart (Figure 5.12 e-f). *Fadd* transcription decreased similarly in both cell types, whilst the remaining transcripts (ASC, BCL10, caspase-1, NAIP5 and NLRC4) exhibited no statistically significant changes post infection (Figure 5.12-3). These findings link CARD9 to the licensing step of NLRP3 inflammasome activation, acting on the availability of pro-IL-1β.

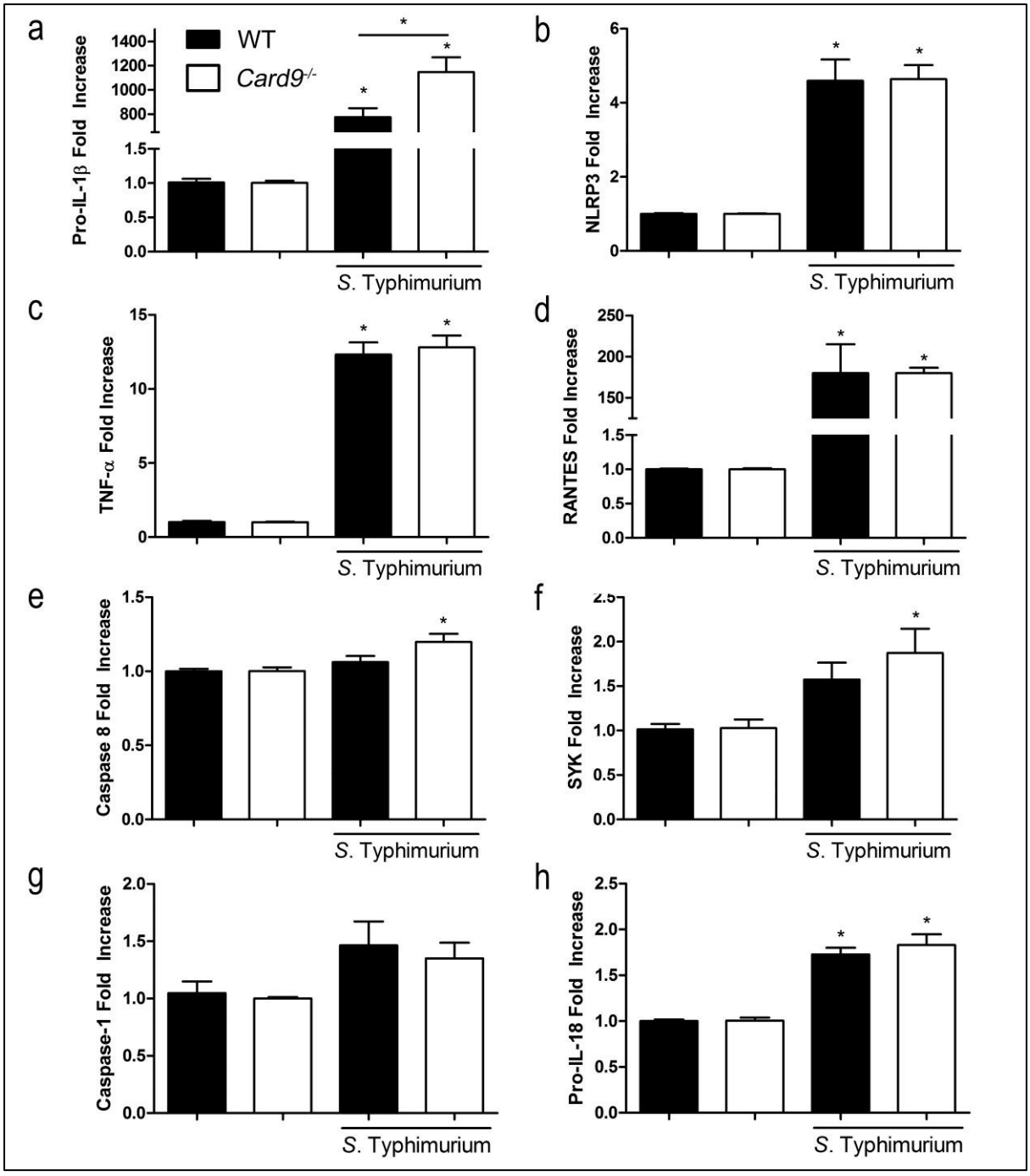

Figure 5.12: CARD9 influences pro-IL-1β transcription during *S.* Typhimurium infection whilst other proinflammatory genes such as TNF-α remain unaffected. qPCR analysis of WT and *Card9*$^{-/-}$ BMDMs infected with *S.* Typhimurium at MOI 5 for 2 hours. Transcription of genes coding for (a) Pro-IL-1β, (b) NLRP3, (c) TNF-α, (d) RANTES, (e) Caspase-8, (f) SYK, (g) Caspase-1, and (h) Pro-IL-18. GAPDH and β-Actin used as reference genes. * $p<0.05$ in relation to respective uninfected control unless otherwise indicated (one-way ANOVA with Tukey's multiple comparisons test). Data represent the mean from three independent experiments while error bars show the s.e.m.

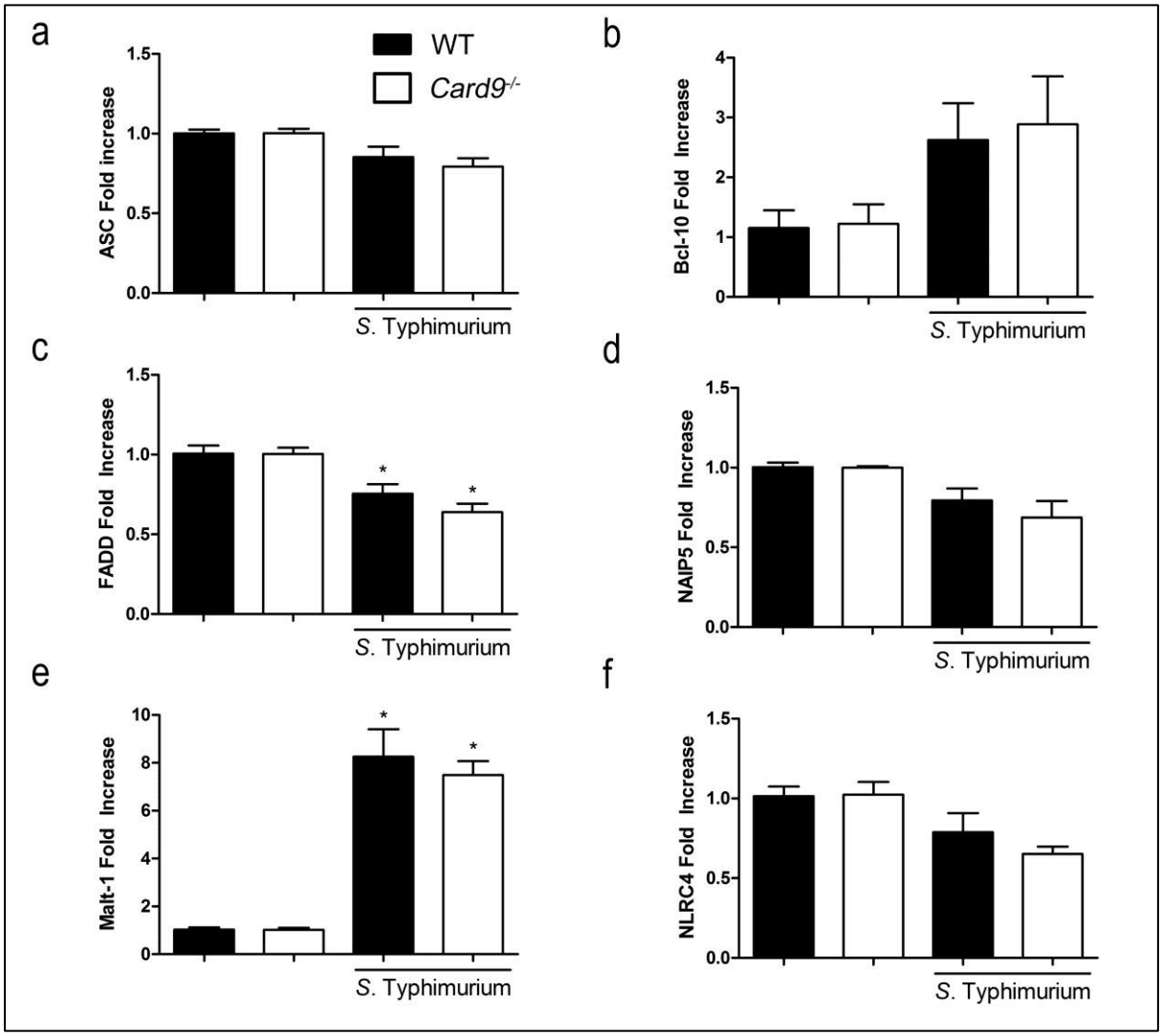

Figure 5.13: Inflammatory genes not influenced by CARD9 during *S.* Typhimurium. qPCR analysis of WT and *Card9*$^{-/-}$ BMDMs infected with *S.* Typhimurium at MOI 5 for 2 hours. Transcription of genes coding for (a) ASC, (b) BCL-10, (c) FADD, (d) NAIP5, (e) MALT-1, and (f) NLRC4. GAPDH and β-Actin used as reference genes. * $p<0.05$ in relation to respective uninfected control (one-way ANOVA with Tukey's multiple comparisons test). Data represent the mean from three independent experiments while error bars show the s.e.m.

CARD9 regulates inflammatory responses downstream of PRRs such as dectin-1, NOD2 and RIG-I, modulating gene transcription by activating NF-κB (such as in the dectin-1 and RIG-I pathways) and the MAPKs p38 and JNK during NOD2 signalling. The CARD9 effects observed on gene transcription are unlikely to be mediated via NF-κB, as TNF-α, a classic readout for NF-κB activity, is produced at comparable levels in WT and CARD9 knockout macrophages. In the NOD2 pathway however, CARD9 is used as an adaptor for activating MAPK but not for NF-κB (Hsu et al., 2007), making NOD2 a prime candidate for explaining my transcriptional data. In this context however, NOD2 would assume a role as a negative modulator of *Il1b* transcription.

To better understand the role that NOD2 undertakes in BMDMs during *Salmonella* infection, I have conducted a GPA in WT and *Nod2*$^{-/-}$ BMDMs using *S.* Typhimuirum (MOI of 10) for 2, 6 and 24 hours and measured the TNF-α and IL-1β output, as well as the cellular viability. Infection of WT and *Nod2*$^{-/-}$ BMDMs with *S*. Typhimurium demonstrated that despite exhibiting similar cellular viability, NOD2 knockout macrophages produce less TNF-α than WT cells (Figure 5.14 a-b). This suggests an impairment in NOD2-mediated NF-κB activation. Surprisingly, *Nod2*$^{-/-}$ macrophages produced more IL-1β than the WT controls, thus supporting the hypothesis that NOD2 has an inhibitory effect on the production of this cytokine (Figure 5.14 c), not unlike the effect observed in *Card9*$^{-/-}$ BMDMs (Figure 3.25).

If NOD2 inhibits IL-1β production via CARD9, then co-stimulation of this NLR during *S.* Typhimurium infection should decrease pro-IL-1β expression in WT but not in *Card9*$^{-/-}$ BMDMs. To test this hypothesis, WT, *Card9*$^{-/-}$ and *Nod2*$^{-/-}$ BMDMs were infected with *S.* Typhimurium for one hour with or without MDP, a classic NOD2 ligand (Girardin et al., 2003). The cells were then lysed, and the protein expression was assessed by immunoblotting. After infection, pro-IL-1β is substantially expressed in all cell types, and co-stimulation with MDP decreases pro-IL-1β levels in WT BMDMs only, having no effect on *Card9*$^{-/-}$ and *Nod2*$^{-/-}$ macrophages (Figure 5.15, Appendix 13). This result, together with the *Nod2*$^{-/-}$ infection assay (Figure 5.14), suggests that in the context of a complex pathogen such as *S*. Typhimurium, NOD2 adopts a CARD9-dependent inhibitory role on pro-IL-1β expression

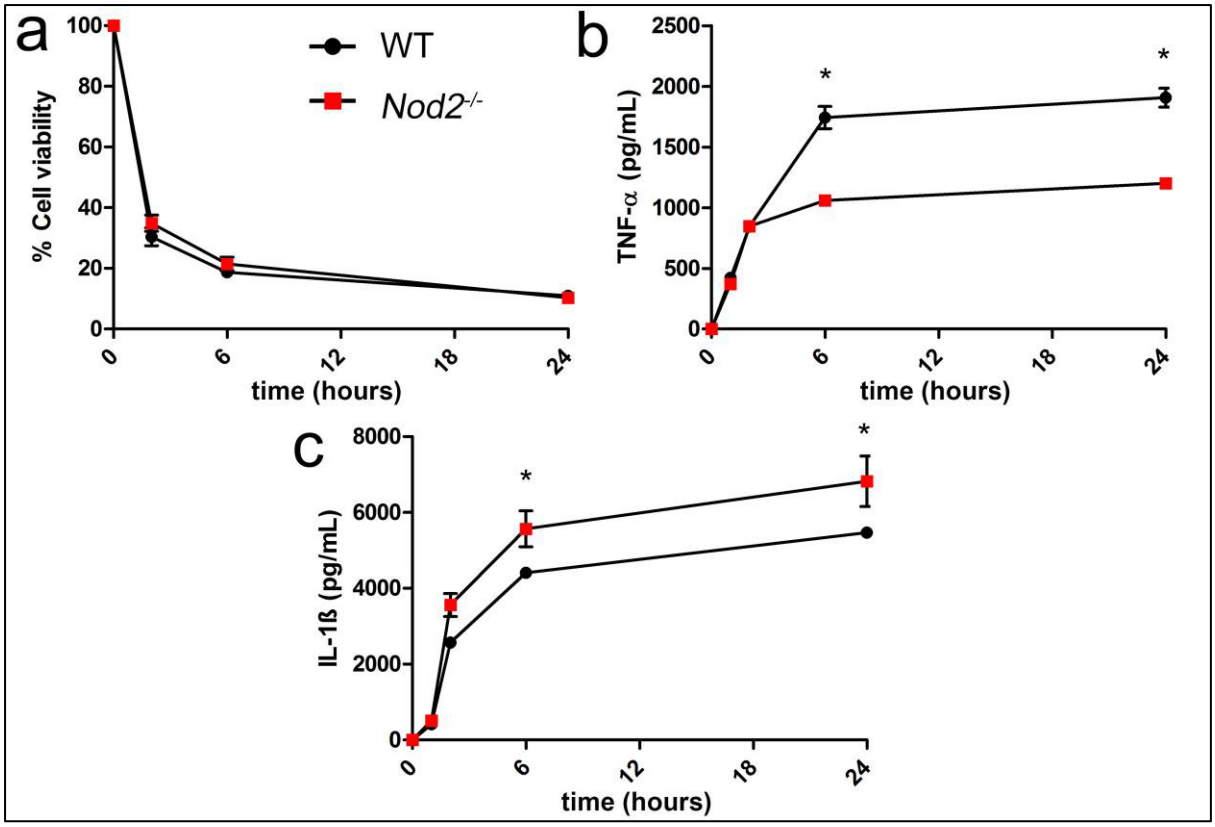

Figure 5.14: NOD2 differentially regulates the production of cytokines during *S.* Typhimurium infection. (a) cellular viability (as measured by LDH release), (b) TNF-α and (c) IL-1β production (as measured by ELISA) in WT and *Nod2*$^{-/-}$ BMDMs infected with *S.* Typhimurium at MOI 10 for 2, 6 and 24 hours. *p<0.05 two-way ANOVA with Bonferroni post-test. Data represent the mean from two independent experiments while error bars show the s.e.m.

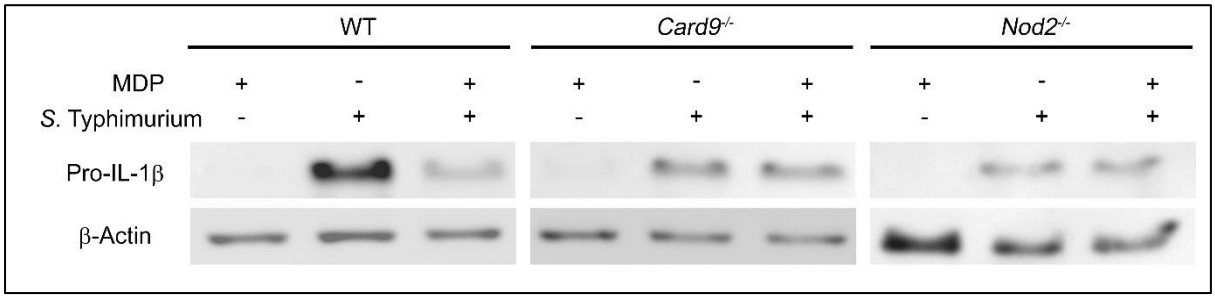

Figure 5.15: NOD2 co-stimulation with MDP decreases pro-IL-1β expression in *S.* Typhimurium-infected WT BMDMs, but not in *Card9*$^{-/-}$ and *Nod2*$^{-/-}$ BMDMs. Pro-IL-1β expression in WT, *Card9*$^{-/-}$ and *Nod2*$^{-/-}$ BMDMs infected with *S.* Typhimurium at MOI 10 for one hour with or without 10 μg/mL MDP co-stimulation. Image representative of two independent experiments.

In the NOD2 pathway, CARD9 acts by modulating the activity of the MAPKs p38 and JNK (Hsu et al., 2007). These MAPKs regulate the activity of AP-1, which in turn acts on *il1b* transcription (Arthur and Ley, 2013; Roman et al., 2000). I hypothesised that AP-1, via p38 and/or JNK in the NOD2 pathway may function as an *Il1b* transcriptional inhibitor. To further elucidate how CARD9 controls pro-IL-1β expression, WT BMDMs were infected with *S.* Typhimurium in presence of MDP to overstimulate the NOD2 pathway. The effect of inhibiting p38, JNK or AP-1 were also tested. The cells were lysed, and the protein lysates were subjected to immunoblotting. Inhibition of AP-1 and JNK led to increased pro-IL-1β expression (Figure 5.16 a-b, Appendix 14). This finding provides further support for activation of the NOD2/CARD9 axis to inhibit pro-IL-1β expression. Blocking AP-1 or JNK in this context would "inhibit the inhibitor", facilitating *Il1b* transcription and subsequent pro-IL-1β expression to occur more efficiently (Figure 5.16 c). The same effect was expected by inhibiting p38, however no pro-IL-1β was detected. Although this is puzzling, it is possible that in this context p38 and JNK have opposite effects. The molecular basis for this difference is unknow but one possibility is that these MAPKs modulate AP-1 activity in different ways, one inhibiting its *Il1b* transcription activity whilst the other enhances it. Another possibility is that this inhibitor is toxic to macrophages in the conditions used for these experiments.

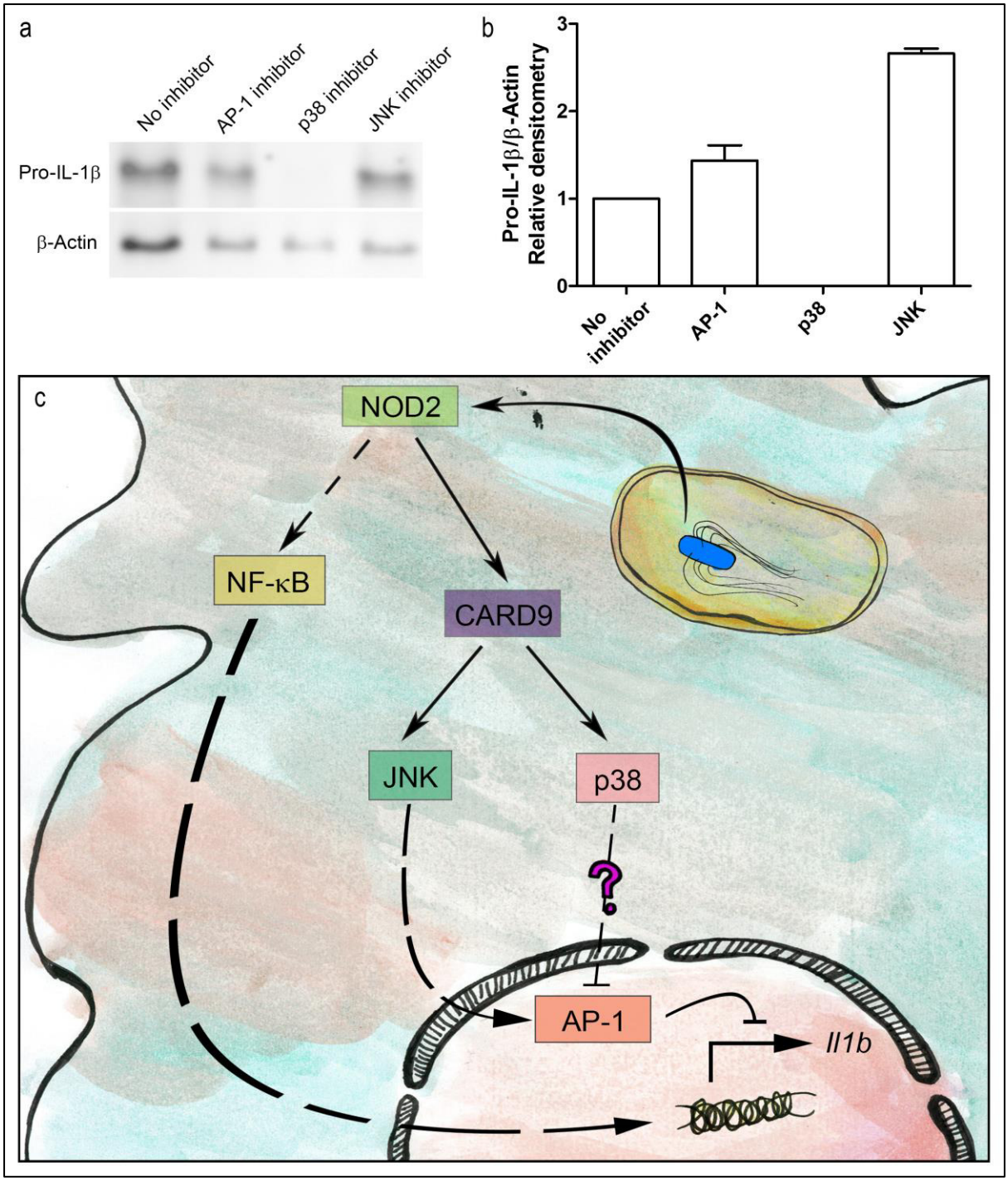

Figure 5.16: Inhibition of AP-1, p38 and JNK in WT BMDMs infected with *S.* Typhimurium during NOD2 stimulation with MDP further suggests an inhibitory role of NOD2 in pro-IL-1β expression. WT BMDMs were infected with *S.* Typhimurium at MOI 10 for one hour in presence of 10 µg/mL MDP and without or with AP-1, p38 and JNK inhibitors. (a) Immunoblot of the cell lysates after stimulations and (b) relative densitometry. (a) Image representative of three independent experiments. (b) Data represent the mean from three independent experiments while error bars show the s.e.m. (c) Possible interpretation of the results in the context of the NOD2 pathway.

The evidence thus far presented in this thesis suggests that CARD9 inhibits the NLRP3 inflammasome by decreasing pro-IL-1β expression via the NOD2 pathway and in addition by decreasing caspase-8 recruitment to the inflammasome via inhibition of SYK. Upon infection however, inflammasome activation is often an outcome advantageous to the host. The production of pro-inflammatory cytokines by the infected cell can modulate important responses that allow the host to combat the infection. With this in mind, I hypothesised that mechanisms capable of "turning off" the CARD9 inhibitory role could potentially exist. To test this hypothesis, I investigated whether the CARD9 expression pattern would change over time upon *S.* Typhimurium infection of WT BMDMs. Consequently, WT macrophages were infected with *S*. Typhimurium at MOI of 5 for 0, 30, 60 and 120 minutes, then lysed and the protein lysates were subjected to immunoblotting and probed for CARD9. Macrophages infected with *Salmonella* showed decreased CARD9 expression in a time-dependent manner, with most of the protein level decreasing within the first hour of infection (Figure 5.17, Appendix 15). This suggests that the cell overcomes the CARD9 inhibition during the infection by decreasing CARD9 expression levels.

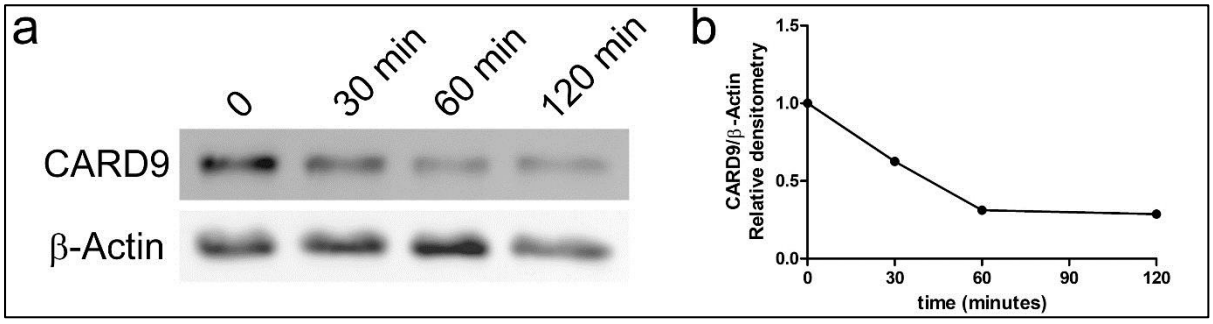

Figure 5.17: CARD9 is progressively degraded during *S*. Typhimurium infection in BMDMs. BMDMs were infected with *S.* Typhimurium at MOI 5, the cells were collected and protein extracted at 0, 30, 60 and 120 minutes post-infection. The lysates were subjected to immunoblot and probed for CARD9 and β-Actin. Immunoblot (a) and its densitometry (b). Image and densitometry are representative of three independent experiments.

Next, I sought to investigate whether the CARD9 expression level is related to inflammasome formation. Unprimed BMDMs derived from WT, *Card9*$^{-/-}$ and *Pycard*$^{-/-}$ (ASC negative) mice were infected with *S*. Typhimurium at MOI 5 for 2 and 6 hours, followed by protein extraction and immunoblotting using anti-CARD9 antibody. The decrease observed in CARD9 expression occurs similarly in WT and *Pycard*$^{-/-}$ macrophages, suggestive of

CARD9 degradation independent of inflammasome formation (Figure 5.18 a, Appendix 15). To further study the link between CARD9 degradation and inflammasome formation, WT, *Card9*$^{-/-}$ and *Pycard*$^{-/-}$ BMDMs were primed with LPS (200 ng/mL for 3 hours) and then stimulated with either nigericin or infected with *S.* Typhimurium. Cells were harvested, and total protein was extracted and analyzed by immunoblotting using anti-CARD9 antibody as the probe. Similar to what was observed in unprimed macrophages, CARD9 degradation occurred at comparable levels in WT and ASC knockout cells infected with *Salmonella*. The use of nigericin, an activator of the canonical NLRP3 inflammasome, did not trigger CARD9 degradation, as cells treated with this reagent had similar CARD9 expression to the untreated controls (Figure 5.18 b, Appendix 15). This suggests that CARD9 degradation occurs independently of inflammasome formation and is triggered by infection.

The decrease in CARD9 expression observed upon *Salmonella* infection could potentially be a consequence of active protein degradation. Amongst the processes commonly used by the host cell to degrade endogenous proteins is proteasome degradation. The proteasome is a barrel-shaped protein complex that remains inaccessible to most proteins. In some cases, proteins are "tagged" for proteasome degradation, usually via ubiquitination, gaining access to the proteasome where they are enzymatically cleaved (Finley, 2009). To investigate whether CARD9 is degraded by proteasomes, WT BMDMs were infected with *S.* Typhimurium for 0, 60 and 120 minutes with or without the addition of epoxomicin, a proteasome inhibitor, and CARD9 expression was assessed by immunoblotting. The CARD9 degradation upon *Salmonella* infection is, surprisingly, increased in the presence of the proteasome inhibitor epoxomicin (Figure 5.19, Appendix 16). This puzzling result suggests either the proteasome is unimportant in regulating CARD9 expression or it could be due to side-effects of this inhibitor on other degradation pathways.

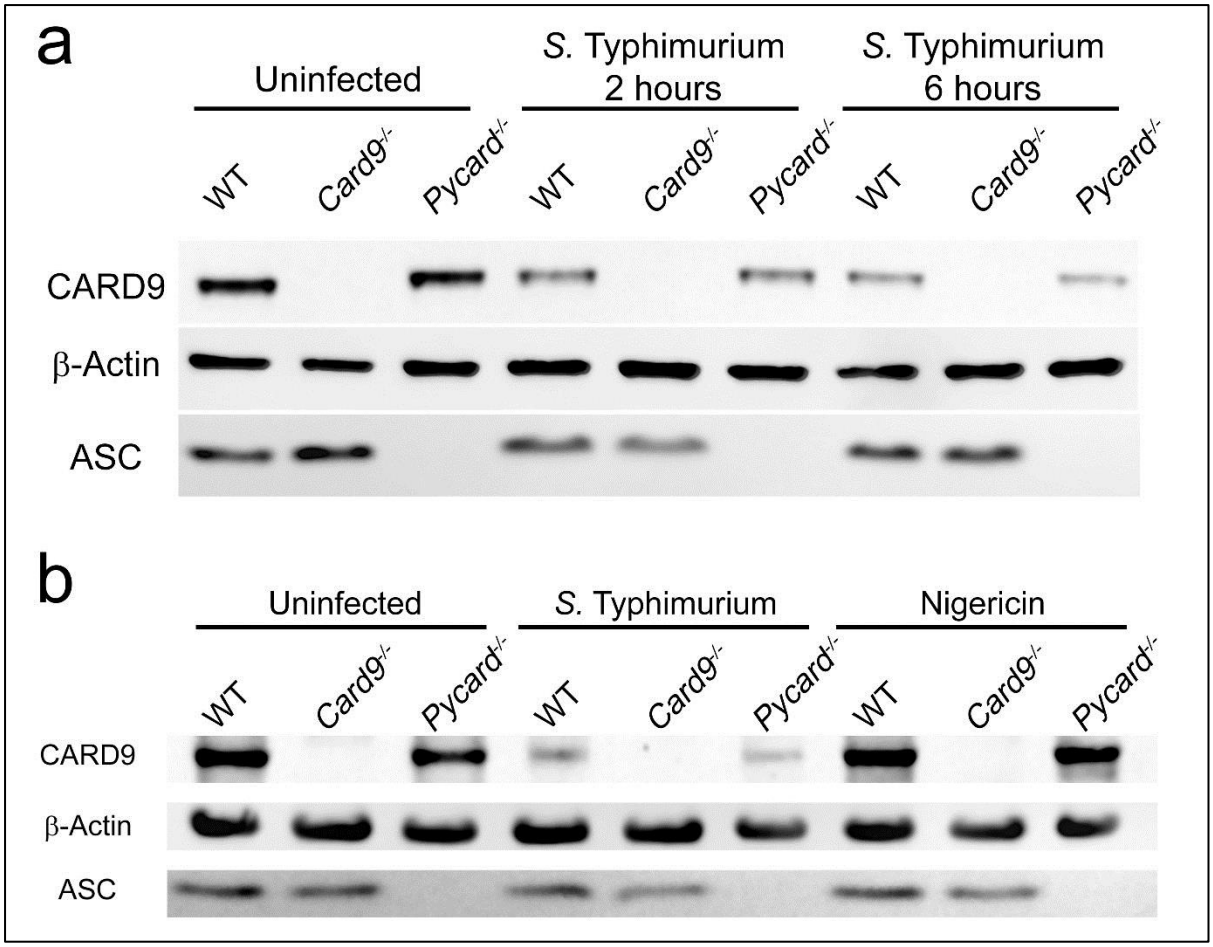

Figure 5.18: CARD9 is degraded during *S.* Typhimurium infection in unprimed and LPS-primed BMDMs independently of ASC and NLRP3 activation. (a) Unprimed WT, *Card9*$^{-/-}$ and *Pycard*$^{-/-}$ BMDMs were infected with *S.* Typhimurium at MOI 5 for 2 and 6 hours and the cell lysates were subjected to immunoblot and probed for CARD9, β-Actin and ASC. (b) LPS-primed (200 ng/mL for 3 hours) WT, *Card9*$^{-/-}$ and *Pycard*$^{-/-}$ BMDMs were infected with *S.* Typhimurium at MOI 5 for 2 hours or stimulated with nigericin 5 μM for 30 minutes and the cell lysates were subjected to immunoblot and probed for CARD9, β-Actin and ASC. Images are representative of three independent experiments.

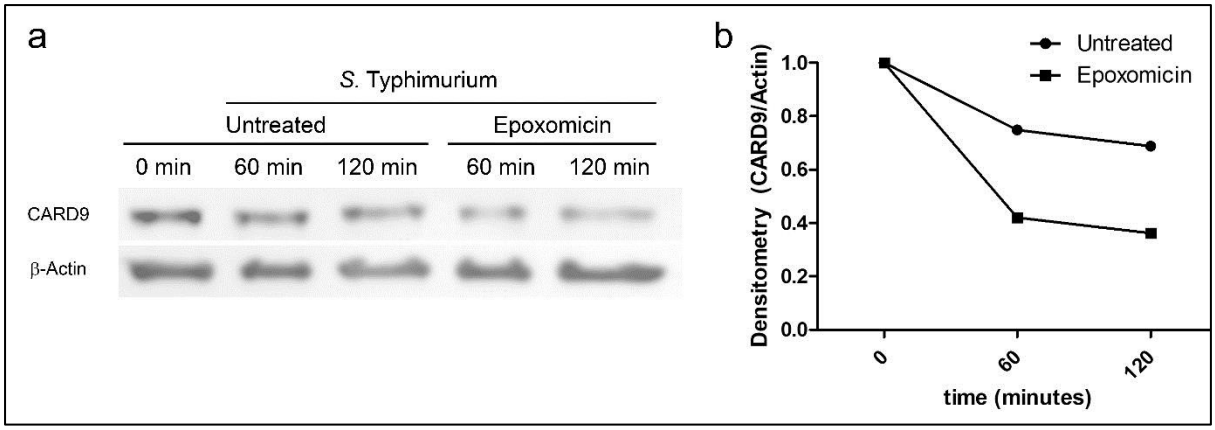

Figure 5.19: Protease inhibition with epoxomicin increases CARD9 degradation in *S.* Typhimurium infected BMDMs. WT BMDMs were infected with *S.* Typhimurium at MOI 5 for 60 and 120 minutes in presence or absence of 1 μM epoxomicin, the cells lysed, and the protein extract subjected to immunoblot probed for CARD9 and β-Actin. (a) Immunoblot and (b) densitometry. Image and densitometry representative of two independent experiments.

Under some conditions, inhibition of proteasome activity can induce autophagy (Lilienbaum, 2013), which could explain why CARD9 degradation increases with addition of epoxomicin. Autophagy is a process responsible for the degradation of cellular components such as organelles and aggregated proteins by the lysosome (Shibutani et al., 2015). To test whether autophagy is the mechanism for the decrease in CARD9 degradation, WT BMDMs were infected with *S.* Typhimurium for one hour with or without the autophagy inhibitor 3-methyladenine (3-MA). The cells were lysed, and the resulting protein lysate was subjected to immunoblotting. No differences in CARD9 expression was observed when using this inhibitor (Figure 5.20, Appendix 17). This may suggest autophagy is not the mechanism for CARD9 degradation, but 3-MA is a phosphoinositide 3-kinase inhibitor and, due its toxicity in macrophages, the concentration used may have been too low for any biological effects to be detected.

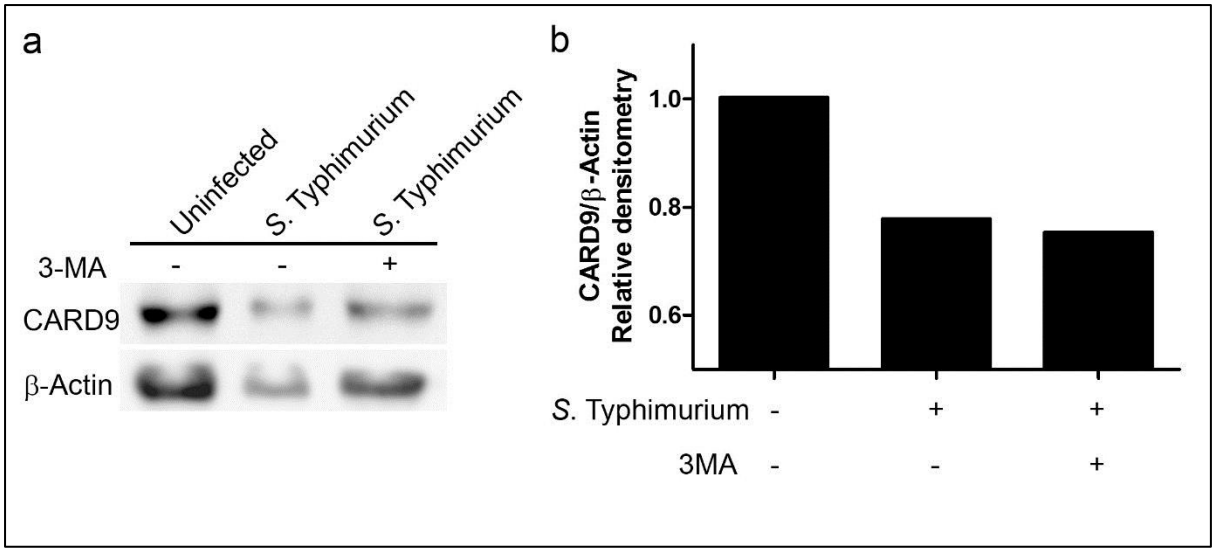

Figure 5.20: Autophagy inhibition with 3MA has no effect on CARD9 degradation during *S.* Typhimurium infection. WT BMDMs were infected for 60 minutes with *S.* Typhimurium at MOI 5 in presence or absence of 2.5 mM 3MA, proteins were extracted and immunoblotted for CARD9 and β-Actin. (a) Immunoblot and (b) densitometry. Image and densitometry representative of two independent experiments.

The preliminary experiments described here sought to investigate whether CARD9 is actively degraded by cellular processes and components such as autophagy and proteasomes. Another possibility however, is that the decrease in CARD9 expression occurs via decrease of *card9* transcription upon infection. To test this possibility, WT BMDMs were infected with *S.* Typhimurium at MOI of 5 for one hour. The mRNA was extracted and *Card9* transcription was quantified pre- and post-infection by qPCR. This approach revealed that BMDMs infected with *Salmonella* showed a statistically significant decrease (20%) in *Card9* mRNA levels (Figure 5.21), suggesting that the CARD9 protein levels are downregulated as a consequence of decreased gene transcription.

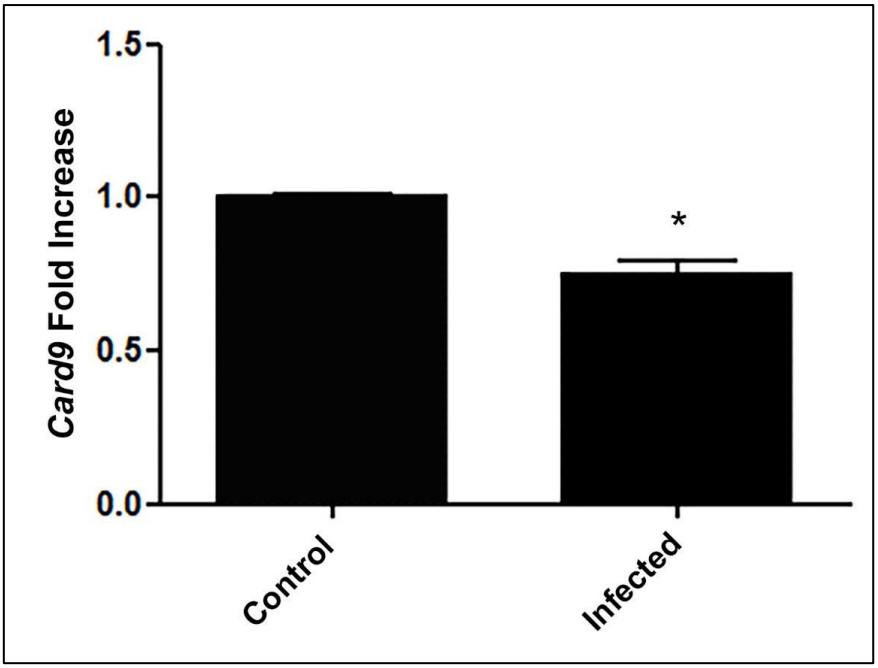

Figure 5.21: *Card9* transcription decreases in WT BMDMs upon infection with *S.* Typhimurium. WT BMDMs were infected for 2 hours with *S.* Typhimurium at MOI 5, the RNA was then extracted and subjected to qPCR using GAPDH and β-Actin as reference genes. * $p<0.05$ (unpaired t-test). Data represent the mean from three independent experiments while error bars show the s.e.m.

5.3 Discussion

Infection of CARD9 knockout macrophages with *S*. Typhimurium revealed that this protein is involved in inhibiting the production of IL-1β whilst not affecting cellular viability or TNF-α production. Evidence presented in Chapter 4 of this thesis suggests that CARD9 is an inhibitor of the canonical NLRP3 inflammasome. Due the nature of this inflammasome, two non-exclusive hypotheses were raised. First, the production of IL-1β is decreased due lower pro-IL-1β availability, meaning that CARD9 fine-tunes the "licensing step" of NLRP3 activation by inhibiting gene transcription. Second, CARD9 inhibits the inflammasome pro-IL-1β processing activity without affecting pyroptosis. In this chapter, my was goal to elucidate which stages(s) of NLRP3 inflammasome activation are inhibited by CARD9 and explore possible mechanisms on how this inhibition occurs.

The first hypothesis was supported by experiments analysing mRNA levels in WT and *Card9*$^{-/-}$ BMDMs upon *S*. Typhimurium infection. This set of experiments revealed that after

infection, CARD9 knockout macrophages upregulate *il1b* transcription to a greater extent than the WT controls, without affecting the transcription level of genes such as *Tnfa and Rantes* (Figure 5.12). This selective effect on *il1b* transcription was puzzling, since TLR4 is the most important PRR involved in NLRP3 licensing during *Salmonella* infection. When TLR4 is activated, NF-κB activation occurs leading to transcription of genes including *Il1b* and *Tnfa* (Hiscott et al., 1993; Shakhov et al., 1990) and later, IRF3-dependent transcription of *Rantes* (Lin et al., 1999). Thus NF-κB is an unlikely candidate for CARD9 regulation in the context of *Salmonella* infection of BMDMs.

The literature on CARD9 suggests an alternative mechanism. A previous study reported that CARD9 functions as an adaptor in the NOD2 signalling pathway (Hsu et al., 2007). In this pathway, NOD2 activation leads to CARD9-independent activation of NF-κB as well as CARD9-dependent activation of the MAPKs p38 and JNK (Figure 1.10). Both p38 and JNK activate AP-1, a transcription factor involved in *il1b* transcription (Roman et al., 2000), whereas *tnfa* transcription is not related to these MAPKs (Baldassare et al., 1999). It is feasible, therefore, that CARD9 controls *il1b* transcription via p38 and/or JNK.

Although NOD2 is classically regarded as an activator of inflammatory responses in response to "pure" ligands such as MDP (Girardin et al., 2003), co-stimulation of this NLR with other PRRs demonstrates that NOD2's role is context dependent (Dahiya et al., 2011; Hedl and Abraham, 2012; Kim et al., 2015; Watanabe et al., 2008, 2006, 2004). For instance, pro-IL-1β expression is inhibited when either TLR2 or TLR4 are co-stimulated with NOD2 (Dahiya et al., 2011; Kim et al., 2015), and *Nod2*$^{-/-}$ splenocytes produce more IL-18 than WT controls upon TLR2 activation (Watanabe et al., 2004). *S.* Typhimurium infection activates primarily TLR4, but NOD2 is also engaged in the response against this pathogen. It is possible that in the context of *Salmonella* infections, NOD2 negatively modulates the production of certain cytokines. Infection assays conducted on *Nod2*$^{-/-}$ BMDMs appear to support this hypothesis as these cells produce less TNF-α, but more IL-1β (Figure 5.14).

To formally link CARD9 to NOD2 in the context of *Salmonella* infections and pro-IL-1β production, the use of primary macrophages derived from CARD9 and NOD2 double knockout mice would be required. Unfortunately, our laboratory does not possess this strain. To circumvent these problems, I have performed *Salmonella* infections whilst co-stimulating NOD2 with its ligand, MDP. The rationale behind this approach was that if NOD2 is indeed an inhibitor of pro-IL-1β in the context of a complex pathogen such as *S.* Typhimurium, then co-stimulation of this PRR would accentuate this inhibitory effect. Indeed, in this experimental setting, pro-IL-1β expression is inhibited by NOD2 overstimulation in WT cells,

but not in *Card9*$^{-/-}$ BMDMs (Figure 5.15) This finding provides further support for a NOD2 inhibitory role using CARD9 as an adaptor.

This inhibitory effect possibly involves the transcription factor AP-1, since it controls *Il1b* transcription and has its activity modulated by the MAPKs p38 and JNK (Arthur and Ley, 2013; Roman et al., 2000). JNK and p38 are in turn controlled by CARD9 in the NOD2 pathway (Hsu et al., 2007). An attempt to link AP-1, JNK and p38 to pro-IL-1β expression was made using pharmacological inhibitors in the context of *S*. Typhimurium infection and NOD2 co-stimulation. The results obtained supports an inhibitory role for AP-1 and JNK in pro-IL-1β expression. The data supporting this claim, however, should be interpreted with caution, as it relies on pharmacological inhibition of kinases and transcription factors involved in numerous biological responses, such that toxicity and adverse effects should be expected (Figure 5.16).

Even though the evidence discussed above supports a role for CARD9 as an inhibitor of *Il1b* transcription, this alone cannot explain all of the data acquired. For instance, LPS-primed macrophages have similar pro-IL-1β expression levels (Figure 5.2), but upon NLRP3 stimulation the amount of IL-1β released by primed *Card9*$^{-/-}$ macrophages is greater than that released by LPS-primed WT controls (Figure 4.10-11), suggesting a role for CARD9 in regulating the second stage of inflammasome activation. Whilst investigating CARD9 interaction with inflammasome components, it was observed that upon inflammasome stimulation, CARD9 preferably interacts with the unphosphorylated form of SYK (Figure 4.17). This finding hinted that this kinase could be involved in the described *Card9*$^{-/-}$ phenotype. Indeed, SYK inhibition in the context of *Salmonella* infection or nigericin stimulation inhibits IL-1β production in both WT and *Card9*$^{-/-}$ BMDMs. Upon inhibition, the IL-1β output is similar between those two cell types. This suggests that the incremental IL-1β production observed in CARD9 knockout macrophages does involve SYK activity (Figure 5.1). Immunoblot analysis of the p-SYK/SYK relation further substantiates this finding. In CARD9 knockout macrophages, a higher percentage of SYK is found in its active form, i.e. phosphorylated, likely increasing IL-1β production via the NLRP3 inflammasome (Figure 5.5). One potential interpretation of this result is that the CARD9 interaction with unphosphorylated SYK “blocks” its phosphorylation, and in *Card9*$^{-/-}$ cells the p-SYK/SYK equilibrium is shifted towards p-SYK. Since SYK is activated by phosphorylation at tyrosine 525/526 (Zhang et al., 2000), the higher p-SYK levels found in *Card9*$^{-/-}$ BMDMs could contribute to the higher IL-1β production.

Despite their many similarities, macrophages and dendritic cells behave differently in many aspects, including NLRP3 (Hara et al., 2013) and CARD9 signalling (Goodridge et al., 2009;

Hara et al., 2008, 2007). One of the differences between the NLRP3 inflammasomes of macrophages and dendritic cells regards the phosphorylation of ASC by SYK. In macrophages, SYK activity enhances cytokine production by the NLRP3 inflammasome, whereas in dendritic cells SYK does not contribute to this activity (Hara et al., 2013). If the CARD9 phenotype indeed involves SYK, it was feasible that the phenotype would be different in dendritic cells. Indeed, infection of WT and CARD9 knockout BMDCs with *S.* Typhimurium revealed no statistically significant differences in relation to cell viability and IL-1β production (Figure 5.3). Similarly, LPS-primed BMDCs from WT and *Card9*$^{-/-}$ mice produced comparable levels of IL-1β in response to nigericin stimulation. Both WT and *Card9*$^{-/-}$ cells were unaffected by SYK inhibition, as previously reported (Hara et al., 2013) (Figure 5.4). This observation illustrates the complexity of signalling pathways in innate immunity and that results obtained in a specific cell types should not be generalised.

The enhanced IL-1β production dissociated from pyroptosis remained puzzling. Often, increased IL-1β production is accompanied by increased cell death via pyroptosis, a characteristic not observed in *Card9*$^{-/-}$ BMDMs (Figure 3.24-35). Previously, however, our research group described caspase-8 as a component of the inflammasome (Man et al., 2014, 2013). In the context of inflammasome activation, caspase-8 undertakes a complementary role in pro-IL-1β processing but is unable to process pro-IL-18 and does not stimulate pyroptosis, roles attributed to caspase-1. This observation raised the hypothesis that in the absence of CARD9, caspase-8-mediated IL-1β production is enhanced. Recent evidence suggests that caspase-8 can trigger cell death downstream NLRC4 activation in the absence of caspase-1 (Lee et al., 2018; Mascarenhas et al., 2017; Schneider et al., 2017). Since caspase-1 remains active in *Card9*$^{-/-}$ macrophages, it is unlikely that caspase-8 contributes significantly to cell death.

The caspase-8/IL-1β hypothesis was tested by stimulating the inflammasome in presence of the caspase-8 inhibitor z-ietd-fmk. This resulted in inhibition of IL-1β production in both WT and *Card9*$^{-/-}$ BMDMs, whilst cellular viability remained unchanged (Figure 5.6). Similar to what is observed in SYK inhibition assays (Figure 5.1), z-ietd-fmk decreased the IL-1β output to similar levels in WT and CARD9 knockout BMDMs, suggesting that the incremental IL-1β produced by *Card9*$^{-/-}$ cells involves caspase-8 (Figure 5.6).

Interestingly, similar results and conclusions were obtained from SYK and caspase-8 inhibition experiments. One explanation for such similar results would be that SYK and caspase-8 are found in the same pathway, and inhibition of either of them has comparable outcomes. Since caspase-8 is found downstream in the NLRP3 inflammasome signalling pathway, where it is responsible for IL-1β production, I hypothesized that SYK activity

influences caspase-8 recruitment to the NLRP3 inflammasome. Analysis of caspase-1 and caspase-8 speck formation upon NLRP3 stimulation supports a link between SYK and caspase-8, but not caspase-1. In presence of SYK inhibitor, caspase-8 specking decreases, whilst caspase-1 specking does not change significantly (Figure 5.9). The outcome of this recruitment pattern would be increased caspase-8-mediated IL-1β production whilst caspase-1-mediated pyroptosis would not change significantly.

It is unclear how SYK activity enhances caspase-8 recruitment to the inflammasome. One possibility is that since SYK phosphorylates ASC in its CARD domain (Hara et al., 2013), it is plausible that this phosphorylation modulates ASC's affinity for caspase-1 and caspase-8. Caspase-1 binds to ASC via CARD/CARD interactions (Srinivasula et al., 2002), a domain absent in Caspase-8 (Muzio et al., 1996). In this scenario, ASC phosphorylation could potentially decrease interaction with caspase-1 due the phosphorylated CARD, and favour the interaction between its PYD domain and caspase-8's DED domain, resulting in enhanced caspase-8 recruitment to the inflammasome. No significant decrease in caspase-1 recruitment, however, was observed using immunofluorescence staining. This could be due the low sensitivity of the technique employed, as it relies on manually enumerating cells positive for caspase-1 and caspase-8 specks. Counting a much greater number of events, either by automation of speck counting or by using techniques such as flow cytometry, could potentially detect differences in caspase-1 specking. Optimization of such techniques is an ongoing effort in our laboratory.

This is not the first time that a functional link between SYK, CARD9 and caspase-8 is reported. In dendritic cells during fungal infections, the dectin-1 receptor is activated and stimulates SYK. This kinase in turn activates PKC-γ which phosphorylates CARD9 leading to the assembly of a non-canonical inflammasome containing CARD9, MALT1, BCL10 and caspase-8 (Gross et al., 2006). This is, however, the first study to link SYK, CARD9 and caspase-8 in the context of a canonical inflammasome. Interestingly, the well-described role that SYK has in the dectin-1 pathway places this kinase upstream of CARD9. This is in contrast with the data presented in this work, which suggests that in the canonical NLRP3 inflammasome, SYK acts downstream of CARD9. Another key difference between the caspase-8 non-canonical inflammasome and the pathway suggested in this chapter is the role played by CARD9. Whilst in the dectin-1 pathway CARD9 has a pro-inflammatory role upregulating IL-1β production in response to fungal pathogens, in the canonical NLRP3 inflammasome CARD9 decreases the production of this cytokine.

The data presented in this thesis and studies previously published in the literature links CARD9 to numerous signalling pathways controlling inflammation including NOD2, Dectin-1,

RIG-I, ROS production and the NLRP3 inflammasome (Gross et al., 2006; Hsu et al., 2007; Poeck et al., 2010; Wu et al., 2009). This suggests that CARD9 is a signalling hub responsible for coordinating inflammatory responses, and its function must be tightly regulated, since both excessive inflammation and lack of inflammatory responses can be detrimental to the host. Not much is known, however, about the signalling events responsible for the modulation of CARD9 function. One example of such regulation involves PKC-γ. In the context of the dectin-1 pathway, this kinase phosphorylates CARD9, allowing it to interact with BCL10 and MALT1 thus positively modulating gene transcription (Gross et al., 2006). In this chapter, another potential mechanism for CARD9 regulation was described: downregulation of protein expression.

CARD9 is a protein constitutively expressed in cells such as macrophages (Heng and Painter, 2008; Hsu et al., 2007), and upon infection, its expression decreases overtime (Figure 5.17). One possible cause for the observed decrease in expression is decreased gene transcription, as *Card9* mRNA was found to be downregulated upon *Salmonella* infection (Figure 5.21). It is unclear if the observed 20% decrease in *Card9* transcription is enough to account for the decrease in protein expression. This would be possible if CARD9 is a protein with a high turnover rate, i.e. short half-life, but unfortunately data regarding CARD9's half-life is lacking. In any case, protein degradation by processes such as autophagy and proteasomes cannot be ruled out. Preliminary experiments using pharmacological inhibitors of these processes were, however, inconclusive (Figure 5.19-20), but remain an avenue for further investigation.

Many other questions regarding the decrease in CARD9 expression remain unanswered. Amongst those questions is what triggers its degradation. Infection experiments using *S.* Typhimurium and stimulation of the canonical NLRP3 inflammasome revealed that this process does not require inflammasome formation, as nigericin alone does not affect CARD9 expression and, equally, ASC plays no role in this phenomenon (Figure 5.18). It is possible that a bacterial factor causes this degradation to occur, perhaps by activating another PRR. If this is the case, it is unlikely to involve TLR4, as LPS-primed cells continues to express CARD9. Another unexplored possibility is that the bacteria itself injects effector protein(s) in the host cytoplasm triggering signalling events that culminates in CARD9 decreased expression.

In summary, data presented in this chapter suggests that CARD9 acts as an inhibitor of the inflammasome by fine-tuning both steps of NLRP3 activation, that is, the transcription of *il1b* via NOD2 and IL-1β production by modulating caspase-8 recruitment to the inflammasome. Additionally, CARD9 itself is downregulated during infection, which probably allows the cell

to overcome its inhibition and produce greater quantities of IL-1β over the course of the infection. Figure 5.22 illustrates the proposed mechanism for CARD9 regulation of the NLRP3 inflammasome.

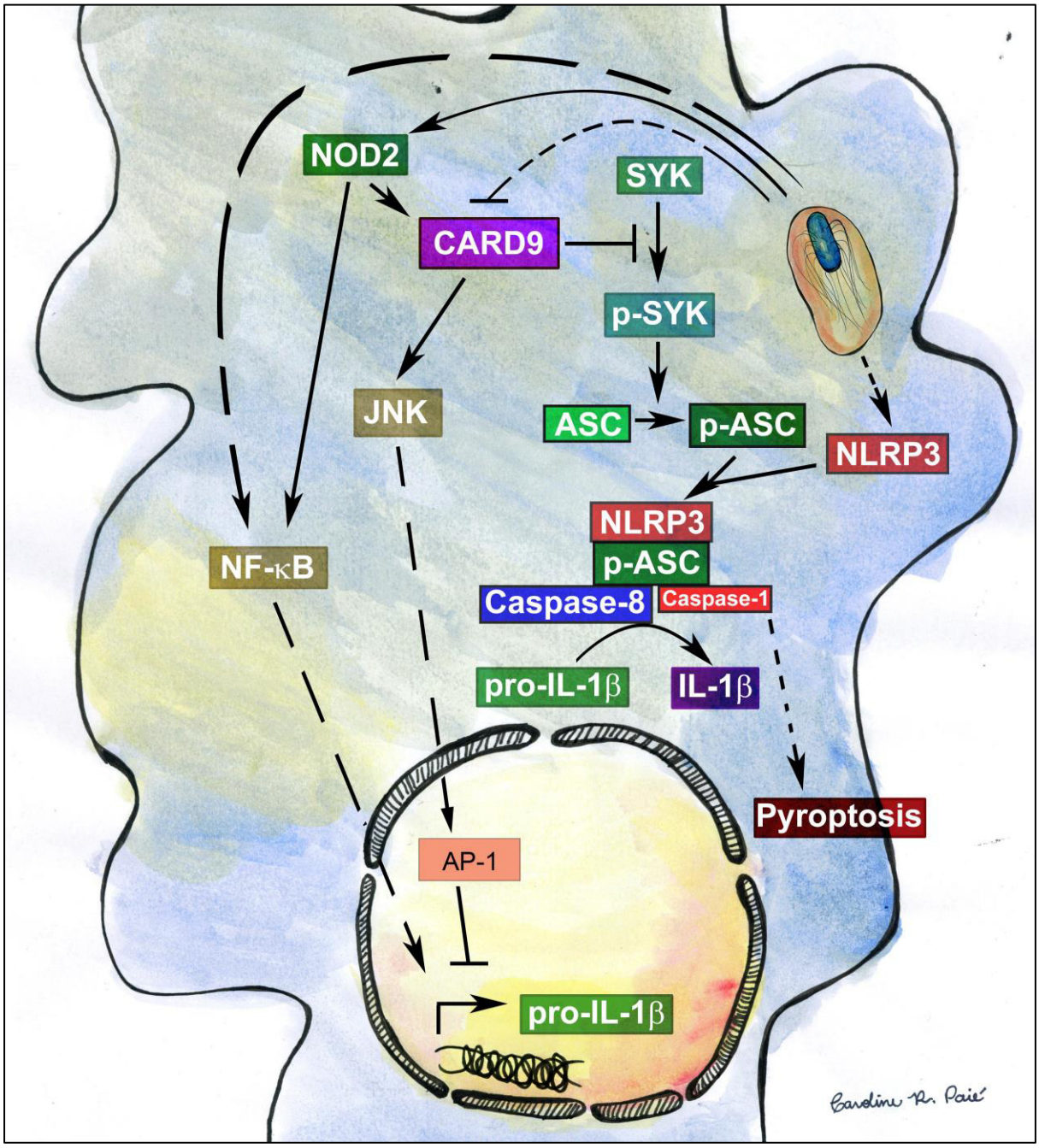

Figure 5.22: Simplified model for CARD9 regulation of IL-1β production in murine macrophages. Infection of BMDMs by *S*. Typhimurium triggers the assembly of the NLRP3 inflammasome in the cytoplasm of BMDMs with subsequent processing of pro-IL-1β to mature IL-1β. CARD9 negatively regulates inflammasome activity at two levels: suppressing pro-IL-1β expression and reducing caspase-8-dependent IL-1β processing.

Chapter 6

General discussion

Inflammation is essential for combating infections. Failing to achieve inflammation resolution, however, can be harmful for the host (Fullerton and Gilroy, 2016). Chronic inflammation is often involved in pathologies such as diabetes, psoriasis, rheumatoid arthritis, ulcerative colitis, Chron's disease, and others (Hotamisligil, 2017; Khor et al., 2011; Lowes et al., 2007), while uncontrolled acute inflammation is one of the hallmarks of sepsis (Cohen, 2002). Inflammation must therefore be tightly regulated.

One mechanism by which this is achieved is by regulating the activity of the inflammasome which triggers an immune response characterised by cell death, secretion of pro-inflammatory cytokines and can drive an eicosanoid storm (Schroder and Tschopp, 2010; von Moltke et al., 2012). Impairment in inflammasome activation is thought to be involved in increased susceptibility to infections while gain of function mutations are involved in autoimmune pathologies including Muckle-Wells Syndrome, familial cold autoinflammatory syndrome, and other diseases featuring symptoms such as fever and cold sensitivity (Aganna et al., 2002; Dodé et al., 2002; Hoffman et al., 2001; Zhong et al., 2013).

In spite of its role in health and disease, the events and molecules regulating inflammasome activity have only started to emerge. The aim of my PhD was, first, to identify proteins that may be linked to inflammasome activation in murine BMDMs infected with *S*. Typhimurium and, second, to characterise how these proteins are involved in inflammasome biology.

A "screening" approach was employed to achieve the first aim. Our laboratory has access to a variety of mice carrying knockout mutations of PRR-associated genes that are related and unrelated to inflammasome biology. Some of these mouse strains had not been studied in the context of *Salmonella*-induced inflammasome activation. I therefore infected BMDMs derived from these animals with *S*. Typhimurium and determined intracellular bacteria counts, cellular viability and IL-1β release as measures of inflammasome activation.

With this approach I found that the NLRs NLRC3 and NLRC5 are involved in inflammasome signalling during *Salmonella* infection by controlling IL-1β production and cell death. Previous research identified NLRC3 and NLRC5 as inhibitors of innate immune pathways such as NF-κB, but how these NLRs impact inflammasome activity remains unknown (Cui et al., 2010; Schneider et al., 2012; Tong et al., 2012; Zhang et al., 2014). Caspase-2 was found to have a similar role to that of caspase-8, that is production of IL-1β independently of

cell death, further illustrating the significant degree of functional redundancy seen amongst caspases (Man et al., 2013). This conflict with a previous study that found that caspase-2 is involved in *Salmonella*-dependent cell death in macrophages. These conflicting findings could be explained by the fact that the experimenters infected macrophages with bacteria transitioning from stationary to logarithmic phase whilst I infected macrophages with bacteria in the logarithmic growth phase, an experimental condition known to better stimulate NLRC4 due the higher expression of SPI-I proteins (Jesenberger et al., 2000; Lara-Tejero et al., 2006). Further studies are required to elucidate the mechanisms via which NLRC3, NLRC5 and caspase-2 affect inflammasome activation during infection. The role of NLRC3 and NLRC5 will be studied in our laboratory in the near future, whilst studies on caspase-2 activity in the context of *Salmonella* infection will be conducted in collaboration with Professor Andreas Strasser (Walter and Eliza Hall Institute of Medical Research, Australia).

I also found evidence that gasdermin D, which is considered the executioner of pyroptosis (Aglietti et al., 2016; Kayagaki et al., 2015; Shi et al., 2015), is not the only player in the context of *Salmonella* infection, as macrophages derived from *GasderminD*$^{-/-}$ mice are only partially protected from *Salmonella*-induced cell death. Previously, gasdermin A, B, C and DFNA5, also known as gasdermin E, were shown to be insensitive to cleavage by caspase-1 (Rogers et al., 2017; Shi et al., 2015). This however does not completely rule out these proteins as potential executioners of cell death in specific contexts, as illustrated by the fact that DFNA5 is cleaved by caspase-3 and is involved in the execution of secondary necrosis and pyroptosis (Rogers et al., 2017; Wang et al., 2017). I was able to show that DFNA5 is not the second player in executing pyroptosis in the context of inflammasome activation, since *Dfna5*$^{-/-}$*GasderminD*$^{-/-}$ and *GasderminD*$^{-/-}$ macrophages had similar phenotypes. In this thesis I was unable to test whether other gasdermin proteins are involved in *Salmonella*-pyroptosis, since mice knockout for other gasdermin family proteins were unavailable. The search for additional pyroptosis executioners is still ongoing.

The most surprising finding of my initial screen, however, was that the adaptor CARD9 inhibited *Salmonella*-induced IL-1β production without affecting cell death and the production of other Toll-like receptor-related cytokines such as TNF-α. I therefore followed up CARD9 for further study. CARD9 is an adaptor protein with multiple roles in cell signalling during innate immunity against, primarily, fungal and viral infections. This includes stimulation of the NF-κB pathway and non-canonical caspase-8 inflammasome assembly (Bertin et al., 2000; Gringhuis et al., 2012; Poeck et al., 2010). My work, however, showed that CARD9 plays an anti-inflammatory role in the context of gram-negative infections in macrophages. Similar findings were independently reported using *in vivo* murine infection models, where increased

inflammation in *Card9*$^{-/-}$ mice was associated with increased *Il1b* transcription in the gut (Lamas et al., 2016). These findings suggest that, depending on the stimulus, CARD9 could have pro-inflammatory or anti-inflammatory properties. It could, therefore, be acting as a central signalling hub modulating inflammatory responses.

The clinical relevance of this protein is illustrated by human genome-wide association studies often correlating CARD9 mutations to pathologies where increased inflammation is observed (Khor et al., 2011), such as inflammatory bowel diseases (IBD). Amongst the clinical relevant CARD9 mutations are non-silent single nucleotide polymorphisms (Beaudoin et al., 2013; Hong et al., 2015; Zhernakova et al., 2008) and splice variants (Rivas et al., 2011) with protective effects. In other pathologies, such as nephropathy, CARD9 mutations are associated with increased risk in developing the disease (Kiryluk et al., 2014). It is unclear at the moment how most of these mutations affect the various CARD9 functions. In the specific case of the CARD9 splice variant CARD9Δ11, NF-κB signalling in response to fungal pathogens is deficient due an impairment in the interaction with the ubiquitin ligase TRIM62 (Cao et al., 2015). This mutation is also associated with increased protein expression and has protective effects on IBD (Pointon et al., 2010; Zhernakova et al., 2008). It is unknown whether the other clinically-relevant CARD9 mutations involve a gain or loss of function.

Further analysis into the mechanisms by which CARD9 inhibits IL-1β production revealed a link to the canonical NLRP3 inflammasome. Upon bacterial infection, CARD9 prevents caspase-8 recruitment to the NLRP3 inflammasome, possibly by modulating SYK activity. In the inflammasome, caspase-8 is involved in processing pro-IL-1β to its mature form, whilst not affecting pyroptotic cell death (Man et al., 2013). Recent studies suggest that caspase-8 can trigger cell death downstream NLRC4 activation (Lee et al., 2018; Mascarenhas et al., 2017; Schneider et al., 2017). The caspase-8 effects on cell death were, however, only significant when cells lacking caspase-1 were used. Since caspase-1 remains active in *Card9*$^{-/-}$ macrophages, it is unlikely that caspase-8 contributes significantly to cell death. The increased IL-1β production in *Card9*$^{-/-}$ cells could be explained by an increase in caspase-8 activity or increased caspase 8 recruitment to the inflammasome. At the moment it is unclear how SYK controls caspase-8 recruitment to the NLRP3 inflammasome, but it is possible that SYK-mediated ASC Y144 phosphorylation (Hara et al., 2013) could be involved in this process. The use of cells that are both CARD9 knockout and ASC Y144F (tyrosine to phenylalanine point mutation, insensitive to phosphorylation) in future experiments could potentially elucidate the links between CARD9, SYK, ASC and caspase-8.

In addition to its inhibitory role on NLRP3-mediated IL-1β production, I have found that CARD9 is involved in controlling *Il1b* transcription, thus affecting pro-IL-1β availability. This effect appeared to be unrelated to other NF-κB target genes such as *Tnfa* and *Rantes*. Previously, in the context of bacterial infections, CARD9 was described as an adaptor in the NOD2 pathway, linking this NLR to gene transcription via MAPKs but not via NF-κB (Hsu et al., 2007). I therefore hypothesized that the CARD9 transcriptional effect occurs downstream the MAPK branch of the NOD2 pathway and does not require NF-κB.

Nod2 was one of the first genes linked to Crohn's disease in human patients (Hugot et al., 2001), a finding that was independently confirmed in a variety of settings and experimental approaches, including unbiased genome-wide association studies (Uniken Venema et al., 2017). The mechanisms mediating how NOD2 links to Crohn's disease are, however, less clear. *In vivo* studies using *Nod2*$^{-/-}$ mice have revealed varying results, such as impairment in the production of α-defensins (Kobayashi et al., 2005), increased production of pro-inflammatory cytokines (Barreau et al., 2007), or no signs of intestinal pathology (Pauleau and Murray, 2003). In recent years however, the precise role of NOD2 is under revaluation: MDP stimulation of the NOD2 pathway reveals a pro-inflammatory role for this protein (Girardin et al., 2003), but opposite results are obtained when NOD2 is co-stimulated with other PRRs, such as TLR2 and TLR4 (Dahiya et al., 2011; Hedl and Abraham, 2012; Kim et al., 2015; Watanabe et al., 2008, 2006, 2004). This is suggestive of a context-dependent role for NOD2.

CARD9 is an adaptor that acts downstream of NOD2 (Hsu et al., 2007). This potentially explains why both proteins are often correlated with IBD. It is also plausible that the clinical data supporting an anti-inflammatory role for CARD9 and NOD2 conflicts with that obtained from *in vitro* trials because in a clinical setting many PRRs are simultaneously stimulated, thus more similar to experiments where NOD2/TLR have been co-stimulated. In this thesis, I have presented data from experiments where I stimulated NOD2 during *Salmonella* infection and found that CARD9 and NOD2 are both involved in suppressing IL-1β by controlling pro-IL-1β expression. This raises the question of whether CARD9 and NOD2 mutations could result in increased IL-1β production in the gut, thus contributing to IBD pathogenesis. Increased IL-1β is observed in IBD patients (Ligumsky et al., 1990), but a definitive link between this cytokine and CARD9 in a clinical setting has yet to be demonstrated. A potential approach could be to use of IBD animal models. This is, however, not a simple task, as IBD is a broad term used to describe multiple diseases such as ulcerative colitis and Chron's disease, and the numerous animal models available have their own limitations (Goyal et al., 2014). Assuming that CARD9 is indeed involved in IBD

pathogenesis by acting as an adaptor in the NOD2 pathway raises the possibility for pharmacological intervention to potentially treat these diseases. The physical interaction between these two proteins requires the NACHT domain and the linker region between CARD and NACHT of NOD2, but the CARD9 domains involved in this interaction are unknown (Parkhouse et al., 2014). To design a drug to target this interaction would require further biochemical studies to determine how CARD9 interacts with NOD2 and/or structural studies on these proteins. Targeting specific CARD9 interactions is feasible, as illustrated by the recent development of a pharmacological inhibitor that targets the CARD9 interaction with the ubiquitin ligase TRIM62. Disrupting this interaction impairs the NF-κB pathway during fungal innate immunity, thus having an anti-inflammatory effect without disrupting other pathways where CARD9 is involved (Cao et al., 2015; Leshchiner et al., 2017).

My data suggests that the inhibitory effect that CARD9 has on IL-1β transcription and production is prevented by CARD9 degradation during infection. Upon BMDM infection with *Salmonella*, CARD9 expression decreases, potentially enhancing NLRP3 inflammasome activity. One of the open questions from my work at the moment is how exactly decreased CARD9 expression occurs and what are its consequences. I saw a decrease in *Card9* transcription, so this is likely to contribute to its decreased expression. Preliminary experiments on autophagy and proteasome degradation were inconclusive and further experimentation is required to establish whether CARD9 degradation also occurs. It is possible that a bacterial factor unrelated to inflammasome activation may trigger the reduction in CARD9 expression, since NLRP3 stimulation with nigericin did not alter CARD9 expression. It is possible that the bacteria actively secrete an effector protein into the cytosol to decrease CARD9 expression. If expression of CARD9 is supressed by a bacterial factor, it is then unclear whether CARD9 expression is beneficial to the bacteria or to the host. *In vivo* infection of *Card9*$^{-/-}$ mice with *S*. Typhimurium showed a marginal, but not statistically significant, increase in bacterial burden in the spleen and liver of infected animals. Closer examination of the cytokine profile of *Salmonella* infected WT and *Card9*$^{-/-}$ mice could provide further clues on CARD9 relevance during infection. Unfortunately, the serum samples from this set of experiments were used in a failed attempt to quantify IL-1β and none was left to quantify other cytokines.

In summary, *Salmonella* infection of cultured macrophages derived from specific knockout mice identified proteins likely to be involved in inflammasome biology, such as NLRC3, NLRC5, caspase-2 and CARD9. While work on NLRC3, NLRC5 and caspase-2 is still ongoing, detailed investigation into CARD9 function during *Salmonella* infection revealed that this protein finely tunes IL-1β production by modulating both pro-IL-1β availability and processing during NLRP3 activation.

Bibliography

Aachoui, Y., Leaf, I.A., Hagar, J.A., Fontana, M.F., Campos, C.G., Zak, D.E., Tan, M.H., Cotter, P.A., Vance, R.E., Aderem, A., Miao, E.A., 2013. Caspase-11 protects against bacteria that escape the vacuole. Science (80-.). 339, 975–978. doi:10.1126/science.1230751

Abbott, D.W., Wilkins, A., Asara, J.M., Cantley, L.C., 2004. The Crohn's Disease Protein, NOD2, Requires RIP2 in Order to Induce Ubiquitinylation of a Novel Site on NEMO. Curr. Biol. 14, 2217–2227. doi:10.1016/j

Abdul-Sater, A.A., Koo, E., Häcker, G., Ojcius, D.M., 2009. Inflammasome-dependent caspase-1 activation in cervical epithelial cells stimulates growth of the intracellular pathogen Chlamydia trachomatis. J. Biol. Chem. 284, 26789–26796. doi:10.1074/jbc.M109.026823

Aganna, E., Martinon, F., Hawkins, P.N., Ross, J.B., Swan, D.C., Booth, D.R., Lachmann, H.J., Gaudet, R., Woo, P., Feighery, C., Cotter, F.E., Thome, M., Hitman, G.A., Tschopp, J., McDermott, M.F., 2002. Association of mutations in the NALP3/CIAS1/PYPAF1 gene with a broad phenotype including recurrent fever, cold sensitivity, sensorineural deafness, and AA amyloidosis. Arthritis Rheum. 46, 2445–2452. doi:10.1002/art.10509

Aglietti, R.A., Estevez, A., Gupta, A., Ramirez, M.G., Liu, P.S., Kayagaki, N., Ciferri, C., Dixit, V.M., Dueber, E.C., 2016. GsdmD p30 elicited by caspase-11 during pyroptosis forms pores in membranes. Proc. Natl. Acad. Sci. U. S. A. 201607769. doi:10.1073/pnas.1607769113

Agostini, L., Martinon, F., Burns, K., McDermott, M.F., Hawkins, P.N., Tschopp, J., 2004. NALP3 forms an IL-1β-processing inflammasome with increased activity in Muckle-Wells autoinflammatory disorder. Immunity 20, 319–325. doi:10.1016/S1074-7613(04)00046-9

Allen, I.C., Moore, C.B., Schneider, M., Lei, Y., Davis, B.K., Scull, M. a, Gris, D., Roney, K.E., Zimmermann, A.G., Bowzard, J.B., Ranjan, P., Monroe, K.M., Pickles, R.J., Sambhara, S., Ting, J.P.Y., 2011. NLRX1 protein attenuates inflammatory responses to infection by interfering with the RIG-I-MAVS and TRAF6-NF-κB signaling pathways. Immunity 34, 854–865. doi:10.1016/j.immuni.2011.03.026

Allen, I.C., Scull, M.A., Moore, C.B., Holl, E.K., McElvania-TeKippe, E., Taxman, D.J., Guthrie, E.H., Pickles, R.J., Ting, J.P.Y., 2009. The NLRP3 Inflammasome Mediates In Vivo Innate Immunity to Influenza A Virus through Recognition of Viral RNA. Immunity 30, 556–565. doi:10.1016/j.immuni.2009.02.005

Amer, A., Franchi, L., Kanneganti, T.D., Body-Malapel, M., Özören, N., Brady, G., Meshinchi, S., Jagirdar, R., Gewirtz, A., Akira, S., Núñez, G., 2006. Regulation of Legionella phagosome maturation and infection through flagellin and host Ipaf. J. Biol. Chem. 281, 35217–35223. doi:10.1074/jbc.M604933200

Anand, P.K., Malireddi, R.K.S., Lukens, J.R., Vogel, P., Bertin, J., Lamkanfi, M., Kanneganti, T.-D., 2012. NLRP6 negatively regulates innate immunity and host defence against bacterial pathogens. Nature 488, 389–93. doi:10.1038/nature11250

Arpaia, N., Godec, J., Lau, L., Sivick, K.E., McLaughlin, L.M., Jones, M.B., Dracheva, T., Peterson, S.N., Monack, D.M., Barton, G.M., 2011. TLR signaling is required for Salmonella typhimurium virulence. Cell 144, 675–688. doi:10.1016/j.cell.2011.01.031

Arthur, J.S.C., Ley, S.C., 2013. Mitogen-activated protein kinases in innate immunity. Nat. Rev. Immunol. 13, 679–92. doi:10.1038/nri3495

Auron, P.E., Webb, A.C., Rosenwasser, L.J., Mucci, S.F., Rich, A., Wolff, S.M., Dinarello, C.A., 1984. Nucleotide sequence of human monocyte interleukin 1 precursor cDNA. Proc. Natl. Acad. Sci. U. S. A. 81, 7907–7911. doi:10.1073/pnas.81.24.7907

Baldassare, J.J., Bi, Y., Bellone, C.J., 1999. The Role of p38 Mitogen-Activated Protein Kinase in IL-1β Transcription. J. Immunol. 162, 5367–5373.

Balzola, F., Bernstein, C., Ho, G.T., Russell, R.K., 2012. Deep resequencing of GWAS loci identifies independent rare variants associated with inflammatory bowel disease. Nat. Genet. 12, 126–127. doi:10.1038/ng.952

Barber, G.N., 2015. STING: infection, inflammation and cancer. Nat. Rev. Immunol. 15, 760–770. doi:10.1038/nri3921

Barreau, F., Meinzer, U., Chareyre, F., Berrebi, D., Niwa-Kawakita, M., Dussaillant, M., Foligne, B., Ollendorff, V., Heyman, M., Bonacorsi, S., Lesuffleur, T., Sterkers, G., Giovannini, M., Hugot, J.P., 2007. CARD15/NOD2 Is Required for Peyer's Patches Homeostasis in Mice. PLoS One 2. doi:10.1371/journal.pone.0000523

Bauernfeind, F.G., Horvath, G., Stutz, A., Alnemri, E.S., MacDonald, K., Speert, D., Fernandes-Alnemri, T., Wu, J., Monks, B.G., Fitzgerald, K.A., Hornung, V., Latz, E., 2009. Cutting edge: NF-kappaB activating pattern recognition and cytokine receptors license NLRP3 inflammasome activation by regulating NLRP3 expression. J. Immunol. 183, 787–791. doi:10.4049/jimmunol.0901363

Beaudoin, M., Goyette, P., Boucher, G., Lo, K.S., Rivas, M.A., Stevens, C., Alikashani, A., Ladouceur, M., Ellinghaus, D., Törkvist, L., Goel, G., Lagacé, C., Annese, V., Bitton, A., Begun, J., Brant, S.R., Bresso, F., Cho, J.H., Duerr, R.H., Halfvarson, J., McGovern, D.P.B., Radford-Smith, G., Schreiber, S., Schumm, P.L., Sharma, Y., Silverberg, M.S., Weersma, R.K., D'Amato, M., Vermeire, S., Franke, A., Lettre, G., Xavier, R.J., Daly, M.J., Rioux, J.D., Aumais, G., Bernard, E.J., Bitton, A., Cohen, A., Deslandres, C., Lahaie, R., Paré, P., Rioux, J.D., Brant, S.R., Cho, J.H., Duerr, R.H., McGovern, D.P.B., Rioux, J.D., Silverberg, M.S., Ellinghaus, D., Franke, A., Targan, S.R., Schumm, P., Rutgeerts, P., Vermeire, S., Silverberg, M.S., Steinhart, a. H., Torkvist, L., D'Amato, M., Schreiber, S., Ahmad, T., Anderson, C. a., Annese, V., Baldassano, R.N., Balschun, T., Barclay, M., Barrett, J.C., Bayless, T.M., Bis, J.C., Brand, S., Brant, S.R., Bumpstead, S., Buning, C., Cho, J.H., Cohen, A., Colombel, J.F., Cottone, M., D'Inca, R., Daly, M.J., Denson, T., Dubinsky, M., Duerr, R.H., Edwards, C., Florin, T., Franchimont, D., Gearry, R., Georges, M., Glas, J., van Gossum, A., Griffiths, A.M., Guthery, S.L., Hakonarson, H., Haritunians, T., Hugot, J.P., de Jong, D.J., Jostins, L., Kugathasan, S., Kullak-Ublick, G., Latiano, A., Laukens, D., Lawrance, I., Lee, J., Lees, C.W., Lemann, M., Levine, A., Libioulle, C., Louis, E., Mansfield, J.C., Mathew, C.G., McGovern, D.P.B., Mitrovic, M., Montgomery, G.W., Mowat, C., Newman, W., Palmieri, O., Panés, J., Parkes, M., Phillips, A., Ponsioen, C.Y., Potocnik, U., Prescott, N.J., Proctor, D.D., Radford-Smith, G.L., Regueiro, M., Rioux, J.D., Roberts, R., Rotter, J.I., Sanderson, J., Sans, M., Satsangi, J., Seibold, F., Sharma, Y., Simms, L.A., Taylor, K.D., Halfvarson, J., Verspaget, H.W., de Vos, M., Walters, T., Wang, K., Weersma, R.K., Whiteman, D., Wijmenga, C., 2013. Deep Resequencing of GWAS Loci Identifies Rare Variants in CARD9, IL23R and RNF186 That Are Associated with Ulcerative Colitis. PLoS Genet. 9. doi:10.1371/journal.pgen.1003723

Bell, B.D., Leverrier, S., Weist, B.M., Newton, R.H., Arechiga, A.F., Luhrs, K.A., Morrissette, N.S., Walsh, C.M., 2008. FADD and caspase-8 control the outcome of autophagic signaling in proliferating T cells. Proc. Natl. Acad. Sci. U. S. A. 105, 16677–16682. doi:10.1073/pnas.0808597105

Bergeron, L., Perez, G.I., Macdonald, G., Shi, L., Sun, Y., Jurisicova, A., Varmuza, S., Latham, K.E., Flaws, J.A., Salter, J.C.M., Hara, H., Moskowitz, M.A., Li, E., Greenberg, A., Tilly, J.L., Yuan, J., 1998. Defects in regulation of apoptosis in caspase-2-deficient mice. Genes Dev. 12, 1304–1314. doi:10.1101/gad.12.9.1304

Bertin, J., Guo, Y., Wang, L., Srinivasula, S.M., Jacobson, M.D., Poyet, J.L., Merriam, S., Du, M.Q., Dyer, M.J.S., Robison, K.E., DiStefano, P.S., Alnemri, E.S., 2000. CARD9 is a novel caspase recruitment domain-containing protein that interacts with BCL10/CLAP and activates NF-kB. J. Biol. Chem. 275, 41082–41086. doi:10.1074/jbc.C000726200

Berube, C., Boucher, L.M., Ma, W., Wakeham, A., Salmena, L., Hakem, R., Yeh, W.C., Mak, T.W., Benchimol, S., 2005. Apoptosis caused by p53-induced protein with death domain (PIDD) depends on the death adapter protein RAIDD. Proc. Natl. Acad. Sci. U. S. A. 102, 14314–14320. doi:10.1073/pnas.0506475102

Boldin, M.P., Varfolomeev, E.E., Pancer, Z., Mett, I.L., Camonis, J.H., Wallach, D., 1995. A novel protein that interacts with the death domain of Fas/APO1 contains a sequence motif related to the death domain. J. Biol. Chem. doi:10.1074/jbc.270.14.7795

Boniface, K., Bak-Jensen, K.S., Li, Y., Blumenschein, W.M., McGeachy, M.J., McClanahan, T.K., McKenzie, B.S., Kastelein, R.A., Cua, D.J., de Waal Malefyt, R., 2009. Prostaglandin E2 regulates Th17 cell differentiation and function through cyclic AMP and EP2/EP4 receptor signaling. J. Exp. Med. 206, 535–548. doi:10.1084/jem.20082293

Boyden, E.D., Deitrich, W.F., 2006. Nalp1b controls mouse macrophage susceptibility to anthrax lethal toxin. Nat. Genet. 38, 240–244. doi:10.1038/ng1724

Brennan, M.A., Cookson, B.T., 2000. Salmonella induces macrophage death by caspase-1-dependent necrosis. Mol. Microbiol. 38, 31–40. doi:10.1046/j.1365-2958.2000.02103.x

Brereton, C.F., Sutton, C.E., Ross, P.J., Iwakura, Y., Pizza, M., Rappuoli, R., Lavelle, E.C., Mills, K.H.G., 2011. Escherichia coli Heat-Labile Enterotoxin Promotes Protective Th17 Responses against Infection by Driving Innate IL-1 and IL-23 Production. J. Immunol. 186, 5896–5906. doi:10.4049/jimmunol.1003789

Brodsky, I.E., Palm, N.W., Sadanand, S., Ryndak, M.B., Sutterwala, F.S., Flavell, R.A., Bliska, J.B., Medzhitov, R., 2010. A Yersinia effector protein promotes virulence by preventing inflammasome recognition of the type III secretion system. Cell Host Microbe 7, 376–387. doi:10.1016/j.chom.2010.04.009

Bronner, D.N., Abuaita, B.H., Chen, X., Fitzgerald, K.A., Nuñez, G., He, Y., Yin, X.-M., O'Riordan, M.X.D., 2015. Endoplasmic Reticulum Stress Activates the Inflammasome via NLRP3- and Caspase-2-Driven Mitochondrial Damage. Immunity 1–12. doi:10.1016/j.immuni.2015.08.008

Broz, P., Newton, K., Lamkanfi, M., Mariathasan, S., Dixit, V.M., Monack, D.M., 2010. Redundant roles for inflammasome receptors NLRP3 and NLRC4 in host defense against Salmonella. J. Exp. Med. 207, 1745–1755. doi:10.1084/jem.20100257

Broz, P., Ruby, T., Belhocine, K., Bouley, D.M., Kayagaki, N., Dixit, V.M., Monack, D.M., 2012. Caspase-11 increases susceptibility to Salmonella infection in the absence of caspase-1. Nature 490, 288–291. doi:10.1038/nature11419

Broz, P., von Moltke, J., Jones, J.W., Vance, R.E., Monack, D.M., 2010b. Differential requirement for Caspase-1 autoproteolysis in pathogen-induced cell death and cytokine processing. Cell Host Microbe 8, 471–83. doi:10.1016/j.chom.2010.11.007

Bryan Coburn, Grassl, G.A., Finlay, B., 2007. Salmonella, the host and disease: a brief review. Immunol. Cell Biol. 85, 112–118. doi:10.1038/sj.icb.7100007

Bürckstümmer, T., Baumann, C., Blüml, S., Dixit, E., Dürnberger, G., Jahn, H., Planyavsky, M., Bilban, M., Colinge, J., Bennett, K.L., Superti-Furga, G., 2009. An orthogonal proteomic-genomic screen identifies AIM2 as a cytoplasmic DNA sensor for the inflammasome. Nat. Immunol. 10, 266–272. doi:10.1038/ni.1702

Burns, K., Martinon, F., Esslinger, C., Pahl, H., Schneider, P., Bodmer, J.L., Di Marco, F., French, L., Tschopp, J., 1998. MyD88, an adapter protein involved in interleukin-1 signaling. J. Biol. Chem. 273, 12203–12209. doi:10.1074/jbc.273.20.12203

Cai, S., Batra, S., Wakamatsu, N., Pacher, P., Jeyaseelan, S., 2012. NLRC4 Inflammasome-Mediated Production of IL-1 Modulates Mucosal Immunity in the Lung against Gram-Negative Bacterial Infection. J. Immunol. 188, 5623–5635. doi:10.4049/jimmunol.1200195

Canna, S.W., de Jesus, A.A., Gouni, S., Brooks, S.R., Marrero, B., Liu, Y., DiMattia, M.A., Zaal, K.J.M., Sanchez, G. a M., Kim, H., Chapelle, D., Plass, N., Huang, Y., Villarino, A. V, Biancotto, A., Fleisher, T.A., Duncan, J.A., O'Shea, J.J., Benseler, S., Grom, A., Deng, Z., Laxer, R.M., Goldbach-Mansky, R., 2014. An activating NLRC4 inflammasome mutation causes autoinflammation with recurrent macrophage activation syndrome. Nat. Genet. 46, 1140–1146. doi:10.1038/ng.3089

Cao, Z., Conway, K.L., Heath, R.J., Rush, J.S., Leshchiner, E.S., Ramirez-Ortiz, Z.G., Nedelsky, N.B., Huang, H., Ng, A., Gardet, A., Cheng, S.C., Shamji, A.F., Rioux, J.D., Wijmenga, C., Netea, M.G., Means, T.K., Daly, M.J., Xavier, R.J., 2015. Ubiquitin Ligase TRIM62 Regulates CARD9-Mediated Anti-fungal Immunity and Intestinal Inflammation. Immunity 43, 715–726. doi:10.1016/j.immuni.2015.10.005

Carlsson, F., Kim, J., Dumitru, C., Barck, K.H., Carano, R.A.D., Sun, M., Diehl, L., Brown, E.J., 2010. Host-detrimental role of Esx-1-mediated inflammasome activation in Mycobacterial infection. PLoS Pathog. 6, 1–12. doi:10.1371/journal.ppat.1000895

Case, C.L., Kohler, L.J., Lima, J.B., Strowig, T., de Zoete, M.R., Flavell, R.A., Zamboni, D.S., Roy, C.R., 2013. Caspase-11 stimulates rapid flagellin-independent pyroptosis in response to Legionella pneumophila. Proc. Natl. Acad. Sci. U. S. A. 110, 1851–1856. doi:10.1073/pnas.1211521110

Cassel, S.L., Eisenbarth, S.C., Iyer, S.S., Sadler, J.L., Colegio, O.R., Tephly, L.A., Carter, A.B., Rothman, P.B., Flavell, R.A., Sutterwala, F.S., 2008. The Nalp3 inflammasome is essential for the development of silicosis. Proc. Natl. Acad. Sci. U. S. A. 105, 9035–9040. doi:10.1073/pnas.0803933105

Cerretti, D., Kozlosky, C., Mosley, B., Nelson, N., Van, N.K., Greenstreet, T., March, C., Kronheim, S., Druck, T., Cannizzaro, L., Huebner, K., Black, R., 1992. Molecular cloning of the interleukin-1 beta converting enzyme. Science (80-.). 256, 97–100.

Chaix, J., Tessmer, M.S., Hoebe, K., Fuseri, N., Ryffel, B., Dalod, M., Alexopoulou, L., Beutler, B., Brossay, L., Vivier, E., Walzer, T., 2008. Cutting edge: Priming of NK cells by IL-18. J. Immunol. 181, 1627–1631. doi:10.4049/jimmunol.181.3.1627

Chamaillard, M., Hashimoto, M., Horie, Y., Masumoto, J., Qiu, S., Saab, L., Ogura, Y., Kawasaki, A., Fukase, K., Kusumoto, S., Valvano, M.A., Foster, S.J., Mak, T.W., Nunez, G., Inohara, N., 2003. An essential role for NOD1 in host recognition of bacterial peptidoglycan containing diaminopimelic acid. Nat. Immunol. 4, 702–707. doi:10.1038/ni945

Chen, F., Ding, X., Ding, Y., Xiang, Z., Li, X., Ghosh, D., Schurig, G.G., Sriranganathan, N., Boyle, S.M., He, Y., 2011. Proinflammatory caspase-2-mediated macrophage cell death induced by a rough attenuated Brucella suis strain. Infect. Immun. 79, 2460–2469. doi:10.1128/IAI.00050-11

Chinnaiyan, A., O'Rourke, K., Tewari, M., Dixit, V., 1995. FADD, a novel death domain-containing protein, interacts with the death domain of Fas and initiates apoptosis. Cell 81, 505–512.

Cho, Y.S., Challa, S., Moquin, D., Genga, R., Ray, T.D., Guildford, M., Chan, F.K.M., 2009. Phosphorylation-Driven Assembly of the RIP1-RIP3 Complex Regulates Programmed Necrosis and Virus-Induced Inflammation. Cell 137, 1112–1123. doi:10.1016/j.cell.2009.05.037

Chung, I.-C., OuYang, C.-N., Yuan, S.-N., Li, H.-P., Chen, J.-T., Shieh, H.-R., Chen, Y.-J., Ojcius, D.M., Chu, C.-L., Yu, J.-S., Chang, Y.-S., Chen, L.-C., 2016. Pyk2 activates the NLRP3 inflammasome by directly phosphorylating ASC and contributes to inflammasome-dependent peritonitis. Sci. Rep. 6, 36214. doi:10.1038/srep36214

Cirelli, K.M., Gorfu, G., Hassan, M.A., Printz, M., Crown, D., Leppla, S.H., Grigg, M.E., Saeij, J.P.J., Moayeri, M., 2014. Inflammasome Sensor NLRP1 Controls Rat Macrophage Susceptibility to Toxoplasma gondii. PLoS Pathog. 10. doi:10.1371/journal.ppat.1003927

Cobrin, G.M., Abreu, M.T., 2005. Defects in mucosal immunity leading to Crohn's disease. Immunol. Rev. 206, 277–295. doi:10.1111/j.0105-2896.2005.00293.x

Cohen, J., 2002. The immunopathogenesis of sepsis. Nature 420, 885–891. doi:10.1038/nature01326

Coll, R.C., Robertson, A.A.B., Chae, J.J., Higgins, S.C., Muñoz-Planillo, R., Inserra, M.C., Vetter, I., Dungan, L.S., Monks, B.G., Stutz, A., Croker, D.E., Butler, M.S., Haneklaus, M., Sutton, C.E., Núñez, G., Latz, E., Kastner, D.L., Mills, K.H.G., Masters, S.L., Schroder, K., Cooper, M.A., O'Neill, L.A.J., 2015. A small-molecule inhibitor of the NLRP3 inflammasome for the treatment of inflammatory diseases. Nat. Med. 21, 248–255. doi:10.1038/nm.3806

Colonna, M., 2007. All roads lead to CARD9. Nat. Immunol. 8, 554–555. doi:S0092-8674(07)00723-4 [pii]\r10.1016/j.cell.2007.05.048

Conti, B.J., Davis, B.K., Zhang, J., O'Connor, W., Williams, K.L., Ting, J.P.Y., 2005. CATERPILLER 16.2 (CLR16.2), a novel NBD/LRR family member that negatively regulates T cell function. J. Biol. Chem. 280, 18375–18385. doi:10.1074/jbc.M413169200

Cordoba-Rodriguez, R., Fang, H., Lankford, C.S.R., Frucht, D.M., 2004. Anthrax lethal toxin rapidly activates Caspase-1/ICE and induces extracellular release of interleukin (IL)-1b and IL-18. J. Biol. Chem. 279, 20563–20566. doi:10.1074/jbc.C300539200

Cosulich, S.C., Worrall, V., Hedge, P.J., Green, S., Clarke, P.R., 1997. Regulation of apoptosis by BH3 domains in a cell-free system. Curr. Biol. 7, 913–920. doi:10.1016/S0960-9822(06)00410-6

Craven, R.R., Gao, X., Allen, I.C., Gris, D., Wardenburg, J.B., McElvania-TeKippe, E., Ting, J.P., Duncan, J.A., 2009. Staphylococcus aureus α-Hemolysin Activates the NLRP3-Inflammasome in Human and Mouse Monocytic Cells. PLoS One 4, e7446. doi:10.1371/journal.pone.0007446

Crump, J.A., Mintz, E.D., 2010. Global trends in typhoid and paratyphoid Fever. Clin. Infect. Dis. 50, 241–246. doi:10.1086/649541

Cruz, C.M., Rinna, A., Forman, H.J., Ventura, A.L.M., Persechini, P.M., Ojcius, D.M., 2007. ATP activates a reactive oxygen species-dependent oxidative stress response and secretion of proinflammatory cytokines in macrophages. J. Biol. Chem. 282, 2871–2879. doi:10.1074/jbc.M608083200

Cui, J., Zhu, L., Xia, X., Wang, H.Y., Legras, X., Hong, J., Ji, J., Shen, P., Zheng, S., Chen, Z.J., Wang, R.-F., 2010. NLRC5 negatively regulates the NF-kappaB and type I interferon signaling pathways. Cell 141, 483–496. doi:10.1016/j.cell.2010.03.040

Cummings, L.A., Barrett, S.L.R., Wilkerson, W.D., Fellnerova, I., Cookson, B.T., 2005. FliC-Specific CD4_ T Cell Responses Are Restricted by Bacterial Regulation of Antigen Expression. J. Immunol. 174, 7929–7938. doi:10.4049/jimmunol.174.12.7929

Cummings, L.A., Wilkerson, W.D., Bergsbaken, T., Cookson, B.T., 2006. In vivo, fliC expression by Salmonella enterica serovar Typhimurium is heterogeneous, regulated by ClpX, and anatomically restricted. Mol. Microbiol. 61, 795–809. doi:10.1111/j.1365-2958.2006.05271.x

Cunha, L.D., Zamboni, D.S., 2013. Subversion of inflammasome activation and pyroptosis by pathogenic bacteria. Front. Cell. Infect. Microbiol. 3, 76. doi:10.3389/fcimb.2013.00076

D'Osualdo, A., Weichenberger, C.X., Wagner, R.N., Godzik, A., Wooley, J., Reed, J.C., 2011. CARD8 and NLRP1 undergo autoproteolytic processing through a ZU5-like domain. PLoS One 6. doi:10.1371/journal.pone.0027396

Dahiya, Y., Pandey, R.K., Sodhi, A., 2011. Nod2 downregulates TLR2/1 mediated IL1b gene expression in mouse peritoneal macrophages. PLoS One 6, 1–11. doi:10.1371/journal.pone.0027828

Dai, X., Sayama, K., Tohyama, M., Shirakata, Y., Hanakawa, Y., Tokumaru, S., Yang, L., Hirakawa, S., Hashimoto, K., 2011. Mite allergen is a danger signal for the skin via activation of inflammasome in keratinocytes. J. Allergy Clin. Immunol. 127, 806–814. doi:10.1016/j.jaci.2010.12.006

Davis, B.K., Roberts, R.A., Huang, M.T., Willingham, S.B., Conti, B.J., Brickey, W.J., Barker, B.R., Kwan, M., Taxman, D.J., Accavitti-Loper, M.-A., Duncan, J.A., Ting, J.P.-Y., 2011a. Cutting edge: NLRC5-dependent activation of the inflammasome. J. Immunol. 186, 1333–7. doi:10.4049/jimmunol.1003111

Davis, B.K., Wen, H., Ting, J.P.-Y., 2011b. The inflammasome NLRs in immunity, inflammation, and associated diseases. Annu. Rev. Immunol. 29, 707–735. doi:10.1146/annurev-immunol-031210-101405

de Jong, H.K., Parry, C.M., van der Poll, T., Wiersinga, W.J., 2012. Host-pathogen interaction in invasive Salmonellosis. PLoS Pathog. 8, e1002933. doi:10.1371/journal.ppat.1002933

Delaloye, J., Roger, T., Steiner-Tardivel, Q.G., Le Roy, D., Reymond, M.K., Akira, S., Petrilli, V., Gomez, C.E., Perdiguero, B., Tschopp, J., Pantaleo, G., Esteban, M., Calandra, T., 2009. Innate immune sensing of modified vaccinia virus Ankara (MVA) is mediated by TLR2-TLR6, MDA-5 and the NALP3 inflammasome. PLoS Pathog. 5. doi:10.1371/journal.ppat.1000480

Deng, L., Wang, C., Spencer, E., Yang, L., Braun, A., You, J., Slaughter, C., Pickart, C., Chen, Z.J., 2000. Activation of the IκB Kinase Complex by TRAF6 Requires a Dimeric Ubiquitin-Conjugating Enzyme Complex and a Unique Polyubiquitin Chain. Cell 103, 351–361. doi:10.1016/S0092-8674(00)00126-4

Diebolder, C.A., Halff, E.F., Koster, A.J., Huizinga, E.G., Koning, R.I., 2015. Cryoelectron Tomography of the NAIP5/NLRC4 Inflammasome: Implications for NLR Activation. Structure 1–9. doi:10.1016/j.str.2015.10.001

Diez, E., Lee, S.-H., Gauthier, S., Yaraghi, Z., Tremblay, M., Vidal, S., Gros, P., 2003. Birc1e is the gene within the Lgn1 locus associated with resistance to Legionella pneumophila. Nat. Genet. 33, 55–60. doi:10.1038/ng1065

Dodé, C., Le Dû, N., Cuisset, L., Letourneur, F., Berthelot, J.-M., Vaudour, G., Meyrier, A., Watts, R.A., Scott, D.G.I., Nicholls, A., Granel, B., Frances, C., Garcier, F., Edery, P., Boulinguez, S., Domergues, J.-P., Delpech, M., Grateau, G., 2002. New Mutations of CIAS1 That Are Responsible for Muckle-Wells Syndrome and Familial Cold Urticaria: A Novel Mutation Underlies Both Syndromes. Am. J. Hum. Genet. 70, 1498–1506. doi:10.1086/340786

Dorhoi, A., Desel, C., Yeremeev, V., Pradl, L., Brinkmann, V., Mollenkopf, H.J., Hanke, K., Gross, O., Ruland, J., Kaufmann, S.H., 2010. The adaptor molecule CARD9 is essential for tuberculosis control. J. Exp. Med. 207, 777–792. doi:10.1084/jem.20090067

Dostert, C., Pétrilli, V., Bruggen, R. Van, Steele, C., Mossman, B.T., Tschopp, J., 2008. Innate immune activation through Nalp3 inflammasome sensing of asbestos and silica. Science (80-.). 674, 674–677. doi:10.1126/science.1156995

Duncan, J.A., Gao, X., Huang, M.T.-H., O'Connor, B.P., Thomas, C.E., Willingham, S.B., Bergstralh, D.T., Jarvis, G.A., Sparling, P.F., Ting, J.P.-Y., 2009. Neisseria gonorrhoeae Activates the Proteinase Cathepsin B to Mediate the Signaling Activities of the NLRP3 and ASC-Containing Inflammasome. J. Immunol. 182, 6460–6469. doi:10.4049/jimmunol.0802696

Enari, M., Talanian, R., Wong, W., Nagata, S., 1996. Sequential activation of ICE-like and CPP32-like proteases during Fas-mediated apoptosis. Nature 25, 723–726.

Fadok, V.A., Voelker, D.R., Campbell, P.A., Cohen, J.J., Bratton, D.L., Henson, P.M., 1992. Exposure of phosphatidylserine on the surface of apoptotic lymphocytes triggers specific recognition and removal by macrophages. J. Immunol. 148, 2207–2216.

Fernandes-Alnemri, T., Kang, S., Anderson, C., Sagara, J., Fitzgerald, K.A., Alnemri, E.S., 2013. Cutting edge: TLR signaling licenses IRAK1 for rapid activation of the NLRP3 inflammasome. J. Immunol. 191, 3995–9. doi:10.4049/jimmunol.1301681

Fernandes-Alnemri, T., Yu, J.-W., Datta, P., Wu, J., Alnemri, E.S., 2009. AIM2 activates the inflammasome and cell death in response to cytoplasmic DNA. Nature 458, 509–513. doi:10.1038/nature07710

Feuillet, V., Medjane, S., 2006. Involvement of Toll-like receptor 5 in the recognition of flagellated bacteria. Proc. Natl. Acad. Sci. U. S. A. 103, 12487–12492.

Finger, J.N., Lich, J.D., Dare, L.C., Cook, M.N., Brown, K.K., Duraiswamis, C., Bertin, J.J., Gough, P.J., 2012. Autolytic proteolysis within the function to find domain (FIIND) is required for NLRP1 inflammasome activity. J. Biol. Chem. 287, 25030–25037. doi:10.1074/jbc.M112.378323

Fink, S.L., Bergsbaken, T., Cookson, B.T., 2008. Anthrax lethal toxin and Salmonella elicit the common cell death pathway of caspase-1-dependent pyroptosis via distinct mechanisms. Proc. Natl. Acad. Sci. U. S. A. 105, 4312–4317. doi:10.1073/pnas.0707370105

Fink, S.L., Cookson, B.T., 2006. Caspase-1-dependent pore formation during pyroptosis leads to osmotic lysis of infected host macrophages. Cell. Microbiol. 8, 1812–1825. doi:10.1111/j.1462-5822.2006.00751.x

Finley, D., 2009. Recognition and Processing of Ubiquitin-Protein Conjugates by the Proteasome. Annu. Rev. Biochem. 78, 477–513. doi:10.1146/annurev.biochem.78.081507.101607

Fitzgerald, K.A., Rowe, D.C., Barnes, B.J., Caffrey, D.R., Visintin, A., Latz, E., Monks, B., Pitha, P.M., Golenbock, D.T., 2003. LPS-TLR4 Signaling to IRF-3/7 and NF-κB Involves the Toll Adapters TRAM and TRIF. J. Exp. Med. 198, 1043–1055. doi:10.1084/jem.20031023

Foster, G.L., Barr, T.A., Grant, A.J., McKinley, T.J., Bryant, C.E., MacDonald, A., Gray, D., Yamamoto, M., Akira, S., Maskell, D.J., Mastroeni, P., 2008. Virulent Salmonella enterica infections can be exacerbated by concomitant infection of the host with a live attenuated S. enterica vaccine via Toll-like receptor 4-dependent interleukin-10 production with the involvement of both TRIF and MyD88. Immunology 124, 469–479. doi:10.1111/j.1365-2567.2007.02798.x

Franchi, L., Amer, A., Body-Malapel, M., Kanneganti, T.-D., Ozören, N., Jagirdar, R., Inohara, N., Vandenabeele, P., Bertin, J., Coyle, A., Grant, E.P., Núñez, G., 2006. Cytosolic flagellin requires Ipaf for activation of caspase-1 and interleukin 1beta in salmonella-infected macrophages. Nat. Immunol. 7, 576–582. doi:10.1038/ni1346

Franchi, L., Kanneganti, T.-D., Dubyak, G.R., Núñez, G., 2007. Differential requirement of P2X7 receptor and intracellular K+ for caspase-1 activation induced by intracellular and extracellular bacteria. J. Biol. Chem. 282, 18810–18818. doi:10.1074/jbc.M610762200

Frew, B.C., Joag, V.R., Mogridge, J., 2012. Proteolytic processing of Nlrp1b is required for inflammasome activity. PLoS Pathog. 8, e1002659. doi:10.1371/journal.ppat.1002659

Fritz, J.H., Ferrero, R.L., Philpott, D.J., Girardin, S.E., 2006. Nod-like proteins in immunity, inflammation and disease. Nat. Immunol. 7, 1250–1257. doi:10.1038/ni1412

Fullerton, J.N., Gilroy, D.W., 2016. Resolution of inflammation: A new therapeutic frontier. Nat. Rev. Drug Discov. 15, 551–567. doi:10.1038/nrd.2016.39

Gaidt, M.M., Ebert, T.S., Chauhan, D., Ramshorn, K., Pinci, F., Zuber, S., O'Duill, F., Schmid-Burgk, J.L., Hoss, F., Buhmann, R., Wittmann, G., Latz, E., Subklewe, M., Hornung, V., 2017. The DNA Inflammasome in Human Myeloid Cells Is Initiated by a STING-Cell Death Program Upstream of NLRP3. Cell 171, 1110–1124.e18. doi:10.1016/j.cell.2017.09.039

Gao, D., Wu, J., Wu, Y., Du, F., Aroh, C., Yan, N., Sun, L., Chen, Z.J., 2013. Cyclic GMP-AMP Synthase Is an Innate Immune Sensor of HIV and Other Retroviruses. Science (80-.). 1375, 903–907.

Geddes, K., Rubino, S., Streutker, C., Cho, J.H., Magalhaes, J.G., Bourhis, L. Le, Selvanantham, T., Girardin, S.E., Philpott, D.J., 2010. Nod1 and Nod2 regulation of inflammation in the Salmonella colitis model. Infect. Immun. 78, 5107–5115. doi:10.1128/IAI.00759-10

Girardin, S.E., Boneca, I.G., Viala, J., Chamaillard, M., Labigne, A., Thomas, G., Philpott, D.J., Sansonetti, P.J., 2003. Nod2 is a general sensor of peptidoglycan through muramyl dipeptide (MDP) detection. J. Biol. Chem. 278, 8869–8872. doi:10.1074/jbc.C200651200

Girardin, S.E., Tournebize, R., Mavris, M., Page, A.L., Li, X., Stark, G.R., Bertin, J., DiStefano, P.S., Yaniv, M., Sansonetti, P.J., Philpott, D.J., 2001. CARD4/Nod1 mediates NF-kappaB and JNK activation by invasive Shigella flexneri. EMBO Rep. 2, 736–742. doi:10.1093/embo-reports/kve155

Gonçalves, V.M., Matteucci, K.C., Buzzo, C.L., Miollo, B.H., Ferrante, D., Torrecilhas, A.C., Rodrigues, M.M., Alvarez, J.M., Bortoluci, K.R., 2013. NLRP3 controls Trypanosoma cruzi infection through a caspase-1-dependent IL-1R-independent NO production. PLoS Negl. Trop. Dis. 7, e2469. doi:10.1371/journal.pntd.0002469

Goodridge, H.S., Shimada, T., Wolf, A.J., Hsu, Y.-M.S., Becker, C.A., Lin, X., Underhill, D.M., 2009. Differential use of CARD9 by dectin-1 in macrophages and dendritic cells. J. Immunol. 182, 1146–1154. doi:10.4049/jimmunol.182.2.1146

Goyal, N., Rana, A., Ahlawat, A., Bijjem, K.R. V., Kumar, P., 2014. Animal models of inflammatory bowel disease: A review. Inflammopharmacology 22, 219–233. doi:10.1007/s10787-014-0207-y

Grenier, J.M., Wang, L., Manji, G.A., Huang, W.J., Al-Garawi, A., Kelly, R., Carlson, A., Merriam, S., Lora, J.M., Briskin, M., DiStefano, P.S., Bertin, J., 2002. Functional screening of five PYPAF family members identifies PYPAF5 as a novel regulator of NF-κB and caspase-1. FEBS Lett. 530, 73–78. doi:10.1016/S0014-5793(02)03416-6

Grimont, P., Weill, F., 2007. Antigenic formulae of the Salmonella serovars, WHO Collaborating Centre for Reference and Research on Salmonella.

Gringhuis, S.I., Kaptein, T.M., Wevers, B.A., Theelen, B., van der Vlist, M., Boekhout, T., Geijtenbeek, T.B.H., 2012. Dectin-1 is an extracellular pathogen sensor for the induction and processing of IL-1β via a noncanonical caspase-8 inflammasome. Nat. Immunol. 13, 246–254. doi:10.1038/ni.2222

Grootjans, S., Vanden Berghe, T., Vandenabeele, P., 2017. Initiation and execution mechanisms of necroptosis: an overview. Cell Death Differ. 24, 1184–1195. doi:10.1038/cdd.2017.65

Gross, O., Gewies, A., Finger, K., Schäfer, M., Sparwasser, T., Peschel, C., Förster, I., Ruland, J., 2006. Card9 controls a non-TLR signalling pathway for innate anti-fungal immunity. Nature 442, 651–6. doi:10.1038/nature04926

Gross, O., Poeck, H., Bscheider, M., Dostert, C., Hannesschläger, N., Endres, S., Hartmann, G., Tardivel, A., Schweighoffer, E., Tybulewicz, V., Mocsai, A., Tschopp, J., Ruland, J., 2009. Syk kinase signalling couples to the Nlrp3 inflammasome for anti-fungal host defence. Nature 459, 433–436. doi:10.1038/nature07965

Guo, H., Ko, R., Deng, M., Duncan, J.A., Chanda, S.K., Ting, J.P., Deng, M., Riess, M., Mo, J., Zhang, L., Petrucelli, A., Yoh, S.M., Barefoot, B., Samo, M., Sempowski, G.D., Zhang, A., Colberg-Poley, A.M., Feng, H., Lemon, S.M., Liu, Y., Zhang, Y., Wen, H., Zhang, Z., Damania, B., Tsao, L.-C., Wang, Q., Su, L., Duncan, J.A., Chanda, S.K., Ting, J.P.-Y., 2016. NLRX1 Sequesters STING to Negatively Regulate the Interferon

Response, Thereby Facilitating the Replication of HIV-1 and DNA Viruses. Cell Host Microbe 19, 515–528. doi:10.1016/j.chom.2016.03.001

Gurung, P., Anand, P.K., Malireddi, R.K.S., Vande Walle, L., Van Opdenbosch, N., Dillon, C.P., Weinlich, R., Green, D.R., Lamkanfi, M., Kanneganti, T.-D., 2014. FADD and caspase-8 mediate priming and activation of the canonical and noncanonical Nlrp3 inflammasomes. J. Immunol. 192, 1835–1846. doi:10.4049/jimmunol.1302839

Hagar, J.A., Powell, D.A., Aachoui, Y., Ernst, R.K., Miao, E.A., 2013. Cytoplasmic LPS activates caspase-11: implications in TLR4-independent endotoxic shock. Science (80-.). 341, 1250–1253. doi:10.1126/science.1240988

Halff, E.F., Diebolder, C. A., Versteeg, M., Schouten, A., Brondijk, T.H.C., Huizinga, E.G., 2012. Formation and structure of a NAIP5-NLRC4 inflammasome induced by direct interactions with conserved N- and C-terminal regions of flagellin. J. Biol. Chem. 287, 38460–38472. doi:10.1074/jbc.M112.393512

Hara, H., Ishihara, C., Takeuchi, A., Imanishi, T., Xue, L., Morris, S.W., Inui, M., Takai, T., Shibuya, A., Saijo, S., Iwakura, Y., Ohno, N., Koseki, H., Yoshida, H., Penninger, J.M., Saito, T., 2007. The adaptor protein CARD9 is essential for the activation of myeloid cells through ITAM-associated and Toll-like receptors. Nat. Immunol. 8, 619–629. doi:10.1038/ni1466

Hara, H., Ishihara, C., Takeuchi, A., Xue, L., Morris, S.W., Penninger, J.M., Yoshida, H., Saito, T., 2008. Cell type-specific regulation of ITAM-mediated NF-kappaB activation by the adaptors, CARMA1 and CARD9. J. Immunol. 181, 918–930.

Hara, H., Saito, T., 2009. CARD9 versus CARMA1 in innate and adaptive immunity. Trends Immunol. 30, 234–242. doi:10.1016/j.it.2009.03.002

Hara, H., Tsuchiya, K., Kawamura, I., Fang, R., Hernandez-Cuellar, E., Shen, Y., Mizuguchi, J., Schweighoffer, E., Tybulewicz, V., Mitsuyama, M., 2013. Phosphorylation of the adaptor ASC acts as a molecular switch that controls the formation of speck-like aggregates and inflammasome activity. Nat. Immunol. 14, 1247–55. doi:10.1038/ni.2749

Hayashi, F., Smith, K.D., Ozinsky, A., Hawn, T.R., Yi, E.C., Goodlett, D.R., Eng, J.K., Akira, S., Underhill, D.M., Aderem, A., 2001. The innate immune response to bacterial flagellin is mediated by Toll-like receptor 5. Nature 410, 1099–1103. doi:10.1038/35074106

He, X., Mekasha, S., Mavrogiorgos, N., Fitzgerald, K.A., Lien, E., Ingalls, R.R., 2010. Inflammation and fibrosis during Chlamydia pneumoniae infection is regulated by IL-1 and the NLRP3/ASC inflammasome. J. Immunol. 184, 5743–5754. doi:10.4049/jimmunol.0903937

Hedl, M., Abraham, C., 2012. Nod2-induced autocrine interleukin-1 alters signaling by ERK and p38 to differentially regulate secretion of inflammatory cytokines. Gastroenterology 143, 1530–1543. doi:10.1053/j.gastro.2012.08.048

Heil, F., 2004. Species-Specific Recognition of Single-Stranded RNA via Toll-like Receptor 7 and 8. Science (80-.). 303, 1526–1529. doi:10.1126/science.1093620

Hemmi, H., Takeuchi, O., Kawai, T., Kaisho, T., Sato, S., Sanjo, H., Matsumoto, M., Hoshino, K., Wagner, H., Takeda, K., Akira, S., 2000. A Toll-like receptor recognizes bacterial DNA. Nature 408, 740–745. doi:10.1038/35047123

Heng, T.S.P., Painter, M.W., 2008. The Immunological Genome Project: networks of gene expression in immune cells. Nat. Immunol. 9, 1091–1094. doi:10.1038/ni1008-1091

Hernandez-Cuellar, E., Tsuchiya, K., Hara, H., Fang, R., Sakai, S., Kawamura, I., Akira, S., Mitsuyama, M., 2012. Cutting edge: nitric oxide inhibits the NLRP3 inflammasome. J. Immunol. 189, 5113–5117. doi:10.4049/jimmunol.1202479

Hersh, D., Monack, D., Smith, M.R., Ghori, N., Falkow, S., Zychlinsky, A., 1999. The Salmonella invasin SipB induces macrophage apoptosis by binding to caspase-1. Proc. Natl. Acad. Sci. U. S. A. 96, 2396–2401.

Hess, D.T., Stamler, J.S., 2012. Regulation by S-nitrosylation of protein post-translational modification. J. Biol. Chem. 287, 4411–4418. doi:10.1074/jbc.R111.285742

Hewinson, J., Moore, S.F., Glover, C., Watts, A.G., MacKenzie, A.B., 2008. A Key Role for Redox Signaling in Rapid P2X7 Receptor-Induced IL-1β Processing in Human Monocytes. J. Immunol. 180, 8410–8420. doi:10.4049/jimmunol.180.12.8410

Hiscott, J., Marois, J., Garoufalis, J., D'Addario, M., Roulston, A., Kwan, I., Pepin, N., Lacoste, J., Nguyen, H., Bensi, G., 1993. Characterization of a functional NF-kappa B site in the human interleukin 1 beta promoter: evidence for a positive autoregulatory loop. Mol. Cell. Biol. 13, 6231–40. doi:10.1128/MCB.13.10.6231

Hoffman, H.M., Mueller, J.L., Broide, D.H., Wanderer, A.A., Kolodner, R.D., 2001. Mutation of a new gene encoding a putative pyrin-like protein causes familial cold

autoinflammatory syndrome and Muckle-Wells syndrome. Nat. Genet. 29, 301–305. doi:10.1038/ng756

Hong, S.N., Park, C., Park, S.J., Lee, C.K., Ye, B.D., Kim, Y.S., Lee, S., Chae, J., Kim, J.-I., Kim, Y.-H., 2015. Deep resequencing of 131 Crohn's disease associated genes in pooled DNA confirmed three reported variants and identified eight novel variants. Gut 1–9. doi:10.1136/gutjnl-2014-308617

Horng, T., Barton, G.M., Flavell, R.A., Medzhitov, R., 2002. The adaptor molecule TIRAP provides signalling specificity for Toll-like receptors. Nature 420, 329–333. doi:10.1038/nature01180

Hornung, V., Ablasser, A., Charrel-Dennis, M., Bauernfeind, F., Horvath, G., Caffrey, D.R., Latz, E., Fitzgerald, K.A., 2009. AIM2 recognizes cytosolic dsDNA and forms a caspase-1-activating inflammasome with ASC. Nature 458, 514–518. doi:10.1038/nature07725

Hoshino, K., Takeuchi, O., Kawai, T., Sanjo, H., Ogawa, T., Takeda, Y., Takeda, K., Akira, S., 1999. Cutting edge: Toll-like receptor 4 (TLR4)-deficient mice are hyporesponsive to lipopolysaccharide: evidence for TLR4 as the Lps gene product. J. Immunol. 162, 3749–3752.

Hotamisligil, G.S., 2017. Inflammation, metaflammation and immunometabolic disorders. Nature 542, 177–185. doi:10.1038/nature21363

Hsu, H., Huang, J., Shu, H.B., Baichwal, V., Goeddel, D. V., 1996a. TNF-dependent recruitment of the protein kinase RIP to the TNF receptor-1 signaling complex. Immunity 4, 387–396. doi:10.1016/S1074-7613(00)80252-6

Hsu, H., Shu, H.B., Pan, M.G., Goeddel, D. V., 1996b. TRADD-TRAF2 and TRADD-FADD interactions define two distinct TNF receptor 1 signal transduction pathways. Cell 84, 299–308. doi:10.1016/S0092-8674(00)80984-8

Hsu, Y.-M.S., Zhang, Y., You, Y., Wang, D., Li, H., Duramad, O., Qin, X.-F., Dong, C., Lin, X., 2007. The adaptor protein CARD9 is required for innate immune responses to intracellular pathogens. Nat. Immunol. 8, 198–205. doi:10.1038/ni1426

Hu, G.-Q., Song, P.-X., Chen, W., Qi, S., Yu, S.-X., Du, C.-T., Deng, X.-M., Ouyang, H.-S., Yang, Y.-J., 2017. Cirtical role for Salmonella effector SopB in regulating inflammasome activation. Mol. Immunol. 90, 280–286. doi:10.1016/j.molimm.2017.07.011

Hu, Z., Yan, C., Liu, P., Huang, Z., Ma, R., Zhang, C., Wang, R., Zhang, Y., Martinon, F., Miao, D., Deng, H., Wang, J., Chang, J., Chai, J., 2013. Crystal structure of NLRC4 reveals its autoinhibition mechanism. Science (80-.). 341, 172–175. doi:10.1126/science.1236381

Hu, Z., Zhou, Q., Zhang, C., Fan, S., Cheng, W., Zhao, Y., Shao, F., Wang, H., Sui, S., Chai, J., 2015. Structural and biochemical basis for induced self-propagation of NLRC4 4, 1–11.

Huang, M.T.-H., Taxman, D.J., Holley-Guthrie, E.A., Moore, C.B., Willingham, S.B., Madden, V., Parsons, R.K., Featherstone, G.L., Arnold, R.R., O'Connor, B.P., Ting, J.P.-Y., 2009. Critical role of apoptotic speck protein containing a caspase recruitment domain (ASC) and NLRP3 in causing necrosis and ASC speck formation induced by Porphyromonas gingivalis in human cells. J. Immunol. 182, 2395–404. doi:10.4049/jimmunol.0800909

Huang, T.T., Kudo, N., Yoshida, M., Miyamoto, S., 1999. A nuclear export signal in the N-terminal regulatory domain of IkappaBalpha controls cytoplasmic localization of inactive NF-kappaB/IkappaBalpha complexes. Proc. Natl. Acad. Sci. U. S. A. 97, 1014–1019.

Hugot, J.P., Chamaillard, M., Zouali, H., Lesage, S., Cézard, J.P., Belaiche, J., Almer, S., Tysk, C., O'Morain, C. a, Gassull, M., Binder, V., Finkel, Y., Cortot, A., Modigliani, R., Laurent-Puig, P., Gower-Rousseau, C., Macry, J., Colombel, J.F., Sahbatou, M., Thomas, G., 2001. Association of NOD2 leucine-rich repeat variants with susceptibility to Crohn's disease. Nature 411, 599–603. doi:10.1038/35079107

Huttenhower, C., Gevers, D., Knight, R., Abubucker, S., Badger, J.H., Chinwalla, A.T., Creasy, H.H., Earl, A.M., FitzGerald, M.G., Fulton, R.S., Giglio, M.G., Hallsworth-Pepin, K., Lobos, E.A., Madupu, R., Magrini, V., Martin, J.C., Mitreva, M., Muzny, D.M., Sodergren, E.J., Versalovic, J., Wollam, A.M., Worley, K.C., Wortman, J.R., Young, S.K., Zeng, Q., Aagaard, K.M., Abolude, O.O., Allen-Vercoe, E., Alm, E.J., Alvarado, L., Andersen, G.L., Anderson, S., Appelbaum, E., Arachchi, H.M., Armitage, G., Arze, C.A., Ayvaz, T., Baker, C.C., Begg, L., Belachew, T., Bhonagiri, V., Bihan, M., Blaser, M.J., Bloom, T., Bonazzi, V., Paul Brooks, J., Buck, G.A., Buhay, C.J., Busam, D.A., Campbell, J.L., Canon, S.R., Cantarel, B.L., Chain, P.S.G., Chen, I.-M.A., Chen, L., Chhibba, S., Chu, K., Ciulla, D.M., Clemente, J.C., Clifton, S.W., Conlan, S., Crabtree, J., Cutting, M.A., Davidovics, N.J., Davis, C.C., DeSantis, T.Z., Deal, C., Delehaunty, K.D., Dewhirst, F.E., Deych, E., Ding, Y., Dooling, D.J., Dugan, S.P., Michael Dunne, W., Scott Durkin, A., Edgar, R.C., Erlich, R.L., Farmer, C.N., Farrell, R.M., Faust, K.,

Feldgarden, M., Felix, V.M., Fisher, S., Fodor, A.A., Forney, L.J., Foster, L., Di Francesco, V., Friedman, J., Friedrich, D.C., Fronick, C.C., Fulton, L.L., Gao, H., Garcia, N., Giannoukos, G., Giblin, C., Giovanni, M.Y., Goldberg, J.M., Goll, J., Gonzalez, A., Griggs, A., Gujja, S., Kinder Haake, S., Haas, B.J., Hamilton, H.A., Harris, E.L., Hepburn, T.A., Herter, B., Hoffmann, D.E., Holder, M.E., Howarth, C., Huang, K.H., Huse, S.M., Izard, J., Jansson, J.K., Jiang, H., Jordan, C., Joshi, V., Katancik, J.A., Keitel, W.A., Kelley, S.T., Kells, C., King, N.B., Knights, D., Kong, H.H., Koren, O., Koren, S., Kota, K.C., Kovar, C.L., Kyrpides, N.C., La Rosa, P.S., Lee, S.L., Lemon, K.P., Lennon, N., Lewis, C.M., Lewis, L., Ley, R.E., Li, K., Liolios, K., Liu, B., Liu, Y., Lo, C.-C., Lozupone, C.A., Dwayne Lunsford, R., Madden, T., Mahurkar, A.A., Mannon, P.J., Mardis, E.R., Markowitz, V.M., Mavromatis, K., McCorrison, J.M., McDonald, D., McEwen, J., McGuire, A.L., McInnes, P., Mehta, T., Mihindukulasuriya, K.A., Miller, J.R., Minx, P.J., Newsham, I., Nusbaum, C., O'Laughlin, M., Orvis, J., Pagani, I., Palaniappan, K., Patel, S.M., Pearson, M., Peterson, J., Podar, M., Pohl, C., Pollard, K.S., Pop, M., Priest, M.E., Proctor, L.M., Qin, X., Raes, J., Ravel, J., Reid, J.G., Rho, M., Rhodes, R., Riehle, K.P., Rivera, M.C., Rodriguez-Mueller, B., Rogers, Y.-H., Ross, M.C., Russ, C., Sanka, R.K., Sankar, P., Fah Sathirapongsasuti, J., Schloss, J.A., Schloss, P.D., Schmidt, T.M., Scholz, M., Schriml, L., Schubert, A.M., Segata, N., Segre, J.A., Shannon, W.D., Sharp, R.R., Sharpton, T.J., Shenoy, N., Sheth, N.U., Simone, G.A., Singh, I., Smillie, C.S., Sobel, J.D., Sommer, D.D., Spicer, P., Sutton, G.G., Sykes, S.M., Tabbaa, D.G., Thiagarajan, M., Tomlinson, C.M., Torralba, M., Treangen, T.J., Truty, R.M., Vishnivetskaya, T.A., Walker, J., Wang, L., Wang, Z., Ward, D. V., Warren, W., Watson, M.A., Wellington, C., Wetterstrand, K.A., White, J.R., Wilczek-Boney, K., Wu, Y., Wylie, K.M., Wylie, T., Yandava, C., Ye, L., Ye, Y., Yooseph, S., Youmans, B.P., Zhang, L., Zhou, Y., Zhu, Y., Zoloth, L., Zucker, J.D., Birren, B.W., Gibbs, R.A., Highlander, S.K., Methé, B.A., Nelson, K.E., Petrosino, J.F., Weinstock, G.M., Wilson, R.K., White, O., 2012. Structure, function and diversity of the healthy human microbiome. Nature 486, 207–214. doi:10.1038/nature11234

Ito, M., Shichita, T., Okada, M., Komine, R., Noguchi, Y., Yoshimura, A., Morita, R., 2015. Bruton's tyrosine kinase is essential for NLRP3 inflammasome activation and contributes to ischaemic brain injury. Nat. Commun. 6, 7360. doi:10.1038/ncomms8360

Jabir, M.S., Ritchie, N.D., Li, D., Bayes, H.K., Tourlomousis, P., Puleston, D., Lupton, A., Hopkins, L., Simon, A.K., Bryant, C., Evans, T.J., 2014. Caspase-1 cleavage of the TLR adaptor TRIF inhibits autophagy and β-interferon production during pseudomonas aeruginosa infection. Cell Host Microbe 15, 214–227. doi:10.1016/j.chom.2014.01.010

Jackson, N., Compton, E., Trowsdale, J., Kelly, A.P., 2014. Recognition of Salmonella by Dectin-1 induces presentation of peptide antigen to type B T cells. Eur. J. Immunol. 44, 962–969. doi:10.1002/eji.201344065

Jacobs, M.D., Harrison, S.C., 1998. Structure of an IκBα/NF-κB Complex. Cell 95, 749–758. doi:10.1016/S0092-8674(00)81698-0

Janeway, C.A., Medzhitov, R., 2002. Innate Immune Recognition. Annu. Rev. Immunol. 20, 197–216. doi:10.1146/annurev.immunol.20.083001.084359

Jennings, E., Thurston, T. L. M., & Holden, D. W. (2017). Salmonella SPI-2 Type III Secretion System Effectors: Molecular Mechanisms And Physiological Consequences. *Cell Host and Microbe*, *22*(2), 217–231.

Jesenberger, V., Procyk, K., Yuan, J., Reipert, S., Baccarini, M., 2000. Salmonella-Induced Caspase-2 Activation in Macrophages A Novel Mechanism in Pathogen-Mediated Apoptosis. J. Exp. Med. 192, 1035–1045.

Jessen, D.L., Osei-Owusu, P., Toosky, M., Roughead, W., Bradley, D.S., Nilles, M.L., 2014. Type III secretion needle proteins induce cell signaling and cytokine secretion via Toll-like receptors. Infect. Immun. 82, 2300–2309. doi:10.1128/IAI.01705-14

Juliana, C., Fernandes-Alnemri, T., Kang, S., Farias, A., Qin, F., Alnemri, E.S., 2012. Non-transcriptional priming and deubiquitination regulate NLRP3 inflammasome activation. J. Biol. Chem. 287, 36617–36622. doi:10.1074/jbc.M112.407130

Julien, O., Wells, J.A., 2017. Caspases and their substrates. Cell Death Differ. 24, 1380–1389. doi:10.1038/cdd.2017.44

Kagan, J.C., Su, T., Horng, T., Chow, A., Akira, S., Medzhitov, R., 2008. TRAM couples endocytosis of Toll-like receptor 4 to the induction of interferon-beta. Nat. Immunol. 9, 361–368. doi:10.1038/ni1569

Kaiser, W.J., Upton, J.W., Long, A.B., Livingston-Rosanoff, D., Daley-Bauer, L.P., Hakem, R., Caspary, T., Mocarski, E.S., 2011. RIP3 mediates the embryonic lethality of caspase-8-deficient mice. Nature 471, 368–372. doi:10.1038/nature09857

Kawai, T., Akira, S., 2010. The role of pattern-recognition receptors in innate immunity: update on Toll-like receptors. Nat. Immunol. 11, 373–384. doi:10.1038/ni.1863

Kayagaki, N., Stowe, I.B., Lee, B.L., O'Rourke, K., Anderson, K., Warming, S., Cuellar, T., Haley, B., Roose-Girma, M., Phung, Q.T., Liu, P.S., Lill, J.R., Li, H., Wu, J.,

Kummerfeld, S., Zhang, J., Lee, W.P., Snipas, S.J., Salvesen, G.S., Morris, L.X., Fitzgerald, L., Zhang, Y., Bertram, E.M., Goodnow, C.C., Dixit, V.M., 2015. Caspase-11 cleaves gasdermin D for non-canonical inflammasome signaling. Nature. doi:10.1038/nature15541

Kayagaki, N., Warming, S., Lamkanfi, M., Vande Walle, L., Louie, S., Dong, J., Newton, K., Qu, Y., Liu, J., Heldens, S., Zhang, J., Lee, W.P., Roose-Girma, M., Dixit, V.M., 2011. Non-canonical inflammasome activation targets caspase-11. Nature 479, 117–121. doi:10.1038/nature10558

Kayagaki, N., Wong, M., Stowe, I., Ramani, S.R., Gonzalez, L.C., Akashi-takamura, S., Miyake, K., Zhang, J., Lee, W.P., Forsberg, L.S., Carlson, R.W., Dixit, V.M., 2013. Noncanonical inflammasome activation by intracellular LPS independent of TLR4. Science (80-.). 1246, 1246–1249. doi:10.5061/dryad.bt51g

Keestra, A.M., Winter, M.G., Klein-douwel, D., Xavier, M.N., Winter, S.E., Kim, A., Tsolis, R.M., Bäumler, A.J., The, A., Salmonella, T.-, 2011. A Salmonella virulence factor activates the NOD1/NOD2 signaling pathway. MBio 2, 1–10. doi:10.1128/mBio.00266-11.Editor

Kerr, J.F.R., Wyllie, A.H., Currie, A.R., 1972. Apoptosis: a Basic Biological Phenomenon With Wide- Ranging Implications in Tissue Kinetics. Br. J. Cancer 258, 479–517. doi:10.1111/j.1365-2796.2005.01570.x

Khor, B., Gardet, A., Xavier, R.J., 2011. Genetics and pathogenesis of inflammatory bowel disease. Nature 474, 307–17. doi:10.1038/nature10209

Kim, H., Zhao, Q., Zheng, H., Li, X., Zhang, T., Ma, X., 2015. A novel crosstalk between TLR4- and NOD2-mediated signaling in the regulation of intestinal inflammation. Sci. Rep. 5, 12018. doi:10.1038/srep12018

Kim, J.H., Park, M.E., Nikapitiya, C., Kim, T.H., Uddin, M.B., Lee, H.C., Kim, E., Ma, J.Y., Jung, J.U., Kim, C.J., Lee, J.S., 2017. FAS-associated factor-1 positively regulates type I interferon response to RNA virus infection by targeting NLRX1. PLoS Pathog. 13, 1–26. doi:10.1371/journal.ppat.1006398

Kim, S., Bauernfeind, F., Ablasser, A., Hartmann, G., Fitzgerald, K. A., Latz, E., Hornung, V., 2010. Listeria monocytogenes is sensed by the NLRP3 and AIM2 inflammasome. Eur. J. Immunol. 40, 1545–1551. doi:10.1002/eji.201040425

Kim, Y.-G., Park, J.-H., Shaw, M.H., Franchi, L., Inohara, N., Núñez, G., 2008. The cytosolic sensors Nod1 and Nod2 are critical for bacterial recognition and host defense after exposure to Toll-like receptor ligands. Immunity 28, 246–257. doi:10.1016/j.immuni.2007.12.012

Kiryluk, K., Li, Y., Scolari, F., Sanna-Cherchi, S., Choi, M., Verbitsky, M., Fasel, D., Lata, S., Prakash, S., Shapiro, S., Fischman, C., Snyder, H.J., Appel, G., Izzi, C., Viola, B.F., Dallera, N., Del Vecchio, L., Barlassina, C., Salvi, E., Bertinetto, F.E., Amoroso, A., Savoldi, S., Rocchietti, M., Amore, A., Peruzzi, L., Coppo, R., Salvadori, M., Ravani, P., Magistroni, R., Ghiggeri, G.M., Caridi, G., Bodria, M., Lugani, F., Allegri, L., Delsante, M., Maiorana, M., Magnano, A., Frasca, G., Boer, E., Boscutti, G., Ponticelli, C., Mignani, R., Marcantoni, C., Di Landro, D., Santoro, D., Pani, A., Polci, R., Feriozzi, S., Chicca, S., Galliani, M., Gigante, M., Gesualdo, L., Zamboli, P., Battaglia, G.G., Garozzo, M., Maixnerová, D., Tesar, V., Eitner, F., Rauen, T., Floege, J., Kovacs, T., Nagy, J., Mucha, K., Pączek, L., Zaniew, M., Mizerska-Wasiak, M., Roszkowska-Blaim, M., Pawlaczyk, K., Gale, D., Barratt, J., Thibaudin, L., Berthoux, F., Canaud, G., Boland, A., Metzger, M., Panzer, U., Suzuki, H., Goto, S., Narita, I., Caliskan, Y., Xie, J., Hou, P., Chen, N., Zhang, H., Wyatt, R.J., Novak, J., Julian, B. a, Feehally, J., Stengel, B., Cusi, D., Lifton, R.P., Gharavi, A.G., 2014. Discovery of new risk loci for IgA nephropathy implicates genes involved in immunity against intestinal pathogens. Nat. Genet. 13. doi:10.1038/ng.3118

Kischkel, F., Hellbardt, S., Behrmann, I., Germer, M., Pawlita, M., Krammer, P.H., Peter, M.E., 1995. Cytotoxicity-dependent APO-1 (Fas/CD95)-associated proteins form a death-inducing signaling complex (DISC) with the receptor. EMBO J. 14, 5579–5588.

Klinman, D.M., Ylt, A., Beaucaget, S.L., Conover, J., Kriegt, A.M., 1996. CpG motifs present in bacterial DNA rapidly induce lymphocytes to secrete interleukin 6, interleukin 12, and interferon y. Proc. Natl. Acad. Sci. U. S. A. 93, 2879–2883.

Knodler, L.A., Crowley, S.M., Sham, H.P., Yang, H., Wrande, M., Ma, C., Ernst, R.K., Steele-Mortimer, O., Celli, J., Vallance, B.A., 2014. Noncanonical Inflammasome Activation of Caspase-4/Caspase-11 Mediates Epithelial Defenses against Enteric Bacterial Pathogens. Cell Host Microbe 16, 249–256. doi:10.1016/j.chom.2014.07.002

Kobayashi, K.S., Chamaillard, M., Ogura, Y., Henegariu, O., Inohara, N., Nuñez, G., Flavell, R. a, 2005. Nod2-dependent regulation of innate and adaptive immunity in the intestinal tract. Science (80-.). 307, 731–734. doi:10.1126/science.1104911

Koblansky, A. A., Jankovic, D., Oh, H., Hieny, S., Sungnak, W., Mathur, R., … Ghosh, S. (2013). Recognition of Profilin by Toll-like Receptor 12 Is Critical for Host Resistance to Toxoplasma gondii. *Immunity*, *38*(1), 119–130.

Kofoed, E.M., Vance, R.E., 2011. Innate immune recognition of bacterial ligands by NAIPs determines inflammasome specificity. Nature 477, 592–5. doi:10.1038/nature10394

Kohka, H., Yoshino, T., Iwagaki, H., Sakuma, I., Tanimoto, T., Matsuo, Y., Kurimoto, M., Orita, K., Akagi, T., Tanaka, N., 1998. Interleukin-18/interferon-γ-inducing factor, a novel cytokine, up-regulates ICAM-1 (CD54) expression in KG-1 cells. J. Leukoc. Biol. 64, 519–527. doi:10.1002/jlb.64.4.519

Koonin, E. V., Aravind, L., 2000. The NACHT family - A new group of predicted NTPases implicated in apoptosis and MHC transcription activation. Trends Biochem. Sci. 25, 223–224. doi:10.1016/S0968-0004(00)01577-2

Korn, T., Mitsdoerffer, M., Croxford, A.L., Awasthi, A., Dardalhon, V.A., Galileos, G., Vollmar, P., Stritesky, G.L., Kaplan, M.H., Waisman, A., Kuchroo, V.K., Oukka, M., 2008. IL-6 controls Th17 immunity in vivo by inhibiting the conversion of conventional T cells into Foxp3+ regulatory T cells. Proc. Natl. Acad. Sci. U. S. A. 105, 18460–18465. doi:10.1073/pnas.0809850105

Krieg, A., Correa, R.G., Garrison, J.B., Le Negrate, G., Welsh, K., Huang, Z., Knoefel, W.T., Reed, J.C., 2009. XIAP mediates NOD signaling via interaction with RIP2. Proc. Natl. Acad. Sci. U. S. A. 106, 14524–14529. doi:10.1073/pnas.0907131106

Krysko, D. V., Vanden Berghe, T., D'Herde, K., Vandenabeele, P., 2008. Apoptosis and necrosis: Detection, discrimination and phagocytosis. Methods 44, 205–221. doi:10.1016/j.ymeth.2007.12.001

Kuenzel, S., Till, A., Winkler, M., Hasler, R., Lipinski, S., Jung, S., Grotzinger, J., Fickenscher, H., Schreiber, S., Rosenstiel, P., 2010. The nucleotide-binding oligomerization domain-like receptor NLRC5 is involved in IFN-dependent antiviral immune responses. J. Immunol. 184, 1990–2000. doi:10.4049/jimmunol.0900557

Kumar, H., Pandey, S., Zou, J., Kumagai, Y., Takahashi, K., Akira, S., Kawai, T., 2011. NLRC5 deficiency does not influence cytokine induction by virus and bacteria infections. J. Immunol. Methods 186, 994–1000. doi:10.4049/jimmunol.1002094

Lage, S.L., Buzzo, C.L., Amaral, E.P., Matteucci, K.C., Massis, L.M., Icimoto, M.Y., Carmona, A.K., D'Império Lima, M.R., Rodrigues, M.M., Ferreira, L.C.S., Amarante-

Mendes, G.P., Bortoluci, K.R., 2013. Cytosolic flagellin-induced lysosomal pathway regulates inflammasome-dependent and -independent macrophage responses. Proc. Natl. Acad. Sci. U. S. A. 110, E3321-30. doi:10.1073/pnas.1305316110

Lai, M.A., Quarles, E.K., López-Yglesias, A.H., Zhao, X., Hajjar, A.M., Smith, K.D., 2013. Innate Immune Detection of Flagellin Positively and Negatively Regulates Salmonella Infection. PLoS One 8, e72047. doi:10.1371/journal.pone.0072047

Lamas, B., Richard, M.L., Leducq, V., Pham, H.-P., Michel, M.-L., Da Costa, G., Bridonneau, C., Jegou, S., Hoffmann, T.W., Natividad, J.M., Brot, L., Taleb, S., Couturier-Maillard, A., Nion-Larmurier, I., Merabtene, F., Seksik, P., Bourrier, A., Cosnes, J., Ryffel, B., Beaugerie, L., Launay, J.-M., Langella, P., Xavier, R.J., Sokol, H., 2016. CARD9 impacts colitis by altering gut microbiota metabolism of tryptophan into aryl hydrocarbon receptor ligands. Nat. Med. 22, 598–605. doi:10.1038/nm.4102

Lamkanfi, M., Declercq, W., Kalai, M., Saelens, X., Vandenabeele, P., 2002. Alice in caspase land. A phylogenetic analysis of caspases from worm to man. Cell Death Differ. 9, 358–61. doi:10.1038/sj/cdd/4400989

Lamkanfi, M., Dixit, V.M., 2012. Inflammasomes and their roles in health and disease. Annu. Rev. Cell Dev. Biol. 28, 137–161. doi:10.1146/annurev-cellbio-101011-155745

Lamkanfi, M., Dixit, V.M., 2014. Mechanisms and functions of inflammasomes. Cell 157, 1013–1022. doi:10.1016/j.cell.2014.04.007

Lamkanfi, M., Kalai, M., Vandenabeele, P., 2004. Caspase-12: an overview. Cell Death Differ. 11, 365–368. doi:10.1038/sj.cdd.4401364

Lamkanfi, M., Mueller, J.L., Vitari, A.C., Misaghi, S., Fedorova, A., Deshayes, K., Lee, W.P., Hoffman, H.M., Dixit, V.M., 2009. Glyburide inhibits the Cryopyrin/Nalp3 inflammasome. J. Cell Biol. 187, 61–70. doi:10.1083/jcb.200903124

Lara-Tejero, M., Sutterwala, F.S., Ogura, Y., Grant, E.P., Bertin, J., Coyle, A.J., Flavell, R. A., Galán, J.E., 2006. Role of the caspase-1 inflammasome in Salmonella typhimurium pathogenesis. J. Exp. Med. 203, 1407–1412. doi:10.1084/jem.20060206

LeBlanc, P.M., Yeretssian, G., Rutherford, N., Doiron, K., Nadiri, A., Zhu, L., Green, D.R., Gruenheid, S., Saleh, M., 2008. Caspase-12 Modulates NOD Signaling and Regulates Antimicrobial Peptide Production and Mucosal Immunity. Cell Host Microbe 3, 146–157. doi:10.1016/j.chom.2008.02.004

Lee, B.L., Mirrashidi, K.M., Stowe, I.B., Kummerfeld, S.K., Watanabe, C., Haley, B., Cuellar, T.L., Reichelt, M., Kayagaki, N., 2018. ASC- And caspase-8-dependent apoptotic pathway diverges from the NLRC4 inflammasome in macrophages. Sci. Rep. 8, 1–12. doi:10.1038/s41598-018-21998-3

LeibundGut-Landmann, S., Gross, O., Robinson, M.J., Osorio, F., Slack, E.C., Tsoni, S.V., Schweighoffer, E., Tybulewicz, V., Brown, G.D., Ruland, J., Reis e Sousa, C., 2007. Syk- and CARD9-dependent coupling of innate immunity to the induction of T helper cells that produce interleukin 17. Nat. Immunol. 8, 630–8. doi:10.1038/ni1460

Leshchiner, E.S., Rush, J.S., Durney, M.A., Cao, Z., Dančík, V., Chittick, B., Wu, H., Petrone, A., Bittker, J.A., Phillips, A., Perez, J.R., Shamji, A.F., Kaushik, V.K., Daly, M.J., Graham, D.B., Schreiber, S.L., Xavier, R.J., 2017. Small-molecule inhibitors directly target CARD9 and mimic its protective variant in inflammatory bowel disease. Proc. Natl. Acad. Sci. 201705748. doi:10.1073/pnas.1705748114

Levinsohn, J.L., Newman, Z.L., Hellmich, K.A., Fattah, R., Getz, M.A., Liu, S., Sastalla, I., Leppla, S.H., Moayeri, M., 2012. Anthrax lethal factor cleavage of Nlrp1 is required for activation of the inflammasome. PLoS Pathog. 8. doi:10.1371/journal.ppat.1002638

Li, H., Zhu, H., Xu, C., Yuan, J., 1998. Cleavage of BID by Caspase 8 Mediates the Mitochondrial Damage in the Fas Pathway of Apoptosis. Cell 94, 491–501. doi:10.1016/S0092-8674(00)81590-1

Li, J., McQuade, T., Siemer, A.B., Napetschnig, J., Moriwaki, K., Hsiao, Y.S., Damko, E., Moquin, D., Walz, T., McDermott, A., Chan, F.K.M., Wu, H., 2012. The RIP1/RIP3 necrosome forms a functional amyloid signaling complex required for programmed necrosis. Cell 150, 339–350. doi:10.1016/j.cell.2012.06.019

Li, P., Nijhawan, D., Budihardjo, I., Srinivasula, S.M., Ahmad, M., Alnemri, E.S., Wang, X., 1997. Cytochrome c and dATP-Dependent Formation of Apaf-1/Caspase-9 Complex Initiates an Apoptotic Protease Cascade. Cell 91, 479–489. doi:10.1016/S0092-8674(00)80434-1

Liao, K.C., Mogridge, J., 2013. Activation of the Nlrp1b inflammasome by reduction of cytosolic ATP. Infect. Immun. 81, 570–579. doi:10.1128/IAI.01003-12

Libermann, T.A., Baltimore, D., 1990. Activation of interleukin-6 gene expression through the NF-kappa B transcription factor. Mol. Cell. Biol. 10, 2327–2334. doi:10.1128/MCB.10.5.2327.Updated

Ligumsky, M., Simon, P.L., Karmeli, F., Rachmilewitz, D., 1990. Role of interleukin 1 in inflammatory bowel disease - enhanced production during active disease. Gut 31(6), 686–689. doi:10.1136/gut.31.6.686

Lilienbaum, A., 2013. Relationship between the proteasomal system and autophagy. Int. J. Biochem. Mol. Biol. 4, 1–26.

Lin, K.-M., Hub, W., Troutmanb, T.D., Jenningsa, M., Brewerb, T., Lic, X., Nandad, S., Cohend, P., Thomasa, J.A., Pasare, C., 2014. IRAK-1 bypasses priming and directly links TLRs to rapid NLRP3 inflammasome activation, Proceedings of the National Academy of Sciences of the United States of America. doi:10.1073/pnas.1324133111

Lin, R., Heylbroeck, C., Genin, P., Pitha, P.M., Hiscott, J., Al, L.I.N.E.T., Iol, M.O.L.C.E.L.L.B., 1999. Essential Role of Interferon Regulatory Factor 3 in Direct Activation of RANTES Chemokine Transcription. Mol. Cell. Biol. 19, 959–966.

Lin, Y., Huang, D., Wang, J., Lin, Y., Hsieh, S., Huang, K., Lin, W., 2015. Syk is involved in NLRP3 inflammasome-mediated caspase-1 activation through adaptor ASC phosphorylation and enhanced oligomerization. J. Leukoc. Biol. 97, 1–11. doi:10.1189/jlb.3HI0814-371RR

Liu, X., Zhang, Z., Ruan, J., Pan, Y., Magupalli, V.G., Wu, H., Lieberman, J., 2016. Inflammasome-activated gasdermin D causes pyroptosis by forming membrane pores. Nature 535, 153–158. doi:10.1038/nature18629

Liu, X., Zhang, Z., Ruan, J., Pan, Y., Magupalli, V.G., Wu, H., Lieberman, J., 2016. Inflammasome-activated gasdermin D causes pyroptosis by forming membrane pores. Nature 535, 153–158. doi:10.1038/nature18629

Locey, K.J., Lennon, J.T., 2016. Scaling laws predict global microbial diversity. Proc. Natl. Acad. Sci. U. S. A. 113, 5970–5975. doi:10.1073/pnas.1521291113

Lowes, M.A., Bowcock, A.M., Krueger, J.G., 2007. Pathogenesis and therapy of psoriasis. Nature 445, 866–873. doi:10.1038/nature05663

Lu, A., Magupalli, V.G., Ruan, J., Yin, Q., Atianand, M.K., Vos, M.R., Schröder, G.F., Fitzgerald, K. A., Wu, H., Egelman, E.H., 2014. Unified polymerization mechanism for the assembly of asc-dependent inflammasomes. Cell 156, 1193–1206. doi:10.1016/j.cell.2014.02.008

Lund, J.M., Alexopoulou, L., Sato, A., Karow, M., Adams, N.C., Gale, N.W., Iwasaki, A., Flavell, R. A., 2004. Recognition of single-stranded RNA viruses by Toll-like receptor 7. Proc. Natl. Acad. Sci. U. S. A. 101, 5598–5603. doi:10.1073/pnas.0400937101 [doi]\r0400937101 [pii]

Maelfait, J., Vercammen, E., Janssens, S., Schotte, P., Haegman, M., Magez, S., Beyaert, R., 2008. Stimulation of Toll-like receptor 3 and 4 induces interleukin-1beta maturation by caspase-8. J. Exp. Med. 205, 1967–1973. doi:10.1084/jem.20071632

Man, S.M., Hopkins, L.J., Nugent, E., Cox, S., Glück, I.M., Tourlomousis, P., Wright, J. A., Cicuta, P., Monie, T.P., Bryant, C.E., 2014. Inflammasome activation causes dual recruitment of NLRC4 and NLRP3 to the same macromolecular complex. Proc. Natl. Acad. Sci. U. S. A. 1–6. doi:10.1073/pnas.1402911111

Man, S.M., Tourlomousis, P., Hopkins, L., Monie, T.P., Fitzgerald, K. A., Bryant, C.E., 2013. Salmonella infection induces recruitment of Caspase-8 to the inflammasome to modulate IL-1β production. J. Immunol. 191, 5239–5246. doi:10.4049/jimmunol.1301581

Marcus, S.L., Brumell, J.H., Pfeifer, C.G., Finlay, B.B., 2000. Salmonella pathogenicity islands: big virulence in small packages. Microbes Infect. 2, 145–156.

Mariathasan, S., Newton, K., Monack, D.M., Vucic, D., French, D.M., Lee, W.P., Roose-Girma, M., Erickson, S., Dixit, V.M., 2004. Differential activation of the inflammasome by caspase-1 adaptors ASC and Ipaf. Nature 430, 213–218. doi:10.1038/nature02664

Mariathasan, S., Weiss, D.S., Newton, K., McBride, J., O'Rourke, K., Roose-Girma, M., Lee, W.P., Weinrauch, Y., Monack, D.M., Dixit, V.M., 2006. Cryopyrin activates the inflammasome in response to toxins and ATP. Nature 440, 228–32. doi:10.1038/nature04515

Martinon, F., Burns, K., Tschopp, J., 2002. The inflammasome: a molecular platform triggering activation of inflammatory caspases and processing of proIL-beta. Mol. Cell 10, 417–26.

Martinon, F., Pétrilli, V., Mayor, A., Tardivel, A., Tschopp, J., 2006. Gout-associated uric acid crystals activate the NALP3 inflammasome. Nature 440, 237–241. doi:10.1038/nature04516

Mascarenhas, D.P.A., Cerqueira, D.M., Pereira, M.S.F., Castanheira, F.V.S., Fernandes, T.D., Manin, G.Z., Cunha, L.D., Zamboni, D.S., 2017. Inhibition of caspase-1 or

gasdermin-D enable caspase-8 activation in the Naip5/NLRC4/ASC inflammasome. PLOS Pathog. 13, e1006502. doi:10.1371/journal.ppat.1006502

Masumoto, J., Dowds, T.A., Schaner, P., Chen, F.F., Ogura, Y., Li, M., Zhu, L., Katsuyama, T., Sagara, J., Taniguchi, S., Gumucio, D.L., Núñez, G., Inohara, N., 2003. ASC is an activating adaptor for NF-kB and caspase-8-dependent apoptosis. Biochem. Biophys. Res. Commun. 303, 69–73. doi:10.1016/S0006-291X(03)00309-7

Masumoto, J., Taniguchi, S., Ayukawa, K., Sarvotham, H., Kishino, T., Niikawa, N., Hidaka, E., Katsuyama, T., Higuchi, T., Sagara, J., 1999. ASC, a novel 22-kDa protein, aggregates during apoptosis of human promyelocytic leukemia HL-60 cells. J. Biol. Chem. 274, 33835–33838. doi:10.1074/jbc.274.48.33835

Mathur, R., Oh, H., Zhang, D., Park, S., Seo, J., Koblansky, A., Hayden, M.S., Ghosh, S., 2012. A Mouse Model of Salmonella Typhi Infection. Cell 151, 590–602. doi:10.1016/j.cell.2012.08.042

Matusiak, M., Van Opdenbosch, N., Vande Walle, L., Sirard, J.C., 2015. Flagellin-induced NLRC4 phosphorylation primes the inflammasome for activation by NAIP5. Proc. Natl. Acad. Sci. U. S. A. 112, 1541–1546. doi:10.1073/pnas.1417945112

Medema, J., Scaffidi, C., Kischkel, F.C., Shevchenko, A., Mann, M., Krammer, P.H., Peter, M.E., 1997. FLICE is activated by association with the CD95 death-inducing signaling complex (DISC). EMBO J. 16, 2794–2804.

Miao, E. A., Leaf, I. A., Treuting, P.M., Mao, D.P., Dors, M., Sarkar, A., Warren, S.E., Wewers, M.D., Aderem, A., 2010. Caspase-1-induced pyroptosis is an innate immune effector mechanism against intracellular bacteria. Nat. Immunol. 11, 1136–1142. doi:10.1038/ni.1960

Miao, E.A., Alpuche-Aranda, C.M., Dors, M., Clark, A.E., Bader, M.W., Miller, S.I., Aderem, A., 2006. Cytoplasmic flagellin activates caspase-1 and secretion of interleukin 1beta via Ipaf. Nat. Immunol. 7, 569–575. doi:10.1038/ni1344

Miao, E.A., Mao, D.P., Yudkovsky, N., Bonneau, R., Lorang, C.G., Warren, S.E., Leaf, I.A., Aderem, A., 2010. Innate immune detection of the type III secretion apparatus through the NLRC4 inflammasome. Proc. Natl. Acad. Sci. U. S. A. 107, 3076–3080. doi:10.1073/pnas.0913087107

Mishra, B.B., Moura-Alves, P., Sonawane, A., Hacohen, N., Griffiths, G., Moita, L.F., Anes, E., 2010. Mycobacterium tuberculosis protein ESAT-6 is a potent activator of the

NLRP3/ASC inflammasome. Cell. Microbiol. 12, 1046–1063. doi:10.1111/j.1462-5822.2010.01450.x

Mishra, B.B., Rathinam, V.A.K., Martens, G.W., Martinot, A.J., Kornfeld, H., Fitzgerald, K.A., Sassetti, C.M., 2012. Nitric oxide controls the immunopathology of tuberculosis by inhibiting NLRP3 inflammasome–dependent processing of IL-1β. Nat. Immunol. 14, 52–60. doi:10.1038/ni.2474

Monack, D., Navarre, W., Falkow, S., 2001. Salmonella-induced macrophage death: the role of caspase-1 in death and inflammation. Microbes Infect. 3, 1201–1212.

Monie, T.P., Bryant, C.E., Gay, N.J., 2009. Activating immunity: lessons from the TLRs and NLRs. Trends Biochem. Sci. 34, 553–561. doi:10.1016/j.tibs.2009.06.011

Moore, C.B., Bergstralh, D.T., Duncan, J.A., Lei, Y., Morrison, T.E., Zimmermann, A.G., Accavitti-Loper, M.A., Madden, V.J., Sun, L., Ye, Z., Lich, J.D., Heise, M.T., Chen, Z., Ting, J.P.-Y., 2008. NLRX1 is a regulator of mitochondrial antiviral immunity. Nature 451, 573–7. doi:10.1038/nature06501

Moore, C.B., Bergstralh, D.T., Duncan, J.A., Lei, Y., Morrison, T.E., Zimmermann, A.G., Accavitti-Loper, M.A., Madden, V.J., Sun, L., Ye, Z., Lich, J.D., Heise, M.T., Chen, Z., Ting, J.P.-Y., 2008. NLRX1 is a regulator of mitochondrial antiviral immunity. Nature 451, 573–7. doi:10.1038/nature06501

Mortimer, L., Moreau, F., Cornick, S., Chadee, K., 2015. The NLRP3 Inflammasome Is a Pathogen Sensor for Invasive Entamoeba histolytica via Activation of α5β1 Integrin at the Macrophage-Amebae Intercellular Junction. PLoS Pathog. 11, 1–26. doi:10.1371/journal.ppat.1004887

Mortimer, L., Moreau, F., MacDonald, J.A., Chadee, K., 2016. NLRP3 inflammasome inhibition is disrupted in a group of auto-inflammatory disease CAPS mutations. Nat. Immunol. 17, 1176–1186. doi:10.1038/ni.3538

Muruve, D.A., Pétrilli, V., Zaiss, A.K., White, L.R., Clark, S.A., Ross, P.J., Parks, R.J., Tschopp, J., 2008. The inflammasome recognizes cytosolic microbial and host DNA and triggers an innate immune response. Nature 452, 103–107. doi:10.1038/nature06664

Muzio, M., 1998. An Induced Proximity Model for Caspase-8 Activation. J. Biol. Chem. 273, 2926–2930. doi:10.1074/jbc.273.5.2926

Muzio, M., Chinnaiyan, A., Kischkel, F., O'Rourke, K., Shevchenko, A., Ni, J., Scaffidi, C., Bretz, J.D., Zhang, M., Gentz, R., Mann, M., Krammer, P.H., Peter, M.E., Dixit, V.M., 1996. FLICE, a novel FADD-homologous ICE/CED-3–like protease, is recruited to the CD95 (Fas/APO-1) death-inducing signaling complex. Cell 85, 817–827.

Nakamura, N., Lill, J.R., Phung, Q., Jiang, Z., Bakalarski, C., de Mazière, A., Klumperman, J., Schlatter, M., Delamarre, L., Mellman, I., 2014. Endosomes are specialized platforms for bacterial sensing and NOD2 signalling. Nature 509, 240–244. doi:10.1038/nature13133

Neerincx, A., Lautz, K., Menning, M., Kremmer, E., Zigrino, P., Hösel, M., Büning, H., Schwarzenbacher, R., Kufer, T.A., 2010. A role for the human nucleotide-binding domain, leucine-rich repeat-containing family member NLRC5 in antiviral responses. J. Biol. Chem. 285, 26223–26232. doi:10.1074/jbc.M110.109736

Neiman-Zenevich, J., Liao, K., Mogridge, J., 2014. Distinct Regions of NLRP1B Are Required To Respond to Anthrax Lethal Toxin and Metabolic Inhibition. Infect. Immun. 82, 3697–3703. doi:10.1128/IAI.02167-14

Nicholson, D., Ali, A., Thornberry, N., Vaillancourt, J., Ding, C., Gallant, M., Gareau, Y., Griffin, P., Labelle, M., Lazebnik, Y., Munday, N., Raju, S., Smulson, M., Yamin, T., Yu, V., Miller, D., 1995. Identification and inhibition of the ICE/CED-3 protease necessary for mammalian apoptosis. Nature 6, 37–43.

Oberst, A., Dillon, C.P., Weinlich, R., McCormick, L.L., Fitzgerald, P., Pop, C., Hakem, R., Salvesen, G.S., Green, D.R., 2011. Catalytic activity of the caspase-8–FLIPL complex inhibits RIPK3-dependent necrosis. Nature 471, 363–367. doi:10.1038/nature09852

Oberst, A., Pop, C., Tremblay, A.G., Blais, V., Denault, J.-B., Salvesen, G.S., Green, D.R., 2010. Inducible dimerization and inducible cleavage reveal a requirement for both processes in caspase-8 activation. J. Biol. Chem. 285, 16632–16642. doi:10.1074/jbc.M109.095083

Oldenburg, M., Krüger, A., Ferstl, R., Kaufmann, A., Nees, G., Sigmund, A., … Kirschning, C. J. (2012). TLR13 Recognizes Bacterial 23 S rRNA Devoid of Erythromycin Resistance–Forming Modification. *Science*, *337*(July), 1111–1115.

Parkhouse, R., Boyle, J.P., Mayle, S., Sawmynaden, K., Rittinger, K., Monie, T.P., 2014. Interaction between NOD2 and CARD9 involves the NOD2 NACHT and the linker

region between the NOD2 CARDs and NACHT domain. FEBS Lett. doi:10.1016/j.febslet.2014.06.035

Parkhouse, R., Boyle, J.P., Mayle, S., Sawmynaden, K., Rittinger, K., Monie, T.P., 2014. Interaction between NOD2 and CARD9 involves the NOD2 NACHT and the linker region between the NOD2 CARDs and NACHT domain. FEBS Lett. doi:10.1016/j.febslet.2014.06.035

Paroni, G., Henderson, C., Schneider, C., Brancolini, C., 2002. Caspase-2 can trigger cytochrome c release and apoptosis from the nucleus. J. Biol. Chem. 277, 15147–15161. doi:10.1074/jbc.M112338200

Paroni, G., Henderson, C., Schneider, C., Brancolini, C., 2002. Caspase-2 can trigger cytochrome c release and apoptosis from the nucleus. J. Biol. Chem. 277, 15147–15161. doi:10.1074/jbc.M112338200

Parry, C.M., Hien, T.T., Dougan, G., White, N.J., Farrar, J.J., 2002. Typhoid fever. N. Engl. J. Med. 347, 1770–1782. doi:10.4269/ajtmh.2010.09-0233

Pauleau, A., Murray, P.J., 2003. Role of Nod2 in the Response of Macrophages to Toll-Like Receptor Agonists Role of Nod2 in the Response of Macrophages to Toll-Like Receptor Agonists. Mol. Cell. Biol. 23, 7531–7539. doi:10.1128/MCB.23.21.7531

Pedra, J.H., Sutterwala, F.S., Sukumaran, B., Ogura, Y., Qian, F., Montgomery, R.R., Flavell, R.A., Fikrig, E., 2007. ASC/PYCARD and caspase-1 regulate the IL-18/IFN-gamma axis during Anaplasma phagocytophilum infection. J Immunol 179, 4783–4791. doi:179/7/4783 [pii]

Pereira, M., Tourlomousis, P., Wright, J., P. Monie, T., Bryant, C.E., 2016. CARD9 negatively regulates NLRP3-induced IL-1β production on Salmonella infection of macrophages. Nat. Commun. 7, 12874. doi:10.1038/ncomms12874

Perez-Lopez, A., Rosales-Reyes, R., Alpuche-Aranda, C.M., Ortiz-Navarrete, V., 2013. Salmonella downregulates Nod-like receptor family CARD domain containing protein 4 expression to promote its survival in B cells by preventing inflammasome activation and cell death. J. Immunol. 190, 1201–1209. doi:10.4049/jimmunol.1200415

Pétrilli, V., Papin, S., Dostert, C., Mayor, A., Martinon, F., Tschopp, J., 2007. Activation of the NALP3 inflammasome is triggered by low intracellular potassium concentration. Cell Death Differ. 14, 1583–1589. doi:10.1038/sj.cdd.4402195

Pfaffl, M.W., 2001. A new mathematical model for relative quantification in real-time RT-PCR. Nucleic Acids Res. 29, 45e–45. doi:10.1093/nar/29.9.e45

Pickard, J.M., Zeng, M.Y., Caruso, R., Núñez, G., 2017. Gut microbiota: Role in pathogen colonization, immune responses, and inflammatory disease. Immunol. Rev. 279, 70–89. doi:10.1111/IMR.12567

Poeck, H., Bscheider, M., Gross, O., Finger, K., Roth, S., Rebsamen, M., Hannesschläger, N., Schlee, M., Rothenfusser, S., Barchet, W., Kato, H., Akira, S., Inoue, S., Endres, S., Peschel, C., Hartmann, G., Hornung, V., Ruland, J., 2010. Recognition of RNA virus by RIG-I results in activation of CARD9 and inflammasome signaling for interleukin 1 beta production. Nat. Immunol. 11, 63–69. doi:10.1038/ni.1824

Pointon, J.J., Harvey, D., Karaderi, T., Appleton, L.H., Farrar, C., Stone, M.A., Sturrock, R.D., Brown, M.A., Wordsworth, B.P., 2010. Elucidating the chromosome 9 association with AS; CARD9 is a candidate gene. Genes Immun. 11, 490–496. doi:10.1038/gene.2010.17

Poltorak, A., He, X., Smirnova, I., Liu, M., Huffel, C. Van, Du, X., Birdwell, D., Alejos, E., Silva, M., Galanos, C., Freudenberg, M., Ricciardi-castagnoli, P., Layton, B., Beutler, B., 1998. Defective LPS Signaling in C3H / HeJ and C57BL / 10ScCr Mice : Mutations in Tlr4 Gene. Science. 282, 2085–2088. doi:10.1126/science.282.5396.2085

Pop, C., Salvesen, G.S., 2009. Human caspases: activation, specificity, and regulation. J. Biol. Chem. 284, 21777–21781. doi:10.1074/jbc.R800084200

Poyet, J.L., Srinivasula, S.M., Tnani, M., Razmara, M., Fernandes-Alnemri, T., Alnemri, E.S., 2001. Identification of Ipaf, a Human Caspase-1-activating Protein Related to Apaf-1. J. Biol. Chem. 276, 28309–28313. doi:10.1074/jbc.C100250200

Proell, M., Riedl, S.J., Fritz, J.H., Rojas, A.M., Schwarzenbacher, R., 2008. The Nod-Like Receptor (NLR) family: A tale of similarities and differences. PLoS One 3, 1–11. doi:10.1371/journal.pone.0002119

Puren, A.J., Fantuzzi, G., Dinarello, C. A., 1999. Gene expression, synthesis, and secretion of interleukin 18 and interleukin 1beta are differentially regulated in human blood mononuclear cells and mouse spleen cells. Proc. Natl. Acad. Sci. U. S. A. 96, 2256–2261. doi:DOI 10.1073/pnas.96.5.2256

Py, B.F., Kim, M.-S., Vakifahmetoglu-Norberg, H., Yuan, J., 2013. Deubiquitination of NLRP3 by BRCC3 critically regulates inflammasome activity. Mol. Cell 49, 331–338. doi:10.1016/j.molcel.2012.11.009

Qu, Y., Misaghi, S., Izrael-Tomasevic, A., Newton, K., Gilmour, L.L., Lamkanfi, M., Louie, S., Kayagaki, N., Liu, J., Kömüves, L., Cupp, J.E., Arnott, D., Monack, D., Dixit, V.M., 2012. Phosphorylation of NLRC4 is critical for inflammasome activation. Nature 490, 539–542. doi:10.1038/nature11429

Qu, Y., Misaghi, S., Newton, K., Maltzman, A., Izrael-Tomasevic, A., Arnott, D., Dixit, V.M., 2016. NLRP3 recruitment by NLRC4 during Salmonella infection. J. Exp. Med. 1, 877–885. doi:10.1084/jem.20132234

Que, F., Wu, S., & Huang, R. (2013). Salmonella pathogenicity Island 1(SPI-1) at work. *Current Microbiology*, *66*(6), 582–587.

Rajan, J. V., Rodriguez, D., Miao, E.A., Aderem, A., 2011. The NLRP3 Inflammasome Detects Encephalomyocarditis Virus and Vesicular Stomatitis Virus Infection. J. Virol. 85, 4167–4172. doi:10.1128/JVI.01687-10

Rathinam, V.A.K., Fitzgerald, K.A., 2016. Inflammasome Complexes: Emerging Mechanisms and Effector Functions. Cell 165, 792–800. doi:10.1016/j.cell.2016.03.046

Rathinam, V.A.K., Jiang, Z., Waggoner, S.N., Sharma, S., Cole, L.E., Waggoner, L., Vanaja, S.K., Monks, B.G., Ganesan, S., Latz, E., Hornung, V., Vogel, S.N., Szomolanyi-Tsuda, E., Fitzgerald, K.A., 2010. The AIM2 inflammasome is essential for host defense against cytosolic bacteria and DNA viruses. Nat. Immunol. 11, 395–402. doi:10.1038/ni.1864

Raupach, B., Peuschel, S.-K., Monack, D.M., Zychlinsky, A., 2006. Caspase-1-mediated activation of interleukin-1beta (IL-1beta) and IL-18 contributes to innate immune defenses against Salmonella enterica serovar Typhimurium infection. Infect. Immun. 74, 4922–4926. doi:10.1128/IAI.00417-06

Rayamajhi, M., Zak, D.E., Chavarria-Smith, J., Vance, R.E., Miao, E.A., 2013. Cutting edge: Mouse NAIP1 detects the type III secretion system needle protein. J. Immunol. 191, 3986–3989. doi:10.4049/jimmunol.1301549

Ritter, M., Gross, O., Kays, S., Ruland, J., Nimmerjahn, F., Saijo, S., Tschopp, J., Layland, L.E., Prazeres da Costa, C., 2010. Schistosoma mansoni triggers Dectin-2, which

activates the Nlrp3 inflammasome and alters adaptive immune responses. Proc. Natl. Acad. Sci. U. S. A. 107, 20459–20464. doi:10.1073/pnas.1010337107

Rivas, M.A., Beaudoin, M., Gardet, A., Stevens, C., Sharma, Y., Zhang, C.K., Boucher, G., Ripke, S., Ellinghaus, D., Burtt, N., Fennell, T., Kirby, A., Latiano, A., Goyette, P., Green, T., Halfvarson, J., Haritunians, T., Korn, J.M., Kuruvilla, F., Lagacé, C., Neale, B., Lo, K.S., Schumm, P., Törkvist, L., Dubinsky, M.C., Brant, S.R., Silverberg, M.S., Duerr, R.H., Altshuler, D., Gabriel, S., Lettre, G., Franke, A., D'Amato, M., McGovern, D.P.B., Cho, J.H., Rioux, J.D., Xavier, R.J., Daly, M.J., 2011. Deep resequencing of GWAS loci identifies independent rare variants associated with inflammatory bowel disease. Nat. Genet. 43, 1066–1073. doi:10.1038/ng.952

Robertson, J.D., Enoksson, M., Suomela, M., Zhivotovsky, B., Orrenius, S., 2002. Caspase-2 acts upstream of mitochondria to promote cytochrome c release during etoposide-induced apoptosis. J. Biol. Chem. 277, 29803–29809. doi:10.1074/jbc.M204185200

Robertson, J.D., Enoksson, M., Suomela, M., Zhivotovsky, B., Orrenius, S., 2002. Caspase-2 acts upstream of mitochondria to promote cytochrome c release during etoposide-induced apoptosis. J. Biol. Chem. 277, 29803–29809. doi:10.1074/jbc.M204185200

Rogers, C., Fernandes-Alnemri, T., Mayes, L., Alnemri, D., Cingolani, G., Alnemri, E.S., 2017. Cleavage of DFNA5 by caspase-3 during apoptosis mediates progression to secondary necrotic/pyroptotic cell death. Nat. Commun. 8, 14128. doi:10.1038/ncomms14128

Rogers, N.C., Slack, E.C., Edwards, A.D., Nolte, M.A., Schulz, O., Schweighoffer, E., Williams, D.L., Gordon, S., Tybulewicz, V.L., Brown, G.D., Reis e Sousa, C., 2005. Syk-dependent cytokine induction by Dectin-1 reveals a novel pattern recognition pathway for C type lectins. Immunity 22, 507–17. doi:10.1016/j.immuni.2005.03.004

Roman, J., Ritzenthaler, J.D., Fenton, M.J., Roser, S., Schuyler, W., 2000. Transcriptional regulation of the human interleukin 1beta gene by fibronectin: role of protein kinase C and activator protein 1 (AP-1). Cytokine 12, 1581–1596. doi:10.1006/cyto.2000.0759

Romberg, N., Al Moussawi, K., Nelson-Williams, C., Stiegler, A.L., Loring, E., Choi, M., Overton, J., Meffre, E., Khokha, M.K., Huttner, A.J., West, B., Podoltsev, N.A., Boggon, T.J., Kazmierczak, B.I., Lifton, R.P., 2014. Mutation of NLRC4 causes a syndrome of enterocolitis and autoinflammation. Nat. Genet. 46, 1135–1139. doi:10.1038/ng.3066

Roth, S., Rottach, A., Lotz-Havla, A.S., Laux, V., Muschaweckh, A., Gersting, S.W., Muntau, A.C., Hopfner, K.-P., Jin, L., Vanness, K., Petrini, J.H.J., Drexler, I., Leonhardt, H., Ruland, J., 2014. Rad50-CARD9 interactions link cytosolic DNA sensing to IL-1β production. Nat. Immunol. 15, 538–545. doi:10.1038/ni.2888

Royle, M., Tötemeyer, S., Alldridge, L., Maskell, D., Bryant, C., 2003. Stimulation of Toll-like receptor 4 by lipopolysaccharide during cellular invasion by live Salmonella typhimurium is a critical but not exclusive event leading to macrophage responses. J. Immunol. 170, 5445–5454.

Saïd-Sadier, N., Padilla, E., Langsley, G., Ojcius, D.M., 2010. Aspergillus fumigatus stimulates the NLRP3 inflammasome through a pathway requiring ROS production and the syk tyrosine kinase. PLoS One 5. doi:10.1371/journal.pone.0010008

Saijo, S., Fujikado, N., Furuta, T., Chung, S., Kotaki, H., Seki, K., Sudo, K., Akira, S., Adachi, Y., Ohno, N., Kinjo, T., Nakamura, K., Kawakami, K., Iwakura, Y., 2007. Dectin-1 is required for host defense against Pneumocystis carinii but not against Candida albicans. Nat. Immunol. 8, 39–46. doi:10.1038/ni1425

Saleh, M., Mathison, J.C., Wolinski, M.K., Bensinger, S.J., Fitzgerald, P., Droin, N., Ulevitch, R.J., Green, D.R., Nicholson, D.W., 2006. Enhanced bacterial clearance and sepsis resistance in caspase-12-deficient mice. Nature 440, 1064–8. doi:10.1038/nature04656

Sander, L.E., Davis, M.J., Boekschoten, M. V, Amsen, D., Dascher, C.C., Ryffel, B., Swanson, J. a, Müller, M., Blander, J.M., 2011. Detection of prokaryotic mRNA signifies microbial viability and promotes immunity. Nature 474, 385–389. doi:10.1038/nature10072

Santos, R.L., 2014. Pathobiology of Salmonella, intestinal microbiota, and the host innate immune response. Front. Immunol. 5, 1–7. doi:10.3389/fimmu.2014.00252

Scaffidi, C., Fulda, S., Srinivasan, A., Friesen, C., Li, F., Tomaselli, K., Debatin, K., Krammer, P., Peter, M., 1998. Two CD95 (APO-1/Fas) signaling pathways. EMBO J. 17, 1675–1687.

Schattgen, S.A., Fitzgerald, K.A., 2011. The PYHIN protein family as mediators of host defenses. Immunol. Rev. 243, 109–118. doi:10.1111/j.1600-065X.2011.01053.x

Schneider, K.S., Groß, C.J., Dreier, R.F., Saller, B.S., Mishra, R., Gorka, O., Heilig, R., Meunier, E., Dick, M.S., Ćiković, T., Sodenkamp, J., Médard, G., Naumann, R., Ruland, J., Kuster, B., Broz, P., Groß, O., 2017. The Inflammasome Drives GSDMD-

Independent Secondary Pyroptosis and IL-1 Release in the Absence of Caspase-1 Protease Activity. Cell Rep. 21, 3846–3859. doi:10.1016/j.celrep.2017.12.018

Schneider, M., Zimmermann, A.G., Roberts, R. a, Zhang, L., Swanson, K. V, Wen, H., Davis, B.K., Allen, I.C., Holl, E.K., Ye, Z., Rahman, A.H., Conti, B.J., Eitas, T.K., Koller, B.H., Ting, J.P.-Y., 2012. The innate immune sensor NLRC3 attenuates Toll-like receptor signaling via modification of the signaling adaptor TRAF6 and transcription factor NF-κB. Nat. Immunol. 13, 823–831. doi:10.1038/ni.2378

Schroder, K., Tschopp, J., 2010. The Inflammasomes. Cell 140, 821–832. doi:10.1016/j.cell.2010.01.040

Scott, F.L., Stec, B., Pop, C., Dobaczewska, M.K., Lee, J.J., Monosov, E., Robinson, H., Salvesen, G.S., Schwarzenbacher, R., Riedl, S.J., 2009. The Fas-FADD death domain complex structure unravels signalling by receptor clustering. Nature 457, 1019–1022. doi:10.1038/nature07606

Sebastiani, G., Blais, V., Sancho, V., Vogel, S.N., Stevenson, M.M., Gros, P., Lapointe, J.-M., Rivest, S., Malo, D., 2002. Host immune response to Salmonella enterica serovar Typhimurium infection in mice derived from wild strains. Infect. Immun. 70, 1997–2009. doi:10.1128/IAI.70.4.1997

Sender, R., Fuchs, S., Milo, R., 2016. Revised Estimates for the Number of Human and Bacteria Cells in the Body. PLoS Biol. 14, 1–14. doi:10.1371/journal.pbio.1002533

Seth, R.B., Sun, L., Ea, C., Chen, Z.J., 2005. Identification and Characterization of MAVS, a Mitochondrial Antiviral Signaling Protein that Activates NF-kB and IRF3. Cell 122, 669–682. doi:10.1016/j.cell.2005.08.012

Shakhov, A., Collart, M., Vassalli, P., Nedospasov, S., Jongeneel, C., 1990. Kappa B-type enhancers are involved in lipopolysaccharide-mediated transcriptional activation of the tumor necrosis factor alpha gene in primary macrophages. J. Exp. Med. 171, 35–47.

Shalini, S., Dorstyn, L., Dawar, S., Kumar, S., 2014. Old, new and emerging functions of caspases. Cell Death Differ. 1–14. doi:10.1038/cdd.2014.216

Shi, C.S., Kehrl, J.H., 2008. MyD88 and Trif target Beclin 1 to trigger autophagy in macrophages. J. Biol. Chem. 283, 33175–33182. doi:10.1074/jbc.M804478200

Shi, C.-S., Shenderov, K., Huang, N.-N., Kabat, J., Abu-Asab, M., Fitzgerald, K.A., Sher, A., Kehrl, J.H., 2012. Activation of autophagy by inflammatory signals limits IL-1β

production by targeting ubiquitinated inflammasomes for destruction. Nat. Immunol. 13, 255–263. doi:10.1038/ni.2215

Shi, J., Zhao, Y., Wang, K., Shi, X., Wang, Y., Huang, H., Zhuang, Y., Cai, T., Wang, F., Shao, F., 2015. Cleavage of GSDMD by inflammatory caspases determines pyroptotic cell death. Nature. doi:10.1038/nature15514

Shi, J., Zhao, Y., Wang, Y., Gao, W., Ding, J., Li, P., Hu, L., Shao, F., 2014. Inflammatory caspases are innate immune receptors for intracellular LPS. Nature. doi:10.1038/nature13683

Shibutani, S.T., Saitoh, T., Nowag, H., Münz, C., Yoshimori, T., 2015. Autophagy and autophagy-related proteins in the immune system. Nat. Immunol. 16, 1014–1024. doi:10.1038/ni.3273

Shimada, K., Crother, T. R., Karlin, J., Dagvadorj, J., Chiba, N., Chen, S., … Arditi, M. (2012). Oxidized Mitochondrial DNA Activates the NLRP3 Inflammasome during Apoptosis. *Immunity*, *36*(3), 401–414.

Shimazu, R., Akashi, S., Ogata, H., Nagai, Y., Fukudome, K., Miyake, K., Kimoto, M., 1999. MD-2, a Molecule that Confers Lipopolysaccharide Responsiveness on Toll-like Receptor 4. J. Exp. Med. 189, 1777–1782. doi:10.1084/jem.189.11.1777

Siegmund, B., Fantuzzi, G., Rieder, F., Gamboni-Robertson, F., Lehr, H.A., Hartmann, G., Dinarello, C.A., Endres, S., Eigler, A., 2001. Neutralization of interleukin-18 reduces severity in murine colitis and intestinal IFN-gamma and TNF-alpha production. Am. J. Physiol. Regul. Integr. Comp. Physiol. 281, R1264-73.

Slaats, J., ten Oever, J., van de Veerdonk, F.L., Netea, M.G., 2016. IL-1β/IL-6/CRP and IL-18/ferritin: Distinct Inflammatory Programs in Infections. PLoS Pathog. 12, 1–13. doi:10.1371/journal.ppat.1005973

Spandidos, A., Wang, X., Wang, H., Seed, B., 2009. PrimerBank: A resource of human and mouse PCR primer pairs for gene expression detection and quantification. Nucleic Acids Res. 38, 792–799. doi:10.1093/nar/gkp1005

Srinivasan, A., Salazar-Gonzalez, R.-M., Jarcho, M., Sandau, M.M., Lefrancois, L., Mcsorley, S.J., 2007. Innate immune activation of CD4 T cells in salmonella-infected mice is dependent on IL-18. J. Immunol. 178, 6342–6349. doi:10.4049/jimmunol.178.10.6342

Srinivasula, S.M., Poyet, J.L., Razmara, M., Datta, P., Zhang, Z., Alnemri, E.S., 2002. The PYRIN-CARD protein ASC is an activating adaptor for caspase-1. J. Biol. Chem. 277, 21119–21122. doi:10.1074/jbc.C200179200

Stanger, B.Z., Leder, P., Lee, T.H., Kim, E., Seed, B., 1995. RIP: A novel protein containing a death domain that interacts with Fas/APO-1 (CD95) in yeast and causes cell death. Cell 81, 513–523. doi:10.1016/0092-8674(95)90072-1

Strasser, D., Neumann, K., Bergmann, H., Marakalala, M.J., Guler, R., Rojowska, A., Hopfner, K.-P., Brombacher, F., Urlaub, H., Baier, G., Brown, G.D., Leitges, M., Ruland, J., 2012. Syk kinase-coupled C-type lectin receptors engage protein kinase C-σ to elicit Card9 adaptor-mediated innate immunity. Immunity 36, 32–42. doi:10.1016/j.immuni.2011.11.015

Sung, K., Khan, S.A., Nawaz, M.S., Khan, A.A., 2003. A simple and efficient Triton X-100 boiling and chloroform extraction method of RNA isolation from Gram-positive and Gram-negative bacteria. FEMS Microbiol. Lett. 229, 97–101. doi:10.1016/S0378-1097(03)00791-2

Sutterwala, F.S., Mijares, L.A., Li, L., Ogura, Y., Kazmierczak, B.I., Flavell, R.A., 2007. Immune recognition of Pseudomonas aeruginosa mediated by the IPAF/NLRC4 inflammasome. J. Exp. Med. 204, 3235–3245. doi:10.1084/jem.20071239

Sutterwala, F.S., Ogura, Y., Szczepanik, M., Lara-Tejero, M., Lichtenberger, G.S., Grant, E.P., Bertin, J., Coyle, A.J., Galán, J.E., Askenase, P.W., Flavell, R.A., 2006. Critical role for NALP3/CIAS1/Cryopyrin in innate and adaptive immunity through its regulation of caspase-1. Immunity 24, 317–327. doi:10.1016/j.immuni.2006.02.004

Suzuki, S., Franchi, L., He, Y., Muñoz-Planillo, R., Mimuro, H., Suzuki, T., Sasakawa, C., Núñez, G., 2014. Shigella Type III Secretion Protein MxiI Is Recognized by Naip2 to Induce Nlrc4 Inflammasome Activation Independently of Pkcδ PLoS Pathog. 10. doi:10.1371/journal.ppat.1003926

Suzuki, T., Franchi, L., Toma, C., Ashida, H., Ogawa, M., Yoshikawa, Y., Mimuro, H., Inohara, N., Sasakawa, C., Nuñez, G., 2007. Differential regulation of caspase-1 activation, pyroptosis, and autophagy via Ipaf and ASC in Shigella-infected macrophages. PLoS Pathog. 3, 1082–1091. doi:10.1371/journal.ppat.0030111

Takeuchi, O., Kawai, T., Mühlradt, P.F., Morr, M., Radolf, J.D., Zychlinsky, A., Takeda, K., Akira, S., 2001. Discrimination of bacterial lipoproteins by Toll-like receptor 6. Int. Immunol. 13, 933–940. doi:10.1093/intimm/13.7.933

Takeuchi, O., Sato, S., Horiuchi, T., Hoshino, K., Takeda, K., Dong, Z., Modlin, R.L., Akira, S., 2002. Cutting edge: role of Toll-like receptor 1 in mediating immune response to microbial lipoproteins. J. Immunol. 169, 10–14. doi:10.4049/jimmunol.169.1.10

Talbot, S., Tötemeyer, S., Yamamoto, M., Akira, S., Hughes, K., Gray, D., Barr, T., Mastroeni, P., Maskell, D.J., Bryant, C.E., 2009. Toll-like receptor 4 signalling through MyD88 is essential to control Salmonella enterica serovar typhimurium infection, but not for the initiation of bacterial clearance. Immunology 128, 472–83. doi:10.1111/j.1365-2567.2009.03146.x

Tattoli, I., Carneiro, L.A., Jéhanno, M., Magalhaes, J.G., Shu, Y., Philpott, D.J., Arnoult, D., Girardin, S.E., 2008. NLRX1 is a mitochondrial NOD-like receptor that amplifies NF-kappaB and JNK pathways by inducing reactive oxygen species production. EMBO Rep. 9, 293–300. doi:10.1038/sj.embor.7401161

Taxman, D.J., Huang, M.T.H., Ting, J.P.Y., 2010. Inflammasome inhibition as a pathogenic stealth mechanism. Cell Host Microbe 8, 7–11. doi:10.1016/j.chom.2010.06.005

Tenthorey, J.L., Haloupek, N., López-blanco, J.R., Grob, P., Adamson, E., Hartenian, E., Lind, N.A., Bourgeois, N.M., Chacón, P., Nogales, E., Vance, R.E., 2017. The structural basis of flagellin detection by NAIP5: A strategy to limit pathogen immune evasion. Science (80-.). 893, 888–893. doi:10.1126/science.aao1140

Tenthorey, J.L., Kofoed, E.M., Daugherty, M.D., Malik, H.S., Vance, R.E., 2014. Molecular basis for specific recognition of bacterial ligands by NAIP/NLRC4 inflammasomes. Mol. Cell 54, 17–29. doi:10.1016/j.molcel.2014.02.018

Tergaonkar, V., 2006. NFkappaB pathway: a good signaling paradigm and therapeutic target. Int. J. Biochem. Cell Biol. 38, 1647–1653. doi:10.1016/j.biocel.2006.03.023

Tinel, A., 2004. The PIDDosome, a Protein Complex Implicated in Activation of Caspase-2 in Response to Genotoxic Stress. Science (80-.). 304, 843–846. doi:10.1126/science.1095432

Tobias, P.S., Soldau, K., Ulevitch, R.J., 1986. Isolation of a lipopolysaccharide-binding acute phase reactant from rabbit serum. J. Exp. Med. 164, 777–93. doi:10.1084/jem.164.3.777

Toma, C., Higa, N., Koizumi, Y., Nakasone, N., Ogura, Y., McCoy, A. J., Franchi, L., Uematsu, S., Sagara, J., Taniguchi, S., Tsutsui, H., Akira, S., Tschopp, J., Nunez, G., Suzuki, T., 2010. Pathogenic Vibrio Activate NLRP3 Inflammasome via Cytotoxins and TLR/Nucleotide-Binding Oligomerization Domain-Mediated NF- B Signaling. J. Immunol. 184, 5287–5297. doi:10.4049/jimmunol.0903536

Tong, Y., Cui, J., Li, Q., Zou, J., Wang, H.Y., Wang, R.-F., 2012. Enhanced TLR-induced NF-κB signaling and type I interferon responses in NLRC5 deficient mice. Cell Res. 22, 822–35. doi:10.1038/cr.2012.53

Tötemeyer, S., Foster, N., Kaiser, P., Duncan, J., Bryant, C.E., 2003. Toll-Like Receptor Expression in C3H/HeN and C3H/HeJ Mice during Salmonella enterica Serovar Typhimurium Infection. Infect. Immun. 71, 6653–6657. doi:10.1128/IAI.71.11.6653

Tötemeyer, S., Kaiser, P., Maskell, D.J., Bryant, C.E., 2005. Sublethal Infection of C57BL / 6 Mice with Salmonella enterica Serovar Typhimurium Leads to an Increase in Levels of Toll-Like as Well as a Decrease in Levels of TLR6 mRNA in Infected Organs Sublethal Infection of C57BL / 6 Mice with Salmonella enterica S. Infect. Immun. 1, 1873–1878. doi:10.1128/IAI.73.3.1873

Tóth, A., Zajta, E., Csonka, K., Vágvölgyi, C., Netea, M.G., Gácser, A., 2017. Specific pathways mediating inflammasome activation by Candida parapsilosis. Sci. Rep. 7, 43129. doi:10.1038/srep43129

Ueda, N., Yamamoto, S., 1995. Transcriptional Roles of Nuclear Factor kB and Nuclear Factor- Interleukin-6 in the Tumor Necrosis Factor a-Dependent Induction of Cyclooxygenase-2 in MC3T3-E1 Cells. J. Biol. Chem. 270, 31315–31320.

Underhill, D.M., Rossnagle, E., Lowell, C.A., Simmons, R.M., 2005. Dectin-1 activates Syk tyrosine kinase in a dynamic subset of macrophages for reactive oxygen production. Blood 106, 2543–50. doi:10.1182/blood-2005-03-1239

Uniken Venema, W.T., Voskuil, M.D., Dijkstra, G., Weersma, R.K., Festen, E.A., 2017. The genetic background of inflammatory bowel disease: from correlation to causality. J. Pathol. 241, 146–158. doi:10.1002/path.4817

Upton, J.W., Kaiser, W.J., Mocarski, E.S., 2008. Cytomegalovirus M45 cell death suppression requires receptor-interacting protein (RIP) homotypic interaction motif (RHIM)-dependent interaction with RIP1. J. Biol. Chem. 283, 16966–16970. doi:10.1074/jbc.C800051200

Van De Craen, M., Vandenabeele, P., Declercq, W., Van Den Brande, I., Van Loo, G., Molemans, F., Schotte, P., Van Criekinge, W., Beyaert, R., Fiers, W., 1997. Characterization of seven murine caspase family members. FEBS Lett. 403, 61–69. doi:10.1016/S0014-5793(97)00026-4

van Raam, B.J., Salvesen, G.S., 2012. Proliferative versus apoptotic functions of caspase-8 Hetero or homo: the caspase-8 dimer controls cell fate. Biochim. Biophys. Acta 1824, 113–122. doi:10.1016/j.bbapap.2011.06.005

Vande Walle, L., Jiménez Fernández, D., Demon, D., Van Laethem, N., Van Hauwermeiren, F., Van Gorp, H., Van Opdenbosch, N., Kayagaki, N., Lamkanfi, M., 2015. Does caspase-12 suppress inflammasome activation? Nature 534, E1–E4. doi:10.1038/nature17649

Varfolomeev, E.E., Schuchmann, M., Luria, V., Chiannilkulchai, N., Beckmann, J.S., Mett, I.L., Rebrikov, D., Brodianski, V.M., Kemper, O.C., Kollet, O., Lapidot, T., Soffer, D., Sobe, T., Avraham, K.B., Goncharov, T., Holtmann, H., Lonai, P., Wallach, D., 1998. Targeted Disruption of the Mouse Caspase 8 Gene Ablates Cell Death Induction by the TNF Receptors, Fas/Apo1, and DR3 and Is Lethal Prenatally. Immunity 9, 267–276. doi:10.1016/S1074-7613(00)80609-3

Vijay-Kumar, M., Wu, H., Jones, R., Grant, G., Babbin, B., King, T.P., Kelly, D., Gewirtz, A.T., Neish, A.S., 2006. Flagellin suppresses epithelial apoptosis and limits disease during enteric infection. Am. J. Pathol. 169, 1686–1700. doi:10.2353/ajpath.2006.060345

von Moltke, J., Trinidad, N.J., Moayeri, M., Kintzer, A.F., Wang, S.B., van Rooijen, N., Brown, C.R., Krantz, B.A., Leppla, S.H., Gronert, K., Vance, R.E., 2012. Rapid induction of inflammatory lipid mediators by the inflammasome in vivo. Nature 490, 107–11. doi:10.1038/nature11351

Walle, L. Vande, Van Opdenbosch, N., Jacques, P., Fossoul, A., Verheugen, E., Vogel, P., Beyaert, R., Elewaut, D., Kanneganti, T.-D., van Loo, G., Lamkanfi, M., 2014. Negative regulation of the NLRP3 inflammasome by A20 protects against arthritis. Nature 512, 69–73. doi:10.1038/nature13322

Wang, L., Yang, J.K., Kabaleeswaran, V., Rice, A.J., Cruz, A.C., Park, A.Y., Yin, Q., Damko, E., Jang, S.B., Raunser, S., Robinson, C. V, Siegel, R.M., Walz, T., Wu, H., 2010. The Fas-FADD death domain complex structure reveals the basis of DISC assembly and disease mutations. Nat. Struct. Mol. Biol. 17, 1324–1329. doi:10.1038/nsmb.1920

Wang, P., Arjona, A., Zhang, Y., Sultana, H., Dai, J., Yang, L., LeBlanc, P.M., Doiron, K., Saleh, M., Fikrig, E., 2010. Caspase-12 controls West Nile virus infection via the viral RNA receptor RIG-I. Nat. Immunol. 11, 912–9. doi:10.1038/ni.1933

Wang, S., Miura, M., Jung, Y., Zhu, H., Li, E., Yuan, J., 1998. Murine Caspase-11, an ICE-Interacting Protease, Is Essential for the Activation of ICE. Cell 92, 501–509. doi:10.1016/S0092-8674(00)80943-5

Wang, Y., Gao, W., Shi, X., Ding, J., Liu, W., He, H., Wang, K., Shao, F., 2017. Chemotherapy drugs induce pyroptosis through caspase-3 cleavage of a gasdermin. Nature 547, 99–103. doi:10.1038/nature22393

Warren, S.E., Armstrong, A., Hamilton, M.K., Mao, D.P., Leaf, I. a, Miao, E. a, Aderem, A., 2010. Cutting edge: Cytosolic bacterial DNA activates the inflammasome via Aim2. J. Immunol. 185, 818–821. doi:10.4049/jimmunol.1000724

Watanabe, T., Asano, N., Murray, P.J., Ozato, K., Tailor, P., Fuss, I.J., Kitani, A., Strober, W., 2008. Muramyl dipeptide activation of nucleotide- binding oligomerization domain 2 protects mice from experimental colitis. J. Clin. Invest. 118, 545–559. doi:10.1172/JCI33145.signaling

Watanabe, T., Kitani, A., Murray, P.J., Strober, W., 2004. NOD2 is a negative regulator of Toll-like receptor 2-mediated T helper type 1 responses. Nat. Immunol. 5, 800–808. doi:10.1038/ni1092

Watanabe, T., Kitani, A., Murray, P.J., Wakatsuki, Y., Fuss, I.J., Strober, W., 2006. Nucleotide Binding Oligomerization Domain 2 Deficiency Leads to Dysregulated TLR2 Signaling and Induction of Antigen-Specific Colitis. Immunity 25, 473–485. doi:10.1016/j.immuni.2006.06.018

Willingham, S.B., Allen, I.C., Bergstralh, D.T., Brickey, W.J., Huang, M.T.-H., Taxman, D.J., Duncan, J.A., Ting, J.P.-Y., 2009. NLRP3 (NALP3, Cryopyrin) Facilitates In Vivo Caspase-1 Activation, Necrosis, and HMGB1 Release via Inflammasome-Dependent and -Independent Pathways. J. Immunol. 183, 2008–2015. doi:10.4049/jimmunol.0900138

Wilson, K.P., Black, J.A., Thomson, J.A., Kim, E.E., Griffith, J.P., Navia, M.A., Murcko, M.A., Chambers, S.P., Aldape, R.A., Raybuck, S.A., et al., 1994. Structure and mechanism of interleukin-1 beta converting enzyme. Nature. doi:10.1038/370270a0

Wolf, A.J., Reyes, C.N., Liang, W., Becker, C., Shimada, K., Wheeler, M.L., Cho, H.C., Popescu, N.I., Coggeshall, K.M., Arditi, M., Underhill, D.M., 2016. Hexokinase Is an Innate Immune Receptor for the Detection of Bacterial Peptidoglycan. Cell 1–13. doi:10.1016/j.cell.2016.05.076

Wright, S., Ramos, R., Tobias, P., Ulevitch, R., Mathison, J., 1990. CD14, a receptor for complexes of lipopolysaccharide (LPS) and LPS binding protein. Science (80-.). 249, 1431–1433. doi:10.1126/science.1698311

Wu, J., Fernandes-Alnemri, T., Alnemri, E.S., 2010. Involvement of the AIM2, NLRC4, and NLRP3 inflammasomes in caspase-1 activation by Listeria monocytogenes. J. Clin. Immunol. 30, 693–702. doi:10.1007/s10875-010-9425-2

Wu, W., Hsu, Y.-M.S., Bi, L., Songyang, Z., Lin, X., 2009. CARD9 facilitates microbe-elicited production of reactive oxygen species by regulating the LyGDI-Rac1 complex. Nat. Immunol. 10, 1208–1214. doi:10.1038/ni.1788

Wynosky-Dolfi, M. a, Snyder, A.G., Philip, N.H., Doonan, P.J., Poffenberger, M.C., Avizonis, D., Zwack, E.E., Riblett, A.M., Hu, B., Strowig, T., Flavell, R. a, Jones, R.G., Freedman, B.D., Brodsky, I.E., 2014. Oxidative metabolism enables Salmonella evasion of the NLRP3 inflammasome. J. Exp. Med. 211, 653–668. doi:10.1084/jem.20130627

Xu, H., Yang, J., Gao, W., Li, L., Li, P., Zhang, L., Gong, Y.-N., Peng, X., Xi, J.J., Chen, S., Wang, F., Shao, F., 2014. Innate immune sensing of bacterial modifications of Rho GTPases by the Pyrin inflammasome. Nature 513, 237–241. doi:10.1038/nature13449

Yamamoto, M., Sato, S., Mori, K., Hoshino, K., Takeuchi, O., Takeda, K., Akira, S., 2002. Cutting edge: a novel Toll/IL-1 receptor domain-containing adapter that preferentially activates the IFN-beta promoter in the Toll-like receptor signaling. J. Immunol. 169, 6668–6672. doi:10.4049/jimmunol.169.12.6668

Yang, C., Kim, J., Kim, T.S., Lee, P.Y., Kim, S.Y., Lee, H., Shin, D., Nguyen, L.T., Lee, M., Jin, H.S., Kim, K., Lee, C., Kim, M.H., Park, S.G., Kim, J., Choi, H., Jo, E., 2015. Small heterodimer partner interacts with NLRP3 and negatively regulates activation of the NLRP3 inflammasome. Nat. Commun. 6, 1–11. doi:10.1038/ncomms7115

Yang, C.S., Rodgers, M., Min, C.K., Lee, J.S., Kingeter, L., Lee, J.Y., Jong, A., Kramnik, I., Lin, X., Jung, J.U., 2012. The autophagy regulator Rubicon is a feedback inhibitor of CARD9-mediated host innate immunity. Cell Host Microbe 11, 277–289. doi:10.1016/j.chom.2012.01.019

Yang, J., Zhao, Y., Shi, J., Shao, F., 2013. Human NAIP and mouse NAIP1 recognize bacterial type III secretion needle protein for inflammasome activation. Proc. Natl. Acad. Sci. U. S. A. 110, 1–6. doi:10.1073/pnas.1306376110/-/DCSupplemental.www.pnas.org/cgi/doi/10.1073/pnas.1306376110

Yoneyama, M., Kikuchi, M., Natsukawa, T., Shinobu, N., Imaizumi, T., Miyagishi, M., Taira, K., Akira, S., Fujita, T., 2004. The RNA helicase RIG-I has an essential function in double-stranded RNA-induced innate antiviral responses. Nat. Immunol. 5, 730–737. doi:10.1038/ni1087

Yoneyama, M., Onomoto, K., Jogi, M., Akaboshi, T., Fujita, T., 2015. Viral RNA detection by RIG-I-like receptors. Curr. Opin. Immunol. 32, 48–53. doi:10.1016/j.coi.2014.12.012

Yoneyama, M., Suhara, W., Fukuhara, Y., Fukuda, M., Nishida, E., Fujita, T., 1998. Direct triggering of the type I interferon system by virus infection : activation of a transcription factor complex containing IRF-3 and CBP / p300. EMBO J. 17, 1087–1095.

Yoshitomi, H., Sakaguchi, N., Kobayashi, K., Brown, G.D., Tagami, T., Sakihama, T., Hirota, K., Tanaka, S., Nomura, T., Miki, I., Gordon, S., Akira, S., Nakamura, T., Sakaguchi, S., 2005. A role for fungal β-glucans and their receptor Dectin-1 in the induction of autoimmune arthritis in genetically susceptible mice. J. Exp. Med. 201, 949–960. doi:10.1084/jem.20041758

Zaki, M.H., Man, S.M., Vogel, P., Lamkanfi, M., Kanneganti, T.-D., 2014. Salmonella exploits NLRP12-dependent innate immune signaling to suppress host defenses during infection. Proc. Natl. Acad. Sci. U. S. A. 111, 385–390. doi:10.1073/pnas.1317643111

Zhang, G., Zhou, B., Li, S., Yue, J., Yang, H., Wen, Y., Zhan, S., Wang, W., Liao, M., Zhang, M., Zeng, G., Feng, C.G., Sassetti, C.M., Chen, X., 2014. Allele-Specific Induction of IL-1β Expression by C/EBPβ and PU.1 Contributes to Increased Tuberculosis Susceptibility. PLoS Pathog. 10. doi:10.1371/journal.ppat.1004426

Zhang, J., Billingsley, M.L., Kincaid, R.L., Siraganian, R.P., 2000. Phosphorylation of Syk activation loop tyrosines is essential Syk function: An in vivo study using a specific anti-Syk activation loop phosphotyrosine antibody. J. Biol. Chem. 275, 35442–35447. doi:10.1074/jbc.M004549200

Zhang, L., Chen, S., Ruan, J., Wu, J., Δ, C.N.N., Tong, A.B., Yin, Q., Li, Y., David, L., Wang, W.L., Marks, C., Ouyang, Q., 2015. Cryo-EM structure of the activated NAIP2- NLRC4 inflammasome reveals nucleated polymerization 4, 12–14.

Zhang, L., Mo, J., Swanson, K. V, Wen, H., Petrucelli, A., Gregory, S.M., Zhang, Z., Schneider, M., Jiang, Y., Fitzgerald, K. a, Ouyang, S., Liu, Z.-J., Damania, B., Shu, H.-B., Duncan, J. a, Ting, J.P.-Y., 2014. NLRC3, a member of the NLR family of proteins, is a negative regulator of innate immune signaling induced by the DNA sensor STING. Immunity 40, 329–341. doi:10.1016/j.immuni.2014.01.010

Zhao, J., Jitkaew, S., Cai, Z., Choksi, S., Li, Q., Luo, J., Liu, Z.-G., 2012. Mixed lineage kinase domain-like is a key receptor interacting protein 3 downstream component of TNF-induced necrosis. Proc. Natl. Acad. Sci. U. S. A. 109, 5322–5327. doi:10.1073/pnas.1200012109

Zhao, Y., Shi, J., Shi, X., Wang, Y., Wang, F., Shao, F., 2016. Genetic functions of the NAIP family of inflammasome receptors for bacterial ligands in mice. J. Exp. Med. 213, 647–656. doi:10.1084/jem.20160006

Zhernakova, A., Festen, E.M., Franke, L., Trynka, G., Diemen, C.C. Van, Monsuur, A.J., Bevova, M., Nijmeijer, R.M., Slot, R. Van, Heijmans, R., Boezen, H.M., Heel, D.A. Van, Bodegraven, A.A. Van, Stokkers, P.C.F., Wijmenga, C., Crusius, J.B.A., Weersma, R.K., 2008. Genetic Analysis of Innate Immunity in Crohn ' s Disease and Ulcerative Colitis Identifies Two Susceptibility Loci Harboring CARD9 and IL18RAP. J. Hum. Genet. 1202–1210. doi:10.1016/j.ajhg.2008.03.016.

Zhong, Y., Kinio, A., Saleh, M., 2013. Functions of NOD-Like Receptors in Human Diseases. Front. Immunol. 4, 1–18. doi:10.3389/fimmu.2013.00333

Zhou, Y., Elleder, D., Diamond, T.L., Bonamy, G.M.C., Irelan, J.T., Chiang, C., Tu, B.P., Jesus, P.D. De, Lilley, C.E., Seidel, S., Opaluch, A.M., Caldwell, J.S., Weitzman, M.D., Kuhen, K.L., Bandyopadhyay, S., Ideker, T., Orth, A.P., Miraglia, L.J., Bushman, F.D., Young, J.A., Chanda, S.K., 2008. Global Analysis of Host-Pathogen Interactions that Regulate Early-Stage HIV-1 Replication. Cell 135, 49–60. doi:10.1016/j.cell.2008.07.032

Zhu, S., Ding, S., Wang, P., Wei, Z., Pan, W., Palm, N.W., Yang, Y., Yu, H., Li, H.-B., Wang, G., Lei, X., de Zoete, M.R., Zhao, J., Zheng, Y., Chen, H., Zhao, Y., Jurado, K.A., Feng, N., Shan, L., Kluger, Y., Lu, J., Abraham, C., Fikrig, E., Greenberg, H.B., Flavell, R.A., 2017. Nlrp9b inflammasome restricts rotavirus infection in intestinal epithelial cells. Nature 546, 667–670. doi:10.1038/nature22967

Zou, H., Li, Y., Liu, X., Wang, X., 1999. An APAf-1 · cytochrome C multimeric complex is a functional apoptosome that activates procaspase-9. J. Biol. Chem. 274, 11549–11556. doi:10.1074/jbc.274.17.11549

Appendices

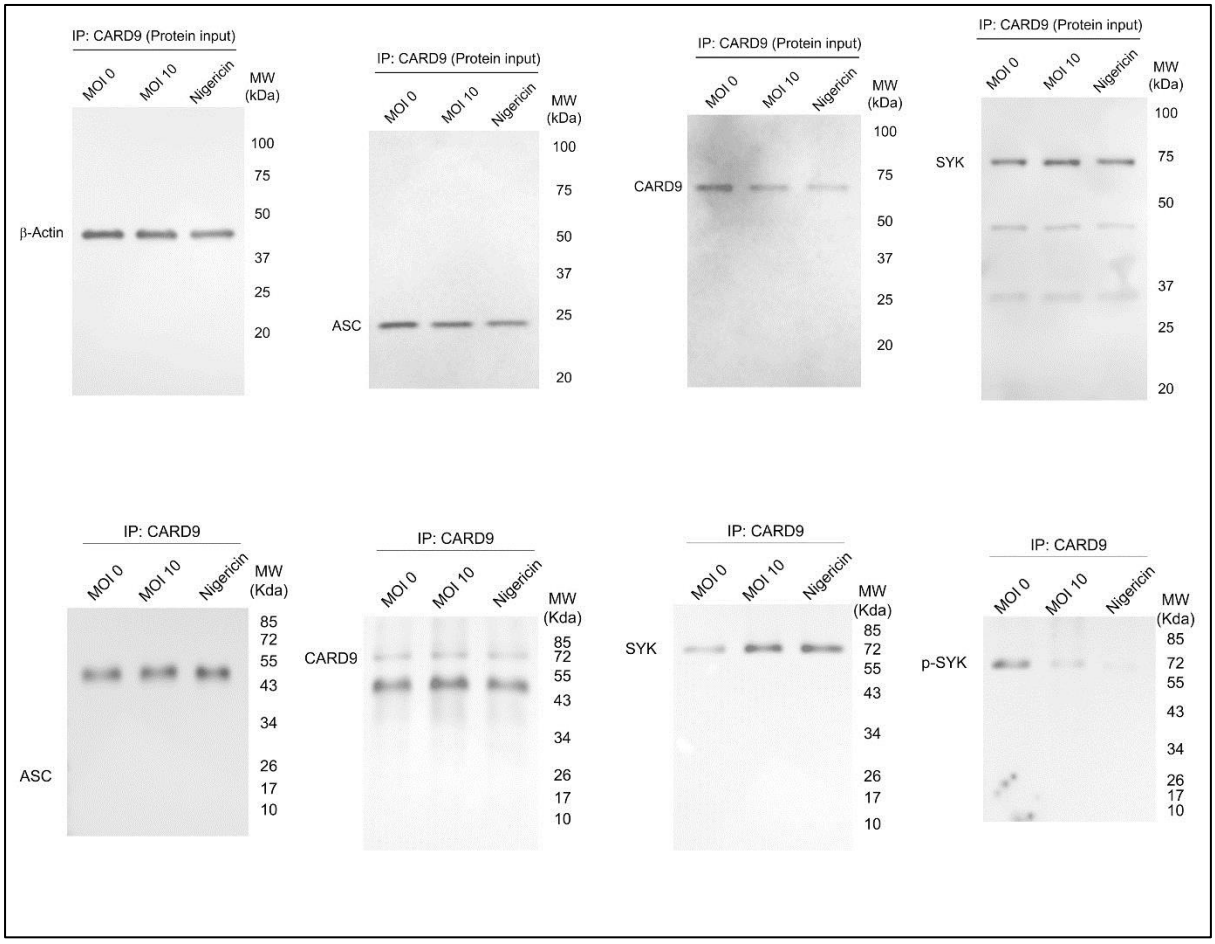

Appendix 1: Uncropped immunoblots presented in Figure 4.17, CARD9 co-immunoprecipitations. Membranes were probed using the indicated antibodies (β-Actin, ASC, CARD9, SYK and p-SYK).

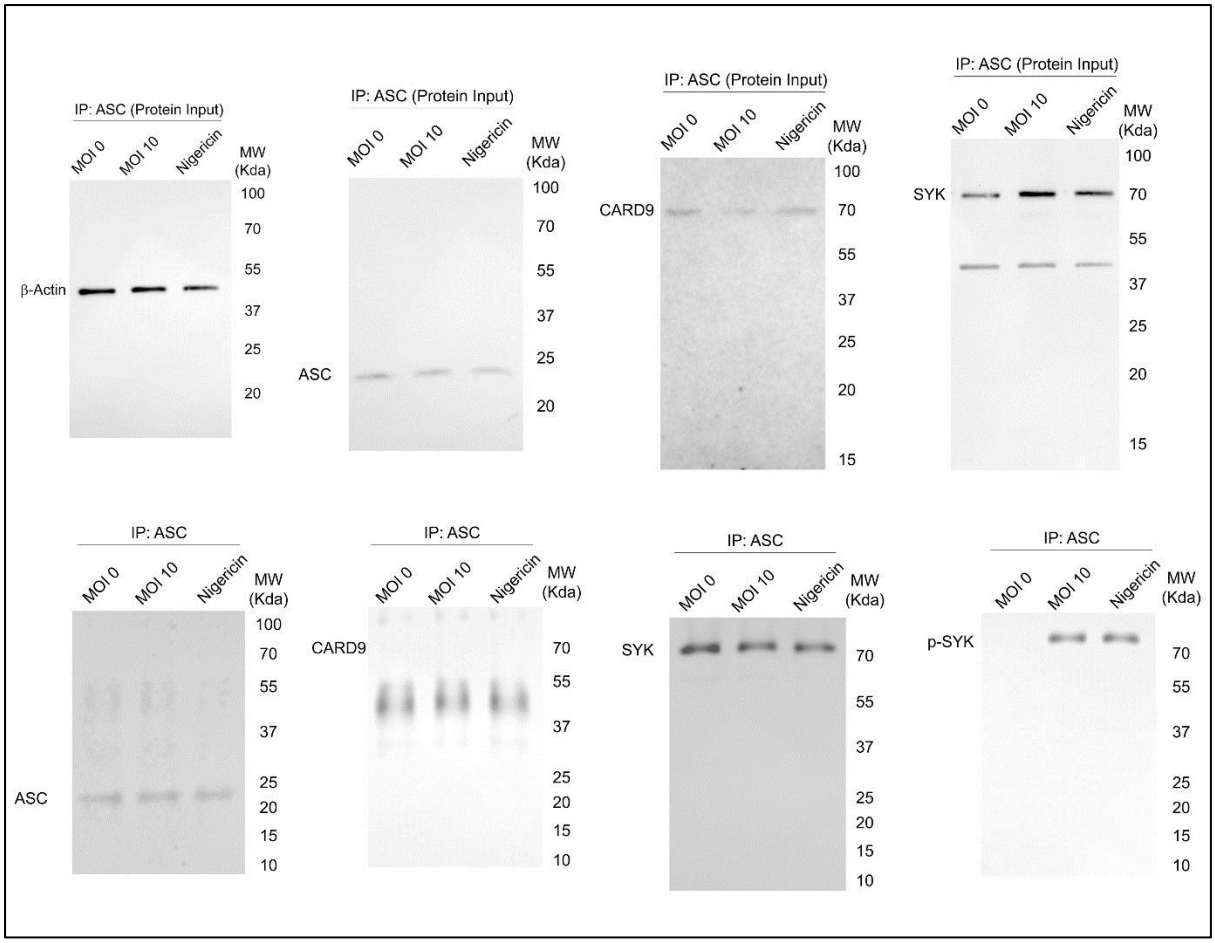

Appendix 2: Uncropped immunoblots presented in Figure 4.17, ASC co-immunoprecipitations. Membranes were probed using the indicated antibodies (β-Actin, ASC, CARD9, SYK and p-SYK).

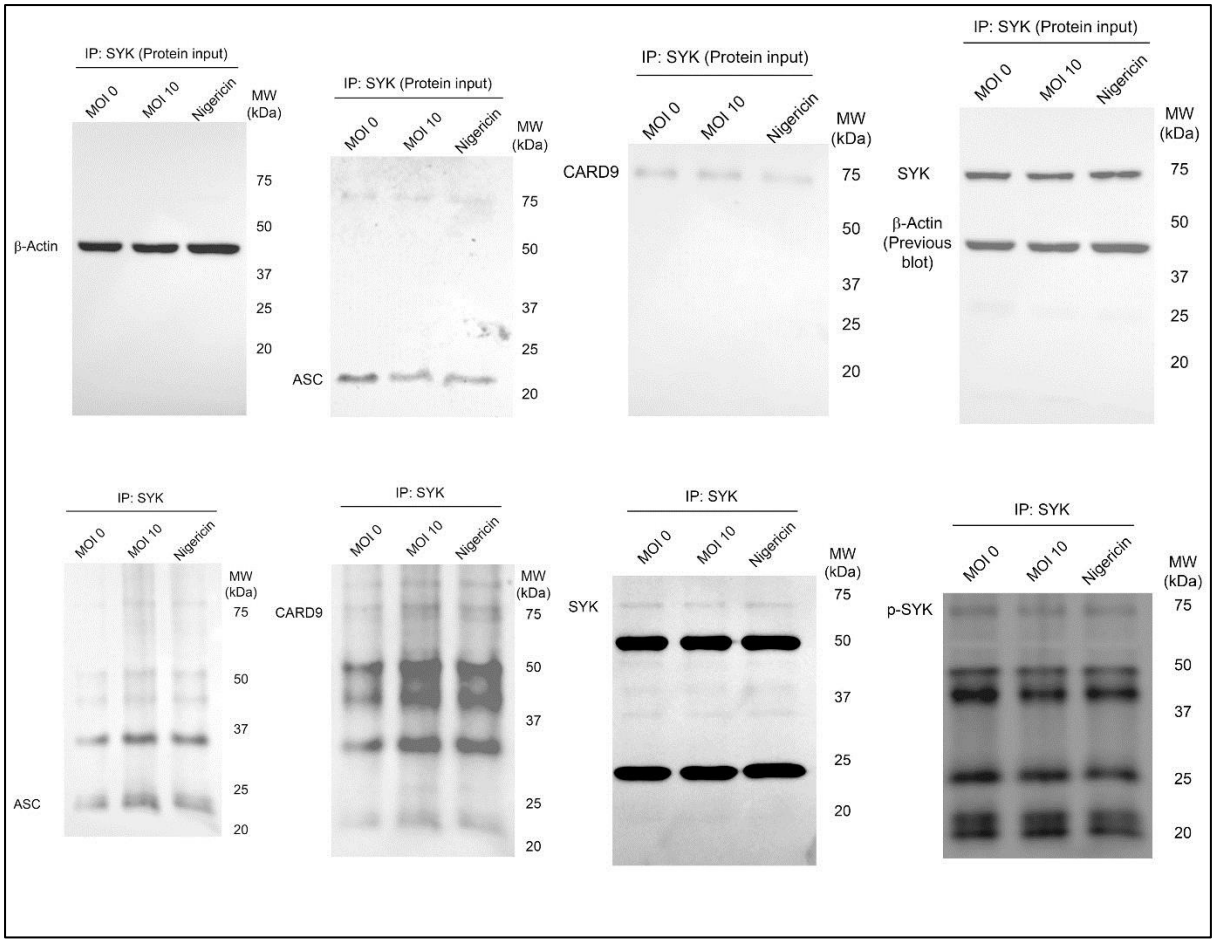

Appendix 3: Uncropped immunoblots presented in Figure 4.17, SYK co-immunoprecipitations. Membranes were probed using the indicated antibodies (β-Actin, ASC, CARD9, SYK and p-SYK).

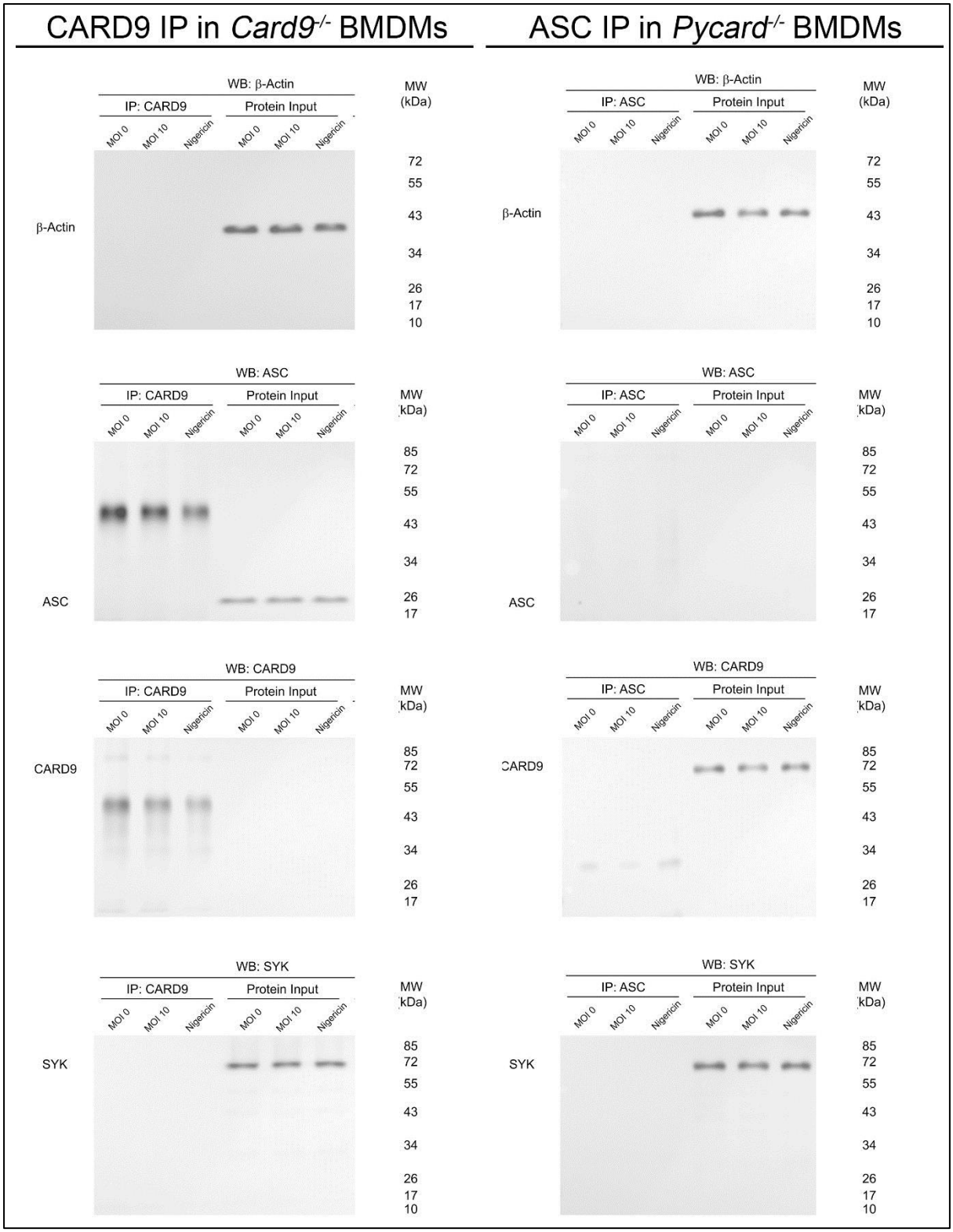

Appendix 4: Uncropped immunoblots presented in Figure 4.18, immunoprecipitations knockout controls. Membranes were probed using the indicated antibodies (ASC, β-Actin, CARD9 and SYK).

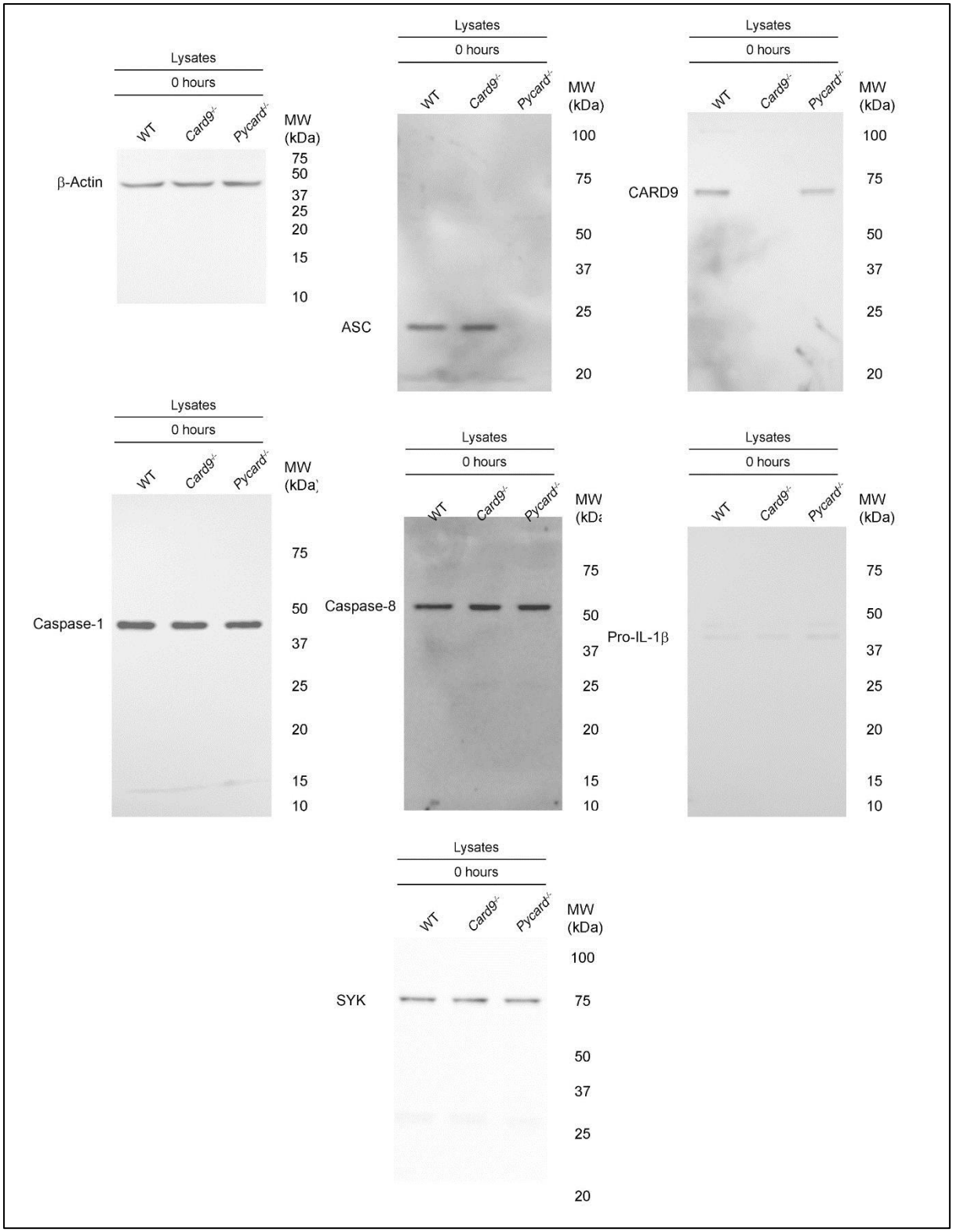

Appendix 5: Uncropped immunoblots presented in Figure 4.20, uninfected cell lysates. Membranes were probed using the indicated antibodies (ASC, β-Actin, CARD9, Caspase-1, Caspase-8, Pro-IL-1β and SYK).

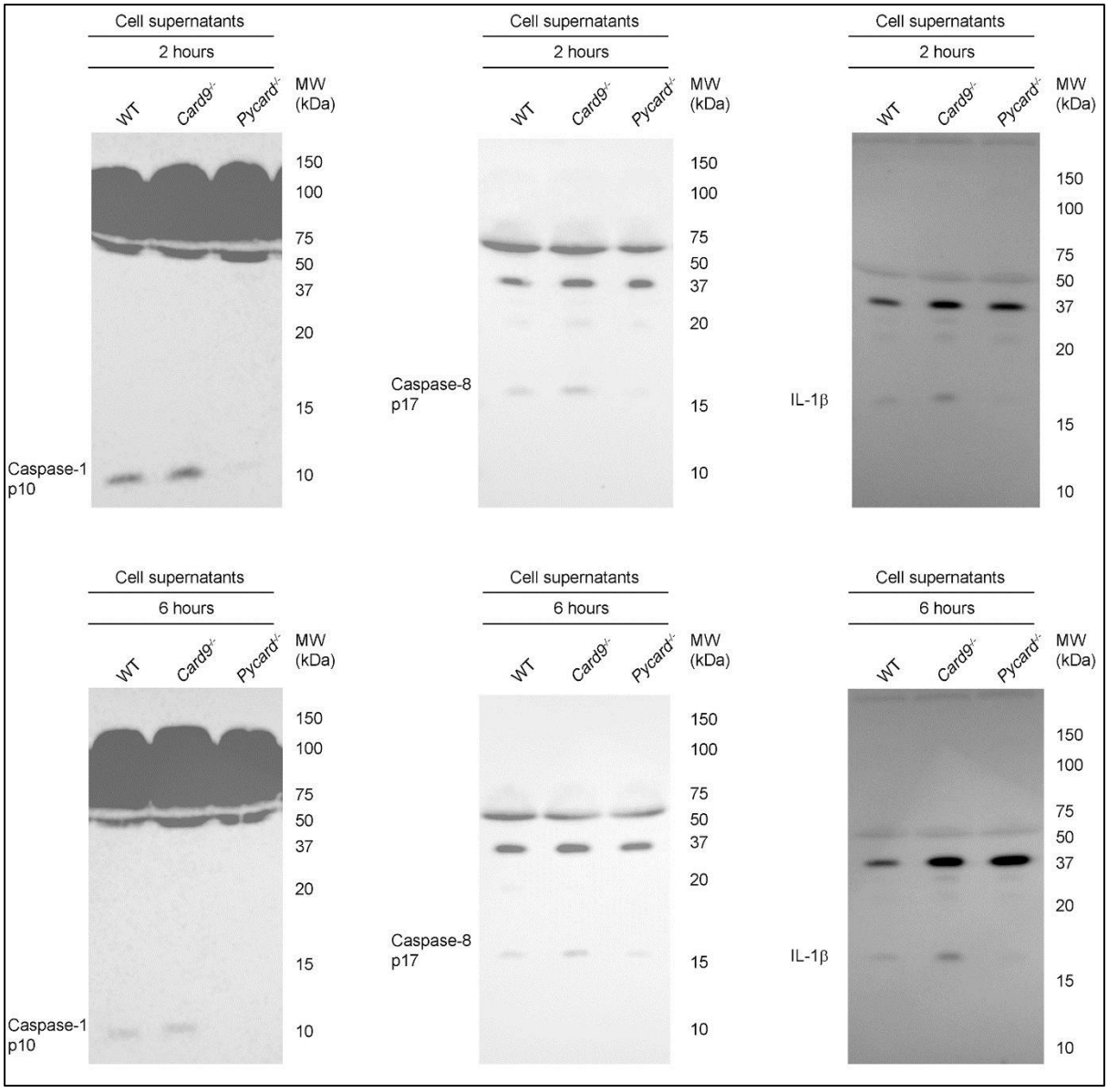

Appendix 6: Uncropped immunoblots presented in Figure 4.21, cell culture supernatants after 2 and 6 hours of *S.* Typhimurium infection. Membranes were probed using the indicated antibodies (ASC, β-Actin, CARD9, Caspase-1, Caspase-8, Pro-IL-1β and SYK).

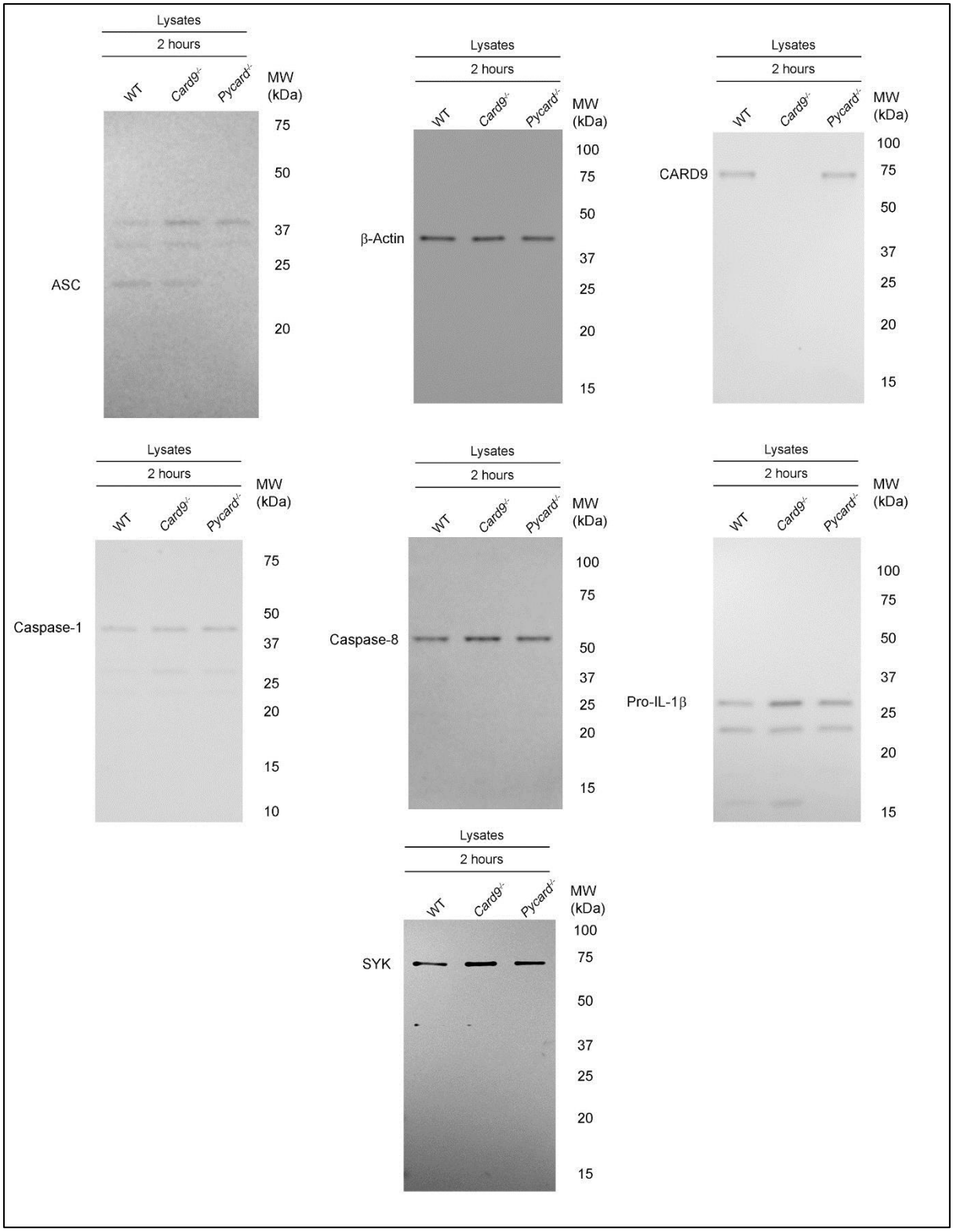

Appendix 7: Uncropped immunoblots presented in Figure 4.21, cell lysates after 2 hours of *S.* Typhimurium infection. Membranes were probed using the indicated antibodies (ASC, β-Actin, CARD9, Caspase-1, Caspase-8, Pro-IL-1β and SYK).

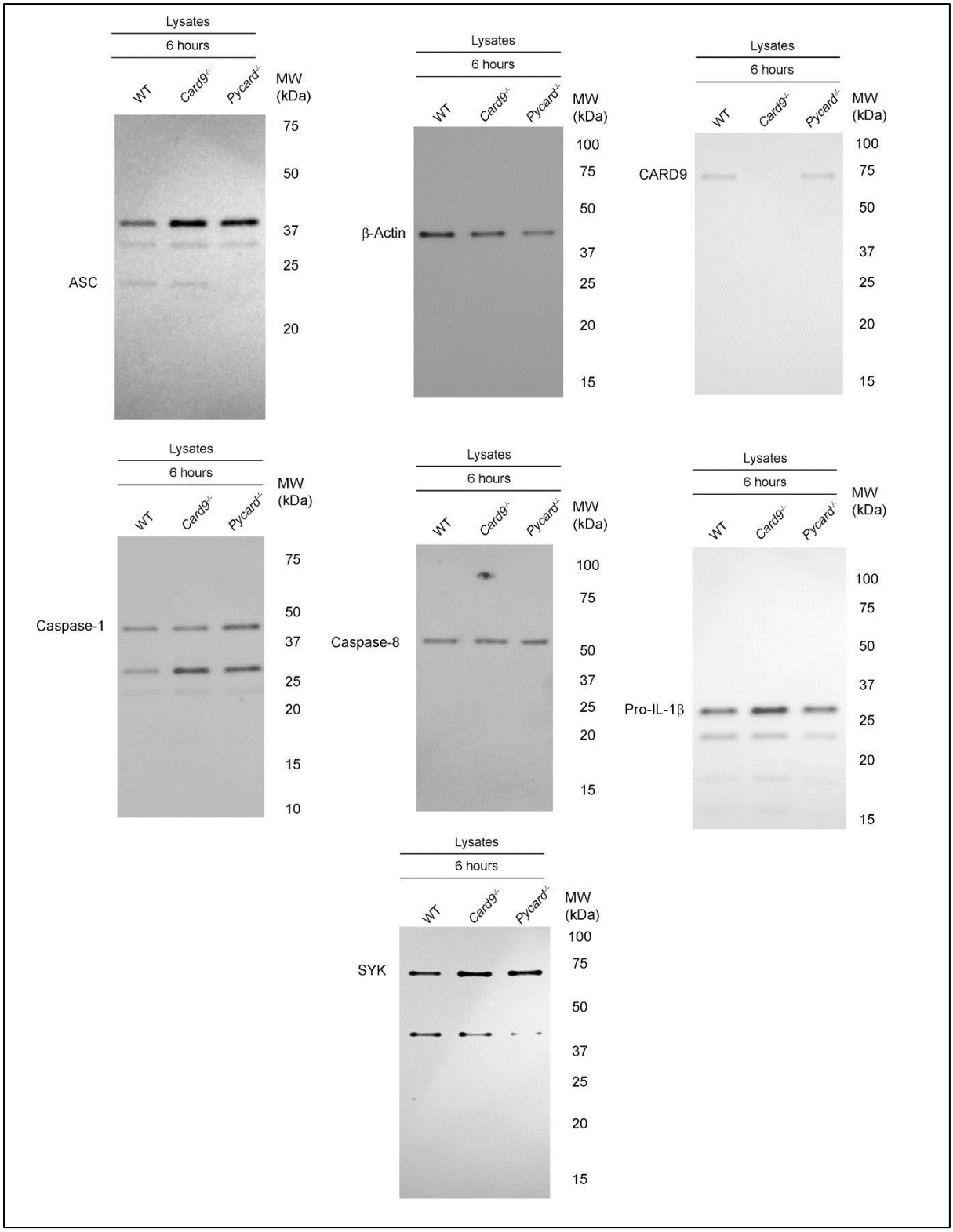

Appendix 8: Uncropped immunoblots presented in Figure 4.21, cell lysates after 6 hours of *S.* Typhimurium infection. Membranes were probed using the indicated antibodies (ASC, β-Actin, CARD9, Caspase-1, Caspase-8, Pro-IL-1β and SYK).

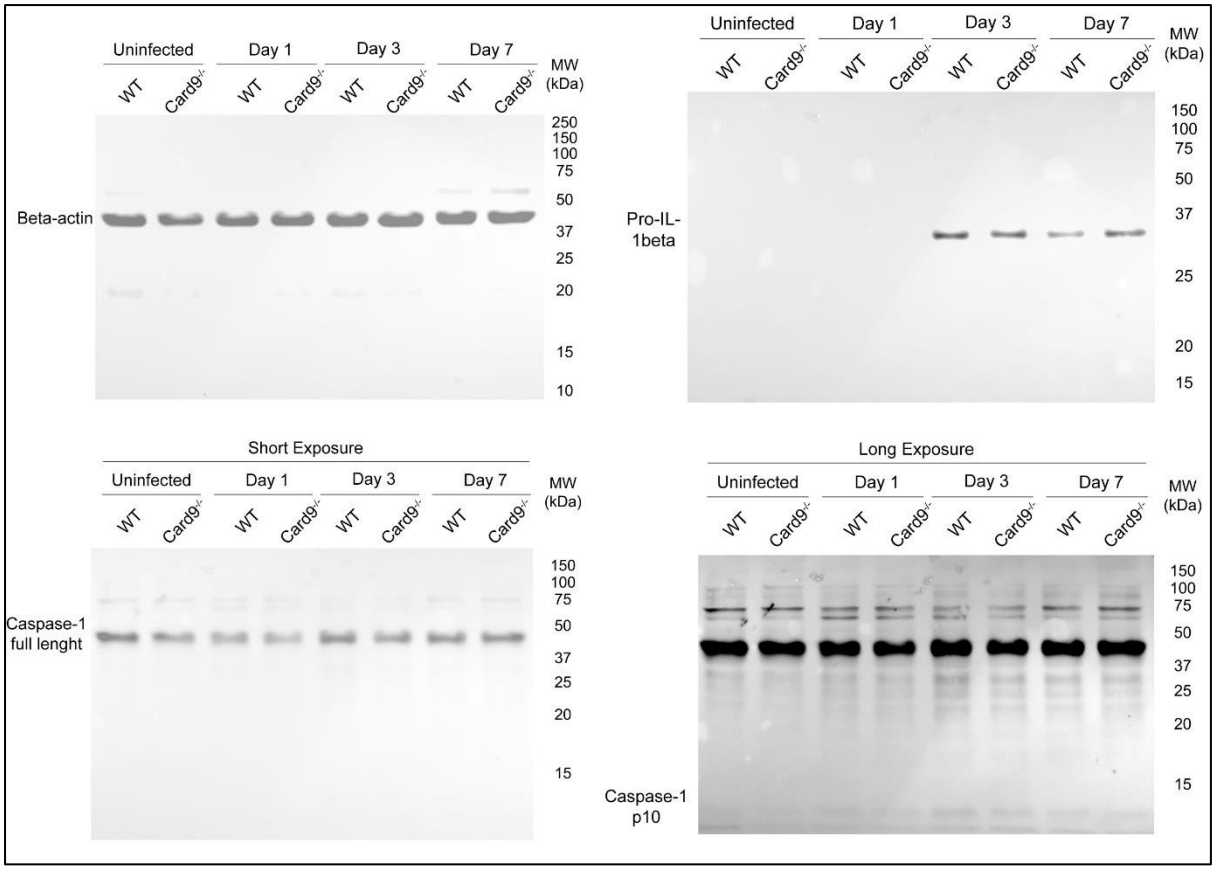

Appendix 9: Uncropped immunoblots presented in Figure 4.23, Pro-IL-1β production in spleen cells derived from *S.* Typhimurium-infected mice. Membranes were probed using the indicated antibodies (β-Actin, Pro-IL-1β and Caspase-1).

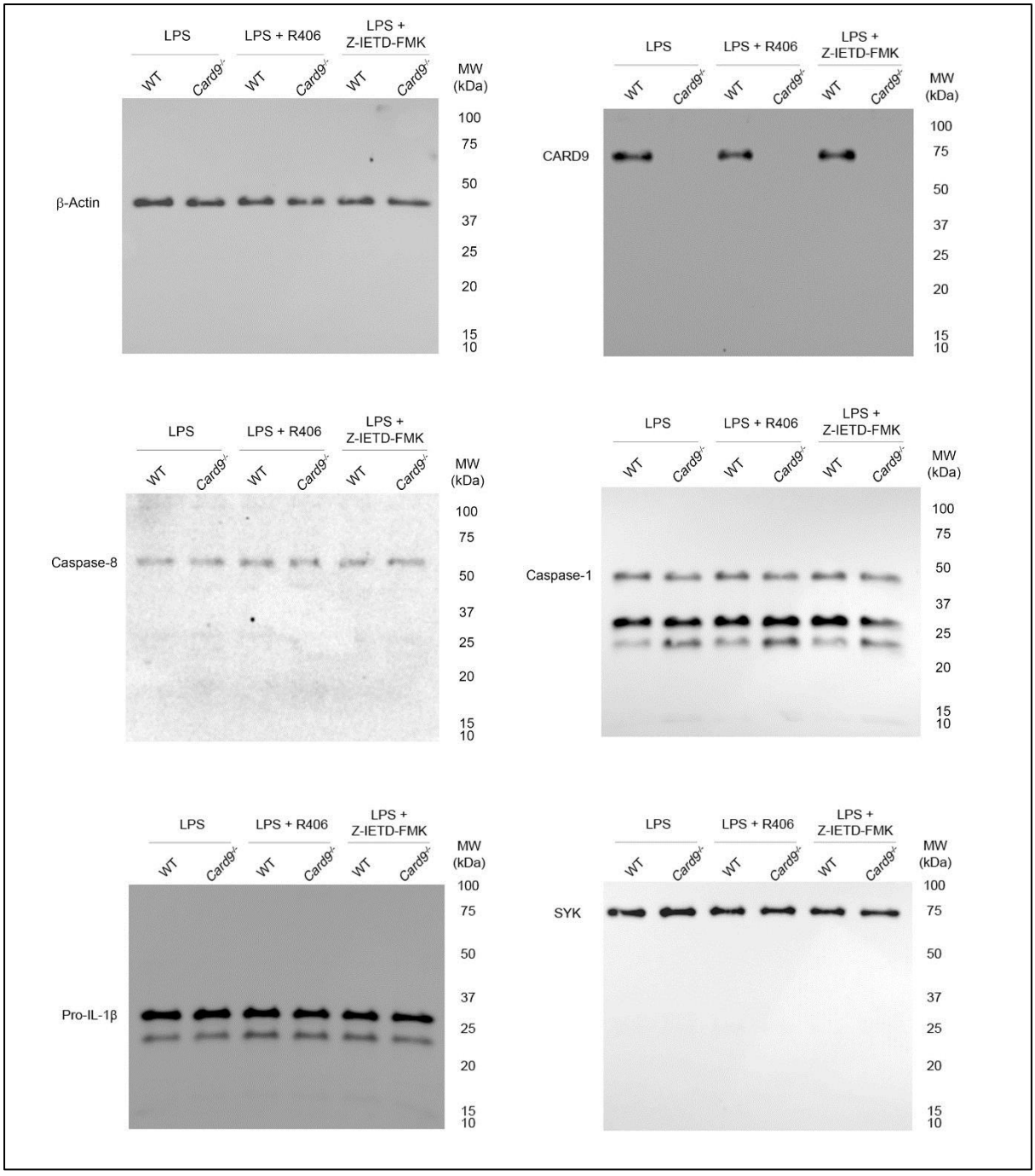

Appendix 10: Uncropped immunoblots presented in Figure 5.2. Membranes were probed using the indicated antibodies (β-Actin, CARD9, Caspase-1, Caspase-8, Pro-IL-1β and SYK).

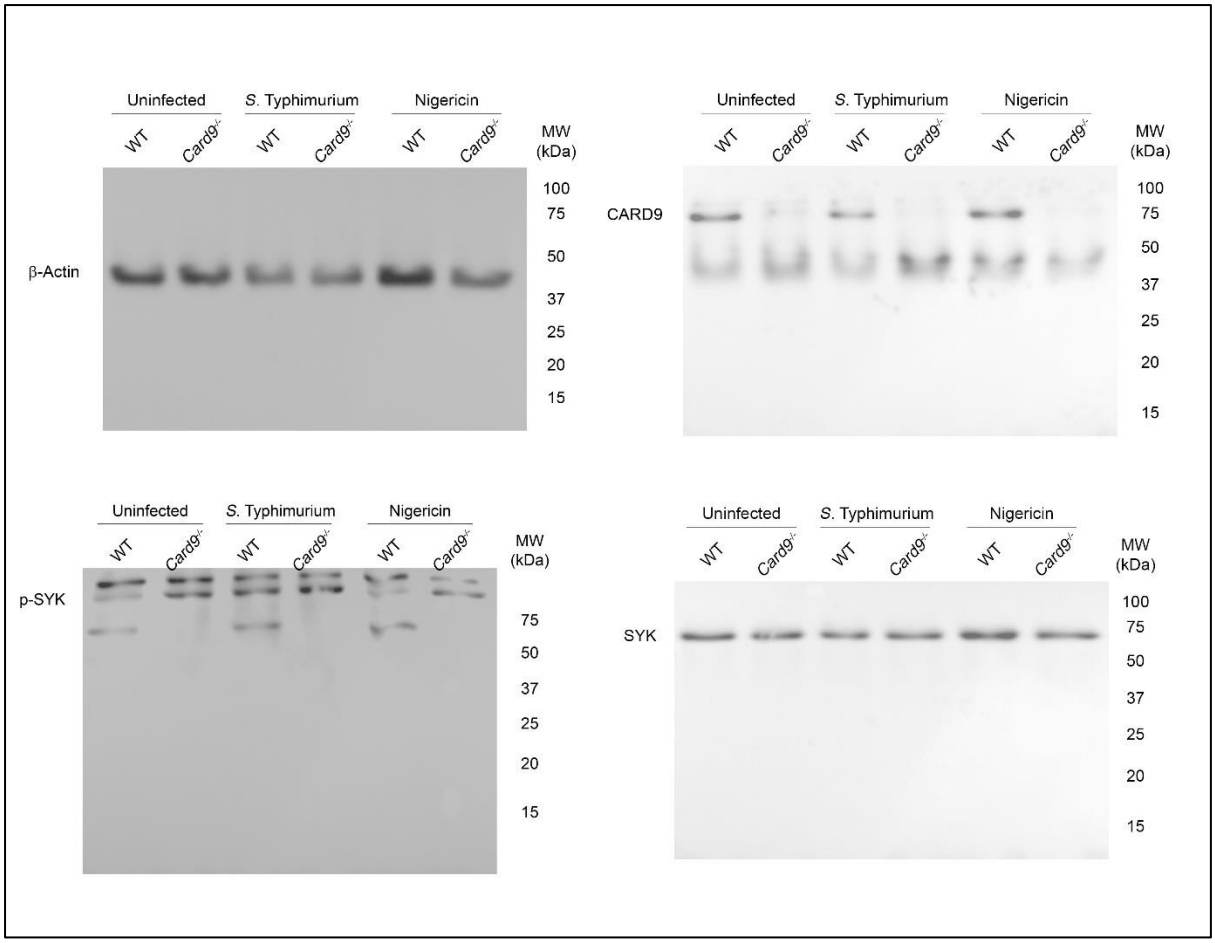

Appendix 11: Uncropped immunoblots presented in Figure 5.5. Membranes were probed using the indicated antibodies (b-Actin, CARD9, SYK and p-SYK).

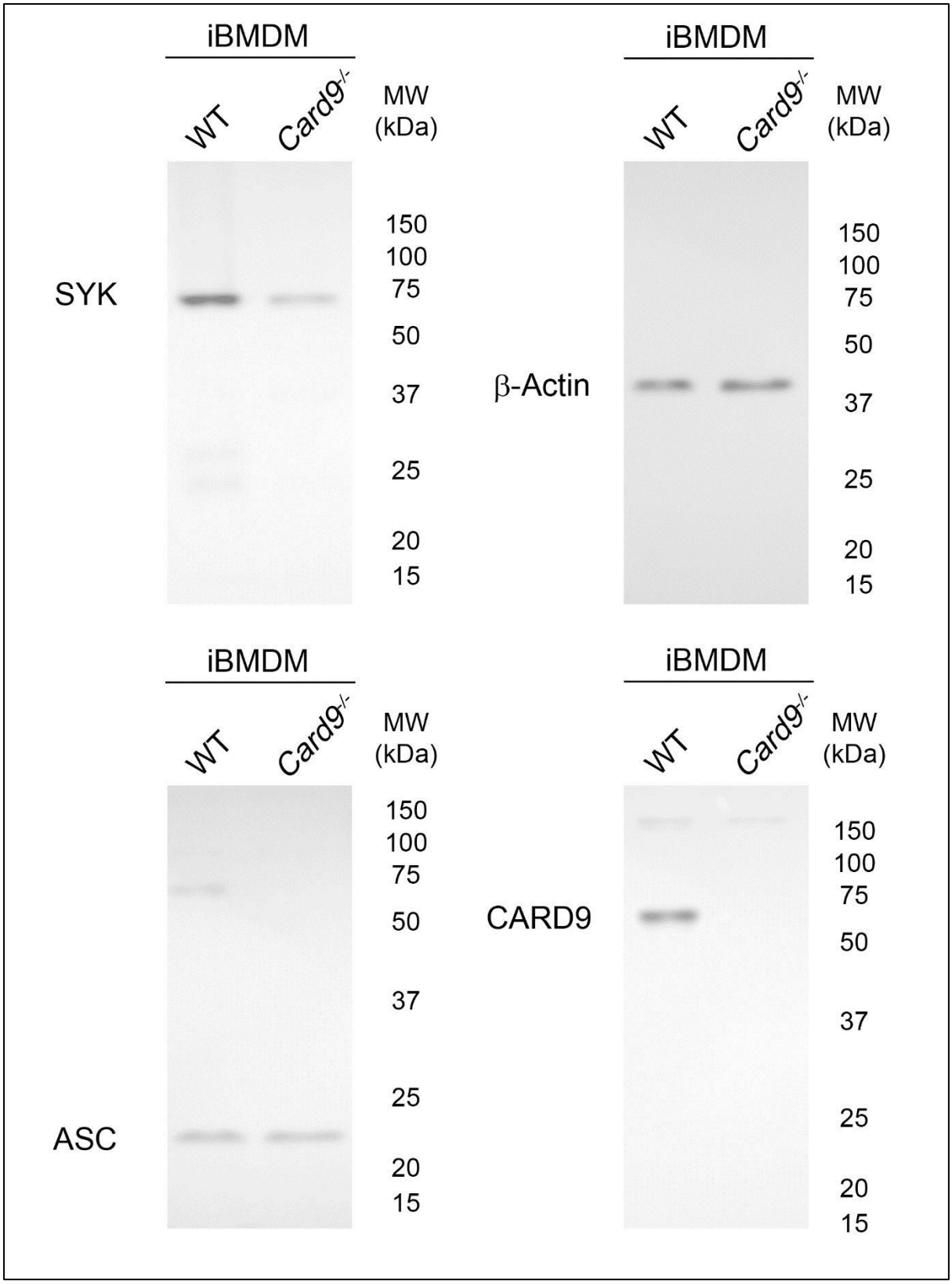

Appendix 12: Uncropped immunoblots presented in Figure 5.8. Membranes were probed using the indicated antibodies (b-Actin, CARD9, SYK and p-SYK).

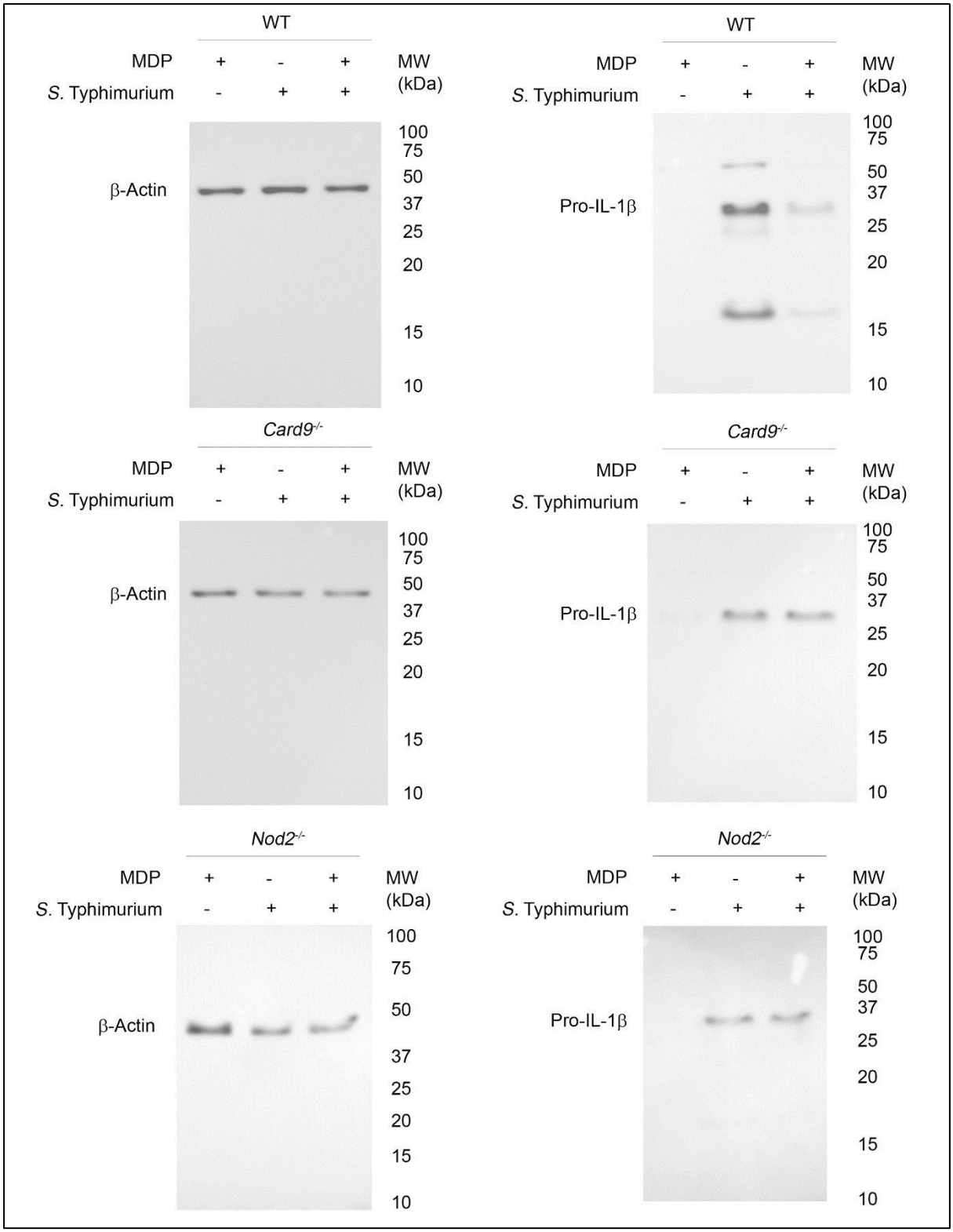

Appendix 13: Uncropped immunoblots presented in Figure 5.15. Membranes were probed using the indicated antibodies (β-Actin and Pro-IL-1β).

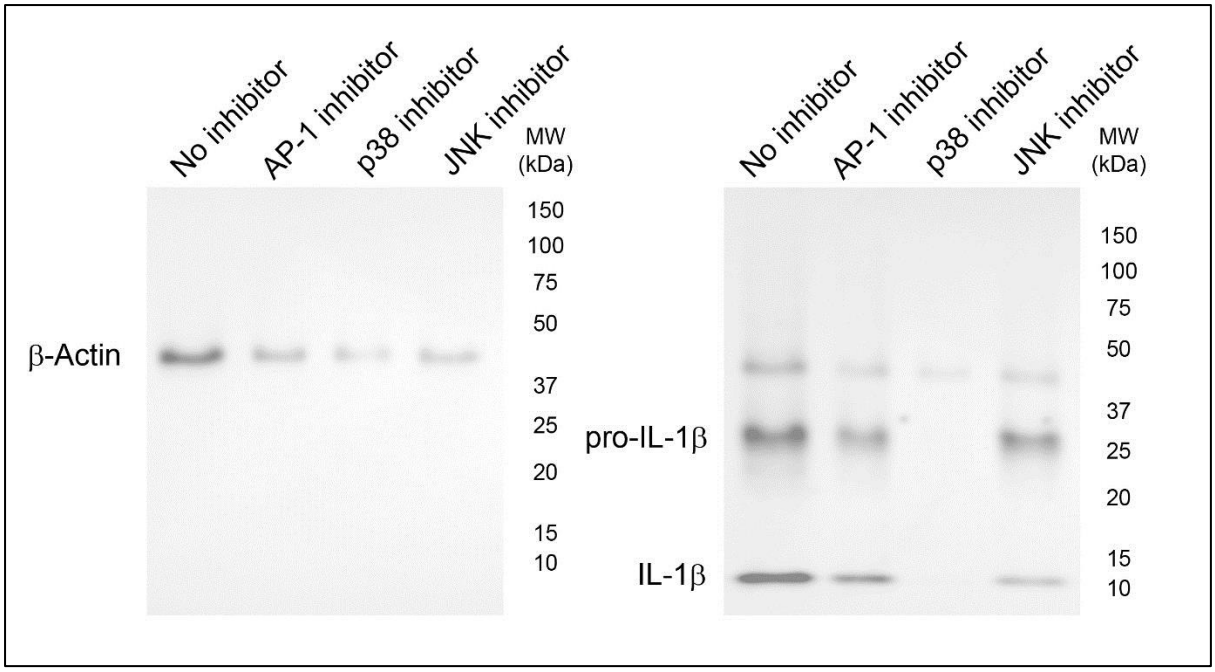

Appendix 14: Uncropped immunoblots presented in Figure 5.16. Membranes were probed using the indicated antibodies (β-Actin and Pro-IL-1β).

Fig. 5.17

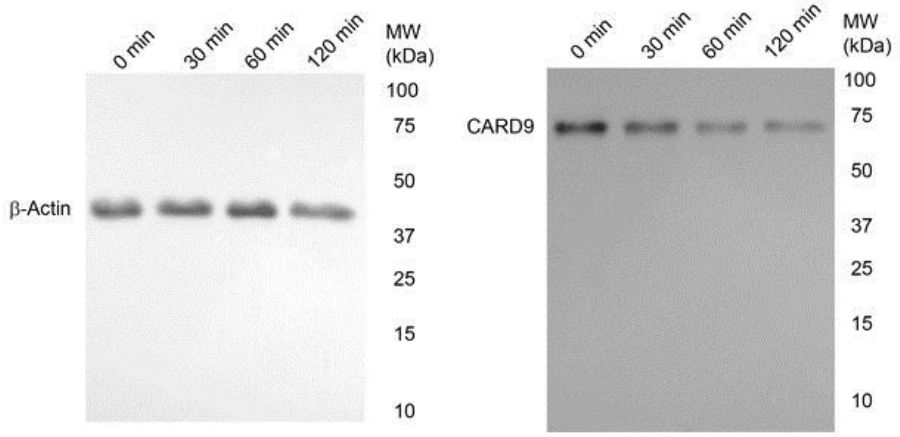

Fig. 5.18-a

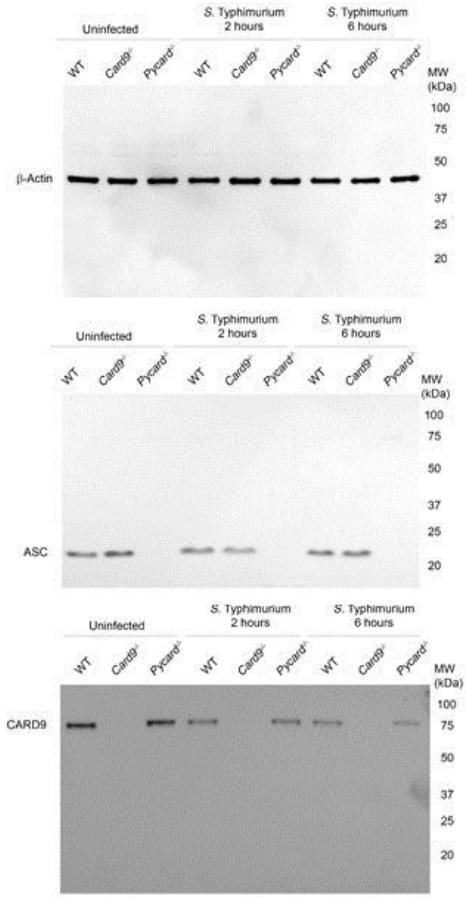

Fig. 5.18-b

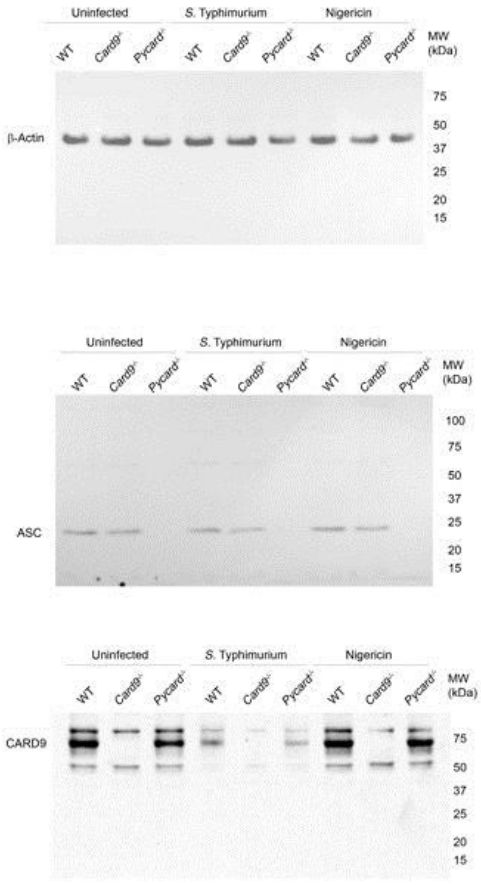

Appendix 15: Uncropped immunoblots presented in Figure 5.17 and 5.18. Membranes were probed using the indicated antibodies (β-Actin, ASC and CARD9).

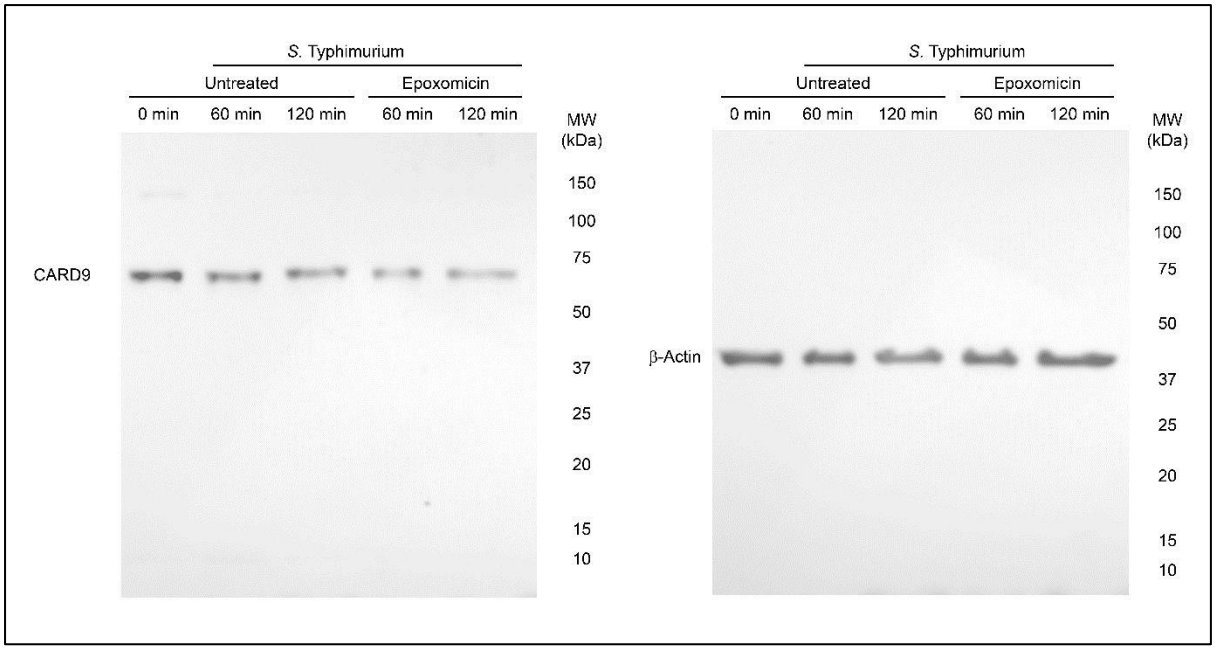

Appendix 16: Uncropped immunoblots presented in Figure 5.19. Membranes were probed using the indicated antibodies (β-Actin and CARD9).

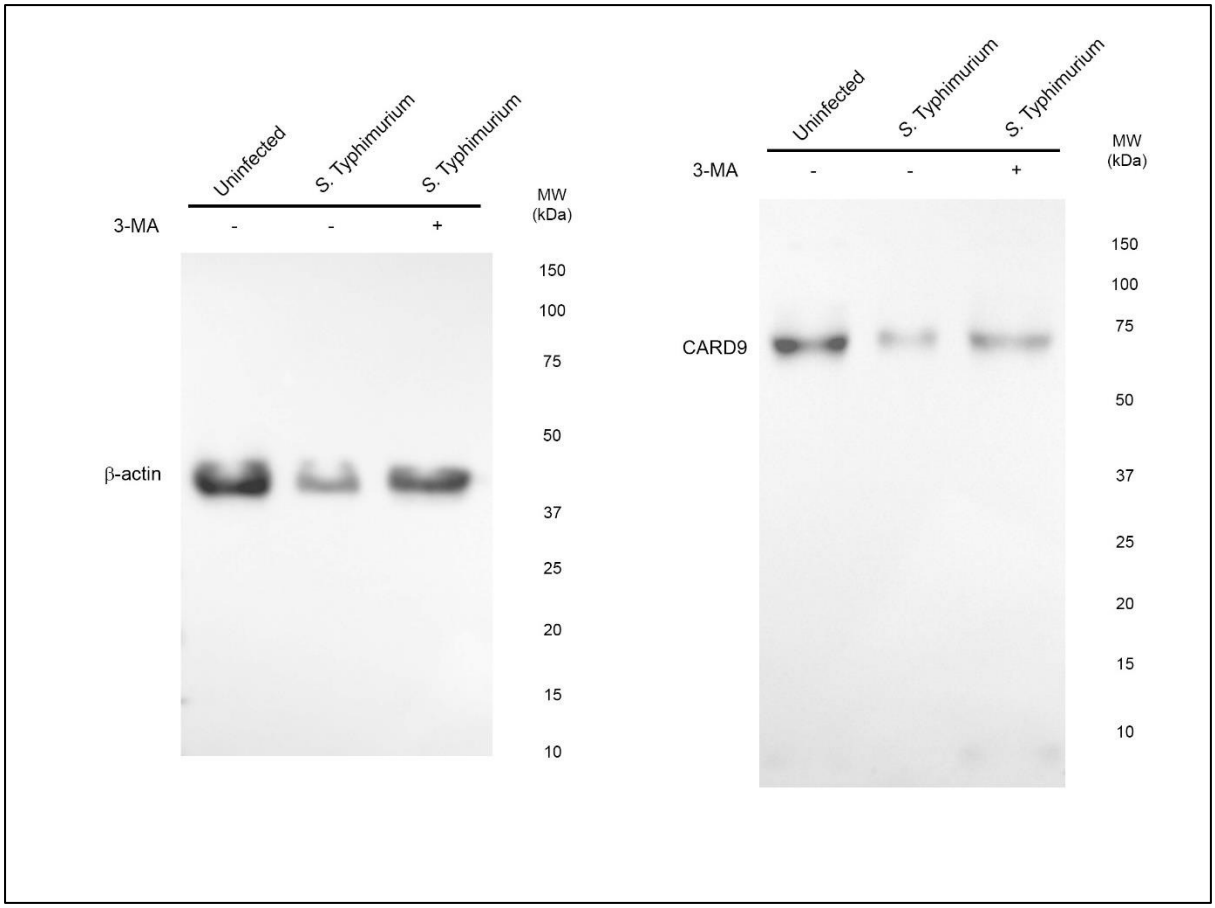

Appendix 17: Uncropped immunoblots presented in Figure 5.20. Membranes were probed using the indicated antibodies (β-Actin and CARD9).

Appendix 18: Published article - Pereira, M., Tourlomousis, P., Wright, J., P. Monie, T., Bryant, C.E., 2016. "CARD9 negatively regulates NLRP3-induced IL-1β production on Salmonella infection of macrophages." Nature Communications. 7, 12874. doi:10.1038/ncomms12874

CARD9 negatively regulates NLRP3-induced IL-1β production upon *Salmonella* infection of macrophages

Milton Pereira[1], Panagiotis Tourlomousis[1], John Wright[1], Tom Monie[2*] and Clare E. Bryant[1*]

[1]Department of Veterinary Medicine, University of Cambridge, Madingley Road, Cambridge CB3 0ES, UK

[2]Medical Research Council Human Nutrition Research, Elsie Widdowson Laboratory, 120 Fulbourn Road, Cambridge, CB1 9NL

*authors for correspondence: ceb27@cam.ac.uk and thomas.monie@mrc-hnr.cam.ac.uk

ABSTRACT

Interleukin 1β (IL-1β) is a proinflammatory cytokine required for host control of bacterial infections, and its production must be tightly regulated to prevent excessive inflammation. Here we show that caspase recruitment domain-containing protein 9 (CARD9), a protein associated with induction of proinflammatory cytokines by fungi, has a negative role on IL-1β production during bacterial infection. Specifically, in response to activation of the nucleotide oligomerization domain receptor pyrin-domain containing protein 3 (NLRP3) by *Salmonella* infection, CARD9 negatively regulates IL-1β by fine-tuning pro-IL-1β expression, spleen tyrosine kinase (SYK)-mediated NLRP3 activation and repressing inflammasome-associated caspase-8 activity. CARD9 is suppressed during *Salmonella enterica* serovar Typhimurium infection, facilitating increased IL-1β production. CARD9 is, therefore, a central signalling hub that coordinates a pathogen-specific host inflammatory response.

INTRODUCTION

Interleukin 1β (IL-1β) is a cytokine of critical importance in inflammatory, infectious and autoimmune diseases. Its powerful proinflammatory effects mean that production of this cytokine must be tightly regulated to prevent excessive inflammation. Pro-IL-1β is cleaved to bioactive IL-1β by several enzymatic complexes, the most important of which are the inflammasomes. Inflammasomes assemble in the cytoplasm of cells and utilize caspases, such as caspase-1 and caspase-8, for cytokine processing[1]. Canonical inflammasomes comprise a nucleotide oligomerisation domain receptor (NLR), an adaptor protein (ASC; apoptosis-associated speck-like protein containing a CARD (caspase recruitment domain)) and effector caspases. Non-canonical inflammasomes are formed in response to activation of other pattern recognition receptors (PRRs), such as the complex formed by dectin-1, spleen tyrosine kinase (SYK) and caspase-8 in response to fungal infection[2,3,4].

Formation of the macromolecular inflammasome structure requires protein-protein interactions, often between CARD domain containing proteins, for example between ASC and caspase-1, NLR family CARD domain-containing protein 4 (NLRC4) and ASC or NLRC4 and caspase-1. Canonical inflammasomes can recruit multiple NLRs and caspases to the same inflammasome complex to tailor a pathogen-specific inflammatory response[5]. This recruitment occurs through multiple domain specific protein interactions, including those mediated by CARDs. Identifying the final composition

of inflammasomes formed in response to specific pathogens or cellular insults, and how this affects inflammasome activity, is likely to be of major clinical importance in infectious and inflammatory disease research.

CARD9 is a CARD-containing adaptor protein with roles in activating innate immune signalling, particularly in response to fungal[6] and viral infections[7,8]. CARD9 regulates dectin-1 stimulation of NF-κB activation[9], reactive oxygen species production[10] and non-canonical inflammasome assembly[3,4], as well as activation of p38 and Jnk during nucleotide-binding oligomerization domain-containing protein 2 (NOD2) signalling[11]. Mutations in CARD9 are associated with chronic inflammatory diseases in humans, including those associated with bacterial rather than fungal infection, such as Crohn's disease and colitis[12–16]. Little is known about whether CARD9 is important in regulating the host response to bacterial infection. CARD9 up-regulates IL-1β production in fungal infections, but whether there is a direct link between this protein and canonical inflammasome activity is unclear.

Infection with *Salmonella enterica* serovar Typhimurium (*S*. Typhimurium) triggers the formation of a complex inflammasome that can include NLRC4, NLR family PYRIN domain-containing protein 3 (NLRP3), ASC, caspase-1 and caspase-8[5,17–19] . Caspase-1 drives IL-18 and IL-1β maturation and gasdermin D processing, which leads to pyroptosis[20,21]. Caspase-8 is important for IL-1β maturation but has no clear role in pyroptosis[17]. The complex composition of the *Salmonella*-induced inflammasome led us to speculate whether other CARD domain containing proteins, such as CARD9, may regulate its activity. CARD9 regulates SYK activity and this kinase phosphorylates the CARD domain of ASC when NLRP3, but not NLRC4, is activated to increase IL-1β and IL-18 production[22–25]. We investigated whether CARD9 could regulate canonical inflammasome activation in response to *S.* Typhimurium infection. Surprisingly, we show that in response to *Salmonella* infection CARD9 negatively regulates NLRP3-induced IL-1β production, but not pyroptosis, in murine bone marrow derived macrophages (BMDM) by two distinct mechanisms: i) by fine-tuning pro-IL-1β expression; and ii) by reducing NLRP3 activation through modulation of SYK and caspase-8 activity. Importantly, we show that CARD9 can negatively regulate canonical NLRP3 inflammasome activity and NOD2-mediated pro-IL-1β synthesis. Our data identify a negative regulatory role for CARD9 on IL-1β production in bacterial infection that contrasts its role in fungal infections in which it drives proinflammatory responses. We propose that CARD9 is a central signalling hub that can negatively or positively regulate proinflammatory signalling to coordinate a pathogen-specific host inflammatory response to infection.

RESULTS

CARD9 negatively regulates IL-1β production from inflammasomes

To evaluate whether CARD9 plays a role in inflammasome activity, we infected BMDMs from wild type, *Card9*$^{-/-}$ and *Nlrc4*$^{-/-}$ C57BL/6 mice with *S*. Typhimurium SL1344. As expected[26], *Nlrc4*$^{-/-}$ BMDMs had reduced IL-1β processing and induction of cell death at all multiplicities of infection (MOI) at early time points, consistent with impaired inflammasome assembly (**Fig. 1a,b,d,e,g,h**). *Card9*$^{-/-}$ BMDMs, however, showed a slight reduction in *S*. Typhimurium-induced cell death. Decreased pyroptosis is usually coupled to reduced IL-1β secretion[1], but here we observed the opposite effect in *Card9*$^{-/-}$ BMDMs. At all time points and MOIs studied, there was an increase in IL-1β in the supernatant from *Card9*$^{-/-}$ BMDMs of up to four times that seen from wild-type (WT) cells (**Fig. 1a,d,g**). The increased cytokine production could not be explained by increased intracellular bacterial load, as both WT and *Card9*$^{-/-}$ BMDMs had comparable intracellular counts (**Supplementary Fig. 1a-c**). We measured TNF-α production from the same cell supernatant and showed that although there is an increase in the production of this cytokine the amount produced is proportional to the increase in cell viability whereas the production of IL-1β is disproportionally enhanced from the infected *Card9*$^{-/-}$ cells. (**Fig. 1c,f,i**). BMDM infection with *Escherichia* coli also showed increased IL-1β production in *Card9*$^{-/-}$ in comparison to WT macrophages without affecting pyroptosis, intracellular bacteria counts and TNF-α production (**Fig. 1j-o, Supplementary Fig. 1d-e**). It is possible that the effects of CARD9 on *Salmonella*-induced inflammasome activity may be indirect, for example by regulating the autocrine production of cytokines such as IL-10 which is reduced in CARD9 deficient neutrophils infected with *Mycobacterium tuberculosis*[27]. An IL-10-mediated effect of CARD9 on *Salmonella*-induced IL-1β production from macrophages is unlikely, however, as elevated IL-1β production occurs within 2 hours of infection, whereas IL-10 production occurs later in infection[28].The increased IL-1β production *in vitro* is also seen in the production of this cytokine from a sub-lethal *in vivo* model of systemic infection with *S.* Typhimurium. WT and *Card9*$^{-/-}$ mice infected with *S*. Typhimurium (strain M525P) had similar bacterial burdens in the spleen at days 1, 3 and 7 post-infection (**Supplementary Fig. 1f-g**). Immunoblotting of cell lysates from isolated spleen cells revealed an upregulation of pro-IL-1β in *Card9*$^{-/-}$ mice at day 7, without an increase in the caspase-1 p10 subunit (**Fig. 1p-q**). The mature cytokine could not be reliably measured in mouse sera at this time point, consistent with other published data[26].

One explanation for these data could be the well-known role of CARD9, during fungal infection, in regulating NF-κB signalling pathways[6] such that enhanced expression of pro-IL-1β could result in an overall increase in IL-1β production without effecting inflammasome-induced cytokine processing and pyroptosis. BMDM were infected with *S.* Typhimurium at an MOI 5 for 2h and, following mRNA extraction, we performed quantitative PCR analysis for genes involved in inflammasome signalling, NF-κB target genes and other genes coding for proteins known to associate with CARD9. Most NF-κB target genes, such as TNF-α and RANTES, were similarly upregulated in WT and *Card9*$^{-/-}$ BMDMs, (**Fig. 2c-d**). Levels of pro-IL-1β, however, whilst significantly upregulated in WT cells (around 800 fold-increase) were even more enhanced in *Card9*$^{-/-}$ cells (1200 fold-increase, $p<0.01$) (**Fig. 2a**). This pattern of enhanced pro-IL-1β was also observed at the protein level (**Fig. 2g**). NLRP3 was upregulated to a similar level in both WT and *Card9*$^{-/-}$ BMDMS (**Fig. 2b**). SYK and caspase-8, proteins know to be involved in non-canonical inflammasome activity and NLRP3 activation[18,24], were also found to be slightly upregulated after infection of *Card9*$^{-/-}$ BMDMs at both the mRNA and protein level (**Fig. 2e-i**). Several other genes (NAIP5, NLRC4, ASC, caspase-1, FADD, Bcl-10, MALT-1 and Pro-IL-18) showed no difference in expression between WT and *Card9*$^{-/-}$ infected BMDMs (**Supplementary Fig. 2a-h**). None of the analyzed transcripts or proteins showed basal differences between uninfected WT and *Card9*$^{-/-}$ cells (**Supplementary Fig. 2i-j**).

To determine whether CARD9 affects inflammasome activation as well as pro-IL-1β expression we analyzed, by immunoblotting, the BMDM supernatants for pro-IL-1β and caspase-1 processing. Our data show increased IL-1β protein expression in *Card9*$^{-/-}$ BMDMs at 2 and 6 hours post-infection compared to WT cells. As expected BMDM from ASC knockout mice (*Pycard*$^{-/-}$) were impaired in the production of IL-1β and the mature forms of both caspase-1 and caspase-8. Caspase-1 processing was similar in both WT and *Card9*$^{-/-}$ BMDMs at 2 and 6 hours, suggesting that the increased IL-1β production in *Card9*$^{-/-}$ cells is not due to an increase in caspase-1 activation. We recently showed that caspase-8 plays an important role in canonical inflammasome processing of IL-1β in response to *S*. Typhimurium, but not pyroptosis which is wholly dependent on caspase-1[17] via cleavage and activation of Gasdermin D[20,21]. The mature form of caspase-8 was increased in *Card9*$^{-/-}$ BMDMs at 2 hours (**Fig. 2g-h**) suggesting that, in the absence of CARD9, increased caspase-8 activity is responsible for the increased conversion pro-IL-1β to its mature form.

CARD9 negatively regulates IL-1β production independently of NLRC4 and AIM2

S. Typhimurium stimulates IL-1β production via both NLRC4 and NLRP3 activation[26]. To assess whether CARD9 affects IL-1β production by each of these NLRs LPS-primed WT, *Nlrc4*$^{-/-}$, *Nlrp3*$^{-/-}$ and *Card9*$^{-/-}$ BMDMs were transfected with ultrapure flagellin from *Salmonella* for one hour, followed by

quantification of IL-1β production. IL-1β was elevated to similar levels in WT, NLRP3 and CARD9 knockout macrophages, but, as expected, was below the detection limit for *Nlrc4*$^{-/-}$ BMDMs (**Fig. 3a**). CARD9 modulation of inflammasome-induced IL-1β production therefore occurs independently of NLRC4.

In order to confirm this observation, we infected WT BMDM with either wild-type *S.* Typhimurium or a mutant strain deficient in NLRC4 activation[5] (ΔfliCΔfljBΔprgJ). Both WT and *Card9*$^{-/-}$ BMDM infected with the ΔfliCΔfljBΔprgJ strain had impaired levels of pyroptosis in comparison to cells infected with WT bacteria (**Fig. 3b-d**). IL-1β secretion was elevated in BMDMs infected with WT *S*. Typhimurium, but markedly reduced, as expected, in BMDMs after infection with the ΔfliCΔfljBΔprgJ mutant. In *Card9*$^{-/-}$ BMDMs, however, IL-1β production was increased after infecting cells with both strains of bacteria (**Fig. 3e-g**). At 2 hours post-infection *Card9*$^{-/-}$ BMDMs produced detectable IL-1β after infection with both bacterial strains although the level was much reduced in cells infected with the ΔfliCΔfljBΔprgJ mutant. No IL-1β was detected in WT cells at this time point infected with the ΔfliCΔfljBΔprgJ strain. *Card9*$^{-/-}$ macrophages secreted 2.5 times more IL-1β than WT BMDMs at both 6 and 24 hours post-infection, time points known to involve NLRP3 activity in response to *Salmonella* infection[5]. This is consistent with our flagellin data suggesting that IL-1β produced via NLRC4 occurs independently of CARD9.

To determine whether AIM2 inflammasome activity could be regulated by CARD9 LPS primed WT and *Card9*$^{-/-}$ BMDMs were stimulated with the AIM2 ligand poly(dA:dT), but no differences in cellular viability or IL-1β secretion were seen (**Supplementary Fig. 3**).

CARD9 negatively regulates IL-1β production through NLRP3

To determine whether the NLRC4-independent impact of CARD9 on IL-1β production resulted from activation of NLRP3 we infected BMDMs with *S*. Typhimurium at an MOI 10 in the presence or absence of either glibenclamide or MCC950[29,30]. At 2 and 6 hours post-infection, both WT and *Card9*$^{-/-}$ BMDMs showed similar levels of cellular viability in the presence or absence of glibenclamide (**Fig. 4a-b**), while MCC950 slightly inhibited cell death in *Card9*$^{-/-}$ BMDM (Fig. 4e-f). Glibenclamide and MCC950 did not affect IL-1β production in WT cells, but they did reduce the enhancement of IL-1β production in *Card9*$^{-/-}$ BMDMs to a level comparable to that seen in WT cells. These data suggest that the increased IL-1β production from *Card9*$^{-/-}$ macrophages after *Salmonella* infection is driven by enhanced NLRP3 activation (**Fig. 4c-d,g-h**).

To verify whether CARD9 regulates IL-1β production via NLRP3, LPS-primed (200 ng/mL for 3 hours) WT, *Nlrc4*$^{-/-}$, *Nlrp3*$^{-/-}$ and *Card9*$^{-/-}$ BMDMs were stimulated for one hour with the NLRP3 activator

nigericin (10 μM, 1 hour). Nigericin, as expected, stimulated cell death and IL-1β secretion in WT and *Nlrc4*$^{-/-}$, but not *Nlrp3*$^{-/-}$, BMDMs (**Fig. 4i-j**). Levels of IL-1β produced by *Card9*$^{-/-}$ BMDMs were greatly enhanced in comparison to WT cells after stimulation with nigericin. Similar levels of cellular viability were seen in nigericin-stimulated WT and *Card9*$^{-/-}$ BMDMs (**Fig. 4i-j).** Similarly, incubation of WT, *Card9*$^{-/-}$ and *Nlrp3*$^{-/-}$ BMDMs with ATP showed no alterations in cellular viability (**Fig. 4k**) and a significant increase in IL-1β production in *Card9*$^{-/-}$ cells in comparison to WT cells, while *Nlrp3*$^{-/-}$ BMDMs showed great impairment in IL-1β production (**Fig. 4l**). These data confirm that the effects of CARD9 on inflammasome function are specific for NLRP3-mediated IL-1β production and are uncoupled from inflammasome-driven pyroptosis.

CARD9 inhibits NLRP3 activation upstream of speck formation

The enhanced production of NLRP3-dependent IL-1β secretion in *Card9*$^{-/-}$ BMDMs is independent of caspase-1 (**Fig. 2g**). How then does the presence of CARD9 inhibit processing of IL-1β? We investigated first whether CARD9 acts upstream or downstream of the canonical inflammasome adaptor protein ASC. WT, *Card9*$^{-/-}$ and *Pycard*$^{-/-}$ LPS-primed BMDMs were stimulated with nigericin (5 μM for 30 minutes), fixed, and stained for ASC and CARD9. Both WT and *Card9*$^{-/-}$ cells formed ASC specks (**Fig. 5a**). Immunolocalisation of endogenous CARD9 suggests that this protein forms aggregates in stimulated and unstimulated WT and *Pycard*$^{-/-}$ BMDMs, but it does not co-localize with ASC specks suggesting that CARD9 is not recruited to the ASC speck (**Fig. 5a**). *Card9*$^{-/-}$ BMDMs show some non-specific background staining, but it is much fainter than the CARD9 immunolocalisation in WT and *Pycard*$^{-/-}$ cells.

To determine whether CARD9 associates with ASC prior to speck formation co-immunoprecipitation analysis of WT BMDM lysate was performed using anti-ASC, anti-CARD9 or anti-SYK antibodies as bait. SYK was targeted because of its involvement in both CARD9 and ASC signalling[22,24]. Co-immunoprecipitations confirmed that both ASC and CARD9 interact with SYK in unstimulated or uninfected WT BMDMs. ASC and CARD9 do not, however, directly interact with one another (**Fig. 5b**). After *Salmonella* infection or nigericin treatment, ASC immunoprecipitated preferentially with the phosphorylated form of SYK (p-SYK) confirming previously published data[25], while CARD9 predominantly interacted with unphosphorylated SYK (**Fig. 5b**). Phosphorylated SYK regulates NLRP3 activation[22–25], so the interaction of CARD9 with unphosphorylated SYK may prevent the its subsequent phosphorylation thereby inhibiting NLRP3 activation. No proteins were pulled down in *Card9*$^{-/-}$ and *Pycard*$^{-/-}$ isotype controls IPs (**Supplementary Fig. 4**). Consistent with this hypothesis we found increased phosphorylation of SYK in unstimulated, infected or nigericin treated BMDM from

Card9$^{-/-}$ mice in comparison to WT cells (**Fig. 5c**). This supports the idea that in the absence of CARD9 there is increased SYK phosphorylation which facilitates NLRP3 activation.

CARD9 inhibits NLRP3 activation through SYK and caspase-8

Our immunoblotting (**Fig 2g)**, co-immunoprecipitation (**Fig. 5b**) and SYK phosphorylation data (**Fig. 5c**) all suggest that CARD9 regulates NLRP3 activation by a SYK and caspase-8-dependent mechanism. To investigate this hypothesis LPS-primed BMDMs were infected in the presence or absence of R406, a specific SYK inhibitor, and Z-IETD-FMK, a caspase-8 inhibitor. The expression of pro-IL-1β, caspase-8, caspase-1, SYK and CARD9 are similar in LPS-primed WT and *Card9*$^{-/-}$ BMDM in the presence or absence of these inhibitors (**Supplementary Fig. 5**). BMDM infection with *S*. Typhimurium (MOI 10) in the presence of the caspase-8 inhibitor Z-IETD-FMK, as expected, had no effect on cell viability as measured by LDH activity (**Fig. 6a**) because caspase-8 does not induce pyroptosis in response to infection with this pathogen[17]. It is possible, however, that caspase-8 may induce cell death in response to infection by other mechanisms[31]. IL-1β production was reduced in both WT and *Card9*$^{-/-}$ macrophages in the presence of Z-IETD-FMK which is consistent with our data suggesting that caspase-8 plays an important role in IL-1β processing during *Salmonella* infection[17]. Importantly IL-1β secretion in infected *Card9*$^{-/-}$ macrophages, in the presence of Z-IETD-FMK, was now no different to that of infected WT BMDM (**Fig. 6b**) supporting the hypothesis that the increased IL-1β production observed in *Card9*$^{-/-}$ cells is indeed mediated by caspase-8. Treatment with Z-IETD-FMK also reduced IL-1β secretion from nigericin stimulated *Card9*$^{-/-}$ BMDMs to the same level as WT cells (**Fig. 6c-d**).

Cell viability in BMDMs infected with *S*. Typhimurium in the presence of the SYK inhibitor R406 was unaffected, as expected, given that SYK activity does not regulate NLRC4 activity (**Fig. 6e**)[24]. SYK inhibition decreased the amount of IL-1β secreted by infected *Card9*$^{-/-}$ BMDMs to similar levels to those seen in WT cells (**Fig. 6f**). SYK inhibition, however, had less effect on IL-1β production than caspase-8 inhibition probably because caspase-8 is activated by both NLRC4 and NLRP3 in response to *Salmonella* infection[17], whereas SYK only regulates NLRP3 activation[24]. Stimulation of LPS-primed WT or *Card9*$^{-/-}$ BMDMs with nigericin in the presence of R406 elicited similar levels of IL-1β production from both cell types (**Fig. 6h**). SYK inhibition led to a small, but statistically significant, increase in cell viability in both WT and CARD9 knockout BMDM stimulated with nigericin probably due to its effect on NLRP3-induced caspase-1 activation[25] (**Fig. 6g**).

SYK regulates NLRP3 activity in BMDM, but it does not affect NLRP3 activation in bone marrow derived dendritic cells (BMDCs)[24]. If CARD9 plays a specific role in regulating NLRP3 activity through

SYK then there should be no difference in NLRP3-stimulated IL-1β production between WT and *Card9*$^{-/-}$ BMDC. Stimulation of LPS-primed BMDCs with nigericin (5 μM, 1 hour) induced similar levels of IL-1β processing and cell death in both *Card9*$^{-/-}$ and WT BMDCs (**Fig. 6i-j**). Similarly, no increase in IL-1β processing was observed in unprimed *Card9*$^{-/-}$ compared to WT BMDCs infected with *S*. Typhimurium (MOI 10) (**Supplementary Fig. 6**). Taken together, these data support a role for CARD9 in regulating SYK activation of NLRP3 to control caspase-8 processing of IL-1β in the canonical inflammasome in BMDMs.

SYK controls caspase-8 recruitment to the inflammasome

How does SYK regulate caspase-8 activity in response to NLRP3 activation? We hypothesized that SYK alters caspase-8 recruitment to the inflammasome speck. To test this hypothesis we stimulated LPS-primed WT, *Card9*$^{-/-}$ and *Pycard*$^{-/-}$ BMDMs with nigericin in the presence or absence of R406, and stained the cells for active caspase-8 and caspase-1. After fixation and counterstaining with DAPI, we observed speck-like structures for both caspase-1 and caspase-8 in WT and CARD9 knockout macrophages, but not in *Pycard*$^{-/-}$BMDM (**Fig. 7a**). Quantification of the number of cells containing specks (1000 cells per treatment, selected from random fields) confirmed that *Card9*$^{-/-}$ BMDMs had more caspase-8 positive specks than WT cells. The number of WT and *Card9*$^{-/-}$ BMDM containing caspase-1 positive specks were very similar to each other (**Fig. 7c**). In the presence of the SYK inhibitor R406 the number of cells containing caspase-8 positive specks was reduced compared to cells without inhibitor, but was the same for WT and *Card9*$^{-/-}$ BMDM (**Fig. 7b**). These observations corroborate the caspase-8 cleavage data (Fig. 2g) and caspase-8 inhibition assays (Fig. 6a-h) supporting the concept that SYK and CARD9 regulate the recruitment of caspase-8 to the inflammasome after NLRP3 activation to process IL-1β.

CARD9 is a central signalling hub for inflammatory signalling

Our data identifies a novel, inhibitory, role for CARD9 in the regulation of NLRP3-induced IL-1β production. CARD9 regulates inflammatory responses downstream of numerous PRRs including NOD2, Dectin-1 and RIG-I. This suggests that CARD9 may function as a signalling hub coordinating the cellular response to infection and permitting a rapid integrated inflammatory response to a range of PRRs. To test this hypothesis we investigated whether *Salmonella* infection alters CARD9 protein expression and thereby potentially alters the resulting level of inflammasome activation. CARD9 is constitutively expressed in many cell types including macrophages[11] and after infection of WT BMDM with *S*. Typhimurium (MOI 10) a progressive decrease in the expression of this protein was observed within 30 minutes after infection (**Fig. 8a**). The decrease in CARD9 expression was

independent of inflammasome assembly, as similar CARD9 expression profiles were seen in infected LPS-primed or unprimed *Pycard*$^{-/-}$ BMDMs (**Fig. 8b**). Nigericin stimulation does not trigger CARD9 downregulation (**Fig. 8c**) supporting our hypothesis that the regulation of CARD9 expression in macrophages is specifically down-regulated upon *Salmonella*-infection possibly to maximize the host inflammasome response to infection.

Our data and other published work supports a role for CARD9 as an important regulator of PRR signalling where it can up- or down-regulate pro-inflammatory cytokine production in a pathogen dependent manner[6,8,32]. If CARD9 is a central regulator of the inflammatory response to pathogens then signalling through other CARD9-dependent PRRs that recognize salmonellae should also be altered in response to infection. NOD2 recruits CARD9 to activate p38 and JNK MAPK signalling[11,33], but NF-κB signalling is activated independently of this adaptor protein. Pro-IL-1β expression is transcriptionally regulated by NF-κB, p38 and JNK MAPK whereas TNF-α transcription is independent of p38 and JNK activity[34]. We investigated whether CARD9 was important in regulating NOD2-induced signalling in response to *S*. Typhimurium infection. WT and *Nod2*$^{-/-}$ BMDMs were infected with *S*. Typhimurium (MOI of 10) and the levels of IL-1β and TNF-α were determined by ELISA. Infection of *Nod2*$^{-/-}$ macrophages induced a small increase in IL-1β production, but suppressed TNF-α production (**Supplementary Fig. 7a-c**). These data are consistent with the NOD2-CARD9 axis negatively regulating pro-IL-1β production through an action on MAPK signalling independently of NOD2 induction of TNF-α. Consistent with this idea, overstimulation of NOD2 at the same time of infection with *S*. Typhimurium leads to a CARD9 and NOD2-dependent decrease in pro-IL-1β expression (**Supplementary Fig. 7d**). Functional association network analysis showed that the primary interactome of CARD9 consists of key immune and death signalling pathways in both mice and humans (**Supplementary Fig. 8**). Collectively these data support the idea that CARD9 functions as a signalling hub to co-ordinate inflammatory responses to pathogens such as *Salmonella*.

DISCUSSION

In this study we have identified a new role for CARD9 as a negative regulator of IL-1β production in response to bacterial infection. This is in stark contrast to the role of CARD9 in fungal signalling where this adaptor is important for driving pro-inflammatory signalling responses to infection[3,6]. The recognition of infection by host cells triggers a series of complex, pathogen specific, signalling events to drive an appropriate inflammatory response. It is increasingly clear that inflammatory signalling pathways do not function in isolation, but form complex networks in which key constituents act as nodes or hubs linking apparently distinct pathways. The data we present here, along with that of other published studies, clearly indicate that CARD9 is one such protein. CARD9

coordinates TLR-dependent and independent NF-κB signalling[6,9,11,35], ROS production[10], autophagy[36], non-canonical inflammasome function[3] and, as we now demonstrate, canonical inflammasome assembly in a context dependent manner. Importantly the specific role of CARD9 differs between cell types, thereby contributing a further level of regulatory control in enabling cell specificity in the host response to infection [32,35,37].

Our data shows CARD9 fine-tunes IL-1β production in two distinct ways (**Supplementary Fig. 9**). During "signal 1", CARD9 specifically downregulates pro-IL-1β transcription without affecting other NF-κB target-genes. This occurs following activation of p38 and JNK signalling via NOD2, and is consistent with reports that NOD2 can have specific inhibitory roles that are dependent upon the context of its activation[38–43]. How CARD9 regulates pro-IL-1β in this context remains to be fully elucidated, but is likely to involve the transcription factor AP-1. AP-1 is a known transcriptional regulator of pro-IL-1β[44] which is itself regulated by p38 and JNK activity[45]. There is, therefore, increased expression of pro-IL-1β during the "signal 1" phase of inflammasome stimulation in *Card9*$^{-/-}$ cells. However, in WT and *Card9*$^{-/-}$ LPS-primed macrophages, which express similar levels of pro-IL-1β, the production of IL-1β is further increased in *Card9*$^{-/-}$ compared to WT cells. This suggests the elevated production of IL-1β from *Card9*$^{-/-}$ cells is not solely due to the increased pro-IL-1β substrate availability, but is also due to an effect of CARD9 during "signal 2" of inflammasome activation. During "signal 2", CARD9 suppresses SYK phosphorylation which consequently reduces ASC phosphorylation and the subsequent assembly and activation of the inflammasome. In macrophages, p-SYK phosphorylates ASC, enhancing NLRP3 inflammasome activity[24,25]; whereas in dendritic cells SYK has no effect on the canonical NLRP3 inflammasome[24]. Consistent with these studies our data clearly shows that CARD9 negatively regulates the activity of NLRP3 in macrophages, but not dendritic cells. Our data suggests that, in addition to the well described regulatory role for CARD9 downstream of SYK, it is also possible that CARD9 can act upstream of SYK during bacterial infection. The regulation of SYK phosphorylation by CARD9 specifically alters caspase-8 recruitment to the inflammasome explaining why we see changes in IL-1β production independently of any effect on pyroptosis. In *Salmonella* infection caspase-8 processes IL-1β but does not affect pyroptosis[17]. Precisely how ASC phosphorylation enhances caspase-8 recruitment is unclear, but as SYK phosphorylates ASC on its CARD domain[24] it is plausible that altering the pattern of ASC phosphorylation could impair the CARD/CARD interaction between ASC and caspase-1[46] and favour interactions between the ASC PYD and Caspase-8 DED[47].

Identification of negative regulators of inflammasome activation may have important clinical implications because dysregulated inflammasome activity is associated with a number of important

diseases[2,48]. Genome-wide association studies found strong correlations between loss of function CARD9 mutations and an increased likelihood of developing inflammatory diseases[12–16]. In a *Mycobacterium tuberculosis* infection model CARD9 knockout mice have an increased bacterial burden and develop exacerbated systemic inflammatory responses[27], further strengthening the link between CARD9 and inflammatory diseases. Similarly, *Card9*$^{-/-}$ mice are deficient in controlling *Candida albicans* infection, a fungal pathogen capable of stimulating NLRP3[6]. These *in vivo* and clinical observations emphasize CARD9 role as a negative regulator for inflammation, possibly by fine-tuning NLRP3-mediated IL-1β production. In conclusion we have identified a novel negative regulatory role for CARD9 on IL-1β production in macrophages by modulating pro-IL-1β expression and caspase-8 recruitment to the inflammasome in response to bacterial infection. These data support a role for CARD9 as a central signalling hub in co-ordinating innate immune inflammatory responses to infection.

Appendix 18

METHODS

Mice

Wild type C57BL/6 mice were obtained from Charles River, UK. *Nlrc4*$^{-/-}$, *Nlrp3*$^{-/-}$ and *Pycard*$^{-/-}$ mice on a C57BL/6 background were produced by Millenium Pharmaceuticals and obtained from Kate Fitzgerald (University of Masschusetts). *Card9*$^{-/-}$ mice on a C57BL/6 background, originally produced by Xin Lin (University of Texas)[11], were provided by David Underhill (Cedars-Sinai Medical Center). *Nod2*$^{-/-}$ mice were provided by Peter Murray (St. Jude Children's Research Hospital). Mice were backcrossed on a C57BL/6 background at least 8 generations. All mice strains were bred independently. All work involving live animals complied with the University of Cambridge Ethics Committee regulations and was performed under the Home Office Project License number 80/2572.

***In vivo* infections**

S. Typhimurium M525P was grown statically for 18 hours at 37 ^{o}C in LB Broth (Sigma), then washed and resuspended in PBS (Sigma). 1.90 to 2.04 x10^{4} CFU/mouse were administered systemically to 8 to 16 weeks-old mice, both male and female, via the lateral tail vein, while control mice were inoculated with PBS only. Mice were euthanized at days 1, 3 and 7 after infection and their spleens and livers were aseptically removed. Organs were homogenized in 10 mL sterile water using a Colworth stomacher. Organ homogenates were then 10-fold serially diluted in PBS, plated on LB agar plates and incubated overnight at 37 °C followed by enumeration of colony-forming units.

To obtain splenocyte cell suspensions, spleens were disrupted through a 70 µm cell strainer (BD Biosciences), washed in RPMI containing 2% Hyclone, resuspended in Red Blood Cell lysis buffer (Sigma), and incubated for 10 minutes at room temperature. The suspension was then centrifuged at 300 G for 10 minutes and the pellet washed twice in RPMI. The purified splenocytes were lysed and the proteins probed by immunoblotting as described below.

All mice were housed in a specific pathogen-free facility and all work involving live animals complied with the University of Cambridge Ethics Committee regulations under Home Office Project License number 80/2572.

Cell culture and stimulation

Primary bone marrow derived macrophages (BMDM) were prepared and cultured for 6-9 days as previously described[17]. Bone marrow derived dendritic cells (BMDCs) were prepared and cultured for 7-10 as previously described[49]. Briefly, mice were killed by cervical dislocation, the skin was sterilized with ethanol (70%) prior to removal of the leg. The tibia and femur were removed, cleaned of

muscle and the proximal and distal epiphysis cut away. For BMDMs, the bone marrow was flushed out using DMEM supplemented with 10% FCS (Thermo Fisher Scientific), 20% L929 conditioned media and 5 mM L-Glutamine (Sigma). For BMDCs, the bone marrow was flushed out using BMDC growth media (RPMI 1640 supplemented with 10% FCS, 50 µM 2-Mercaptoethanol and 1000 U/mL GM-CSF (Thermo Fisher Scientific). The bone marrow cells were centrifuged (300 x G for 10 minutes at 15 ^{o}C) and ressuspended in appropriate growth media. Cells were cultured at 37 ^{o}C in 5% CO_2 and growth media replaced every 2 days.Infection of BMDM with *S.* Typhimurium strain SL1344 and Δ*fliC*Δ*fljB*Δ*prgJ* was performed as previously described[17]. For NLRP3 inhibition assay, the cells were pre-incubated with glibenclamide (Sigma) 200 µM, MCC950 10 µM (Cayman Chemical) or vehicle control (DMSO) for 15 minutes and infection was carried out as described above. For NOD2 co-stimulation assay, the cells were infected with *S*. Typhimurium in the presence or absence of muramyl dipeptide 10 µg/mL (Invivogen).

Selected experiments required BMDMs primed with LPS. This was performed by incubating the cells in growth media containing 200 ng/mL ultrapure LPS from *Escherichia coli* O111:B4 (InvivoGen) for 3 hours at 37 ^{o}C and 5% CO_2, followed by washes in media alone. For stimulation experiments, the LPS-primed BMDM were incubated with nigericin 10 µM (Sigma), 5 mM ATP (Sigma) or 60 ng ultrapure flagellin from *S.* Typhimurium (Invivogen), after incubation at room temperature for 20 minutes with Profect-P1 reagent (Target Systems) for transfection complex formation. AIM2 stimulation was performed using Poly(dA:dT)/LyoVec (Invivogen) 2 µg/mL for 4 hours. Caspase-8 inhibition experiments were performed in LPS-primed cells by the addition of the stimuli with or without 10 µM Z-IETD-FMK (MBL International). SYK inhibition experiments were conducted by pre-incubating the LPS-primed cells for 1 hour with or without 1 µM R406 (Invivogen), followed by stimulation in presence or absence of 1 µM R406.

Quantitative PCR

Following stimulation, cells were treated with RNAprotect Cell Reagent (Qiagen) and total RNA was isolated using the RNeasy Mini kit (Qiagen) according to manufacturer's instructions. Genomic DNA was removed using the TURBO DNA-free kit (ThemoFisher Scientific). The primers used (**Supplementary Table 1**) were selected based on data submitted to the primer bank database (http://pga.mgh.harvard.edu/primerbank/index.html)[50]. The quantitative RT-PCR was performed with the SensiFAST™ One-Step Real-Time PCR kit (Bioline) using a Rotor-Gene Q real-time PCR cycler (Qiagen). Data analysis was carried out using the mean of glyceraldehyde 3-phosphate dehydrogenase (GAPDH) and β-actin as reference genes, employing Pfaffl method to correct for reaction efficiency[51].

Immunoprecipitation, protein precipitation and immunoblot

Cell culture supernatant and spleen homogenate proteins were precipitated using methanol and chloroform. Briefly, a volume of the sample was vortexed with one volume of ice-cold methanol and 0.25 volume of chloroform, followed by centrifugation (4 ^{o}C, 16000 G, 12 minutes). The intermediate phase was collected, washed two times in ice-cold methanol, and ressuspended in Pierce™ Lane Marker Reducing Sample Buffer (Life Technologies).

Cells were lysed in lysis buffer containing 10 mM Tris pH 7.4, 150 mM NaCl, 5 mM EDTA, 1% Triton X-100, 10 mM NaF, 1 mM $NaVO_4$, 20 mM PMSF, Phosphatase inhibitor cocktail 3 (1 in 100 dilution, Sigma) and Protease inhibitor cocktail (1 in 100 dilution, P8340, Sigma). Protein levels were quantified using Pierce™ BCA Protein Assay Kit (Life Technologies). The samples were used for co-immunoprecipitation or incubated for 5 minutes at 100 ^{o}C with Pierce™ Lane Marker Reducing Sample Buffer (Life Technologies) for immunoblotting.

For co-immunoprecipitation analysis cells were reversibly cross-linked with 5 mM DTBP (Fisher Scientific) for 30 minutes at 4 ^{o}C then lysed as described above. Protein concentration was adjusted to 600 µg/mL and 800 µL was incubated overnight with 2 µL antibody (goat anti-ASC, (sc-33958, Santa Cruz); rabbit anti-CARD9 mouse preferred (12283, Cell Signaling); mouse anti-SYK (MA1-19332, Thermo Scientific)) and 20 µL of Protein A/G PLUS-agarose beads (Santa Cruz). The remainder of the protein sample was stored for immunoblotting. After incubation, the beads were washed four times in lysis buffer, ressuspended with Pierce™ Lane Marker Reducing Sample Buffer (Life Technologies), incubated for 5 minutes at 100 ^{o}C, centrifuged for 1 minute at 5000 G and the supernatant used for immunoblotting.

Immunoblots were probed using the following primary antibodies: caspase-1 p10 (mouse) (sc-514, Santa Cruz) 1 in 500; cleaved caspase-8 (rabbit) (8592, Cell Signaling) 1 in 500; caspase-8 (rabbit) (IG12, Enzo) 1 in 500; IL-1β (goat) (AF-401, R&D Systems) 1 in 1000; SYK (mouse) (MA1-19332, Thermo Scientific) 1 in 1000; p-SYK (rabbit) (2711, Cell Signaling) 1 in 1000; ASC (rabbit) (AL177, Enzo) 1 in 2000; B-Actin (mouse) (AB3280, ABCAM) 1 in 2500; CARD9, mouse preferred (rabbit) 1 in 1000 (12283, Cell Signaling). The secondary antibodies used were: anti-goat IgG-HRP (sc-2922, Santa Cruz) 1 in 5000; anti-mouse IgG-HRP (7076, Cell Signaling) 1 in 6000; anti-rabbit IgG-HRP (A24537, Thermo Scientific) 1 in 6000 as appropriate.

Immunofluorescence microscopy

To label CARD9 and ASC, stimulated cells were fixed in -20 ^{o}C methanol for 5 minutes, after washing with PBS, non specific labeling was blocked by incubation at 37 ^{o}C for one hour in 10% normal goat

serum (Dako) containing 0.1% saponin (Sigma). ASC was labeled with anti-ASC primary (1:500 dilution, AL177; Enzo) and Alexa-fluor 568 secondary antibody (1:1000 dilution, anti-rabbit Alexa-fluor 568 (Invitrogen)). To label CARD9 the cells were subsequently blocked in PBS containing 1% BSA and 0.1% saponin. Immunolabelling was performed with anti-CARD9 (1:300 dilution, sc-49408, Santa Cruz) and anti-Rabbit-Alexa 430 (1:1000 dilution, Invitrogen). Cells were counterstained using DAPI mounting medium (Vecta Labs).

Speck enumeration was performed in cells stimulated with nigericin in presence of FAM-FLICA™ Caspase 8 Assay Kit, green (1:150, Immunochemistry Technologies) and FAM-FLICA™ Caspase 8 Assay Kit, red (1:150, Immunochemistry Technologies), followed by fixation with 4% paraformaldehyde for 15 minutes at room temperature. Non-specific labeling was prevented by incubating cells with 10% normal goat serum (Dako) and 0.1% saponin (Sigma) for one hour. 1000 cells per treatment were selected from random fields and the specks counted.

Cellular viability assays and intracellular bacteria counts

Cytotoxicity was quantified by measuring LDH activity after being released from live cells. Uninfected BMDMs (ranging from 12.500 to 200.000 cells/well) were used as standards. After treatment, the cells were washed three times with pre-warmed PBS and the intracellular LDH was released by lysing the cells with Triton X-100 1.2% for 1 hour at 37^{o} C. LDH activity was them measured using CytoTox 96 Non-Radioactive Cytotoxicity Assay (Promega)[17]. Cellular viability was them calculated in relation to the uninfected control containing 200.000 cells (100% viability). Intracellular bacteria counts were performed using LB agar plates after overnight incubation.

Cytokine quantification

Secreted cytokines were measured in the culture supernatants. All cytokines were measured according to the manufacturer's instructions. For IL-1β OptEIA Mouse IL-1β Set (BD Biosciences) was used and TNF-α using the DuoSet ELISA kit (R&D Systems).

Computational analysis

Functional association network analysis was performed using STRING v10[52] and either murine or human CARD9 as search proteins. Primary interactomes were initially established using a high confidence cut-off score of 0.7 and a maximum of 50 fifty interaction partners. These interactomes were further expanded by relaxing the inclusion criteria to a cut-off value of 0.4. Data are presented with the thickness of the line between protein nodes representing the confidence level associated with that interaction.

Statistical analysis

Statistical significance was determined by one-way analysis of variance (ANOVA) with Tukey post-comparison tests using a confidence interval of 95%. *In vivo* data was analyzed by two-way ANOVA with Bonferroni post-test using a CI of 95%.

Data availability

The data presented in this study have been deposited in the University of Cambridge data repository and are available with the DOI 10.17863/CAM.778 (http://dx.doi.org/10.17863/CAM.778).

REFERENCES

1. Lamkanfi, M. & Dixit, V. M. Mechanisms and functions of inflammasomes. *Cell* **157,** 1013–1022 (2014).
2. Lamkanfi, M. & Dixit, V. M. Inflammasomes and their roles in health and disease. *Annu. Rev. Cell Dev. Biol.* **28,** 137–161 (2012).
3. Gringhuis, S. I. *et al.* Dectin-1 is an extracellular pathogen sensor for the induction and processing of IL-1β via a noncanonical caspase-8 inflammasome. *Nat. Immunol.* **13,** 246–254 (2012).
4. Zwolanek, F. *et al.* The Non-receptor Tyrosine Kinase Tec Controls Assembly and Activity of the Noncanonical Caspase-8 Inflammasome. *PLoS Pathog.* **10,** e1004525 (2014).
5. Man, S. M. *et al.* Inflammasome activation causes dual recruitment of NLRC4 and NLRP3 to the same macromolecular complex. *Proc. Natl. Acad. Sci. U. S. A.* 1–6 (2014). doi:10.1073/pnas.1402911111
6. Gross, O. *et al.* Card9 controls a non-TLR signalling pathway for innate anti-fungal immunity. *Nature* **442,** 651–6 (2006).
7. Poeck, H. *et al.* Recognition of RNA virus by RIG-I results in activation of CARD9 and inflammasome signaling for interleukin 1 beta production. *Nat. Immunol.* **11,** 63–69 (2010).
8. Roth, S. *et al.* Rad50-CARD9 interactions link cytosolic DNA sensing to IL-1β production. *Nat. Immunol.* **15,** 538–545 (2014).
9. Bertin, J. *et al.* CARD9 is a novel caspase recruitment domain-containing protein that interacts with BCL10/CLAP and activates NF-kB. *J. Biol. Chem.* **275,** 41082–41086 (2000).
10. Wu, W., Hsu, Y.-M. S., Bi, L., Songyang, Z. & Lin, X. CARD9 facilitates microbe-elicited production of reactive oxygen species by regulating the LyGDI-Rac1 complex. *Nat. Immunol.* **10,** 1208–1214 (2009).
11. Hsu, Y.-M. S. *et al.* The adaptor protein CARD9 is required for innate immune responses to intracellular pathogens. *Nat. Immunol.* **8,** 198–205 (2007).
12. Beaudoin, M. *et al.* Deep Resequencing of GWAS Loci Identifies Rare Variants in CARD9, IL23R and RNF186 That Are Associated with Ulcerative Colitis. *PLoS Genet.* **9,** (2013).
13. Zhernakova, A. *et al.* Genetic Analysis of Innate Immunity in Crohn ' s Disease and Ulcerative Colitis Identifies Two Susceptibility Loci Harboring CARD9 and IL18RAP. *J. Hum. Genet.* 1202–1210 (2008). doi:10.1016/j.ajhg.2008.03.016.
14. Balzola, F., Bernstein, C., Ho, G. T. & Russell, R. K. Deep resequencing of GWAS loci identifies independent rare variants associated with inflammatory bowel disease. *Nat. Genet.* **12,** 126–127 (2012).
15. Kiryluk, K. *et al.* Discovery of new risk loci for IgA nephropathy implicates genes involved in immunity against intestinal pathogens. *Nat. Genet.* **13,** (2014).
16. Hong, S. N. *et al.* Deep resequencing of 131 Crohn's disease associated genes in pooled DNA confirmed three reported variants and identified eight novel variants. *Gut* 1–9 (2015). doi:10.1136/gutjnl-2014-308617
17. Man, S. M. *et al.* Salmonella infection induces recruitment of Caspase-8 to the inflammasome

to modulate IL-1β production. *J. Immunol.* **191,** 5239–5246 (2013).

18. Gurung, P. *et al.* FADD and caspase-8 mediate priming and activation of the canonical and noncanonical Nlrp3 inflammasomes. *J. Immunol.* **192,** 1835–1846 (2014).

19. Philip, N. H. *et al.* Caspase-8 mediates caspase-1 processing and innate immune defense in response to bacterial blockade of NF-κB and MAPK signaling. *Proc. Natl. Acad. Sci. U. S. A.* **111,** 7385–7390 (2014).

20. Kayagaki, N. *et al.* Caspase-11 cleaves gasdermin D for non-canonical inflammasome signaling. *Nature* (2015). doi:10.1038/nature15541

21. Shi, J. *et al.* Cleavage of GSDMD by inflammatory caspases determines pyroptotic cell death. *Nature* (2015). doi:10.1038/nature15514

22. Gross, O. *et al.* Syk kinase signalling couples to the Nlrp3 inflammasome for anti-fungal host defence. *Nature* **459,** 433–436 (2009).

23. Tiemi Shio, M. *et al.* Malarial hemozoin activates the NLRP3 inflammasome through Lyn and Syk kinases. *PLoS Pathog.* **5,** (2009).

24. Hara, H. *et al.* Phosphorylation of the adaptor ASC acts as a molecular switch that controls the formation of speck-like aggregates and inflammasome activity. *Nat. Immunol.* **14,** 1247–55 (2013).

25. Lin, Y. *et al.* Syk is involved in NLRP3 inflammasome-mediated caspase-1 activation through adaptor ASC phosphorylation and enhanced oligomerization. *J. Leukoc. Biol.* **97,** 1–11 (2015).

26. Broz, P. *et al.* Redundant roles for inflammasome receptors NLRP3 and NLRC4 in host defense against Salmonella. *J. Exp. Med.* **207,** 1745–1755 (2010).

27. Dorhoi, A. *et al.* The adaptor molecule CARD9 is essential for tuberculosis control. *J Exp Med* **207,** 777–792 (2010).

28. Foster, G. L. *et al.* Virulent Salmonella enterica infections can be exacerbated by concomitant infection of the host with a live attenuated S. enterica vaccine via Toll-like receptor 4-dependent interleukin-10 production with the involvement of both TRIF and MyD88. *Immunology* **124,** 469–479 (2008).

29. Lamkanfi, M. *et al.* Glyburide inhibits the Cryopyrin/Nalp3 inflammasome. *J. Cell Biol.* **187,** 61–70 (2009).

30. Coll, R. C. *et al.* A small-molecule inhibitor of the NLRP3 inflammasome for the treatment of inflammatory diseases. *Nat. Med.* (2015). doi:10.1038/nm.3806

31. Sagulenko, V. *et al.* AIM2 and NLRP3 inflammasomes activate both apoptotic and pyroptotic death pathways via ASC. *Cell Death Differ* **20,** 1149–1160 (2013).

32. Goodridge, H. S. *et al.* Differential use of CARD9 by dectin-1 in macrophages and dendritic cells. *J. Immunol.* **182,** 1146–1154 (2009).

33. Parkhouse, R. *et al.* Interaction between NOD2 and CARD9 involves the NOD2 NACHT and the linker region between the NOD2 CARDs and NACHT domain. *FEBS Lett.* (2014). doi:10.1016/j.febslet.2014.06.035

34. Baldassare, J. J., Bi, Y. & Bellone, C. J. The Role of p38 Mitogen-Activated Protein Kinase in IL-1β Transcription. *J. Immunol.* **162,** 5367–5373 (1999).

35. Hara, H. *et al.* The adaptor protein CARD9 is essential for the activation of myeloid cells through ITAM-associated and Toll-like receptors. *Nat. Immunol.* **8,** 619–629 (2007).

36. Yang, C. S. *et al.* The autophagy regulator Rubicon is a feedback inhibitor of CARD9-mediated host innate immunity. *Cell Host Microbe* **11,** 277–289 (2012).

37. Hara, H. *et al.* Cell type-specific regulation of ITAM-mediated NF-kappaB activation by the adaptors, CARMA1 and CARD9. *J. Immunol.* **181,** 918–930 (2008).

38. Watanabe, T., Kitani, A., Murray, P. J. & Strober, W. NOD2 is a negative regulator of Toll-like receptor 2-mediated T helper type 1 responses. *Nat. Immunol.* **5,** 800–808 (2004).

39. Watanabe, T. *et al.* Nucleotide Binding Oligomerization Domain 2 Deficiency Leads to Dysregulated TLR2 Signaling and Induction of Antigen-Specific Colitis. *Immunity* **25,** 473–485 (2006).

40. Watanabe, T. *et al.* Muramyl dipeptide activation of nucleotide- binding oligomerization domain 2 protects mice from experimental colitis. *J. Clin. Invest.* **118,** 545–559 (2008).

41. Dahiya, Y., Pandey, R. K. & Sodhi, A. Nod2 downregulates TLR2/1 mediated IL1b gene expression in mouse peritoneal macrophages. *PLoS One* **6,** 1–11 (2011).

42. Hedl, M. & Abraham, C. Nod2-induced autocrine interleukin-1 alters signaling by ERK and p38 to differentially regulate secretion of inflammatory cytokines. *Gastroenterology* **143,** 1530–1543 (2012).

43. Kim, H. *et al.* A novel crosstalk between TLR4- and NOD2-mediated signaling in the regulation of intestinal inflammation. *Sci. Rep.* **5,** 12018 (2015).

44. Roman, J., Ritzenthaler, J. D., Fenton, M. J., Roser, S. & Schuyler, W. Transcriptional regulation of the human interleukin 1beta gene by fibronectin: role of protein kinase C and activator protein 1 (AP-1). *Cytokine* **12,** 1581–1596 (2000).

45. Arthur, J. S. C. & Ley, S. C. Mitogen-activated protein kinases in innate immunity. *Nat. Rev. Immunol.* **13,** 679–92 (2013).

46. Srinivasula, S. M. *et al.* The PYRIN-CARD protein ASC is an activating adaptor for caspase-1. *J. Biol. Chem.* **277,** 21119–21122 (2002).

47. Muzio, M. *et al.* FLICE, a novel FADD-homologous ICE/CED-3–like protease, is recruited to the CD95 (Fas/APO-1) death-inducing signaling complex. *Cell* **85,** 817–827 (1996).

48. Davis, B. K., Wen, H. & Ting, J. P.-Y. The inflammasome NLRs in immunity, inflammation, and associated diseases. *Annu. Rev. Immunol.* **29,** 707–735 (2011).

49. Inaba, K. *et al.* Generation of large numbers of dendritic cells from mouse bone marrow cultures supplemented with granulocyte/macrophage colony-stimulating factor. *J. Exp. Med.* **176,** 1693–1702 (1992).

50. Spandidos, A., Wang, X., Wang, H. & Seed, B. PrimerBank: A resource of human and mouse PCR primer pairs for gene expression detection and quantification. *Nucleic Acids Res.* **38,** 792–799 (2009).

51. Pfaffl, M. W. A new mathematical model for relative quantification in real-time RT-PCR. *Nucleic Acids Res.* **29,** 45e–45 (2001).

52. Jensen, L. J. *et al.* STRING 8 - a global view on proteins and their functional interactions in 630 organisms. *Nucleic Acids Res.* **37,** D412–D416 (2009).

ACKNOWLEDGEMENTS

We thank Dr. Martyn F. Symmons for his suggestions and Caroline R. Paié for the drawing used in the supplementary diagram. M.P. was supported by CAPES (Coordenação de Aperfeiçoamento de Pessoal de Nível Superior, Brazil). This work was supported by a grant from the BBSRC BB/K006436/1 and a Wellcome Trust Investigator 108045/Z/15/Z award to CEB.

AUTHOR CONTRIBUTIONS

The experiments were performed and the results analyzed by M.P. and P.T. The experiments designed by M.P., P.T., J.A.W. and C.E.B. Manuscript written by M.P., J.A.W., T.P.M. and C.E.B.

ADDITIONAL INFORMATION

Competing financial interests: The authors declare no competing financial interests.

Figures

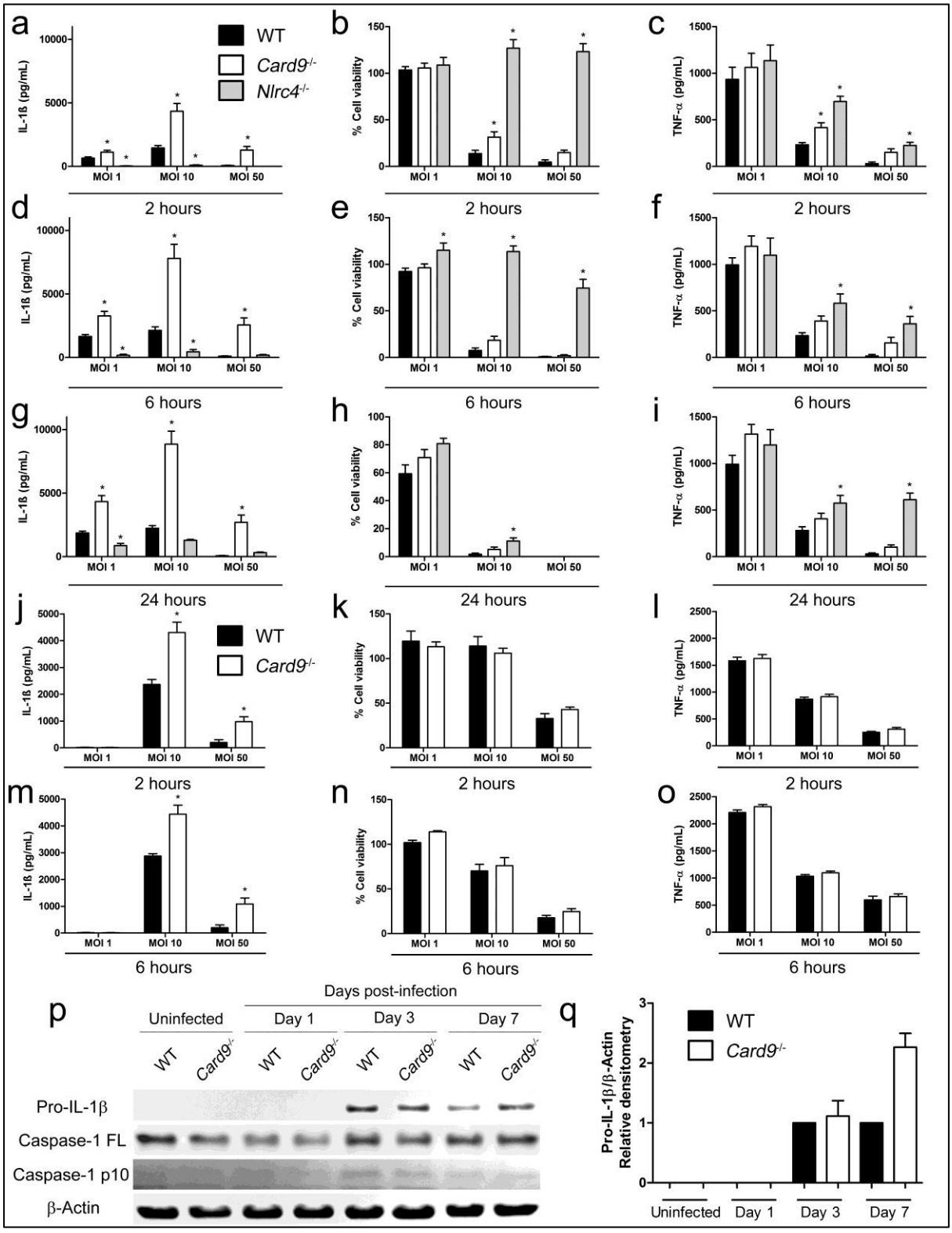

Figure 1: CARD9 negatively regulates IL-1β production *in vitro* and *in vivo*. (a,d,g) IL-1β secretion (as measured by ELISA), (b,e,h) cellular viability (as measured by LDH release) and (c,f,i) TNF-α (as measured by ELISA) of WT, *Nlrc4*$^{-/-}$ and *Card9*$^{-/-}$ BMDMs after infection with *S*. Typhimurium SL1344

at MOIs 1, 10 and 50 for 2 (a-c), 6 (d-f) and 24 (g-i) hours. (j,m) IL-1β secretion, (k,n) cellular viability and TNF-α (l,o) after infection of WT and *Card9*$^{-/-}$ BMDMs with *E*. coli P19A at MOIs 1, 10 and 50 for 2 (j-l) and 6 (m-o) hours. (p) Immunoblot analysis of pro-IL-1β, caspase-1 and β-actin in spleen cells isolated from infected WT and *Card9*$^{-/-}$ C57BL/6 mice after intravenous infection with *S*. Typhimurium M525P ($4x10^3$ CFU) (q) densitometric analysis of this immunoblot. * $p<0.05$ (one-way analysis of variance (ANOVA) with Tukey's multiple comparisons test). (a-i) Data from five independent experiments (mean and s.e.m.). (j-o, q) Data from two independent experiments (mean and s.e.m). (p) Representative data from two independent experiments, using cells pooled from four to six mice per genotype, plus two negative controls per genotype. Mice were from 8 to 16 weeks old, both male and female.

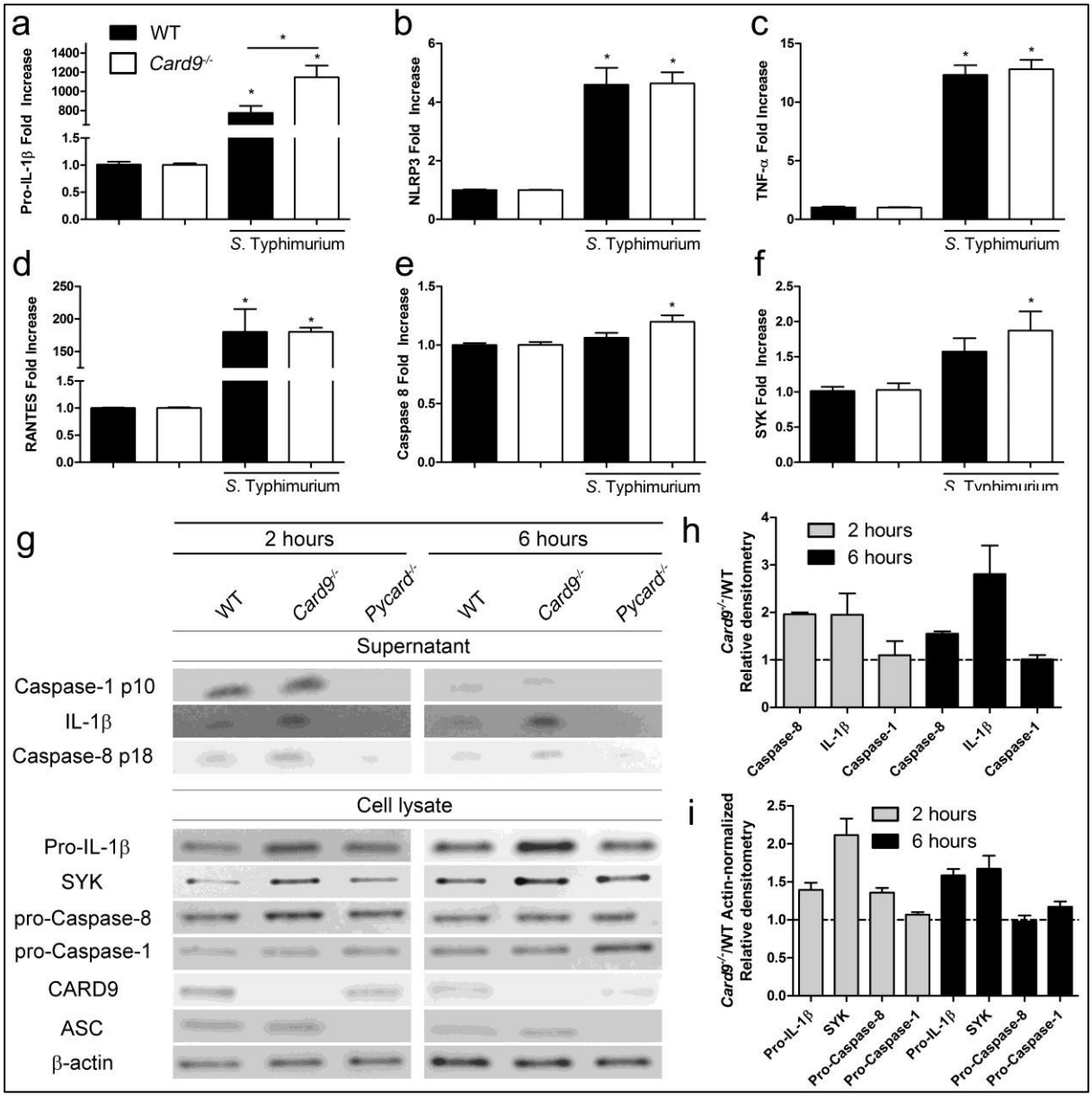

Figure 2: CARD9 modulates pro-IL-1β expression. (a-f) qPCR analysis of WT and *Card9*$^{-/-}$ BMDMs infected with *S*. Typhimurium (MOI 5) for 2 hours, compared to uninfected controls. (a) pro-IL-1β, (b) NLRP3, (c) TNF-α, (d) RANTES, (e) Caspase-8 , (f) SYK. (g) Expression of pro-IL-1β, SYK, pro-caspase-8, pro-caspase-1, CARD9, ASC, β-actin in cell lysates and caspase-1 p10, caspase-8 p18 and IL-1β in culture supernatants from WT, *Card9*$^{-/-}$ and *Pycard*$^{-/-}$ BMDMs after 2 or 6 hours of infection with *S*. Typhimurium (MOI 5) and relative densitometry (*Card9*$^{-/-}$/WT) in culture supernatants (h) or cell lysates (*Card9*$^{-/-}$/WT, actin-normalized) (i). * $p<0.05$ in comparison to uninfected control, unless stated in the graph (one-way ANOVA with Tukey's multiple comparisons test). (a-f, h-i) Data from three independent experiments (mean and s.e.m.). (g) Image is representative of three independent experiments.

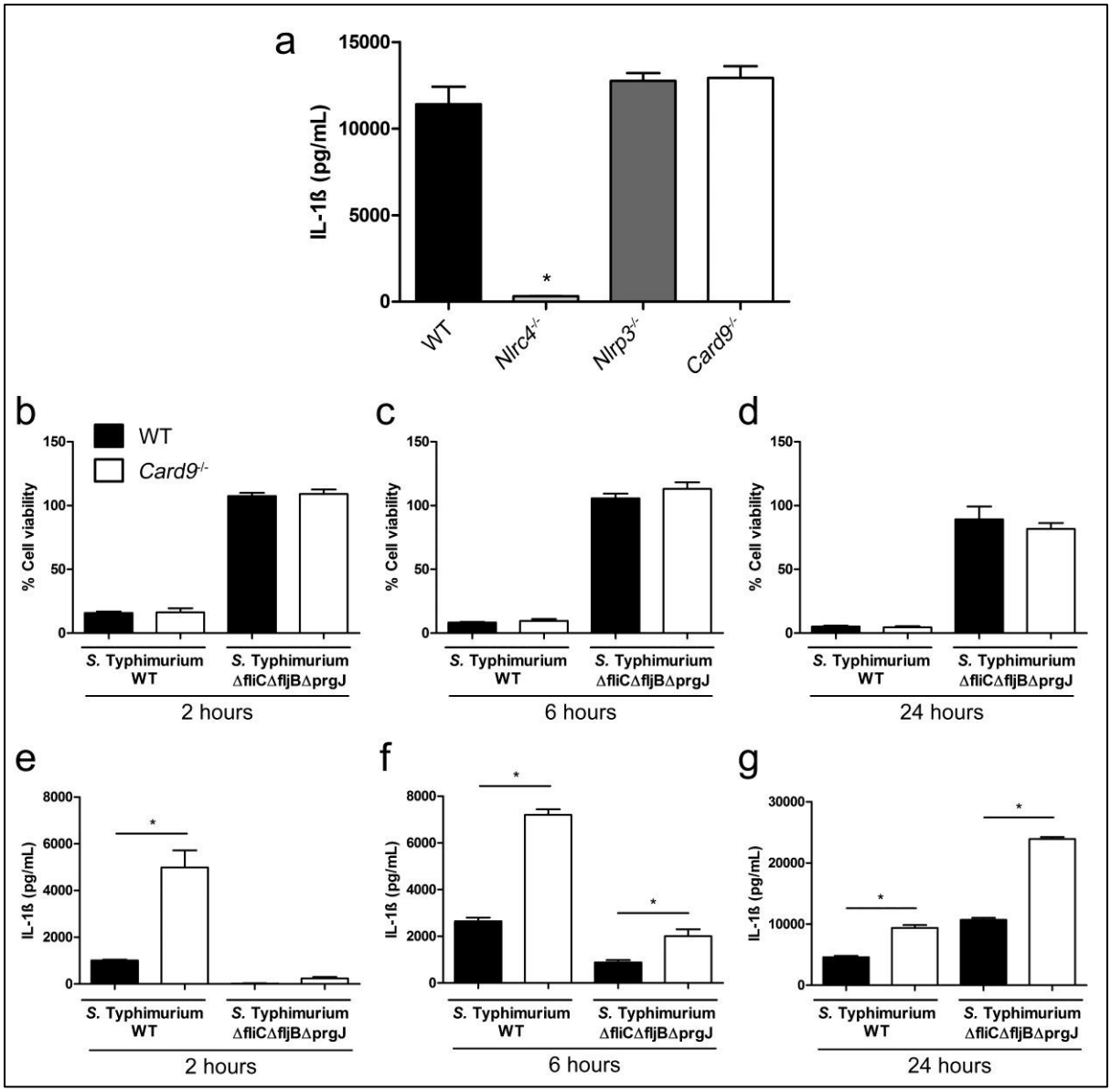

Figure 3: CARD9 does not control IL-1β produced via NLRC4. (a) IL-1β production from LPS-primed BMDMs after transfection with ultrapure flagellin. (b-d) Cellular viability and (e-g) IL-1β production from unprimed BMDMs after infection with *S*. Typhimurium WT or ΔfliCΔfljBΔprgJ (deficient in NLRC4 activation) at an MOI 10 for 2 (c,f), 6 (d,g) and 24 (e,h) hours. * $p<0.05$ in comparison to WT (one-way ANOVA with Tukey's multiple comparisons test). (a-h) Data from three independent experiments (mean and s.e.m.).

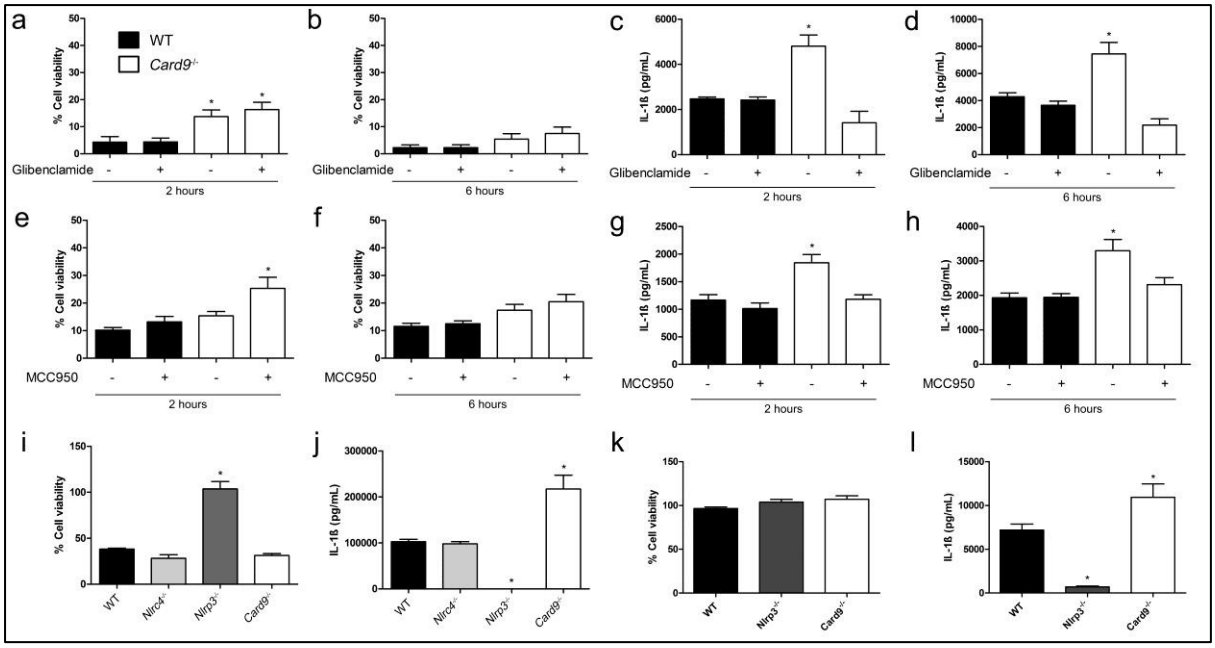

Figure 4: CARD9 selectively negatively regulates NLRP3-induced IL-1β production. (a-b, e-f) Cellular viability and (c-d, g-h) IL-1β secretion from unprimed WT and *Card9*$^{-/-}$ BMDMs infected with *S*. Typhimurium at MOI 10 for 2 (a,c,e,g) and 6 (b,d,f,h) hours in presence or absence of NLRP3 inhibitors glibenclamide (a-d) and MCC950 (e-h). (i-j) Cellular viability (i) and IL-1β secretion (j) from LPS-primed BMDMs after nigericin stimulation (10 µM, 1 hour). IL-1β from LPS-primed cells without nigericin stimulation was below the level of detection. (k-l) Cellular viability (k) and IL-1β secretion (l) from LPS-primed BMDMs after ATP stimulation (5 mM, 30 minutes). * $p<0.05$ in comparison to WT (one-way ANOVA with Tukey's multiple comparisons test). (a-f) Data from three independent experiments (mean and s.e.m.).

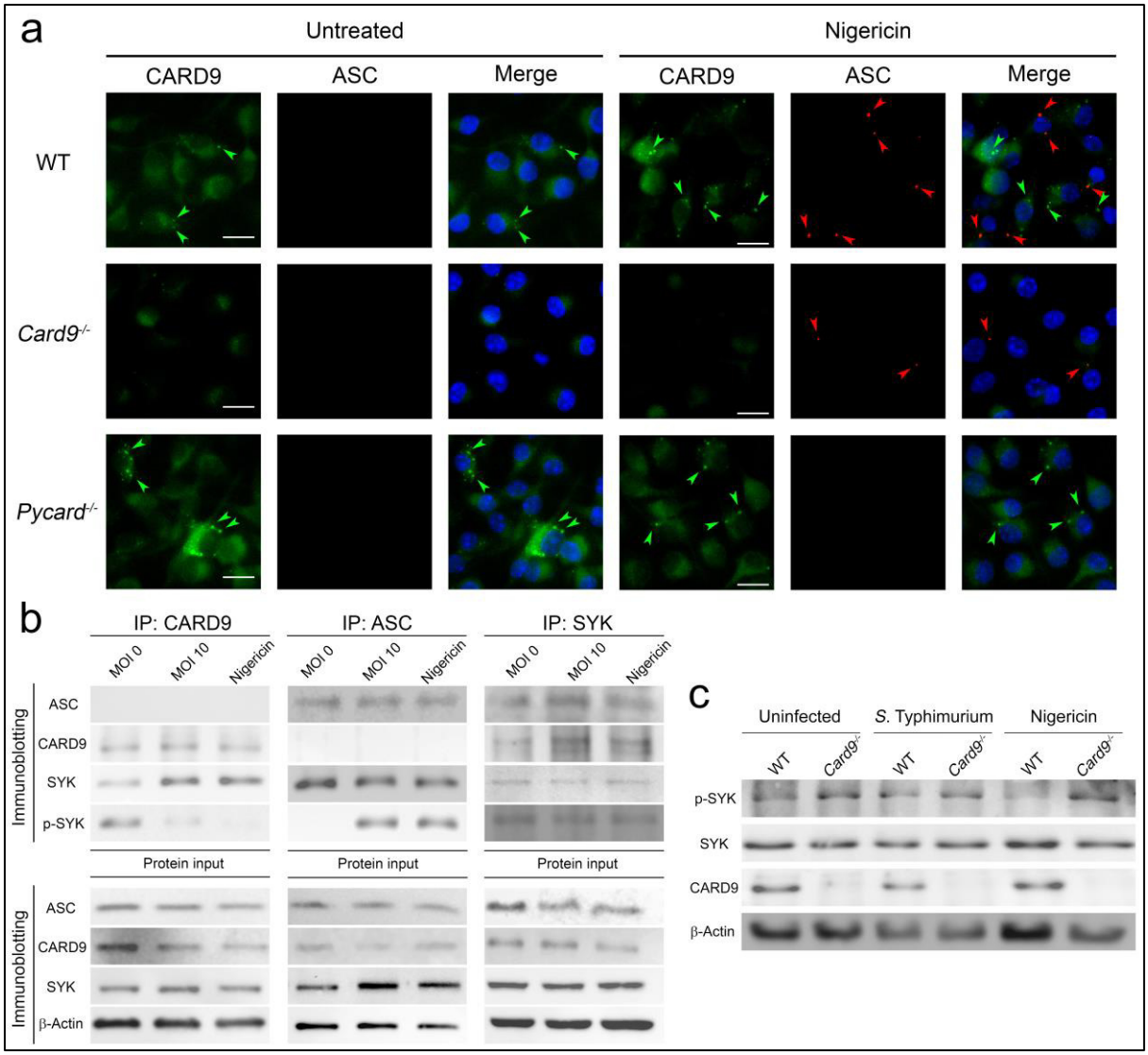

Figure 5: CARD9 and SYK regulates NLRP3 activation upstream to speck formation. (a) CARD9 and ASC were immuno-labelled in WT, *Card9*$^{-/-}$ and *Pycard*$^{-/-}$ LPS-primed macrophages after nigericin stimulation (5 µM, 30 minutes). Green arrows indicates CARD9 aggregates. Red arrows indicates ASC specks. (b) Co-immunoprecipitation of ASC, CARD9 and SYK from cell lysates of uninfected, *S*. Typhimurium (MOI 10, 30 minutes) infected or nigericin (10 µM, 30 minutes) stimulated LPS-primed BMDMs. (c) Immunoblot analysis of LPS-primed WT and *Card9*$^{-/-}$ uninfected, *S*. Typhimurium (MOI 10, 2 hours) infected or nigericin (10 µM, 30 minutes) stimulated BMDMs. (a-c) Images are representative of three independent experiments. Scale bar represents 10 µm.

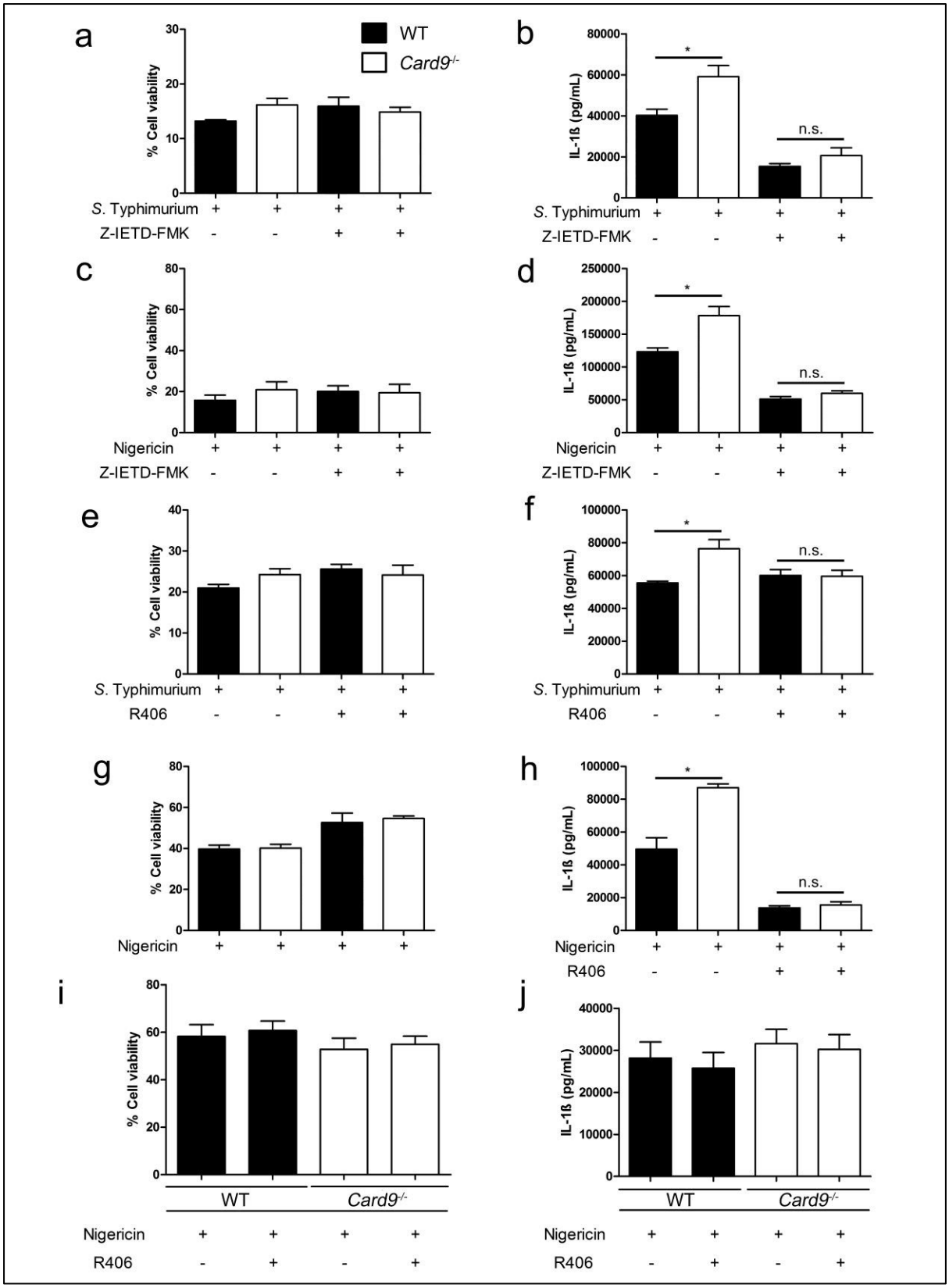

Figure 6: SYK and Caspase-8 activity are important for CARD-9 regulation of NLRP3 activity in BMDMs, but not BMDCs. (a-d) Effects of caspase-8 inhibition by Z-IETD-FMK on LPS-primed WT and *Card9*$^{-/-}$ LPS-primed BMDMs on cellular viability (a,c) and IL-1β production (b,d) during *S.*

Typhimurium infection (MOI 10, 1 hour) (a-b) or nigericin (10 µM, 1 hour) stimulation (c-d). (e-h) Effects of SYK inhibition by R406 on WT and *Card9*$^{-/-}$ LPS-primed BMDMs on cellular viability (e,g) and IL-1β secretion (f,h) in response to *S*. Typhimurium infection (MOI 10, 1 hour) (e-f) or nigericin stimulation (5 µM, 1 hour) (g-h). (i-j) Stimulation of WT or *Card9*$^{-/-}$ BMDCs with Nigericin (5 µM, 1 hour). Cellular viability (i) and IL-1β secretion (j). *p<0.05 (one-way ANOVA with Tukey's multiple comparisons test. (a-j) Data from three independent experiments (mean and s.e.m.).

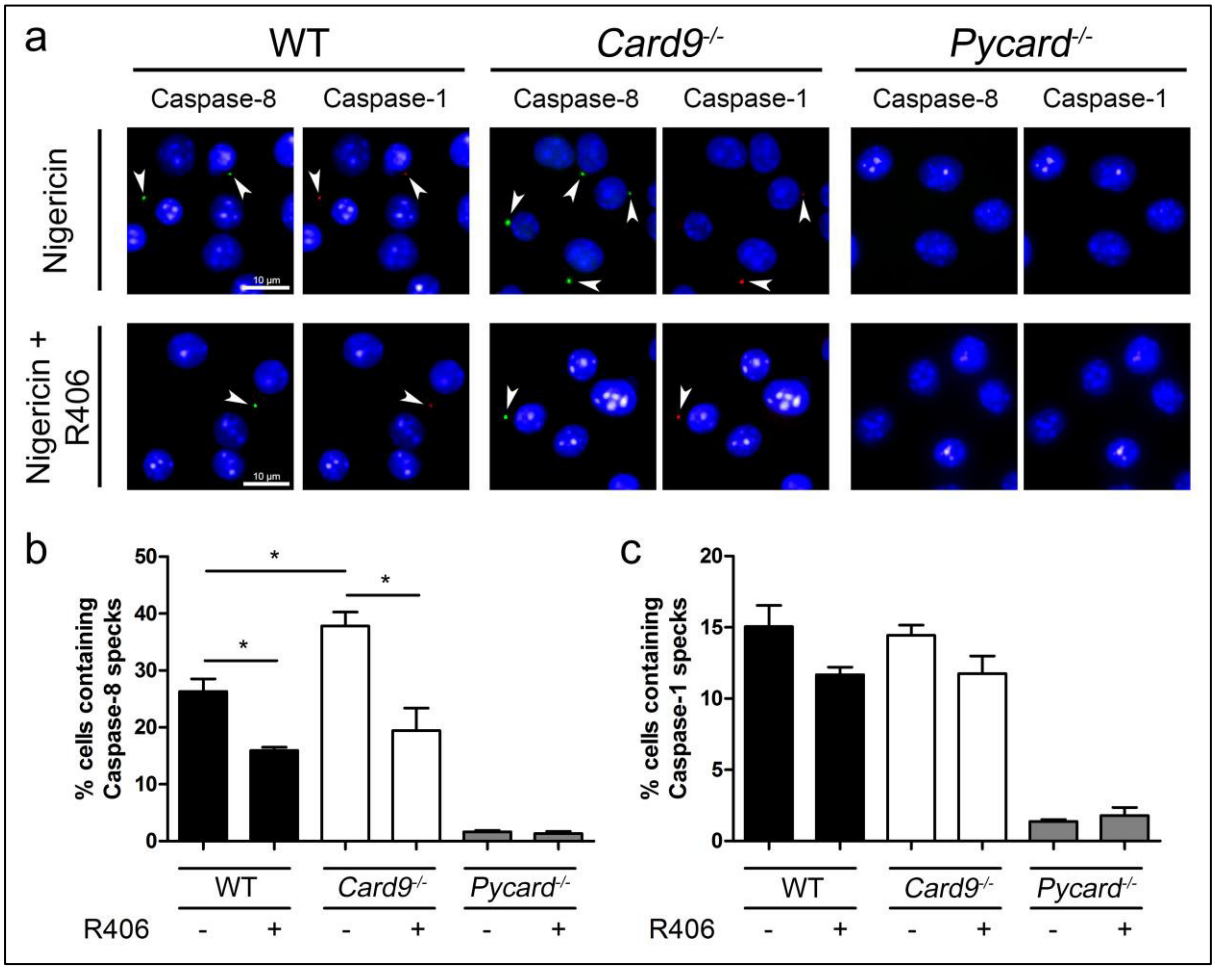

Figure 7: SYK activity increases the number of caspase-8 specks in response to NLRP3 stimulation in *Card9*$^{-/-}$ BMDMs. (a-c) WT, *Card9*$^{-/-}$ or *Pycard*$^{-/-}$ LPS-primed BMDMs were incubated with nigericin (5 µM, 30 minutes) in the presence of caspase-1 and caspase-8 FLICA substrates, with or without the SYK inhibitor R406. (a) Pattern of caspase-1 and caspase-8 specks observed by immunofluorescence labelling of this protein. (b) Percentage of cells containing caspase-8 or (c) caspase-1 specks. * p<0.05 (one-way ANOVA with Tukey's multiple comparisons test). (a) Image is representative of three independent experiments. (b-c) Data from three independent experiments (mean and s.e.m.). Scale bar represents 10 µm.

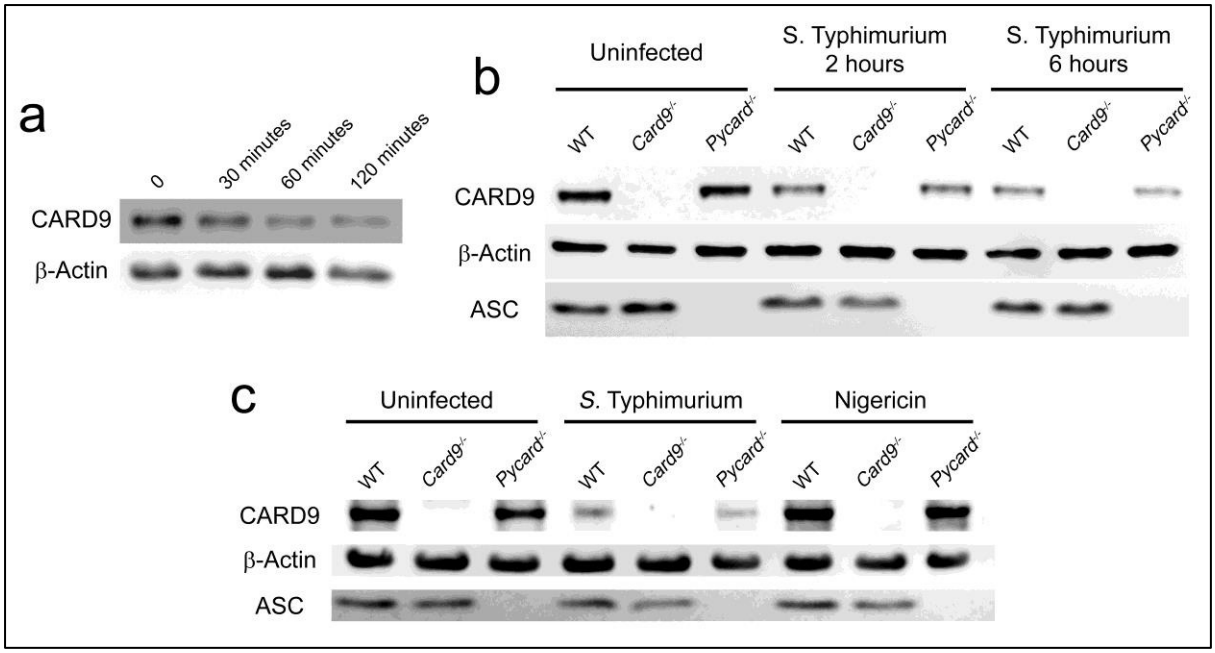

Figure 8: CARD9 acts as a regulatory switch during infection. (a) Immunoblotting of CARD9 and ASC in cell lysates from unprimed WT BMDMs after infection with *S*. Typhimurium (MOI 5) for 0, 30, 60 and 120 minutes. (b) Immunoblotting of CARD9 and ASC in cell lysates from unprimed BMDMs (WT, *Card9*$^{-/-}$ or *Pycard*$^{-/-}$) after infection with *S*. Typhimurium (MOI 5) for 0, 2 and 6 hours. (c) Immunoblotting of CARD9 and ASC in cell lysates from uninfected, *S*. Typhimurium infected (MOI 5 for 2 hours), or nigericin stimulated (5 µM, 30 minutes) LPS-primed BMDMs (WT, *Card9*$^{-/-}$ or *Pycard*$^{-/-}$). (a-c) Images are representative of three independent experiments.

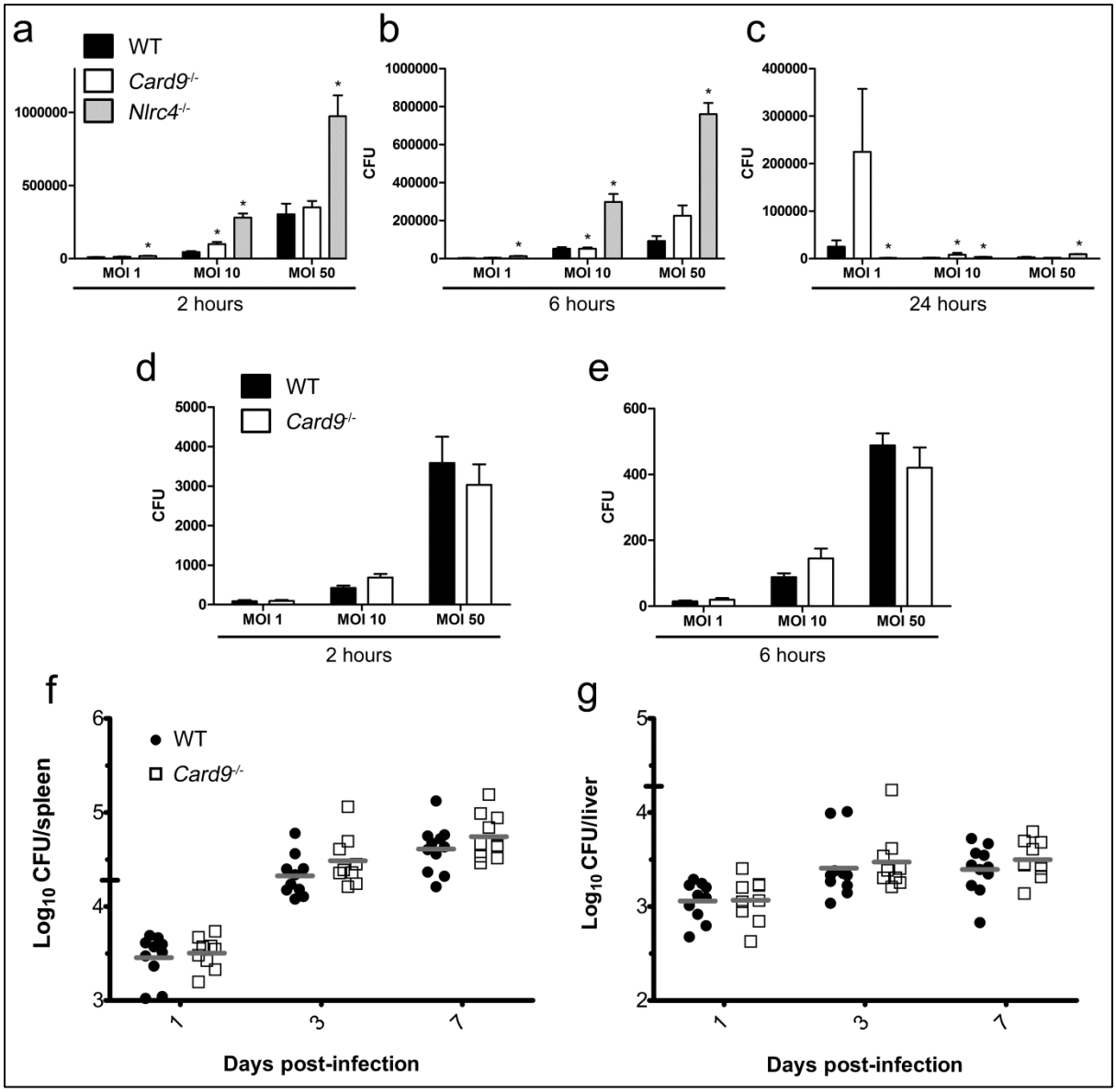

Supplementary Figure 1: CARD9 does not influence bacteria counts *in vitro* and *in vivo.* (a-c) intracellular bacteria counts of WT, *Nlrc4*$^{-/-}$ and *Card9*$^{-/-}$ BMDMs after infection with *S*. Typhimurium SL1344 at MOIs 1, 10 and 50 for 2 (a), 6 (b) and 24 (c) hours. (g-h) Bacteria burden in the spleen (g) and liver (h) after C57BL/6 WT and *Card9*$^{-/-}$ infection with *S*. Typhimurium M525P ($4x10^3$ CFU). * $p<0.05$ in comparison to WT (one-way ANOVA with Tukey's multiple comparisons test). (a-e) Data from two independent experiments (mean and s.e.m.). (g-h) Data from two independent experiments using from four to six mice per genotype, plus two negative controls per genotype. Mice were from 8 to 16 weeks old, both male and female.

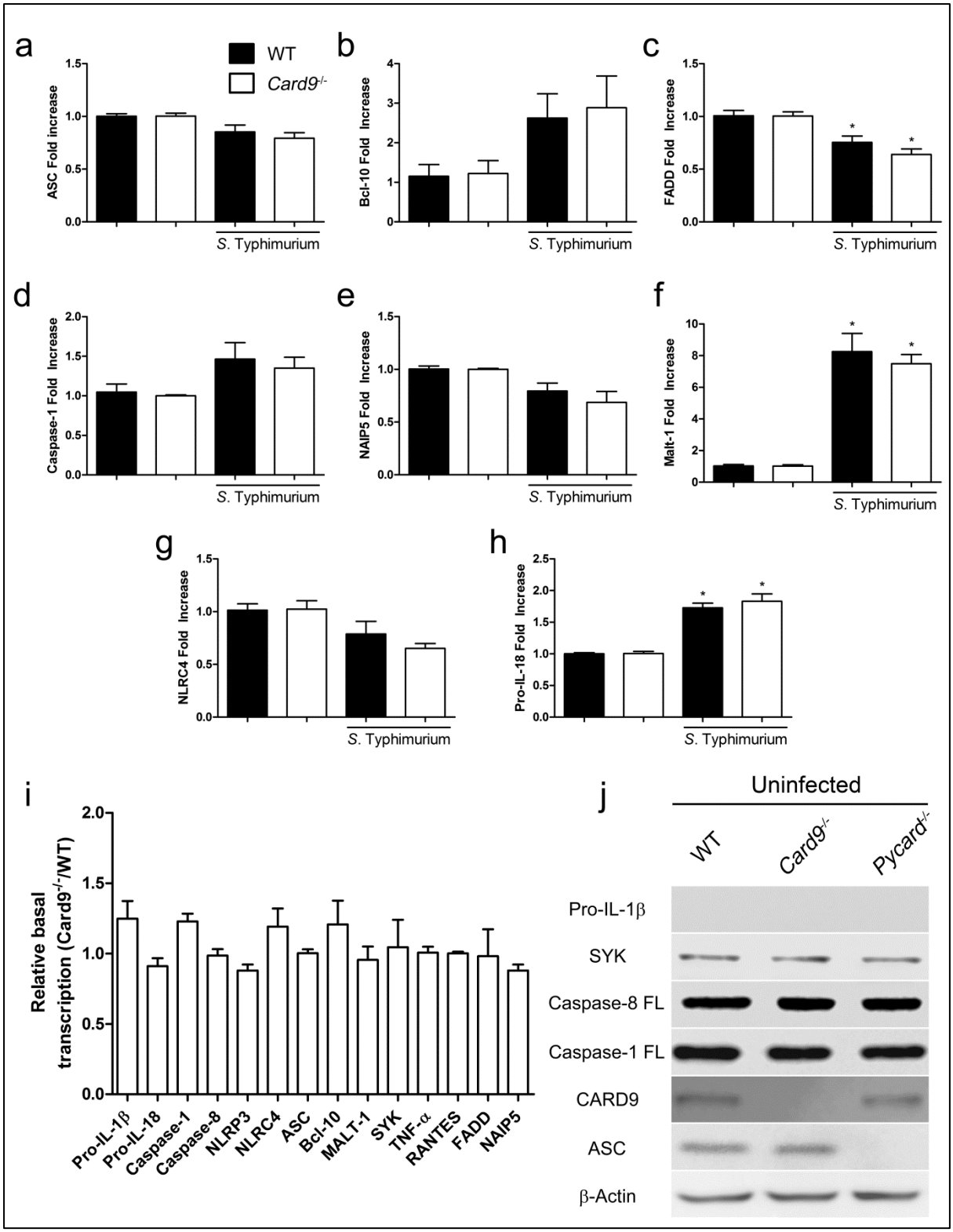

Supplementary Figure 2: Transcription and expression analysis of WT and *Card9*$^{-/-}$ BMDMs. (a-h) qPCR analysis of WT and *Card9*$^{-/-}$ BMDMs infected with *S*. Typhimurium (MOI 5) for 2 hours, in relation to their respective uninfected controls. (a) ASC, (b) Bcl-10, (c) FADD, (d) Caspase-1, (e) NAIP5 , (f) Malt-1, (g) NLRC4, (h) pro-IL-18. (i) Basal transcriptional levels in uninfected *Card9*$^{-/-}$ BMDMs in relation to uninfected WT cells. (j) Basal expression of pro-IL-1β, SYK, Caspase-8 Full Length, Caspase-1 Full Length, CARD9, ASC, β-actin in WT, *Card9*$^{-/-}$ and *Pycard*$^{-/-}$ BMDMs cell lysates. * $p<0.05$ in

comparison to uninfected control (one-way ANOVA with Tukey's multiple comparisons test). (a-i) Data from three independent experiments (mean and s.e.m.). (j) Image is representative of three independent experiments.

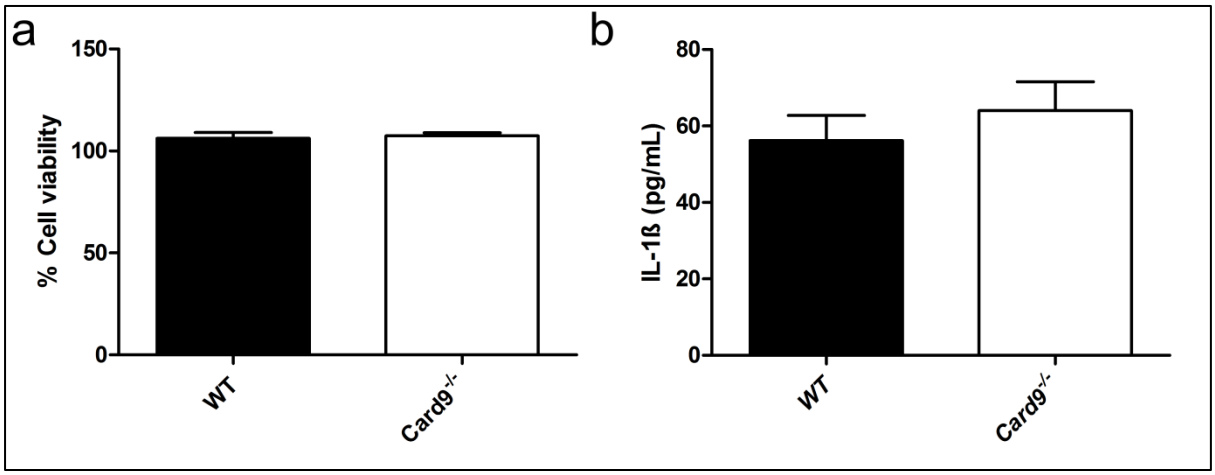

Supplementary Figure 3: CARD9 does not control IL-1β produced via AIM2. (a) Cellular viability and (b) IL-1β from LPS-primed BMDMs after transfection with poly(dA:dT) for 4 hours. Data from three independent experiments (mean and s.e.m.).

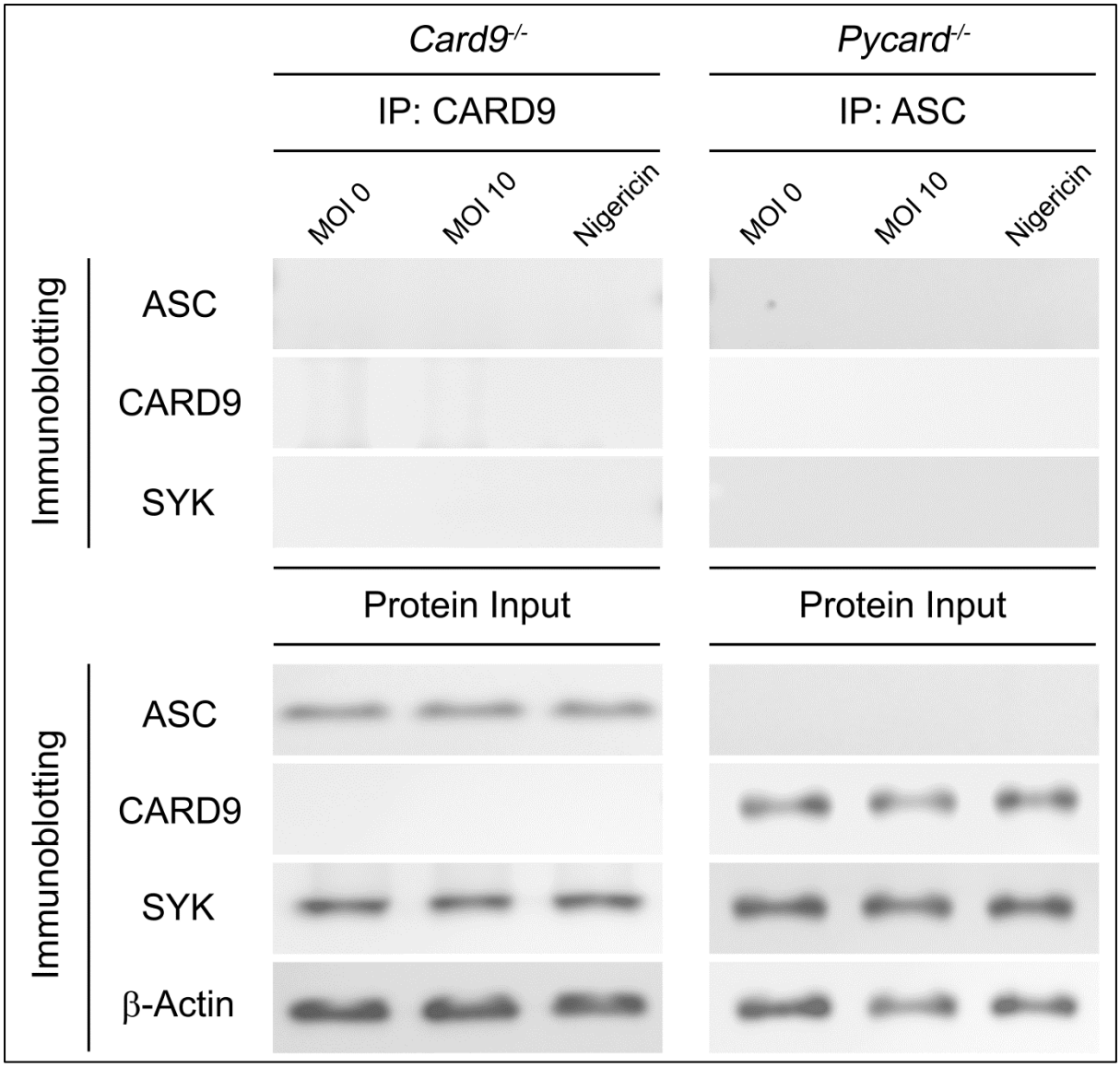

Supplementary Figure 4: CARD9 and ASC co-IPs isotype controls. *Card9*$^{-/-}$ and *Pycard*$^{-/-}$ BMDMs were primed with LPS (200 ng/mL) for 3 hours and incubated with *S*. Typhimurium (MOI 10, 30 minutes) or with Nigericin (10 µM, 30 minutes). IPs were then performed as indicated using anti-CARD9 (for *Card9*$^{-/-}$ BMDMs) or anti-ASC (for *Pycard*$^{-/-}$ BMDMs), followed by immunoblotting. No IPs or co-IPs are observed. Images are representative of three independent experiments.

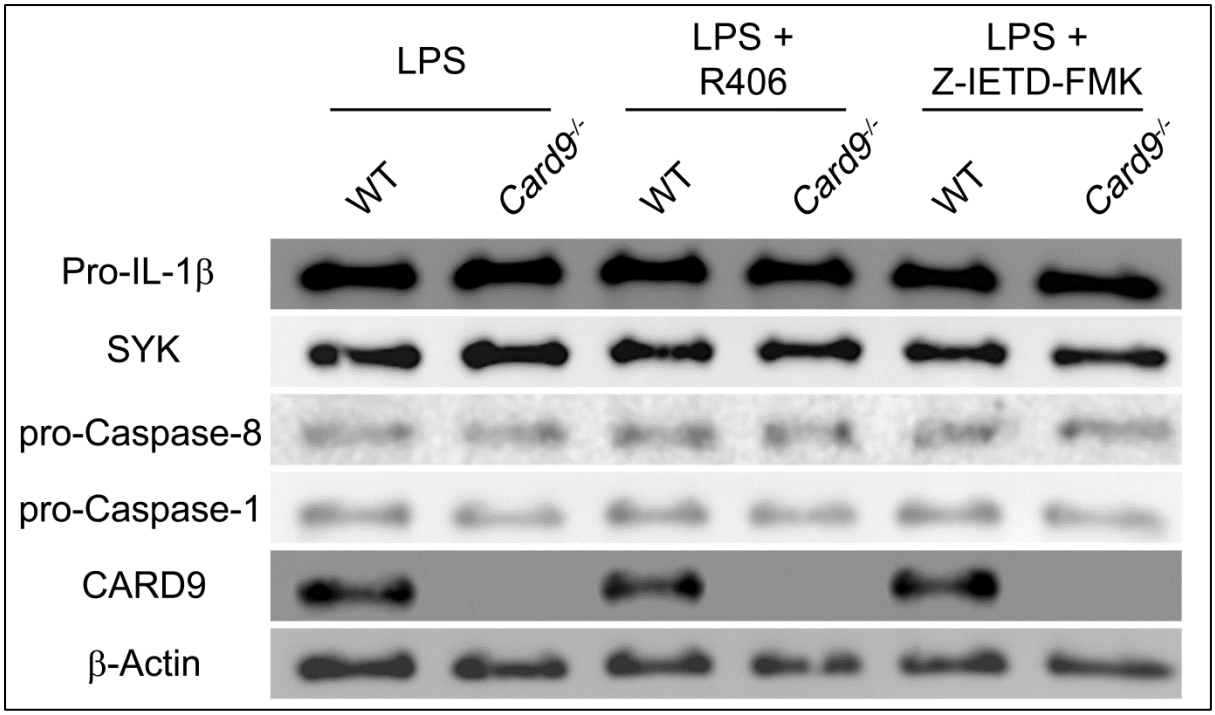

Supplementary Figure 5: LPS-priming by itself or use of Z-IETD-FMK and R406 do not cause different expression in WT and *Card9*$^{-/-}$ BMDMs. Expression of pro-IL-1β, SYK, pro-caspase-8, pro-caspase-1, CARD9, β-actin in of cell lysates from WT and *Card9*$^{-/-}$ BMDMs incubated for 3 hours with LPS (200 ng/mL) or 3 hours with LPS with and additional hour of incubation with Z-IETD-FMK (10 μM) or R406 (1 μM). Figure is representative of three independent experiments.

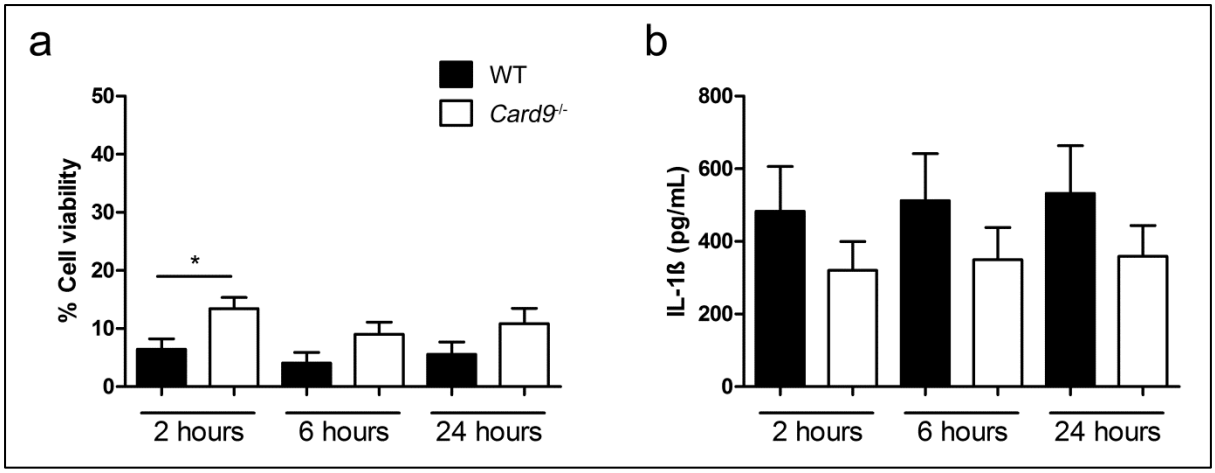

Supplementary Figure 6: CARD9 plays no role in controlling IL-1β production in BMDCs. (a) cellular viability (as measured by LDH release) and (b) IL-1β secretion (as measured by ELISA), of WT and *Card9*$^{-/-}$ BMDCs after infection with *S*. Typhimurium SL1344 at MOI 10 for 2, 6 and 24 hours. (a-b) Data from three independent experiments (mean and s.e.m.).

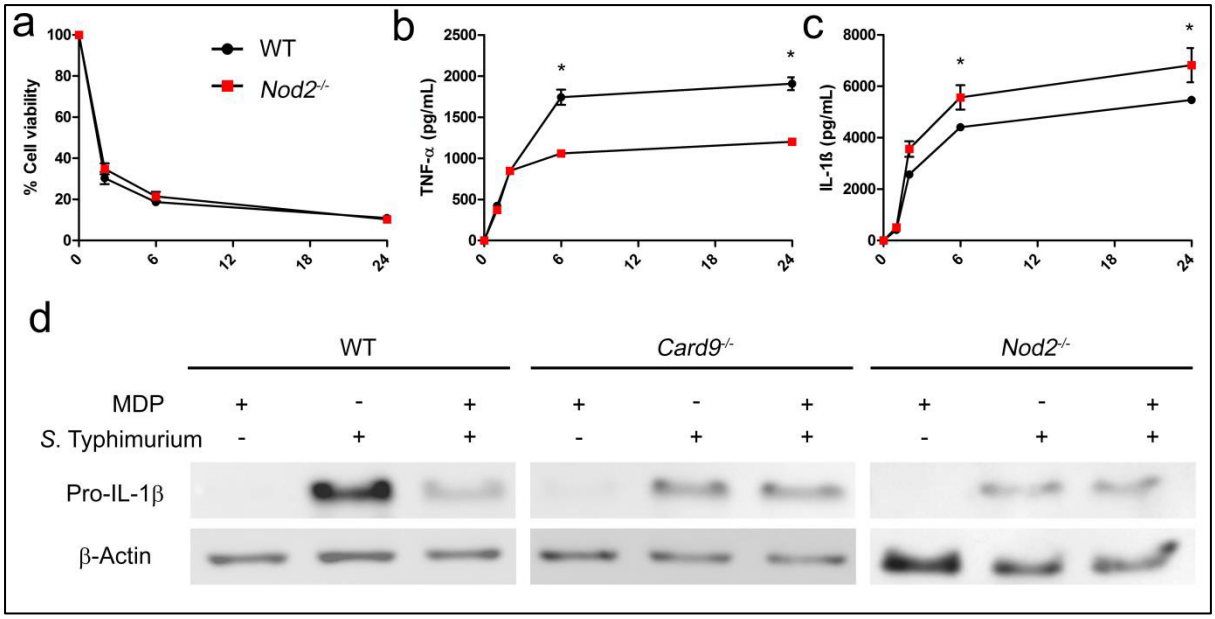

Supplementary Figure 7: NOD2 up- and down-regulates the expression of different cytokines during *S*. Typhimurium infection. (a) Cellular viability (as measured by LDH release) (b) IL-1β secretion (as measured by ELISA) and (c) TNF-α (as measured by ELISA) of WT and *Nod2*$^{-/-}$ BMDMs after infection with *S*. Typhimurium SL1344 at MOI 10 for 2, 6 and 24 hours. (d) Pro-IL-1β expression in WT, *Nod2*$^{-/-}$ and *Card9*$^{-/-}$ BMDMs infected with S. Typhimurium (MOI 10) with or without MDP co-stimulation (10 µg/mL) (a-c) Data from two independent experiments (mean and s.e.m.). (d) Figure is representative of three independent experiments. * $p<0.05$ (two-way ANOVA) with Bonferroni post-test.

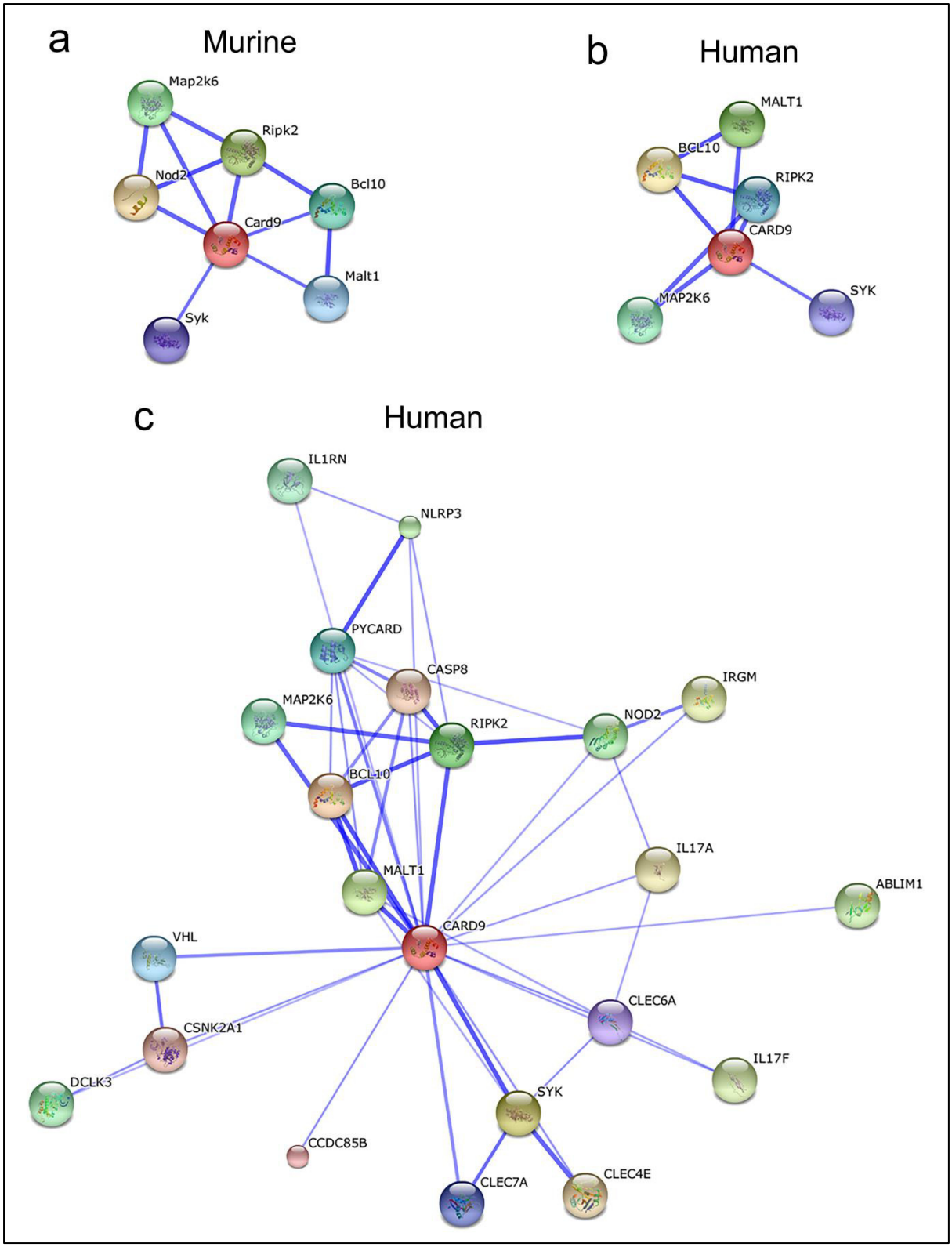

Supplementary Figure 8: CARD9 interfaces with multiple inflammatory and death-related signalling pathways. Functional association network analysis of the primary CARD9 interactome was performed using STRINGv10. High confidence interaction partners (score > 0.7) for murine (a) and human (b) CARD9. Reducing the stringency of the inclusion criteria to include medium confidence

interaction partners (score > 0.4) confirms the expansive signalling network in which CARD9 is involved supporting its assignment as a critical inflammatory signalling node (c).

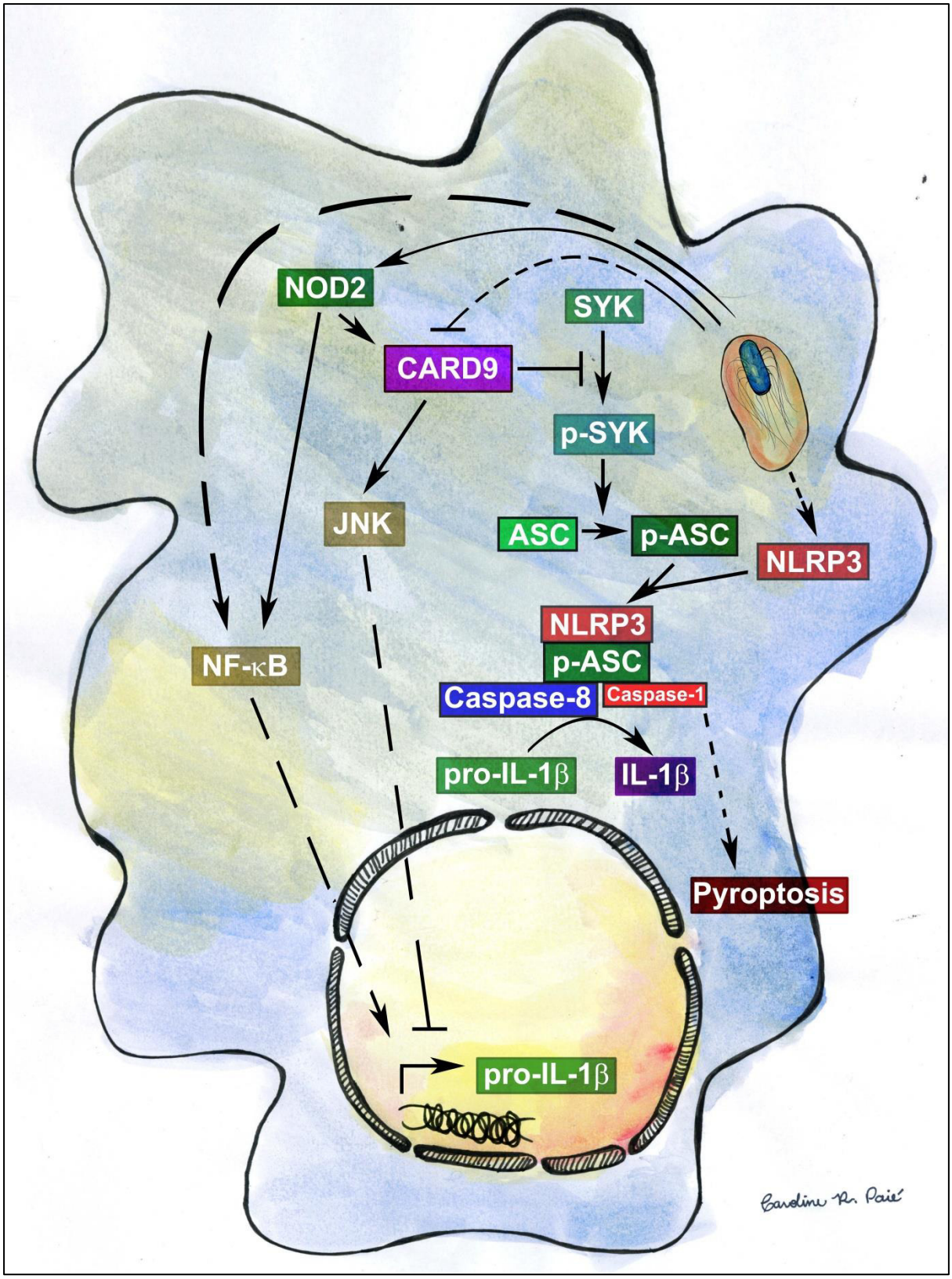

Supplementary Figure 9: Simplified model for CARD9 regulation of IL-1β production. Infection by *S.* Typhimurium triggers the assembly of the NLRP3 inflammasome in the cytoplasm of BMDMs with subsequent processing of pro-IL-1β to mature IL-1β. CARD9 negatively regulates inflammasome activity at two levels: suppressing pro-IL-1β expression and reducing caspase-8-dependent IL-1β processing.

Supplementary Table 1: Pairs of primers used for the qPCR experiments.

Gene	Forward (5'-3')	Reverse (5'-3')	Amplicon size (bp)	Primer Bank ID
β-actin	GGCTGTATTCCCCTCCATCG	CCAGTTGGTAACAATGCCATGT	154	6671509a1
ASC	CTTGTCAGGGGATGAACTCAAAA	GCCATACGACTCCAGATAGTAGC	154	31560222a1
Bcl-10	CTTCAAGTAGAAAACGGGCTGG	GCACCTAGAGAGGTTGTTGGT	233	6753166a1
Caspase-1	ACAAGGCACGGGACCTATG	TCCCAGTCAGTCCTGGAAATG	237	6753282a1
Caspase-8	TGCTTGGACTACATCCCACAC	TGCAGTCTAGGAAGTTGACCA	169	33859520a1
FADD	GCGCCGACACGATCTACTG	TTACCCGCTCACTCAGACTTC	215	6753812a1
GAPDH	AGGTCGGTGTGAACGGATTTG	TGTAGACCATGTAGTTGAGGTCA	123	6679937a1
MALT-1	GGACAAAGTCGCCCTTTTGAT	TCCACAGCGTTACACATCTCA	165	27370250a1
NAIP5	TGCCAAACCTACAAGAGCTGA	CAAGCGTTTAGACTGGGGATG	203	5932014a1
NLRC4	TTGAAGGCGAGTCTGGCAAAG	GGCGCTTCTCAGGTGGATG	125	146198620c2
NLRP3	ATTACCCGCCCGAGAAAGG	TCGCAGCAAAGATCCACACAG	141	22003870a1
Pro-IL-18	GTGAACCCCAGACCAGACTG	CCTGGAACACGTTTCTGAAAGA	202	6680412c1
Pro-IL-1β	TTCAGGCAGGCAGTATCACTC	GAAGGTCCACGGGAAAGACAC	75	118130747c2
RANTES	GCTGCTTTGCCTACCTCTCC	TCGAGTGACAAACACGACTGC	104	7305461a1
SYK	CTACCTGCTACGCCAGAGC	GCCATTAAGTTCCCTCTCGATG	103	6755706a1
TNF-α	CCCTCACACTCAGATCATCTTCT	GCTACGACGTGGGCTACAG	61	7305585a1